frontiers | Research Topics

Needs and potential application of one health approach in the control of vector-borne and zoonotic infectious disease

Edited by
Xinyu Feng, Sibao Wang, Gong Cheng, Xiao-kui Guo and Xiao-Nong Zhou

Published in
Frontiers in Microbiology
Frontiers in Veterinary Science

ISSN 1664-8714
ISBN 978-2-83250-956-2
DOI 10.3389/978-2-83250-956-2

About Frontiers

Frontiers is more than just an open access publisher of scholarly articles: it is a pioneering approach to the world of academia, radically improving the way scholarly research is managed. The grand vision of Frontiers is a world where all people have an equal opportunity to seek, share and generate knowledge. Frontiers provides immediate and permanent online open access to all its publications, but this alone is not enough to realize our grand goals.

Frontiers journal series

The Frontiers journal series is a multi-tier and interdisciplinary set of open-access, online journals, promising a paradigm shift from the current review, selection and dissemination processes in academic publishing. All Frontiers journals are driven by researchers for researchers; therefore, they constitute a service to the scholarly community. At the same time, the *Frontiers journal series* operates on a revolutionary invention, the tiered publishing system, initially addressing specific communities of scholars, and gradually climbing up to broader public understanding, thus serving the interests of the lay society, too.

Dedication to quality

Each Frontiers article is a landmark of the highest quality, thanks to genuinely collaborative interactions between authors and review editors, who include some of the world's best academicians. Research must be certified by peers before entering a stream of knowledge that may eventually reach the public - and shape society; therefore, Frontiers only applies the most rigorous and unbiased reviews. Frontiers revolutionizes research publishing by freely delivering the most outstanding research, evaluated with no bias from both the academic and social point of view. By applying the most advanced information technologies, Frontiers is catapulting scholarly publishing into a new generation.

What are Frontiers Research Topics?

Frontiers Research Topics are very popular trademarks of the *Frontiers journals series*: they are collections of at least ten articles, all centered on a particular subject. With their unique mix of varied contributions from Original Research to Review Articles, Frontiers Research Topics unify the most influential researchers, the latest key findings and historical advances in a hot research area.

Find out more on how to host your own Frontiers Research Topic or contribute to one as an author by contacting the Frontiers editorial office: frontiersin.org/about/contact

Needs and potential application of one health approach in the control of vector-borne and zoonotic infectious disease

Topic editors

Xinyu Feng — Chinese Center For Disease Control and Prevention, China
Sibao Wang — Key Laboratory of Insect Developmental and Evolutionary Biology, Institute of Plant Physiology and Ecology, Shanghai Institutes for Biological Sciences (CAS), China
Gong Cheng — Tsinghua University, China
Xiao-kui Guo — Shanghai Jiao Tong University, China
Xiao-Nong Zhou — National Institute of Parasitic Diseases (China), China

Citation

Feng, X., Wang, S., Cheng, G., Guo, X.-k., Zhou, X.-N., eds. (2022). *Needs and potential application of one health approach in the control of vector-borne and zoonotic infectious disease*. Lausanne: Frontiers Media SA.
doi: 10.3389/978-2-83250-956-2

Table of contents

frontiers | Frontiers in Microbiology

TYPE Editorial
PUBLISHED 22 November 2022
DOI 10.3389/fmicb.2022.1089174

OPEN ACCESS

EDITED AND REVIEWED BY
Axel Cloeckaert,
Institut National de recherche pour l'agriculture, l'alimentation et l'environnement (INRAE), France

*CORRESPONDENCE
Xiaonong Zhou
zhouxn1@chinacdc.cn

SPECIALTY SECTION
This article was submitted to Infectious Agents and Disease, a section of the journal Frontiers in Microbiology

RECEIVED 04 November 2022
ACCEPTED 08 November 2022
PUBLISHED 22 November 2022

CITATION
Feng X, Wang S, Cheng G, Guo X and Zhou X (2022) Editorial: Needs and potential application of One Health approach in the control of vector-borne and zoonotic infectious disease. *Front. Microbiol.* 13:1089174. doi: 10.3389/fmicb.2022.1089174

Editorial: Needs and potential application of One Health approach in the control of vector-borne and zoonotic infectious disease

Xinyu Feng[1,2,3,4,5,6,7], Sibao Wang[8,9], Gong Cheng[10], Xiaokui Guo[5,6] and Xiaonong Zhou[1,2,3,4,5,6]*

[1]National Institute of Parasitic Diseases, Chinese Center for Disease Control and Prevention (Chinese Center for Tropical Diseases Research), Beijing, China, [2]National Health Commission (NHC) Key Laboratory of Parasite and Vector Biology, Beijing, China, [3]World Health Organization (WHO) Collaborating Centre for Tropical Diseases, Beijing, China, [4]National Center for International Research on Tropical Diseases, Beijing, China, [5]School of Global Health, Chinese Center for Tropical Diseases Research, Shanghai Jiao Tong University School of Medicine, Shanghai, China, [6]One Health Center, Shanghai Jiao Tong University-The University of Edinburgh, Shanghai, China, [7]Department of Biology, College of Life Sciences, Inner Mongolia University, Hohhot, China, [8]Chinese Academy of Sciences (CAS) Key Laboratory of Insect Developmental and Evolutionary Biology, CAS Center for Excellence in Molecular Plant Sciences, Institute of Plant Physiology and Ecology, Chinese Academy of Sciences, Shanghai, China, [9]CAS Center for Excellence in Biotic Interactions, University of Chinese Academy of Sciences, Beijing, China, [10]Tsinghua-Peking Center for Life Sciences, School of Medicine, Tsinghua University, Beijing, China

KEYWORDS

One Health, global health, microbiology, vector-borne disease, zoonotic disease

Editorial on the Research Topic
Needs and potential application of One Health approach in the control of vector-borne and zoonotic infectious disease

In view of the unbridled outbreaks and increasing prevalence of zoonotic diseases and other infectious diseases, the global health community advocates adopting the "One Health" approach to prevent and cope with these challenges (Jones et al., 2008; Keusch et al., 2022). Some countries have adopted relevant strategies in the campaign against zoonotic diseases and achieved some initial success (Bird and Mazet, 2018; Acharya et al., 2020). For example, from 2013 to 2019, Tamil Nadu in India established a "One Health" committee to address the challenge of dog and human rabies. Finally, the intervention measures developed by the committee reduced the human rabies mortality rate economically and effectively (Fitzpatrick et al., 2016; Gibson et al., 2022). Also, integrated measures against echinococcosis based on the concept of One Health were deployed in Shiqu County, Sichuan Province, China, which significantly reduced the prevalence of echinococcosis after long-term monitoring (Tiaoying et al., 2005; Wang et al., 2021). In addition, since 2009, Switzerland, New Zealand, and other countries have built campylobacteriosis surveillance and management systems by implementing the "One Health" strategy, and the campylobacteriosis epidemic has been effectively

contained (Babo Martins et al., 2017; Schiaffino et al., 2019). All the evidence showed that the application of the "One Health" strategy in controlling infectious diseases and zoonoses has achieved good results and led to substantially more significant socio-economic benefits worldwide (Ajuwon et al., 2021). Therefore, this topic discussed the needs and potential application of the One Health approach in practice, program, and policy of vector-borne and zoonotic infectious diseases.

Zoonotic and vector-borne diseases contribute significantly to the global burden of diseases. For instance, malaria, the most important vector-borne disease, affects millions of people and contributes significantly to the disadvantage of public health and socioeconomic development. In this Research Topic, Kassegne et al. characterized different species of plasmodium parasites (*Plasmodium ovale* and *Plasmodium malaria*), which were not previously reported, in high-transmission areas of southern Togo of tropical Africa. The molecular survey of malaria infections in the area helped reveal the natural malaria's epidemiological status. It provided helpful information to improve disease control/surveillance strategies and policies in such areas of endemic malaria. Besides, Rift Valley fever virus (RVFV) is a mosquito-borne viral zoonosis causing severe disease in humans and ruminants. Although the disease is classified as a priority disease by the World Health Organization, licensed vaccines are presently unavailable or contraindicated. Zhang et al. constructed a bacterium-like particle vaccine (BLP), RVFV-BLPs. They also determined that mice immunized with RVFV-BLPs produced both humoral and cellular immunity. RVFV-BLPs represent a novel and promising vaccine candidate for the prevention of RVF infection in both humans and veterinary animals. The described RVFV-BLPs were also found to have the advantage of large-scale use and relatively low cost. In addition, the Japanese encephalitis virus (JEV) is one of the most important emerging pathogens, which causes not only fatal neurological disease in humans but also causes reproductive failure in pigs. By comparing pathogenicity between Japanese encephalitis virus strains (SA14 and BJB), Xing et al. found that the SL-IV and DB1 regions of 3′UTR were essential for JEV replication, neural invasiveness, and viral pathogenicity. They confirmed that some mutations at sites 248, 254, 258, and 307 in the 3′UTR of JEV play a vital role in the viral life cycle. This study offered a new perspective for designing and formulating a candidate vaccine.

Increasing environmental change, global migration, acts of bioterrorism, and human social behavior change may increase the risk of pathogen spill over, such as from wildlife reservoirs to humans, from abundant domestic reservoir hosts to the susceptible animal populations, and from living organisms to the environment and vice versa. More comprehensive prevention and control strategies and meaningful risk management tools are essential to reduce disease spillovers and prevent disease emergence. Olaya-Galán et al. evaluated a zoonotic infection of bovine leukemia virus (BLV) in human beings by gathering experimental evidence about the susceptibility of human cell lines to BLV infection. Several human cell lines (iSLK and MCF7) produced a stable infection throughout the 3 months, supporting the hypothesis of a natural transmission from cattle to humans. This study provided *in vitro* experimental evidence of BLV as an exogenous etiological agent of human breast cancer.

Previous research has reported non-human primates (NHPs) as reservoirs for human intestinal protozoa infection. Li J. et al. investigated the prevalence of pathogenic intestinal protozoan infections in macaques and humans and conducted a risk evaluation of interspecies transmission among laboratory macaques, animal facility workers, and nearby villagers from One Health Perspective. They found that the facility workers had direct contact with macaques and had a significantly higher intestinal protozoa infection rate. Furthermore, some shared haplotypes confirmed the presence of zoonotic subtypes in NHPs and humans. These results warrant the utility of One Health frameworks to characterize infection risk and to offer relevant and comprehensive control strategies in the future.

Microbiological hazards form a major source of food-borne diseases in humans. Solís et al. reported that pet food, especially new feeding practices, such as raw meat-based diets, can be a potential source of microbiological hazards that might affect companion animals and owners. Therefore, microbiological hazards of foodborne pathogens in raw and extruded canine diets may facilitate the causative agent spillover by transmission from a reservoir population, which implies a significant concern for humans and pets.

Emerging infectious diseases (EID) have rapidly increased in recent years and expanded in geographic range. Many EIDs (∼60%) are zoonotic, including HIV-AIDS, Ebola and SARS, and COVID-19. Yeo et al. investigated the prevalence of emerging or re-emerging human enteric viruses in porcine stools and swabs in the Republic of Korea. The study demonstrated that human enteric viruses detected in pigs and some porcine enteric viruses are genetically related to human enteric viruses, indicating the zoonotic potential of porcine enteric viruses as potential EIDs.

Generally, influenza A viruses (IAVs) infections are refractory to mammals because of species barriers. On rare occasions, however, IAVs can break the species barrier and spill over to mammalian species. Except for a small number of viruses known to infect animals, including swine, bats, and humans, the emergence of H3N2 canine influenza viruses (CIVs) provides a new perspective for interspecies transmission of the virus. Given this, Li X. et al. screened for amino acid transitions involved in adapting IAVs to canine and other mammalian hosts. They found that the H3N2 influenza virus has host-adaptive signatures in canines and can establish persistent transmission in lower mammals. All these studies highlight the necessity of identifying and monitoring the emerging pathogen spillover effects by enhanced surveillance and further studies to ensure an integrated "One Health" approach that

aims to balance and optimize the health of humans, animals, and ecosystems.

Timely and sensitive detection is particularly important for the detection of potential pathogens. Molecular methods offer improved sensitivity for detecting pathogens through a diverse context. Herein, Yao et al. developed a cost-effective, multi pathogen and high-throughput method for simultaneously detecting the Ebola virus and 16 other pathogens associated with hemorrhagic fever. The simultaneous detection assay would provide a reliable and sensitive diagnostic method and aid the surveillance and epidemiological study of the Ebola Virus.

One Health approach has immense potential to improve human, animal, and environmental health and combat future global health crises by creating collaborative processes connecting expertise. As a paradigm, One Health needs to involve a broad transdisciplinary effort working locally, nationally, and globally. The strategy are being discussed in our Research Topic by Tucker et al. and Yasmeen et al. Through analysis and comparison between African Swine Fever (ASF) and subsequently emerged COVID-19 pandemic, Tucker et al. pointed out that both pandemics highlight the difficulties in adequately preparing for and containing an outbreak in the face of complicated social and political factors. There are temporal and thematic links, such as similar patterns in these two threats and factors associated with ASF that compounded the COVID-19 pandemic. Moreover, two pandemics likely had asymmetric effects on each other, many of which are difficult to quantify. These two pandemics underscore the need to use a One Health framework to overcome threats from surrounding transmission to and from wildlife, exacerbating food insecurity and bottlenecks in disease surveillance capacity.

Yasmeen et al. indicated that the concept is not widely accepted in impoverished areas where zoonotic diseases often occur due to close contact with domestic or wild animals. They raised a Pakistan perspective on how to use the One Health paradigm to confront zoonotic health threats. Firstly, the study provided an overview of Pakistan's most common zoonotic diseases. Subsequently, they listed several potential factors necessary to overcome zoonotic disease prevalence, including disease outbreak surveillance, infectious waste management, disposal of hazardous materials, food safety, vector control, and health education. Finally, the authors emphasized the collaboration of governmental agencies between and with the private sector and NGOs to adopt innovative and practical practices to deal with zoonotic diseases in Pakistan.

There are some specific strategies to assist the implementation of the One Health strategy. Potential drug strategies to target vital organelles in eukaryotic cells have been identified as potential resources for novel drug design and therapy. The endoplasmic reticulum (ER) and its application as the target for drug design were summarized in reviews by Peng et al. The review clarified the role of ER stress pathways and related molecules in parasites for their survival and development, the parasitic infection-induced pathological damage in hosts and the drug resistance of parasite, which provides potential drug design targets to inhibit the development of parasites and effective treatment approaches for anti-parasite drugs.

The increasing microbial drug resistance has been the most extensive public health in recent years. Biofilms are complex microbial microcolonies of planktonic and dormant bacteria bound to a surface. Biofilm formation increases the resistance of bacteria to antibiotics and helps bacteria escape from host immune attack, which leads to clinical persistent chronic infection and other problems. Chang et al. demonstrated the advantages and challenges of bacteriophage therapy on biofilm removal, as well as the potential usage of combination therapy and genetically modified phages in a nosocomial setting, especially on artificial joint restorations and catheters. Within the One Health framework, it is crucial to combine multimodal strategies and channels to offer more access to health between humans, animals, and the environment.

In conclusion, our Research Topic focuses on the epidemiological status of primary vector-borne and zoonotic infectious diseases, the risk of pathogen spillover, novel pathogens detection system and vaccine design, concerns on One Health paradigm and application, and has generated meaningful collection in the field. Taken together, the Research Topic highlighted an urgent need to re-examine existing knowledge in the One Health approach to expand our understanding toward unraveling the underlying interplay of humans, animals, and the environment.

Author contributions

XF contributed to the original idea and conceived the paper. XF and XZ wrote the initial draft of the paper. XF, SW, GC, XG, and XZ reviewed the final version. All authors contributed to the article and approved the submitted version.

Funding

This work was supported in part by grants from the China Postdoctoral Science Foundation (No. 2021M692107) and the National Natural Science Foundation of China (No. 81802039).

Conflict of interest

The authors declare that the research was conducted in the absence of any commercial or financial relationships that could be construed as a potential conflict of interest.

Publisher's note

References

Acharya, K. P., Acharya, N., Phuyal, S., Upadhyaya, M., and Lasee, S. (2020). One-health approach: a best possible way to control rabies. *One Health* 10, 100161. doi: 10.1016/j.onehlt.2020.100161

Ajuwon, B. I., Roper, K., Richardson, A., and Lidbury, B. A. (2021). One Health approach: a data-driven priority for mitigating outbreaks of emerging and re-emerging zoonotic infectious diseases. *Trop. Med. Infect. Dis.* 7, 4. doi: 10.3390/tropicalmed7010004

Babo Martins, S., Rushton, J., and Stärk, K. D. (2017). Economics of zoonoses surveillance in a 'One Health' context: an assessment of Campylobacter surveillance in Switzerland. *Epidemiol. Infect.* 145, 1148–1158. doi: 10.1017/S0950268816003320

Bird, B. H., and Mazet, J. A. K. (2018). Detection of emerging zoonotic pathogens: an integrated One Health approach. *Annu. Rev. Anim. Biosci.* 6, 121–139. doi: 10.1146/annurev-animal-030117-014628

Fitzpatrick, M. C., Shah, H. A., Pandey, A., Bilinski, A. M., Kakkar, M., Clark, A. D., et al. (2016). One Health approach to cost-effective rabies control in India. *Proc. Natl. Acad. Sci. U. S. A.* 113, 14574–14581. doi: 10.1073/pnas.1604975113

Gibson, A. D., Yale, G., Corfmat, J., Appupillai, M., Gigante, C. M., Lopes, M., et al. (2022). Elimination of human rabies in Goa, India through an integrated One Health approach. *Nat. Commun.* 13, 2788. doi: 10.1038/s41467-022-30371-y

Jones, K. E., Patel, N. G., Levy, M. A., Storeygard, A., Balk, D., Gittleman, J. L., et al. (2008). Global trends in emerging infectious diseases. *Nature* 451, 990–993. doi: 10.1038/nature06536

Keusch, G. T., Amuasi, J. H., Anderson, D. E., Daszak, P., Eckerle, I., Field, H., et al. (2022). Pandemic origins and a One Health approach to preparedness and prevention: solutions based on SARS-CoV-2 and other RNA viruses. *Proc. Natl. Acad. Sci. U. S. A.* 119, e2202871119. doi: 10.1073/pnas.2202871119

Schiaffino, F., Platts-Mills, J., and Kosek, M. N. (2019). A One Health approach to prevention, treatment, and control of campylobacteriosis. *Curr. Opin. Infect. Dis.* 32, 453–460. doi: 10.1097/QCO.0000000000000570

Tiaoying, L., Jiamin, Q., Wen, Y., Craig, P. S., Xingwang, C., Ning, X., et al. (2005). Echinococcosis in Tibetan populations, western Sichuan Province, China. *Emerging infectious diseases* 11, 1866–1873. doi: 10.3201/eid1112.050079

Wang, Q., Zhong, B., Yu, W., Zhang, G., Budke, C. M., Liao, S., et al. (2021). Assessment of a 10-year dog deworming programme on the transmission of *Echinococcus multilocularis* in Tibetan communities in Sichuan Province, China. *Int. J. Parasitol.* 51, 159–166. doi: 10.1016/j.ijpara.2020.08.010

frontiers in Microbiology

REVIEW
published: 31 May 2021
doi: 10.3389/fmicb.2021.670874

Endoplasmic Reticulum Stress, a Target for Drug Design and Drug Resistance in Parasitosis

Mei Peng[1,2,3], *Fang Chen*[4], *Zhongdao Wu*[1,2,3] *and Jia Shen*[1,2,3]*

[1] Department of Parasitology of Zhongshan School of Medicine, Sun Yat-sen University, Guangzhou, China, [2] Key Laboratory of Tropical Disease Control (SYSU), Ministry of Education, Guangzhou, China, [3] Provincial Engineering Technology Research Center for Biological Vector Control, Guangzhou, China, [4] School of Medicine, South China University of Technology, Guangzhou, China

Endoplasmic reticulum stress (ER stress) can be induced when cellular protein homeostasis is damaged, and cells can activate the unfolded protein response (UPR) to restore protein homeostasis or induce cell death to facilitate the survival of the whole system. Globally, parasites are a constant threat to human health and are therefore considered a serious public health problem. Parasitic infection can cause ER stress in host cells, and parasites also possess part or all of the UPR under ER stress conditions. In this review, we aim to clarify the role of ER stress pathways and related molecules in parasites for their survival and development, the pathogenesis of parasitosis in hosts, and the artemisinin resistance of *Plasmodium*, which provides some potential drug design targets to inhibit survival of parasites, relieves pathological damage of parasitosis, and solves the problem of artemisinin resistance.

Keywords: endoplasmic reticulum stress, drug targets, parasite, parasitosis, drug resistance

OPEN ACCESS

Edited by:
Karl Kuchler,
Medical University of Vienna, Austria

Reviewed by:
Cláudia Pereira,
University of Coimbra, Portugal
Madhu Sudhan Ravindran,
Biocon, India

***Correspondence:**
Jia Shen
shenj29@mail.sysu.edu.cn

Specialty section:
This article was submitted to Infectious Diseases, a section of the journal Frontiers in Microbiology

Received: *22 February 2021*
Accepted: *03 May 2021*
Published: *31 May 2021*

Citation:
Peng M, Chen F, Wu Z and Shen J (2021) Endoplasmic Reticulum Stress, a Target for Drug Design and Drug Resistance in Parasitosis. Front. Microbiol. 12:670874. doi: 10.3389/fmicb.2021.670874

ER STRESS AND UPR

The endoplasmic reticulum (ER), a vital organelle in eukaryotic cells, is the site of synthesis and processing of membrane and secretory proteins, synthesis of lipids, and storage of Ca^{2+} (Dolai and Adak, 2014). Therefore, it is important to maintain ER homeostasis. Yet, many factors influence the protein homeostasis of ER, such as plasma cell differentiation (Gass et al., 2002), tunicamycin (Pahl and Baeuerle, 1995), and parasite infection (Galluzzi et al., 2017) which result in accumulated misfolded or unfolded proteins that exceed the folding capacity of ER and trigger endoplasmic reticulum stress (ER stress). Endoplasmic reticulum-associated degradation (ERAD) and unfolded protein response (UPR) are the two major quality control processes of ER stress (Bukau et al., 2006). UPR reduces the synthesis of proteins and eliminates misfolded proteins within the ER by increasing the expression of the ER chaperone proteins.

In mammalian cells, the UPR is mediated by three signaling pathways and activated by three ER-transmembrane proteins: inositol-requiring kinase/endoribonuclease 1 (IRE1), protein kinase RNA-like ER kinase (PERK), and activating transcription factor 6 (ATF6) (**Figure 1**; Hwang and Qi, 2018). Glucose-regulated proteins 78 (GRP78) (Bertolotti et al., 2000; Shen et al., 2002), also called immunoglobulin heavy chain binding protein (Bip) (Bertolotti et al., 2000; Shen et al., 2002), binds to these transmembrane proteins in unstressed cells, while it dissociates from them and binds to unfolded or misfolded proteins in stressed cells (Bertolotti et al., 2000; Shen et al., 2002; Grootjans et al., 2016). After dissociation from Bip, IRE1α will be activated by forming IRE1α

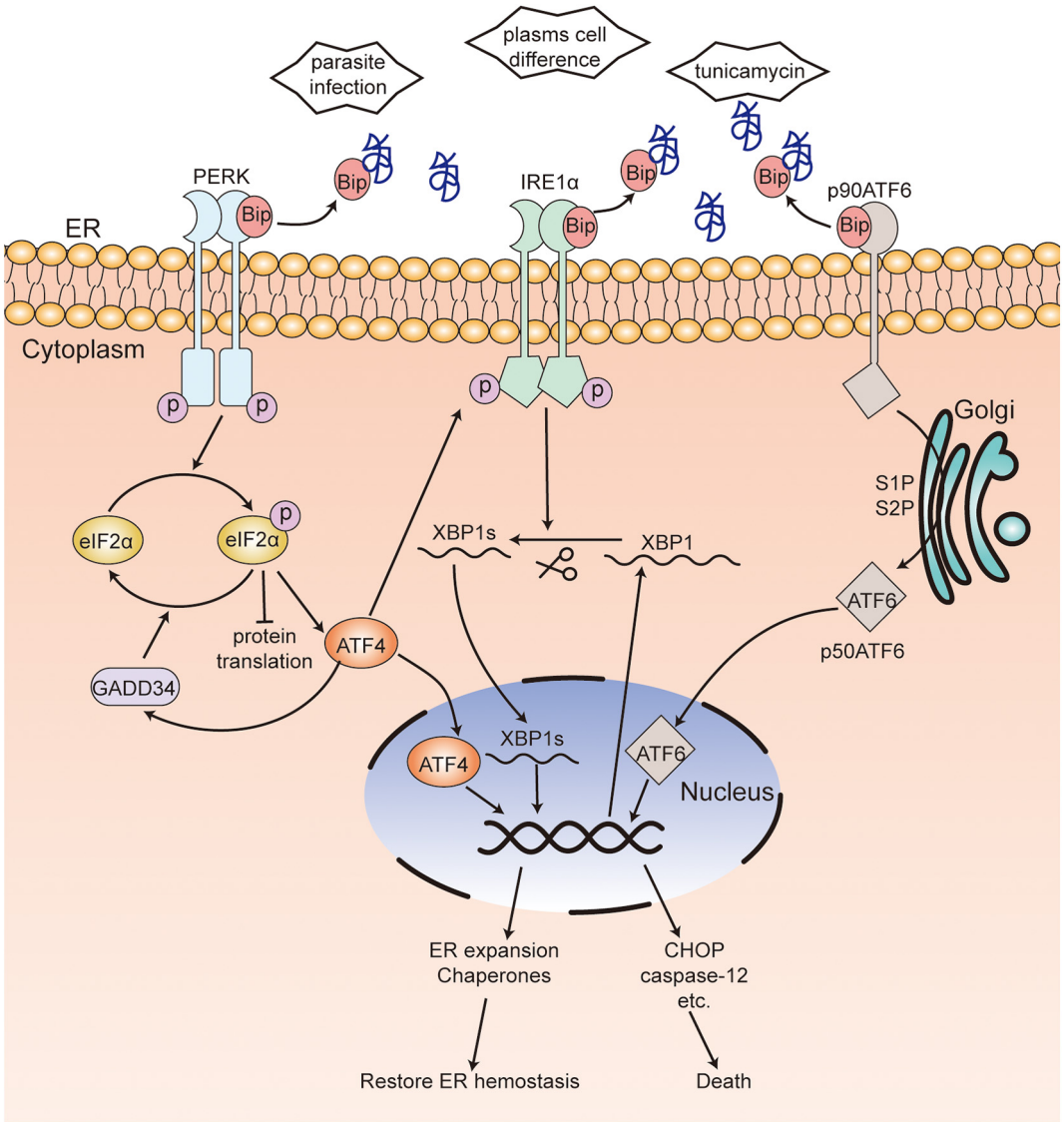

FIGURE 1 | Unfolded protein response in mammalian cells. In unstressed cells, Bip binds to three transmembrane proteins PERK, IRE1α and ATF6. When ER stress occurs, Bip dissociates from these transmembrane proteins and binds to unfolded or misfolded proteins. Activated PERK, induced by oligomerization following dissociation from Bip, phosphorylates eIF2α, which reduces protein translation while upregulating the expression of ATF4. eIF2α phosphorylation can be dephosphorylated by GADD34. After dissociation from Bip, IRE1α is activated by forming IRE1α homodimers and incises XBP1 mRNA into XBP1s. Bip releases from ATF6, which leads to the translocation to Golgi and activation of ATF6. ATF4, XBP1s, and activated ATF6 enter the nucleus and activate the transcription of ER chaperones or various death effectors, which results in the restoration of ER hemostasis or cell death. [公]], unfolded or misfolded proteins; PERK, protein kinase RNA-like ER kinase; IRE1, inositol-requiring kinase/endoribonuclease 1; eIF2α, α-subunit of eukaryotic translational initiation factor 2; ATF6, activating transcription factor 6; ATF4, activating transcription factor 4; XBP1, X box-binding protein 1; CHOP, C/EBP-homologous protein; Bip, immunoglobulin heavy chain binding protein; GADD34, DNA damage-inducible protein-34.

homodimers and incise the transcription factor X box-binding protein 1 (XBP1) mRNA into spliced XBP1 (XBP1s) (Bertolotti et al., 2000; Calfon et al., 2002). The function of XBP1s is to maintain the ER function and response to UPR and regulate the expansion of the secretory apparatus (Acosta-Alvear et al., 2007). Activated PERK, induced by oligomerization and autophosphorylation following dissociation from Bip (Bertolotti et al., 2000), phosphorylates the α-subunit of eukaryotic translational initiation factor 2 (eIF2α) and attenuates protein translation, which will reduce the load of newly synthesized proteins within the ER while upregulating the expression of activating transcription factor 4 (ATF4). In addition, the phosphorylation of eIF2α can be dephosphorylated by growth arrest and DNA damage-inducible protein-34 (GADD34). Further, ATF4 is required for the transactivation of GADD34, which will promote the recovery of translation

(Novoa et al., 2001; Ma and Hendershot, 2003). Under ER stress, ATF6 translocates from the ER to the Golgi apparatus (Shen et al., 2002). A 90-kDa protein ATF6 (p90ATF6) is converted to a 50-kDa protein ATF6 (p50ATF6, an active and mature form of ATF6) through the cleavage of Golgi-resident proteases—site 1 protease (S1P) and site 2 protease (S2P). P50ATF6 further activates the transcription of ER chaperone genes after entering the nucleus (Haze et al., 1999; Ron and Walter, 2007). Interactions among the three UPR pathways have been found, wherein ATF6 induces the transcription of XBP1 (Yoshida et al., 2001) and PERK-ATF4 upregulates the expression of IRE1α (Tsuru et al., 2016). These interactions will promote UPR to be stronger and more persistent in order to deal with various types of ER stress. Nevertheless, prolonged and severe ER stress can activate various cell death effectors such as BAK, BAX, caspase-12, C/EBP-homologous protein (CHOP), and GADD34 and induce cell death (Ron and Walter, 2007). The mechanism of UPR is evolutionary conservatism across eukaryotes.

PARASITIC INFECTION AND UPR

Parasitosis, caused by parasitic infections, has been harmful to human health and economic development since very long and is still a major global public health problem. As is known, the effective control of parasitic diseases is mainly dependent on the application of parasitic drugs and disruption of the pathogen's life cycle, such as praziquantel and artemisinin. Unfortunately, drug resistance of parasitic drugs has been reported in recent years (Fallon and Doenhoff, 1994; Dondorp et al., 2009). Therefore, new anti-parasitic drugs including those to alleviate the pathology of the host caused by parasite infection and those to kill parasites should be identified urgently, along with determination of the mechanisms of drug resistance.

When parasites infect the host and obtain nutrients, they will perturb ER homeostasis and induce ER stress and UPR of the host. On the one hand, the induced ER stress of the host is beneficial to the survival and infection of the parasites. For instance, it has been reported that *Plasmodium berghei* infection induced ER stress of hepatocytes and activated UPR through the XBP1 and cAMP responsive element-binding protein (CREBH, a hepatocyte specific UPR mediator) pathways, which contributed to the infection of *Plasmodium* by providing phosphatidylcholine and regulating iron level (Inacio et al., 2015). In addition, *Leishmania* infection induced ER stress of the host to facilitate infection through the PERK-eIF2α-ATF4 and IRE1-XBP1 pathways (Dias-Teixeira et al., 2016, 2017; Galluzzi et al., 2016; Abhishek et al., 2018). And *Toxoplasma* triggered the UPR in host cells, which affected calcium release from ER, can enhance host cell migration and dissemination of the parasite to host organs (Augusto et al., 2020). However, Poncet et al. (2021) have showed that the IRE1a/XBP1s branch of the UPR was a key regulator of host defense upon *Toxoplasma gondii* infection, that mice deficient for IRE1a and XBP1 in DCs displayed a severe susceptibility to *T. gondii* infection, which indicates that the UPR induced by parasites also plays an important role in host immune defense. Anyhow, on the other hand, excessive ER stress and UPR will cause severe pathological damage to the host. Yu et al. (2014) found that the levels of GRP78, CHOP, cleaved caspase-12, and phosphorylated-JNK in the intestine of *Trichinella spiralis*-infected mice were significantly upregulated, which indicated that the ER stress-induced apoptotic pathway participated in intestinal lesions caused by *T. spiralis* infection. Thus, inhibition of excessive UPR in the host may be a therapeutic target to alleviate the pathological symptoms.

Additionally, the parasites can sense ER stress and either induce UPR to facilitate their survival when attacked by the host immune system or adapt to the host environment (such as changes in pH and temperature, oxidative stress, nutrient deficiency) (Zuzarte-Luís and Mota, 2018). Therefore, the UPR signaling pathway may be a potential target for inhibiting the survival and development of parasites.

THE UPR IN THE HOST MAY BE A THERAPEUTIC TARGET FOR RELIEVING PATHOLOGICAL DAMAGE OF PARASITOSIS

Different parasitic infections result in different pathological damage to different host tissues and organs. Nowadays, increasing reports show that ER stress and UPR play an important role in the development of pathology of parasitosis (Anand and Babu, 2013; Ayyappan et al., 2019).

Plasmodium

Plasmodium spp., which are the causative agents of malaria, are obligate intracellular protozoan parasites. Anand and Babu (2013) reported that experimental cerebral malaria (ECM), caused by *P. berghei* ANKA (PbA) infection, was related to ER stress. They found that PbA infection-induced ER stress could cause the apoptosis of neuronal cells in mice by activating the three branches of UPR—PERK-eIF2α-ATF4/GADD34, IRE1-XBP1s, and ATF6—along with upregulating the levels of CHOP, cleaved caspase-3 and caspase-12 and downregulating the expression of Bip, calreticulin, and calnexin.

Trypanosome

Trypanosome cruzi is the causative pathogen of Chagas disease in humans. Reportedly, the trypomastigotes of *T. cruzi* infection could induce ER stress in the heart of mice, with an increase in the levels of Bip, PERK, eIF2α, ATF4, and CHOP, thereby causing damage to the host. Interestingly, 2-aminopurine (2-APB, an ER stress inhibitor) treatment could alleviate the pathological damage to the heart by decreasing the phosphorylation of eIF2α and its downstream signaling. Therefore, this indicates that inhibition of ER stress may be a therapeutic target for cardiomyopathy in Chagas patients (Ayyappan et al., 2019).

Toxoplasma

Toxoplasma is an obligate intracellular parasite and opportunistic pathogenic parasite (Sullivan et al., 2004). *Toxoplasma* encephalitis is the most serious outcome of toxoplasmosis,

which may be fatal to immunocompromised individuals. Some studies have found that *Toxoplasma* encephalitis was related to ER stress. It has been reported that the tachyzoites of *T. gondii* RH strain and TgCtwh3 (a representative Chinese 1 *Toxoplasma* strain) induced apoptosis of neural stem cells and neural stem cell line C17.2 by activating CHOP, caspase-12, and JNK (Wang et al., 2014; Zhou et al., 2015). Pretreatment with tauroursodeoxycholic acid (TUDCA, an ER stress inhibitor) and Z-ATAD-FMK (a caspase-12 inhibitor) led to the inhibition of apoptosis (Wang et al., 2014; Zhou et al., 2015), which suggested that neural stem cell apoptosis induced by both TgCtwh3 and RH strain infection was dependent on the ER stress pathway, and ER stress inhibitors could be used to alleviate *Toxoplasma* encephalitis. In addition, Wan et al. (2015) showed that virulence factor rhoptry protein 18 (ROP18) secreted by *T. gondii* was involved in nerve cell apoptosis *via* the ER stress pathway, characterized by an increase in the expression of cleaved caspase-12, CHOP, and cleaved caspase-3. Ran et al. further indicated that ROP18 induced apoptosis of neural cells by phosphorylating reticulon 1-C [RTN1-C, a protein localized in the ER that is preferentially expressed in the neural cells of the central nervous system (CNS) at Ser7/134 and Thr4/8/118], which led to the acetylation of GRP78 and induced ER stress (An et al., 2018). These results suggest that inhibition of ROP18 of *T. gondii* can be used as a drug target for the treatment of *Toxoplasma* encephalitis to inhibit the ER stress-induced apoptosis of host cells.

Schistosoma japonicum

Schistosoma japonicum is the causative agent of schistosomiasis. The pathogenic mechanism of schistosomiasis is primarily attributed to egg-induced hepatic granuloma and fibrosis and cirrhosis (Yu et al., 2016; Duan et al., 2019). Duan et al. (2019) showed that the level of CHOP, a vital factor in the ER stress-mediated apoptosis pathway, was significantly increased in mice at 6 and 10 weeks following infection with *S. japonicum*. The study indicated that ER stress may be involved in *S. japonicum* infection-induced hepatic fibrosis. Moreover, Yu et al. (2016) showed that treatment with taurine, an inhibitor of ER stress, significantly suppressed the egg-induced hepatic granuloma and alleviated hepatic fibrosis in mice at 8 weeks post-infection, along with marked reduction of the expression of GRP78. Therefore, ER stress inhibitors may be a therapeutic drug for hepatic fibrosis.

The summary of ER stress in hosts caused by parasitic infection is shown in **Figure 2**. Therefore, the UPR signaling pathway may be a therapeutic target to alleviate pathological symptoms.

THE UPR IN PARASITES SUGGESTS POTENTIAL DRUG TARGETS FOR INHIBITING THE SURVIVAL AND DEVELOPMENT OF PARASITES

Parasites can sense ER stress and induce UPR of themselves to facilitate their survival and development. Different parasites may have different components of ER stress pathway.

Plasmodium

Plasmodium has a complicated life cycle, including the merozoite, ring, trophozoite, schizont, and gametophyte stages in humans and the ookinete and sporozoite stages in mosquitoes. Chaubey et al. (2014) showed that *Plasmodium falciparum* lacked the orthologs of XBP1, IRE1, ATF6, and ATF4, and only retained the PERK-eIF2α pathway to regulate translation under ER stress. Three eIF2α kinases have been identified, namely IK1, IK2, and PK4 (eIF2α kinase of *Plasmodium* (Möhrle et al., 1997), a PERK homolog of mammals) (Ward et al., 2004). It has been reported that increased phosphorylation of eIF2α leads to reduced levels of protein translation, which is associated with the formation of *P. falciparum* gametophytes and the conversion of the *P. berghei* gametophytes into ookinetes when treated with dithiothreitol (DTT) (Chaubey et al., 2014; Duran-Bedolla et al., 2017). In addition, Zhang et al. (2012) have shown that PK4 was involved in the invasion of new red blood cells of merozoite-containing schizonts and the gametocyte infecting *Anopheles* mosquitoes. The inhibition of PK4 of *P. berghei* by generating a PK4 conditional mutant (PbPK4cKO) would alleviate the symptoms of malaria and inhibit disease transmission. Another study indicated that treatment of GSK2606414 (a small molecule inhibitor of PERK (Axten et al., 2012), which specifically inhibits PK4 instead of IK1 and IK2 *in vitro*) could block the transformation of *P. falciparum* from trophozoites to schizonts (Zhang et al., 2017). The transformation between different forms increased the ability of translational regulation of *Plasmodium*. In addition, Chen et al. (2018) reported that apoptozole, a novel chemical scaffold, was lethal to the chloroquine-sensitive and chloroquine -resistant *P. falciparum* parasite strains by inhibiting GRP78 function *in vitro*. Compared to human GRP78, *P. falciparum* GRP78 showed a lower affinity to the endogenous ligands, ADP and ATP, which indicated that the competitive inhibitors of GRP78 can be investigated for *P. falciparum* control (Chen et al., 2018).

According to the above mentioned studies, it appears that the PK4-eIF2α pathway plays an important role in both morphological transformation and host transmission in *Plasmodium*. Thus, PK4 inhibition would inhibit the development of *Plasmodium*, which implies that PK4 inhibitors may be a potential target in malaria treatment. However, Bridgford et al. (2018) found that dihydroartemisinin (DHA) increased the toxicity to *Plasmodium* by prolonging PK4 activation and eIF2α phosphorylation. Therefore, appropriate ER stress is beneficial to the development of *Plasmodium*, while excessive ER stress would be lethal to the parasites.

Leishmania

Leishmania is the pathogen causing Leishmaniasis and has two forms—promastigote and amastigote. Gosline et al. (2011) proved that *Leishmania* lacked a transcriptional regulation response to UPR, and only retained the translational regulation in ER stress. They also showed an increased level of phosphorylation of eIF2α in *L. donovani* after treatment of DTT (Gosline et al., 2011). Moreover, Chow et al. (2011) found that the PERK homolog of *Leishmania* largely colocalized with Bip in

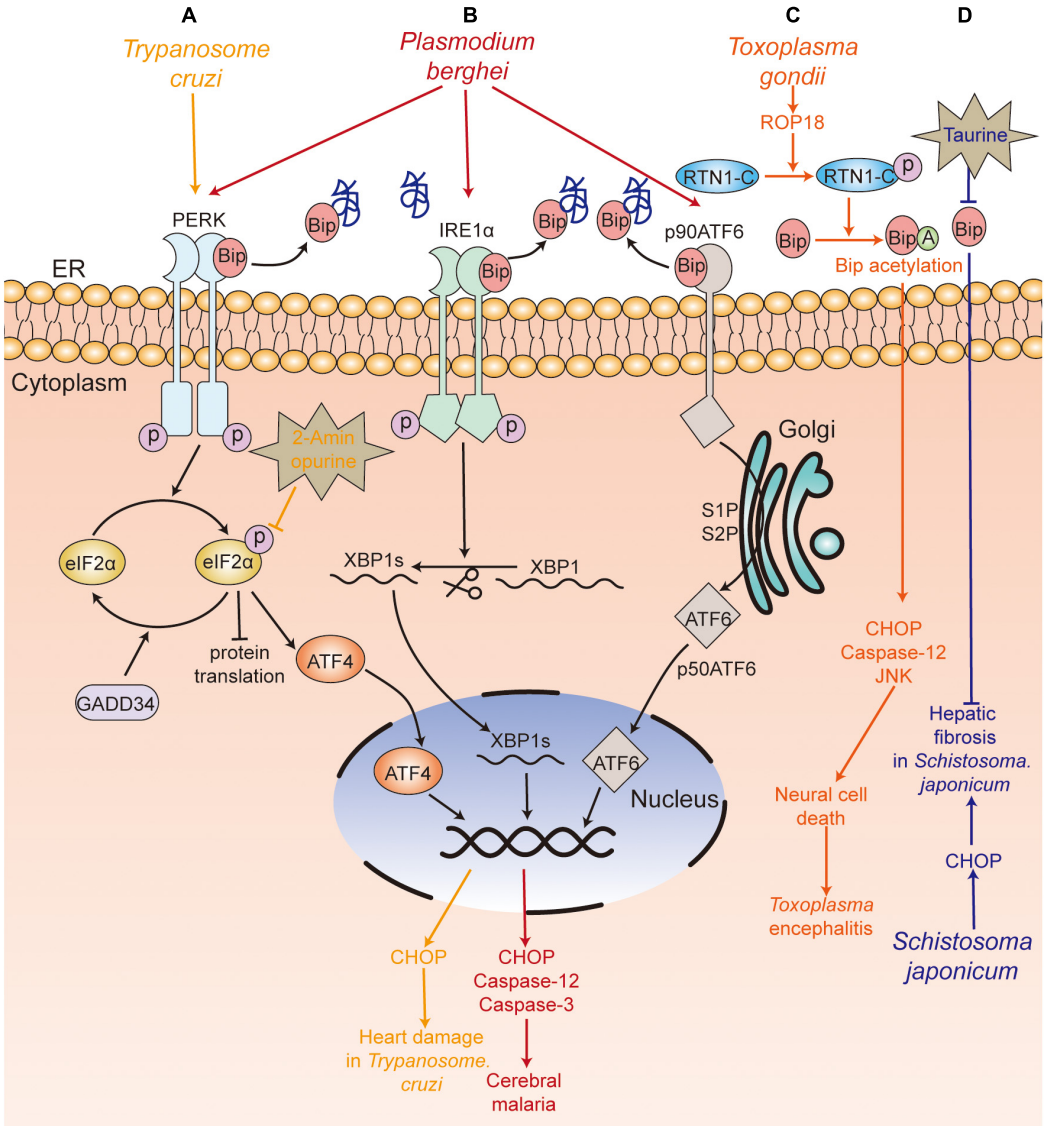

FIGURE 2 | UPR participates in the pathological damage caused by parasite infection. **(A)** *T. Cruzi* (yellow) infection caused heart damage, with upregulation of PERK-eIF2α-ATF4-CHOP pathway, and 2-aminopurine treatment alleviated the heart's pathological damage. **(B)** *P. berghei* (red) infection induced neuronal cell death and caused experimental cerebral malaria by activating the three branches of the UPR (PERK-eIF2α-ATF4/GADD34, IRE1-XBP1s, ATF6). **(C)** Rhoptry protein 18 (ROP18) of *T. gondii* (orange) phosphorylated reticulon 1-C (RTN1-C), which led to the acetylation of GRP78 and further upregulated the expression of cleaved caspase-12, CHOP, cleaved caspase-3, and induced the apoptosis of neural cells. **(D)** *S. japonicum* (blue) infection led to increased levels of CHOP, which was involved in hepatic fibrosis, and the treatment with taurine suppressed the egg-induced hepatic granuloma and fibrosis. PERK, protein kinase RNA-like ER kinase; IRE1, inositol-requiring kinase/endoribonuclease 1; eIF2α, α-subunit of eukaryotic translational initiation factor 2; ATF6, activating transcription factor 6; ATF4, activating transcription factor 4; XBP1, X box-binding protein 1; CHOP, C/EBP-homologous protein; Bip, immunoglobulin heavy chain binding protein;GADD34, DNA damage-inducible protein-34.

ER, which can phosphorylate eIF2α at threonine 166. They further confirmed that PERK-dependent eIF2α phosphorylation was vital for *Leishmania* to switch from the promastigote to amastigote form *in vitro* (Chow et al., 2011). Unlike host macrophages having intact UPR pathway, the mere presence of the PERK pathway in *L. donovani* promoted the parasite's susceptibility to DTT-induced ER stress (Gosline et al., 2011), which suggests that inhibition of the PERK pathway and induction of ER stress in *Leishmania* are both potential targets to kill the parasite. Dolai et al. (2011) proved that tunicamycin treatment induced apoptosis of *Leishmania major*, with an increase in the level of Bip.

Trypanosome

Trypanosome brucei is a protozoan parasite that cycles between the tsetse fly (procyclic form) and mammalian host (blood stream form), which causes African sleeping sickness in humans and nagana in livestock (Zhang et al., 2019). Goldshmidt et al. (2010)

reported that the expression of Bip of *T. brucei* was increased in both procyclic and blood stream forms in DTT-induced ER stress, and irrecoverable ER stress could induce spliced leader RNA silencing pathway (SLS pathway, a unique process in *T. brucei*), which may accelerate programmed cell death (PCD). Besides, Messias Sandes et al. (2019) showed that both DTT and tunicamycin could induce PCD in *T. cruzi*.

There were three putative eIF2α kinases (TbeIF2K1-K3) in *T. brucei*, though its genome lacked the homologs of IRE1/XBP1. It was reported that TbeIF2K2, a transmembrane glycoprotein expressed both in the procyclic and bloodstream forms of *Trypanosome* (Moraes et al., 2007), shared no similar sequence with known eIF2 kinases of mammals and was localized to the flagellar pocket, where endocytosis and exocytosis occur, and all proteins were transported from the flagellar pocket to the cell membrane (Gull, 2003). Therefore, the localization of TbeIF2K2 indicated that it could sense proteins and regulate protein synthesis near the flagellar pocket of the *Trypanosome* (Moraes et al., 2007), which suggests that TbeIF2K2 may be a good drug target to destroy *T. brucei*. In addition, Hope et al. (2014) showed that SEC63 (a factor participating in protein translocation machinery in ER) silence-induced ER stress could activate PK3 (TbeIF2K3) and trigger the release of PK3 from the ER to nucleus in the procyclic form of *T. brucei*. The deletion of PK3 reduced the death of *T. brucei* in SEC63 silence-induced ER stress, which suggests that PK3 is required for ER stress-induced PCD. Thus, the results indicate that TbeIF2K2 and TbeIF2K3 could be potential drug targets to eliminate *T. brucei*.

The PERK-eIF2α pathway is also involved in the form transformation of *T. cruzi* at different developmental stages. Tonelli et al. (2011) reported that the differentiation of non-infective epimastigotes into infective metacyclic trypomastigotes in *T. cruzi* requires the phosphorylation of Tc-eIF2α .

In conclusion, the results show that eIF2α phosphorylation plays an important role in the survival and development of *Trypanosome*, while excessive ER stress induced by DTT or tunicamycin can lead to the death of *Trypanosome*.

Toxoplasma

Toxoplasma shows two forms in the human host: tachyzoite (a rapidly growing form) and bradyzoite (a quiescent cyst form) (Black and Boothroyd, 2000; Sullivan et al., 2004). It has been reported that *T. gondii* lacked the homologs of IRE1 and ATF6 (Joyce et al., 2013), while it possessed four TgIF2α kinases, namely TgIF2K-A, TgIF2K-B, TgIF2K-C, and TgIF2K-D (Narasimhan et al., 2008; Konrad et al., 2014). Narasimhan et al. (2008) showed that only TgIF2K-A was a transmembrane protein localized in the ER and bonded to Bip under unstressed conditions. When ER stress occurred, the binding of Bip to TgIF2K-A was reduced, similar to the binding of BiP to PERK in mammals, which suggests that part of the UPR was conserved in *T. gondii* (Narasimhan et al., 2008).

ER stress is also involved in the differentiation of *Toxoplasma*. Narasimhan et al. (2008) reported that the phosphorylation of TgIF2α induced by tunicamycin treatment resulted in the differentiation of *T. gondii* from tachyzoite to bradyzoite cysts. Treatment with salubrinal, an inhibitor of eIF2α dephosphorylation, could also induce the differentiation of bradyzoite cysts, which indicated that TgIF2α phosphorylation was involved in the differentiation of bradyzoite cysts (Narasimhan et al., 2008). Cyst formation is a good way to escape from the host's immune attack. Therefore, the formation of bradyzoite cysts induced by TgIF2α phosphorylation promotes the survival of *T. gondii* under stressful conditions. Similar results were confirmed by Joyce et al. (2013). Besides, Joyce et al. (2010) reported that the TgIF2α mutant strain of *Toxoplasma* (i.e., TgIF2α-S71A, which cannot be phosphorylated) showed a lower virulence to the host cell, a lower survival rate and a slower transmitting speed, compared with the control strain of *Toxoplasma*. Moreover, Augusto et al. (2018) showed that specific inhibition of TgIF2K-A with GSK2606414 could inhibit the lytic cycle of tachyzoites, including attachment/invasion, replication, egress, and differentiation, which prolonged the survival time of mice with acute toxoplasmosis at a lethal dose of 100 RH strain tachyzoites. Interestingly, GSK2606414 did not show apparent detrimental effects on the host cell though with a high concentration *in vitro*. Therefore, the results suggest that TgIF2K-A and TgIF2α can be used as drug targets to inhibit *Toxoplasma* survival.

However, DTT treatment and stearoyl-coenzyme A (CoA) desaturase (SCD) accumulation at the ER could trigger ER stress with increasing phosphorylation of TgIF2α and mediated the apoptosis or autophagy of *T. gondii* (Nguyen et al., 2017; Hao et al., 2019). Therefore, although the TgIF2K-A/TgIF2α pathway plays a protective role in *T. gondii* under stress conditions, severe disruption of ER homeostasis can lead to the death of *T. gondii*.

Entamoeba histolytica

Entamoeba histolytica infection, caused by ingestion of cysts in contaminated water and food, usually induces amoebic dysentery and liver abscesses in humans (Pineda and Perdomo, 2017). Santi-Rocca et al. (2012) found that no genes encoded the orthologs of PERK and ATF6 in *E. histolytica* amoeba, while the expression of gene encoding eIF2α was upregulated upon treatment with nitric oxide (NO). Hendrick et al. (2016) showed that eIF2α could be phosphorylated at serine-59 in *E. histolytica*, with a decrease in translation levels during long-term serum starvation, long-term heat shock, and oxidative stress instead of short-term serum starvation, short-term heat shock, and glucose deprivation, and the viability of EheIF2α-S59D (a phosphomimetic variant of eIF2α) was significantly increased during long-term serum starvation. This study suggests that EheIF2α phosphorylation promotes the survival of *E. histolytica* under stress conditions. DTT treatment can also induce distinct fragmentation of ER and phosphorylation of EheIF2α, while treatment with SNP and DPTA-NON-Oate (NO donors) did not induce phosphorylation of EheIF2α (Walters et al., 2019). Besides, Kumari et al. (2018) identified the ortholog of IRE1 in *E. histolytica* (EhIre1) and reported that treatment with

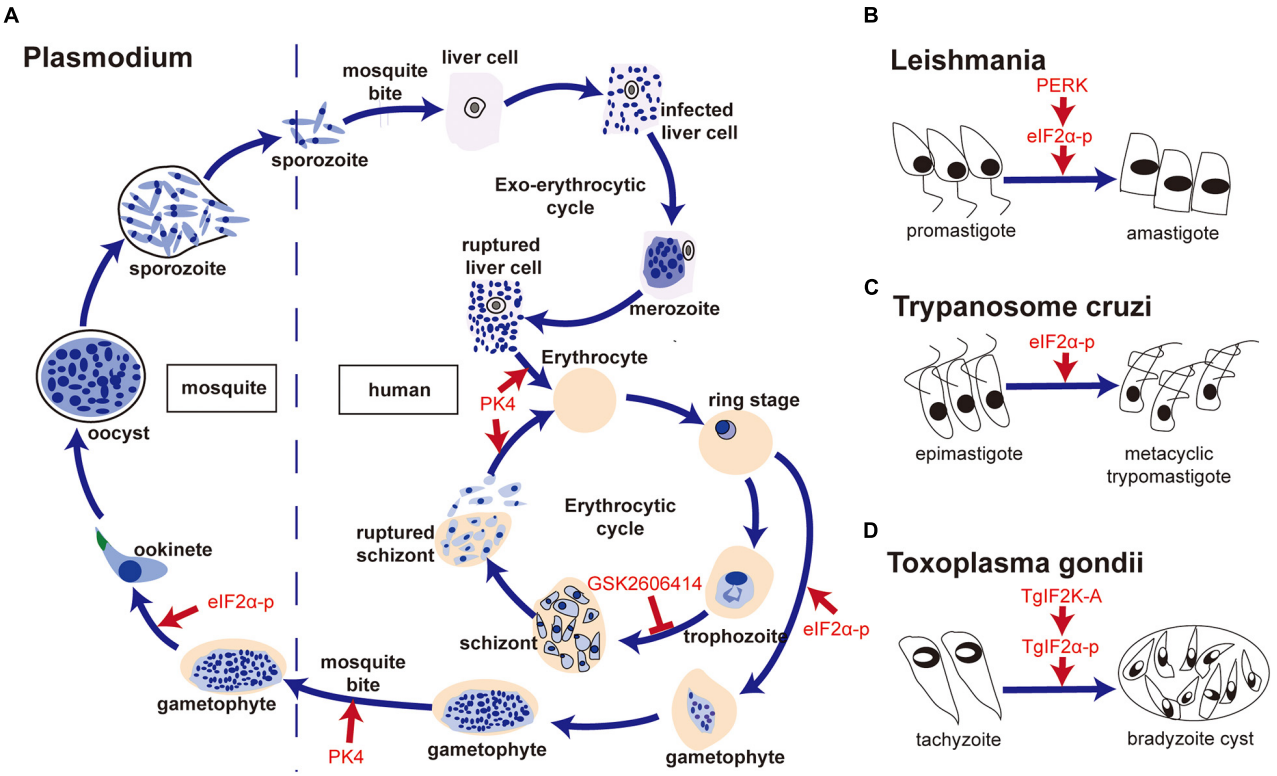

FIGURE 3 | The PERK-eIF2α pathway is involved in forms transformation of parasites. **(A)** PK4-eIF2α was associated with the formation of gametophytes, conversion of *Plasmodium* gametophytes into ookinetes, invasion of new red blood cells by merozoite-containing schizonts and the infection of *Anopheles* mosquitoes by gametocytes; **(B)** PERK- eIF2α phosphorylation was vital for the switch from promastigote to amastigote in *Leishmania*; **(C)** Tc-eIF2α phosphorylation was required for the differentiation of non-infective epimastigotes into infective metacyclic trypomastigotes of *T. cruzi*; **(D)** TgIF2K-A/TgIF2α phosphorylation was related to bradyzoite cyst differentiation in *T. gondii*.

tunicamycin resulted in the upregulation of EhIre1. In addition, the level of eIF2α phosphorylation was increased during encystation of *Entamoeba invadens*, but whether eIF2α is necessary for encystation still needs further investigation (Hendrick et al., 2016).

Echinococcus granulosus

Echinococcus granulosus is the causative cestode of hydatidosis or cystic echinococcosis (CE) and is a worldwide zoonotic infection that affects many organs in human and mammals (Loos et al., 2018). Nicolao et al. (2017) have identified the ortholog of IRE2, XBP1, and ATF6 in the genome of *E. granulosus*, but the ortholog of PERK/ATF4 was not found. Treatment with bortezomib (a proteasome inhibitor) led to lower viability of *E. granulosus* in the larval stage *in vitro* than that in the control group, with an increase of EgGRP78 and EgIRE2/EgXBP1 mRNA levels in protoscoleces; however, no changes were found in the metacestodes (Nicolao et al., 2017). Another study also showed that arsenic trioxide (As_2O_3) could disturb the intracellular Ca^{2+} homeostasis and activated ER stress-related apoptosis of protoscoleces *in vitro*, with an increase in the expression of GRP78, caspase-3, and caspase-12 (Li et al., 2018). These studies show that the induction of ER stress can lead to the apoptosis of protoscoleces *in vitro*.

In sum, the components of the UPR response such as the PERK-eIF2α pathway of some parasites (**Figures 3**, **4**), including *Plasmodium*, *Leishmania*, *Trypanosome*, *Toxoplasma*, and *E. histolytica,* play an important role in their survival and development. However, excessive ER stress could induce the death of parasites such as *Plasmodium*, *Leishmania*, *Trypanosome*, *Toxoplasma,* and *E. granulosus* (**Figure 4**). Considering the toxicity of commonly used ER stress inducers such as DTT and tunicamycin, it is difficult to use them to kill parasites *in vivo*. For those parasites that are more sensitive to ER stress inducers than their hosts, it is necessary to explore the appropriate concentration of these inducers. TUDCA, a bile salt and chemical chaperone used to treat biliary cirrhosis clinically (Lazaridis et al., 2001), partially inhibits ER stress by lowering the levels of PERK, Bip (Malo et al., 2010; Liu et al., 2015; Li et al., 2019). Thus, TUDCA may be an alternative therapy for parasitosis.

Endoplasmic reticulum-associated degradation is another way for maintaining ER homeostasis, which can degrade misfolded protein (Hwang and Qi, 2018). And ERAD also exists in parasites, such as trypanosomes (Tiengwe et al., 2016). In addition, some apicomplexan parasites, including *P. falciparum*, *T. gondii* and *cryptosporidium,* harbor an apicoplast, which is important for parasite survival (Agrawal et al., 2013). Reportedly, ERAD

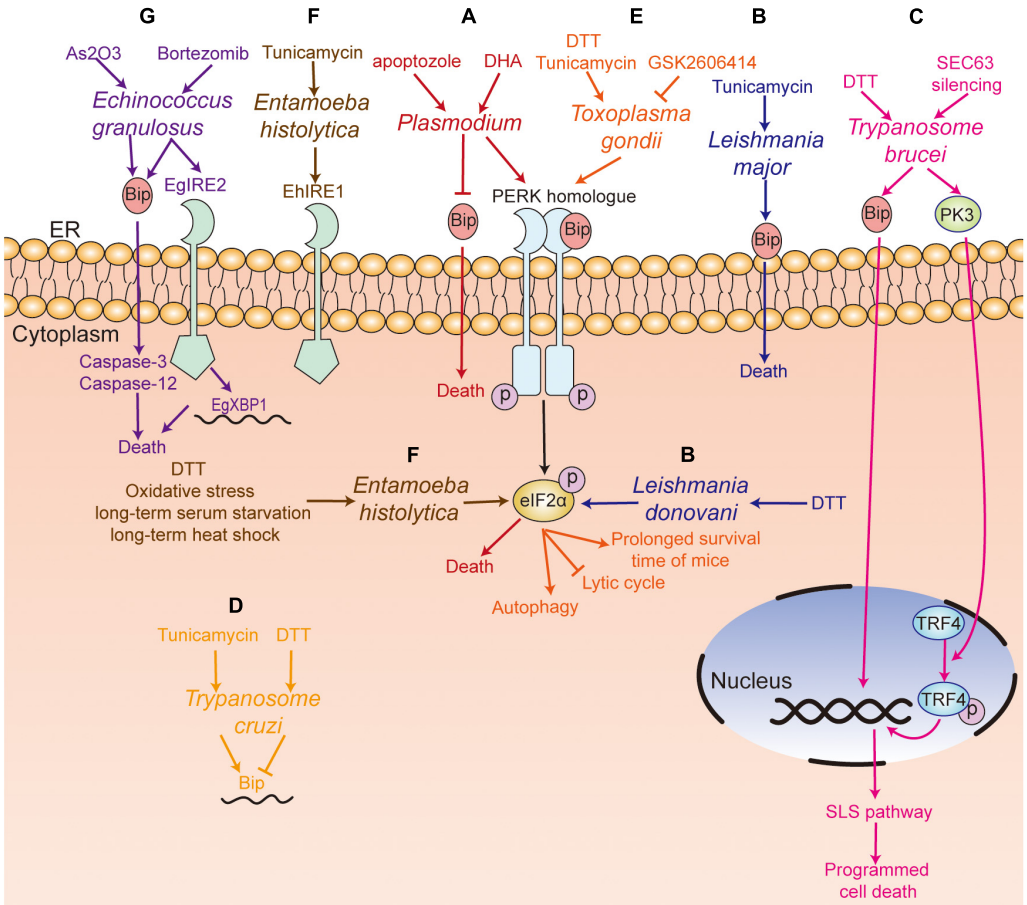

FIGURE 4 | UPR pathway in parasites. **(A)** *Plasmodium* spp. (red) with the PERK homolog; apoptozole was lethal to the chloroquine-sensitive and chloroquine-resistant *P. falciparum* parasite strains by inhibiting GRP78 function *in vitro*, and DHA treatment could induce the death of *P. falciparum* through the PERK-eIF2α pathway; **(B)** Tunicamycin treatment induced the death of *L. major* (blue) with an increased level of Bip, and DTT treatment upregulated the phosphorylation of eIF2α in *L. donovani*; **(C)** DTT treatment induced programmed cell death. SEC63 silencing activated PK3, which further induced programmed cell death by phosphorylating TRF4 and inducing the SLS pathway in *T. brucei* (pink); **(D)** Tunicamycin treatment increased the level of Bip mRNA, while DTT treatment decreased the level of Bip in *T. Cruzi* (yellow); **(E)** GSK2606414 inhibited the lytic cycle of tachyzoites, including attachment/invasion, replication, egress, and prolonged the survival time of infected mice. DTT treatment mediated the apoptosis or autophagy of *T. gondii* (orange) by increasing the phosphorylation of TgIF2α; **(F)** DTT treatment, long-term serum starvation, long-term heat shock and oxidative stress induced the phosphorylation of eIF2α, and the ortholog of IRE1 in *E. histolytica* (EhIre1) (gray) was identified; **(G)** Bortezomib treatment induced the death of *E. granulosus* (purple) with an increase of EgGRP78 and EgIRE2/EgXBP1 mRNA. Arsenic trioxide treatment induced the death of *E. granulosus* (purple) with upregulation of the expression of GRP78, caspase-3, and caspase-12 in protoscoleces. PERK, protein kinase RNA-like ER kinase; IRE1, inositol-requiring kinase/endoribonuclease 1; XBP1, X box-binding protein 1; Bip, immunoglobulin heavy chain binding protein; eIF2α, α-subunit of eukaryotic translational initiation factor 2; TRF4, TBP-related factor 4; SLS pathway, spliced leader RNA silencing pathway; DTT, dithiothreitol; DHA, dihydroartemisinin.

components were associated with importing the apicoplast protein, and lose of ERAD components would lead to the death of parasites (Agrawal et al., 2009; Spork et al., 2009). Thus, apicoplast is a potential anti-parasitic drug target. Ubiquitin-dependent ERAD is essential for the survival of *Plasmodium* (Chung et al., 2012). Harbut et al. found that the inhibitors of signal peptide peptidase (SPP, a protein of ERAD) was lethal to *P. falciparum* (Harbut et al., 2012). It was reported that NITD731, a SPP inhibitor, was effective against *T. cruzi* and *T. gondii*, and it showed no toxicity to human cell lines (Harbut et al., 2012). Above studies further showed that parasites were much more sensitive to the disruption of protein homeostasis. Thus, inhibition of the two key quality-control mechanisms, UPR and ERAD, may be a potential way for parasites control.

UPR IN PARASITES IS INVOLVED IN ARTEMISININ RESISTANCE AND RECRUDESCENCE OF *Plasmodium*

As is well known, UPR can restore ER homeostasis. Therefore, when parasites are exposed to external risk factors such as drugs, they are capable of restoring their own homeostasis by inducing ER stress and activating UPR; hence, it is not surprising that ER stress and UPR are involved in the mechanism of drug resistance.

TABLE 1 | Potential drug targets of UPR for treatment of parasitosis.

Inhibitors	Target molecules	Function/mechanism of inhibitor	Effects	References
2-aminopurine	PERK-eIF2α- CHOP pathway	Inhibiting eIF2α phosphorylation and its downstream signaling	Alleviating *T. cruzi* infection induced-heart damage	Ayyappan et al., 2019
TUDCA/Taurine	CHOP-cleaved caspase-12 pathway; GRP78-CHOP pathway	Inhibiting ER stress induced cell apoptosis	Alleviating *T. gondii* infection induced-*Toxoplasma* encephalitis; Alleviating *S. japonicum* infection induced-hepatic granuloma and fibrosis	Wang et al., 2014; Yu et al., 2016
ROP18 inhibitors	ROP18 of *T. gondii*	Inhibiting *T. gondii* infection induced-nerve cell apoptosis by ER stress pathway	Alleviating *Toxoplasma* encephalitis	Wan et al., 2015; Tang et al., 2017; An et al., 2018
GSK2606414	PERK homolog PK4 of *Plasmodium;* PERK homolog TgIF2K-A of *Toxoplasma*	Inhibiting the activation of PK4 and phosphorylation of eIF2α; inhibiting the lytic cycle of tachyzoites	Alleviating the symptoms of malaria, preventing the recurrence of *Plasmodium* and inhibit the transmission of this disease; Inhibiting the invasion, replication and differentiation of *T. gondii*	Zhang et al., 2017; Augusto et al., 2018
apoptozole	GRP78 of *P. falciparum*	Inhibiting GRP78 function	Leading to the death of chloroquine-sensitive and -resistant *P. falciparum* strains	Chen et al., 2018
ER stress inducer	PERK pathway of *Leishmania*; eIF2α of *Plasmodium*; Bip of *T. brucei;* PERK pathway of *T. gondii;* TgIF2α of *T. gondii;* Bip of *Leishmania major*	Inducing eIF2α phosphorylation; Inducing eIF2α phosphorylation of *Plasmodium;* Increasing the expression of Bip of *T. brucei;* Inducing eIF2α phosphorylation of *T. gondii;* Inducing the phosphorylation of TgIF2α; Increasing the expression of Bip of *Leishmania major*	Kill parasites (The parasite is more susceptible to ER stress than host due to the mere presence of the PERK pathway); Participating in the formation of *P. falciparum* gametophytes and the conversion of the *P. berghei;* Inducing programmed cell death of *T. brucei;* Inducing apoptosis or autophagy of *T. gondii;* Inhibiting the differentiation of *T. gondii* from tachyzoite to bradyzoite cysts; Inducing the apoptosis of *Leishmania major*	Narasimhan et al., 2008; Goldshmidt et al., 2010; Dolai et al., 2011; Gosline et al., 2011; Chaubey et al., 2014; Duran-Bedolla et al., 2017; Nguyen et al., 2017; Hao et al., 2019
TbeIF2K2 inhibitors	PERK homolog TbeIF2K2 of *T. brucei*	May suppress the function of sensing protein and regulating protein synthesis near flagellar pocket of *Trypanosome*	Inhibiting the survival of parasites	Gull, 2003; Moraes et al., 2007
PK3 activator	PERK homolog PK3 of *T. brucei*	Increasing ER stress-induced PCD	Lead to the death of *T. brucei*	Hope et al., 2014
Tc-eIF2α phosphorylation inhibitor	Tc-eIF2α of *T. cruzi*	Inhibiting the phosphorylation of Tc-eIF2α	Inhibiting the differentiation of non-infective epimastigotes into infective metacyclic trypomastigotes	Tonelli et al., 2011
TgIF2α phosphorylation inhibitor Salubrinal	TgIF2α of *T. gondii*	Inhibiting the phosphorylation of TgIF2α	Inhibiting the survival of *Toxoplasma* and decreasing virulence to host cell	Narasimhan et al., 2008; Joyce et al., 2010
Bortezomib	GRP78- IRE2/XBP1 pathway of protoscoleces of *E. granulosus*	Inducing ER stress and apoptosis	Reducing the viability of *E. granulosus*	Nicolao et al., 2017
PI3P tubules/vesicles inhibitor	PI3P tubules/vesicles of *Plasmodium*	Inhibiting the formation and diffusion of PI3P tubules/vesicles	Inhibiting UPR mediated artemisinin resistance	Mok et al., 2015; Bhattacharjee et al., 2018

PERK, protein kinase RNA-like ER kinase; IRE1, inositol-requiring kinase/endoribonuclease 1; ATF6, activating transcription factor 6; ATF4, activating transcription factor 4; XBP1, X box-binding protein 1; CHOP, C/EBP-homologous protein; GRP78, Glucose regulated proteins 78; TUDCA, tauroursodeoxycholic acid; ROP18, rhoptry protein 18; eIF2α, α-subunit of eukaryotic translational initiation factor 2; PCD, programmed cell death; PI3P, phosphatidylinositol-3-phosphate.

Artemisinin-based combination therapies (ACTs) are efficient frontline drugs to treat malaria. However, since artemisinin resistance was first discovered *in vivo* in western Cambodia (Dondorp et al., 2009), it gradually become a great challenge in malaria treatment. In recent years, many researches have focused on the mechanism of artemisinin resistance, and some of them have suggested that UPR is an important mechanism for artemisinin resistance. By analyzing 1,043 *P. falciparum* samples isolated from the peripheral blood of patients with acute malaria, Mok et al. (2015) found that artemisinin-resistant parasites exhibited decelerated development in the early ring stage and the expression of two molecular chaperone complexes of UPR were upregulated, such as *Plasmodium* reactive oxidative stress complex (PROSC, BiP belonging to the family) (Haldar et al., 2018) and TCP-1 ring complex (TRiC) (Mok et al., 2015). Thus, they speculated that the decelerated development of artemisinin-resistant *P. falciparum* may be associated with the upregulation of their UPR, which as a proteostatic mechanism that can repair the artemisinin induced impaired protein and reduce artemisinin-induced toxic proteopathy (Mok et al., 2015). Souvik et al. further clarified that the amplified phosphatidylinositol-3-phosphate (PI3P) tubules/vesicles in the parasite's ER in infected red cells extensively spread the proteostatic capacity of UPR, which may neutralize artemisinin's toxic proteopathy and participate in artemisinin resistance (Bhattacharjee et al., 2018). Therefore, ER stress inhibitors or PI3P tubules/vesicles inhibitors may be used in patients with artemisinin resistance.

Zhang et al. (2017) studied the relationship between PK4-eIF2α pathway and recrudescence of *Plasmodium* and found that treatment of ARTs could activate the phosphorylation of PK4-eIF2α and promote latency in the ring stage. Treatment with salubrinal significantly increased the recrudescence rate, while the PK4 inhibitor GSK2606414 abolished recrudescence after ARTs treatment in *P. berghei*-infected mice. Furthermore, they also showed that eIF2α phosphorylation was only observed in the young ring stage of $Dd2^{C580Y}$ but not in Dd2, an ART-sensitive and chloroquine-resistant *Plasmodium* line. This study indicated that the recrudescence of *Plasmodium* was related to the activation of PK4 and phosphorylation of eIF2α following ART treatment. The results show that artemisinin can be combined with PK4 inhibitor to prevent the recurrence of *Plasmodium*.

CONCLUSION AND PERSPECTIVES

Parasitic infection-induced pathological damage in hosts largely depends on ER stress. Therefore, inhibition of ER stress in hosts can be an effective treatment approach for parasitic diseases. In addition, considering that ER stress of parasites participates in their survival, development, and infection, the components or molecules of ER stress of parasites may be used as drug targets to kill or inhibit the development of parasites. The ER stress components or molecules that may be potential targets for the treatment of parasitic diseases are summarized in **Table 1**. Chemical chaperones TUDCA, trehalose, and 4-phenylbutyrate (4-PBA) have been used to reduce ER stress (Hetz et al., 2013), and they may be available for clinical application. Besides, clinical trials have shown that TUDCA therapy improved the sensitivity of insulin in the liver and muscle of insulin-resistant obese patients by affecting ER stress (Kars et al., 2010). Low dose of naltrexone treatment improved the function of epithelial barrier in IBD patients by reducing ER stress (Lie et al., 2018). These studies further demonstrate the feasibility of ER stress inhibitors as a treatment for parasitic diseases. In addition, the selectively target molecules of ER stress are more likely to be used, such as the inhibitors of ER stress molecules that play a key role in the survival and development of parasites (e.g., GSK2606414, PERK inhibitor) (Zhang et al., 2017), or the molecules of ER stress of parasites that are different from the host genes (e.g., GRP78 of *P. falciparum*) (Chen et al., 2018), or the parasites that are more sensitive to ER stress inducers than the host (e.g., DTT-induced ER stress in *Leishmania*) (Gosline et al., 2011). Moreover, because ER stress is involved in drug resistance, the inhibitors of ER stress molecules can be used in combination with anti-parasite drugs, such as ER stress inhibitors or PI3P tubules/vesicles inhibitors that may be used in patients with artemisinin resistance (Mok et al., 2015; Bhattacharjee et al., 2018).

AUTHOR CONTRIBUTIONS

JS advocated writing this review, reviewed, edited, and approved its final version. MP collected literature and wrote the manuscript. FC collected and reviewed literature. ZW provided some suggestions for this review. All authors contributed to the article and approved the submitted version.

FUNDING

This work was supported by grants from National Natural Science Foundation of China (grant nos. 81802036 and 81871682), the Natural Science Foundation of Guangdong Province, China (2020A1515010896), the China Postdoctoral Science Foundation (nos. 2018M631027 and 2019T120770), and the Fundamental Research Funds for the Central Universities (no. 19ykpy165).

REFERENCES

Abhishek, K., Das, S., Kumar, A., Kumar, A., Kumar, V., Saini, S., et al. (2018). *Leishmania donovani* induced unfolded protein response delays host cell apoptosis in PERK dependent manner. *PLoS Neglect. Trop. Dis.* 12:e0006646. doi: 10.1371/journal.pntd.0006646

Acosta-Alvear, D., Zhou, Y., Blais, A., Tsikitis, M., Lents, N. H., Arias, C., et al. (2007). XBP1 controls diverse cell type- and condition-specific transcriptional regulatory networks. *Mol. Cell* 27, 53–66.

Agrawal, S., Chung, D. W. D., Ponts, N., van Dooren, G. G., Prudhomme, J., Brooks, C. F., et al. (2013). An apicoplast localized Ubiquitylation system is required for the import of nuclear-encoded plastid proteins. *PLoS Pathog.* 9:e1003426. doi: 10.1371/journal.ppat.1003426

Agrawal, S., van Dooren, G. G., Beatty, W. L., and Striepen, B. (2009). Genetic evidence that an endosymbiont-derived endoplasmic reticulum-associated protein degradation (ERAD) system functions in import of apicoplast proteins. *J. Biol. Chem.* 284, 33683–33691. doi: 10.1074/jbc.M109.044024

An, R., Tang, Y., Chen, L., Cai, H., Lai, D.-H., Liu, K., et al. (2018). Encephalitis is mediated by ROP18 of, a severe pathogen in AIDS patients. *Proc.Natl. Acad. Sci. U.S.A.* 115, E5344–E5352. doi: 10.1073/pnas.1801118115

Anand, S. S., and Babu, P. P. (2013). Endoplasmic reticulum stress and neurodegeneration in experimental cerebral malaria. *Neuro Signals* 21:79. doi: 10.1159/000336970

Augusto, L., Martynowicz, J., Amin, P. H., Alakhras, N. S., Kaplan, M. H., Wek, R. C., et al. (2020). *Toxoplasma gondii* Co-opts the unfolded protein response to enhance migration and dissemination of infected host cells. *mBio* 11:e00915-20. doi: 10.1128/mBio.00915-20

Augusto, L., Martynowicz, J., Staschke, K. A., Wek, R. C., and Sullivan, W. J. (2018). Effects of PERK eIF2α kinase inhibitor against *Toxoplasma gondii*. *Antimicrob. Agents Chemother.* 62:e001442-18. doi: 10.1128/AAC.01442-18

Axten, J. M., Medina, J. R., Feng, Y., Shu, A., Romeril, S. P., Grant, S. W., et al. (2012). Discovery of 7-methyl-5-(1-{[3-(trifluoromethyl)phenyl]acetyl}-2,3-dihydro-1H-indol-5-yl)-7H-pyrrolo[2,3-d]pyrimidin-4-amine (GSK2606414), a potent and selective first-in-class inhibitor of protein kinase R (PKR)-like endoplasmic reticulum kinase (PERK). *J. Med. Chem.* 55, 7193–7207. doi: 10.1021/jm300713s

Ayyappan, J. P., Lizardo, K., Wang, S., Yurkow, E., and Nagajyothi, J. F. (2019). Inhibition of ER stress by 2-aminopurine treatment modulates cardiomyopathy in a murine chronic chagas disease model. *Biomol. Ther.* 27, 386–394. doi: 10.4062/biomolther.2018.193

Bertolotti, A., Zhang, Y., Hendershot, L. M., Harding, H. P., and Ron, D. (2000). Dynamic interaction of BiP and ER stress transducers in the unfolded-protein response. *Nat. Cell Biol.* 2, 326–332.

Bhattacharjee, S., Coppens, I., Mbengue, A., Suresh, N., Ghorbal, M., Slouka, Z., et al. (2018). Remodeling of the malaria parasite and host human red cell by vesicle amplification that induces artemisinin resistance. *Blood* 131, 1234–1247. doi: 10.1182/blood-2017-11-814665

Black, M. W., and Boothroyd, J. C. (2000). Lytic cycle of *Toxoplasma gondii*. *Microbiol. Mol. Biol. Rev.* 64, 607–623.

Bridgford, J. L., Xie, S. C., Cobbold, S. A., Pasaje, C. F. A., Herrmann, S., Yang, T., et al. (2018). Artemisinin kills malaria parasites by damaging proteins and inhibiting the proteasome. *Nat. Commun.* 9:3801. doi: 10.1038/s41467-018-06221-1

Bukau, B., Weissman, J., and Horwich, A. (2006). Molecular chaperones and protein quality control. *Cell* 125, 443–451.

Calfon, M., Zeng, H., Urano, F., Till, J. H., Hubbard, S. R., Harding, H. P., et al. (2002). IRE1 couples endoplasmic reticulum load to secretory capacity by processing the XBP-1 mRNA. *Nature* 415, 92–96.

Chaubey, S., Grover, M., and Tatu, U. (2014). Endoplasmic reticulum stress triggers gametocytogenesis in the malaria parasite. *J. Biol. Chem.* 289, 16662–16674. doi: 10.1074/jbc.M114.551549

Chen, Y., Murillo-Solano, C., Kirkpatrick, M. G., Antoshchenko, T., Park, H. W., and Pizarro, J. C. (2018). Repurposing drugs to target the malaria parasite unfolding protein response. *Sci. Rep.* 8:10333. doi: 10.1038/s41598-018-28608-2

Chow, C., Cloutier, S., Dumas, C., Chou, M.-N., and Papadopoulou, B. (2011). Promastigote to amastigote differentiation of *Leishmania* is markedly delayed in the absence of PERK eIF2alpha kinase-dependent eIF2alpha phosphorylation. *Cell. Microbiol.* 13, 1059–1077. doi: 10.1111/j.1462-5822.2011.01602.x

Chung, D.-W. D., Ponts, N., Prudhomme, J., Rodrigues, E. M., and Le Roch, K. G. (2012). Characterization of the ubiquitylating components of the human malaria parasite's protein degradation pathway. *PLoS One* 7:e43477. doi: 10.1371/journal.pone.0043477

Dias-Teixeira, K. L., Calegari-Silva, T. C., dos Santos, G. R. R. M., Vitorino Dos Santos, J., Lima, C., Medina, J. M., et al. (2016). The integrated endoplasmic reticulum stress response in *Leishmania amazonensis* macrophage infection: the role of X-box binding protein 1 transcription factor. *FASEB J.* 30, 1557–1565. doi: 10.1096/fj.15-281550

Dias-Teixeira, K. L., Calegari-Silva, T. C., Medina, J. M., Vivarini, A. C., Cavalcanti, A., Teteo, N., et al. (2017). Emerging role for the PERK/eIF2alpha/ATF4 in human Cutaneous *Leishmaniasis*. *Sci. Rep.* 7:17074. doi: 10.1038/s41598-017-17252-x

Dolai, S., and Adak, S. (2014). Endoplasmic reticulum stress responses in *Leishmania*. *Mol. Biochem. Parasitol.* 197, 1–8. doi: 10.1016/j.molbiopara.2014.09.002

Dolai, S., Pal, S., Yadav, R. K., and Adak, S. (2011). Endoplasmic reticulum stress-induced apoptosis in *Leishmania* through Ca2+-dependent and caspase-independent mechanism. *J. Biol. Chem.* 286, 13638–13646. doi: 10.1074/jbc.M110.201889

Dondorp, A. M., Nosten, F., Yi, P., Das, D., Phyo, A. P., Tarning, J., et al. (2009). Artemisinin resistance in *Plasmodium falciparum* malaria. *New Engl. J. Med.* 361, 455–467. doi: 10.1056/NEJMoa0808859

Duan, M., Yang, Y., Peng, S., Liu, X., Zhong, J., Guo, Y., et al. (2019). C/EBP homologous protein (CHOP) activates macrophages and promotes liver fibrosis in *Schistosoma japonicum*-infected mice. *J. Immunol. Res.* 2019:5148575. doi: 10.1155/2019/5148575

Duran-Bedolla, J., Tellez-Sosa, J., Valdovinos-Torres, H., Pavon, N., Buelna-Chontal, M., Tello-Lopez, A. T., et al. (2017). Cellular stress associated with the differentiation of *Plasmodium berghei* ookinetes. *Biochem. Cell Biol.* 95, 310–317. doi: 10.1139/bcb-2016-0028

Fallon, P. G., and Doenhoff, M. J. (1994). Drug-resistant schistosomiasis: resistance to praziquantel and oxamniquine induced in *Schistosoma mansoni* in mice is drug specific. *Am. J. Trop. Med. Hyg.* 51, 83–88.

Galluzzi, L., Diotallevi, A., De Santi, M., Ceccarelli, M., Vitale, F., Brandi, G., et al. (2016). *Leishmania infantum* induces mild unfolded protein response in infected macrophages. *PLoS One* 11:e0168339. doi: 10.1371/journal.pone.0168339

Galluzzi, L., Diotallevi, A., and Magnani, M. (2017). Endoplasmic reticulum stress and unfolded protein response in infection by intracellular parasites. *Future Sci. OA* 3:FSO198. doi: 10.4155/fsoa-2017-0020

Gass, J. N., Gifford, N. M., and Brewer, J. W. (2002). Activation of an unfolded protein response during differentiation of antibody-secreting B cells. *J. Biol. Chem.* 277, 49047–49054.

Goldshmidt, H., Matas, D., Kabi, A., Carmi, S., Hope, R., and Michaeli, S. (2010). Persistent ER stress induces the spliced leader RNA silencing pathway (SLS), leading to programmed cell death in *Trypanosoma brucei*. *PLoS Pathog.* 6:e1000731. doi: 10.1371/journal.ppat.1000731

Gosline, S. J. C., Nascimento, M., McCall, L.-I., Zilberstein, D., Thomas, D. Y., Matlashewski, G., et al. (2011). Intracellular eukaryotic parasites have a distinct unfolded protein response. *PLoS One* 6:e19118. doi: 10.1371/journal.pone.0019118

Grootjans, J., Kaser, A., Kaufman, R. J., and Blumberg, R. S. (2016). The unfolded protein response in immunity and inflammation. *Nat. Rev. Immunol.* 16, 469–484. doi: 10.1038/nri.2016.62

Gull, K. (2003). Host-parasite interactions and *trypanosome* morphogenesis: a flagellar pocketful of goodies. *Curr. Opin. Microbiol.* 6, 365–370.

Haldar, K., Bhattacharjee, S., and Safeukui, I. (2018). Drug resistance in *Plasmodium*. *Nat. Rev. Microbiol.* 16, 156–170. doi: 10.1038/nrmicro.2017.161

Hao, P., Cui, X., Liu, J., Li, M., Fu, Y., and Liu, Q. (2019). Identification and characterization of stearoyl-CoA desaturase in *Toxoplasma gondii*. *Acta Biochim. Biophys. Sinica* 51, 615–626. doi: 10.1093/abbs/gmz040

Harbut, M. B., Patel, B. A., Yeung, B. K., McNamara, C. W., Bright, A. T., Ballard, J., et al. (2012). Targeting the ERAD pathway via inhibition of signal peptide peptidase for antiparasitic therapeutic design. *Proc. Natl. Acad. Sci. U.S.A.* 109, 21486–21491. doi: 10.1073/pnas.1216016110

Haze, K., Yoshida, H., Yanagi, H., Yura, T., and Mori, K. (1999). Mammalian transcription factor ATF6 is synthesized as a transmembrane protein and activated by proteolysis in response to endoplasmic reticulum stress. *Mol. Biol. Cell* 10, 3787–3799.

Hendrick, H. M., Welter, B. H., Hapstack, M. A., Sykes, S. E., Sullivan, W. J., and Temesvari, L. A. (2016). Phosphorylation of eukaryotic initiation factor-2α during Stress and encystation in *Entamoeba* Species. *PLoS Pathog.* 12:e1006085. doi: 10.1371/journal.ppat.1006085

Hetz, C., Chevet, E., and Harding, H. P. (2013). Targeting the unfolded protein response in disease. *Nat. Rev. Drug Discov.* 12, 703–719. doi: 10.1038/nrd3976

Hope, R., Ben-Mayor, E., Friedman, N., Voloshin, K., Biswas, D., Matas, D., et al. (2014). Phosphorylation of the TATA-binding protein activates the spliced

leader silencing pathway in *Trypanosoma brucei*. *Sci. Signal.* 7:ra85. doi: 10.1126/scisignal.2005234

Hwang, J., and Qi, L. (2018). Quality control in the endoplasmic reticulum: crosstalk between ERAD and UPR pathways. *Trends Biochem. Sci.* 43, 593–605. doi: 10.1016/j.tibs.2018.06.005

Inacio, P., Zuzarte-Luis, V., Ruivo, M. T., Falkard, B., Nagaraj, N., Rooijers, K., et al. (2015). Parasite-induced ER stress response in hepatocytes facilitates *Plasmodium* liver stage infection. *EMBO Rep.* 16, 955–964. doi: 10.15252/embr.201439979

Joyce, B. R., Queener, S. F., Wek, R. C., and Sullivan, W. J. (2010). Phosphorylation of eukaryotic initiation factor-2{alpha} promotes the extracellular survival of obligate intracellular parasite *Toxoplasma gondii*. *Proc. Natl. Acad. Sci. U.S.A.* 107, 17200–17205. doi: 10.1073/pnas.1007610107

Joyce, B. R., Tampaki, Z., Kim, K., Wek, R. C., and Sullivan, W. J. (2013). The unfolded protein response in the protozoan parasite *Toxoplasma gondii* features translational and transcriptional control. *Eukaryot. Cell* 12, 979–989. doi: 10.1128/EC.00021-13

Kars, M., Yang, L., Gregor, M. F., Mohammed, B. S., Pietka, T. A., Finck, B. N., et al. (2010). Tauroursodeoxycholic Acid may improve liver and muscle but not adipose tissue insulin sensitivity in obese men and women. *Diabetes* 59, 1899–1905. doi: 10.2337/db10-0308

Konrad, C., Wek, R. C., and Sullivan, W. J. (2014). GCN2-like eIF2α kinase manages the amino acid starvation response in *Toxoplasma gondii*. *Intern. J. Parasitol.* 44, 139–146. doi: 10.1016/j.ijpara.2013.08.005

Kumari, R., Gupta, P., and Tiwari, S. (2018). Ubc7/Ube2g2 ortholog in *Entamoeba histolytica*: connection with the plasma membrane and phagocytosis. *Parasitol. Res.* 117, 1599–1611. doi: 10.1007/s00436-018-5842-6

Lazaridis, K. N., Gores, G. J., and Lindor, K. D. (2001). Ursodeoxycholic acid 'mechanisms of action and clinical use in hepatobiliary disorders'. *J. Hepatol.* 35, 134–146.

Li, J., Tang, G., Qin, W., Yang, R., Ma, R., Ma, B., et al. (2018). Toxic effects of arsenic trioxide on *Echinococcus granulosus* protoscoleces through ROS production, and Ca2+-ER stress-dependent apoptosis. *Acta Biochimi. Biophys. Sinica* 50, 579–585. doi: 10.1093/abbs/gmy041

Li, P., Fu, D., Sheng, Q., Yu, S., Bao, X., and Lv, Z. (2019). TUDCA attenuates intestinal injury and inhibits endoplasmic reticulum stress-mediated intestinal cell apoptosis in necrotizing enterocolitis. *Intern. Immunopharmacol.* 74:105665. doi: 10.1016/j.intimp.2019.05.050

Lie, M. R. K. L., van der Giessen, J., Fuhler, G. M., de Lima, A., Peppelenbosch, M. P., van der Ent, C., et al. (2018). Low dose Naltrexone for induction of remission in inflammatory bowel disease patients. *J. Transl. Med.* 16:55. doi: 10.1186/s12967-018-1427-5

Liu, F., Cui, Y., Ge, P., Luan, J., Zhou, X., and Han, J. (2015). Tauroursodeoxycholic acid attenuates inorganic phosphate-induced osteoblastic differentiation and mineralization in NIH3T3 fibroblasts by inhibiting the ER stress response PERK-eIF2α-ATF4 pathway. *Drug Discov. Therap.* 9, 38–44.

Loos, J. A., Nicolao, M. C., and Cumino, A. C. (2018). Metformin promotes autophagy in *Echinococcus granulosus* larval stage. *Mol. Biochem. Parasitol.* 224, 61–70. doi: 10.1016/j.molbiopara.2018.07.003

Ma, Y., and Hendershot, L. M. (2003). Delineation of a negative feedback regulatory loop that controls protein translation during endoplasmic reticulum stress. *J. Biol. Chem.* 278, 34864–34873.

Malo, A., Krüger, B., Seyhun, E., Schäfer, C., Hoffmann, R. T., Göke, B., et al. (2010). Tauroursodeoxycholic acid reduces endoplasmic reticulum stress, trypsin activation, and acinar cell apoptosis while increasing secretion in rat pancreatic acini. *Am. J. Physiol. Gastrointest. Liver Physiol.* 299, G877–G886. doi: 10.1152/ajpgi.00423.2009

Messias Sandes, J., Nascimento Moura, D. M., Divina da Silva Santiago, M., Barbosa de Lima, G., Cabral Filho, P. E., da Cunha Goncalves de Albuquerque, S., et al. (2019). The effects of endoplasmic reticulum stressors, tunicamycin and dithiothreitol on *Trypanosoma cruzi*. *Exp. Cell Res.* 383:111560. doi: 10.1016/j.yexcr.2019.111560

Möhrle, J. J., Zhao, Y., Wernli, B., Franklin, R. M., and Kappes, B. (1997). Molecular cloning, characterization and localization of PfPK4, an eIF-2alpha kinase-related enzyme from the malarial parasite *Plasmodium falciparum*. *Biochem. J.* 328(Pt 2), 677–687.

Mok, S., Ashley, E. A., Ferreira, P. E., Zhu, L., Lin, Z., Yeo, T., et al. (2015). Drug resistance. Population transcriptomics of human malaria parasites reveals the mechanism of artemisinin resistance. *Science* 347, 431–435. doi: 10.1126/science.1260403

Moraes, M. C. S., Jesus, T. C. L., Hashimoto, N. N., Dey, M., Schwartz, K. J., Alves, V. S., et al. (2007). Novel membrane-bound eIF2alpha kinase in the flagellar pocket of *Trypanosoma brucei*. *Eukaryot. Cell* 6, 1979–1991.

Narasimhan, J., Joyce, B. R., Naguleswaran, A., Smith, A. T., Livingston, M. R., Dixon, S. E., et al. (2008). Translation regulation by eukaryotic initiation factor-2 kinases in the development of latent cysts in *Toxoplasma gondii*. *J. Biol. Chem.* 283, 16591–16601. doi: 10.1074/jbc.M800681200

Nguyen, H. M., Berry, L., Sullivan, W. J., and Besteiro, S. (2017). Autophagy participates in the unfolded protein response in *Toxoplasma gondii*. *FEMS Microbiol. Lett.* 364:fnx153. doi: 10.1093/femsle/fnx153

Nicolao, M. C., Loos, J. A., Rodriguez Rodrigues, C., Beas, V., and Cumino, A. C. (2017). Bortezomib initiates endoplasmic reticulum stress, elicits autophagy and death in *Echinococcus granulosus* larval stage. *PLoS One* 12:e0181528. doi: 10.1371/journal.pone.0181528

Novoa, I., Zeng, H., Harding, H. P., and Ron, D. (2001). Feedback inhibition of the unfolded protein response by GADD34-mediated dephosphorylation of eIF2alpha. *J. Cell Biol.* 153, 1011–1022.

Pahl, H. L., and Baeuerle, P. A. (1995). A novel signal transduction pathway from the endoplasmic reticulum to the nucleus is mediated by transcription factor NF-kappa B. *EMBO J.* 14, 2580–2588.

Pineda, E., and Perdomo, D. (2017). *Entamoeba histolytica* under oxidative stress: what countermeasure mechanisms are in place? *Cells* 6:44. doi: 10.3390/cells6040044

Poncet, A. F., Bosteels, V., Hoffmann, E., Chehade, S., Rennen, S., Huot, L., et al. (2021). The UPR sensor IRE1α promotes dendritic cell responses to control *Toxoplasma gondii* infection. *EMBO Rep.* 22:e49617. doi: 10.15252/embr.201949617

Ron, D., and Walter, P. (2007). Signal integration in the endoplasmic reticulum unfolded protein response. *Nat. Rev. Mol. Cell Biol.* 8, 519–529.

Santi-Rocca, J., Smith, S., Weber, C., Pineda, E., Hon, C.-C., Saavedra, E., et al. (2012). Endoplasmic reticulum stress-sensing mechanism is activated in *Entamoeba histolytica* upon treatment with nitric oxide. *PLoS One* 7:e31777. doi: 10.1371/journal.pone.0031777

Shen, J., Chen, X., Hendershot, L., and Prywes, R. (2002). ER stress regulation of ATF6 localization by dissociation of BiP/GRP78 binding and unmasking of Golgi localization signals. *Dev. Cell* 3, 99–111.

Spork, S., Hiss, J. A., Mandel, K., Sommer, M., Kooij, T. W. A., Chu, T., et al. (2009). An unusual ERAD-Like complex is targeted to the apicoplast of *Plasmodium falciparum*. *Eukaryot. Cell* 8, 1134–1145. doi: 10.1128/Ec.00083-09

Sullivan, W. J., Narasimhan, J., Bhatti, M. M., and Wek, R. C. (2004). Parasite-specific eIF2 (eukaryotic initiation factor-2) kinase required for stress-induced translation control. *Biochem. J.* 380(Pt 2), 523–531.

Tang, Y. W., Zheng, M. J., An, R., Chen, L. J., Gong, L. L., Cai, H. J., et al. (2017). Proteasomal degradation of *T. gondii* ROP18 requires Derlin2. *Acta Trop.* 174, 106–113. doi: 10.1016/j.actatropica.2017.06.027

Tiengwe, C., Muratore, K. A., and Bangs, J. D. (2016). Surface proteins, ERAD and antigenic variation in *Trypanosoma brucei*. *Cell. Microbiol.* 18, 1673–1688. doi: 10.1111/cmi.12605

Tonelli, R. R., Augusto Lda, S., Castilho, B. A., and Schenkman, S. (2011). Protein synthesis attenuation by phosphorylation of eIF2alpha is required for the differentiation of *Trypanosoma cruzi* into infective forms. *PLoS One* 6:e27904. doi: 10.1371/journal.pone.0027904

Tsuru, A., Imai, Y., Saito, M., and Kohno, K. (2016). Novel mechanism of enhancing IRE1α-XBP1 signalling via the PERK-ATF4 pathway. *Sci. Rep.* 6:24217. doi: 10.1038/srep24217

Walters, H. A., Welter, B. H., Sullivan, W. J., and Temesvari, L. A. (2019). Phosphorylation of eukaryotic initiation factor-2α in response to endoplasmic reticulum and nitrosative stress in the human protozoan parasite, *Entamoeba histolytica*. *Mol. Biochem. Parasitol.* 234:111223. doi: 10.1016/j.molbiopara.2019.111223

Wan, L., Gong, L., Wang, W., An, R., Zheng, M., Jiang, Z., et al. (2015). *T. gondii* rhoptry protein ROP18 induces apoptosis of neural cells via endoplasmic reticulum stress pathway. *Parasit. Vect.* 8:554. doi: 10.1186/s13071-015-1103-z

Wang, T., Zhou, J., Gan, X., Wang, H., Ding, X., Chen, L., et al. (2014). *Toxoplasma gondii* induce apoptosis of neural stem cells via endoplasmic reticulum stress pathway. *Parasitology* 141, 988–995. doi: 10.1017/S0031182014000183

Ward, P., Equinet, L., Packer, J., and Doerig, C. (2004). Protein kinases of the human malaria parasite *Plasmodium falciparum*: the kinome of a divergent eukaryote. *BMC Genom.* 5:79. doi: 10.1186/1471-2164-5-79

Yoshida, H., Matsui, T., Yamamoto, A., Okada, T., and Mori, K. (2001). XBP1 mRNA is induced by ATF6 and spliced by IRE1 in response to ER stress to produce a highly active transcription factor. *Cell* 107, 881–891.

Yu, Y.-R., Deng, M.-J., Lu, W.-W., Zhang, J.-S., Jia, M.-Z., Huang, J., et al. (2014). Endoplasmic reticulum stress-mediated apoptosis is activated in intestines of mice with *Trichinella spiralis* infection. *Exper. Parasitol.* 145, 1–6. doi: 10.1016/j.exppara.2014.06.017

Yu, Y.-R., Ni, X.-Q., Huang, J., Zhu, Y.-H., and Qi, Y.-F. (2016). Taurine drinking ameliorates hepatic granuloma and fibrosis in mice infected with *Schistosoma japonicum*. *Intern. J. Parasitol. Drugs Drug Resist.* 6, 35–43. doi: 10.1016/j.ijpddr.2016.01.003

Zhang, M., Gallego-Delgado, J., Fernandez-Arias, C., Waters, N. C., Rodriguez, A., Tsuji, M., et al. (2017). Inhibiting the *Plasmodium* eIF2alpha Kinase PK4 prevents artemisinin-induced latency. *Cell Host Microb.* 22, 766–776.e764. doi: 10.1016/j.chom.2017.11.005

Zhang, M., Mishra, S., Sakthivel, R., Rojas, M., Ranjan, R., Sullivan, W. J., et al. (2012). PK4, a eukaryotic initiation factor 2 (eIF2) kinase, is essential for the development of the erythrocytic cycle of *Plasmodium*. *Proc. Natl. Acad. Sci. U.S.A.* 109, 3956–3961. doi: 10.1073/pnas.1121567109

Zhang, X., An, T., Pham, K. T. M., Lun, Z.-R., and Li, Z. (2019). Functional analyses of cytokinesis regulators in bloodstream stage *Trypanosoma brucei* parasites identify functions and regulations specific to the life cycle stage. *mSphere* 4:e0199-19. doi: 10.1128/mSphere.00199-19

Zhou, J., Gan, X., Wang, Y., Zhang, X., Ding, X., Chen, L., et al. (2015). *Toxoplasma gondii* prevalent in China induce weaker apoptosis of neural stem cells C17.2 via endoplasmic reticulum stress (ERS) signaling pathways. *Parasit. Vect.* 8:73. doi: 10.1186/s13071-015-0670-3

Zuzarte-Luís, V., and Mota, M. M. (2018). Parasite sensing of host nutrients and environmental cues. *Cell Host Microb.* 23, 749–758. doi: 10.1016/j.chom.2018.05.018

Conflict of Interest: The authors declare that the research was conducted in the absence of any commercial or financial relationships that could be construed as a potential conflict of interest.

frontiers in Microbiology

ORIGINAL RESEARCH
published: 30 July 2021
doi: 10.3389/fmicb.2021.713372

Simultaneous Detection of Ebola Virus and Pathogens Associated With Hemorrhagic Fever by an Oligonucleotide Microarray

Wenwu Yao†, Zhangnv Yang†, Xiuyu Lou, Haiyan Mao, Hao Yan and Yanjun Zhang**

Zhejiang Provincial Center for Disease Control and Prevention, Hangzhou, China

Ebola virus infection causes severe hemorrhagic fever, and its mortality rates varied from 25 to 90% in the previous outbreaks. The highly infectious and lethal nature of this virus highlights the need for reliable and sensitive diagnostic methods to distinguish it from other diseases present with similar clinical symptoms. Based on multiplex polymerase chain reaction (PCR) and oligonucleotide microarray technology, a cost-effective, multipathogen and high-throughput method was developed for simultaneous detection of Ebola virus and other pathogens associated with hemorrhagic fever, including Marburg virus, Lassa fever virus, Junin virus, Machupo virus, Rift Valley fever virus, Crimean-Congo hemorrhagic fever virus, malaria parasite, hantavirus, severe fever with thrombocytopenia syndrome virus, dengue virus, yellow fever virus, Chikungunya virus, influenza A virus, and influenza B virus. This assay had an excellent specificity for target pathogens, without overlap signal between the probes. The limit of detection was approximately 10^3 pathogen copies/μl. A total of 60 positive nucleic acid samples for different pathogens were detected, a concordance of 100% was observed between microarray assay and real-time PCR analysis. Consequently, the described oligonucleotide microarray may be specific and sensitive assay for diagnosis and surveillance of infections caused by Ebola virus and other species of hemorrhagic fever pathogens.

Keywords: Ebola virus, hemorrhagic fever, microarray, detection, pathogen

OPEN ACCESS

Edited by:
Gong Cheng,
Tsinghua University, China

Reviewed by:
Yasushi Itoh,
Shiga University of Medical Science, Japan
Felix Broecker,
Idorsia Pharmaceuticals Ltd., Switzerland

****Correspondence:***
Hao Yan
hyan@cdc.zj.cn
Yanjun Zhang
yjzhang@cdc.zj.cn

† These authors have contributed equally to this work

Specialty section:
This article was submitted to Infectious Diseases, a section of the journal Frontiers in Microbiology

Received: *22 May 2021*
Accepted: *05 July 2021*
Published: *30 July 2021*

Citation:
Yao W, Yang Z, Lou X, Mao H, Yan H and Zhang Y (2021) Simultaneous Detection of Ebola Virus and Pathogens Associated With Hemorrhagic Fever by an Oligonucleotide Microarray. Front. Microbiol. 12:713372. doi: 10.3389/fmicb.2021.713372

INTRODUCTION

Ebola virus disease (EVD), formerly known as Ebola hemorrhagic fever, is a severe, often fatal illness in humans. The first outbreaks of Ebola virus were documented in Sudan and the Democratic Republic of Congo in 1976 (Gire et al., 2014). Since its reemergence in 2013, Ebola virus has infected more than 32,000 people in Africa, resulting in more than 13,000 deaths (Tong et al., 2015; Maxmen, 2020). Similar to other viral hemorrhagic fever (VHF), following an incubation period of EVD, infected patients commonly develop non-specific flulike symptoms of fever, chills, malaise, and myalgia. The subsequent signs and symptoms indicate multisystem involvement and include systemic, gastrointestinal, respiratory, vascular, and neurological manifestations. Haemorrhagic manifestations occur during the peak of the illness and include petechiae, ecchymoses, uncontrolled oozing from venepuncture sites,

mucosal hemorrhages, and postmortem evidence of visceral haemorrhagic effusions (Feldmann and Geisbert, 2011). The typical clinical symptoms of VHF include fever and bleeding disorders which are often accompanied with headache, muscle joint pain and convulsions which can progress to severe disseminated intravascular coagulation (DIC), central nervous system damage, shock, and even death (Marty et al., 2006). Many people throughout the world are exposed to the threat of hemorrhagic fever viruses, including Ebola virus, Marburg virus, Lassa fever virus, Junin virus, Machupo virus, Rift Valley fever virus, Crimean-Congo hemorrhagic fever virus, hantavirus, severe fever with thrombocytopenia syndrome virus, dengue virus, yellow fever virus, Chikungunya virus, etc. Most of the infections lacking specific clinical features at early stage of the disease must rely on laboratory diagnostic methods for identification, as the symptoms are similar to influenza or malaria.

There is a persistent need for cost-effective and reliable approaches for distinguishing Ebola virus from other pathogens associated with hemorrhagic fever. Currently, the laboratory methods for detecting Ebola virus include polymerase chain reaction (PCR), enzyme-linked immunosorbent assay (ELISA), indirect immunofluorescence assay (IFA), immunohistochemistry, virus isolation, etc. (Huang et al., 2014; Liu et al., 2015; Martin et al., 2015). However, the major disadvantage of each method mentioned above is that each assay can only test one infectious agent of the specimens. Although the multiple PCR can simultaneously detect more than one pathogen in one reaction, the quantity of pathogen is limited and this method cannot meet the requirement of high throughput, further it is also time consuming, costly, and requires large amount of samples.

Oligonucleotide microarray, a highthroughput technology that is accurate, speedy, and low-cost has been used for disease diagnosis, pathogenic microorganism detection, gene expression analysis, single-nucleotide polymorphism (SNP) detection, and genome sequencing (Leski et al., 2009; Chen et al., 2011; Kolquist et al., 2011; Mazzatti et al., 2012; Zhang et al., 2013; Katoski et al., 2015; Hardick et al., 2016). In this study, we report the establishment of an oligonucleotide microarray method for simultaneous identification of 16 pathogens associated with hemorrhagic fever, including Zaire ebolavirus (ZEBOV), Sudan ebolavirus (SEBOV), Marburg virus (MARV), Lassa fever virus (LFV), Junin virus (JUNV), Machupo virus (MACV), Rift Valley fever virus (RVFV), Crimean-Congo hemorrhagic fever virus (CCHFV), malaria parasite (MP), hantavirus (HV), severe fever with thrombocytopenia syndrome virus (SFTSV), dengue virus (DENV), yellow fever virus (YFV), Chikungunya virus (CHIKV), influenza A virus (FluA), and influenza B virus (FluB).

METERIALS AND METHODS

Specimen Collection and Processing

Serum or plasma specimens, blood samples, and clinical throat swab samples were collected from the Zhejiang Provincial Center for Disease Control and Prevention (CDC) and Chinese PLA Academy of Military Medical Sciences (AMMS). Total RNA or DNA were extracted by QIAamp MinElute Virus Spin Kit or QIAamp DNA Blood Mini Kit (Qiagen, Hilden, Germany).

Primer and Probe Design

Gene sequences for ZEBOV, SEBOV, MARV, LFV, JUNV, MACV, RVFV, CCHFV, MP, HV, SFTSV, DENV, YFV, CHIKV, FluA, and FluB were downloaded from the nucleotide database of NCBI.[1] The sequences were then aligned using AlignX (a component of the Vector NTI Advance 10.3.0). We designed primers to amplify the specific sequences of each pathogen mentioned above. Moreover, microarray probes ranging from 19 to 45 nucleotides were designed to detect targeted sequences of the 16 pathogens. Eventually, 29 primers and 16 were selected that accurately identified targeted pathogens. All the primers and probes were verified by BLAST[2], and the sequences are shown in **Tables 1**, **2**.

Microarray Preparation

All microarray probes were synthesized by Sangon Biotech Co., Ltd. (Shanghai, China), and a repeat sequence of 12T with an amino-labeled 3′end was connected to the 3′-end of all the probes for fixation to the aldehyde-chip surface. The microarray was composed of 10 multiwell grid holes, and each multiwell grid holes was composed of 48 points. Probes, at a 50 mM final concentration, were spotted onto the aldehyde chip after mixing with uniform proportional printing buffer [6 × saline-sodium citrate buffer (SSC), 5% glycerol, and 0.1% sodium dodecyl sulfate (SDS)]. The microarray was placed in a dryer for 24 h at room temperature, and unbound probes were removed by washing once with 0.2% SDS and once with distilled water for 30 s each at room temperature prior to use. The microarray layout is shown in **Figure 1**.

RT-PCR Amplification

The 16 pathogens associated with hemorrhagic fever were divided into three groups for higher amplification efficiency. The specific fragment of each pathogen in each group was respectively amplified by a multiplex RT-PCR system. Each multiplex RT-PCR was performed in a 25-μl reaction volume containing 12.5 μl of 2 × One Step Buffer, 5 μl of template nucleic acid, and 1 μl of PrimeScript One Step Enzyme Mix (Takara Biotechnology Co., Ltd., Dalian, China). The primers for the three different RT-PCR systems are listed in **Table 1**. Amplifications were performed with a Veritil 96-Well Thermal Cycler PCR system (Applied Biosystems, Waltham, MA, United States) using the following conditions: 30 min at 50°C; 2 min at 94°C; 45 cycles of 20 s at 94°C, 20 s at 55°C, and 20 s at 72°C; with a final extension of 5 min at 72°C.

Hybridization and Signal Detection

After the targeted fragments were amplified, 2 μl of each amplification product of the three reactions was mixed with 6 μl of hybridization buffer (8 × SSC, 1.2% SDS, 10% formylamine,

[1]http://www.ncbi.nlm.nih.gov/genomes

[2]http://blast.ncbi.nlm.nih.gov/

TABLE 1 | The primers and their concentrations in multiplex PCR.

Group ID	Primers[a]	Sequence (5′–3′)[b]	Primer conc. in multiplex PCR (mM)	Targeted genes	Pathogens	GenBank accession no.
A tube	EBO-F	TCTTGAAATMAARAAACCTGAC	0.14	GP	ZEBOV and SEBOV	KM233101
	EBO-R	ACCGGGGRAAGCCYCGAATC	0.7			KC589025
	MAR-F	AATAAGAAAGTGATATTATTTGACACAA	0.1	NP	MARV	Z12132
	MAR-R	TGTTGAATTTATCCTTATCAGAATT	0.5			
	LF-F	TCAAGGACTTCAATAACA	0.1	NP	LFV	AY628201
	LF-R	CCCTGCAGACTGCAAGGATTTG	0.5			
	JUN-F	CCATCAGGTTATGTTAAGG	0.1	L	JUNV	JN801477
	JUN-R	CTATGGTGGTGGTGCTG	0.5			
	MAC-F	ATATGAAGGGAGGTGTGAACA	0.1	GP1	MACV	AY571930
	MAC-R	GCTTGAGTCAGACTTATTGAGACA	0.5			
B tube	RVF-F	GGAGAATTCCCATACCGAGTCG	0.08	NS	RVFV	KF648860
	RVF-R	GTGAAATCACTGAGAGTCATATGG	0.4			
	CCHFV-F1	TCTCAAAGAAACACGTGC	0.1	NP	CCHFV	AF362080
	CCHFV-R1	CACAAGTCCATTTCCTTTCTTGAAC	0.5			
	MAL-F1	GTAATCTTAACCATAAACTATGC	0.1	18s rRNA	MP	HQ283215
	MAL-R1	TGTCAATCCTACTCTTGTCTTA	0.5			
	HV-MFO	AAAAGTAGGTGITAYATCYTIACAATGTGG	0.16	M	HV	AF288298
	HV-MRO	GTACAICCTGTRCCIACCCC	0.8			
	SFTSV-F	AGCATGAATTCTCACGGAGC	0.12	L	SFTSV	KP202163
	SFTSV-R	CGCTCTTCAAGGTTCTGCTT	0.6			
C tube	DEN-F	TCCACCTGAGAAGGTGTAARAAATCCG	0.1	3′UTR	DENV	GQ398257
	YFV-F1	GACTCCACACATTGAATAGA	0.1	3′UTR	YFV	U54798
	FLA-R[c]	ATGTCTCCTCTACCCTCTAGWACT	0.5	3′UTR	Flavivirus	GQ398257
	CHIKV-F1	GATCATAGATGCAGTTGTAT	0.1	NSP4	CHIKV	DQ443544
	CHIKV-R2	CGCCGTACAAAGTTATGACG	0.5			
	FA-MF2	GGCCCCCTCAAAGCCGAGAT	0.1	M	Flu A	HQ664927
	FA-MR2	CAAAGCGTCTACGCTGCAGT	0.5			
	FB-F1	ATGGCCATCGGATCCTCAACTCACTC	0.1	NS	Flu B	CY099917
	FB-R1	TCATGTCAGCTATTATGGAGCTGTT	0.5			

[a] *F, forward primers; R, reverse primers.*
[b] *All the reverse primers with a biotin-labeled 5′-end.*
[c] *Consensus reverse primer for DENV and YFV.*
ZEBOV, Zaire ebolavirus; SEBOV, Sudan ebolavirus; MARV, Marburg virus; LFV, Lassa fever virus; JUNV, Junin virus; MACV, Machupo virus; RVFV, Rift Valley fever virus; CCHFV, Crimean-Congo hemorrhagic fever virus; MP, malaria parasite; HV, hantavirus; SFTSV, severe fever with thrombocytopenia syndrome virus; DENV, Dengue virus, YFV, yellow fever virus; CHIKV, Chikungunya virus, FluA, influenza A virus; FluB, influenza B virus; JEV, Japanese encephalitis virus; HPIV, human parainfluenza virus.

and 10 × Denhardt's). A total of 10 μl of hybridization mixture was added to the hybridization region on the microarray, then the chip was placed in a hybrid box, and incubated for 1 h at 45°C. Subsequently, the chip was washed once for 20 s with 1 × SSC and 0.2% SDS, followed by 0.2 × SSC, and 0.1 × SSC at room temperature.

In this assay, we introduced a chemiluminescence approach for signal detector. After hybridization and washing were complete, the chip was incubated with 15 μl of 25 nM streptavidin-horseradish peroxidase (Str-HRP, Sigma-Aldrich Co., LLC, St Louis, MO, United States) for 30 min at 37°C. Then, the chip was washed with phosphate buffered saline with 0.05% Tween 20 (PBST) for 20 s at room temperature. Subsequently, 20 μl of Chemiluminescent HRP Substrate (Millipore Corporation, Billerica, MA, United States) prepared before use was added, and the chip was scanned by Chemiluminescent Imager (Academy of Military Medical Sciences, Tianjin, China). The probe signal densities were quantified by Arrayvision 7.0. The cutoff value for each probe was calculated through the mean of the spot intensity in order to determine the signals objectively.

Specificity and Sensitivity Evaluation

Clinical specimens that were confirmed and genotyped previously by Department of Microbiology, Zhejiang CDC, were used as positive controls for MP, HV, SFTSV, DENV, CHIKV, FluA, and FluB. The targeted genes of the remaining pathogens were synthesized by Sangon Biotech Co., Ltd. (Shanghai, China) and used for plasmid construction. Then, the RNAs were transcribed *in vitro* and also used as templates to assess the specificity of the microarray. The sensitivity of the microarray analysis was evaluated by serial 10-fold dilutions of *in vitro*-transcribed RNAs (ranging from 10^5 to 10^1 copies/μl). Ebola virus (Zaire) Nucleic Acid Detection Kit (real-time PCR)

TABLE 2 | The probes sequences for microarray.

Pathogens	Probes	Sequence (5′–3′)[a]
ZEBOV	ZEBO-P	GGACGGGAGCGAATGCTTAC
SEBOV	SEBO-P	TGGTGTCAGAGGCTTTCCA
MARV	MAR-P	GAGATCTCCTAGAAGGGGGTTTGCTGAC
LFV	LF-P	AGCCACAATAAATTGGGAGCAACAACTCCA
JUNV	JUN-P	CACAATCACAGTGCCGGTGGAGCCA
MACV	MAC-P	TATCAGTCTATGAACCAGAAGACCTTGGAAA
RVFV	RVF-P	GCCTTTTCAGAGACTTGTTGATCT
CCHFV	CCHFV-P	GTGTTCTCTTGAGTGCTAGCAAAATGG
MP	MAL-P	AATCAAAGTCTTTGGGTTCTGGGGCGAGTA
HV	HV-MP	GAATCCATCCTGTGGGCWGCAAGTG
SFTSV	SFTSV-P	TCCTCAGAGCTGCWTGCTCATCTC
DENV	DEN-P	CTAGCGGTTAGAGGAGACCCCTCCCTTACA GATCGCAGCAACAAT
YFV	YFV-P	CCACATGGGCTCTGCCACTGC
CHIKV	CHIKV-P	TATCAGTTGTGGTAATGTCC
Flu A	FluA-P	CTCATGGAATGGCTAAAGACAAGACCAA
Flu B	FluB-P	AATGAAGGACATTCAAAGCCAATTCGAGCAG CTGAAACTGCG
Quality control[b]	20T	TTTTTTTTTTTTTTTTTTT

[a] *A repeat sequence of 12T with an amino-labeled 3′-end was connected to the 3′-end of all the probes.*
[b] *A repeat sequence of 20T with an amino-labeled 3′-end and biotin-labeled 5′-end was used as microarray quality control.*

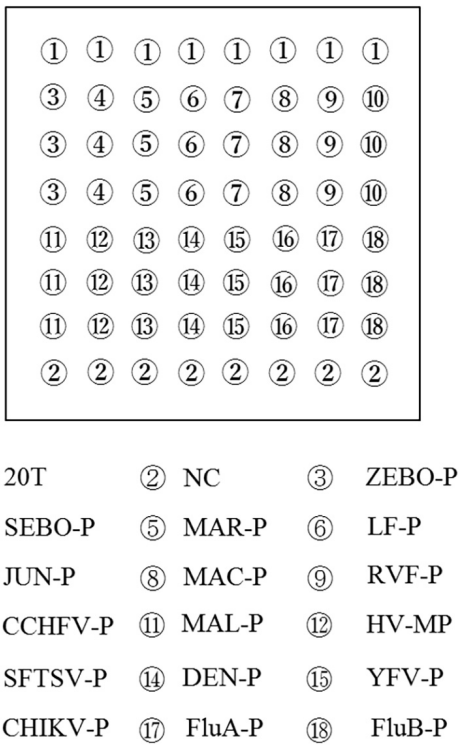

FIGURE 1 | Microarray layout. Capture probes were spotted in triplicate in columns. The sequence of biotin-labeled 20 T was repeated eight times for quality control and indicated the situations of capture probes. NC, negative control.

(Puruikang Biotech Co., Ltd., Shenzhen, China) was also used as references for sensitivity evaluation.

Samples Detection

Sixty positive samples with nucleic acid of different pathogens (including 45 Zaire ebolavirus RNAs which were extracted from inactivated Zaire ebolavirus culture samples), were provided by the Chinese People's Liberation Army (PLA), Academy of Military Medical Sciences (AMMS), and Zhejiang CDC, were detected by microarray analysis and commercial PCR kits. These dangerous infectious agents were handled in BSL-3 facilities of Zhejiang CDC for safety and surety. Agreement between the microarray assay and Real-Time RT-PCR assay was assessed.

RESULTS

Specificity of the Microarray

The microarray assay was able to well distinguish nucleic acid of ZEBOV, SEBOV, MARV, LFV, JUNV, MACV, RVFV, CCHFV, MP, HV, SFTSV, DENV, YFV, CHIKV, FluA, and FluB. Also, no overlapping signal between the probes was observed. Results are shown in **Figure 2**.

Sensitivity of the Microarray

To determine the detection limits of the microarray assays, we prepared 10-fold serial dilutions of *in vitro* transcribed RNAs (ranging from 10^5 to 10^1 copies/μl). Based on the positive signals generated, the sensitivity of the assay was 10^3 gene copies for ZEBOV, SEBOV, MARV, LFV, JUNV, RVFV, CCHFV, HV, SFTSV, DENV, YFV, CHIKV, FluA, and FluB. For MACV and MP, the detection limit was 10^2 gene copies (**Table 3**). We also compared the microarray detection methods with the real-time RT-PCR method, and we discovered that our method possessed similar detection sensitivities as the real-time RT-PCR method. The sensitivity comparison results of Zaire ebolavirus genomic template are shown in **Figure 3A**. The relationship between microarray signals and PCR cycles were analyzed and showed in **Figure 3B**.

Detection of Samples

The cutoff value is an index to determine hybridization results. The value was calculated by the average intensity of signals from negative pathogens and blank control plus three SD value for each probe (data not shown). A total of 60 positive samples with nucleic acid of different pathogens were tested by our microarray and commercial kits (**Table 4**). The ZEBOV testing results of microarray assay were 41 positive and four negative and had no cross-reactive signal with SEBOV and probes for other pathogens. The real-Ttime RT-PCR method also identified 41 samples as positive and four as negative. The results of the microarray had 100% concordance with the results of the Real-Time RT-PCR (kappa = 1.00).

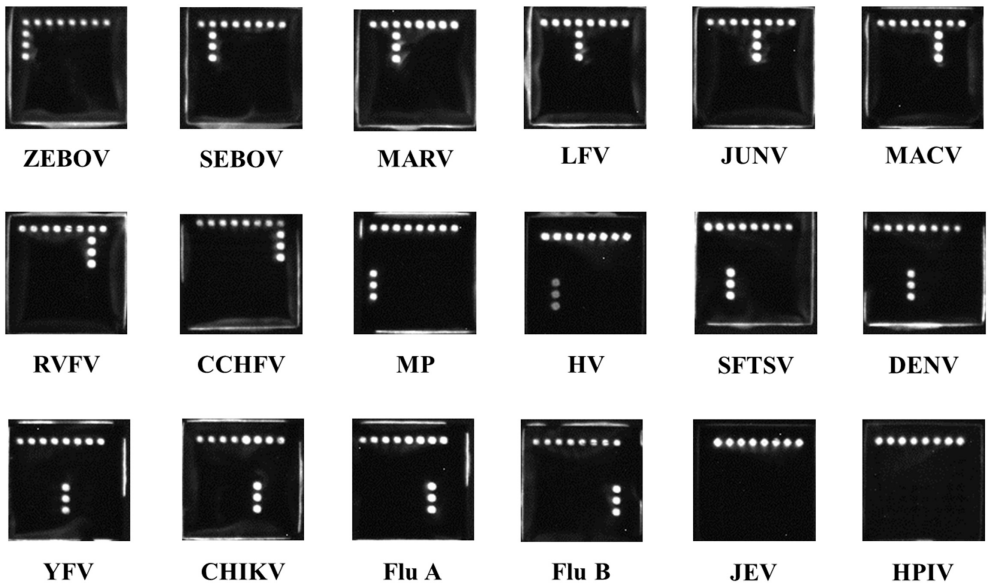

FIGURE 2 | Chemiluminescence images of typical patterns for each pathogens associated with hemorrhagic fever. ZEBOV, Zaire ebolavirus; SEBOV, Sudan ebolavirus; MARV, Marburg virus; LFV, Lassa fever virus; JUNV, Junin virus; MACV, Machupo virus; RVFV, Rift Valley fever virus; CCHFV, Crimean-Congo hemorrhagic fever virus; MP, malaria parasite; HV, hantavirus; SFTSV, severe fever with thrombocytopenia syndrome virus; DENV, dengue virus; YFV, yellow fever virus; CHIKV, Chikungunya virus; FluA, influenza A virus; FluB, influenza B virus; JEV, Japanese encephalitis virus; HPIV, human parainfluenza virus.

TABLE 3 | Results for the serial dilutions of each genomic template.

Genomic template	Sensitivity (copies/μ l)				
	10^5	10^4	10^3	10^2	10^1
ZEBOV	+	+	+	−	−
SEBOV	+	+	+	−	−
MARV	+	+	+	−	−
LFV	+	+	+	−	−
JUNV	+	+	+	−	−
MACV	+	+	+	+	−
RVFV	+	+	+	−	−
CCHFV	+	+	+	−	−
MP	+	+	+	+	−
HV	+	+	+	−	−
SFTSV	+	+	+	−	−
DENV	+	+	+	−	−
YFV	+	+	+	−	−
CHIKV	+	+	+	−	−
Flu A	+	+	+	−	−
Flu B	+	+	+	−	−

DISCUSSION

The Ebola virus is one of the greatest human infectious disease threats, with an average EVD case fatality rate approximating 50%, varing from 25 to 90% in past outbreaks (Kucharski and Edmunds, 2014; World Health Organization, 2021) according to the World Health Organization (WHO). There are numerous diseases with similar clinical syndromes (other VHFs, malaria, and influenza), their diagnosis can be a great challenge (Matua et al., 2015). Cycles of hemorrhagic fever viruses outbreak continue to be a major concern from a public health perspective and biodefense as few licensed therapeutic agents or vaccines are available. There is a persistent need for sensitive and reliable laboratory approaches for identification. A number of methods including virus culture, transmission electron microscopy, simple or multiplex PCR, IFA, and ELISA, have been utilized; however, these methods can be operationally complex, time consuming, or with low sensitivity. Most of these methods cannot meet the requirement of high throughput. Recently, serological approaches were developed for high-throughput detection of Ebola and other hemorrhagic fever viruses (Kamata et al., 2014; Wu et al., 2014). However, antibody cross-reaction between the recombinant antigens limited the application. By contrast, the advantages of the oligonucleotide microarray has distinct advantages.

In order to improve the sensitivity, we adopted the chemiluminescence detection technology widely used for ELISA (Maiolini et al., 2014), liquid hybridization assay (Hommatsu et al., 2013), and capillary electrophoresis (Jiang et al., 2013). The sensitivity of our microarray was evaluated based on cutoff values, with hybridization signals were demonstrated to be positive for samples that contained at least 10^3 copies/μl (**Table 3**). These are greater detection limits labeled by fluorescence (Cy3/Cy5) (Li et al., 2009) and had similar sensitivity as the real-time RT-PCR kit (**Figure 3**). However, compared with other RT-PCR systems, the sensitivity of our method was much lower (Wölfel et al., 2007; Rieger et al., 2016). The reason may be due to the interaction

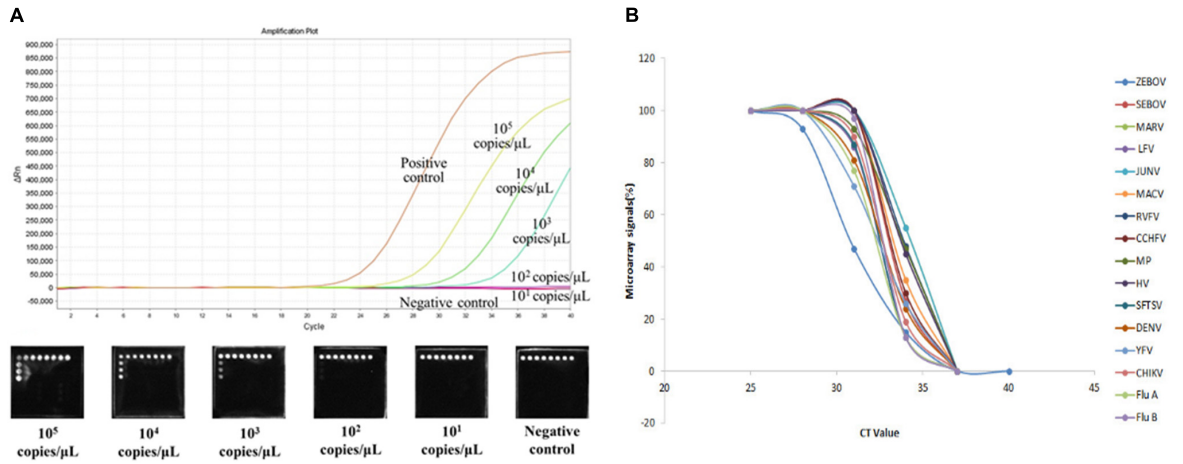

FIGURE 3 | (A) Sensitivity comparison results of Zaire ebolavirus. The real-time RT-PCRs were amplified by the 7,500 Real-Time PCR System (ABI, Foster City, CA, United States). Five dilutions (ranging from 10^5 to 10^1 copies/μl) of Zaire ebolavirus *in vitro*-transcribed RNA templates were amplified to compare the sensitivity of our microarray with that of the Ebola virus (Zaire) Nucleic Acid Detection Kit (real-time PCR) (Shenzhen Puruikang Biotech Co., Ltd.). **(B)** Relationship between microarray signals and PCR cycles. Real-time RT-PCR and microarray of 16 pathogens were performed simultaneously, and the diagram display the relationship between microarray signals and PCR cycles obtained.

TABLE 4 | Results for all positive samples tested in the two different assays.

Nucleic acid samples	No.	PCR		Microarray	
		+	−	+	−
ZEBOV	45	41	4	41	4
Plasmodium falciparum	1	1	0	1	0
Plasmodium vivax	1	1	0	1	0
HV	2	2	0	2	0
SFTSV	4	4	0	4	0
DENV-1	1	1	0	1	0
DENV-4	1	1	0	1	0
CHIKV	1	1	0	1	0
Flu A (H1)	1	1	0	1	0
Flu A (H3)	1	1	0	1	0
Flu B (BV)	1	1	0	1	0
Flu B (Y)	1	1	0	1	0
Total	60	56	4	56	4

between primers for different pathogens, and compared with other microarray systems, our microarray had a similar or better sensitivity for detecting part of these pathogens (Leski et al., 2009).

Since most of the targeted viruses are extremely dangerous, the collection of corresponding clinical sample or nucleic acid is unavailable. In order to determine the reliability of the microarray, *in vitro*-transcribed RNAs were prepared and used as templates to verify the detection results. By testing positive controls, we found that the microarray was able to distinguish all the targeted pathogens. In addition, the positive control of each pathogen could be negative control for other probes, showing an excellent specificity, without any overlapping signal between the probes (**Figure 2**). However, since a sufficient length of identical sequence for all 16 pathogens was not available, we had not got an internal control to verify nucleic acid templates of these pathogens extracted and the PCR reaction carried out successfully or not. This may be the disadvantage of microarray.

The GP gene of Ebola virus was chosen as an assay target for several reasons: (1) the GP protein of Ebola virus is required for entry into cells, (2) the membrane-bound GP is an important virulence factor of Ebola virus and plays a central role in the virus-mediated cytotoxicity of endothelial cells, and (3) sequence analysis of the GP genes of Ebola virus revealed that regions within this gene would be relatively conservative in evolution (Kibuuka et al., 2015; Tong et al., 2015). As more than 88% outbreaks of EVD were caused by Zaire and Sudan ebolavirus (Leroy et al., 2011; World Health Organization, 2021), we designed consensus primers for their PCR amplification and used specific probe for subtyping. The reliability of the method was also verified by detection of Ebola virus in specimens and in positive control samples.

A total of 60 samples of Ebola virus and other pathogens were tested by our microarray and compared with commercial real-time RT-PCR kits. A concordance of 100% was observed between the two methods (**Table 4**). However, these two methods did not positively identify four Zaire ebolavirus nucleic acid samples. These negative results may be due to low nucleic acid load or degradation of nucleic acid for inappropriate sample preservation.

CONCLUSION

In conclusion, a cost-effective, multipathogen, specific, and sensitive oligonucleotide microarray assay was developed to

detect Ebola virus and pathogens associated with hemorrhagic fever. This microarray was fast and high throughput, with the entire procedure, from extraction to microarray detection, could be completed within 5.5 h. The detection cost per sample was less than five US dollars. This oligonucleotide microarray will prove to be useful for treatment, prevention, surveillance, and epidemiological studies of Ebola virus.

DATA AVAILABILITY STATEMENT

The raw data supporting the conclusions of this article will be made available by the authors, without undue reservation.

ETHICS STATEMENT

This study was approved by the Academic Committee of Zhejiang Provincial Center for Disease Control and Prevention and all experiments were carried out in accordance with the approved guidelines. The human materials used were serum or plasma specimens, blood samples and throat swab samples, and all patients provided written informed consent.

AUTHOR CONTRIBUTIONS

HY and YZ designed the study. HY and WY performed the experiments. ZY analyzed the data and wrote the discussion part of the manuscript. XL and HM wrote the "Results" section of the manuscript. All authors reviewed the manuscript.

FUNDING

This study was supported by the Health Leading Talents Program of Zhejiang Province [2018(22)], Key Disciplinary of Health and Family Planning Commission of Zhejiang Province (CX-9), the National Key Research and Development of China (2017YFC1601503), and Medical Science and Technology Program of Zhejiang Province (2020KY092 and 2018KY341).

REFERENCES

Chen, E. C., Miller, S. A., DeRisi, J. L., and Chiu, C. Y. (2011). Using a pan-viral microarray assay (Virochip) to screen clinical samples for viral pathogens. *J. Vis. Exp*. 50:2536.

Feldmann, H., and Geisbert, T. W. (2011). Ebola haemorrhagic fever. *Lancet* 377, 849–862. doi: 10.1016/s0140-6736(10)60667-8

Gire, S. K., Goba, A., Andersen, K. G., Sealfon, R. S., Park, D. J., Kanneh, L., et al. (2014). Genomic surveillance elucidates Ebola virus origin and transmission during the 2014 outbreak. *Science* 345, 1369–1372.

Hardick, J., Woelfel, R., Gardner, W., and Ibrahim, S. (2016). Sequencing ebola and marburg viruses genomes using microarrays. *J. Med. Virol*. 88, 1303–1308. doi: 10.1002/jmv.24487

Hommatsu, M., Okahashi, H., Ohta, K., Tamai, Y., Tsukagoshi, K., and Hashimoto, M. (2013). Development of a PCR/LDR/flow-through hybridization assay using a capillary tube, probe DNA-immobilized magnetic beads and chemiluminescence detection. *Anal. Sci*. 29, 689–695. doi: 10.2116/analsci.29.689

Huang, Y., Zhu, Y., Yang, M., Zhang, Z., Song, D., and Yuan, Z. (2014). Nucleoprotein-based indirect enzyme-linked immunosorbent assay (indirect ELISA) for detecting antibodies specific to Ebola virus and Marbug virus. *Virol. Sin*. 29, 372–380. doi: 10.1007/s12250-014-3512-0

Jiang, J., Zhao, S., Huang, Y., Qin, G., and Ye, F. (2013). Highly sensitive immunoassay of carcinoembryonic antigen by capillary electrophoresis with gold nanoparticles amplified chemiluminescence detection. *J. Chromatogr. A*. 1282, 161–166. doi: 10.1016/j.chroma.2013.01.066

Kamata, T., Natesan, M., Warfield, K., Aman, M. J., and Ulrich, R. G. (2014). Determination of specific antibody responses to the six species of ebola and marburg viruses by multiplexed protein microarrays. *Clin. Vaccine Immunol*. 21, 1605–1612. doi: 10.1128/cvi.00484-14

Katoski, S. E., Meyer, H., and Ibrahim, S. (2015). An approach for identification of unknown viruses using sequencing-by-hybridization. *J. Med. Virol*. 87, 1616–1624. doi: 10.1002/jmv.24196

Kibuuka, H., Berkowitz, N. M., Millard, M., Enama, M. E., Tindikahwa, A., Sekiziyivu, A. B., et al. (2015). Safety and immunogenicity of Ebola virus and Marburg virus glycoprotein DNA vaccines assessed separately and concomitantly in healthy Ugandan adults: a phase 1b, randomised, double-blind, placebo-controlled clinical trial. *Lancet* 385, 1545–1554. doi: 10.1016/s0140-6736(14)62385-0

Kolquist, K. A., Chultz, R. A., Furrow, A., Brown, T. C., Han, J. Y., and Campbell, L. J. (2011). Microarray-based comparative genomic hybridization of cancer targets reveals novel, recurrent genetic aberrations in the myelodysplastic syndromes. *Cancer Genet*. 204, 603–628. doi: 10.1016/j.cancergen.2011.10.004

Kucharski, A. J., and Edmunds, W. J. (2014). Case fatality rate for Ebola virus disease in west Africa. *Lancet* 384:1260. doi: 10.1016/s0140-6736(14)61706-2

Leroy, E. M., Gonzalez, J. P., and Baize, S. (2011). Ebola and Marburg haemorrhagic fever viruses: major scientific advances, but a relatively minor public health threat for Africa. *Clin. Microbiol. Infect*. 17, 964–976. doi: 10.1111/j.1469-0691.2011.03535.x

Leski, T. A., Lin, B., Malanoski, A. P., Wang, Z., Long, N. C., Meador, C. E., et al. (2009). Testing and validation of high density resequencing microarray for broad range biothreat agents detection. *PLoS One* 4:e6569. doi: 10.1371/journal.pone.0006569

Li, X., Qi, X., Miao, L., Wang, Y., Liu, F., Gu, H., et al. (2009). Detection and subtyping of influenza A virus based on a short oligonucleotide microarray. *Diagn. Microbiol. Infect. Dis*. 65, 261–270. doi: 10.1016/j.diagmicrobio.2009.07.016

Liu, L., Sun, Y., Kargbo, B., Zhang, C., Feng, H., Lu, H., et al. (2015). Detection of Zaire Ebola virus by real-time reverse transcription-polymerase chain reaction, Sierra Leone, 2014. *J. Virol. Methods* 222, 62–65. doi: 10.1016/j.jviromet.2015.05.005

Maiolini, E., Ferri, E., Pitasi, A. L., Montoya, A., Di Giovanni, M., Errani, E., et al. (2014). Bisphenol A determination in baby bottles by chemiluminescence enzyme-linked immunosorbent assay, lateral flow immunoassay and liquid chromatography tandem mass spectrometry. *Analyst* 139, 318–324. doi: 10.1039/c3an00552f

Martin, P., Laupland, K. B., Frost, E. H., and Valiquette, L. (2015). Laboratory diagnosis of Ebola virus disease. *Intens. Care Med*. 41, 895–898.

Marty, A. M., Jahrling, P. B., and Geisbert, T. W. (2006). Viral hemorrhagic fevers. *Clin. Lab. Med*. 26, 345–386.

Matua, G. A., Van der Wal, D. M., and Locsin, R. C. (2015). Ebolavirus and Haemorrhagic Syndrome. *Sultan. Qaboos Univ. Med. J*. 15, e171–e176.

Maxmen, A. (2020). World's second-deadliest Ebola outbreak ends in Democratic Republic of the Congo. *Nature* doi: 10.1038/d41586-020-01950-0

Mazzatti, D., Lim, F. L., O'Hara, A., Wood, I. S., and Trayhurn, P. A. (2012). microarray analysis of the hypoxia-induced modulation of gene expression in human adipocytes. *Arch. Physiol. Biochem*. 118, 112–120. doi: 10.3109/13813455.2012.654611

Rieger, T., Kerber, R., El Halas, H., Pallasch, E., Duraffour, S., Günther, S., et al. (2016). Evaluation of RealStar reverse transcription-polymerase chain reaction

kits for Filovirus detection in the laboratory and field. *J. Infect. Dis.* 214, S243–S249.

Tong, Y. G., Shi, W. F., Liu, D., Qian, J., Liang, L., Bo, X. C., et al. (2015). Genetic diversity and evolutionary dynamics of Ebola virus in Sierra Leone. *Nature* 524, 93–96.

Wölfel, R., Paweska, J. T., Petersen, N., Grobbelaar, A. A., Leman, P. A., Hewson, R., et al. (2007). Virus detection and monitoring of viral load in Crimean-Congo hemorrhagic fever virus patients. *Emerg. Infect. Dis.* 13, 1097–1100. doi: 10.3201/eid1307.070068

World Health Organization (2021). *Ebola Virus Disease*. Available online at: https://www.who.int/news-room/fact-sheets/detail/ebola-virus-disease (accessed February 27, 2021).

Wu, W., Zhang, S., Qu, J., Zhang, Q., Li, C., Li, J., et al. (2014). Simultaneous detection of IgG antibodies associated with viral hemorrhagic fever by a multiplexed Luminex-based immunoassay. *Virus Res.* 187, 84–90. doi: 10.1016/j.virusres.2013.12.037

Zhang, Y., Liu, Q., Wang, D., Chen, S., and Wang, S. (2013). Simultaneous detection of oseltamivir- and amantadine-resistant influenza by oligonucleotide microarray visualization. *PLoS One* 8:e57154. doi: 10.1371/journal.pone.0057154

Conflict of Interest: The authors declare that the research was conducted in the absence of any commercial or financial relationships that could be construed as a potential conflict of interest.

Publisher's Note: All claims expressed in this article are solely those of the authors and do not necessarily represent those of their affiliated organizations, or those of the publisher, the editors and the reviewers. Any product that may be evaluated in this article, or claim that may be made by its manufacturer, is not guaranteed or endorsed by the publisher.

frontiers in Veterinary Science

ORIGINAL RESEARCH
published: 02 August 2021
doi: 10.3389/fvets.2021.703147

3′UTR SL-IV and DB1 Regions Contribute to Japanese Encephalitis Virus Replication and Pathogenicity

Jinchao Xing[1,2,3†], *Youyue Zhang*[1,2,3†], *Ziying Lin*[1,2], *Lele Liu*[1,2], *Qiang Xu*[1,2], *Jiaqi Liang*[1,2], *Zhaoxia Yuan*[4], *Cuiqin Huang*[5], *Ming Liao*[1,2,3,6*] *and Wenbao Qi*[1,2,3,6*]

[1] *Key Laboratory of Zoonoses, Ministry of Agriculture and Rural Affairs, South China Agricultural University, Guangzhou, China,* [2] *National and Regional Joint Engineering Laboratory for Medicament of Zoonoses Prevention and Control, Guangzhou, China,* [3] *Guangdong Laboratory for Lingnan Modern Agriculture, Guangzhou, China,* [4] *College of Animal Sciences and Technology, Zhongkai University of Agriculture and Engineering, Guangzhou, China,* [5] *The Key Laboratory of Fujian Animal Diseases Control, Longyan University, Longyan, China,* [6] *Key Laboratory of Zoonoses Prevention and Control of Guangdong Province, Guangzhou, China*

OPEN ACCESS

Edited by:
Gong Cheng,
Tsinghua University, China

Reviewed by:
Fengwei Bai,
University of Southern Mississippi, United States
Tongling Shan,
Shanghai Veterinary Research Institute, Chinese Academy of Agricultural Sciences (CAAS), China

****Correspondence:***
Ming Liao
mliao@scau.edu.cn
Wenbao Qi
qiwenbao@scau.edu.cn

† These authors have contributed equally to this work

Specialty section:
This article was submitted to Veterinary Infectious Diseases, a section of the journal Frontiers in Veterinary Science

Received: *30 April 2021*
Accepted: *07 July 2021*
Published: *02 August 2021*

Citation:
Xing J, Zhang Y, Lin Z, Liu L, Xu Q, Liang J, Yuan Z, Huang C, Liao M and Qi W (2021) 3′UTR SL-IV and DB1 Regions Contribute to Japanese Encephalitis Virus Replication and Pathogenicity. Front. Vet. Sci. 8:703147. doi: 10.3389/fvets.2021.703147

Japanese encephalitis virus (JEV), a mosquito-borne flavivirus that causes fatal neurological disease in humans, is one of the most important emerging pathogens of public health significance. JEV is maintained in an enzootic cycle and causes reproductive failure in pigs. Notably, the shift in JEV genotypes is not fully protected by existing vaccines, so the development of a candidate vaccine is urgently needed. In this study, we compared pathogenicity between Japanese encephalitis virus SA14 and BJB (isolated from humans in the 1970s) strains. We found that the BJB strain was attenuated in mice and that there was no case fatality rate. The growth rate of BJB was higher than SA14 virus in BHK-21 cells. Based on the sequence alignment of the viral genome between the SA14 and BJB virus strains, some mutations at sites 248, 254, 258, and 307 were observed in the 3′ untranslated region (3′UTR). The 3′UTR of JEV plays a very important role in the viral life cycle. Furthermore, using a reverse genetic system, we conducted and rescued the parental JEV strain SA14 (T248, A254, and A258) and the mutant virus rSA14-3′UTRmut (T248C, A254G, A258G, and 307G). Through an analysis of the RNA secondary structure model of the 3′UTR, we discovered that the mutations of T248C, A254G, and A258G reduced the apiculus ring and increased the lateral ring significantly in the stem-loop structures IV (SL-IV) structure region of 3′UTR. Moreover, the insertion of 307G added a ring to the dumbbell structure 1 (DB1) structure region. Strikingly, these RNA secondary structure changes in 3′UTR of rSA14-3′UTRmut increased viral negative chain RNA production and enhanced the replication ability of the virus in BHK-21 cells. However, *in vivo* mouse experiments illustrated that the rSA14-3′UTRmut virus significantly decreased the neurovirulence of JEV. These results affirmed that the JEV SL-IV and DB1 regions play an important role in viral proliferation and pathogenicity. Taken together, we complement the study of RNA element function in the 3′UTR region of JEV by providing a new target for the rational design of live attenuated candidate vaccines and the increase of virus production.

Keywords: Japanese encephalitis virus, 3′ untranslated region, stem-loop IV, virus replication, pathogenicity

INTRODUCTION

Japanese encephalitis virus (JEV) belongs to the genus *Flavivirus* in the family *Flaviviridae*. Flaviviruses such as dengue virus (DENV), Zika virus (ZIKV), and West Nile virus (WNV) can cause viral encephalitis, Guillain-Barré syndrome, and infant microcephaly (1). JEV is maintained in an enzootic cycle involving mosquito vectors (particularly *Culex tritaeniorhynchus*) and amplified in the main vertebrate of host pigs and wading birds (2, 3). The JEV exists as five distinguishable genotypes (G-I, G-II, G-III, G-IV, and G-V) based on nucleotide homology in the E protein gene (4, 5). JEV G-III was the historically dominant genotype throughout most of Asia, but it has been gradually replaced over the last 20 years by G-I in many Asian countries (6, 7). However, the shift in JEV genotypes is not fully protected by existing vaccines (8, 9). The need for new JE vaccine strategies is urgent.

The JEV genome is a single-stranded, positive-sense RNA about 11 kb in length, and it encodes a single polyprotein that is processed post-translationally into structural and non-structural proteins by cellular and viral proteases (10). The structural proteins make up the virion (11), and the non-structural proteins have multiple functions during the virus life cycle, including virus replication and host immune evasion (12–14). Significantly, highly conserved secondary structures are formed by the 5′ and 3′ untranslated regions (UTR) and are implicated in virus replication, translation and packaging of the genome (15).

Recently, studies on flaviviruses have shown that the *cis*-RNA structural elements of the untranslated region of the flavivirus play an important role in immune escape and virus replication in host cells (16–18). For the synthesis of the genomic RNA to take place, the replicase complex must specifically recognize viral *cis*-acting RNA elements, defined by primary sequences or secondary/tertiary structures (19). These RNA elements are found in various locations within the genome but most frequently are located in the 5′ and 3′UTRs (17). The hairpin structure of 3′UTR is specific to the host for DENV, and the point mutation in the hairpin structure eliminated infection by the virus in mosquito cells but did not affect the replication of the virus in mammalian cells (20, 21). In vertebrate and invertebrate cells infected with DENV, the restriction of host cells results in selective genetic mutation of the virus, and the virus 3′UTR often has a hot spot for mutation (22, 23). The 3′UTR includes four stem-loop structures (SL, named SLI, SLII, SLIII, and SLIV) and two dumbbell structures (DB, named DB1 and DB2). SL and DB structures are essential in the initial virus replication process. SL-II structures are the main components that prevent 5′-3′ RNA Xrn1 from degrading and that produce subgenomic flavivirus RNA (sfRNA) (24). This sfRNA plays an important role in causing cell lesions and pathogenicity by participating in the apoptosis of host cells and regulating the host's antiviral type I interferon response (25–27). The growth efficiency of DENV which deleted DB1 or DB2 was reduced (28). In addition, while deletion of DB1 reduced replication of DENV, viruses lacking DB2 displayed a great increase of fitness in mosquitoes (29). Although research on flavivirus UTR has been carried out in depth, the current studies mainly focus on the RNA elements SL-II and DB2 in the 3′UTR. Research on the RNA element SL-IV and DB1 structures of JEV is still rare.

In this study, we found that the BJB strain, isolated from human in the 1970s, was attenuated in mice, and that there was no case fatality rate. Based on the sequence alignment of the viral genome, we found some mutations at sites 248, 254, and 258, as well as an insert at site 307 in the 3′UTR. Through analysis of the RNA secondary structure model of the 3′UTR, it was found that the nucleotide mutations of rSA14-3′UTRmut caused the top loop to shrink and the side loop to increase in the SL-IV structure region, and a ring was added to the DB1 structure region. These RNA secondary structure changes enhanced the replication of the virus in BHK-21 cells and significantly reduced pathogenicity in mice as well as the ability of neuron invasion. Collectively, this study provides a new perspective for the weakening of candidate vaccine strains and the increase of virus production.

MATERIALS AND METHODS

Cells and Viruses

Baby hamster kidney cells (BHK-21) were maintained in Dulbecco's modified Eagle's medium (DMEM; Gibco), supplemented with 5% fetal bovine serum (FBS; Biological Industries, Israel) at 37°C in 5% CO_2. The Japanese encephalitis virus (JEV) strains SA14 (pACYC-SA14, U14163) and BJB were kindly provided separately by Dr. Bo Zhang (Wuhan Institute of Virology, Chinese Academy of Sciences, China) and Dr. Changwen Ke (Guangdong Center for Disease Control and Prevention).

Plasmid Construction

An infectious cDNA clone of JEV (pACYC-SA14) was used as the parental JEV strain for mutations. The mutant fragment was synthesized by the GENEWIZ company. The infectious cDNA clones pACYC-rSA14-3′UTRmut were handled using *Xba*I and *Xho*I sites to clone on the vector, pACYC. The following primers were used (5′-3′): 3′UTR -F:GGGTCATCTAGTG TGATTTAAGGTAGAAAA, 3′UTR -R: CCGACCCAGATCT TGTGTTCTTCCTCACCA, HDVr-F: ACTAGGCACAGAG CGCCGAAGTA, *Xho*I-R: ATTCAACGGGAAACGTCTTGCT CGA, *Xba*I-F: CATTTGGTTCATGTGGCTTGGAGCACGGTA, NS5-R: CTTAAATCACACTAGATGACCCTGTCTTCC.

RNA Transcription *in vitro* and Transfection

The plasmids for the infectious clone were linearized using *Xho*I, followed in purification by phenol-chloroform extraction. RNA was then transcribed from the linearized plasmids using a T7 mMESSAGE mMACHINE kit (Ambion) according to the manufacturer's instructions. BHK-21 cells in 12- well plates were transfected with *vitro*-transcribed RNA using the Lipofectamine 2000 transfection reagent (Invitrogen) according to the manufacturer's instructions.

Virus Replication in BHK-21 Cells

BHK-21 cells were infected with viruses at a multiplicity of infection (MOI) of 0.01 for 1 h and washed twice with phosphate-buffered saline (PBS) (Gibco), followed by the addition of

medium. At 24, 48, and 72 h post-infection (hpi), the medium was harvested, and virus titer was determined in the BHK-21 cells.

Virus Titer by $TCID_{50}$ Method

Confluent monolayers of BHK-21 cells on 12-well plates were infected with wild-type and recombinant JEV and harvested at different time points post-infection. BHK-21 cells on 96-well plates were infected with 10-fold serial dilutions of the viral stock. 2 days post-inoculation, the infection situation of cells was examined by immunocytochemistry. BHK-21 cells on 96-well plates infected with JEV were washed three times with PBS and fixed with pre-cold methanol for 30 min at −20°C. Then, the cells were washed three times with PBS, incubated with primary antibody NS1 (ascitic fluid secreting mouse monoclonal anti-JEV NS1 by hybridoma cells) for 1.5 h at room temperature (RT), and followed by the appropriate secondary antibody HRP (Jackson ImmunoResearch, 115-035-003) for 1 h at RT. Finally, the cells were chemically stained with preparation mixture (1mL 3-Amino-9-ethylcarbazole solution (0.4g 3-Amino-9-ethylcarbazol powder, 100 mL Dimethylformamide), 15 mL 0.1 mol NaAc, and 0.15 mL 3% H_2O_2) for 30 min at RT and the number of infected wells were then counted using a microscope. The 50% tissue culture infection dose ($TCID_{50}$) of each sample was determined using the Reed and Muench method.

Real-Time Reverse Transcription (RT)-PCR

Total RNA was extracted from cells and tissues with Total RNA Kit I R6834 (OMEGA). The obtained RNA was subjected by using Moloney murine leukemia virus reverse transcriptase (M-MLV) (Takara) for specific reverse transcription of the positive and negative strands, respectively. The JEV positive-chain RNA was reverse transcribed using the JEV-Tag-R primer, and GAPDH-R, was amplified using the tag sequence as the reverse primer and JEV-F as the forward primer. The JEV negative-chain RNA was reverse transcribed synthesis using the JEV-Tag-F primer and GAPDH-R, was amplified using the tag sequence as the forward primer and JEV-R as the forward primer. The viral RNA levels were measured using a one-step real-time reverse transcription (RT)-PCR with SYBR Premix Ex Taq kit (TaKaRa), and the following primers were used (5′-3′): Tag sequence: TTTGCTAGCTTTAGGACCTACTATATCTACCT, JEV-Tag-F primer: TTTGCTAGCTTTAGGACCTACTATATCTACCTG GAATTTGAAGAGGCGCAC JEV-Tag-R primer: TTTGCTAG CTTTAGGACCTACTATATCTACCTGTACTCCACCACGAT GGCTC, JEV-F primer: GGAATTTGAAGAGGCGCAC, JEV-R primer: GTACTCCACCACGATGGCTC, GAPDH-F: AAGGCC ATCACCATCTTCCA, GAPDH-R: GCCAGTAGACTCCACA ACATAC.

In vivo Mouse Experiment

3-week-old female BALB/c mice were obtained from the Vitalriver Company in Beijing, housed in an environmentally controlled room, and maintained on standard laboratory food and water *ad libitum* throughout the study. To assess the virulence of the JEV mutant, intraperitoneal (i.p.) injections (10^6 $TCID_{50}$ /200 μL) and intracerebral (i.c.) injections (10^2 $TCID_{50}$ /30 μL) were used. Mouse survival and body weight were monitored daily. Then, three mice were randomly selected from each group after day 7 (i.p.) or 3 (i.c.) post-injection. Mice brain tissues were harvested separately, the virus solution was infected into BHK-21 cells, and brain virus titer was measured using the $TCID_{50}$ method.

Ethics Statement and Biosafety

All animal experiments involving recombinant JEV were reviewed and approved by the Institutional Animal Care and Use Committee at South China Agricultural University (SCAU) and were carried out in accordance with the approved guidelines.

Statistical Analyses

Differences between experimental groups were determined using an unpaired *t*-test and analysis of variance (ANOVA) in GraphPad Prism software (GraphPad Software Inc.).

RESULTS

The Pathogenicity *in vivo* and Growth Rate *in vitro* Are Compared Between SA14 and BJB Viruses

To explore the pathogenicity of BJB strains isolated from humans, 3-week-old female BALB/c mice were infected with the SA14 and BJB virus strains using 10^6 $TCID_{50}$ by intraperitoneal (i.p.) injection. Mice infected with SA14 virus began to die from 9 days post-infection (dpi), and resulting in a 100% case fatality rate (**Figure 1A**). However, mice infected with BJB virus did not die, nor did they display obvious clinical symptoms or weight loss (**Figures 1A,B**).

In vitro, BHK-21 cells were infected with SA14 or BJB at a multiplicity of infection (MOI) of 0.001. Supernatants and cells were harvested at 24, 48, and 72 hpi. The viral titers were determined by $TCID_{50}$. As shown in **Figure 1C**, the growth rate of BJB was higher than SA14 virus.

The Nucleotide Mutations of 3′UTR Significantly Alter the RNA Secondary Structure of SL-IV and DB1 Structure Regions

The complete genome sequences for the SA14 and BJB virus strains were compared in order to identify nucleotides that consistently differ between these viruses. Through sequence analysis, some mutations at sites 248, 254, 258, and 307 were observed in the 3′UTR (**Table 1**). In order to explore the impact of these differences on viral characteristics, we used an infectious cDNA clone pACYC-SA14/U14163 as the parental JEV strain for engineering 3′UTR (T248C, A254G, A258G, and 307G). The parental virus SA14 (T248, A254, and A258) and recombinant virus rSA14-3′UTRmut (T248C, A254G, A258G and 307G) were rescued, biologically cloned, and sequenced in BHK-21 cells.

Subsequently, we explored whether the mutation of 3′UTR would affect the secondary structure of RNA. RNAfold was performed structural prediction of the 3′UTR mutant region. According to the prediction of two viral 3′UTR secondary

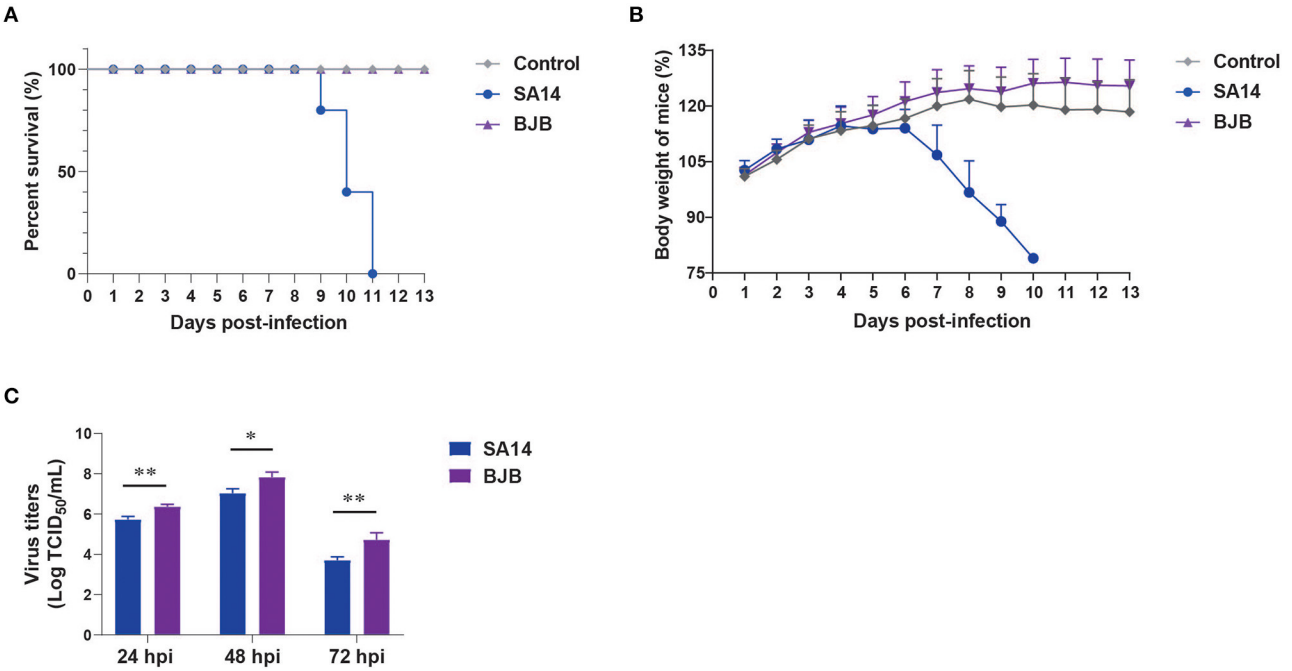

FIGURE 1 | The pathogenicity and growth rate of SA14 and BJB viruses *in vivo* and *in vitro*. The SA14 and BJB viruses were injected intraperitoneal into SPF BALB/c ($n = 5$) mice using a dose of 10^6 $TCID_{50}$/200 μL. Survival rate **(A)** and body weight **(B)** were monitored daily for 13 days. Mice that lost more than 25% of their initial weight were euthanized. **(C)** BHK-21 cells seeded in 12-well plates were infected with SA14 or BJB viruses at a multiplicity of infection (MOI) of 0.001. Culture supernatant was then collected at 24, 48, and 72 hpi and subjected to $TCID_{50}$ on BHK-21 cells. Data are shown as means ± SD ($n = 3$), and significance was calculated using an unpaired *t*-test (*$P < 0.05$; **$P < 0.01$).

TABLE 1 | Differences of nucleotide in the 3′UTR between SA14 and BJB.

	Nucleotide position[a] in the 3′UTR			
Virus	**248**	**254**	**258**	**307**
SA14	T	A	A	-[b]
BJB	C	G	G	G

[a] *The nucleotide numbering refers to the start of the 3′UTR.*
[b] *"-" is indicated for a deletion of nucleotides.*

structures, the nucleotide sites 248, 254, and 258 were located in the SL-IV structure region, and the nucleotide site 307 was located in the DB1 structure region. The mutations of T248C, A254G, and A258G reduced the apiculus ring and increased the lateral ring significantly in the SL-IV structure region of 3′UTR (**Figures 2A,B**). Moreover, the insertion of 307G added a ring to the DB1 structure region. These differences suggested that the nucleotide mutations (T248C, A254G, A258G, and 307G) in 3′UTR significantly alter the RNA secondary structure SL-IV and DB1 regions.

The Nucleotide Mutations of 3′UTR Promote Viral Growth Rate

To examine the growth properties of SA14 and rSA14-3′UTRmut *in vitro*, BHK-21 cells were infected with SA14 or rSA14-3′UTRmut at a MOI of 0.001. Supernatants and cells were harvested at 24, 48, and 72 hpi. The viral titers were determined by $TCID_{50}$. As shown in **Figure 3A**, the titer of rSA14-3′UTRmut virus was higher than the parental virus SA14 by approximately 18-fold at 72 hpi. Subsequently, replication ability was compared by detecting the level of positive- and negative-chain RNA at 24 hpi, revealing that the positive- (**Figure 3B**) and negative-chain (**Figure 3C**) RNA levels of rSA14-3′UTRmut were higher than SA14 by approximately 2.5-fold. These results showed that the nucleotide mutations (T248C, A254G, A258G, and 307G) in 3′UTR promote viral replication.

The Nucleotide Mutations of 3′UTR Reduce the Ability of Neuron Invasion

In order to investigate changes in the neural invasiveness of the virus in mice, 3-week-old female BALB/c mice were infected with the SA14 and rSA14-3′UTRmut viruses with 10^6 $TCID_{50}$ by i.p., injection. Mice infected with the SA14 virus died beginning at 11 dpi, showing signs of illness and weight loss (**Figure 4A**). Conversely, the rSA14-3′UTRmut virus was attenuated in mice, including only slight weight loss and no case fatality rate. Three mice were randomly selected from each group at 7 dpi to detect the viral burdens in the brain. The titer of SA14 in mice brains reached approximately 10^6 $TCID_{50}$. However, no virus was detected in mice brains infected with rSA14-3′UTRmut (**Figure 4A**). These results signified that the nucleotide mutations (T248C, A254G, A258G, and 307G) in 3′UTR reduce neuron invasion.

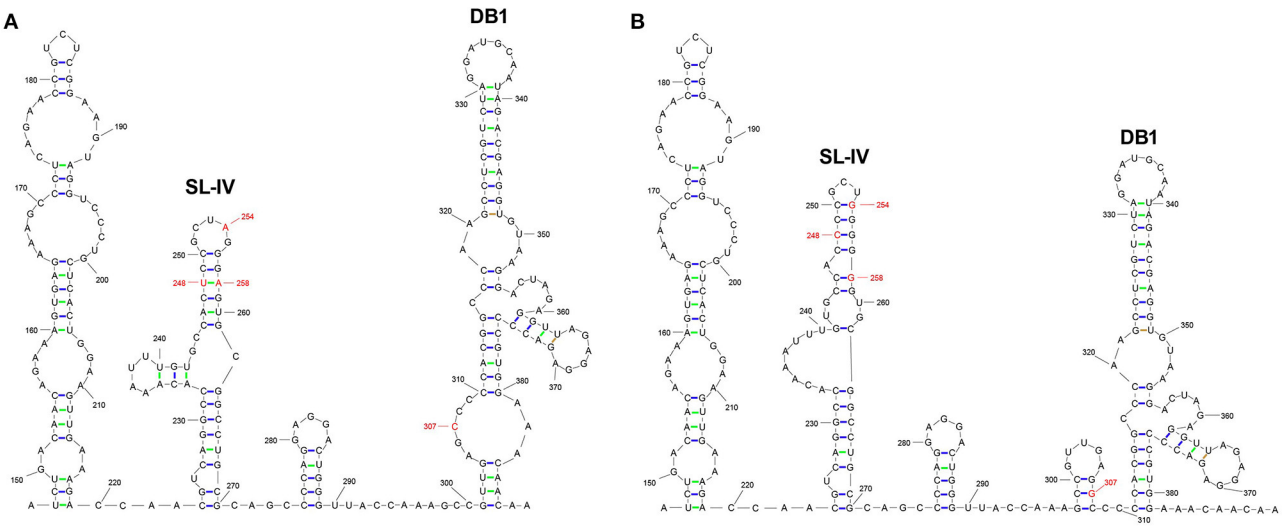

FIGURE 2 | The prediction of RNA secondary structures in 3′UTR SL-IV and DB1 structure regions. The RNA secondary structures with the location of 3′UTR differences between JEV strains SA14 **(A)** and rSA14-3′UTRmut **(B)**. RNA structure was used to predict the RNAfold (http://rna.tbi.univie.ac.at//cgi-bin/RNAWebSuite/RNAfold.cgi) in the mutated regions.

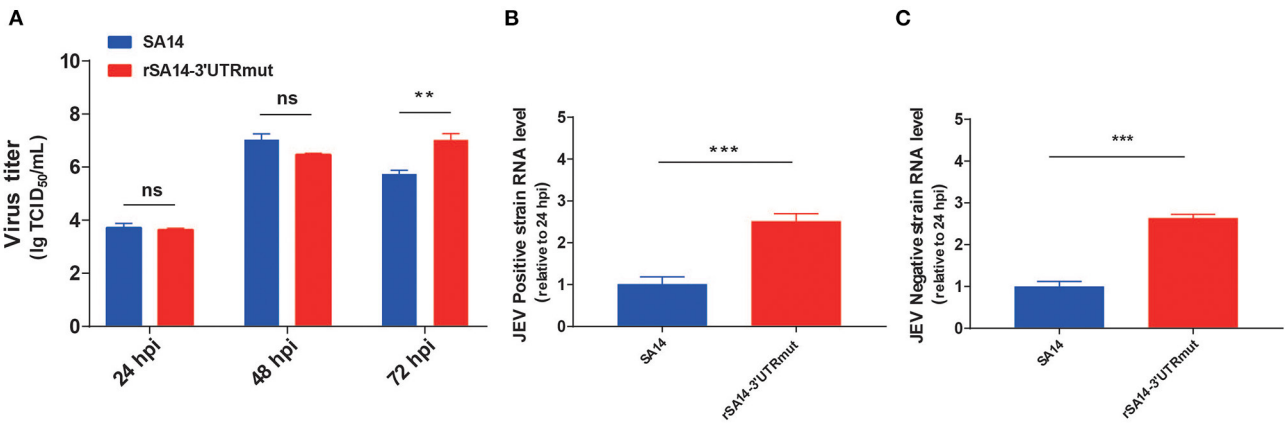

FIGURE 3 | Virus replication of SA14 and rSA14-3′UTRmut. **(A)** BHK-21 cells seeded in 12-well plates were infected with rSA14-3′UTRmut or parental virus SA14 at a MOI of 0.001. Culture supernatant was then collected at 24, 48, and 72 hpi and subjected to $TCID_{50}$ on BHK-21 cells. BHK-21 cells were infected with viruses at a MOI of 0.001, and then cells were harvested to extract total RNA. The obtained RNA was subjected to specific reverse transcription of the positive and negative strands, respectively. The viral positive strands **(B)** and negative strands **(C)** RNA levels were measured using a one-step real-time reverse transcription (RT)-PCR. Data are shown as means ± SD ($n = 3$), and significance was calculated using an unpaired *t*-test ($^{**}P < 0.01$; $^{***}P < 0.001$).

The Nucleotide Mutations of 3′UTR Decrease Pathogenicity in Mice

As the above results proved that the nucleotide mutations (T248C, A254G, A258G, and 307G) in 3′UTR are responsible for neural tropism *in vivo*, we explored the effects of neural pathogenicity in mice. 3-week-old female BALB/c mice were infected with the SA14 and rSA14-3′UTRmut viruses with 10^2 $TCID_{50}$ by intracranially (i.c.) injection. SA14 was virulent in the mice, causing severe weight loss and 100% mortality (**Figure 4B**). However, the mortality rate of the rSA14-3′UTRmut virus reached just 20%, with only a slight weight loss. Three mice were randomly selected from each group at 3 dpi to detect the viral burdens in the brain. Strikingly, the rSA14-3′UTRmut virus decreased titers in mice brains by approximately 200-fold compared with SA14 in mice brains (**Figure 4B**). These results revealed that the nucleotide mutations (T248C, A254G, A258G, and 307G) in 3′UTR decrease pathogenicity in mice.

DISCUSSION

In China, before the 1970s and 1980s, the mainstream genotype was G-III. Around 1979, the G-I strains began to be introduced into China and gradually replaced G-III as the mainstream genotype (6, 7). Most existing vaccines in the world are G-III,

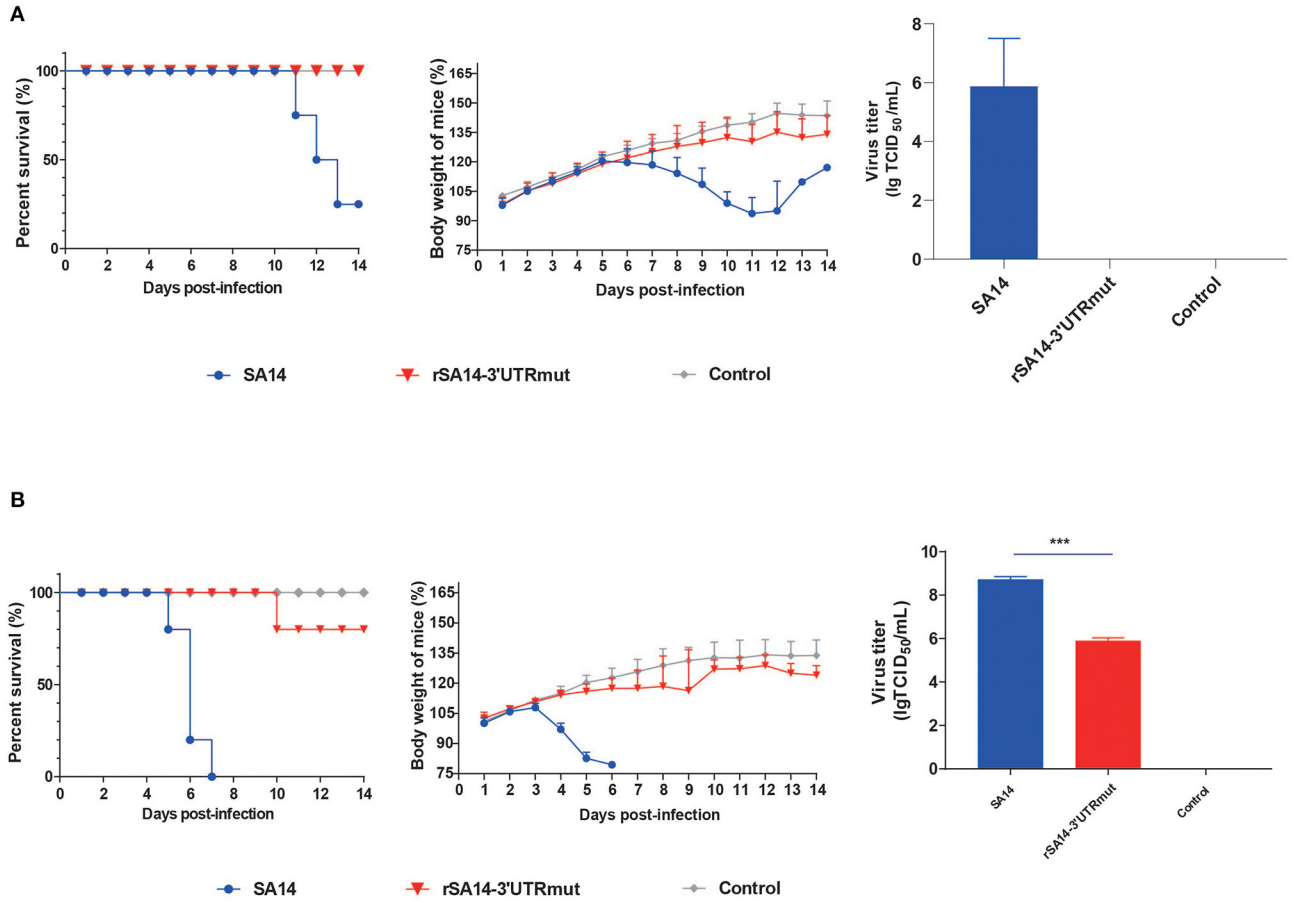

FIGURE 4 | The neuron invasion and pathogenicity in mice. **(A)** The ability of the virus to invade neurons by the intraperitoneal inoculation route in mice. The SA14 and rSA14-3′UTRmut viruses were injected intraperitoneal into SPF BALB/c mice ($n = 8$) using a dose of 10^6 $TCID_{50}$/200 μL. Survival rate and body weight were monitored daily for 14 days. Then three mice were randomly selected from each group at day seven post-injection. Mouse brain tissues were harvested separately; the virus solution was infected into BHK-21 cells, and the brain virus titer was measured. **(B)** The pathogenicity of the virus by the intracranially inoculation route in mice. The SA14 and rSA14-3′UTRmut viruses were injected intracranially into SPF BALB/c mice ($n = 8$) using a dose of 10^2 $TCID_{50}$ /30 μL. Survival rate and body weight were monitored daily for 14 days. Then three mice were randomly selected from each group at day 3 post-injection. Mouse brain tissues were harvested separately; the virus solution was infected into BHK-21 cells, and the brain virus titer was measured. Mice that lost more than 25% of their initial weight were euthanized. The percentage weight from each group and each time point are presented as means ± SD ($n = 3$) and the significance was calculated using an unpaired *t*-test ($^{***}P < 0.001$).

which can completely protect against the G-III strain. However, studies have shown that the current G-III vaccine does not provide complete protection against the G-I strain, and the G-I vaccine also does not provide complete protection against the G-III strain (8, 9). Hence, the development of a new vaccine is particularly important. However, the requirements for the new vaccine include low virulence, high replication and strong immunogenicity. In this study, we compared pathogenicity between Japanese encephalitis virus SA14 and BJB (isolated from humans in the 1970s) strains, and we found that the BJB strain was attenuated in mice, with no case fatality rate. Strinkingly, the growth rate of BJB was higher than SA14.

Based on the sequence alignment of the viral genome between SA14 and BJB virus strains, some mutations at sites 248, 254, 258, as well as an insert at site 307 were observed in 3′UTR. The untranslated regions of flavivirus play a significant role in the virus life cycle. The study of RNA elements formed in the untranslated regions of other members of the Flaviviridae family (DENV, WNV, etc.) revealed the important functions in virus replication and significant impacts on lesion and mice pathogenicity (17, 29–31).

Subsequently, we predicte RNA secondary structure using RNAfold. The analysis showed that the nucleotide sites 248, 254, and 258 are located in the SL-IV structure region, and the nucleotide mutation 307 is located in the DB1 structure region. The nucleotide mutations T248C, A254G, and A258G cause the top loop of the SL-IV structure to shrink and the side loop to increase. The insertion of 307G adds a ring to the DB1 structure.

We became curious as to whether this secondary structure change affects the biological properties of the virus. We used an

infectious cDNA clone (pACYC-SA14/U14163) as the parental JEV strain for engineering 3′UTR (T248C, A254G, A258G and 307G), and we rescued the mutant virus, which was named rSA14-3′UTRmut. The growth rate of the rSA14-3′UTRmut virus was higher than the parental virus SA14 at 72 hpi. However, there was no significant difference between 24 and 48 hpi. We speculated that the mutant virus would cause less cell lesions in the later growth period, which was conducive to the replication of the virus. The positive- and negative-chain RNA levels of rSA14-3′UTRmut were significantly higher than SA14 at 24 hpi. These results showed that the nucleotide mutations (T248C, A254G, A258G and 307G) in 3′UTR promote viral replication.

Subsequently, we investigated the changes in the neural invasiveness of the virus in mice. We found that the rSA14-3′UTRmut virus was attenuated in mice, including only slight weight loss and no case fatality rate, this compared to SA14, which caused death, illness and weight loss. The mice infected with SA14 started to die at 11 dpi not at 6 dpi as **Figure 1A**. We speculated that it might be due to individual differences, as well as differences in ambient temperature and humidity. Further, no virus was detected in mice brains infected with rSA14-3′UTRmut at 7 dpi. This indicated that the nucleotide mutations (T248C, A254G, A258G, and 307G) in 3′UTR reduce the ability of neuron invasion. We then explored the effects of the neural pathogenicity in mice. SA14 was virulent in mice, including severe weight loss and 100% mortality. However, the mortality rate of the rSA14-3′UTRmut virus reached just 20% with only slight weight loss. The rSA14-3′UTRmut virus decreased viral burdens in mice brains by approximately 200-fold compared with SA14. The neuron tropism of the rSA14-3′UTRmut virus in neuron cells *in vitro* needs further study. The reduction in mouse pathogenicity caused by changes in secondary structure may be due to SL-IV preventing Xrn1 from reducing the efficiency of viral RNA degradation and reducing sfRNA production, making the virus more susceptible to natural immunity and clearance (19, 32). The specific mechanism still needs further exploration and verification.

In summary, our study found that the SL-IV and DB1 regions of 3′UTR are essential for JEV replication, neural invasiveness, and viral pathogenicity. Our results confirm that the nucleotide mutations (T248C, A254G, A258G, and 307G) in 3′UTR can promote viral replication in BHK-21 cells, reduce the ability of neuron invasion, and decrease pathogenicity in mice. This study provides a new perspective for weakening candidate vaccine strains and increasing virus production.

DATA AVAILABILITY STATEMENT

The original contributions generated for this study are included in the article/supplementary material, further inquiries can be directed to the corresponding author/s.

ETHICS STATEMENT

All animal experiments involving recombinant JEV were reviewed and approved by the Institutional Animal Care and Use Committee at South China Agricultural University (SCAU) and were carried out in accordance with the approved guidelines.

AUTHOR CONTRIBUTIONS

JX, YZ, WQ, and ML conceived and designed the experiments and wrote the manuscript. JX, YZ, ZL, LL, QX, and JL performed the experiments. JX, YZ, ZY, CH, and WQ analyzed the results of the experiments. All authors read and approved the final manuscript.

FUNDING

This work was partially supported by The National Key Research and Development Program of China (2016YFD0500405), the National Natural Science Foundation (NSFC) of China (31272563), the Key Laboratory of Fujian Animal Diseases Control (2017), Guangdong Province Universities and Colleges Pearl River Scholar Funded Scheme (2018), and Young Scholars of Yangtze River Scholar Professor Program (2019, WQ).

REFERENCES

1. Weaver SC, Reisen WK. Present and future arboviral threats. *Antivir Res.* (2010) 85:328–45. doi: 10.1016/j.antiviral.2009.10.008
2. van den Hurk AF, Ritchie SA, Mackenzie JS. Ecology and geographical expansion of Japanese encephalitis virus. *Annu Rev Entomol.* (2009) 54:17–35. doi: 10.1146/annurev.ento.54.110807.090510
3. Vaughn DW, Hoke CH. The epidemiology of Japanese encephalitis: prospects for prevention. *Epidemiol Rev.* (1992) 14:197–221. doi: 10.1093/oxfordjournals.epirev.a036087
4. Tsarev SA, Sanders ML, Vaughn DW, Innis BL. Phylogenetic analysis suggests only one serotype of Japanese encephalitis virus. *Vaccine.* (2000) 18(Suppl. 2):36–43. doi: 10.1016/S0264-410X(00)00039-6
5. Uchil PD, Satchidanandam V. Phylogenetic analysis of Japanese encephalitis virus: envelope gene based analysis reveals a fifth genotype, geographic clustering, and multiple introductions of the virus into the Indian subcontinent. *Am J Trop Med Hyg.* (2001) 65:242–51. doi: 10.4269/ajtmh.2001.65.242
6. Han N, Adams J, Chen P, Guo Z, Zhong X, Fang W, et al. Comparison of genotypes I and III in Japanese encephalitis virus reveals distinct differences in their genetic and host diversity. *J Virol.* (2014) 88:11469–79. doi: 10.1128/JVI.02050-14
7. Schuh AJ, Ward MJ, Leigh Brown AJ, Barrett ADT. Dynamics of the emergence and establishment of a newly dominant genotype of Japanese encephalitis virus throughout Asia. *J Virol.* (2014) 88:4522–32. doi: 10.1128/JVI.02686-13
8. Fan Y, Chen J, Chen Y, Lin J, Chiou S. Reduced neutralizing antibody titer against genotype I virus in swine immunized with a live-attenuated genotype III Japanese encephalitis virus vaccine. *Vet Microbiol.* (2013) 163:248–56. doi: 10.1016/j.vetmic.2013.01.017
9. Wei J, Wang X, Zhang J, Guo S, Pang L, Shi K, et al. Partial cross-protection between Japanese encephalitis virus genotype I and III in mice. *PLoS Neglect Trop. D.* (2019) 13:e7601. doi: 10.1371/journal.pntd.0007601
10. Sampath A, Padmanabhan R. Molecular targets for flavivirus drug discovery. *Antivir Res.* (2009) 81:6–15. doi: 10.1016/j.antiviral.2008.08.004

11. Wang X, Li S, Zhu L, Nian Q, Yuan S, Gao Q, et al. Near-atomic structure of Japanese encephalitis virus reveals critical determinants of virulence and stability. *Nat Commun.* (2017) 8:14. doi: 10.1038/s41467-017-00024-6
12. Avirutnan P, Punyadee N, Noisakran S, Komoltri C, Thiemmeca S, Auethavornanan K, et al. Vascular leakage in severe dengue virus infections: a potential role for the nonstructural viral protein NS1 complement. [Comparative Study; Journal Article; Research Support, Non-U.S. Gov't]. *J Infect Dis.* (2006) 193:1078–88. doi: 10.1086/500949
13. Ye J, Zhu B, Fu ZF, Chen H, Cao S. Immune evasion strategies of flaviviruses. *Vaccine.* (2013) 31:461–71. doi: 10.1016/j.vaccine.2012.11.015
14. Ye Q, Li XF, Zhao H, Li SH, Deng YQ, Cao RY, et al. A single nucleotide mutation in NS2A of Japanese encephalitis-live vaccine virus (SA14-14-2) ablates NS1' formation contributes to attenuation. *J Gen Virol.* (2012) 93:1959–64. doi: 10.1099/vir.0.043844-0
15. Shi PY, Brinton MA, Veal JM, Zhong YY, Wilson WD. Evidence for the existence of a pseudoknot structure at the 3' terminus of the flavivirus genomic RNA. [Journal Article; Research Support, Non-U.S. Gov't; Research Support, Gov't US. P.H.S.]. *Biochemistry.* (1996) 35:4222–30. doi: 10.1021/bi952398v
16. Chang R, Hsu T, Chen Y, Liu S, Tsai Y, Lin Y, et al. Japanese encephalitis virus non-coding RNA inhibits activation of interferon by blocking nuclear translocation of interferon regulatory factor 3. *Vet Microbiol.* (2013) 166:11–21. doi: 10.1016/j.vetmic.2013.04.026
17. Roby JA, Pijlman GP, Wilusz J, Khromykh AA. Noncoding subgenomic flavivirus RNA: multiple functions in West Nile virus pathogenesis and modulation of host responses. *Viruses.* (2014) 6:404–27. doi: 10.3390/v6020404
18. Uzri D, Gehrke L. Nucleotide sequences and modifications that determine RIG-I/RNA binding and signaling activities. *J Virol.* (2009) 83:4174–84. doi: 10.1128/JVI.02449-08
19. Clarke BD, Roby JA, Slonchak A, Khromykh AA. Functional non-coding RNAs derived from the flavivirus 3′ untranslated region. *Virus Res.* (2015) 206:53–61. doi: 10.1016/j.virusres.2015.01.026
20. Alvarez DE, De Lella Ezcurra AL, Fucito S, Gamarnik AV. Role of RNA structures present at the 3′UTR of dengue virus on translation, RNA synthesis, viral replication. *Virology.* (2005) 339:200–12. doi: 10.1016/j.virol.2005.06.009
21. Göertz GP, Fros JJ, Miesen P, Vogels CBF, van der Bent ML, Geertsema C, et al. Noncoding subgenomic flavivirus RNA is processed by the mosquito RNA interference machinery determines west nile virus transmission by culex pipiens mosquitoes. *J Virol.* (2016) 90:10145–59. doi: 10.1128/JVI.00930-16
22. Tajima S, Nukui Y, Takasaki T, Kurane I. Characterization of the variable region in the 3′ non-translated region of dengue type 1 virus. *J Gen Virol.* (2007) 88:2214–22. doi: 10.1099/vir.0.82661-0
23. Tumban E, Mitzel DN, Maes NE, Hanson CT, Whitehead SS, Hanley KA. Replacement of the 3' untranslated variable region of mosquito-borne dengue virus with that of tick-borne Langat virus does not alter vector specificity. *J Gen Virol.* (2011) 92:841–8. doi: 10.1099/vir.0.026997-0
24. Yun S, Choi Y, Song B, Lee Y. 3′ cis-Acting elements that contribute to the competence efficiency of japanese encephalitis virus genome replication: functional importance of sequence duplications, deletions, substitutions. *J Virol.* (2009) 83:7909–30. doi: 10.1128/JVI.02541-08
25. Cumberworth SL, Clark JJ, Kohl A, Donald CL. Inhibition of type I interferon induction and signalling by mosquito-borne flaviviruses. [Journal Article; Review; Research Support, Non-U.S. Gov't]. *Cell Microbiol.* (2017) 19:e12737. doi: 10.1111/cmi.12737
26. Moon SL, Anderson JR, Kumagai Y, Wilusz CJ, Akira S, Khromykh AA, et al. A noncoding RNA produced by arthropod-borne flaviviruses inhibits the cellular exoribonuclease XRN1 and alters host mRNA stability. *RNA.* (2012) 18:2029–40. doi: 10.1261/rna.034330.112
27. Schuessler A, Funk A, Lazear HM, Cooper DA, Torres S, Daffis S, et al. West nile virus noncoding subgenomic RNA contributes to viral evasion of the type i Interferon-Mediated antiviral response. *J Virol.* (2012) 86:5708–18. doi: 10.1128/JVI.00207-12
28. Men R, Bray M, Clark D, Chanock RM, Lai CJ. Dengue type 4 virus mutants containing deletions in the 3′ noncoding region of the RNA genome: analysis of growth restriction in cell culture and altered viremia pattern and immunogenicity in rhesus monkeys. *J Virol.* (1996) 70:3930–7. doi: 10.1128/jvi.70.6.3930-3937.1996
29. de Borba L, Villordo SM, Marsico FL, Carballeda JM, Filomatori CV, Gebhard LG. et al. RNA structure duplication in the dengue virus 3′ UTR: redundancy or host specificity? *mBio.* (2019) 10:e2506–18. doi: 10.1128/mBio.02506-18
30. Ng WC, Soto-Acosta R, Bradrick SS, Garcia-Blanco MA, Ooi EE. The 5' and 3' untranslated regions of the flaviviral genome. *Viruses.* (2017) 9:137. doi: 10.3390/v9060137
31. Villordo SM, Carballeda JM, Filomatori CV, Gamarnik AV. RNA structure duplications and flavivirus host adaptation. *Trends Microbiol.* (2016) 24:270–83. doi: 10.1016/j.tim.2016.01.002
32. Funk A, Truong K, Nagasaki T, Torres S, Floden N, Balmori Melian E, et al. RNA structures required for production of subgenomic flavivirus RNA. *J Virol.* (2010) 84:11407–17. doi: 10.1128/JVI.01159-10

Conflict of Interest: The authors declare that the research was conducted in the absence of any commercial or financial relationships that could be construed as a potential conflict of interest.

frontiers in Veterinary Science

ORIGINAL RESEARCH
published: 29 September 2021
doi: 10.3389/fvets.2021.696568

Risk Evaluation of Pathogenic Intestinal Protozoa Infection Among Laboratory Macaques, Animal Facility Workers, and Nearby Villagers From One Health Perspective

Jian Li[1,2], *Yijing Ren*[3], *Haiying Chen*[1], *Weiyi Huang*[3], *Xinyu Feng*[4,5,6,7,8,9,10,11]* *and Wei Hu*[2,4,5,6,7,8,11]*

[1] Department of Pathogen Biology, Basic Medical College, Guangxi Traditional Chinese Medical University, Nanning, China, [2] Department of Infectious Diseases, Huashan Hospital, State Key Laboratory of Genetic Engineering, Ministry of Education Key Laboratory for Biodiversity Science and Ecological Engineering, Ministry of Education Key Laboratory of Contemporary Anthropology, School of Life Sciences, Fudan University, Shanghai, China, [3] Department of Veterinary Preventive Medicine, College of Animal Science and Technology, Guangxi University, Nanning, China, [4] National Institute of Parasitic Diseases, Chinese Center for Disease Control and Prevention (Chinese Center for Tropical Diseases Research), Shanghai, China, [5] NHC Key Laboratory of Parasite and Vector Biology, Shanghai, China, [6] WHO Collaborating Centre for Tropical Diseases, Shanghai, China, [7] National Center for International Research on Tropical Diseases, Shanghai, China, [8] Joint Research Laboratory of Genetics and Ecology on Parasite-Host Interaction, Chinese Center for Disease Control and Prevention & Fudan University, Shanghai, China, [9] School of Global Health, Chinese Center for Tropical Diseases Research, Shanghai Jiao Tong University School of Medicine, Shanghai, China, [10] One Health Center, Shanghai Jiao Tong University-The University of Edinburgh, Shanghai, China, [11] Department of Biology, College of Life Sciences, Inner Mongolia University, Hohhot, China

OPEN ACCESS

Edited by:
Michael Kogut,
United States Department of Agriculture, United States

Reviewed by:
Manigandan Lejeune,
Cornell University, United States
Faham Khamesipour,
Shahid Beheshti University of Medical Sciences, Iran

***Correspondence:**
Xinyu Feng
fengxinyu2013@163.com
Wei Hu
huw@fudan.edu.cn

Specialty section:
This article was submitted to Veterinary Infectious Diseases, a section of the journal Frontiers in Veterinary Science

Received: 08 May 2021
Accepted: 25 August 2021
Published: 29 September 2021

Citation:
Li J, Ren Y, Chen H, Huang W, Feng X and Hu W (2021) Risk Evaluation of Pathogenic Intestinal Protozoa Infection Among Laboratory Macaques, Animal Facility Workers, and Nearby Villagers From One Health Perspective. Front. Vet. Sci. 8:696568. doi: 10.3389/fvets.2021.696568

Background: Previous epidemiological studies have confirmed non-human primates (NHPs) as reservoirs for *Cryptosporidium* spp. , *Giardia intestinalis*, and *Enterocytozoon bieneusi*. It highlights the possibility of interspecies transmission between humans and macaques in laboratory animal facilities. This study aimed to investigate the prevalence of pathogenic intestinal protozoan infections in macaques and humans and to determine the risk of cross-species transmission from One Health view.

Materials and Methods: A total of 360 fecal samples, including 310 from the four *Macaca mulatta* groups, 25 from the facility workers in a laboratory animal facility, and 25 from the villagers nearby in Yongfu country, southeast China, were collected. Nested PCR assays were done for detecting protozoan pathogens from all the specimens. Furthermore, potential risk factors (gender, age, and direct contact) on the occurrence of intestinal protozoa infection among different sub-groups were evaluated. A phylogenetic and haplotype network analysis was conducted to examine the genetic structure and shared patterns of *E. bieneusi* and *Cyclospora cayetanensis*.

Results: The pathogenic intestinal protozoa were detected in both human and macaque fecal samples. A total of 134 (37.2%) samples were tested positive, which included 113 (36.4%) macaques, 14 (56.0%) facility workers, and 7 (28.0%) villagers, respectively. There was no significant difference in four intestinal protozoa infections between facility workers and villagers ($\chi^2 = 2.4$, $P > 0.05$). However, the positive rate of pathogenic intestinal protozoa in the facility workers,

who had direct contact with macaques, was significantly higher [odds ratio (OR) = 0.31, 95% confidence interval (CI): 0.09–1.00, $P < 0.05$).Thirty-three *ITS* genotypes of *E. bieneusi* were identified, including five known genotypes (PigEBITS7, Peru8, Henan V, D, and CM1) and six novel genotypes (MEB1–6). Seven haplotypes were identified in the network analysis from *C. cayetanensis*-positive samples. Meanwhile, a phylogenetic and haplotype analysis confirmed the presence of zoonotic subtypes in NHPs and humans.

Conclusion: The data collected from this study confirmed a high prevalence of intestinal protozoan infection in humans and macaques. These results warrant workers of such facilities and residents to limit contact with infected animals in order to minimize related health risks. The need for comprehensive strategies to mitigate the risk of zoonotic transmission, especially from a One Health perspective, is recommended.

Keywords: intestinal protozoan, *Macaca mulatta*, epidemiology, genotype, haplotype, one health

INTRODUCTION

Several pathogenic intestinal protozoa, including *Enterocytozoon bieneusi*, *Cyclospora cayetanensis*, *Cryptosporidium* spp., and *Giardia intestinalis*, are the causative agents of gastrointestinal diseases with a primary clinical symptom of diarrhea in humans and animals worldwide (1, 2). Many of these pathogens can be transmitted to humans by direct contact or the ingestion of contaminated food and water and are therefore usually defined as foodborne or waterborne parasites (3–5). Elders, children, and immunocompromised individuals are more susceptible to these pathogenic intestinal protozoa (6–8).

The application of molecular tools to identify species, genotypes, and sub-genotypes of the intestinal protozoa has dramatically improved their classification, transmission, and virulence. For example, the *ITS2* gene-based identification of the genotypes facilitates the taxonomy of *E. bieneusi* and identified potential zoonotic species (9, 10). Similarly, employing *Giardia duodenalis* genes (genetic loci), only the assemblages A and B of *Giardia* spp. were found to be zoonotic (4). Furthermore, the *60-kDa glycoprotein* (*gp60*) was used in subtyping the *Cryptosporidium* spp., which helps to identify the hyper-transmissible IIaA15G2R1 subtype in *Cryptosporidium parvum* and the virulent IbA10G2 subtype in *Cryptosporidium hominis* (11). With the increased usage and the integration of molecular tools, an improved understanding of zoonotic transmission will aid research and prevent infection in the future.

The studies of life sciences require many laboratory animals; among which, non-human primates (NHPs) are the essential living experimental animals by similarity in their physiological characteristics to humans (12). China has become a significant supplier of NHPs since the 1970s after India banned their export. More than 39 commercial NHP facilities have been established, mainly raising cynomolgus macaques (*Macaca fascicularis*) and rhesus macaques (*Macaca mulatta*). Therefore, there is a risk of interspecies transmission of pathogens between humans and macaques. For example, macacine herpesvirus 1 (MaHV1; B virus) can lead to fatal encephalitis in humans if they encounter animal-related exposures such as being bitten or scratched by an infected macaque monkey (13). Recently, a simian malaria parasite, *Plasmodium cynomolgi*, has made the jump to infect humans and become zoonotic (14) naturally. In the context of the COVID-19 pandemic, One Health provides a unique perspective and primary care on the health of humans and the health of animals and closely connected our shared environment (14). The present study was conducted to detect and characterize intestinal protozoa (*E. bieneusi*, *Cyclospora* spp., *Cryptosporidium* spp., and *G. intestinalis*) in rhesus macaques, facility workers, and residents in nearby villages in order to better inform the potential health risk for both human and animal, which would have great public health significance.

MATERIALS AND METHODS

Ethics Statement

This study was conducted following the Regulations for the Administration of Laboratory Animal in China. The research protocol was reviewed and approved by the Ethics Committee of Fudan University. Before the sampling, appropriate permission was obtained from the director of animals and properties.

Sample Collection

The commercial laboratory animal facility is located in Guangxi Autonomous Region in China. Mountains surround it on three sides, and a village called Qinmu is next to the fourth side. The farmhouse contained 24 door-to-door independent feeding rooms in two rows. The separate rooms are about 15 m^2 with an iron mesh of about 1 m above the ground. The facility was established in 2001, where over 5,000 animals were reared at the time of sampling.

The macaque fecal samples, taken from a total of 310 rhesus macaques (*M. mulatta*) in August 2015, were divided into four groups according to rearing mode and defined as follows: (1) the breeding macaques (BreM) group contained mainly sexually mature females. (2) The fattening macaques (FatM) group included monkeys of 6 months−2 years old. (3) The teenage macaques (TeeM) were composed of monkeys of 2–3.5 years of age. They were primary commercial monkeys. (4) The adult male macaque group (AduM) includes male aged over 3.5 years

old. A single fresh fecal sample was collected from each macaque immediately following the defecation in a labeled and sterile fecal container. Additionally, 25 stool samples were collected from the workers in the facility, and 25 stools samples were from the villagers in Qinmu country. Each piece (about 10 g) was collected into a plastic container and labeled. The samples were stored in 2.5% (*w*/*v*) potassium dichromate at 4°C before DNA extraction.

DNA Extraction and PCR Amplification

Approximately 200 mg/ml of each sample was used for the extraction of parasite genomic DNA using E.Z.N.A.R® Stool DNA Kit (Omega Biotek Inc., Norcross, GA, USA), according to the manufacturer's instructions. The extracted DNA samples were stored at −20°C until PCR amplification.

The nested PCR assay targeting the sequence of the *ITS* rRNA gene was used to amplify *C. cayetanensis* from specimens. The specific primer pairs were designed as described by Sulaiman et al. (15). The genotypes were named based on an established nomenclature system (9). A *C. cayetanensis*-specific nested PCR of the *SSU* rRNA gene was performed on macaque samples as previously published (16). Nested PCR assay was also done for detecting *Cryptosporidium* spp. and *G. intestinalis* by amplifying *SSU* rRNA (17) and the *SSU* rRNA gene (18), respectively.

All the secondary PCR products, which were positive and corresponding to the protozoan parasites, were directly sequenced using a set of primers used for secondary PCR after being purified. The obtained sequences were edited using DNASTAR software (www.dnastar.com/software/lasergene/) and aligned using ClustalX (http://www.clustal.org/clustal2/). The genotypes of *E. bieneusi*, acquired in the present study, were given the published name if they were identical to the known genotypes in GenBank. New genotypes were named according to the established nomenclature system based on 243 bp of the *ITS* gene region of *E. bieneusi* (9). The genotypes of *C. cayetanensis* are based on 445 bp of the *SSU rRNA* gene. The species of *Cryptosporidium* spp. and *Giardia* spp. were identified using BLAST (blast.ncbi.nlm.nih.gov/Blast.cgi) with the highest identity. The nucleotide sequences obtained in the present study have been deposited in GenBank database under the accession numbers MN890022-MN890026 (*E. bieneusi*), MN893885-MN893894 (*C. cayetanensis*), MN893902-MN893909 (*Cryptosporidium andersoni*), MN894004-MN894009 (*C. parvum*), and MN897749-MN897750 (*G. intestinalis*).

Haplotype Network Analysis and Phylogenetic Reconstruction

To visualize the genetic structure characteristics of the intestinal protozoa, we included the *E. bieneusi ITS2* sequences dataset, containing all the zoonosis genotypes and NHP genotypes (15, 19–21). We also included *C. cayetanensis* partial *SSU rRNA* sequences dataset, containing the genotypes of human and non-human primates (22–25). The multiple sequence alignment of both datasets was performed using ClustalW implemented in MEGAX (www.megasoftware.net) (26). The unique haplotypes were identified in DnaSP27 prior to the network analysis. The network reconstruction was carried out using a statistical parsimony network analysis with the connection probability set to 95%. The haplotype networks were analyzed in the TCS Networks (27), and the frequencies of specimens were displayed in PopART (28).

Phylogenetic trees were constructed using the neighbor-joining (NJ) method in MEGAX (26). Haplotypes with frequencies >1% were selected for analysis. The genotype PtEbIX (DQ885585), isolated from a dog, was used as an out-group for the construction of the phylogenetic trees of *E. bieneusi*. For the construction of phylogenetic tree of *C. cayetanensis*, the *Eimeria perforans* (EF694017), *Eimeria langebarteli* (AF311640), *Eimeria catronensis* (AF324213), and *Eimeria meleagrimitis* (AF041437) were used as out-groups. The phylogeny was tested with 1,000 bootstrap replicates, using the Kimura two-parameter model as a nucleotide substitution model and gamma distribution as rates among sites.

Statistical Analysis

Chi-square tests were used to calculate the *P*-value with odds ratios (OR) and 95% confidence intervals (CI) to determine the prevalence of intestinal protozoan infections among different groups. All statistical significance was set to a value of $P < 0.05$. GraphPad Prism (Version 8.02, GraphPad Software Inc.) was used for the analysis.

RESULTS

Prevalence of Pathogenic Intestinal Protozoa in Macaques and Humans

The overall intestinal protozoa prevalence of parasitic infection was 37.2%. There were 28.7% (89/310) of macaques, 56.0% (14/25) of facility workers, and 28.0% (7/25) of villagers infected with one or more protozoa (*E. bieneusi*, *C. cayetanensis*, *Cryptosporidium* spp., and *G. intestinalis*).

A total of 31 (8.6%) of the samples were *E. bieneusi* positive (7, 6.5% in humans; 24, 7.7% in macaque). Five known genotypes (PigEBITS7, Peru8, Henan V, D, and CM1) and six novel genotypes (MEB1–6) were found. *C. cayetanensis* was detected in 5 (10.0%) human samples and 23 (7.4%) macaque samples. The highest prevalence of *E. bieneusi* and *C. cayetanensis* was found in facility workers (**Table 1**). Three species of *Cryptosporidium* spp. were detected, which included *C. parvum* (7.5%), *C. andersoni* (5.3%), and *C. hominis* (1.4%). *C. parvum* was only found in facility workers (16.0%), but the other two species were found in the villagers (3.4% and 8.6%, respectively). The *G. intestinalis* was observed in 7.2% (26/360) of the fecal samples tested. The coinfection rate was relatively low, occurring at a rate of 36.1% (co-occurrence of *C. cayetanensis* and *G. intestinalis* accounted for 30.7%).

Factors Associated With the Prevalence of Pathogenic Intestinal Protozoa

The positive rate of pathogenic intestinal protozoa in the facility workers, who were in contact with macaques, was significantly higher than that in the villagers (OR = 0.31, 95% CI: 0.09–1.00, $P < 0.05$). However, no significant difference was detected in each kind of intestinal protozoa infection rate between the two groups (*E. bieneusi*: $\chi^2 = 2.6$, $P > 0.05$; *C. cayetanensis:* $\chi^2 = 0.9$,

TABLE 1 | Occurrence of *Enterocytozoon bieneusi*, *Cyclospora cayetanensis*, *Cryptosporidium* spp., and *Giardia duodenalis* in humans and macaques.

	Intestinal protozoa	***Enterocytozoon bieneusi***		***Cyclospora cayetanensis***	***Cryptosporidium* spp.**			***Giardia intestinalis***
	Group	**No. of positive/No. of examined (%)**	**Genotype (*n*)**	**No. of positive/No. of examined (%)**	***C. parvum* No. of positive/No. of examined (%)**	***C. andersoni* No. of positive/No. of examined (%)**	***C. hominis* No. of positive/No. of examined (%)**	**No. of positive/No. of examined (%)**
Humans	Facility worker	6/25 (24.0)	D (3), CM1 (2), MEB5(1)	4/25 (16.0)	4/25 (16.0)	0/25 (0.0)	0/25 (0.0)	2/25 (8.0)
	Villager	1/25 (4.0)	D(1)	1/25 (4.0)	0/25 (0.0)	4/25 (16.0)	0/25 (0.0)	2/25 (8.0)
	Sub-total	7/50 (6.5)		5/50 (10.0)	4/50 (8.0)	4/50 (8.0)	0/50 (0.0)	4/50 (8.0)
Macaques	Breeding	5/99 (5.1)	D (1), CM1 (3), MEB2 (1)	6/99 (6.0)	4/99 (4.0)	7/99 (7.1)	1/99 (1.0)	5/99 (5. 1)
	Fattening	10/58 (17.2)	D (1), CM1 (4), PigEBITS7 (1), MEB3 (2), MEB4 (1), MEB6 (1)	6/58 (10.3)	5/58 (8.6)	2/58 (3.4)	5/58 (8.6)	5/58 (8.6)
	Teenage	1/79 (1.3)	CM1 (1)	11/79 (13.9)	7/79 (9.0)	5/79 (6.3)	0/79 (0.0)	5/79 (6.3)
	Adult male	8/74 (10.8)	D (2), CM1 (1), Peru8 (2), Henan V (1), MEB1 (1), MEB3 (1)	0/74 (0.0)	7/74 (9.5)	1/74 (1.4)	0/74 (0.0)	7/74 (9.5)
	Sub-total	24/310 (7.7)		23/310 (7.4)	23/310 (7.4)	15/310 (4.8)	6/310 (1.9)	22/310 (7.1)
Total		31/360 (8.6)		28/360 (7.8)	27/360 (7.5)	19/360 (5.3)	6/360 (1.6)	26/360 (7.2)

$P > 0.05$; *Cryptosporidium* spp.: $\chi^2 = 0.0$, $P > 0.05$; and *G. intestinalis:* $\chi^2 = 0.0$, $P > 0.05$). Among the different groups in macaques, Pearson's chi-squared test showed no statistically significant difference between the male and female macaques (BreM vs. AduM, $\chi^2 = 0.2$, $P > 0.05$). There was a significant difference in infection rate between macaque of different age groups. Notably, the infection rate decreased with age, and the infection rate in the FatM group aged between 6 months and 2 years was almost two times higher than that in the AduM group aged above 3.5 years (48.3% vs 23.0%; OR = 0.32, 95% CI: 0.15–0.68, $P < 0.05$). Additionally, no significant difference in four intestinal protozoa infection rates was identified between different subgroups, except in TeeM ($\chi^2 = 12.3$, $P < 0.05$) (**Table 2**).

Phylogenetic Relationship and Haplotype Analysis of *E. bieneusi*

A total of 24 and 7 *ITS* sequences were obtained from the *E. bieneusi* of macaques and humans, respectively. All the sequences were trimmed to 243 bp and aligned to the reference sequences. The phylogenetic tree was reconstructed using the 10 unique haplotypes and main genotypes of *E. bieneusi* from previous studies (19, 21) (**Figure 1A**). All the haplotypes identified in this study belonged to potential zoonotic species. Twenty-five haplotypes were shown in the networks, and 10 unique haplotypes were collapsed. Three haplotypes (Hap1, Hap19, and Hap25) were detected from humans, while the Hap1 is the most common haplotype, accounting for 57.1% of the total known genotype D. A total of nine haplotypes (Hap1, Hap8, Hap9, and Hap18–24) were detected in macaques; among them, Hap19 was the most common haplotype, accounting for 37.5% of the known genotype CM1. Five unique new haplotypes were found from macaques, and one unique new haplotype was found from humans (**Supplementary Table S1**; **Figure 1B**).

Phylogenetic Relationship and Haplotype Analysis of *C. cayetanensis*

A total of 23 and 5 partial *SSU rRNA* gene sequences of *C. cayetanensis* were obtained from macaques and humans, respectively (**Figure 2A**). The phylogenetic tree was reconstructed using all the sequences after trimming, and *C. cayetanensis* from the previous studies (24) were used as the reference sequences. All the *Cyclospora* species identified in this study belonged to *C. cayetanensis* cluster, which differed from the other *Cyclospora* spp. found in the NHPs at 96% bootstrap values. Moreover, the three sub-clusters presented in the *C. cayetanensis* cluster were consistent with the results from the analysis of haplotype networks (**Figure 2A**). A total of seven haplotypes were shown in the network analysis. Four haplotypes (Hap1–4) were detected in the human samples, while five haplotypes (Hap1 and Hap4–7) were

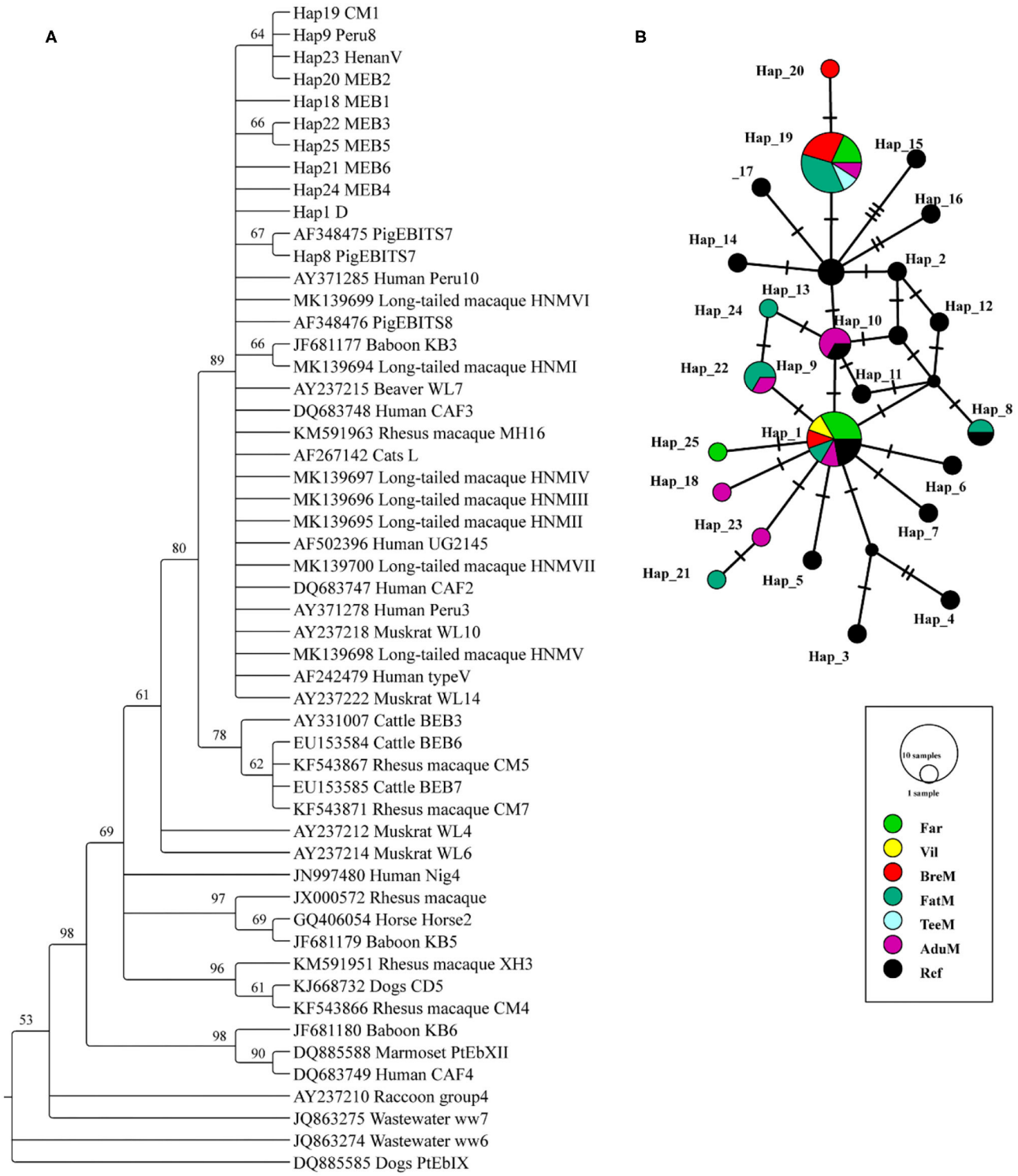

FIGURE 1 | Phylogenetic tree constructed using neighbor-joining (NJ) method and haplotype analysis network of *Enterocytozoon bieneusi* based on ~243 bp sequence of the internal transcribed spacer 2 (*ITS2*) region. **(A)** The phylogenetic analysis tree was constructed using the Kimura two-parameter model with 100 bootstrap replications. Eleven haplotypes were used in tree construction. **(B)** All the 31 sequences in this study and 19 published sequences in group 1 cluster were used to generate haplotype data. The network was constructed using TCS Network algorithm. Various colors represent different groups and the sizes of the circle represent the numbers of haplotypes. Far, facility workers; Vil, villagers; BreM, breeding macaques; FatM, fattening macaques; TeeM, teenage macaques; AduM, adult male macaques; Ref, reference published sequences.

TABLE 2 | Prevalence and risk factors for intestinal protozoan infections in humans and macaques.

Variable	Groups	No. tested	No. positive	% (95% CI)	OR (95% CI)	*P*-value
Occupation	Villagers	25	7	28.00 (10.40–45.60)		
	Workers	25	14	56.00 (36.54–75.46)	0.31 (0.09–1.00)	$P < 0.05$
Human-macaques contact	Macaques	310	113	36.45 (31.09–41.81)		
	Workers	25	14	56.00 (36.54–75.46)	0.45 (0.21–1.00)	$P > 0.05$
Macaques	BreM (vs. AduM)	99	20	20.20 (12.29–28.11)	1.18 (0.57–2.36)	$P > 0.05$
	FatM (vs. TeeM)	58	28	48.28 (35.41–61.14)	0.47 (0.23–0.95)	$P < 0.05$
	TeeM (vs. AduM)	79	24	30.38 (20.24–40.52)	0.68 (0.33–1.41)	$P > 0.05$
	AduM (vs. FatM)	74	17	22.97 (13.39–2.56)	0.32 (0.15–0.68)	$P < 0.05$

detected in macaques. Hap5 was the most common haplotype, accounting for 52.2% of all the haplotypes in macaques (**Supplementary Table S2**). Moreover, Hap1 was shared among humans, macaques, and the reference sequence from previous studies (**Figure 2B**).

DISCUSSION

Our study documented a relatively high prevalence of enteric parasites in NHPs in the Guangxi district, southwest China. Four pathogenic intestinal protozoan species were identified and analyzed. More than 36% of the macaques (in 310 tested macaque samples) in laboratory animal facilities were infected with at least one intestinal protozoa. Among them, the infection rate of *E. bieneusi* was 7.7%. This result is similar to other studies performed previously at the laboratory NHP facility or wild fields (20, 25, 29). For example, the previous studies indicated that *E. bieneusi* was the most common intestinal protozoan infection in the NHPs (29, 30), and Ye et al. revealed the prevalence rate of 18.53% for *E. bieneusi* in a laboratory animal facility in Guangxi (29). Another study of 197 fresh fecal samples obtained from eight NHP species in the Qinling Mountains revealed an *E. bieneusi* prevalence of 12.7% (20). However, we should notice that the composition of the group size and population structure may affect prevalence results.

Three species of zoonotic *Cryptosporidium* spp., including *C. parvum*, *C. hominis*, and *C. andersoni*, were detected in this study. The first two accounted for over 90% of the infections in the specified host (11). In previous studies, the most prevalent species infecting the NHPs was *C. hominis* (25), inconsistent with the results of this study. In our study, the positive rate of *Cryptosporidium* spp. was 14.4%, much higher than 0.5% in the study of Ye et al. (29), 0.7% (19/2,660) in the study of Karim et al. (31), and 3.0% (6/197) in the study of Du et al. (20). We speculated that this might be due to the long-term semi-closed environment in the facility, which led to repeated infections, and the positive rate also increased in the absence of better prevention and control strategies.

C. cayetanensis is the only species of the genus *Cyclospora* with strict host adaptation only known to infect humans, which has not been found in any of the animals studied before (2). Notably, the sequence analysis of the *SSU rRNA* gene showed the prevalence of *C. cayetanensis* in NHPs in our study. The overall prevalence of *C. cayetanensis* was 7.4% (23/310) in macaques but not detected in the AduM group. The phylogenetic analysis clearly showed that the sequences from our study differed from the previous characterization of *Cyclospora* spp. in NHPs such as *Cyclospora papionis*, *Cyclospora cercopitheci*, *Cyclospora colobi*, and *Cyclospora macacae* (16, 22, 32, 33). Considering the failure to establish the experimental *C. cayetanensis* infection in *M. mulatta* and *M. fascicularis* (34), the question regarding its host specificity is still unanswered. In contrast, one study reported the detection of *Cyclospora* sp. and *C. cayetanensis* in three *Pan troglodytes* (13.6%) and nine (9.3%) *M. fascicularis* in Europe (23). The results of haplotype network analysis in this study showed two common haplotypes found in macaques. The Hap5 was the most common haplotype (52.2%) observed in macaques only, but not in humans. Moreover, the sequence of Hap5 had only one single nucleotide difference from Hap1 at position 69 in the 423-bp partial *SSU rRNA* gene (T → C). It was speculated that this transition might result in the transmission from humans to macaques, and then the parasites circulate effectively in the population of macaques, forming their unique haplotypes. Since the Hap5 was not detected in humans, this raised a worrying question of whether this haplotype is transmissible to humans or not.

NHPs are commonly infected with *G. intestinalis*. However, understanding of its epidemiology remains incomplete and is primarily based on microscopical analysis. Giardia cysts were found in 31% of macaque samples (belonging to assemblage B, by sequencing PCR products) in wild rhesus macaques (*M. mulatta*) living in urban and semi-rural North-West India. Meanwhile, a molecular prevalence of *Giardia* spp. was recorded about 1% in bonnet macaque in another Indian study (35). We also noticed a total *G. duodenalis* infection rate of 7% among 200 long-tailed macaques' fecal samples (*M. fascicularis*) in Thailand in 2004 (36). Karim et al. (30) investigated the intestinal protozoa from 26 NHP species in China and found that the positive rate of *G. duodenum* was 2.2% (30/1,386).

Similarly, *G. intestinalis* infection was noticed in 7.1% of the macaques under our investigation, and there was no significant difference in infetion rate among different groups. Although,

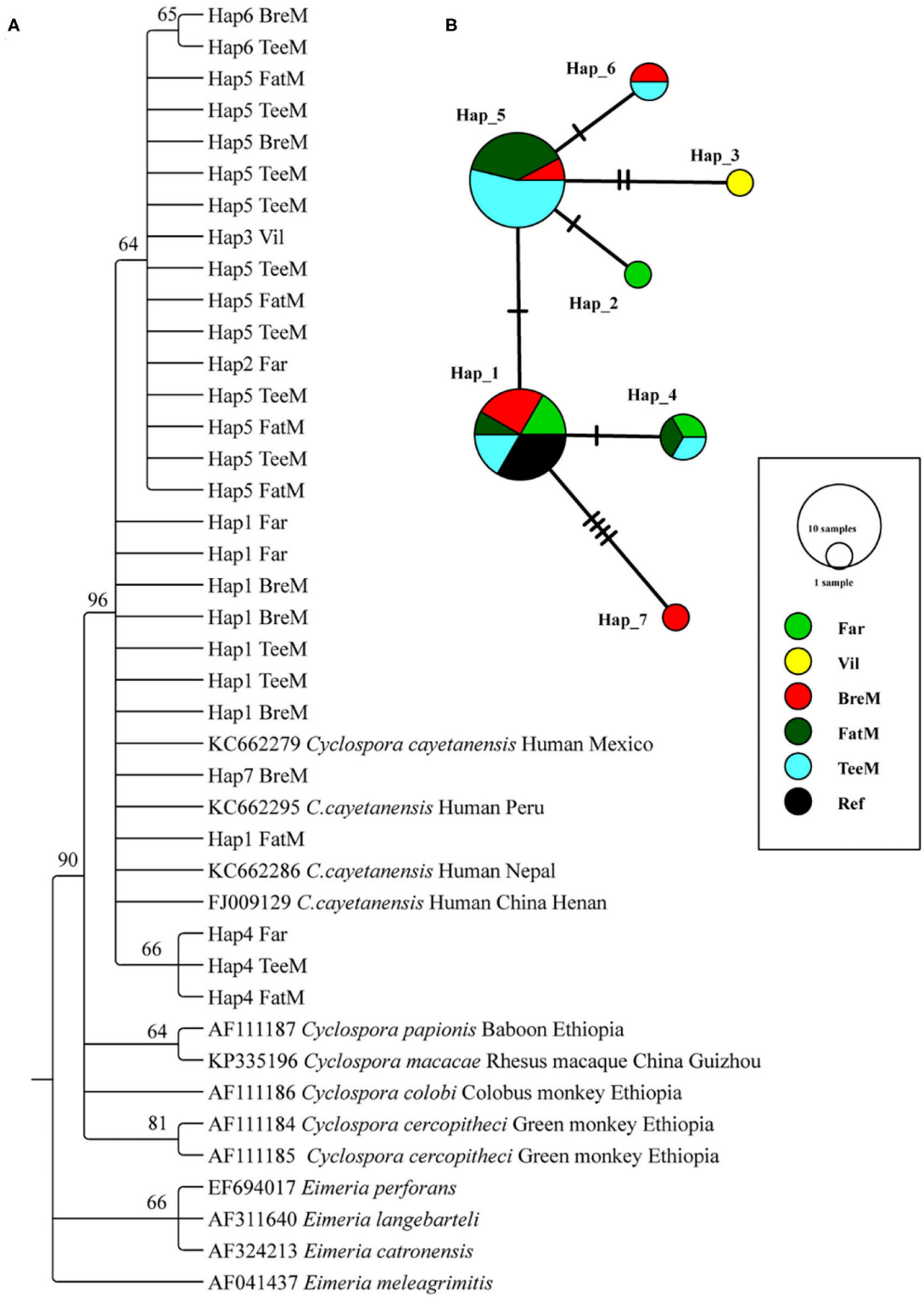

FIGURE 2 | Phylogenetic tree constructed using neighbor-joining (NJ) method and haplotype analysis network of *Cyclospora cayetanensis* based on 423 bp sequence of the partial *SSU rRNA* gene. **(A)** The phylogenetic analysis tree was constructed using the Kimura two-parameter model with 100 bootstrap replications. Eleven haplotype sequences were used in tree construction. **(B)** All the 28 sequences in this study and 4 published sequences of *C. cayetanensis* cluster were used to generate haplotype data. The network was constructed using TCS Network algorithm. Various colors represent different groups and the sizes of the circle represent the numbers of haplotypes. Far, facility worker; Vil, villager; BreM, breeding macaques; FatM, fattening macaques; TeeM, teenage macaques; AduM, adult male macaques; Ref, reference published sequences.

the percent prevalence of *Giardia* spp. varied across the above studies. However, these facts indicate that these animals may potentially contribute to the transmission of human giardiasis. The sequence analysis of the *ITS* gene identified five known genotypes (PigEBITS7, Peru8, Henan V, D, and CM1) in *E. bieneusi* in macaques, which were previously reported in humans (21). The genotype CM1 was the most prevalent genotype (9/24) identified in the stool samples of macaques. Similar results have also been reported in the 23 NHP species from five provinces of China, which considered the CM1, D, and IV as the dominant genotypes (30). All these genotypes were also the members of the group 1 cluster, thereby indicating the zoonotic potential. In our study, the most prevalent *E. bieneusi* genotype in humans was genotype D, with 57.1% (4/7) prevalence. In addition, it was worth noticing that the genotype CM1 was only identified in the facility workers but not in the villagers, which implied that this might be attributed to their direct contact with macaques.

In this study, we investigated the prevalence of intestinal protozoans and related risk factors in both humans and macaques. In two different human populations, the OR of facility workers was higher as compared to the villagers. This result was not surprising since the workers have already been exposed to several risk factors, including direct contact with animals and possible soil, water, and other environmental contamination. From this perspective, health awareness and education among the facility workers are required to prevent and control potential intestinal protozoan infections in this and other similar facilities (7, 37). In the different macaque groups, the OR in the FatM group was higher than that in the AduM group, which may be attributed to their nutrition support or high feeding density. These findings could also provide guidance for the veterinarian to pay attention to animal health caused by such kind of potential risk factors.

Understanding the pathogenic intestinal protozoa infection among humans and animals is a prerequisite for comprehending pathogen and host interactions and dynamics of interspecies dissemination. Our findings added some valuable shreds of evidence indispensable for comprehensive strategy making to reduce zoonosis. However, there are several limitations in the present study. First, the small sample number is a limitation of the present study, especially the villages in this area, decreasing the statistical credibility of finding divergence between different groups. It is necessary to repeat these tests with more samples and in more NHP facilities in future studies. Second, intestinal protozoa are among the most relevant pathogens of foodborne or waterborne disease. Environmental factors such as water supply infection test is overlooked in our study. There is a possibility that unsuspected ecological factors contribute to the risk associated with infection. One Health concept initiative needs to be well established to identify relevant environmental and socio-economic factors that may provide a unique perspective to zoonosis and reverse zoonosis interventions. Third, unfortunately, we failed to amplify the *gp60* gene, the most commonly used genetic locus for subtyping. The molecular subtyping of intestinal protozoa could offer beneficial insights into disease pathogenesis and interspecies transmission. Therefore, it is necessary to confirm the exhaustive information about the subtypes in future investigations.

CONCLUSIONS

This study revealed a relatively high prevalence of intestinal protozoa infections in macaques, facility workers, and villages nearby. The presence of potentially zoonotic intestinal protozoa, in particular the shared haplotypes, could pose health risks between wildlife and humans. Understanding protozoan epidemiology is essential for the health of animals and also for public health. Close contact with wild or captive NPHs is a risk factor for infection, as identified by various studies suggesting that we should limit contact with animal or their excreta. If exposed, we need to take hygienic precautions to mitigate the risk of zoonotic infection and appropriate strategies to control transmission adequately. The utility of One Health frameworks is recommended to characterize infection risk and to offer relevant and comprehensive control strategies in the future.

DATA AVAILABILITY STATEMENT

The datasets presented in this study can be found in online repositories. The names of the repository/repositories and accession number(s) can be found in the article/**Supplementary Material**.

ETHICS STATEMENT

The studies involving human participants were reviewed and approved by Ethics Committee of Fudan University. The patients/participants provided their written informed consent to participate in this study. The animal study was reviewed and approved by Ethics Committee of Fudan University.

AUTHOR CONTRIBUTIONS

JL, YJR, and HYC conceptualized the study. JL and YJR made significant contributions in the methodology. JL, YJR, and WYH made significant contributions in the investigation. JL and YJR were responsible for writing and preparation of the original draft. XYF and JL were responsible for reviewing

and editing the manuscript. XYF and WH supervised the study. All authors contributed to the article and approved the submitted version.

FUNDING

This study was supported by the Guangxi Traditional Chinese Medical University Scientific Research Project (XP021059); National Parasitic Resources Center (NPRC-2019-194-30); Key Technology Project of Inner Mongolia Science and Technology Department (2021GG0171).

SUPPLEMENTARY MATERIAL

The Supplementary Material for this article can be found online at: https://www.frontiersin.org/articles/10.3389/fvets.2021.696568/full#supplementary-material

REFERENCES

1. Thellier M, Breton J. Enterocytozoon bieneusi in human and animals, focus on laboratory identification and molecular epidemiology. *Parasite*. (2008) 15:349–58. doi: 10.1051/parasite/20081 53349
2. Giangaspero A, Gasser RB. Human cyclosporiasis. *Lancet Infect Dis*. (2019) 19:e226–36. doi: 10.1016/S1473-3099(18) 30789-8
3. Bouree P, Lancon A, Bisaro F, Bonnot G. Six human cyclosporiasis: with general review. *J Egypt Soc Parasitol*. (2007) 37:349–60.
4. Feng Y, Xiao L. Zoonotic potential and molecular epidemiology of Giardia species and giardiasis. *Clin Microbiol Rev*. (2011) 24:110–40. doi: 10.1128/CMR.00033-10
5. Putignani L, Menichella D. Global distribution, public health and clinical impact of the protozoan pathogen cryptosporidium. *Interdiscip Perspect Infect Dis*. (2010) 2010:753512. doi: 10.1155/2010/7 53512
6. Cegielski JP, Ortega YR, McKee S, Madden JF, Gaido L, Schwartz DA, et al. Cryptosporidium, enterocytozoon, and cyclospora infections in pediatric and adult patients with diarrhea in Tanzania. *Clin Infect Dis*. (1999) 28:314–21. doi: 10.1086/515131
7. Liu H, Shen Y, Yin J, Yuan Z, Jiang Y, Xu Y, et al. Prevalence and genetic characterization of cryptosporidium, enterocytozoon, Giardia and cyclospora in diarrheal outpatients in China. *BMC Infect Dis*. (2014) 14:25. doi: 10.1186/1471-2334-14-25
8. Maikai BV, Umoh JU, Lawal IA, Kudi AC, Ejembi CL, Xiao L. Molecular characterizations of cryptosporidium, giardia, and enterocytozoon in humans in Kaduna state, Nigeria. E*xp Parasitol*. (2012) 131:452–6. doi: 10.1016/j.exppara.2012.05.011
9. Santin M, Fayer R. Enterocytozoon bieneusi genotype nomenclature based on the internal transcribed spacer sequence: a consensus. *J Eukaryot Microbiol*. (2009) 56:34–8. doi: 10.1111/j.1550-7408.2008.00380.x
10. Li W, Cama V, Feng Y, Gilman RH, Bern C, Zhang X, et al. Population genetic analysis of enterocytozoon bieneusi in humans. *Int J Parasitol*. (2012) 42:287–93. doi: 10.1016/j.ijpara.2012.01.003
11. Feng Y, Ryan UM, Xiao L. Genetic diversity and population structure of cryptosporidium. *Trends Parasitol*. (2018) 34:997–1011. doi: 10.1016/j.pt.2018.07.009
12. Zhang X-L, Wei P, Xin-Tian H, Jia-Li L, Yong-Gang Y, Zheng Y-T. Experimental primates and non-human primate (NHP) models of human diseases in China: current status and progress. *Zoological Research*. (2014) 35:447. doi: 10.13918/j.issn.2095-8137.2014.6.447
13. Muehlenbein MP, Angelo KM, Schlagenhauf P, Chen L, Grobusch MP, Gautret P, et al. Traveller exposures to animals: a GeoSentinel analysis. *J Travel Med*. (2020) 27:taaa010. doi: 10.1093/jtm/taaa010
14. Salkeld D. One health and the COVID-19 pandemic. *Front Ecol Environ*. (2020) 18:311. doi: 10.1002/fee.2235
15. Sulaiman IM, Fayer R, Lal AA, Trout JM, Schaefer FW, Xiao LH. Molecular characterization of microsporidia indicates that wild mammals harbor host-adapted Enterocytozoon spp. as well as human-pathogenic enterocytozoon bieneusi. *Appl Environ Microb*. (2003) 69:4495–501. doi: 10.1128/AEM.69.8.4495-4501.2003
16. Li W, Kiulia NM, Mwenda JM, Nyachieo A, Taylor MB, Zhang X, et al. Cyclospora papionis, cryptosporidium hominis, and human-pathogenic enterocytozoon bieneusi in captive baboons in Kenya. *J Clin Microbiol*. (2011) 49:4326–9. doi: 10.1128/JCM.05051-11
17. Ryan U, Xiao L, Read C, Zhou L, Lal AA, Pavlasek I. Identification of novel cryptosporidium genotypes from the czech republic. *Appl Environ Microbiol*. (2003) 69:4302–7. doi: 10.1128/AEM.69.7.4302-430 7.2003
18. Hopkins RM, Meloni BP, Groth DM, Wetherall JD, Reynoldson JA, Thompson RC. Ribosomal RNA sequencing reveals differences between the genotypes of Giardia isolates recovered from humans and dogs living in the same locality. *J Parasitol*. (1997) 83:44–51. doi: 10.2307/32 84315
19. Wu J, Han JQ, Shi LQ, Zou Y, Li Z, Yang JF, et al. Prevalence, genotypes, and risk factors of enterocytozoon bieneusi in asiatic black bear (Ursus thibetanus) in yunnan province, southwestern China. *Parasitol Res*. (2018) 117:1139–45. doi: 10.1007/s00436-018-5791-0
20. Du SZ, Zhao GH, Shao JF, Fang YQ, Tian GR, Zhang LX, et al. Cryptosporidium spp., giardia intestinalis, and enterocytozoon bieneusi in captive non-human primates in qinling mountains. *Korean J Parasitol*. (2015) 53:395–402. doi: 10.3347/kjp.2015.53.4.395
21. Chen L, Zhao J, Li N, Guo Y, Feng Y, Feng Y, Xiao L. Genotypes and public health potential of enterocytozoon bieneusi and giardia duodenalis in crab-eating macaques. *Parasit Vectors*. (2019) 12:254. doi: 10.1186/s13071-019-3511-y
22. Li N, Ye J, Arrowood MJ, Ma J, Wang L, Xu H, et al. Identification and morphologic and molecular characterization of cyclospora macacae n. sp. from rhesus monkeys in China. *Parasitol Res*. (2015) 114:1811–6. doi: 10.1007/s00436-015-4367-5
23. Marangi M, Koehler AV, Zanzani SA, Manfredi MT, Brianti E, Giangaspero A, et al. Detection of cyclospora in captive chimpanzees and macaques by a quantitative PCR-based mutation scanning approach. *Parasit Vectors*. (2015) 8:274. doi: 10.1186/s13071-015-0872-8
24. Guo Y, Li N, Ortega YR, Zhang L, Roellig DM, Feng Y, et al. Population genetic characterization of cyclospora cayetanensis from discrete geographical regions. *Exp Parasitol*. (2018) 184:121–7. doi: 10.1016/j.exppara.2017.12.006
25. Li J, Dong H, Wang R, Yu F, Wu Y, Chang Y, et al. An investigation of parasitic infections and review of molecular characterization of the intestinal protozoa in nonhuman primates in China from 2009 to 2015. *Int J Parasitol Parasites Wildl*. (2017) 6:8–15. doi: 10.1016/j.ijppaw.2016.12.003
26. Thompson JD, Higgins DG, Gibson TJ. CLUSTAL W: improving the sensitivity of progressive multiple sequence alignment through sequence weighting, position-specific gap penalties and weight matrix choice. *Nucleic Acids Res*. (1994) 22:4673–80. doi: 10.1093/nar/22.22.4673
27. Clement M, Posada D, Crandall KA. TCS: a computer program to estimate gene genealogies. *Mol Ecol*. (2000) 9:1657–9. doi: 10.1046/j.1365-294x.2000.01020.x
28. Leigh JW, Bryant D. Popart: full-feature software for haplotype network construction. *Methods Ecol Evol*. (2015) 6:1110–6. doi: 10.1111/2041-210X.12410
29. Ye J, Xiao L, Li J, Huang W, Amer SE, Guo Y, et al. Occurrence of human-pathogenic enterocytozoon bieneusi, Giardia duodenalis

and cryptosporidium genotypes in laboratory macaques in Guangxi, China. *Parasitol Int*. (2014) 63:132–7. doi: 10.1016/j.parint.2013.10.007
30. Karim MR, Wang R, Dong H, Zhang L, Li J, Zhang S, et al. Genetic polymorphism and zoonotic potential of enterocytozoon bieneusi from nonhuman primates in China. *Appl Environ Microbiol*. (2014) 80:1893–8. doi: 10.1128/AEM.03845-13
31. Karim MR, Zhang S, Jian F, Li J, Zhou C, Zhang L, et al. Multilocus typing of cryptosporidium spp. and giardia duodenalis from non-human primates in China. *Int J Parasitol*. (2014) 44:1039–47. doi: 10.1016/j.ijpara.2014.07.006
32. Eberhard ML, da Silva AJ, Lilley BG, Pieniazek NJ, Morphologic and molecular characterization of new Cyclospora species from Ethiopian monkeys: C. cercopitheci sp.n., C. colobi sp.n., and C. papionis sp.n. *Emerg Infect Dis*. (1999) 5:651–8. doi: 10.3201/eid0505.990506
33. Eberhard ML, Njenga MN, DaSilva AJ, Owino D, Nace EK, Won KY, Mwenda JM. A survey for cyclospora spp. in kenyan primates, with some notes on its biology. *J Parasitol*. (2001) 87:1394–7. doi: 10.1645/0022-3395(2001)087[1394:ASFCSI]2.0.CO
34. Eberhard ML, Ortega YR, Hanes DE, Nace EK, Do RQ, Robl MG, et al. Attempts to establish experimental cyclospora cayetanensis infection in laboratory animals. *J Parasitol*. (2000) 86:577–82. doi: 10.2307/3284875
35. Kumar S, Sundararaj P, Kumara HN, Pal A, Santhosh K, Vinoth S. Prevalence of gastrointestinal parasites in bonnet macaque and possible consequences of their unmanaged relocations. *PloS ONE*. (2018) 13:e0207495. doi: 10.1371/journal.pone.0207495
36. Sricharern W, Inpankaew T, Keawmongkol S, Supanam J, Stich RW, Jittapalapong S. Molecular detection and prevalence of giardia duodenalis and cryptosporidium spp. among long-tailed macaques (macaca fascicularis) in thailand. I*nfect Genet Evol*. (2016) 40:310–4. doi: 10.1016/j.meegid.2016.02.004
37. Yang Y, Zhou Y-B, Xiao P-L, Shi Y, Chen Y, Liang S, et al. Prevalence of and risk factors associated with cryptosporidium infection in an underdeveloped rural community of southwest China. *Infect Dis Poverty*. (2017) 6:2. doi: 10.1186/s40249-016-0223-9

Conflict of Interest: The authors declare that the research was conducted in the absence of any commercial or financial relationships that could be construed as a potential conflict of interest.

Publisher's Note: All claims expressed in this article are solely those of the authors and do not necessarily represent those of their affiliated organizations, or those of the publisher, the editors and the reviewers. Any product that may be evaluated in this article, or claim that may be made by its manufacturer, is not guaranteed or endorsed by the publisher.

frontiers in Microbiology

PERSPECTIVE
published: 08 October 2021
doi: 10.3389/fmicb.2021.718546

Parallel Pandemics Illustrate the Need for One Health Solutions

*Claire Tucker[1], Anna Fagre[1], George Wittemyer[2], Tracy Webb[3], Edward Okoth Abworo[4] and Sue VandeWoude[1]**

[1] Department of Microbiology, Immunology, and Pathology, College of Veterinary Medicine and Biomedical Sciences, Colorado State University, Fort Collins, CO, United States, [2] Department of Fish, Wildlife, and Conservation Biology, Warner College of Natural Resources, Colorado State University, Fort Collins, CO, United States, [3] Department of Clinical Sciences, College of Veterinary Medicine and Biomedical Sciences, Colorado State University, Fort Collins, CO, United States, [4] Department of Animal and Human Health, International Livestock Research Institute, Nairobi, Kenya

African Swine Fever (ASF) was reported in domestic pigs in China in 2018. This highly contagious viral infection with no effective vaccine reached pandemic proportions by 2019, substantially impacting protein availability in the same region where the COVID-19 pandemic subsequently emerged. We discuss the genesis, spread, and wide-reaching impacts of this epidemic in a vital livestock species, noting parallels and potential contributions to ignition of COVID-19. We speculate about impacts of these pandemics on global public health infrastructure and suggest intervention strategies using a cost: benefit approach for low-risk, massive-impact events. We note that substantive changes in how the world reacts to potential threats will be required to overcome catastrophes driven by climate change, food insecurity, lack of surveillance infrastructure, and other gaps. A One Health approach creating collaborative processes connecting expertise in human, animal, and environmental health is essential for combating future global health crises.

Keywords: African Swine Fever, COVID-19, One Health, disease surveillance and control, public health

OPEN ACCESS

Edited by:
Jakob Zinsstag, Swiss Tropical and Public Health Institute (Swiss TPH), Switzerland

Reviewed by:
Shawn Babiuk, National Centre for Foreign Animal Disease (NCFAD), Canada
Juan C. De La Torre, The Scripps Research Institute, United States

***Correspondence:**
Sue VandeWoude
sue.vandewoude@colostate.edu

Specialty section:
This article was submitted to Infectious Diseases, a section of the journal Frontiers in Microbiology

Received: *01 June 2021*
Accepted: *19 August 2021*
Published: *08 October 2021*

Citation:
Tucker C, Fagre A, Wittemyer G, Webb T, Abworo EO and VandeWoude S (2021) Parallel Pandemics Illustrate the Need for One Health Solutions. Front. Microbiol. 12:718546. doi: 10.3389/fmicb.2021.718546

INTRODUCTION

The Centers for Disease Control and Prevention (CDC), the One Health Commission, the United States Department of Agriculture (USDA), and the National Institutes of Health (NIH) define One Health as an approach, involving health of humans, animals (domestic and wild), and the environment (ecosystem and sometimes plants), and involving a wide lens and transdisciplinary effort (Centers for Disease Control, 2020a). The One Health Initiative Task Force, convened by the American Veterinary Medical Association (AVMA), defines One Health succinctly as: "the collaborative efforts of multiple disciplines working locally, nationally, and globally, to attain optimal health for people, animals and our environment" (American Veterinary Medical Association, 2008).

The COVID-19 pandemic, resulting from transmission of the newly discovered SARS-CoV, is one of the most severe crises of the Anthropocene. Examining the reasons underlying the emergence of SARS-CoV-2, its epidemic spread, effective control measures, and unforeseen consequences of COVID-19 will occupy us for decades. Yet the COVID-19 pandemic did not arise in a vacuum. A second pandemic caused by African Swine Fever virus (ASFV) emerged in domestic swine populations in China just prior to COVID-19, spreading to Mongolia, Vietnam, and Eastern Europe by mid-2019. The ASF panzootic, while caused by a different virus in a different species, has strikingly parallel drivers to the COVID-19 pandemic, and impacts of both infections

have multiplied far beyond the original threat, overwhelming government and agency capacity to monitor and mitigate their initial spread.

Here we describe the temporal and thematic links that reveal similar patterns in these two threats and discuss factors associated with ASF that compounded the COVID-19 pandemic. Commonalities between these pandemics include concerns surrounding transmission to and from wildlife, interconnected global networks, and concomitant stresses on food supply and disease surveillance capacity. Future consequences of these pandemics include exacerbation of food insecurity and bottlenecks in disease surveillance capacity. These two pandemics underscore the need to use a One Health framework, incorporating diverse experts cooperating globally, to overcome continuing threats.

AFRICAN SWINE FEVER

With Chinese citizens consuming 28% of the global meat production, China has emerged as the primary pork-producing country, with half of the world's pigs – upward of 700 million head per year – being raised in China. While Chinese pork production has historically been managed by smaller farming units, modern intensive swine facilities have flourished over the last decade to meet growing demands (Cheng et al., 2011).

The Chinese pork market had been largely unhindered by serious disease during its expansion and intensification. However, production was decimated by the recent emergence of ASF, a viral infection endemic in domestic and wild suids that results in fever, gastrointestinal disease, and respiratory illness typically leading to death (Penrith and Vosloo, 2009; O'Neill et al., 2020). ASF has been associated with serious economic ramifications during outbreaks due to high mortality, the use of culling as for primary control, and trade restrictions with unaffected countries. Unlike diseases like classical swine fever and pseudorabies, ASF does not have an efficacious vaccine to control its impact.

The first case of ASF reported in the domestic pigs in China was in August 2018 (Wang et al., 2019). In order to halt the spread of the infection, the Chinese government mandated strict culling laws, with a recommendation to slaughter every pig within 3 km of a known infection (Staff, 2019). Despite these aggressive control measures, ASF spread to all mainland provinces. Estimates of the number of slaughtered pigs range from 150–200 million, which represents 30% of all Chinese pigs, though the true figure may approach 50–70% of the total pig population (Berthe, 2020; Good, 2021). Although the economic impacts of ASF are still being tallied, some scenarios have calculated a 1% reduction in China's GDP ($100 billion USD) (Ma et al., 2020). It is also estimated that the incursion of ASF into China killed half of breeding sow stocks, resulting in lower production of pigs (China Ministry of Agriculture). The virus has additionally spread to many Asian countries including Vietnam, Cambodia, Indonesia, and India, causing significant impacts to pork production across Asia and Europe (Mazur-Panasiuk et al., 2019), and ASF was recently reported in several feral swine in Eastern Germany (Standaert, 2020a). ASF has not however, spread globally, because of strict trade restrictions with other countries and the aforementioned culling policies. However, there is a very real threat the United States pig industry could be affected by deliberate or accidental introduction of ASF virus.

The rapid spread of ASF has been influenced by many factors, some intrinsically related to the virus and others to governance, culture, and economy (**Figure 1**). The economic trend for consolidation of pork production in intensive rearing conditions increases risk of disease, with pig density identified as the most important predictor of an ASF outbreak (Ma et al., 2020). ASF is a hardy and stable virus, reported to survive high temperatures and freezing, and can live for days on food products, fomites, and other pigs (Mazur-Panasiuk et al., 2019). The feeding of kitchen waste (including both raw and cooked pork) is a common cultural practice in China, which results in a rapid chain of transmission between animals, if the waste is contaminated with ASF virus. Pig density was identified as the most important predictor of an ASF outbreak; thus, the economic drive trend for consolidation of pork production in intensive rearing conditions has also contributed to the spread of the epidemic (Rabobank, 2020).

Unique aspects of the Chinese food economy also contributed to the spread of ASF. The Chinese pork market is largely non-automated and dependent upon "warm meat" processing (**Figure 1**). This system of slaughter and transport relies on truck-based refrigeration that delivers pork to markets within 24 h of slaughter (Standaert, 2020a), presenting challenges for disease outbreak tracing and containment. The food culture of China is based upon "wet market" distribution, meaning that fresh meat (usually domestic species, but sometimes including wildlife), seafood, and produce are offered at a specific location. Though the terms are often used interchangeably, wet markers differ from "wildlife markets," which specialize in the sale of live farmed and wild-caught wildlife (Warchol, 2004). Wet markets complicate ASF control as live pigs and pig products may be closely associated at these sites (Standaert, 2020a).

Stability of the Chinese pork market faltered as ASF decreased pork supply. Government actors and suppliers looked to other protein sources to meet demand, which rapidly induced global impacts on other commodity markets (Rabobank, 2020). The demand for alternative protein sources may have also impacted wildlife markets and production systems. The Chinese government historically encouraged wildlife trade as a form of rural economic development, enhancing through policy rather than investment both farmed wildlife production and wild harvest (Standaert, 2020b). Given its unofficial status, this sector is prone to poor regulation, and official statistics on pricing or production are scarce. While it is unclear how disruption to pork markets may have affected activity at wildlife markets, the convergence of circumstances outlined here, with first the incursion of ASF virus into China followed closely with the first detection of SARS-CoV-2 virus, suggest that acceleration of COVID-19 cases due to severe disruption of the Chinese pork market is plausible, possibly through increased congregation of vendors and consumers at the markets.

The ASF outbreak illustrates the broad need for the use a One Health approach in disease management in that a convergence

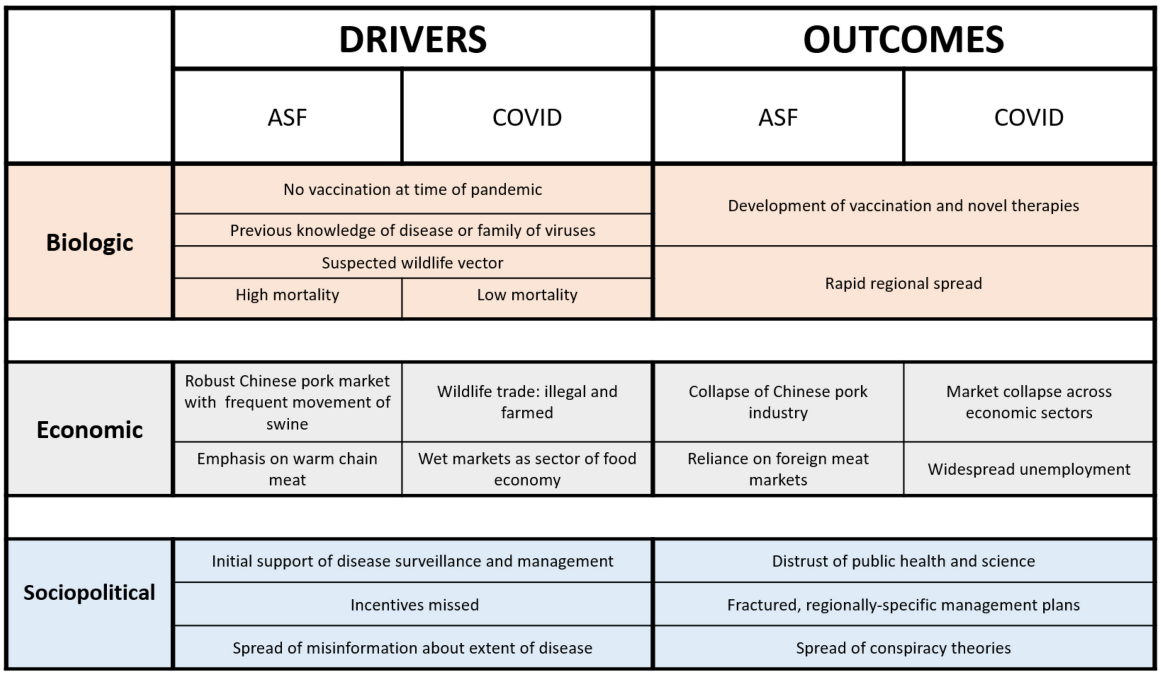

FIGURE 1 | Drivers and outcomes of ASF and COVID have animal, human, and environmental health implications. This comparative framework identifies commonalities and predictable aspects of One Health pandemics.

of animal, human, and environmental conditions resulted in its ignition and subsequent epidemic spread (**Figure 1**). Addressing the consequences of the outbreak relating to food insecurity and potential indirect amplification of SARS-CoV-2 emergence and the continuing spread of ASF across the globe will require a focused effort among basic scientists, epidemiologists, industry, and governmental representatives. Convergence of specific technologies in vaccine development in both the veterinary and human medical fields, for example, could be a solution to the control of both diseases (Vrba et al., 2020).

COVID-19

During the ASF outbreak in Chinese swine markets, a cluster of pneumonia cases were reported in Wuhan city, Hubei province, China, starting in late 2019, and reported to the World Health Organization (WHO) on December 31, 2019 (Wu et al., 2020). Initial cases were linked to Huanan Seafood Wholesale Market, causing public health officials to suspect a zoonotic origin.

Throughout the early stages of the pandemic, there was a great degree of speculation as to the evolutionary origins of SARS-CoV-2 and the animal species involved in the spillover event to humans (Zhang and Holmes, 2020; Good, 2021). Virologists and epidemiologists conducted extensive environmental and animal sampling at the Huanan seafood market to determine whether SARS-CoV-2 was present at the Huanan market in December 2019. In May 2020, the director of the Chinese Centers for Disease Control and Prevention announced that all animal samples tested for SARS-CoV-2 were negative, suggesting that the Huanan Seafood Wholesale Market was likely a point-source outbreak sourcing additional human-to-human transmission chains rather than the location where the initial animal-to-human transmission event took place. On February 24, 2020, the Chinese government instituted a ban on the trade and consumption of non-aquatic wildlife modeled on prohibitions instituted after the 2003 SARS-CoV outbreak, linked to trade in civet cats, that had since been relaxed in the face of mounting social and economic pressures (Mitchell et al., 2020). The WHO-convened global study of origins of SARS-CoV-2: China Part evaluated several possible wildlife sources for the virus, ultimately drawing no significant conclusions (WHO, 2021). Additional studies are ongoing to continue to unravel the details of the origins of SARS-CoV-2.

The spillover event that initiated the COVID-19 pandemic extended well beyond the boundaries of wet markets, moving around the globe in a way that altered the fabric of society. The scope of economic, political, and social consequences of the COVID-19 pandemic is engrained in public consciousness. However, the comparison and interdependence of the ASF outbreak and COVID-19 pandemic, has not been widely evaluated, particularly under the lens of defining One Health solutions.

DISCUSSION: COMPARISON OF PARALLEL PANDEMICS

African Swine Fever and COVID-19 are strong examples of the need for applying a One Health approach to disease control as they demonstrate the devastating results of contagious

spread of a virulent infection across a significant portion of the globe owing to animal, human, and environmental interactions. Prediction, prevention, mitigation, and restoration phases of such outbreaks require consideration of cultural, political, industrial, economic, nutritional, and psychological components of complex, overlapping societies and habitats. It is impossible to "solve" One Health pandemics unilaterally. Instead, the effort required to manage a pandemic requires resilience, unity, and foresight.

We have outlined striking similarities between the complex biological histories and complicating factors that resulted in rapid spread and stymied mitigation efforts in the coincident ASF and COVID-19 pandemics. Both viruses are multi-host pathogens, complicating our understanding of the origins and/or epidemiology of the virus within larger-scale systems. Both viruses have a suspected connection to wildlife disease spillover. ASF is enzootic in many wild boar populations at a prevalence high enough to facilitate periodic spillover into domestic swine populations, while SARS-CoV-2 is speculated to have its origins in *Rhinolophus* spp. Bats (Andersen et al., 2020; BBC News, 2020).

Both pandemics highlight the difficulties in adequately preparing for and containing an outbreak in the face of complicating social and political factors. China published an ASF contingency plan in 2015 requiring the culling of all pigs within a 3 km radius of the initial site (Wang et al., 2019). However, initiation of this plan resulted in stigmatization of reporting and adversely impacted compliance (Patton, 2020). Governmental subsidies were inadequate to support farmers with culled herds, and enforcement of transport and slaughter regulations was sometimes poor (Patton, 2020). Aggressive testing and contact tracing were critical to the early containment of COVID-19, as reflected by the discrepancy in outcomes in different regions. For example, Vietnam, Singapore, and Taiwan – having been significantly affected by the 2003 SARS outbreak and avian influenza – had developed infrastructure to deal with a highly transmissible respiratory pathogen (Institute of Medicine, 2004). As a result, these countries witnessed lower fatality rates than the United States, Italy, and other countries that implemented less aggressive diagnostic protocols and social distancing measures (Villani et al., 2020). As the second and third waves of the virus have crested, rapid detection and quarantine have been repeatedly shown as the most effective measures of control (Lotfi et al., 2020).

Controversies have arisen over implementation of control measures for human-to-human transmission of SARS-CoV-2 in the United States including quarantine time, mask-wearing, and social distancing. Similarly, there has been debate about eliminating backyard pig production systems to prevent ASF, as these operations lack appropriate biosecurity measures and are therefore a risk factor for swine epidemics and zoonotic disease emergence and spread. However, because these systems support the welfare and livelihoods of smallholder farmers, their loss would negatively impact resource-restricted communities (Huang et al., 2012). Personal freedom, mental health issues, and economic concerns are all cited as reasons to decrease protective regulations even in the face of active disease spread. Under-reporting of disease incidence and misinformation about risk factors could have contributed to the rapid growth of COVID-19 outbreaks in the United States and other countries, indicating that the challenges noted in China's official response to both ASF and COVID-19 also occurred in other countries with different governing systems (Patton, 2020; Ruinyan et al., 2020).

The ASF and COVID-19 pandemics likely had asymmetric effects on each other, many of which are difficult to quantify. As the ASF epidemic preceded COVID-19, it likely influenced the spread and severity of the burgeoning COVID-19 pandemic. As previously noted, pork shortages possibly drove dietary changes to other protein sources, potentially increasing human-to-human contact and reliance on wildlife farming that may have exposed individuals to reservoir or intermediate hosts for SARS-CoV-2 (Woonwong et al., 2020). Slaughterhouses were also found to be the location of point source outbreaks, both in China and around the world (Taylor et al., 2020). The influence of COVID-19 on the spread of ASF is not as significant but still conceivable. The pork processing industry in China is highly reliant on manual labor (Pan et al., 2020). The spread of COVID-19 sharply limited the availability of the labor force at a time when the inspection, testing, and culling of pigs demanded an increase. In addition, imports of meat in the 2019–2020 winter were unable to be promptly transported from Chinese ports due to COVID-19 transportation disruptions and labor shortages (Chandran, 2020). The impacts of the compounded economic, dietary, and psychological stressors caused by the two pandemics are difficult to quantify, and the indirect and downstream effects of the pandemics on both provisioning of public health resources and exacerbation of health inequities will be delineated by public health agencies worldwide for years to come.

The ASFV and SARS-CoV-2 outbreaks illustrate the importance of having scalable vaccination technologies available. Due to lack of an effective vaccine, ASF is extremely difficult to control or prevent; therefore, outbreak control relies on drastic measures like culling infected animals. Although highly impactful, the non-zoonotic ASFV lacked the political urgency of SARS-CoV-2. The development of a COVID-19 vaccine relied on years of coronavirus and vaccine efficacy research spurred by SARS-CoV and MERS-CoV outbreaks, unprecedented funding from private industry and government, and an acceleration of regulatory process (Ball, 2020).

Finally, genetic mutations have arisen in both SARS-CoV-2 and ASFV owing to evolutionary processes that occur when a virus circulates through large swaths of naïve populations (Chen et al., 2020; Lauring and Hodcroft, 2021). The advent of more transmissible SARS-CoV-2 variants has complicated control efforts globally. Similarly, ASFV has lingered in parts of Hong Kong and mainland China because a new variant resulting in milder disease makes detection far more difficult. While this variant is associated with decreased mortality in swine, infection results in increased abortion and long-term unthriftiness, both of which have devastating impacts on the industry (Sánchez-Cordón et al., 2018; Friends of the Global Fight, 2020).

The ASF and COVID-19 outbreaks have demonstrated that non-pharmaceutical interventions – such as quarantine and stamping out – have the most impact on whether an outbreak was contained. It has been shown that ASFV likely spread

from Georgia (isolates identified in 2007) through Russia and then through wild swine into China (Rowlands et al., 2008). If strict control measures had been implemented along that chain, the eventual epidemic in China could have been minimized. The economic benefits of those initial measures are difficult to quantify, but the concept of them is not. Similarly, the initial COVID-19 outbreak expanded quickly due to weak quarantine protocols and movement restrictions. The delay to instigate these measures – amplified by delayed reporting and misinformation – led to the global pandemic we are experiencing.

DOWNSTREAM CONSEQUENCES OF COVID-19 AND ASF

There are many consequences of the both COVID-19 and ASF outbreaks, including economic and social upheavals (**Supplementary Table S1**). A better understanding of these consequences could aid in risk reduction of future scenarios, promoting positive outcomes and resiliency. Additional emerging infectious disease outbreaks are a significant concern, as medical and diagnostic supply infrastructure is currently stressed by urgent needs of these two pandemics. In the United States, many national animal health and veterinary diagnostic laboratories assisted with SARS-CoV-2 diagnosis, limiting capacity to surveil for ongoing zoonotic and endemic diseases of animals. Changes in human behavior during the pandemic have resulted in record numbers of salmonella outbreaks (from backyard chicken rearing) and a fear of increased cases of Lyme disease (attributed to increased outdoor activities in the midst of climate patterns favoring tick populations) as well as increased risk of health consequences due to inactivity, weight gain, and mental health issues (Centers for Disease Control, 2020b; Mock, 2020). Additionally, increased death rates have been noted and are suspected to be due to "medical distancing" secondary to restricted access to health care and/or fear of SARS-CoV-2 infection at health care facilities (Mihaljevic and Farrugia, 2020).

Civil and social unrest, permanent modification of workplace and educational frameworks, and changes in protein consumption patterns are likely to be key outcomes of these two pandemics. On the positive side, investments to advance diagnostics, therapeutics, vaccines, and other solutions for infectious disease mitigation are rapidly developing, likely with impact far beyond COVID-19 and ASF (**Figure 1**).

HOW DO WE PREPARE A ONE HEALTH APPROACH FOR THE NEXT PANDEMIC?

Why has it been so hard to prepare for pandemics that have been repeatedly documented as a threat to the lives of millions of animals and humans? And, what can we do to reverse this predictable trend?

Social, cultural, and political factors underlie our seeming inability to prepare for disease outbreaks. Pandemics are exceedingly rare events relative to the number of human-animal-environmental interactions. For example, primary factors leading to SARS-CoV-2 emergence (human-animal interactions at wild-urban interface) and ASFV spread (transport of food products across international borders) are events that happen routinely around the world. Low-risk, high-impact events resulting in infection in a target population cause outbreaks that do not usually amount to epidemics. However, the frequency of pandemics will likely increase in the future. There have been at least three zoonotic coronaviruses in the last two decades. Potent drivers like globalization, expanding population, and pressure on the human-wildlife interface will increase this likelihood. Investment in detection of human illness (versus preventing the myriad of interactions with exceedingly small probabilities of ignition) would overcome the need to eliminate practices and behaviors that are vital to community identity. Development of strong local and regional surveillance networks, with incentivized data sharing and open communications, is essential to change outcomes of future spillover events.

Successful pandemic preparedness, however, must expand beyond local and regional borders. Disease is not constrained by boundaries of country or category. ASFV may not be zoonotic, but it has far-reaching impacts on the human population that involve economics, nutrition, environmental management, trade, food security, wildlife interactions, etc. Similarly, the impact of SARS-CoV-2 is far from just a human health concern and has affected nearly all aspects of human life around the globe–including airline travel, consumption trends, environmental impacts, and mental health. The multifaceted impacts of the ASF and COVID-19 pandemics strongly support the need for a One Health approach to pandemic management that incorporates a team of diverse and transdisciplinary experts to cooperatively solve complex problems (**Figure 2**).

One Health requires an inclusive process that breaks down barriers and brings together professions. Creating a funded network of One Health teams and Centers of Excellence across the United States that link to other networks such as those in Africa (African One Health University Network) and Southeast Asia (Southeast Asia One Health University Network) would provide a stronger, more coordinated means of addressing worldwide problems. Areas for investment to influence early phases of pandemics include: (1) enhancement of local surveillance efforts, with capacity for data storage and analysis to detect new infections; (2) communication strategies at local, regional, national, and global scales, incentivized by investment of resources and recognition of scientific expertise and public health management; (3) international training programs that inspire disciplinarily diverse early-career scientists collaborate; and (4) One Health legislation and investment to operationalize roadmaps that outline plans for mitigation of future pandemics. Understanding and mobilizing a One Health framework allows for the lessons and structures from one outbreak to be utilized and improved for the next one, regardless of whether the disease impacts humans or animals.

A One Health approach has immense potential to improve future outcomes not only for infectious diseases but other shared problems too. Creating a One Health framework that facilitates

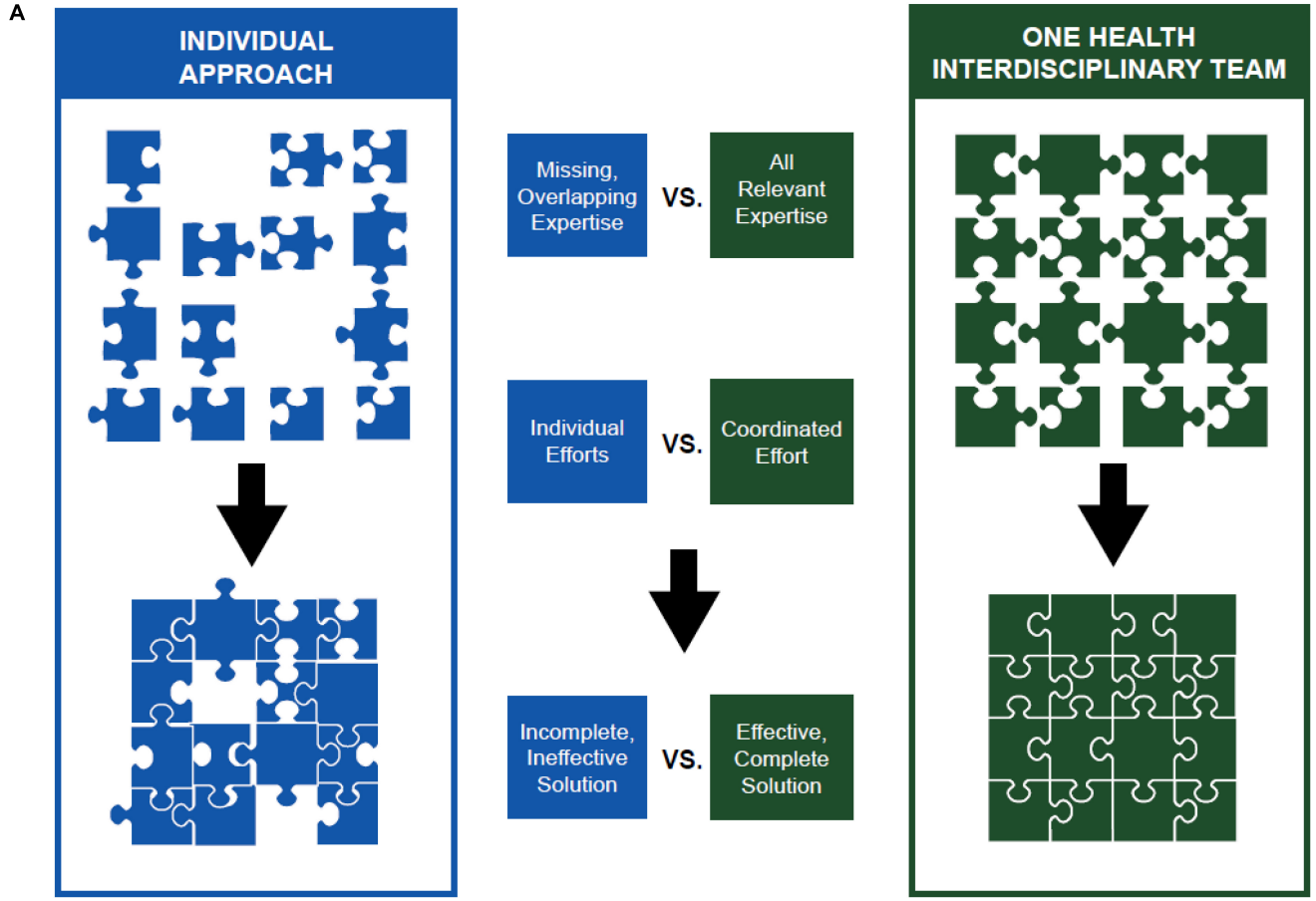

B

Local public health departments embrace One Health. In the United States, the intersections of animal, human, and environmental health are shaped at the local level. For example, the Harris County Public Health Department representing Houston, TX (the fourth largest city in the U.S.), has adopted a One Health framework. The Department hosts an annual One Health Conference, developing a network of stakeholders among human and animal health professionals. Because those connections were already fostered, Harris County Public Health was able to respond quickly and multilaterally to the COVID-19 pandemic. (Chu and Guidry, 2017)

C

Novel One Health programs support capacity development. The Field Epidemiology Training Network in Southeast Asia allows professionals with training in medical, veterinary medical, and other health sciences to gain skills in surveillance and outbreak investigation. These programs have demonstrated improved identification of disease risk and containment of the spread of disease. In Thailand, the FarmResist project conducted an epidemiologic analysis of fecal samples of animals and humans from small farms to identify patterns of resistance associated with occupational contact with animals. Additionally, Thailand has piloted a crowd-sourcing phone application called FARMER to identify zoonotic disease risk. The project is expanding and will be key to future outbreak investigations. (Iamsirithaworn et al., 2014; Centers for Disease Control and Prevention, 2021; Sudatip et al., 2021)

D

Tackling an epidemic with a One Health approach brings readiness for the next. Sub-Saharan Africa was devastated by the Ebola virus in the past decade, leading to socioeconomic instability and high mortality. When the COVID-19 pandemic threatened the region, the response was quicker and more coordinated than anticipated. Public health measures like social distancing and hand hygiene were familiar. Surveillance and diagnostic capabilities were improved. Community-based research on cultural perceptions of disease had been performed during Ebola and was leveraged to provide better care. The protracted nature and variant emergence during COVID-19 pandemic has highlighted the need to strengthen resources and coordination. (Masumbuko Claude et al., 2019; World Health Organization, 2020; Afolabi et al., 2021)

FIGURE 2 | A One Health Approach: Framework and Vignettes. **(A)** A One Health approach brings together a diverse, inclusive, multidisciplinary team of experts to address complex problems resulting in coordinated, effective, complete solutions. One Health teams incorporate individuals from all science disciplines including but not limited to data, math, computer, engineering, behavioral, social, economic, cultural, natural, applied, biomedical, agricultural, and environmental sciences. Creating a framework for One Health teams with international connections can decrease the challenges and costs associated with multiple individual efforts. **(B–D)** Vignettes representing a One Health Approach.

finding solutions to the "other shared problems" may be the key to truly successful disease outcomes. As Peter J. Hotez, a physician and vaccine developer, is quoted saying, "We must remove the conditions in which new diseases arise: poverty has more impact than any of our technical interventions. . ..Political collapse, climate change, urbanization, deforestation: these are

what's holding us back. We can develop all the vaccines and drugs we want, but unless we figure out a way to deal with these other issues, we'll always be behind" (Mckenna, 2020).

DATA AVAILABILITY STATEMENT

The original contributions presented in the study are included in the article/**Supplementary Material**, further inquiries can be directed to the corresponding author/s.

AUTHOR CONTRIBUTIONS

SV, CT, AF, TW, and GW wrote the manuscript. SV and TW conceived of the manuscript idea and discussion. GW contributed on content about wildlife trade. AF researched and wrote about COVID-19 and designed **Supplementary Figure S1**. CT researched and wrote about African Swine Fever, designed **Figure 1**, and prepared the manuscript. TW designed **Figure 2**. EA reviewed the manuscript and contributed to discussion of implications. All authors contributed extensively to the work presented in this manuscript.

ACKNOWLEDGMENTS

The authors wish to thank Maddi Funk from the Colorado State University CATS Laboratory for her help with actualizing **Figure 2**.

SUPPLEMENTARY MATERIAL

The Supplementary Material for this article can be found online at: https://www.frontiersin.org/articles/10.3389/fmicb.2021.718546/full#supplementary-material

REFERENCES

Afolabi, M. O., Folayan, M. O., Munung, N. S., Yakubu, A., Ndow, G., Jegede, A., et al. (2021). Lessons from the Ebola epidemics and their applications for COVID-19 pandemic response in sub-Saharan Africa. *Dev. World Bioeth.* 21, 25–30. doi: 10.1111/dewb.12275

American Veterinary Medical Association (2008). *AVMA Task Force Initiative Task Force. 'One Health: A New Professional Imperative'*. Schaumburg, IL: American Veterinary Medical Association.

Andersen, K. G., Rambaut, A., Lipkin, W. I., Holmes, E. C., and Garry, R. F. (2020). The proximal origin of SARS-CoV-2. *Nat. Med.* 26, 450–452. doi: 10.1038/s41591-020-0820-9

Ball, P. (2020). The lightning-fast quest for COVID vaccines - and what it means for other diseases. *Nature* 589, 16–18. doi: 10.1038/d41586-020-03626-1

BBC News (2020). *Coronavirus: Vietnam Bans Wildlife Trade Over Pandemic Risk*. Available online at: https://www.bbc.com/news/world-asia-53525954?fbclid=IwAR0sX6dzbC7i1qpF8H4rcLVhhhkCCVZORtau-Dvh-jwD2B0R_SfMfO4Bvzk (accessed August 23, 2020).

Berthe, F. (2020). The global impact of ASF. *OIE Bull* doi: 10.20506/bull.2020.1.3119

Centers for Disease Control (2020a). *One Health*. Atlanta, GA: Centers for Disease Control.

Centers for Disease Control (2020b). *Outbreak of Salmonella Infections Linked to Backyard Poultry | CDC*. Atlanta, GA: Centers for Disease Control.

Centers for Disease Control and Prevention (2018). *Crowdsourcing for Zoonotic Diseases*. Atlanta, GA: Centers for Disease Control and Prevention.

Chandran, R. (2020). *Traditional Markets Blamed for Virus Outbreak Are Lifeline for Asia's poor*. Canary Wharf: Reuters.

Chen, W., Zhao, D., He, X., Liu, R., Wang, Z., Zhang, X., et al. (2020). A seven-gene-deleted African swine fever virus is safe and effective as a live attenuated vaccine in pigs. *Sci. China Life Sci.* 63, 623–634. doi: 10.1007/s11427-020-1657-9

Cheng, H., Wang, Y., Meng, Q., Guo, J., and Wang, Y. P. (2011). Pork production system and its development in mainland china. *Int. J. Fish. Aquac.* 3, 166–174.

Chu, B., and Guidry, T. (2017). *A Local Health Department's One Health Approach to Bridging the Gap Between Veterinary and Medical Professional*. Available online at: https://www.onehealthcommission.org/documents/filelibrary/resources/Harris_Co_OH_Conf_2017_Summary_4218055B080D8.pdf

Friends of the Global Fight (2020). *How COVID-19 is Affecting the Global Response to AIDS, Tuberculosis and Malaria*. Available online at: https://www.theglobalfight.org/covid-aids-tb-malaria/ (accessed September 5, 2020).

Good, K. (2021). *Observers Watching ASF in China, Herd Size a Variable Impacting Demand for Feed and Pork. Illinois Farm Policy News*. Available online at: https://farmpolicynews.illinois.edu/2021/03/observers-watching-asf-in-china-herd-size-a-variable-impacting-demand-for-feed-and-pork/ (accessed May 28, 2021).

Huang, J., Wang, X., and Qui, H. (2012). *Small-Scale Farmers in China in the Face of Modernisation and Globalisation*. London: IIED.

Iamsirithaworn, S., Chanachai, K., and Castellan, D. (2014). Field epidemiology and one health: Thailand's experience. *Confronting Emerging Zoonoses*. 19, 191–212. doi: 10.1007/978-4-431-55120-1_9

Institute of Medicine (2004). *Learning from SARS: Preparing for the Next Disease Outbreak: Workshop Summary*. Washington, DC: National Academies Press.

Lauring, A. S., and Hodcroft, E. B. (2021). Genetic variants of SARS-CoV-2 - what do they mean? *JAMA* 325, 529–531. doi: 10.1001/jama.2020.27124

Lotfi, M., Hamblin, M. R., and Rezaei, N. (2020). COVID-19: transmission, prevention, and potential therapeutic opportunities. *Clin. Chim. Acta.* 508, 254–266. doi: 10.1016/j.cca.2020.05.044

Ma, J., Chen, H., Gao, X., Xiao, J., and Wang, H. (2020). African swine fever emerging in China: distribution characteristics and high-risk areas. *Prev. Vet. Med.* 175:104861. doi: 10.1016/j.prevetmed.2019.104861

Masumbuko Claude, K., Underschultz, J., and Hawkes, M. T. (2019). Social resistance drives persistent transmission of Ebola virus disease in Eastern Democratic Republic of Congo: a mixed-methods study. *PLoS One* 14:e0223104. doi: 10.1371/journal.pone.0223104

Mazur-Panasiuk, N., Śmudzki, J., and Woźniakowski, G. (2019). African swine fever virus – persistence in different environmental conditions and the possibility of its indirect transmission. *J. Vet. Res.* 63, 303–310. doi: 10.2478/jvetres-2019-0058

Mckenna, M. (2020). *In the Fight Against Infectious Disease, Social Changes Are the New Medicine. Scientific American*. Available online at: https://www.scientificamerican.com/article/in-the-fight-against-infectious-disease-social-changes-are-the-new-medicine/ (accessed September 5, 2020).

Mihaljevic, T., and Farrugia, G. (2020). *The Coronavirus Pandemic's Needless Deaths*. New York, NY: New York Times.

Mitchell, S. L., St. George, K., Rhoads, D. D., Butler-Wu, S. M., Dharmarha, V., McNult, P., et al. (2020). Understanding, verifying, and implementing emergency use authorization molecular diagnostics for the detection of SARS-CoV-2 RNA. *J. Clin. Microbiol.* 58, e796–e720.

Mock, J. (2020). *With More People Getting Outside This Summer, Scientists Wonder if Lyme Disease Cases Will Jump. Discover Magazine*. Available online at: https://www.discovermagazine.com/health/with-more-people-getting-outside-this-summer-scientists-wonder-if-lyme (accessed September 5, 2020).

O'Neill, X., White, A., Ruiz-Fon, F., and Gortázar, C. (2020). Modelling the transmission and persistence of African swine fever in wild boar in contrasting European scenarios. *Sci. Rep.* 10:5895.

Pan, D., Yang, J., Zhou, G., and Kong, F. (2020). The influence of COVID-19 on agricultural economy and emergency mitigation measures in China: a text mining analysis. *PLoS One* 15:e0241167. doi: 10.1371/journal.pone.0241167

Patton, D. (2020). *Before Coronavirus, China Bungled Swine Epidemic With Secrecy*. Canary Wharf: Reuters.

Penrith, M.-L., and Vosloo, W. (2009). Review of African swine fever: transmission, spread and control. *J. S. Afr. Vet. Assoc.* 80, 58–62. doi: 10.4102/jsava.v80i2.172

Rabobank (2020). *African Swine Fever Losses to Lift All Protein Boats*. Utrecht: Rabobank.

Rowlands, R. J., Michaud, V., Heath, L., Hutchings, G., Oura, C., Vosloo, W., et al. (2008). African swine fever virus isolate, Georgia 2007. *Emerg Infect Dis.* 14, 1870–1874.

Ruinyan, L., Sen, P., Bin, C., Yimeng, S., Tao, Z., Wan, Y., et al. (2020). Substantial undocumented infection facilitates the rapid dissemination of novel coronavirus (SARS-CoV-2). *Science* 368, 489–493. doi: 10.1126/science.abb3221

Sánchez-Cordón, P. J., Montoya, M., Reis, A. L., and Dixon, L. K. (2018). African swine fever: a re-emerging viral disease threatening the global pig industry. *Vet J.* 233, 41–48. doi: 10.1016/j.tvjl.2017.12.025

Staff, R. (2019). *China Has Shown 'Shortcomings' in Bid to Contain African Swine Fever*. Canary Wharf: Reuters.

Standaert, M. (2020a). *Appetite for 'Warm Meat' Drives Risk of Disease in Hong Kong and China*. London: The Guardian.

Standaert, M. (2020b). *Coronavirus Closures Reveal Vast Scale of China's Secretive Wildlife Farm Industry*. London: The Guardian.

Sudatip, D., Chasiri, K., Kritiyakan, A., Phanprasit, W., Thinphovong, C., Tiengrim, S., et al. (2021). A One Health approach to assessing occupational exposure to antimicrobial resistance in Thailand: THE FarmResist project. *PLoS One* 16:e0245250. doi: 10.1371/journal.pone.0245250

Taylor, C. A., Boulos, C., and Almond, D. (2020). Livestock plants and COVID-19 transmission. *Proc. Natl. Acad. Sci. U.S.A.* 117:31706.

Villani, L., McKee, M., Cascini, F., Ricciardi, W., and Boccia, S. (2020). Comparison of deaths rates for COVID-19 across Europe during the first wave of the COVID-19 pandemic. *Front. Public Health* 8:620416.

Vrba, S. M., Kirk, N. M., Brisse, M. E., Liang, Y., and Ly, H. (2020). Development and applications of viral vectored vaccines to combat zoonotic and emerging public health threats. *Vaccines* 8:680. doi: 10.3390/vaccines8040680

Wang, T., Sun, Y., and Qiu, H.-J. (2019). African swine fever: an unprecedented disaster and challenge to China. *Infect. Dis. Poverty* 7:111.

Warchol, G. L. (2004). The transnational illegal wildlife trade. *Crim. Justice Stud.* 17, 57–73. doi: 10.1080/0888431042000167933 4

WHO (2021). *WHO-Convened Global Study of Origins of SARS-CoV-2: China Part*. Joint WHO-China Study Team report. 2021. Geneva: WHO.

Woonwong, Y., Do Tien, D., and Thanawongnuwech, R. (2020). The future of the pig industry after the introduction of African swine fever into Asia. *Anim. Front.* 10, 30–37. doi: 10.1093/af/vfaa037

World Health Organization (2020). *Social Science Research Projects for the Ebola Response in the DRC and Neighbouring Countries*. Geneva: World Health Organization.

Wu, Y., Ho, W., Huang, Y., Jin, D.-Y., Li, S., Liu, S.-L., et al. (2020). SARS-CoV-2 is an appropriate name for the new coronavirus. *Lancet* 395, 949–950. doi: 10.1016/s0140-6736(20)30557-2

Zhang, Y. Z., and Holmes, E. C. (2020). A genomic perspective on the origin and emergence of SARS-CoV-2. *Cell* 181, 223–227. doi: 10.1016/j.cell.2020.03.035

Conflict of Interest: The authors declare that the research was conducted in the absence of any commercial or financial relationships that could be construed as a potential conflict of interest.

Publisher's Note: All claims expressed in this article are solely those of the authors and do not necessarily represent those of their affiliated organizations, or those of the publisher, the editors and the reviewers. Any product that may be evaluated in this article, or claim that may be made by its manufacturer, is not guaranteed or endorsed by the publisher.

frontiers in Veterinary Science

ORIGINAL RESEARCH
published: 20 October 2021
doi: 10.3389/fvets.2021.740472

Host-Adaptive Signatures of H3N2 Influenza Virus in Canine

Xueyun Li[1], *Jia Liu*[2], *Zengzhao Qiu*[1], *Qijun Liao*[1], *Yani Peng*[1], *Yongkun Chen*[1]* and *Yuelong Shu*[1]*

[1] School of Public Health (Shenzhen), Sun Yat-sen University, Shenzhen, China, [2] National Institute for Viral Disease Control and Prevention, Chinese Center for Disease Control and Prevention, Beijing, China

Wild aquatic birds are the primary natural reservoir of influenza A viruses (IAVs), although a small number of viruses can spill over to mammals and circulate. The focus of IAV infection in mammals was largely limited to humans and swine variants, until the emergence of H3N2 canine influenza viruses (CIVs), which provides new perspective for interspecies transmission of the virus. In this study, we captured 54 canine-adaptive signatures in H3N2 CIVs through entropy computation, which were largely concentrated in the interaction region of polymerase proteins on ribonucleoprotein complex. The receiver operating characteristic curves of these sites showed >95% accuracy in distinguishing between the hosts. Nine of the 54 canine-adaptive signatures were shared in avian–human/equine or equine–canine (PB2-82; PB1-361; PA-277; HA-81, 111, 172, 196, 222, 489), suggesting their involvement in canine adaptation. Furthermore, we found that IAVs can establish persistent transmission in lower mammals with greater ease compared to higher mammals, and 25 common adaptation signatures of H3 IAVs were observed in diverse avian–mammals comparison. There were few human-like residues in H3N2 CIVs, which suggested a low risk of human infection. Our study highlights the necessity of identifying and monitoring the emerging adaptive mutations in companion animals by enhanced surveillance and provides a basis for mammal adaptation of avian influenza viruses.

Keywords: host-adaptive signatures, IAVs, H3N2, evolution, canine

OPEN ACCESS

Edited by:
Xinyu Feng,
Chinese Center for Disease Control and Prevention, China

Reviewed by:
Yang Yang,
Inner Mongolia University, China
Yongzhang Zhu,
Shanghai Jiao Tong University, China

***Correspondence:**
Yuelong Shu
shuylong@mail.sysu.edu.cn
Yongkun Chen
chenyk8@mail.sysu.edu.cn

Specialty section:
This article was submitted to Veterinary Infectious Diseases, a section of the journal Frontiers in Veterinary Science

Received: *13 July 2021*
Accepted: *13 September 2021*
Published: *20 October 2021*

Citation:
Li X, Liu J, Qiu Z, Liao Q, Peng Y, Chen Y and Shu Y (2021) Host-Adaptive Signatures of H3N2 Influenza Virus in Canine. Front. Vet. Sci. 8:740472. doi: 10.3389/fvets.2021.740472

INTRODUCTION

Based on the surface glycoprotein hemagglutinin (HA) and neuraminidase (NA), influenza A viruses (IAVs) are classified into 18 HA subtypes and 11 NA subtypes (1). Although avian species are the natural reservoir of IAVs, mutations and genetic reassortments can facilitate sporadic infection in mammals. Because of species barriers, most IAVs infections in mammals are "dead-end" infections. On rare occasions, however, IAVs can break the species barrier and establish an independent lineage in mammalian species, as exemplified by seasonal H3N2 influenza virus. The first recorded outbreak of H3N2 influenza was caused by influenza A/Hong Kong/1968 (H3N2) virus in 1968 in Hong Kong. This virus comprised two genes from avian influenza virus (AIV) and six genes from the human influenza virus (H2N2). It was not until the early 21st century that H3N2 made another avian-to-mammal "host jump" in canines, and H3N2 and H3N8 are the two major influenza A subtypes that currently circulate in canine hosts (2, 3).

Both avian-like α-2,3–linked sialic-acid receptors and human-like α-2,6-linked sialic-acid receptors were detected in the endothelial cells of the respiratory tract and other organs of dogs (4), suggesting that they may act as "mixing vessels" for the generation of novel reassorted viruses. Indeed, except for the 2009 pandemic H1N1 and various avian influenza viruses (AIVs) were isolated from canines (5, 6), reassorted viruses between swine origin H1N1 and H3N2 canine influenza viruses (CIVs) were occurred in canines in Guangxi, China (7). The *in vitro* experiments indicated that H3 CIVs preferred to bind α-2,3–linked sialic acids ("avian-like receptors") yet replicated in primary human nasal and bronchial epithelial cells, which suggested CIVs may pose a risk of infection to humans as well (8).

H3N2 CIVs were first reported in South Korea in 2007 (3) and have since rapidly spread to China and Thailand (9, 10). They originate from avian lineages and undergo mutations that might be responsible for host adaptation (11). However, little is known regarding the amino acid substitutions in H3N2 CIVs that are related to canine adaptation. W222L in HA facilitates H3N2 CIV infection in dogs, and K576E in PB2 enhances replication ability of H3N2 CIVs in mice (12, 13). Another prevalent subtype of influenza in canine is H3N8, which predominantly circulates in America. It derived from avian-origin H3N8 equine influenza virus (EIV), presenting as an "avian–equine–canine" host shift event in influenza virus (14, 15). Despite their diverged evolution, H3N8 CIV and H3N8 EIV appeared phenotypically equivalent (16). Just as in H3N2 CIVs, mutation at 222 position of HA facilitated viral adaption from H3N8 EIV to dogs (17), indicating that HA-222 plays a crucial role in canine adaptation of influenza virus. Thus, a wide range of comparisons between sequences from multiple hosts may provide clues for molecular markers in host tropism of IAVs.

Several techniques were developed to compute the adaptive strategies of IAVs in humans. For instance, information entropy was used to identify characteristic conserved sites in human IAVs (18), and 42 human-adaptive PB2 markers were detected in the seasonal H1N1 and H3N2 viruses (19). A nonhomogeneous phylogenetic model was used to count equilibrium frequencies of amino acids in different hosts and locations, which identified 172 amino acid sites that are strongly related to the avian to human host shift (20). However, a comprehensive adaptive signature mapping of H3N2 influenza virus in mammals, especially canines, was still lacking. In this study, we rebuilt the evolution history of H3N2 CIVs and used entropy to identify mammalian- and canine-adaptive sites in H3N2 influenza viruses.

MATERIALS AND METHODS

Phylogenetic Analysis

The sequences of the individual segments of H3N2 CIVs were downloaded from the NCBI influenza database (https,//www.ncbi.nlm.nih.gov/genomes/FLU/Database/nph-select.cgi) using "full length plus" and "collapse identical sequences" as the filtering parameters (available on January 27, 2021). After Blasting in NCBI, the first 5,000 sequences of IAVs closest to CIVs were downloaded. H3 and N2 sequences were retrieved, and the sequences of internal genes of all subtypes were selected. Redundant sequences were removed using cd-hit-est before aligning with MAFFT v7.222 (21, 22). Low-quality sequences with degenerate base >5 or gap frequency of more than 20 were excluded. The phylogenetic trees were generated with maximum likelihood method and the general time-reversible substitution model using MEGA v7.0.

Protein Genome Dataset and Alignment

The protein sequences of the eight gene segments of IAVs were downloaded from NCBI influenza database. In the AIV dataset, all available internal protein sequences were downloaded except that for HA and NA, which only comprised H3N2 subtype. The sequences of canine, equine, human, and swine viruses were downloaded using H3N2/H3N8 subtype as the filtering parameter. A total of 1,131,554 protein sequences, including 207,745 from the AIV dataset, 3,992 from CIVs, 6,326 from EIVs, 879,788 from human and 33,703 from swine influenza virus (SIV) dataset, were downloaded. Target sequences <95% of the full-length and AIVs isolated from humans were excluded, and the number of sequences of each protein finally included in the analysis is shown in **Table 1**. Then, protein sequence alignments were performed with sequence alignment program.

Host-Adaptive Signature Prediction

Forty-seven avian–human signatures were computed using the formula $-\Sigma P_i \times \ln(P_i)$, as described by Chen et al. (19) based on Shannon entropy that has been used to evaluate the diversity of a system. The conservation of amino acids was measured by entropy value (X) of dominant amino acid residue in the position, which has experimentally validated cross-species association. An amino acid is defined as a host-adaptive marker if the entropy value of the dominant amino acid at the given site is (i) less than or equal to X (22) and (ii) inconsistent between the two species. The substitution at position 222 in the HA gene of H3N2 AIVs with entropy value of 0.351 was used as the threshold when screening for host-specific signatures between avian and canine/equine viruses. To compare avian and human viruses, the dominant amino acid value at position PB2-627, which is a widely reported species-associated position in various subtypes of IAVs, was selected as the threshold. The entropy value of dominant amino acid in PB2-627 is 0.147 and 0.677 in the AIVs and human influenza viruses, respectively. As applying any one value as the threshold would lead to the loss of meaningful sites or result in too many irrelevant signatures, a position harboring entropy value $\leq$0.147 and $\leq$0.677 in two-host sequence calculation, respectively, were considered the avian–human signature. The same threshold was used for avian–swine/swine–human analysis. The analysis workflow is outlined in **Figure 1**. All data were calculated using the Python software 3.7.

Entropy Evaluation, Receiver Operating Characteristic Curves

Receiver operating characteristic (ROC) curves and area under the curve with 95% confidence intervals were used to evaluate the

TABLE 1 | The number of protein sequences of target finally used in this study.

	Avian	Canine (H3N2)/(H3N8)	Equine (H3N8)	Human (H3N2)	Swine (H3N2)
PB2	22,742	236/53	175	38,958	2,501
PB1	19,871	222/50	179	40,167	2,039
PB1-F2	12,628	214/43	110	32,452	1,585
PA	12,175	236/53	159	5,930	934
HA	412 (H3N2)/1,421 (H3N8)	235/92	243	66,542	3,921
NP	23,224	252/74	177	40,586	2,589
NA	393 (H3N2)/1,063 (H3N8)	211/89	158	58,732	3,938
M1	23,858	251/189	219	51,988	3,192
M2	23,837	251/203	200	51,833	3,127
NS1	26,378	210/195	242	37,130	2,630
NS2	21,383	199/193	200	21,383	2,439
Total	189,385	2,517/1,234	2,062	445,701	28,895

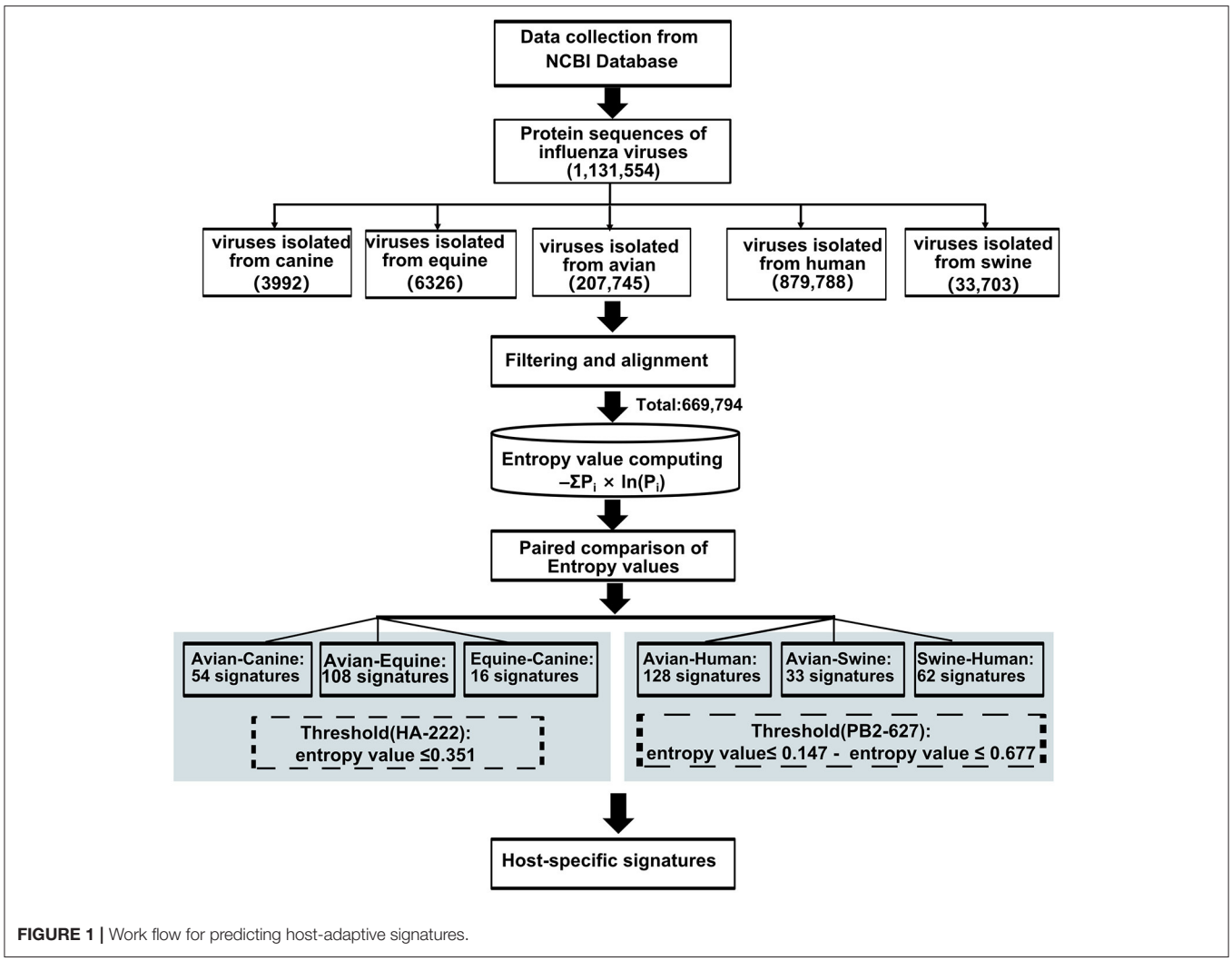

FIGURE 1 | Work flow for predicting host-adaptive signatures.

entropy model. The ROC curves were generated by the MedCalc program. The positions of canine-adaptive signatures were used to calculate true-positive pairs and false-positive pairs in AIVs and H3N2 CIV sequences dataset. The accuracy reflected the efficacy of those positions to distinguish between avian-adaptive or canine-adaptive sequences.

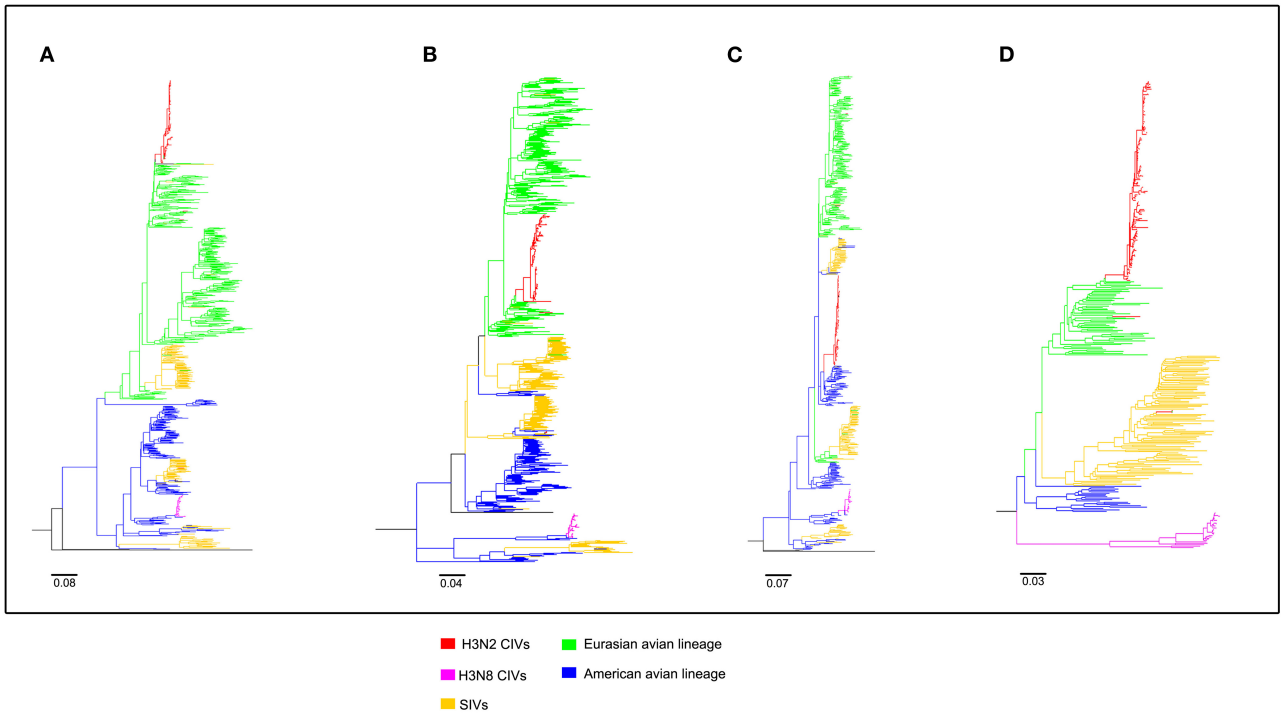

FIGURE 2 | Maximum likelihood trees of segment 1-4 of H3N2 CIVs. **(A)** PB2; **(B)** PB1; **(C)** PA; **(D)** HA. Colored branches represent distinct lineages. H3N2 CIVs: red, H3N8 CIVs: purple, SIVs: yellow, Eurasian avian lineage: green, and American avian lineage: blue. The bars are drawn to scale.

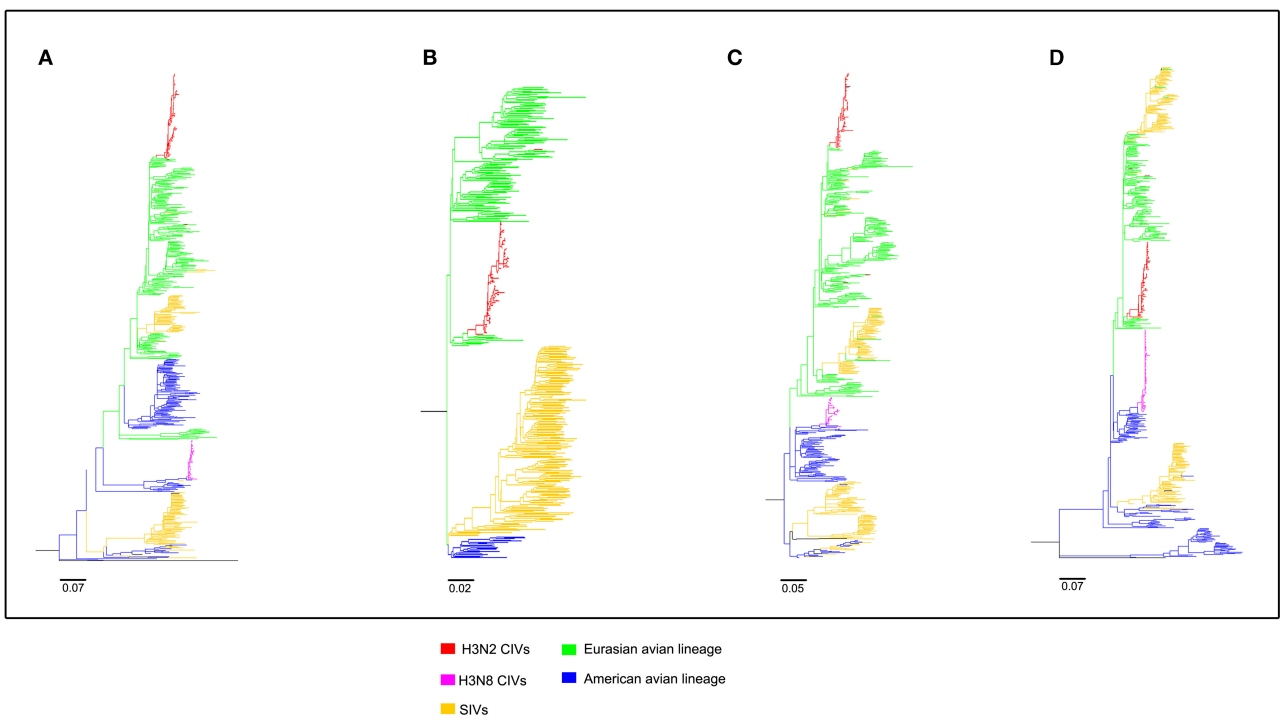

FIGURE 3 | Maximum likelihood trees of segment 5-8 of H3N2 CIVs. **(A)** NP; **(B)** NA; **(C)** M; **(D)** NS. Colored branches represent distinct lineages. H3N2 CIVs: red, H3N8 CIVs : purple, SIVs: yellow, Eurasian avian lineage: green, and American avian lineage: blue. The bars are drawn to scale.

TABLE 2 | The positions of adaptive amino acid substitutions in different host-pair calculations.

	Avian–canine (H3N2)	Equine–canine (H3N8)	Avian–equine (H3N8)	Avian–human (H3N2)	Avian–swine (H3N2)	Swine–human (H3N2)
PB2	82,195,334,365,511,570	107,221,292	/	9,44,67,81,82,120,194, 199,227,271,353,382, 456,463,475,526,567, 569,627,682,697	271,456,591,645	120,199,353,475,526, 567,569,627,674,682
PB1	108,361,397,469,517,723, 744	/	61,157,164,175,261, 429,587,642	212,327,336,361,486,576, 581,586,587,619,709,741	336,339,433,486, 581,741	576,586,619,709
PB1-F2	13	/	10,38,51,52,68,69,74	76	76	8,18,20,62
PA	208,234,243,277,369,432, 441,615	27,256,675	55,57,99,118,216,217, 244,277,336,437,683, 689	28,55,57,62,65,66,225,268, 311,332,383,385,552, 557,573,668	254,362	311,573
HA	10,45,81,111,128,172, 196,222,232,261,326, 435,489,496	29,54,83,118, **222**,328,483	25,56,63,70,81,83,88, 102,111,121,122,143,146, 160,182,207,244,252, 278,300,304,309,328, 331,347,355,387,442, 464,479,489,541	31,33,48,53,75,172, 186,192,196,198,202, 212,223,225,227, 361,384,452,489,530	/	33
NP	125,159,374,418,428,473	375	41,50,117,146,245,293, 305,312,319,345,351,374, 453,496,498	16,18,31,61,65,100,131, 197,214,280,283,286,293, 305,312,313,343,344,357, 422,423,442,455,459,472	21,119,189,190, 289,305,357,400, 425,444,456	18,52,65,131,214,239, 280,283,286,312, 344,372,406,422,442, 455,459
NA	9,24,54,65,156,208,372, 380,432	62,147	19,22,43,47,82,91,93,160, 199,211,233,250,258, 260,266,301,311,319, 321,339,359,374, 386,393,415,454	18,23,42,152,217,223, 247,249,312,369,374, 389,404,439	/	152,217,247,249,312, 389
M1	/	/	85	115,121,137,174,218,239	116,209,214	115,137,167,174, 218,230,239
M2	/	/	50	54,57,78,86,93	77	57,78,86,89,93
NS1	75,172,230	/	96,156,186,214	41,82,125,135,144,196,	125,189	28,82,135,144,196
NS2	/	/	33,35	57,107	32,34,57	107

The position of signature shared in CIVs was shown in bold. /, no host-specific amino acid substitutions in the protein.

RESULTS

Phylogenetic Analysis of CIVs

To clearly map the evolutionary background of H3N2 CIVs, the sequences of different avian influenza lineages were included in phylogenetic analyses. As shown in **Figures 2**, **3**, the H3N2 CIVs (red cluster) and H3N8 CIVs (purple cluster) were clustered into two branches respectively, revealing that they have different origins. H3N2 CIVs mainly originated from Eurasian avian viruses and circulated for a long time in Eurasia, HA (**Figure 2D**) and NA (**Figure 3B**) segment exhibited a monophyletic origin nested within the H3N2 avian influenza lineage. Consistent with previous studies, we found that the H3N2 CIVs emerged from cross-species transmission of AIVs. In contrast, H3N8 CIVs originated from EIVs.

Host-Adaptive Signatures of Avian–Canine in H3N2

We next screened for the species-specific amino acid changes associated with host adaptation in H3N2 CIVs. A total of 54 amino acid signatures separated H3N2 CIVs from AIVs on the basis of the Shannon entropy value of the HA-222 position of H3N2 AIVs (**Table 2** and **Supplementary Table 1**). HA (14/54) was most frequently mutated, followed by NA (9/54) and PA (8/54). H3N2 has consistently circulated in the canine population and spread to other mammals such as humans and swine. We compared the positions of the host-adaptive signatures of H3N2 in canine with these mammals. Five amino acid sites were common to avian–canine (H3N2) and avian–human (H3N2) entropy results, including 82 in PB2, 361 in PB1, and positions 172,196, and 489 in HA protein. These results suggest that adaptive mutations at these sites may be important for AIVs to cross the species barrier and infect mammals. Zhu et al. identified 45 mutations based on the H3N2 CIV lineage and avian lineages (11), of which 31 were identified in our study as well. In addition, 23 novel genomic signatures were also discovered. Previous studies have demonstrated that the most adaptive mutations conferring enhanced polymerase activity are localized in two clusters, the N and C termini of PB2 (especially in NP-binding and the PB1-binding domain of C-terminus), for example, the positions 627 and 701 (23, 24). We identified mutations at sites 82 and 195 located in the N-terminal NP/PB1-binding region of PB2 protein, along with

sites 334 and 365 in the C-terminal cap-binding domain. No mutations were detected in the C terminal NP/PB1-binding region (**Figure 4A**).

Of the seven characteristic sites in PB1, four (108, 361, 397, 469) were located in the cRNA-binding region and three (517, 723, 744) in the vRNA-binding region (**Figure 4B**). The C-terminal region in the PA subunit has protease activity and plays a critical role in the transcription and replication of influenza ribonucleoprotein (RNP)–encoding genes (25). Several sites were identified in the C-terminal region, including 277, 432, 441 and 615, along with 208, 234, and 243 in the linker domain (**Figure 4C**). We detected most signatures in HA, with mutations at positions 196 and 222 in the receptor-binding domain (RBD) (**Figure 5A**). Four of six characteristic sites were located in PB2-binding domain of the NP protein (**Figure 5B**). NA protein is the second major transmembrane protein responsible for virion release from the surface of infected cells. We identified two signatures (54 and 65) in the stalk region of NA, and the remaining most in the head region (**Figure 5C**).

Host-Adaptive Signatures of Equine–Canine in H3N8

The emergence of H3N8 CIVs was shown to be a cross-species transmission event of influenza virus from equine to canine (15). To further explore the adaptability of influenza virus in the canine host and the key host-specific signatures in H3N2 CIVs, we further identified 16 signatures that separate H3N8 CIVs from H3N8 EIVs (**Table 2** and **Supplementary Table 2**). The HA contains 7 species-associated amino acid substitutions, of which position 222 was common to the avian–canine and equine–canine comparisons. Three amino acid changes were found in PB2 and PA protein, and one- and two-species–associated signatures were found in NP and NA, respectively. However, no common mutated sites were observed within these four segments compared to H3N2 CIVs. The positions of equine–canine signatures of H3N8 are shown in **Figures 4–6** (blue circles). No study, so far, has focused on the equine–canine adaptation sites, although some characteristic sites in AIVs have been verified. For example, the isoleucine (Ile) to valine (Val) mutation at position 292 in H9N2 increased polymerase activity in a mammalian cell line and enhanced virus virulence in mice (26). In addition, the E83K mutation in HA of H5N1 virus facilitates virus binding to α-2,6 receptor (27). The mutation in these sites may also play an important role in equine-to-canine adaptation.

Host-Adaptive Signatures of Avian–Equine in H3N8

As shown in **Table 2** and **Supplementary Table 3**, the adaptive signatures in avian–equine were much more abundant than in avian–canine (H3N2), indicating greater biological distance between avian and equine. HA contained the most signatures, followed by NA (32/26). Notably, there was not any characteristic site in PB2. Besides, compared to other avian–mammals, the markers in PB1-F2 was the most, suggesting that the selective constraints in PB2 gene may be higher than in other genes; further, PB1-F2 may play a significant role in cross-transmission of AIVs to equine. PA-277 and HA-81,111 were three common signatures between this group and avian–canine. The HA-146 was located in 150-loop of RBD, and its nearby site 143 have an increasing effect on the binding capacity of α-2,6 receptor in H5N1 (27). As reported, the NP-41 could enhance the polymerase activity of AIVs in mammalian cell (28). Such documented sites may also be associated with adaptation of AIVs in equine population.

Host-Adaptive Signatures of Avian–Human/Swine–Human in H3N2

A total of 128 positions with distinct amino acid residues were identified between human and avian H3N2 influenza viruses (**Table 2** and **Supplementary Table 4**), and most were located in the RNP complex. We obtained fewer signatures compared to a previous study, which can be attributed to different evaluation models used in the studies (29). As shown in **Figures 4**, **5** most of the characteristic sites in the PB1/NP-binding region of PB2 were similar to that identified in a previous study (30), of which positions 9 and 199 are related to increased virulence of H5N1 in mice (31, 32). In the PB1 protein, most of the adaptation sites were located in the vRNA-binding region. There were 16 human-adaptive signatures in the PA protein, and most were located in the PA-C domain. The mutation at 383 (N→D) in H5N1 increased the polymerase activity of virus in mammalian and avian cell lines (33). The NP protein harbored the most signatures in all proteins that were mainly concentrated in the PB2 interaction areas. Of the 25 characteristic sites, mutations at positions 357 and 627 in H5N1 are associated with increased virulence in mice (31). The number of human-adaptive sites in other proteins like M1/M2 and NS1/NS2 were fewer, and the positions of these signatures were mainly mapped to the second half part of the target protein (**Figure 6**).

In addition, we found 62 swine–human host-adaptive signatures (**Table 2** and **Supplementary Table 6**), of which 17 were in NP and 10 were mapped to PB2. The RNP complex contained the most characteristic sites, of which 28 were common to the avian–human and swine–human results. PB2-526, in particular, was associated with increased adaptability of the avian strains to mammalian cell lines (34).

Host-Adaptive Signatures of Avian–Swine in H3N2

Swine is a "mixing vessel" for the reassortment of influenza viruses, and the ancestor of H3N2 that circulates in swine is of avian origin. In this study, we identified 33 swine-adaptive signatures in H3N2 (**Table 2** and **Supplementary Table 5**), 11 in NP, 6 in PB1, and 4 in PB2. As shown in **Figures 4–6**, most of these sites were located in the polymerase genome interaction region (green squares). Among the 33 signatures we identified, 4 sites (PB2-271,591;HA-186;NP-357) have been experimentally verified to be associated with host adaptation of influenza viruses to mammals (31, 35–37).

In conclusion, as shown in **Table 3**, there were 25 common signatures observed in different avian–mammals

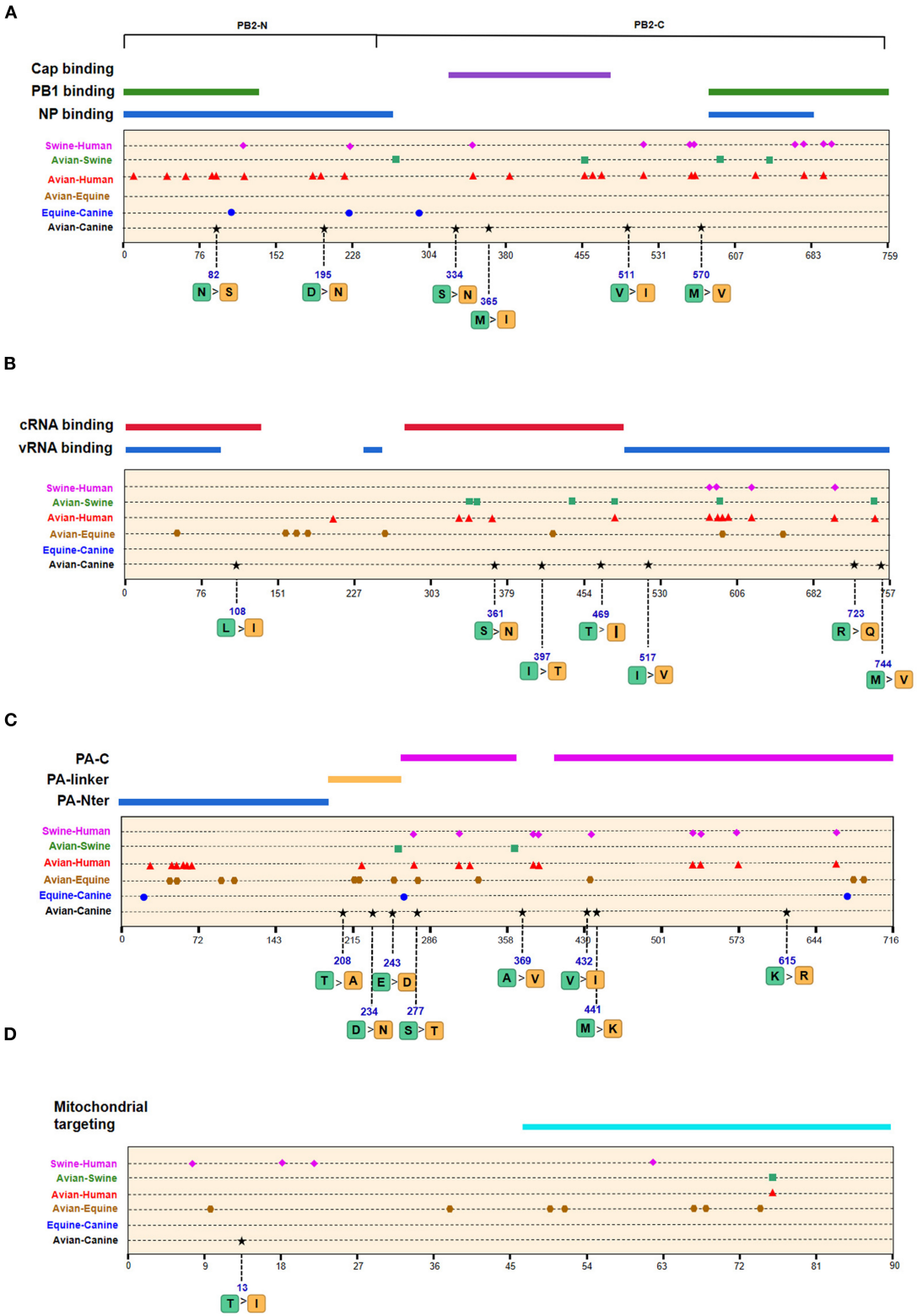

FIGURE 4 | Positions of identified signatures in the structural and functional domains of PB2 **(A)**, PB1 **(B)**, PA **(C)**, and PB1-F2 **(D)** proteins. The positions and dominant amino acid residues of Avian→ Canine (H3N2) signatures are placed below the pale-yellow bar. Black star: Avian→ Canine (H3N2), blue circle: Equine→ Canine (H3N8), brown hexagon: Avian→ Equine (H3N8), red triangle: Avian→ Human (H3N2), green square: Avian→ Swine (H3N2), and purple triangle rhomb: Swine→ Human (H3N2). The detail of these signatures are in **Table 2**.

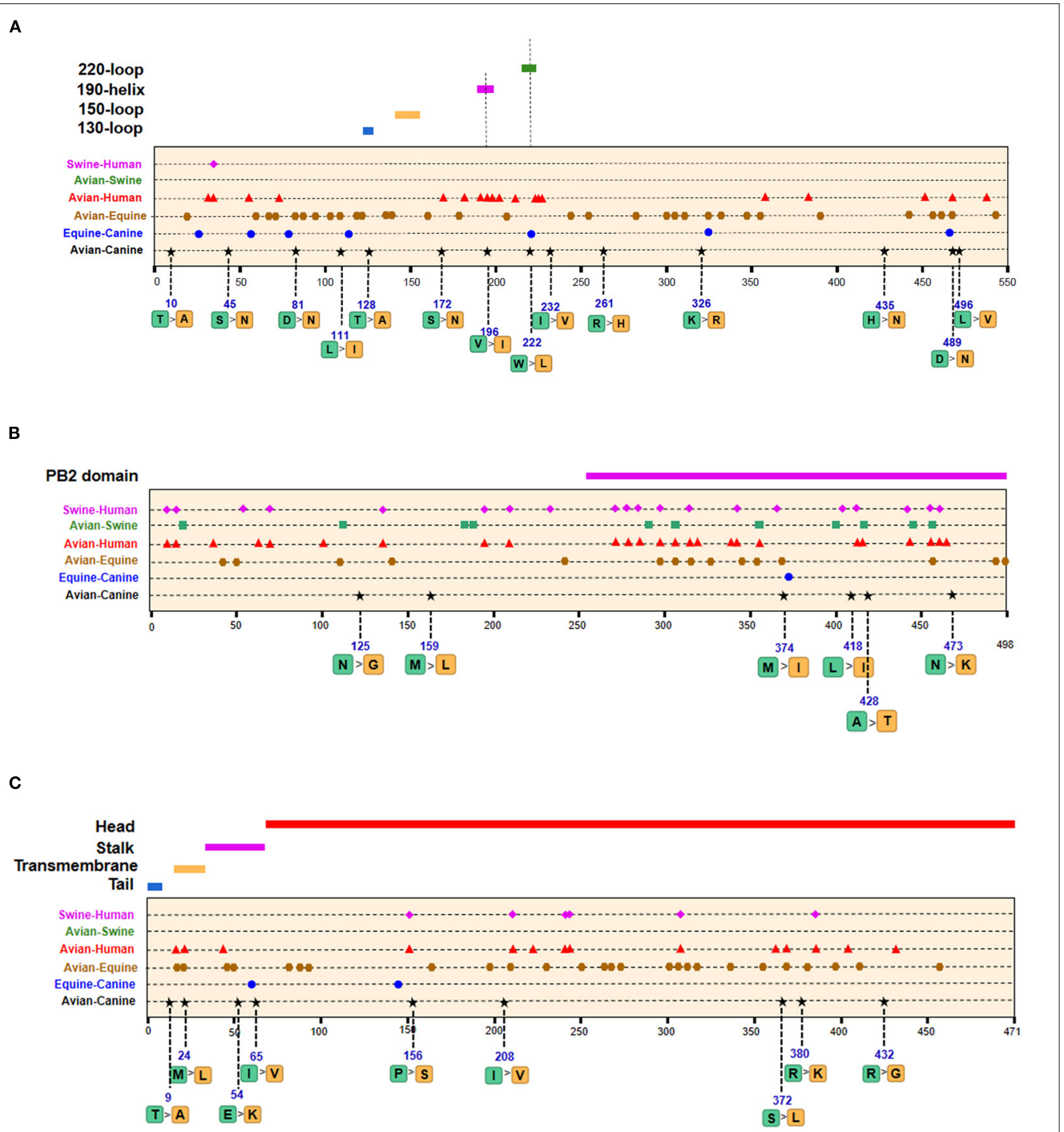

FIGURE 5 | Positions of identified signatures in structural and functional domains of HA **(A)**, NP **(B)**, and NA **(C)** proteins. The positions and dominant amino acid residues of Avian→ Canine (H3N2) signatures are placed below the pale-yellow bar. Black star: Avian→ Canine (H3N2), blue circle: Equine→ Canine (H3N8), brown hexagon: Avian→ Equine (H3N8), red triangle: Avian→ Human (H3N2), green square: Avian→ Swine (H3N2), and purple triangle rhomb: Swine→ Human (H3N2). The detail of these signatures are in **Table 2**.

calculation results of H3 IAVs, most of which were captured through pairwise comparisons, with the largest number in avian–human and avian–swine. In addition, two notable sites were common in triple comparison, with HA-489 in avian–canine/equine/human and NP-305 in avian–equine/human/swine. Among these sites, PB2-271, HA-196, and NP-357 were identified involved in AIV adaption to mammals (31, 35, 38).

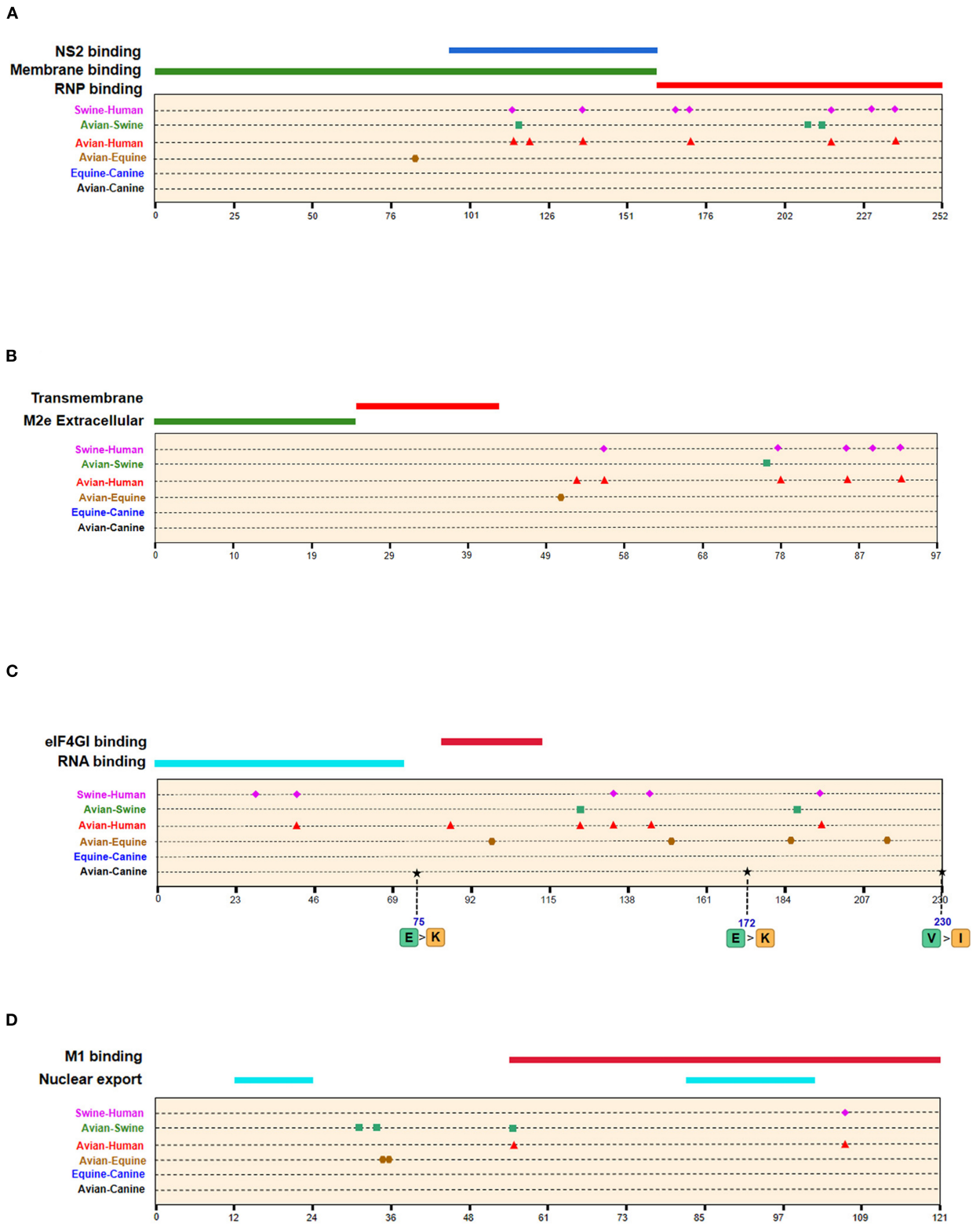

FIGURE 6 | Positions of identified signatures in structural and functional domains of M1 **(A)**, M2 **(B)**, NS1 **(C)**, and NS2 **(D)** proteins. The positions and dominant amino acid residues of Avian→ Canine (H3N2) signatures are placed below the pale-yellow bar. Black star: Avian→ Canine (H3N2), blue circle: Equine→ Canine (H3N8), brown hexagon: Avian→ Equine (H3N8), red triangle: Avian→ Human (H3N2), green square: Avian→ Swine (H3N2), and purple triangle rhomb: Swine→ Human (H3N2). The detail of these signatures are in **Table 2**.

TABLE 3 | Common signatures in different avian–mammal calculation results of H3 IAVs.

Avian–mammals comparison	Signature
Avian–canine (H3N2) and avian–human (H3N2)	PB2-82;PB1-361;HA-172,196,489
Avian–canine (H3N2) and avian–equine (H3N8)	PA-277;HA-81,111,489
Avian–equine (H3N8) and avian–human (H3N2)	PB1-587;PA-55,57;HA-489;NP-293,305,312;NA-374
Avian–equine (H3N8) and avian–swine (H3N2)	NP-305
Avian–human (H3N2) and avian–swine (H3N2)	PB2-271,456;PB1-336,486,581,714;PB1-F2-76;NP-305,357;NS1-125;NS2-57
Avian–canine (H3N2), avian–equine (H3N8) and avian–human (H3N2)	HA-489
Avian–equine (H3N8), avian–human (H3N2) and avian–swine (H3N2)	NP-305

The Risk of H3N2 CIVs to Human

Although no human cases of CIV infection have been reported to date, the risk of zoonotic influenza virus infection needs continuous surveillance and evaluation. To predict the risk of H3N2 CIV infection in humans, we studied the amino acid composition of H3N2 CIVs at positions corresponding to the human-adaptive signatures of H3N2 viruses. As shown in **Supplementary Table 4**, 123 positions had the same amino acid residues in AIVs and H3N2 CIVs, whereas five positions were distinct. PB2-82 was similar to the human IAV, whereas positions 361 in PB1, 65 in PA, and 172 and 196 in HA exhibited canine-like signatures that were completely distinct from that of avian and human viruses, suggesting a canine-adaptive role of these positions. Given that only few sites in H3N2 CIVs exhibited human-like features at the positions corresponding to avian–human signatures, and based on previous findings (8), we hypothesize that H3N2 CIVs pose a low risk to human. Overall, of the 54 avian–canine signatures identified in H3N2, the amino acid mutations in PB2-82; PB1-361; PA-277; and HA-81,111,172,196,222,489 were common to avian–equine/human or equine–canine signatures and may therefore be important for the canine adaptation of avian viruses.

DISCUSSION

Little is known regarding the mammal-specific gene signatures in avian viruses. In this study, we screened for amino acid transitions that are involved in the adaptation of IAVs to canine and other mammalian hosts. The molecular markers of host adaptability are usually identified using phylogenetic and statistical models, which have several disadvantages. The adjusted Rand index can identify distinct sites between the sequences of different hosts, although it is associated with an increase in the false-positive rate (30). Likewise, the results of phylogenetic models are affected if an intermediate host is present, and the selective constraints in this intermediate host are strong (20). In this study, we relied on an entropy threshold to discriminate signatures from nonsignatures as described by Chen et al. Low entropy indicated well-conserved amino acid residues at a site. Although this method has the disadvantage that one single threshold may overlook potential characteristic sites, the substantial sequence data from NCBI database can improve the sensitivity of these calculations. The ROC curves showed that canine-adaptive sites in all proteins except PB1-F2 can distinguish the source sequences with an accuracy higher than 98% (**Figure 7**). The lower accuracy of PB1-F2 can be attributed to the fewer sites in this protein. Overall, the sensitivity and specificity of identifying host-specific signatures by entropy algorithm were satisfactory.

Currently, H3N2 is the predominant CIV subtype circulating in China. Consistent with previous studies, we identified avian and equine lineages of CIVs. The HA and NA segments of H3N2 CIVs are likely derived from H3N2 avian viruses circulating in Eurasia and the internal segments, originated from Eurasian AIVs. Although we analyzed evolutionary history of H3N2 CIVs, the geographical and seasonal patterns of CIV infection need to be further explored in greater detail.

Adaptive mutation sites were detected in six of the nine internal canine H3N2 proteins, whereas all internal proteins in the human and swine had mutated sites, indicating that the host adaptation of influenza virus is highly complex and requires the entire genomic ensemble. A higher number of signatures indicated greater difficult in transmission and adaption of a viral protein to a new species (30). Our results show that it is more challenging for AIVs to adapt to higher as opposed to lower mammals. For example, there were fewer loci for avian–canine/equine/swine adaptation compared to avian–human adaptation. Notably, some sites were shared in mammal hosts, which raises the possibility that these particular sites carried higher correlation with H3 AIV adaptation to mammals, and HA-489 and NP-305 may deserve more attention. However, it is unclear whether these sites are critical for adaptation or simply coevolve. In addition, the shared sites in different mammalian hosts were few, indicating that the adaptive changes required for AIVs to establish stable lineages vary in different mammals.

We obtained 54 host-specific signatures that distinguish AIVs from H3N2 CIVs by entropy calculating, which encompasses 31 *in silico* markers documented in prior studies, as well as 23 novel markers. However, several proteins of the CIV lack any adaptive mutations, which suggests that the mutations in other proteins are sufficient for the virus to establish a stable linage in canine species. Another possibility is that the number of sequences used to calculate was relatively small, as only limited sequences have been isolated from canine and equine viruses. Besides, in another similar study, 54 characterized genetic substitutions were found to be accumulated and fixed in H3N2 CIV during its circulation in dogs (39). However, there were only five markers observed in our study. Different from the previous study, which calculated the accumulated frequencies of each amino acid over time in CIV sequences, our study explored extremely conservative and inconsistent amino acids sites through the comparison between H3N2 AIVs and CIVs. The divergency of the studies may attribute to the differences in analysis targets and methods.

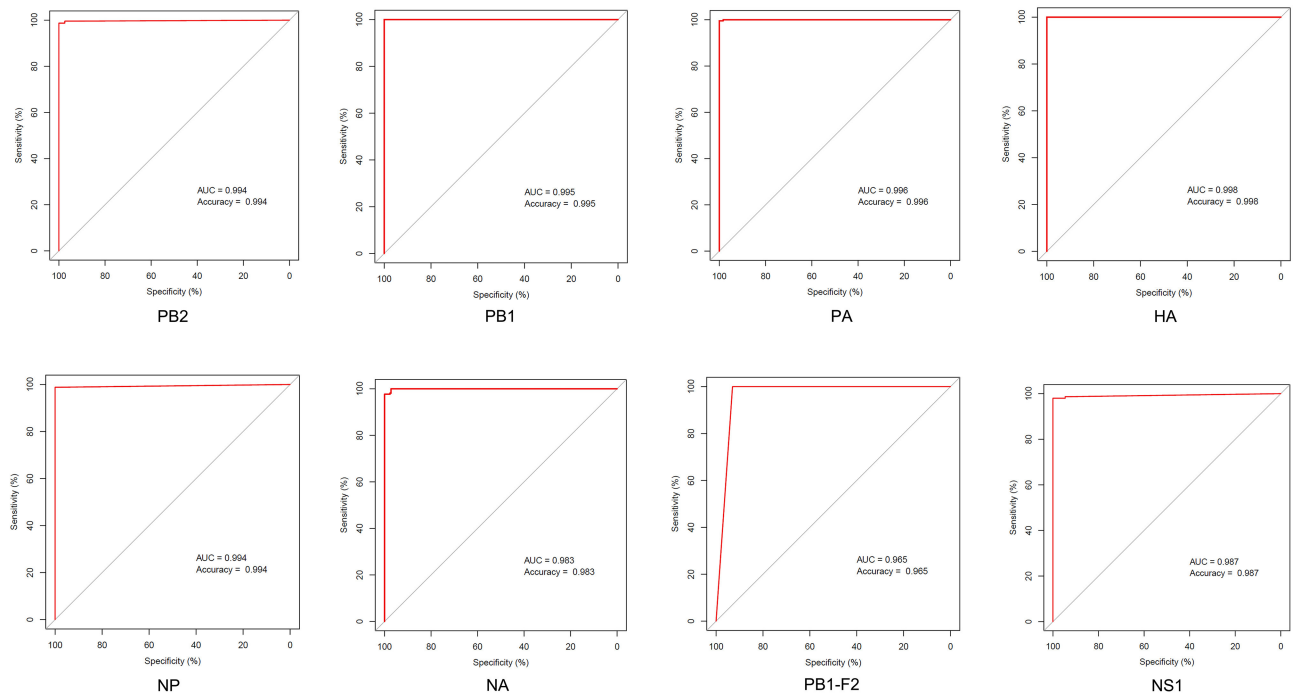

FIGURE 7 | ROC curve of host identification by the avian–canine signatures of different proteins.

In this study, we not only elucidated the evolutionary history of H3N2 CIVs but also mapped canine-specific signatures to known functional domain of proteins. As the polymerase of IAV is crucial for replication and transcription, any mutations into these four proteins may improve viral fitness in the new host. We detected six host-restricted sites in PB2 that separated AIVs and H3N2 CIVs, of which two were located in the NP- and PB1-binding domains that regulate RNP assembly and virus replication (40). Several mutations in this region, such as E192K in H5N1 and E158K in H4N6, increase virus replication and virulence in mammals (36, 41). Therefore, the substitutions in 82 and 195 are likely more important compared to other mutations.

We identified seven canine-adaptive signatures in PB1 protein, of which three were located in vRNA-binding region that regulates vRNP complex activity and viral replication. A previous study showed that the SUMOylation-defective K612R mutation in PB1 impaired vRNA binding and activity and inhibited viral replication *in vitro* and *in vivo* (42). It remains to be elucidated whether mutations at positions 517, 723, and 744 affect the pathogenic characteristics of CIVs.

The non-essential viral protein PB1-F2 promotes apoptosis, antagonizes the interferon response, and exacerbates secondary bacterial infections, all of which increase virus virulence (43, 44). We identified a canine-adaptive mutation T13I in this protein. Only a few experimentally verified mammalian adaptive sites are known for this protein, and the N66S substitution in the 1,918 pandemic virus was partly responsible for its high pathogenicity (45). The PA-K615N substitution of H7N7 considerably increases its polymerase activity in mammalian cell lines and increases virulence in mice (46). The K615R located in the C-terminal region of PA protein may play an important role in canine adaption of the virus.

The viral nucleoprotein is crucial for the switch between transcription and replication (47). Some mutations in NP have been identified that are required for the efficient growth of AIVs in mammalian hosts, for example, N319K in H7N7 (46) and K470R in H5N1 (48). Although there were no reported verified sites in our results for AIVs-H3N2 CIVs in NP protein, the virulence marker NP-Q357K known to enhance the pathogenicity of Eurasian H1N1 SIVs (49) was common to avian–human and avian–swine transitions, which is indicative of the reliability of our analysis.

The HA protein initiates influenza virus infection by recognizing and binding to sialylated glycans on the surface of host cells (50). There are four key secondary structure elements in these glycans—150 loop (residues 147–152), 190 helix (residues 190–198), 130 loop (residues 135–138), and 220 loop (residues 221–228) (51). CIVs with mutation W222L in receptor-binding pocket enhanced the binding to canine respiratory receptors (12, 17). Furthermore, H5N1 with Q196R increased virus binding to α-2,6 receptor (52). In this study, V196I and W222L were identified, both of which were located at the receptor binding site and V196I warrants further investigation.

The head domain of the HA molecule is the main target of neutralizing antibodies. T128D is an important determinant of antigenic change during A/H2N2 virus evolution (53). In our study, we found a transition from T to A at position HA-128 after

canine adaptation of AIVs, which may result in antigenic changes of the virus.

We obtained nine canine-adaptive signatures in the NA protein, of which five were located in head region. A previous study showed that tolerant substitutions that enabled the NA protein to retain at least 20% of its NA activity are frequently present in the stalk region, indicating that the mutations in the head domain led to NA inactivation. Interestingly, the probability of a mutation leasing to the loss of NA activity decreased with increasing distance from the structural center of the enzyme active site (Y406-N2) (54). Therefore, the mutations at positions 372, 380, and 432 are likely more crucial. The S372A and R403W substitutions in NA enhance the ability of the virus to cross the species barrier and adapt to a mammalian host (55). These substitutions have also been detected in H9N2, H2N2, and H3N2 subtypes (56). Chen et al. demonstrated that mouse-adapted H7N7 virus harbored amino acid changes in the PB2 (E627K), PB1 (R118I), PA (L550M), HA (G214R), and NA (S372N) proteins, which enhanced its ability to replicate in mammalian cells (57). The S372L substitution identified in the NA protein identified in this study may be related to the avian–canine adaptation of AIVs.

Most of the signatures identified in this study were not verified in experimental studies. Furthermore, we were unable to map the mutation sites accurately given the lack of protein structure data currently. We also evaluated the zoonotic transmission risk of H3N2 CIVs, and most signatures exhibited avian–like residues at positions where avian–human signatures were located, which indicate a low risk of H3N2 CIV infection in humans. In summary, we have characterized the adaptive signatures of H3N2 associated with transmission to new mammalian hosts, especially canines. The host-specific sites and canine-adaptive signatures identified by the entropy method exhibited moderate specificity and sensitivity in distinguishing the host source of sequences. It is less challenging for influenza viruses to spread to lower mammals compared to higher mammals, and some common signatures exist in the process of AIV adaption to diverse hosts' environment. The host-adaptation sites on RNP complex are the most abundant and are concentrated in the polymerase proteins interaction domain in canines and other mammals. Of the 54 characteristic sites in H3N2 CIVs, nine were shared between avian–human/equine or equine–canine (PB2-82; PB1-361; PA-277; HA-81,111,172,196,222,489), indicating a crucial role in adapting to canine hosts. Further studies are needed to elucidate the complex mechanisms underlying mammalian adaptation of AIVs.

DATA AVAILABILITY STATEMENT

The original contributions presented in the study are included in the article/**Supplementary Material**, further inquiries can be directed to the corresponding authors.

AUTHOR CONTRIBUTIONS

XL conceived and wrote the manuscript. JL performed phylogenetic analysis. ZQ performed host-adaptive signatures computing and analysis. QL performed model evaluation and YP collated the data. YC and YS checked and revised the manuscript. All the authors read and approved the final manuscript.

FUNDING

This work is supported by the Shenzhen Science and Technology Program (KQTD20180411143323605 to YS), National Mega-projects for Infectious Diseases (2018ZX10305409-004-003 to YC), and Guangdong Province Science and Technology Innovation Strategy Special Fund (2018A030310337 to YC).

ACKNOWLEDGMENTS

We thank all the scientists and teachers of School of Public Health (Shenzhen), Sun Yat-sen University for their support.

SUPPLEMENTARY MATERIAL

The Supplementary Material for this article can be found online at: https://www.frontiersin.org/articles/10.3389/fvets.2021.740472/full#supplementary-material

REFERENCES

1. Tong S, Zhu X, Li Y, Shi M, Zhang J, Bourgeois M, et al. New world bats harbor diverse influenza A viruses. *PLoS Pathog*. (2013) 9:e1003657. doi: 10.1371/journal.ppat.1003657
2. Crawford PC, Dubovi EJ, Castleman WL, Stephenson I, Gibbs EPJ, Chen L, et al. Transmission of equine influenza virus to dogs. *Science*. (2005) 310:482–5. doi: 10.1126/science.1117950
3. Song D, Kang B, Lee C, Jung K, Ha G, Kang D, et al. Transmission of avian influenza virus (H3N2) to dogs. *Emerg Infect Dis*. (2008) 14:741–6. doi: 10.3201/eid1405.071471
4. Suzuki Y, Ito T, Suzuki T, Holland RE, Chambers TM, Kiso M, et al. Sialic acid species as a determinant of the host range of influenza A viruses. *J Virol*. (2000) 74:11825–31. doi: 10.1128/JVI.74.24.11825-11831.2000
5. Songserm T, Amonsin A, Jam-on R, Sae-Heng N, Pariyothorn N, Payungporn S, et al. Fatal avian influenza A H5N1 in a dog. *Emerg Infect Dis*. (2006) 12:1744–7. doi: 10.3201/eid1211.060542
6. Lin D, Sun S, Du L, Ma J, Fan L, Pu J, et al. Natural and experimental infection of dogs with pandemic H1N1/2009 influenza virus. *J Gen Virol*. (2012) 93:119–23. doi: 10.1099/vir.0.037358-0
7. Chen Y, Trovão NS, Wang G, Zhao W, He P, Zhou H, et al. Emergence and evolution of novel reassortant influenza A viruses in Canines in Southern China. *mBio*. (2018) 9:e00909-18. doi: 10.1128/mBio.00909-18
8. Martinez-Sobrido L, Blanco-Lobo P, Rodriguez L, Fitzgerald T, Zhang H, Nguyen P, et al. Characterizing emerging canine H3 influenza viruses. *PLoS Pathog*. (2020) 16:e1008409. doi: 10.1371/journal.ppat.1008409
9. Bunpapong N, Nonthabenjawan N, Chaiwong S, Tangwangvivat R, Boonyapisitsopa S, Jairak W, et al. Genetic characterization of canine influenza A virus (H3N2) in Thailand. *Virus Genes*. (2014) 48:56–63. doi: 10.1007/s11262-013-0978-z
10. Li S, Shi Z, Jiao P, Zhang G, Zhong Z, Tian W, et al. Avian-origin H3N2 canine influenza A viruses in Southern China. *Infect Genet Evol*. (2010) 10:1286–8. doi: 10.1016/j.meegid.2010.08.010

11. Zhu H, Hughes J, Murcia PR. Origins and evolutionary dynamics of H3N2 canine influenza virus. *J Virol*. (2015) 89:5406–18. doi: 10.1128/JVI.03395-14
12. Yang G, Li S, Blackmon S, Ye J, Bradley KC, Cooley J, et al. Mutation tryptophan to leucine at position 222 of haemagglutinin could facilitate H3N2 influenza A virus infection in dogs. *J Gen Virol*. (2013) 94:2599–608. doi: 10.1099/vir.0.054692-0
13. Shi X. Effect of PB2 protein 576E on H3N2 canine influenza virus mammalian adaptability and its mechanism. [dissertation/master's thesis]. [Shanghai]: Chinese Academy of Agricultural Sciences (2020).
14. Chambers TM. A Brief introduction to equine influenza and equine influenza viruses. *Methods Mol Biol*. (2020) 2123:355–60. doi: 10.1007/978-1-0716-0346-8_26
15. He W, Li G, Wang R, Shi W, Li K, Wang S, et al. Host-range shift of H3N8 canine influenza virus: a phylodynamic analysis of its origin and adaptation from equine to canine host. *Vet Res*. (2019) 50:87. doi: 10.1186/s13567-019-0707-2
16. Feng KH, Gonzalez G, Deng L, Yu H, Tse VL, Huang L, et al. Equine and canine influenza H3N8 viruses show minimal biological differences despite phylogenetic divergence. *J Virol*. (2015) 89:6860–73. doi: 10.1128/JVI.00521-15
17. Wen F, Blackmon S, Olivier AK, Li L, Guan M, Sun H, et al. Mutation W222L at the receptor binding site of hemagglutinin could facilitate viral adaption from equine influenza A(H3N8) virus to dogs. *J Virol*. (2018) 92:e01115–18. doi: 10.1128/JVI.01115-18
18. Chen G-W, Chang S-C, Mok CK, Lo Y-L, Kung Y-N, Huang J-H, et al. Genomic signatures of human versus avian influenza A viruses. *Emerg Infect Dis*. (2006) 12:1353–60. doi: 10.3201/eid1209.060276
19. Chen G-W, Shih S-R. Genomic signatures of influenza A pandemic (H1N1) 2009 virus. *Emerg Infect Dis*. (2009) 15:1897–903. doi: 10.3201/eid1512.090845
20. Tamuri AU, Dos Reis M, Hay AJ, Goldstein RA. Identifying changes in selective constraints: host shifts in influenza. *PLoS Comput Biol*. (2009) 5:e1000564. doi: 10.1371/journal.pcbi.1000564
21. Fu L, Niu B, Zhu Z, Wu S, Li W. CD-HIT: accelerated for clustering the next-generation sequencing data. *Bioinformatics*. (2012) 28:3150–2. doi: 10.1093/bioinformatics/bts565
22. Nakamura T, Yamada KD, Tomii K, Katoh K. Parallelization of MAFFT for large-scale multiple sequence alignments. *Bioinformatics*. (2018) 34:2490–2. doi: 10.1093/bioinformatics/bty121
23. Herfst S, Schrauwen EJA, Linster M, Chutinimitkul S, de Wit E, Munster VJ, et al. Airborne transmission of influenza A/H5N1 virus between ferrets. *Science*. (2012) 336:1534–41. doi: 10.1126/science.1213362
24. Yu Z, Ren Z, Zhao Y, Cheng K, Sun W, Zhang X, et al. PB2 and hemagglutinin mutations confer a virulent phenotype on an H1N2 avian influenza virus in mice. *Arch Virol*. (2019) 164:2023–9. doi: 10.1007/s00705-019-04283-0
25. Lo C-Y, Li OT-W, Tang W-P, Hu C, Wang GX, Ngo JC-K, et al. Identification of influenza polymerase inhibitors targeting C-terminal domain of PA through surface plasmon resonance screening. *Sci Rep*. (2018) 8:2280. doi: 10.1038/s41598-018-20772-9
26. Gao W, Zu Z, Liu J, Song J, Wang X, Wang C, et al. Prevailing I292V PB2 mutation in avian influenza H9N2 virus increases viral polymerase function and attenuates IFN-β induction in human cells. *J Gen Virol*. (2019) 100:1273–81. doi: 10.1099/jgv.0.001294
27. Yamada S, Suzuki Y, Suzuki T, Le MQ, Nidom CA, Sakai-Tagawa Y, et al. Haemagglutinin mutations responsible for the binding of H5N1 influenza A viruses to human-type receptors. *Nature*. (2006) 444:378–82. doi: 10.1038/nature05264
28. Zhu W, Zou X, Zhou J, Tang J, Shu Y. Residues 41V and/or 210D in the NP protein enhance polymerase activities and potential replication of novel influenza (H7N9) viruses at low temperature. *Virol J*. (2015) 12:71. doi: 10.1186/s12985-015-0304-6
29. Khaliq Z, Leijon M, Belák S, Komorowski J. Identification of combinatorial host-specific signatures with a potential to affect host adaptation in influenza A H1N1 and H3N2 subtypes. *BMC Genomics*. (2016) 17:529. doi: 10.1186/s12864-016-2919-4
30. Hu Y-J, Tu P-C, Lin C-S, Guo S-T. Identification and chronological analysis of genomic signatures in influenza A viruses. *PLoS ONE*. (2014) 9:e84638. doi: 10.1371/journal.pone.0084638
31. Kim JH, Hatta M, Watanabe S, Neumann G, Watanabe T, Kawaoka Y. Role of host-specific amino acids in the pathogenicity of avian H5N1 influenza viruses in mice. *J Gen Virol*. (2010) 91:1284–9. doi: 10.1099/vir.0.018143-0
32. Graef KM, Vreede FT, Lau Y-F, McCall AW, Carr SM, Subbarao K, et al. The PB2 subunit of the influenza virus RNA polymerase affects virulence by interacting with the mitochondrial antiviral signaling protein and inhibiting expression of beta interferon. *J Virol*. (2010) 84:8433–45. doi: 10.1128/JVI.00879-10
33. Song J, Xu J, Shi J, Li Y, Chen H. Synergistic effect of S224P and N383D substitutions in the PA of H5N1 avian influenza virus contributes to mammalian adaptation. *Sci Rep*. (2015) 5:10510. doi: 10.1038/srep10510
34. Song W, Wang P, Mok BW-Y, Lau S-Y, Huang X, Wu W-L, et al. The K526R substitution in viral protein PB2 enhances the effects of E627K on influenza virus replication. *Nat Commun*. (2014) 5:5509. doi: 10.1038/ncomms6509
35. Bussey KA, Bousse TL, Desmet EA, Kim B, Takimoto T. PB2 residue 271 plays a key role in enhanced polymerase activity of influenza A viruses in mammalian host cells. *J Virol*. (2010) 84:4395–406. doi: 10.1128/JVI.02642-09
36. Taft AS, Ozawa M, Fitch A, Depasse JV, Halfmann PJ, Hill-Batorski L, et al. Identification of mammalian-adapting mutations in the polymerase complex of an avian H5N1 influenza virus. *Nat Commun*. (2015) 6:7491. doi: 10.1038/ncomms8491
37. Dortmans JCFM, Dekkers J, Wickramasinghe INA, Verheije MH, Rottier PJM, van Kuppeveld FJM, et al. Adaptation of novel H7N9 influenza A virus to human receptors. *Sci Rep*. (2013) 3:3058. doi: 10.1038/srep03058
38. Chutinimitkul S, van Riel D, Munster VJ, van den Brand JMA, Rimmelzwaan GF, Kuiken T, et al. *In vitro* assessment of attachment pattern and replication efficiency of H5N1 influenza A viruses with altered receptor specificity. *J Virol*. (2010) 84:6825–33. doi: 10.1128/JVI.02737-09
39. Guo F, Roy A, Wang R, Yang J, Zhang Z, Luo W, et al. Host adaptive evolution of avian-origin H3N2 canine influenza virus. *Front Microbiol*. (2021) 12:655228. doi: 10.3389/fmicb.2021.655228
40. Poole E, Elton D, Medcalf L, Digard P. Functional domains of the influenza A virus PB2 protein: identification of NP- and PB1-binding sites. *Virology*. (2004) 321:120–33. doi: 10.1016/j.virol.2003.12.022
41. Xu G, Wang F, Li Q, Bing G, Xie S, Sun S, et al. Mutations in PB2 and HA enhanced pathogenicity of H4N6 avian influenza virus in mice. *J Gen Virol*. (2020) 101:910–20. doi: 10.1099/jgv.0.001192
42. Li J, Liang L, Jiang L, Wang Q, Wen X, Zhao Y, et al. Viral RNA-binding ability conferred by SUMOylation at PB1 K612 of influenza A virus is essential for viral pathogenesis and transmission. *PLoS Pathog*. (2021) 17:e1009336. doi: 10.1371/journal.ppat.1009336
43. Xiao Y, Evseev D, Stevens CA, Moghrabi A, Miranzo-Navarro D, Fleming-Canepa X, et al. Influenza PB1-F2 inhibits avian MAVS signaling. *Viruses*. (2020) 12:409. doi: 10.3390/v12040409
44. Zamarin D, Ortigoza MB, Palese P. Influenza A virus PB1-F2 protein contributes to viral pathogenesis in mice. *J Virol*. (2006) 80:7976–83. doi: 10.1128/JVI.00415-06
45. Conenello GM, Zamarin D, Perrone LA, Tumpey T, Palese P. A single mutation in the PB1-F2 of H5N1 (HK/97) and 1918 influenza A viruses contributes to increased virulence. *PLoS Pathog*. (2007) 3:1414–21. doi: 10.1371/journal.ppat.0030141
46. Gabriel G, Dauber B, Wolff T, Planz O, Klenk HD, Stech J. The viral polymerase mediates adaptation of an avian influenza virus to a mammalian host. *Proc Natl Acad Sci USA*. (2005) 102:18590–5. doi: 10.1073/pnas.0507415102
47. Portela A, Digard P. The influenza virus nucleoprotein: a multifunctional RNA-binding protein pivotal to virus replication. *J Gen Virol*. (2002) 83:723–34. doi: 10.1099/0022-1317-83-4-723
48. Chen L, Wang C, Luo J, Li M, Liu H, Zhao N, et al. Amino acid substitution K470R in the nucleoprotein increases the virulence of H5N1 influenza A virus in mammals. *Front Microbiol*. (2017) 8:1308. doi: 10.3389/fmicb.2017.01308
49. Zhu W, Feng Z, Chen Y, Yang L, Liu J, Li X, et al. Mammalian-adaptive mutation NP-Q357K in Eurasian H1N1 Swine Influenza viruses determines the virulence phenotype in mice. *Emerg Microbes Infect*. (2019) 8:989–99. doi: 10.1080/22221751.2019.1635873

50. Suttie A, Deng Y-M, Greenhill AR, Dussart P, Horwood PF, Karlsson EA. Inventory of molecular markers affecting biological characteristics of avian influenza A viruses. *Virus Genes*. (2019) 55:739–68. doi: 10.1007/s11262-019-01700-z
51. Gamblin SJ, Haire LF, Russell RJ, Stevens DJ, Xiao B, Ha Y, et al. The structure and receptor binding properties of the 1918 influenza hemagglutinin. *Science*. (2004) 303:1838–42. doi: 10.1126/science.1093155
52. Chen L-M, Blixt O, Stevens J, Lipatov AS, Davis CT, Collins BE, et al. *In vitro* evolution of H5N1 avian influenza virus toward human-type receptor specificity. *Virology*. (2012) 422:105–13. doi: 10.1016/j.virol.2011.10.006
53. Linster M, Schrauwen EJA, van der Vliet S, Burke DF, Lexmond P, Bestebroer TM, et al. The molecular basis for antigenic drift of human A/H2N2 influenza viruses. *J Virol*. (2019) 93:e01907–18. doi: 10.1128/JVI.01907-18
54. Yano T, Nobusawa E, Nagy A, Nakajima S, Nakajima K. Effects of single-point amino acid substitutions on the structure and function neuraminidase proteins in influenza A virus. *Microbiol Immunol*. (2008) 52:216–23. doi: 10.1111/j.1348-0421.2008.00034.x
55. Barberis A, Boudaoud A, Gorrill A, Loupias J, Ghram A, Lachheb J, et al. Full-length genome sequences of the first H9N2 avian influenza viruses isolated in the Northeast of Algeria. *Virol J*. (2020) 17:108. doi: 10.1186/s12985-020-01377-z
56. Rashid S, Naeem K, Ahmed Z, Saddique N, Abbas MA, Malik SA. Multiplex polymerase chain reaction for the detection and differentiation of avian influenza viruses and other poultry respiratory pathogens. *Poult Sci*. (2009) 88:2526–31. doi: 10.3382/ps.2009-00262
57. Chen Q, Yu Z, Sun W, Li X, Chai H, Gao X, et al. Adaptive amino acid substitutions enhance the virulence of an H7N7 avian influenza virus isolated from wild waterfowl in mice. *Vet Microbiol*. (2015) 177:18–24. doi: 10.1016/j.vetmic.2015.02.016

Conflict of Interest: The authors declare that the research was conducted in the absence of any commercial or financial relationships that could be construed as a potential conflict of interest.

frontiers in Microbiology

ORIGINAL RESEARCH
published: 02 December 2021
doi: 10.3389/fmicb.2021.732923

A Molecular Investigation of Malaria Infections From High-Transmission Areas of Southern Togo Reveals Different Species of *Plasmodium* Parasites

Kokouvi Kassegne[1,2], Si-Wei Fei[1], Koffigan Ananou[3], Kokou Sépénou Noussougnon[4†], Komi Komi Koukoura[5], Eniola Michael Abe[6], Xiao-Kui Guo[1], Jun-Hu Chen[2]* and Xiao-Nong Zhou[1,2]*

[1] School of Global Health, Chinese Center for Tropical Diseases Research, Shanghai Jiao Tong University School of Medicine, Shanghai, China, [2] National Institute of Parasitic Diseases, Chinese Center for Diseases Control and Prevention (Chinese Center for Tropical Diseases Research), National Health Commission of the People's Republic of China (NHC) Key Laboratory of Parasite and Vector Biology, World Health Organization (WHO) Collaborating Center for Tropical Diseases, National Center for International Research on Tropical Diseases, Shanghai, China, [3] Centre Médico-Social Notre Dame de la Consolation, Atakpamé, Togo, [4] Hôpital Bethesda d'Agou Nyogbo, Agou, Togo, [5] Laboratoire des Sciences Biomédicales, Alimentaires et Santé Environnementale, Département des Analyses Biomédicales, Ecole Supérieure des Techniques Biologiques et Alimentaires, Université de Lomé, Lomé, Togo, [6] Department of Social Work, Education and Community Wellbeing, Faculty of Health and Life Sciences, Northumbria University, Newcastle upon Tyne, United Kingdom

Malaria particularly burdens people in poor and neglected settings across the tropics of Africa. Meanwhile, a large proportion of the Togo population have poor understanding of malaria epidemiology and parasites. This study carried out a molecular survey of malaria cases in southern Togo during 2017–2019. We estimated *Plasmodium* species infection rates and microscopic examination compliance with nested PCR results. Sensitivity and specificity analyses were performed in conjunction with predictive values. Also, phylogenetic characterization of species of malaria parasites was assessed. *Plasmodium* genus-specific nested PCR identified 565 positive cases including 536/611 (87.8%) confirmed cases from the microscopy-positive group and 29/199 (14.6%) diagnosed malaria cases from the microscopy-negative group. Our findings revealed a disease prevalence (69.8%) higher than that reported (25.5–55.1%) for the country. The diagnostic test had 94.9% sensitivity and 69.4% specificity, i.e., it missed 120 of the people who had malaria and about one-third of the people tested positive for the disease, which they did not have, respectively. In conjunction, the test showed 87.7% positive predictive value and 85.4% negative predictive value, which, from a clinical perspective, indicates the chance that a person with a positive diagnostic test truly has the disease and the probability that a person with a negative test does not have the disease, respectively. Further species-specific nested PCR followed by analysis of gene sequences confirmed species of malaria parasites and indicated infection rates for *Plasmodium falciparum* (Pf), 95.5% (540/565); *P. ovale* (Po), 0.5% (3/565); and *P. malariae* (Pm), 0.4% (2/565). In addition, 20 cases were coinfection cases of Pf-Po (15/565) and Pf-Pm (5/565). This study publicly reports, for the first time, a molecular

OPEN ACCESS

Edited by:
Aparup Das, ICMR-National Institute of Research in Tribal Health, India

Reviewed by:
William Harold Witola, University of Illinois at Urbana–Champaign, United States
Farah Aini Abdullah, Universiti Sains Malaysia (USM), Malaysia

***Correspondence:**
Kokouvi Kassegne
kassegnek@sjtu.edu.cn
Jun-Hu Chen
chenjh@nipd.chinacdc.cn

†Present address:
Kokou Sépénou Noussougnon, Centre Hospitalier Préfectoral d'Agou Gare, Agou, Togo

Specialty section:
This article was submitted to Infectious Agents and Disease, a section of the journal Frontiers in Microbiology

Received: *29 June 2021*
Accepted: *25 October 2021*
Published: *02 December 2021*

Citation:
Kassegne K, Fei S-W, Ananou K, Noussougnon KS, Komi Koukoura K, Abe EM, Guo X-K, Chen J-H and Zhou X-N (2021) A Molecular Investigation of Malaria Infections From High-Transmission Areas of Southern Togo Reveals Different Species of Plasmodium Parasites. Front. Microbiol. 12:732923. doi: 10.3389/fmicb.2021.732923

survey of malaria cases in Togo and reveals the presence of other malaria parasites (Po and Pm) other than Pf. These findings might provide answers to some basic questions on the malaria scenario and, knowledge gained could help with intervention deployment for effective malaria control in Togo.

Keywords: malaria, molecular surveillance, *Plasmodium* species, phylogeny, Togo

INTRODUCTION

Malaria is a major debilitating infectious disease that affects millions of people and impedes public health and socioeconomic development in Africa (Kassegne et al., 2017). In tropical Africa, nearly 90% of deaths among young children are related to malaria (World Health Organization [WHO], 2018b).

Malaria transmission occurs throughout the year in Togo and is usually characterized by seasonal outbreaks with a peak during the rainy season. An estimated nearly 100% of the population of Togo lives in areas endemic for malaria—all the five administrative regions of the country having populations at risk of malaria—with disease prevalence rate estimated between 25.5 and 55.1% (World Health Organization [WHO], 2018a). In 2016, uncomplicated malaria was the first cause (41.7%) of outpatient consultations in public health centers and, hospitalization rate related to severe disease accounted for 20.5%, with 3.8% hospital mortality (Thomas et al., 2020). In Togo mortality rate associated with severe malaria is underestimated because most of the cases do not adhere to clinical consultations. For example, in 2017, > 60% of severe cases have not been to the hospital (Programe National de Lutte contre le Paludisme [PNLP], 2019). Children under 5 years old remain highly affected by malaria, with 35.4% uncomplicated outpatient cases, 58.4% hospitalized severe cases, and 69.7% deaths reported in 2017 (Programe National de Lutte contre le Paludisme [PNLP], 2019). Pregnant women accounted for 5% uncomplicated outpatients and 6% hospitalized severe cases (Programe National de Lutte contre le Paludisme [PNLP], 2019). To combat the disease, the country has developed and implemented several interventions based on prevention, care, and support strategies in accordance with the World Health Organization guidelines (World Health Organization [WHO], 2015; Programme National de Lutte contre le Paludisme [PNLP], 2018). However, malaria epidemiology is poorly understood in Togo, with a paucity of information on species of *Plasmodium* that are responsible for disease transmission. Studies on disease burden erroneously made believe that malaria cases are only related to *Plasmodium falciparum* (Pf) infection in Togo (Bakai et al., 2020; Thomas et al., 2020), making the standards of care unilateral with important implications in disease epidemiology.

Routine diagnosis using the standard method for the detection of *Plasmodium* species by examining Giemsa-stained blood smears under a microscope is the major approach being used in malaria control programmes of many tropical African settings. The method is effective and inexpensive, but it is laborious and time consuming. In addition, its sensitivity is doubtful with low parasitemia during low-transmission periods and also with the shortage of experienced technicians (Agabani et al., 1994). Polymerase chain reaction (PCR) is one of the highly sensitive methods, which has been widely used for molecular detection and identification of malaria parasites. Its effectiveness is unquestionable as it had been successfully used to detect cases of mixed infections or low parasitemia (Snounou et al., 1993c; Zhou et al., 2014). A range of PCR-based assays has been described for malaria detection including species of *Plasmodium* that regularly infect humans [Pf, *Plasmodium vivax* (Pv), *Plasmodium ovale* (Po), *Plasmodium malariae* (Pm), and *Plasmodium knowlesi* (Pk)] (Snounou et al., 1993a,b; Singh et al., 2004; Chen et al., 2017). In addition, nested PCR is used for the amplification of the small subunit ribosomal RNA (ssrRNA) gene of *Plasmodium* species (Snounou and Singh, 2002).

In order to advance knowledge of diagnosis efficacy and species of malaria parasites in Togo, this study carried out a molecular investigation on malaria clinical samples in comparison with light microscopic examination and assessed the phylogeny of *Plasmodium* species from southern Togo.

MATERIALS AND METHODS

Study Sites

This study was conducted in the two southern regions (Maritime and Plateaux) of Togo (Togo Confidentiel, 2021) where malaria is endemic (World Health Organization [WHO], 2018a). Urban and periurban areas of Lomé (N 6°12′56″; E 1°22′54″) in Golfe Prefecture (Maritime Region), Atakpamé (N 7°52′87″; E 1°13′05″) in Ogou Prefecture and Agou-Gadzépé (N 7°28′01″; E 1°55′01″) in Agou Prefecture (Plateaux Region) were selected (**Figure 1**).

Lomé is the capital of Togo and lies on the Gulf of Guinea (Atlantic coast) in the extreme southwestern corner of the country. Its urban population was estimated at 837,437 inhabitants as of the 2010 census (Direction Générale de la Statistique et de la Compatibilité Nationale, 2010). Lomé has a tropical savanna climate despite its latitude close to the equator, which is characterized by one dry season (November–March) and two rainy seasons (April–October), with two rainfall peaks in June and September (Encyclopædia Britannica, Inc., 2021). Lomé is relatively dry, with an annual average rainfall of 800–900 mm and a mean temperature above 27.5°C (Encyclopædia Britannica, Inc., 2021). Agou-Gadzépé and Atakpamé (the largest city in Plateaux Region) are located at 80 and 161 km, respectively, from Lomé, with estimated populations of 11,000 and 84,979, respectively, as indicated in the 2006 population census (Encyclopædia Britannica, Inc., 2021). The climate in Plateaux is generally tropical characterized by dry and rainy

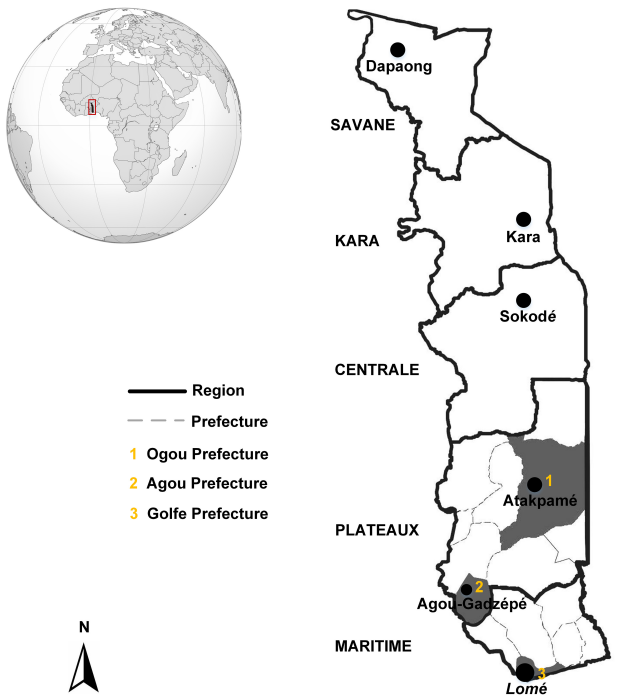

FIGURE 1 | Togo, showing the geographic area of the municipalities involved in this study (dark gray shading). Atakpamé (Ogou Prefecture), Agou-Gadzépé (Agou Prefecture), and Lomé (Golfe Prefecture) are located in the Plateaux and Maritime Regions, respectively.

seasons (as described above), with peaks of malaria transmission related to rainfall. The western part of Plateaux receives the highest amount of precipitation—about 1,800 mm annually (up to 2,000 mm in Agou) and, the rainfall amounts to 1,300–1,400 mm per year in Atakpamé, with annual average temperatures of 23.5 and 26°C, respectively (Encyclopædia Britannica, Inc., 2021).

Ethics Statement

Ethical approval for malaria samples collection was assented by the Togolese Ministry of Health's Bioethics Committee following the institutional ethical guidelines by the Ethics Committee at the National Institute of Parasitic Diseases, Chinese Center for Disease Control and Prevention, as reported previously (Kassegne et al., 2020). Informed consent was sought from all participants or their parents or guardians. Information obtained from all the participants were kept confidential.

Patient Samples and Microscopic Examination

Lomé, Agou-Gadzépé, and Atakpamé inhabitants usually access regional hospitals, polyclinics, and community health centers experienced in the management of malaria cases for treatment and medical attention. Blood samples were collected from *Centre Médico-Social de Doumassessé* and *Clinique Chirurgicale Martin Luther-King*, Lomé; *Centre Médico-Social Notre Dame de la Consolation d'Agbonou Campement*, Atakpamé; and *Hôpital Bethesda d'Agou Nyogbo* and *Centre Hospitalier Préfectoral d'Agou Gare*, Agou in September 2017 to December 2019. Individuals diagnosed by microscopic examination were referred to our study and samples were collected from those who consented to the study. The end of specimen collection was not determined by any factor other than the defined period of the study.

Sample collection involved febrile and suspected malaria cases including asymptomatic individuals, aged between 3 months and 70 years old. Clinical malaria patients were subjects who presented themselves to health facilities with fever or a history of fever (oral $\geq$ 37°C, rectal $\geq$ 38°C) in the last 24 h and were confirmed for Pf infection by microscopy (parasite density ranging from 2,500 to 1,000,000 asexual parasites/μl). Suspected malaria cases were persons who complained of fever of less than 2 days or having a history of fever, diagnosed either negative or positive by microscopy, and received treatment with antimalarial drugs.

Finger prick/venipuncture blood samples were obtained from individuals who received parasitological diagnosis at the health facilities, using the Giemsa-stained thick blood smear microscopic examination under × 1,000 magnification. Asexual stages of malaria parasites were counted per 200 leukocytes and, parasite density was calculated as the number of parasites per microliter by assuming a fixed leukocyte count of 8,000 cells/μl of blood. The thick film was considered positive when malaria parasites were present and negative if no parasites were seen after 500 leukocytes were counted. A total of 810 blood samples were collected including 610 Pf confirmed cases and 199 microscopy-negative cases. Except one Pm case that was detected by microscopy, no infection case of other *Plasmodium* species or case of coinfection of *Plasmodium* species was recorded from microscopy. All participants that were positive for malaria after diagnosis by parasitological blood smear test were treated with antimalarial drugs according to the national malaria programme guidelines.

Blood Sampling and DNA Extraction

Fresh whole blood and serum samples were collected and sampled as dried blood spots (DBSs) and dried serum spots (DSSs) on Whatman FTA and 903 Protein Saving Cards (GE Healthcare, NJ, United States), respectively, according to the instructions of the manufacturer. They were then packed in transparent zip-lock airtight plastic bags with silica gel desiccant to ensure quality of spots storage. Genomic DNA was extracted from the blood samples applied to FTA Cards using the QIAGEN DNeasy Blood and Tissue Kit (Qiagen, Germany) according to the instructions of the manufacturer and as reported by Chen et al. (2017) and Shen et al. (2018). Approximately 100 μl of blood from 12 punched-out circles of 3-mm (1/8 inch) diameter each were used per filter spot. Negative controls were also included to ensure lack of contamination. A final volume of 100-μl DNA template was eluted after extraction, followed by concentration measurement using a NanoDrop ND-2000 Spectrophotometer (Thermo Fisher Scientific, NH, United States) for downstream processing.

Polymerase Chain Reaction Amplification

T100 Thermal Cycler (BioRad, CA, United States) was used to perform nested PCR amplification of *Plasmodium* species ssrRNA genes with primers as reported previously (Zhou et al., 2014). For first-round nested PCR amplification, 2 μl of extracted genomic DNA template was added to a 25-μl PCR mixture, consisting of 0.4 M of each genus-specific primer (rPLU1 and rPLU5), 12.5 μl of 2 × Taq PCR MasterMix (Tiangen, China), which contains 0.1 U of Taq polymerase/μl, 500 μM deoxynucleotide triphosphates (dNTP), 3 mM $MgCl_2$, 100 mM KCl, 20 mM Tris-HCl, and pH 8.3. Amplification of DNA targets was carried out under conditions as follows: 94°C for 5 min, 35 cycles of (94°C for 30 s, 58°C for 30 s, and 72°C for 2 min), followed by a final extension at 72°C for 10 min. Two microliters of the first PCR product were used for the second-round amplification, with conditions and concentrations identical to those used for the first, except that rPLU3 and rPLU4 were used as inner primers (**Table 1**) and amplification was performed at 40 cycles. The size of the amplicons using outer and inner primers during the first and nested PCRs are about 1,600–1,700 and 235 bp, respectively. These primers are genus specific and therefore, can amplify target sequences of the five species of *Plasmodium* parasites that regularly infect humans (**Table 1**). The first nested PCR products were used as templates for the next species-specific nested PCR amplification under the same conditions. Negative control reaction was performed in each amplification reaction. In addition, positive controls consisting of the 3D7 strain of Pf and Pv isolates from the China–Myanmar border (Yunnan Province, China), which were preserved in our laboratory, were also used.

Sequencing and Analysis of DNA Targets

Two percent agarose gel electrophoresis of the PCR products was performed followed by GoldView staining and visualized under UV light using Molecular Imager Gel Doc XR$^+$ Imaging System (BioRad, CA, United States). All positive results of *Plasmodium*-infected cases were confirmed again through direct sequencing of the second round nested-PCR products by the BGI Company (China), using nested primers. Sequencing reads were imported into the EditSeq module of Lasergene-Ver7.1[1] to construct ssrRNA gene sequences of the nested-PCR products, which were then blasted at https://blast.ncbi.nlm.nih.gov/. Partial sequences of *18S ribosomal RNA* genes of the Togo isolates were aligned with those of other *Plasmodium* isolates obtained from blast analysis, using the ClustalW method (EMBL-EBI, Hixton and Cambridge, United Kingdom) of MEGA-Ver7.0[2] to generate a phylogenetic tree based on the neighbor-joining method (Uwase et al., 2020).

Analysis of Sensitivity, Specificity, and Predictive Values

Sensitivity and specificity are characteristics of a diagnostic test. Sensitivity is the probability that a diagnostic test indicates "disease" among those with the disease. Specificity is the fraction of those without disease who have a negative test result. Thus, sensitivity and specificity analyses for the tested population were performed as follows:

$$\text{Sensitivity} = \frac{\text{True Positive}}{\text{True Positive} + \text{False Negative}} \times 100$$

$$\text{Specificity} = \frac{\text{True Negative}}{\text{True Negative} + \text{False Positive}} \times 100$$

In addition, from a clinical perspective, in order to estimate the chance that a person with a positive diagnostic test truly has the disease or the probability that a person with a negative test does not have the disease, positive and negative predictive values (PPV and NPV, respectively) were also calculated for the population

[1]https://lasergene.software.informer.com/7.1

[2]http://mega.software.informer.com/7.0/

TABLE 1 | Primer sequences used in this study for PCR detection of malaria parasites.

PCR reaction—*Plasmodium* spp.	Primers	Primer sequences (5′–3′)	Amplicon size (bp)
Nested I—Genus specific	rPLU1	TCAAAGATTAAGCCATGCAAGTGA	1,600–1,700
	rPLU5	CCTGTTGTTGCCTTAAACTTC	
Nested II—Genus specific	rPLU3	TTTTTATAAGGATAACTACGGAAAAGCTGT	235
	rPLU4	TACCCGTCATAGCCATGTTAGGCCAATACC	
Nested II—*P. vivax*	rVIV1	CGCTTCTAGCTTAATCCACATAACTGATAC	121
	rVIV2	ACTTCCAAGCCGAAGCAAAGAAAGTCCTTA	
Nested II—*P. falciparum*	rFAL1	TTAAACTGGTTTGGGAAAACCAAATATATT	206
	rFAL2	ACACAATGAACTCAATCATGACTACCCGTC	
Nested II—*P. ovale*	rOVA1	ATCTCTTTTGCTATTTTTTAGTATTGGAGA	226
	rPLU2	ATCTAAGAATTTCACCTCTGACATCTG	
Nested II—*P. malariae*	rMAL1	ATAACATAGTTGTACGTTAAGAATAACCCC	145
	rMAL2	AAAATTCCCATGCATAAAAATTATACAAA	
Nested II—*P. knowlesi*	Pmk8	GTTAGCGAGAGCCACAAAAAAGCGAAT	153
	Pmkr9	ACTCAAAGTAACAAAATCTTCCGTA	

bp, base pairs; PCR, polymerase chain reaction.

that was tested in this study.

$$\text{Positive Predictive Value} = \frac{\text{True Positive}}{\text{True Positive} + \text{False Positive}} \times 100$$

$$\text{Negative Predictive Value} = \frac{\text{True Negative}}{\text{True Negative} + \text{False Negative}} \times 100$$

RESULTS

A total of 810 blood specimens were collected in this study. Following the diagnosis results (hereinafter referred to as test results) with Giemsa-stained thick blood smear microscopic examination, we obtained 611 positive malaria cases [referred to as microscopy-positive group (MPG)] including 610 cases of Pf and one case of Pm, while the remaining 199 cases were tested malaria negative and were referred to as the microscopy-negative group (MNG). The use of *Plasmodium* genus-specific nested PCR identified 565 malaria-positive cases including 536 and 29 cases from the MPG and MNG groups, respectively. In other words, nested PCR confirmed 536 out of 611 (87%) cases that were true positive from the MPG and identified 29/199 (14.6%) malaria cases that were found negative (**Table 2**) in the MNG. Such a finding reveals that there were 75/245 false-positive cases (30.6% error in species diagnosis) in the MPG and 29/565 (5.1%) undiagnosed cases in the MNG. This was reflected in the sensitivity and specificity values obtained (94.9 and 69.4%, respectively), suggesting that the test missed 5% of the people who had malaria and 31% of the people tested positive for the disease which they did not have. Such errors in microscopic test might be related to inadequacy of precision in parasite-based diagnosis by microscopy or low parasitemia conditions. In conjunction, PPV and NPV for the population tested in this study were 87.7 and 85.4%, respectively (**Table 2**). Clinically speaking, this implies that among the people who tested positive, the chance that a person with a positive diagnostic test truly has the disease was 88% and among those who tested negative, the probability that a person with a negative test does not has the disease was 85%.

Further species-specific nested PCR and species confirmation through direct sequencing of the nested-PCR products identified higher infection rate [95.5% (540/565)] for Pf than those for other species, which were 0.5% (3/565) for Po and 0.4% (2/565) for Pm. In addition, 20 cases were coinfection cases of Pf and Po [2.7% (15/565)] and Pf and Pm [0.9% (5/565)] (**Table 3**). However, there was no malaria case of Pv or Pk found in this study (**Figure 2**).

Phylogenetic relationships of unique sequences that were amplified were constructed on the basis of similarities with published homologous sequences from different countries based on neighbor-joining analysis of the *18S rRNA* locus. Phylogenetic analysis of the fragments of *18S SSu rRNA* gene sequences of the sample cases tested in this study showed species specificity and clustered with homologous sequences of isolates of *Plasmodium* species from different countries (**Figure 3**). Gene sequences of malaria samples that were used for the phylogenetic analysis were deposited in the National Center for Biotechnology Information (NCBI), under GenBank accession numbers [MW490726, MW492389, MW492390, MW492391, and MW504628 (Pf); MW492393 and MW492394 (Po); MW492392 and MW504627 (Pm)].

DISCUSSION

Togo, an integral part of tropical Africa where malaria is endemic, has its entire population at risk of malaria infection and disease transmission occurs all year round (World Health Organization [WHO], 2018a; Kassegne et al., 2020, 2021). Sustainable efforts have been engaged to reduce malaria burden in Togo; however, effective disease control toward elimination requires novel and innovative approaches among which diagnostics, monitoring, and surveillance are of capital importance (Chen et al., 2012; Kassegne et al., 2016, 2019).

Microscopic analysis is currently being used as the appropriate test for routine clinical diagnosis of malaria, especially in low-income settings. However, the sensitivity of the detection of malaria parasites by microscopy is approximately 50–200 parasites/μl of blood (Mbanefo and Kumar, 2020). Molecular tests are very sensitive to detect *Plasmodium* species, and a number of studies demonstrated that PCR is more reliable than microscopy in detecting malaria parasites in infected individuals, especially in those with low parasite density (Roper et al., 1996; Singh et al., 1996; Zhou et al., 2014). While the population tested in this study only focused on the southern Togo, the findings revealed disease prevalence (69.8%) higher than that reported

TABLE 2 | Sensitivity, specificity, and predictive values of diagnosis for the population tested in this study.

	Test result (microscopic test)	True condition (PCR test)	
	Total (number)	**Diseases (number)**	**Non-Diseases (number)**
Positive (number)	$T_{\text{Test Positive}}$ (611)	True Positive (536)	False Positive (75)
Negative (number)	$T_{\text{Test Negative}}$ (199)	False Negative (29)	True Negative (170)
	Total (810)	T_{Disease} (565)	$T_{\text{Non-Disease}}$ (245)
Sensitivity (94.9%*), Specificity (69.4%*), PPV (87.7%), NPV: 85.4%			

T, total.

**Sensitivity and specificity percentages of the diagnostic test compared with PCR.*

TABLE 3 | *Plasmodium* species identified in 565 malaria patients from high transmission areas in southern Togo, 2017–2019.

	Microscopy positive		Microscopy negative	
	P. falciparum	*P. malariae*		
	610	1	199	
PCR-based species specific	**536**		**29**	**T_{number} (%)**
P. falciparum	514	0	26	540 (95.5)
P. ovale	0	0	3	3 (0.5)
P. malariae	1	1	0	2 (0.4)
P. falciparum/P. ovale	15	0	0	15 (2.7)
P. falciparum/P. malariae	5	0	0	5 (0.9)

T, total.

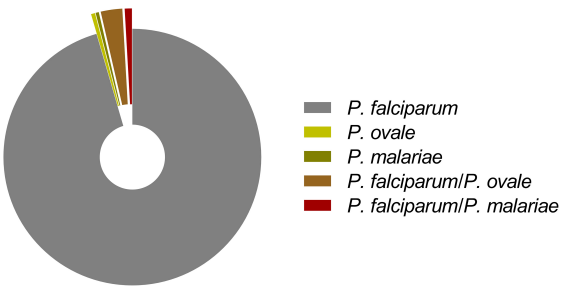

FIGURE 2 | Distribution of *Plasmodium* species identified in 565 malaria infections from high-transmission areas in southern Togo, 2017–2019.

(25.5–55.1%) for the entire country (World Health Organization [WHO], 2018a). Microscopic examination had 94.9% sensitivity and 69.4% specificity, showing that the test missed 120 of the people who had malaria, and one-third of the people tested positive for the disease, which they did not have, respectively. Similar observations of misdiagnosed malaria cases by microscopy have also been reported from a molecular survey of febrile cases in malaria-endemic areas along the China–Myanmar border (Zhou et al., 2014). In this study, the test showed sensitivity aligning onto that generally estimated (95%), whereas its specificity was relatively lower (69.4%) than expected (98%) as reviewed in a recent study (Mbanefo and Kumar, 2020). That is to say, the microscopic diagnosis for this study population tested people false positive for the disease they did not have. These misdiagnoses could be attributed to lack of precision and expertise in identifying species of malaria parasites, low parasite density conditions, or inadequate staining/poorly maintained microscopes. Such an interpretation is consistent with the fact that the subset of microscopy-positive PCR-negative specimens were recorded for low parasitemia from individuals who have been under antimalarial medication. Since 2005, the Togo National Malaria Control Programme has recommended two different formulations of artemisinin-based combination therapy (ACT), artesunate–amodiaquine (ASAQ) and artemether-lumefantrine (AL), for the treatment of uncomplicated malaria as well as for the treatment of unconfirmed malaria (World Health Organization [WHO], 2018a). In other words, the same care is given irrespective of whether a falciparum or unconfirmed malaria diagnosis is made. In addition, given that routine microscopic diagnosis usually does fall short in identifying other species of *Plasmodium* than Pf, no specific drugs effective against ovale relapse or malariae infection have been reported being used in Togo. Thus, the potential misdiagnosis of malaria parasite species by microscopy does not affect current treatment standards but, instead, has important implications in malaria epidemiology because it would identify individuals without disease but for whom the test indicates "disease" or individuals who test positive for a disease which they do not have. This may prompt resistance to artemisinin or delay in parasite clearance as patients would have been given inappropriate treatment to their ailments. Another public health consequence would be that untreated patients could become carriers for malaria transmission in areas where disease diagnosis may be already "problematic".

PCR-based molecular methods are able to detect malaria cases that are "truly positive" as well as those with mixed infections of *Plasmodium* parasites (Snounou et al., 1993b; Zhou et al., 2014). In this study, nested PCR was very specific and helped detect different monospecies of malaria cases or cases of mixed infections that were not diagnosed by microscopy. Among the five known species of *Plasmodium* that infect humans, Pf infection (and to a lesser extent Po and Pm) is the essential cause of malaria burden in tropical Africa (World Health Organization [WHO], 2018b). In West Africa, both Po and Pm malaria cases have been identified in Benin, Ghana, and Senegal (Browne et al., 2000; Roucher et al., 2014; Trape et al., 2014; Doritchamou et al., 2018), as well as Po in Cote d'Ivoire and Comoros Islands (Bauffe et al., 2012), to mention a few. However, there have been no information publicly reported yet on Po and Pm from Togo. In this study, Pf was the most prevalent *Plasmodium* species detected (95.5%) among the sample cases, aligning onto the evidence that Pf is always highly endemic in West African countries because the region usually experiences long periods of rainy reason which enhances perennial or semiperennial *Anopheles* breeding sites. We, also detected low infection rates of both ovale and malariae cases (0.5 and 0.4%, respectively). The detection of these two "bashful" malaria parasites in such a Pf-endemic area is consistent with previous studies from West Africa, which reported that Po and Pm are often associated with Pf infections, especially in areas where falciparum is highly endemic (Mueller et al., 2007; Roucher et al., 2014). However, the Po and Pm infection rates found in this study were much lower than those reported from studies in other West African countries [e.g., 15.5% Po and 10.4% Pm infections in a community-based survey in Ashanti Region of Ghana (Browne et al., 2000); 9.2% Pm and 5.8% Po infections in a cohort in Beninese pregnant women (Doritchamou et al., 2018), or 2.5% Po and 12.2% Pm infections in a longitudinal study in Dielmo Village, Senegal (Roucher et al., 2014)]. The large-scale cohorts conducted over the years in such malarious areas might explain the high infection rates observed for both Po and Pm. Furthermore, there was evidence that Po and Pm are sympatric with Pf across the African continent and are frequently present as coinfections

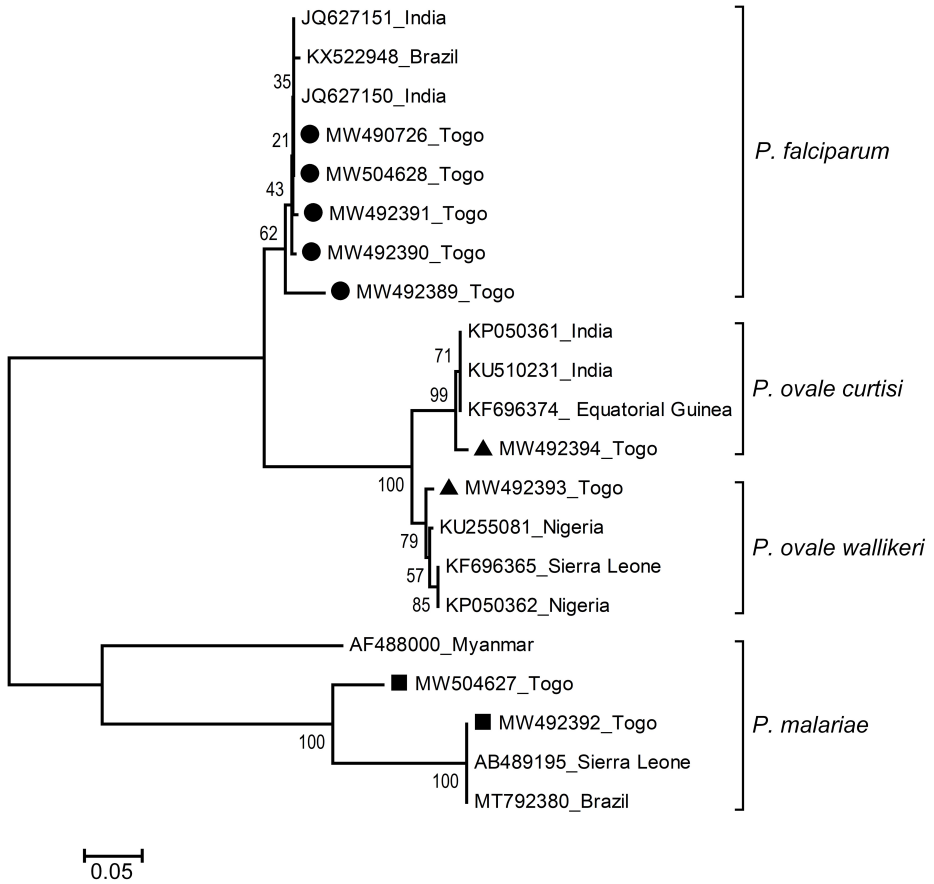

FIGURE 3 | Genetic and geographical relationships of *Plasmodium* species from high-transmission areas in southern Togo based on the *18S rRNA* locus. The relationships were inferred by a neighbor-joining analysis of *18S SSu rRNA* partial gene sequences of *Plasmodium* species isolates from different countries. The numbers on the branches are percent bootstrapping values from 1,000 replicates. Each sequence of *Plasmodium* species is identified by its accession number and geographical location (country). Gene sequences of the present study are highlighted (black circles for Pf, black triangles for Po, and black rectangles for Pm). Scale bar indicates nucleotide substitutions per site.

(Fancony et al., 2012). Low-level infection rate with Po or Pm seems to be common across tropical Africa in areas where malaria is endemic and often as complex mixed infections with Pf. The rate of Pf coinfections with Po or Pm was reported to be about 24% in the rainforest area of Ghana (Browne et al., 2000), while the proportion was much lower in other parts of West Africa such as Dielmo Village, Senegal (7.9% Pf/Pm and 1.1% Pf/Po mixed infections) (Roucher et al., 2014) or among Beninese pregnant women (6.6% Pf/Pm and 2.3% Pf/Po mixed infections) (Doritchamou et al., 2018). The low mixed infection rates that we observed in this study may be related to that all the samples were mainly collected in urban areas. However, we found infection rates of coinfection cases for both Po and Pm with Pf higher than the rates for single Po or Pm infection cases. This was consistent with previous findings from Ghana where it has been found that cases infected with Pf are more likely to carry Po or Pm than those who were not infected with Pf (Browne et al., 2000). Such a finding suggests evidence for interactions between Pm or possibly Po, with Pf infections (Mueller et al., 2007).

A series of comprehensive studies have investigated Pf in different parts of tropical Africa where malaria is endemic. However, morbidity associated with Po and Pm infections has received relatively little attention and was, therefore, markedly underestimated and unreported because they are generally regarded as a benign cause of malaria. Such interpretations could be attributed to the following reasons: (i) low incidence of the disease, (ii) lack or rarity of severe cases as they are regarded less important to Pf in terms of public health issues, or (iii) practical difficulties in microscopic identification as Po and Pm share morphological characteristics resembling those of Pf (young ring forms of the three species may be difficult to distinguish in thick blood films, especially during coinfections) (Roucher et al., 2014). Thus, in malaria-endemic areas of tropical Africa including Togo, most of all malaria attacks are erroneously attributed to Pf, probably due to underdiagnoses of Po and Pm clinical attacks. This study showed evidence of Po and Pm coexistence with Pf in southern Togo. More so, ovale or malariae malaria would have already been diagnosed by microscopy as falciparum malaria due to similarities in symptoms and species morphology.

PCR-based diagnostic tests of clinical cases are therefore required for accurate species discrimination and detection.

Although considered "mild," Po and Pm may constitute an important cause of morbidity and high risk of mortality. For example, fever episodes related to parasitemia peaks of Pm (in Liberia and The Gambia) or Po (in Senegal), in both children and adults have been reported (Miller, 1958; Greenwood et al., 1987; Faye et al., 2002). Also, Pm can cause chronic infections that can persist in the host for many years and reoccur after living in endemic areas (Siala et al., 2005); e.g., a chronic nephrotic syndrome that, once established, does not respond to treatment and carries a high rate of mortality (Mueller et al., 2007). Po shares peculiarity with Pv to form the latent stage in the liver—hypnozoite, which causes late relapse of the parasite, with new febrile episodes (after months or years) without recent exposures (Coldren et al., 2007). The reinforcement of malaria control policies for accurate diagnosis of parasites species in Togo should be, therefore, prioritized, to ensure deployment of appropriate treatment regimen for malaria patients and to provide a better knowledge on epidemiological assessments to guide control interventions.

CONCLUSION

This study publicly reports, for the first time, a molecular survey of malaria infections in Togo and also reveals the presence of other species of malaria parasites—Po and Pm, which were not previously reported. In addition, findings from this study indicated errors in microscopic examination including error in species diagnosis and undiagnosed cases. For example, in this study population, one-third of the people were microscopically tested positive for the disease they did not have. Thus, overlaps of different species of malaria could further aggravate the disease burden in Togo if appropriate actions are not taken, especially in situations where diagnosis of monospecies of malaria cases seems already "problematic." Collectively, this preliminary study advanced our understanding of the malaria epidemiology in southern Togo and provided information to improve disease control/surveillance policy. However, large-scale studies across the whole country are required in the future to assess malariae and ovale malaria epidemiology.

DATA AVAILABILITY STATEMENT

The datasets presented in this study can be found in online repositories. The names of the repository/repositories and accession number(s) can be found below: https://www.ncbi.nlm.nih.gov/, MW490726, MW492389, MW492390, MW492391, MW504628, MW492393, MW492394, MW492392, and MW504627.

ETHICS STATEMENT

Permission was obtained from all malaria subjects before collecting the specimens. Blood collection was made under a study protocol reviewed and approved by the Togo Ministry of Health's Bioethics Committee (Authorization N°019/2019/MSHP/CBRS), following institutional ethical guidelines by the Ethics Committee at the National Institute of Parasitic Diseases, Chinese Center for Disease Control and Prevention, as reported previously (Kassegne et al., 2020).

AUTHOR CONTRIBUTIONS

KK and J-HC conceptualized the study. KK, KA, KN, and KKK collected and analyzed the specimens. KK, S-WF, and KKK conducted the experiments. KK interpreted the data and wrote the manuscript. EMA, X-KG, and X-NZ revised the manuscript critically for intellectual content. All authors contributed to the article and approved the submitted version.

FUNDING

This work was, in part, financially supported by the Young Faculty Start-up Project Fund of Shanghai Jiao Tong University (Grant No. 21X010501074), the Intradisciplinary Platform Fund of Shanghai Jiao Tong University (Grant No. 20200927), the National Key Research and Development Program of China (Grant Nos. 2018YFE0121600 and 2016YFC1202000), and the National Sharing Service Platform for Parasite Resources (Grant No. TDRC-2019-194-30). The sponsor played no roles in the study design or in the collection, analysis, or interpretation of the data, in writing the report, or in the decision to submit the article for publication.

ACKNOWLEDGMENTS

We are grateful to the Ministry of Health of Togo for giving the permission to conduct this study and to Mrs. Emidzo Teteh Tedokou and Gatigbene Bomboma for their help in collecting clinical samples. We would also thank the health centers including *Centre Médico-Social de Doumassessé*, Lomé; *Clinique Chirurgicale Martin Luther-King*, Lomé; *Centre Médico-Social Notre Dame de la Consolation d'Agbonou Campement*, Atakpamé; *Hôpital Bethesda d'Agou Nyogbo, Agou*; and *Centre Hospitalier Préfectoral d'Agou Gare*, Agou for allowing us to collect the malaria samples.

REFERENCES

Agabani, H. M., el Hag, I. A., el Toum, I. A., Satti, M., and el Hassan, A. M. (1994). Fluorescence microscopy using a light microscope fitted with an interference filter for the diagnosis of malaria. *Trans. R. Soc. Trop. Med. Hyg.* 88:61. doi: 10.1016/0035-9203(94)90501-0

Bakai, T. A., Thomas, A., Iwaz, J., Atcha-Oubou, T., Tchadjobo, T., Khanafer, N., et al. (2020). Changes in registered malaria cases and deaths in Togo

from 2008 to 2017. *Int. J. Infect. Dis.* 101, 298–305. doi: 10.1016/j.ijid.2020.10.006

Bauffe, F., Desplans, J., Fraisier, C., and Parzy, D. (2012). Real-time PCR assay for discrimination of *Plasmodium ovale curtisi* and *Plasmodium ovale wallikeri* in the Ivory Coast and in the Comoros Islands. *Malar. J.* 11:307. doi: 10.1186/1475-2875-11-307

Browne, E. N., Frimpong, E., Sievertsen, J., Hagen, J., Hamelmann, C., Dietz, K., et al. (2000). Malariometric update for the rainforest and savanna of Ashanti region, Ghana. *Ann. Trop. Med. Parasitol.* 94, 15–22.

Chen, J. H., Wang, H., Chen, J. X., Bergquist, R., Tanner, M., Utzinger, J., et al. (2012). Frontiers of parasitology research in the People's Republic of China: infection, diagnosis, protection and surveillance. *Parasit. Vectors* 5:221. doi: 10.1186/1756-3305-5-221

Chen, S. B., Wang, Y., Kassegne, K., Xu, B., Shen, H. M., and Chen, J. H. (2017). Whole-genome sequencing of a *Plasmodium vivax* clinical isolate exhibits geographical characteristics and high genetic variation in China-Myanmar border area. *BMC Genomics* 18:131. doi: 10.1186/s12864-017-3523-y

Coldren, R. L., Jongsakul, K., Vayakornvichit, S., Noedl, H., and Fukudas, M. M. (2007). Apparent relapse of imported *Plasmodium ovale* malaria in a pregnant woman. *Am. J. Trop. Med. Hyg.* 77, 992–994.

Direction Générale de la Statistique et de la Compatibilité Nationale (2010). Quatrième Recensement Général de la Population et de l'Habitat 2010. Lomé: Direction Générale de la Statistique et de la Compatibilité Nationale.

Doritchamou, J. Y. A., Akuffo, R. A., Moussiliou, A., Luty, A. J. F., Massougbodji, A., Deloron, P., et al. (2018). Submicroscopic placental infection by non-falciparum *Plasmodium* spp. *PLoS Negl. Trop. Dis.* 12:e0006279. doi: 10.1371/journal.pntd.0006279

Encyclopædia Britannica, Inc. (2021). *Encyclopædia Britannica*. Chicago, IL: Encyclopædia Britannica, Inc.

Fancony, C., Gamboa, D., Sebastiao, Y., Hallett, R., Sutherland, C., Sousa-Figueiredo, J. C., et al. (2012). Various pfcrt and pfmdr1 genotypes of *Plasmodium falciparum* cocirculate with *P. malariae*, *P. ovale* spp., and *P. vivax* in northern Angola. *Antimicrob. Agents Chemother.* 56, 5271–5277. doi: 10.1128/AAC.00559-12

Faye, F. B., Spiegel, A., Tall, A., Sokhna, C., Fontenille, D., Rogier, C., et al. (2002). Diagnostic criteria and risk factors for *Plasmodium ovale* malaria. *J. Infect. Dis.* 186, 690–695. doi: 10.1086/342395

Greenwood, B. M., Bradley, A. K., Greenwood, A. M., Byass, P., Jammeh, K., Marsh, K., et al. (1987). Mortality and morbidity from malaria among children in a rural area of The Gambia, West Africa. *Trans. R. Soc. Trop. Med. Hyg.* 81, 478–486. doi: 10.1016/0035-9203(87)90170-2

Kassegne, K., Abe, E. M., Chen, J. H., and Zhou, X. N. (2016). Immunomic approaches for antigen discovery of human parasites. *Expert Rev. Proteomics* 13, 1091–1101. doi: 10.1080/14789450.2016.1252675

Kassegne, K., Abe, E. M., Cui, Y. B., Chen, S. B., Xu, B., Deng, W. P., et al. (2019). Contribution of *Plasmodium* immunomics: potential impact for serological testing and surveillance of malaria. *Expert Rev. Proteomics* 16, 117–129. doi: 10.1080/14789450.2019.1554441

Kassegne, K., Komi Koukoura, K., Shen, H. M., Chen, S. B., Fu, H. T., Chen, Y. Q., et al. (2020). Genome-wide analysis of the malaria parasite *Plasmodium falciparum* isolates from Togo reveals selective signals in immune selection-related antigen genes. *Front. Immunol.* 11:552698. doi: 10.3389/fimmu.2020.552698

Kassegne, K., Zhang, T., Chen, S. B., Xu, B., Dang, Z. S., Deng, W. P., et al. (2017). Study roadmap for high-throughput development of easy to use and affordable biomarkers as diagnostics for tropical diseases: a focus on malaria and schistosomiasis. *Infect. Dis. Poverty* 6, 130. doi: 10.1186/s40249-017-0344-9

Kassegne, K., Zhou, X. N., and Chen, J. H. (2021). Editorial: vectors and vector-borne parasitic diseases: infection, immunity, and evolution. *Front. Immunol.* 12:729415. doi: 10.3389/fimmu.2021.729415

Mbanefo, A., and Kumar, N. (2020). Evaluation of malaria diagnostic methods as a key for successful control and elimination programs. *Trop. Med. Infect. Dis.* 5, 102. doi: 10.3390/tropicalmed5020102

Miller, M. J. (1958). Observations on the natural history of malaria in the semi-resistant West African. *Trans. R. Soc. Trop. Med. Hyg.* 52, 152–168. doi: 10.1016/0035-9203(58)90036-1

Mueller, I., Zimmerman, P. A., and Reeder, J. C. (2007). Plasmodium malariae and *Plasmodium ovale*—the "bashful" malaria parasites. *Trends Parasitol.* 23, 278–283. doi: 10.1016/j.pt.2007.04.009

Programe National de Lutte contre le Paludisme, PNLP (2019). *Rapport Annuel 2018*. Lomé: Programme National de Lutte contre le Paludisme.

Programme National de Lutte contre le Paludisme, PNLP (2018). *Plan Stratégique National de Lutte contre le Paludisme 2017–2022*. Lomé: Programme National de Lutte contre le Paludisme.

Roper, C., Elhassan, I. M., Hviid, L., Giha, H., Richardson, W., Babiker, H., et al. (1996). Detection of very low level *Plasmodium falciparum* infections using the nested polymerase chain reaction and a reassessment of the epidemiology of unstable malaria in Sudan. *Am. J. Trop. Med. Hyg.* 54, 325–331. doi: 10.4269/ajtmh.1996.54.325

Roucher, C., Rogier, C., Sokhna, C., Tall, A., and Trape, J. F. (2014). A 20-year longitudinal study of *Plasmodium ovale* and *Plasmodium malariae* prevalence and morbidity in a West African population. *PLoS One* 9:e87169. doi: 10.1371/journal.pone.0087169

Shen, H. M., Chen, S. B., Cui, Y. B., Xu, B., Kassegne, K., Abe, E. M., et al. (2018). Whole-genome sequencing and analysis of *Plasmodium falciparum* isolates from China-Myanmar border area. *Infect. Dis. Poverty* 7, 118. doi: 10.1186/s40249-018-0493-5

Siala, E., Khalfaoui, M., Bouratbine, A., Hamdi, S., Hili, K., and Aoun, K. (2005). [Relapse of *Plasmodium malariae* malaria 20 years after living in an endemic area]. *Presse Med.* 34, 371–372. doi: 10.1016/s0755-4982(05)83926-0

Singh, B., Cox-Singh, J., Miller, A. O., Abdullah, M. S., Snounou, G., and Rahman, H. A. (1996). Detection of malaria in Malaysia by nested polymerase chain reaction amplification of dried blood spots on filter papers. *Trans. R. Soc. Trop. Med. Hyg.* 90, 519–521. doi: 10.1016/s0035-9203(96)90302-8

Singh, B., Kim Sung, L., Matusop, A., Radhakrishnan, A., Shamsul, S. S., Cox-Singh, J., et al. (2004). A large focus of naturally acquired *Plasmodium knowlesi* infections in human beings. *Lancet* 363, 1017–1024. doi: 10.1016/S0140-6736(04)15836-4

Snounou, G., Viriyakosol, S., Zhu, X. P., Jarra, W., Pinheiro, L., do Rosario, V. E., et al. (1993c). High sensitivity of detection of human malaria parasites by the use of nested polymerase chain reaction. *Mol. Biochem. Parasitol.* 61, 315–320. doi: 10.1016/0166-6851(93)90077-b

Snounou, G., Pinheiro, L., Goncalves, A., Fonseca, L., Dias, F., Brown, K. N., et al. (1993a). The importance of sensitive detection of malaria parasites in the human and insect hosts in epidemiological studies, as shown by the analysis of field samples from Guinea Bissau. *Trans. R. Soc. Trop. Med. Hyg.* 87, 649–653. doi: 10.1016/0035-9203(93)90274-t

Snounou, G., Viriyakosol, S., Jarra, W., Thaithong, S., and Brown, K. N. (1993b). Identification of the four human malaria parasite species in field samples by the polymerase chain reaction and detection of a high prevalence of mixed infections. *Mol. Biochem. Parasitol.* 58, 283–292. doi: 10.1016/0166-6851(93)90050-8

Snounou, G., and Singh, B. (2002). Nested PCR analysis of *Plasmodium parasites*. *Methods Mol. Med.* 72, 189–203. doi: 10.1385/1-59259-271-6:189

Thomas, A., Bakai, T. A., Atcha-Oubou, T., Tchadjobo, T., and Voirin, N. (2020). Implementation of a malaria sentinel surveillance system in Togo: a pilot study. *Malar. J.* 19:330. doi: 10.1186/s12936-020-03399-y

Togo Confidentiel (2021). *Togo: Info & Service–Division Administrative*. Available online at: http://www.togo-confidentiel.com/texte/Info&Service/Divisions_admin (accessed April 30, 2021).

Trape, J. F., Tall, A., Sokhna, C., Ly, A. B., Diagne, N., Ndiath, O., et al. (2014). The rise and fall of malaria in a West African rural community, Dielmo, Senegal, from 1990 to 2012: a 22 year longitudinal

study. *Lancet Infect. Dis.* 14, 476–488. doi: 10.1016/S1473-3099(14)70712-1

Uwase, J., Chu, R., Kassegne, K., Lei, Y., Shen, F., Fu, H., et al. (2020). Immunogenicity analysis of conserved fragments in *Plasmodium ovale* species merozoite surface protein 4. *Malar. J.* 19:126. doi: 10.1186/s12936-020-03207-7

World Health Organization [WHO] (2015). *Global Technical Strategy for Malaria, 2016–2030*. Geneva: World Health Organization.

World Health Organization [WHO] (2018b). *World Malaria Report 2018*. Geneva: World Health Organization.

World Health Organization [WHO] (2018a). *Malaria Profile in Togo 2018*. Geneva: World Health Organization.

Zhou, X., Huang, J. L., Njuabe, M. T., Li, S. G., Chen, J. H., and Zhou, X. N. (2014). A molecular survey of febrile cases in malaria-endemic areas along China-Myanmar border in Yunnan province, People's Republic of China. *Parasite* 21:27. doi: 10.1051/parasite/2014030

Conflict of Interest: The authors declare that the research was conducted in the absence of any commercial or financial relationships that could be construed as a potential conflict of interest.

Publisher's Note: All claims expressed in this article are solely those of the authors and do not necessarily represent those of their affiliated organizations, or those of the publisher, the editors and the reviewers. Any product that may be evaluated in this article, or claim that may be made by its manufacturer, is not guaranteed or endorsed by the publisher.

frontiers in Microbiology

REVIEW
published: 08 February 2022
doi: 10.3389/fmicb.2021.719334

One Health Paradigm to Confront Zoonotic Health Threats: A Pakistan Prospective

Nafeesa Yasmeen[1,2†], Abdul Jabbar[3†], Taif Shah[3], Liang-xing Fang[1,2], Bilal Aslam[4], Iqra Naseeb[5], Faiqa Shakeel[5], Hafiz Ishfaq Ahmad[6], Zulqarnain Baloch[2] and Yahong Liu[1,2]*

[1] National Risk Assessment Laboratory for Antimicrobial Resistance of Animal Original Bacteria, South China Agricultural University, Guangzhou, China, [2] Guangdong Provincial Key Laboratory of Veterinary Pharmaceutics Development and Safety Evaluation, South China Agricultural University, Guangzhou, China, [3] Faculty of Life Science and Technology, Kunming University of Science and Technology, Kunming, China, [4] Department of Microbiology, Government College University, Faisalabad, Pakistan, [5] Institute of Applied Microbiology, University of Veterinary and Animal Sciences, Punjab, Pakistan, [6] Department of Animal Breeding and Genetics, University of Veterinary and Animal Sciences, Punjab, Pakistan

OPEN ACCESS

Edited by:
Sibao Wang, Institute of Plant Physiology and Ecology, Shanghai Institutes for Biological Sciences, Chinese Academy of Sciences (CAS), China

Reviewed by:
Krishna Prasad Acharya, Department of Livestock Services, Nepal
Lloyd Reeve-Johnson, University of the Sunshine Coast, Australia
Peter MacGarr Rabinowitz, University of Washington, United States

***Correspondence:**
Yahong Liu
lyh@scau.edu.cn

† These authors have contributed equally to this work

Specialty section:
This article was submitted to Infectious Agents and Disease, a section of the journal Frontiers in Microbiology

Received: *02 June 2021*
Accepted: *21 December 2021*
Published: *08 February 2022*

Citation:
Yasmeen N, Jabbar A, Shah T, Fang L-x, Aslam B, Naseeb I, Shakeel F, Ahmad HI, Baloch Z and Liu Y (2022) One Health Paradigm to Confront Zoonotic Health Threats: A Pakistan Prospective. Front. Microbiol. 12:719334. doi: 10.3389/fmicb.2021.719334

The emergence and re-emergence of zoonotic diseases significantly impact human health, particularly those who live in impoverished areas and have close contact with domestic or wild animals. Nearly 75% of zoonotic diseases are transmitted directly from animals to humans or indirectly *via* vector/agent interactions between animals and humans. Growing populations, globalization, urbanization, and the interaction of the environment with humans and livestock all play roles in the emergence and spread of zoonotic diseases. "One Health" is a multidisciplinary concept aimed at improving human, animal, and environmental health, but this concept is not widely accepted in developing countries. In Pakistan, environmental, human, and animal health are severely affected due to a lack of sufficient resources. This review article provides an overview of the most common zoonotic diseases found in Pakistan and emphasizes the importance of the "One Health" concept in managing these diseases. Given the current situation, interdisciplinary research efforts are required to implement and sustain effective and long-term control measures in animal, human, and environmental health surveillance and accurate diagnostic methods.

Keywords: zoonotic disease, One Health, human, livestock, Pakistan

INTRODUCTION

Zoonotic diseases (zoonoses) are caused by microbes that are naturally transmitted from animals to humans. The ongoing occurrence of zoonoses pose significant threats to public health since nearly 60% of all infectious diseases are zoonotic and animal origins account for 75% of emerging transmissible infections (Mangili et al., 2016; Supramaniam et al., 2018; Espinosa et al., 2020). Zoonotic diseases are most commonly spread through direct contact from animals to humans or indirect contact (**Figure 1**) *via* vector/agent interactions (McArthur, 2019). Global environmental changes, increased populations, urbanization, animal migration, and tourism all play roles in the emergence of zoonotic diseases (Rahman et al., 2020). The "One Health" initiative that has been

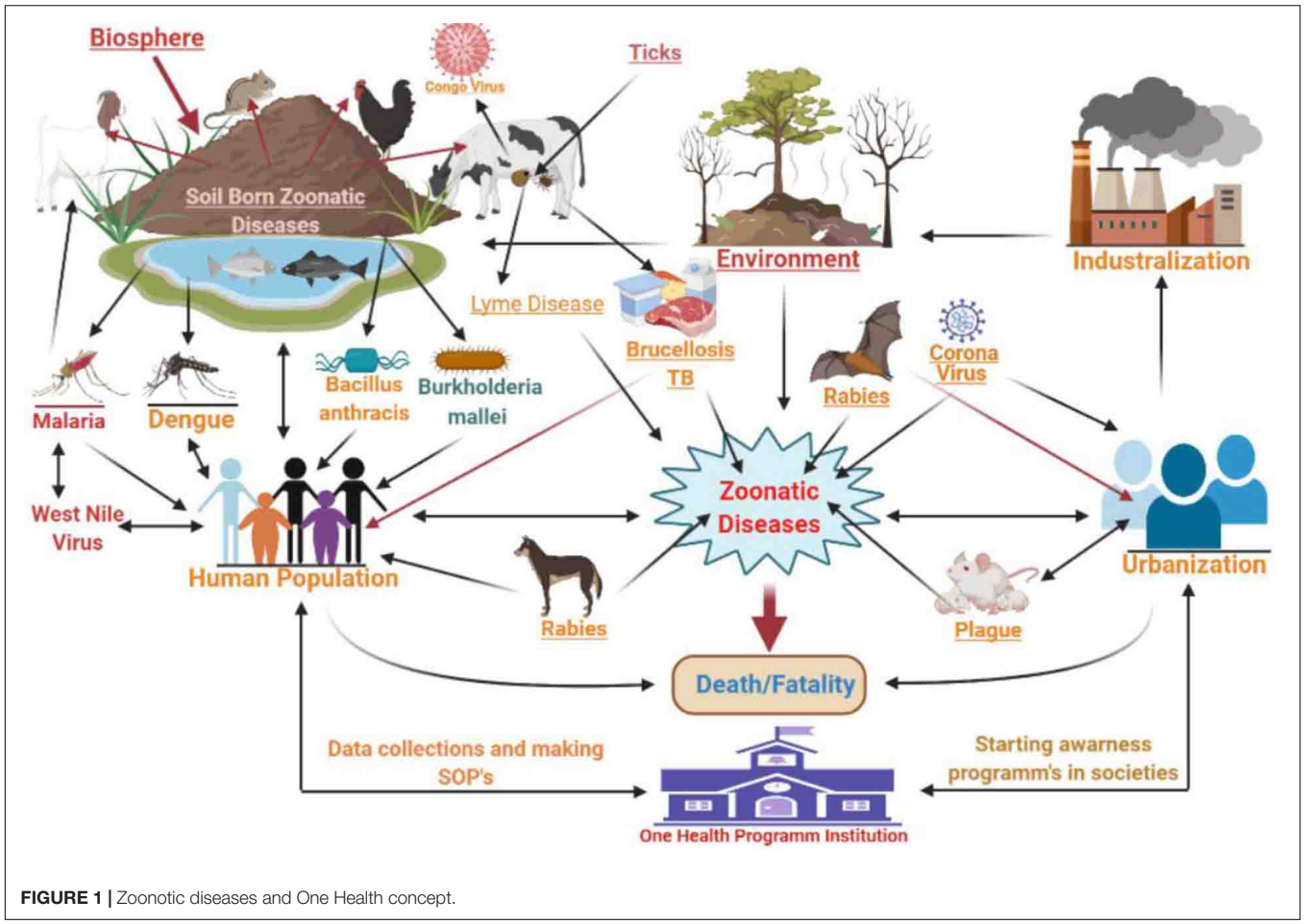

FIGURE 1 | Zoonotic diseases and One Health concept.

adopted by most industrialized countries allows for different sectors to collaborate in an effort to improve health outcomes. The goals are to promote and encourage a global health network by refining effective collaboration, cooperation, and contribution at the human-animal-environmental interface (McEwen and Collignon, 2018; Barton, 2019).

Pakistan is located near the Arabian Sea in South Asia and has the world's sixth-largest population (208 million) (Pakistan Bureau of Statistics [PBS], 2017). Pakistan's livestock population exceeds 300 M that includes 83 M large and 103 M small ruminants and 147 M poultry (Central Intelligence Agency [CIA], 2016). Regional conflicts in Afghanistan over the past 4 decades have resulted in massive refugee movements from Afghanistan to Pakistan (World Health Organization [WHO], 2004). Pakistan has a diverse natural topography, climate, and a wide range of domestic and wild animal species (Turnbull, 2008). Similarly, climate change, ecosystem diversity, poverty, social inequality, regional conflicts, and lack of a political will can all disrupt disease surveillance systems and public health (Ashraf et al., 2014).

The "One Health" concept has yet to be widely accepted in developing countries including Pakistan, where the prevalence of infectious diseases and hazardous biological materials has significantly negatively affected the environment and human and animal welfare. For example, a WHO report in 2017 documented >800 cases of Chikungunya virus infections in humans across Pakistan (World Health Organization [WHO], 2017). Similarly, Crimean–Congo Hemorrhagic Fever (CCHF) infected 63 people in Pakistan resulting in 11 fatalities (Altmann et al., 2019). Interactions between humans, animals, and the environment provide opportunities for pathogenic microbes to spread in any direction. Government institutions including the Ministries of Climate Change, Education, Industry and Food Safety as well as numerous non-governmental organizations (NGO) are responsible for designing and implementing innovative and practical strategies to control or prevent zoonotic diseases in Pakistan (Bartges et al., 2017). The current review provides an overview of the most common zoonotic diseases in Pakistan, and we focused on the importance of government and private sector collaborations to mitigate zoonotic threats according to the "One Health" concept.

An Overview of Zoonotic Diseases in Pakistan

In Pakistan, common zoonotic diseases include tuberculosis (TB), rabies, encephalitis, Lyme disease, CCHF, foot and

mouth disease, Brucellosis, Q fever, Leishmaniosis, Chagas disease/Trypanosomiasis, Balantidiasis, avian influenza, *Giardia*, and anthrax (**Table 1**; Feng and Xiao, 2011; Shabbir et al., 2015; Yousaf et al., 2018; Ahmed et al., 2020b; Iqbal et al., 2020a). Soil-borne zoonotic pathogens such as *Bacillus anthracis* and *Burkholderia mallei* have been reported in humans and animals in Punjab province (Shabbir et al., 2015). Moreover, DNA-based studies have revealed that *B. anthracis* has a high prevalence in Pakistan (Shabbir et al., 2015).

A significant proportion of human TB infections throughout the 19th and 20th centuries were caused by *Mycobacterium bovis* and raw cow milk consumption (Jafar et al., 2014). The large Pakistani livestock population is well-adapted to local environmental conditions and the source of 1.6 M tons of meat annually. Bovine TB infections are devastating for cattle (Jafar et al., 2014) and can transmitted to humans *via* aerosols in coughs, sneezes, or raw cow milk consumption. Pakistan ranks fifth among countries with a high TB burden (Shah et al., 2017) with 510,000 new TB cases emerging annually. For instance, a study of 3 primary abattoirs in Peshawar city that included lung and liver tissue samples from 121 buffaloes and 30 cattle indicated the presence of *M. bovis* in 4 cattle and 17 buffaloes with an overall prevalence of 10.18 and 11.53%, respectively (Jafar et al., 2014). This high prevalence of bovine TB was linked to a lack of preventive treatments, but the presence of the diseased animals in abattoirs indicates a lack of quality veterinary inspection and monitoring for the prevention and control of animal TB. Proper inspection and monitoring should be implemented to improve the quality of animal meat and to prevent TB transmission from diseased animals to humans.

Rabies virus belongs to the Rhabdoviridae family and is one of the deadliest single-stranded RNA viruses that infect both humans and warm-blooded mammals. These infections are most prevalent in bats, dogs, and raccoons, and these species spread the infection to humans. There are 5 million cases reported annually and 50,000 fatalities due to dog bites (World Health Organization [WHO], 2018). According to the National Rabies Control Program of Pakistan (NRCP), many rural areas in Pakistan are still at high risk of rabies and 54.7% of dogs that bit humans were not vaccinated against rabies (Noureen, 2018). In addition, another report indicated that 70 canine bite victims are treated in public and private hospitals daily. Therefore, the total incidence of rabies is likely in the range of 9 million (World Health Organization [WHO], 2018).

Multiple dengue outbreaks have been reported from different regions of Pakistan during the last three decades since the first outbreak was reported in 1994 (Khan and Khan, 2015; Abdullah et al., 2019; Junaidi, 2019; Fatima et al., 2021). In particular, the 2005 outbreak in Karachi involved >6000 cases and 52 fatalities In 2011, in Lahore there were >21,000 dengue cases and 350 fatalities (Junaidi, 2019), and in 2019, 44,415 people were affected and 66 died (Junaidi, 2019). Although the prevalence rate of the dengue virus has increased yearly, the overall mortality has decreased. This milestone has been achieved with the collaborative efforts of the WHO, local public and private institutions to promote screening, door-to-door surveillance, staff training, and to conduct organized awareness sessions with the public.

Salmonella Typhi causes typhoid fever and is commonly spread *via* contaminated water and food as well as through animal-to-human and person-to-person contact. Every year, 11–12 M typhoid cases are reported worldwide, and the estimated prevalence of typhoid fever is 451.7/100,000 (Ochiai et al., 2008). Therefore, there is a need for proper surveillance and monitoring strategies to control this disease (Fatima et al., 2021).

Bacillus anthracis causes anthrax and has a tremendous impact on animal health especially for cattle, sheep, and goats, and the infection is easily spread to humans. The likelihood of *B. anthracis* infections is greater in areas with many interactions between animals and humans such as slaughterhouses. An essential part of an effective disease surveillance program is animal vaccination and is needed for the prevention of future outbreaks.

Crimean–Congo Hemorrhagic Fever is one of Pakistan's most lethal tick-borne viral diseases and is characterized by fever and hemorrhage. Rapid climate change has resulted in an increased prevalence of CCHF in Pakistan due to increased industrialization, agricultural and occupational activities, and population density. Factors that contribute to CCHF spread include poor sanitation in farms, villages, and cities, the unsanitary transportation and slaughter of animals within cities, ineffective tick-control programs, nomadic lifestyles, and a lack of trained healthcare staff. CCHF is present in most major cities including Karachi, Quetta, Peshawar, and Multan, and its transmission in Pakistan is linked to a lack of an effective disease surveillance system (Yousaf et al., 2018). The general public, farmers, and healthcare workers should be educated about CCHF transmission and its consequences by local and provincial governments. Implementation of a disease surveillance system, preventive measures, detection, and treatment are all urgently required to control and eradicate this lethal disease from the country.

Potential Factors Necessary to Overcome Zoonotic Disease Prevalence in Pakistan

Surveillance of Disease Outbreaks

Zoonotic diseases are disseminated through animals, and disease outbreak surveillance helps to determine the cause, transmission, and pathogenesis and to guide prevention efforts (Supramaniam et al., 2018). Epidemiological surveillance is vital for population health management to determine associated risk factors responsible for disease persistence and spread. However, the collection of population-based data related to zoonotic disease prevalence in Pakistan is rare. Generally, hospital-based surveillance data has been used and indicates a high prevalence of numerous zoonotic diseases. Clinicians, epidemiologists, and specialists in environmental health and veterinary medicine can be brought together to formulate policies that address disease persistence. Awareness campaigns and vaccination programs that educate the general public should be instituted as well. Tools for programs such as these are included in the "One Health"

TABLE 1 | List of common zoonotic diseases in Pakistan.

Zoonotic disease	Symptoms in human	Source of transmission	Risk factors	References
Direct transmission/contamination				
Salmonellosis	Fever, abdominal pain, diarrhea, vomiting, nausea	contaminated food, water, livestock products, contact with infected animals	Poor living conditions, lack of hygiene	Altaf Hussain et al., 2020; Petrin et al., 2020
Anthrax	Fever, headache, chills, nausea, sore throat, swelling of the neck, hoarseness, painful swallowing, vomiting, diarrhea	*Bacillus anthracis*: a soil-borne bacteria, transmitted *via* herbivores, spores, or *via* an infected carcass		Ahmad et al., 2004; Doganay and Demiraslan, 2015; Kim et al., 2015; Moayeri et al., 2015; Saad-Roy et al., 2017; Kolton et al., 2019
Food-borne *E. coli* infection	Fever, diarrhea, vomiting, respiratory disorders	Contaminated water, food, livestock products, contact with infected animals	Living conditions, lack of hygiene	Bokhari et al., 2013; Ishaq et al., 2021
Hepatitis E	Fever, yellow skin, tiredness, vomiting, nausea, abdominal pain, loss of appetite, liver failure	Food and water contaminated with human sewage, eating uncooked pig meat	Living conditions, lack of hygiene	Bosan et al., 2010; Butt and Sharif, 2016
Leptospirosis	Fever, headache, nausea, loss of appetite, jaundice, swollen limbs, chest pain, shortness of breath, coughing blood	contaminated soil and water with animal urine	Skin lesions/injuries, occupational exposure	Ijaz et al., 2018; Sohail et al., 2018
Bovine TB	Fever, weakness, loss of appetite, weight loss, intermittent cough, diarrhea, large prominent lymph nodes	Contaminated water, food, livestock products, unpasteurized dairy products, direct contact with infected animals	Animal husbandry; living conditions; occupational exposure; wildlife reservoirs	Awah Ndukum et al., 2010; Jafar et al., 2014
Brucellosis	Fever, weight loss, abdominal pain, weakness, body ache	Contact with aborted fetuses, vaginal fluids, placenta, milk, urine, semen, feces	Occupational exposure, ingesting unpasteurized dairy products	Bilal et al., 2009; Garshasbi et al., 2014; Mohammadi and Golchin, 2018; Qin et al., 2019
Rabies	Encephalitis, hyper-excitability, hydrophobia, motor neuron weakness, and paralysis	Animal bites (for example, dogs)	Free-roaming dogs, rarely pets	Ondrejková et al., 2015; Jackson, 2018; Singh and Ahmad, 2018; World Health Organization [WHO], 2018; Dascalu et al., 2019; Torquato et al., 2020
Vector-borne diseases				
Leishmaniosis	Fever, cutaneous leishmaniosis: skin lesions, weight loss, spleen, liver enlargement	Leishmania parasite transmission *via* female phlebotomine sandfly bite which feeds on blood; 70 animal species are natural reservoirs, including humans	Environmental changes, urbanization, malnutrition, people migration, unhygienic lifestyle, poor health status, poverty	Tiwananthagorn et al., 2012; Khan et al., 2016; Kämink et al., 2019
Chikungunya	Fever, joint pain/swelling, headache, muscle pain, skin rashes	This virus is maintained in the environment between humans, animals, and mosquitoes	Aedes mosquitoes transmit the chikungunya virus from infected to healthy people.	Ali and Dasti, 2018
Crimean-Congo hemorrhagic fever	Fever, myalgia, dizziness, neck pain/stiffness, headache, backache, nausea, vomiting, diarrhea, abdominal pain, sore throat, confusion, sleepiness, liver enlargement, petechial rash, liver failure	Tick bites, contact with infected livestock	Occupational exposure, human migration	Yousaf et al., 2018; Hatami et al., 2019; Kasi et al., 2020
Rift Valley Fever	Range from mild flu-like symptoms to severe hemorrhagic fever	Contact with infected livestock blood/organs, mosquito bites, unpasteurized milk	Occupational exposure	Atif et al., 2012
Foot and mouth disease	Fever, sore throat, pain, loss of appetite, red lesions on the tongue, gums, rashes on the palms, soles, buttocks, irritability in infants and toddlers	Cloven-hoofed animals, such as domestic and wild Bovidae, cattle, sheep, swine, humans	Small ruminants like sheep and goats can spread the virus	Ur-Rehman et al., 2014; Dubie and Amare, 2020

system mapping and analysis resource toolkit (Breslin et al., 2017; Brown and Nading, 2019; Iqbal et al., 2020a). In addition, routine surveillance or the continuous declaration or reporting of diseases related to public health can also play an important role in preventing zoonotic diseases (George et al., 2020). Pakistan is an agricultural country, so it is also necessary to determine the prevalence and risks associated with new zoonotic pathogens in soil, plants, vegetables, and fruits and to have formulated an action plan for their prevention (Ahmed et al., 2017).

Environmental Change and the "One Health" Concept

Human expansion has increased atmospheric carbon emissions, resulting in an elevation of the global temperature that has disrupted normal lifecycles and ecosystems. Urbanization has accelerated the close contact of humans with animals such as squirrels, mice, jackals, foxes, and pigs. These are favorable circumstances for the emergence or re-emergence of zoonotic diseases (Sleeman et al., 2019). Deforestation and the loss of ecosystem diversity, air pollution from crop and coal combustion, melting ice due to global warming, extremes of temperature, over-population, increased humidity and temperatures, and decreased food production are having catastrophic effects on the natural diversity of the environment. These conditions also aid zoonotic pathogen survival and spread (El-Sayed and Kamel, 2020; Majeed and Munir, 2020). For instance, humidity and temperature directly influence the spread of the coronavirus through aerosols and the virus can be found in an active state for at least 2 weeks on most surfaces (Lin et al., 2020).

In Pakistan, inadequate infectious waste management is a major source of contamination in communities and facilitates infectious disease dissemination on a wide scale. Many hospitals and industries do not separate different types of waste materials such as chemicals, pulp, biologicals, textiles, and leather. These pollutants can act as carriers of hepatitis A and E, intestinal pathogens such as *Salmonella*, and acute respiratory disease pathogens (Rab et al., 1997; Qasim et al., 2014). The lack of proper industrial, hospital, farm, and household disposal can combine with natural events such as floods to contaminate drinking water supplies (Daud et al., 2017).

Enteric zoonotic diseases are often transmitted by the food chain and the environment (Klumb et al., 2020) such as bacteria residing in contaminated soil and surface waters (Vincent et al., 2019). Wildlife can also spread zoonotic pathogens to humans (Rothenburger et al., 2019). Disease burden is also tightly linked to poverty in Pakistan, and examples are dengue, *Vibrio cholera*, malaria, Lyme disease, COVID-19, influenza virus, respiratory syncytial virus, TB, and skin cancer (Baudouin et al., 2002; Patz et al., 2003; Khaliq et al., 2015; Velraj and Haghighat, 2020). Disease transmission due to the improper disposal of hazardous materials can be prevented, and this can begin at the community hospital level and successes can be used as examples for other areas including improvements for public trash disposal and limiting agricultural and industrial runoff (Ali, 2018; Hussain et al., 2020; Majeed and Munir, 2020). The "One Health" process has strategic plans that can be implemented to achieve these targets (Cunningham et al., 2017).

Animals and Food Safety

The prevalence of food-borne infections caused by *Listeria monocytogenes*, *Campylobacter* spp., *Salmonella* spp., *Toxoplasma gondii*, and Norovirus is common in Pakistan (Nisar et al., 2018). Furthermore, food is exposed to a variety of toxic chemicals during its preparation, processing, handling, and storage (Javed, 2016; Ishaq et al., 2021). Pakistan is one of the top milk and halal meat-producing states in the world, although the quality of these products is often not good. Therefore, diseases such as brucellosis and bovine TB begin at the farm level are transmitted during animal handling, milking, slaughtering, and processing (Claeys et al., 2013). The most successful method for improving milk production is pasteurization. Residual antibiotics as well as microbes and other contaminants in milk can be easily screened using Raman spectroscopic techniques (He et al., 2019). Pasteurization extends the shelf life of milk, and untreated or raw milk can contain infectious pathogens. Therefore, the latest milk production and processing techniques must be implemented on a country-wide basis to control milk-related zoonotic disease transmission in Pakistan.

Meat is a primary protein source and is consumed massively all over the world. The spread of food-borne illnesses such as Bovine Spongiform Encephalopathy (BSE), hepatitis, and typhoid has been linked to inappropriate meat processing (Ozawa, 2003; Javed, 2016), and standard operating procedures for farm and abattoir sanitation are necessary for healthy meat production. Environmental health practitioners play a crucial role in meat safety and the fulfillment of hygienic conditions. Food inspections are also required for meat labeled for export, and technologies like multiplex PCR for meat screening are relatively easy to implement (Iqbal et al., 2020b). All these safety procedures also apply to organic food production (Akbar et al., 2019). Safe meat for the consumer requires that quality standards are applied to animal handling, slaughtering, dressing, and storage (Ishaq et al., 2021).

Vectors and Their Controls

Climate change is a key player in the global spread of vector-borne diseases. According to WHO estimates, climate change will most likely cause 250,000 extra deaths annually due to malaria, malnutrition, heat stress, and diarrhea from 2030 to 2050. These climatic alterations result in heavy and unpredictable rainfalls, flooding, and high humidity, and all these are conducive for the propagation of disease vectors such as rodents, fleas, and mosquitoes (Ngeleja et al., 2017). Furthermore, air pollution from excessive gas emissions, the greenhouse effect, increased hydrocarbon combustion, and deforestation all contribute to a greater risk for zoonotic disease transmission (Rossati, 2017). Approximately half of the human population is at risk of vector-borne disease, and these diseases account for >17% of all infectious diseases and 1 M deaths worldwide each year. Increased temperature and humidity levels are linked to the surge in the prevalence of insect vector-borne diseases such as malaria, plaque, leishmaniosis, African trypanosomiasis, Japanese

encephalitis, and diseases of viral origin like Rift Valley Fever. Additionally, health professional negligence has also been cited as a contributing factor to increased disease prevalence (Fouque and Reeder, 2019).

Pakistan is vulnerable to the impacts of climate change. The exact figure of vector-borne diseases in Pakistan is unclear, although there are currently 1.5 million malaria cases in Pakistan and these levels are comparable to Somalia, Afghanistan, and Djibouti. Inadequate housing, water, sanitation, and limited access to health facilities are the most direct possible causes of the prevalence of vector-borne diseases in Pakistan. The re-emergence of Leishmaniosis caused by the female phlebotomine sand fly (Khan et al., 2019), CCHF acquired *via* tick bites (Altmann et al., 2019), and Rift Valley Fever *via* mosquito bites or consumption of unpasteurized milk (Fouque and Reeder, 2019) are the major causes for morbidity and mortality levels that can all be addressed by the "One Health" Initiative. New strategies and collaborations with health administrations, the environmental ministry, entomologists, zoologists, veterinarians, and NGOs can assist vector-borne zoonotic disease management in Pakistan (Bostan et al., 2017; Huang et al., 2019).

Importance of Health Education

Health education is the building block of "One Health" where its motto is to educate the public about their health. Factors such as malnourishment, food insecurity, poverty, crowding, late reporting of disease, and poor observance of sanitary treatment measures as well as lack of vaccination and contaminated drinking water are major obstacles in securing Pakistan's health security. In March 2002, 300 attorneys from 35 countries gathered to increase awareness and provide alertness related to environmental hazards and their effects on public health. Healthcare facilities should be updated in Pakistan, and awareness of these problems must be communicated through human resources to improve management systems particularly in rural areas (Ahmed and Shaikh, 2011). Information concerning food safety awareness and dietary guidelines to prevent zoonotic disease should be readily available to the general public. Further, policies for the improvement of farm production, sanitation, and food storage conditions should be implemented. Local authorities can develop collaborations with the Ministry of Health and Livestock for proper vaccination against zoonotic diseases, and overall, these measures will improve public health (Suk et al., 2003). This type of process would also assist in educating farmers and consumers in maintaining animal health. The focus on education is crucial because an understanding of a process is more likely to result in the acceptance of the values suggested by health services. But unfortunately, the Pakistani community is less likely to be aware of the basic issues due to a low literacy rate and a lack of understanding of how diseases spread and how these are connected with health parameters, socio-cultural and environmental problems, as well as political issues. Therefore, to overcome and halt this dangerous situation, it is necessary to adopt, enforce, and implement awareness campaigns especially related to health-seeking behavior and conduct in person surveys and develop assessment exercises with private and public sector collaborators (Shaikh and Hatcher, 2005; Zahid, 2018).

Population Density

The close association of humans and their livestock is linked to the transmission of zoonotic pathogens (Kilpatrick and Randolph, 2012; Suk et al., 2014), and these risks are elevated in areas where animals and humans share living areas (Nieto et al., 2012; Owczarczak-Garstecka, 2018) and those with inadequate sanitation facilities (Gayer et al., 2007; Warraich et al., 2011). When a disease has become established in a human population (Paterson et al., 2018; Braam et al., 2021), sedentary conditions in camps and informal settlements increase the risk of zoonotic pathogen transmission and population size and density affect a pathogen's ability to infect susceptible hosts (Brooker et al., 2004; Hammer et al., 2018). Strengthening the standards for improving hygiene and sanitation in local food markets will decrease the risk of zoonotic disease transmission. In market settings, policies for crowd control, physical distancing measures, and handwashing and sanitizing stations should be implemented and enforced.

Poverty and Socio-Economic Inequities

Poverty and socioeconomic inequalities are associated with poor health (Vincent, 2016; Khan and Hussain, 2020). Disasters and displacement affect access to education, employment, and lifestyle choices and exacerbates poverty (Du et al., 2018). Displaced populations are frequently subjected to structural discrimination, violence, and a lack of equitable access to services (Castañeda et al., 2015). Furthermore, displaced communities are frequently located in geographically marginalized areas with limited resources (McMichael et al., 1998). For example, communities along the Pakistan-Afghan border bear the brunt of vector-borne disease due to human displacement (Nieto et al., 2012). Numerous events should encourage dialogue and collaboration with local representatives, academics, policymakers, and medical practitioners. Seminars and conferences should be held in various cities to raise public awareness about disease prevention, protect and strengthen investments in health and unemployment insurance, make tax systems less regressive, safeguard worker rights, and expand medical care facilities.

Importance of Food and Water Safety and Its Hygiene Practices

Food is an important source of zoonotic disease. Zoonoses with a food-borne reservoir are typically caused by consuming food or contaminated water. Additionally, many zoonotic microbes exist in the gastrointestinal tracts of food-producing animals and poses a farm to fork risk of contamination. Therefore, food safety is a major concern for global public health (Gizaw, 2019) and pro-active strategies are required to mitigate the spread of these diseases (Chapman and Gunter, 2018; Ishaq et al., 2021). Food handling is a major factor in controlling the spread of food-borne diseases. It has always been challenging to control zoonotic diseases in countries (Ma et al., 2019), particularly Pakistan, where food is commonly sold in the streets under unsanitary conditions. Additionally, food safety knowledge in the general population is poor (Ma et al., 2019). These factors elevate the risk of zoonotic diseases such as the major pathogens *Salmonella*, *Campylobacter*, *Listeria*, *E. coli* O157:H7, *Bacillus cereus*, *and*

Clostridium (Lammie and Hughes, 2016; Samad et al., 2018). The "One Health" concept promotes the wellbeing of humans and animals including farm and wild animals. This concept can decrease the prevalence of most food-borne diseases by using the combined efforts of environmental health professionals.

Water is the most fundamental resource, and pure drinking water is one of the most important components for life (Pandey, 2006). Unsafe or contaminated water can expose animals and humans to pathogens and pollutants resulting in gastrointestinal, neurological, and reproductive disorders (Lee and Murphy, 2020). Most of the water resources in the world have been polluted due to urbanization, industrialization, and environmental changes (Pandey, 2006). Therefore, approximately 2.2 billion people are using unsafe drinking water in the world (World Health Organization [WHO], 2019).

Pakistan is a developing country located in South Asia. Urbanization, industrialization, and population growth have polluted water resources in Pakistan. Therefore, only 20% of the population has access to safe drinking water in Pakistan (Daud et al., 2017). In terms of potable water quality, Pakistan has been ranked 80th out of 122 countries. If water quality issues are not addressed, then a 60% potable water shortage may soon be confronted due to the mixing of community, sewerage, and industrial waste without treatment (Aziz, 2005; Azizullah et al., 2011; Bhowmik et al., 2015; Khalid et al., 2018; Ilyas et al., 2019). In 2020, 400+ schools were randomly tested in Pakistan to examine the quality of the water and >50% of the samples were contaminated with highly pathogenic microorganisms (Ahmed et al., 2020a). Another study reported that drinking water in Sibi district, Baluchistan was highly contaminated with fluoride and arsenic (Chandio et al., 2020). Contaminated or untreated water originating from agriculture is also a major issue in Pakistan (Shahid et al., 2020), and crops produced from contaminated water are not fit for human consumption. In Pakistan, water supplies have been adversely influenced by climate change, chemical and biological pollutants due to pipe cracks, poor sewage systems, and a lack of water quality control testing systems (Aziz, 2005). Governments and NGOs have adopted different rules and regulations to control the risk of water contamination such as the WASH interventions, Water and Sanitation Extension Programs (WASEP) projects, Oxfam GB, Quantitative Microbiological Risk Assessment (QMRA), Punjab Saaf Pani project, and the Changa Pani scheme (Nanan et al., 2003; Baig et al., 2012; Ahmed et al., 2020a,c; Als et al., 2020). WASEP projects are particularly enforced at the rural level to enhance or rectify water supplies for consumers (Nanan et al., 2003). Similarly, the NGO Oxfam GB is putting its efforts into evaluating major problems associated with the quality of potable water (Baig et al., 2012). In addition, the Punjab Saaf Pani and Changa Pani projects are contributing to the improvement of water quality in rural and urban areas (Ahmed et al., 2020c).

Organizations such as the Pakistan Environmental Protection Council (PEPC) and the Pakistan Environmental Protection Agency (Pak-EPA) are contributing their efforts to implementing protective standards such as the National Environmental Quality Standard (NEQS). The primary concern is how to perform technical assessments of water quality and provide microbiologically certified safe water by following the recommended procedures of the Environment, Health and Safety (EHS) ministry. Unfortunately, these organizations were unable to apply those environmental safety standards to all industrial and non-industrial sectors (Azizullah et al., 2011). This situation can be remedied by implementing suitable holistic solutions and legislation through proper monitoring systems in all national, local, and individual sectors.

CONCLUSION

Zoonotic diseases pose the largest challenge for developing countries because humans, animals, and the environment all play roles in their transmission. Pakistan faces huge challenges due to a lack of strategic planning for responses to zoonotic disease infections. The "One Health" strategy can assist governmental agencies such as the Ministries of Climate Change, Education, Industry and Production and Food Safety by collaborating with the private sector and NGOs to adopt innovative and practical plans to control or prevent zoonotic diseases in Pakistan. The environmental health and food supply chains require a "One Health" approach to deal with zoonotic diseases (Lammie and Hughes, 2016).

AUTHOR CONTRIBUTIONS

YL designed the study. NY, AJ, and ZB wrote the initial version of the manuscript. ZB, TS, L-XF, and BA revised the final draft of the manuscript. IN, FS, and HA searched the literature and designed the table and figure.

FUNDING

This study was supported by grants from "Guangdong Special Support Program innovation team 2019BT02N054" and the Major Science and Technology Special Project of Yunnan Province, No. 2019ZF004.

ACKNOWLEDGMENTS

We thank all the participants involved in this study.

REFERENCES

Abdullah, Ali, S., Salman, M., Din, M., Khan, K., Ahmad, M., et al. (2019). Dengue Outbreaks in Khyber Pakhtunkhwa (KPK), Pakistan in 2017: an Integrated Disease Surveillance and Response System (IDSRS)-Based Report. *Pol. J. Microbiol.* 68, 115–119. doi: 10.21307/pjm-2019-013

Ahmad, K., Kazi, B., Us-Saba, N., Ansari, J., and Nomani, K. (2004). Pakistan's experience of a bioterrorism-related anthrax scare. *East. Mediterr. Health J.* 10, 19–26.

Ahmed, H., Ali, S., Afzal, M. S., Khan, A. A., Raza, H., Shah, Z. H., et al. (2017). Why more research needs to be done on echinococcosis in Pakistan. *Infect. Dis. Poverty* 6, 1–5. doi: 10.1186/s40249-017-0309-z

Ahmed, J., and Shaikh, B. (2011). The state of affairs at primary health care facilities in Pakistan: where is the State's stewardship? *East. Mediterr. Health J.* 17, 619–623.

Ahmed, T., Hussain, S., Rinchen, S., Yasir, A., Ahmed, S., Khan, W. A., et al. (2020b). Knowledge, attitude and practice (KAP) survey of canine rabies in Khyber Pakhtunkhwa and Punjab Province of Pakistan. *BMC Public Health* 20:1293. doi: 10.1186/s12889-020-09388-9

Ahmed, J., Wong, L. P., Chua, Y. P., Channa, N., Mahar, R. B., Yasmin, A., et al. (2020a). Quantitative Microbial Risk Assessment of Drinking Water Quality to Predict the Risk of Waterborne Diseases in Primary-School Children. *Int. J. Environ. Res. Public Health* 17:2774. doi: 10.3390/ijerph17082774

Ahmed, T., Zounemat-Kermani, M., and Scholz, M. (2020c). Climate change, water quality and water-related challenges: a review with focus on Pakistan. *Int. J. Environ. Res. Public Health* 17:8518. doi: 10.3390/ijerph17228518

Akbar, A., Ali, S., Ahmad, M. A., Akbar, M., and Danish, M. (2019). Understanding the Antecedents of Organic Food Consumption in Pakistan: moderating Role of Food Neophobia. *Int. J. Environ. Res. Public Health* 16:4043. doi: 10.3390/ijerph16204043

Ali, I., and Dasti, J. I. (2018). Chikungunya virus; an emerging arbovirus in Pakistan. *J. Pak. Med. Assoc.* 68, 252–257.

Ali, M. (2018). Field lessons in surveying healthcare waste management activities in Pakistan. *East. Mediterr. Health J.* 25, 213–217. doi: 10.26719/emhj.18.024

Als, D., Meteke, S., Stefopulos, M., Gaffey, M. F., Kamali, M., Munyuzangabo, M., et al. (2020). Delivering water, sanitation and hygiene interventions to women and children in conflict settings: a systematic review. *BMJ Glob. Health* 5:e002064. doi: 10.1136/bmjgh-2019-002064

Altaf Hussain, M., Wang, W., Sun, C., Gu, L., Liu, Z., Yu, T., et al. (2020). Molecular Characterization Of Pathogenic *Salmonella* Spp From Raw Beef In Karachi, Pakistan. *Antibiotics* 9:73. doi: 10.3390/antibiotics9020073

Altmann, M., Nahapetyan, K., and Asghar, H. (2019). Identifying hotspots of viral haemorrhagic fevers in the Eastern Mediterranean Region: perspectives for the Emerging and Dangerous Pathogens Laboratory Network. *East. Mediterr. Health J.* 24, 1049–1057. doi: 10.26719/emhj.18.002

Ashraf, S., Chaudhry, H. R., Chaudhry, M., Iqbal, Z., Ali, M., Jamil, T., et al. (2014). Prevalence of common diseases in camels of Cholistan desert, Pakistan. *IUFS J. Biol.* 2, 49–52. doi: 10.1016/j.micpath.2017.04.011

Atif, F. A., Khan, M. S., Iqbal, H. J., Ali, Z., and Ullah, S. (2012). Prevalence of cattle tick infestation in three districts of the Punjab, Pakistan. *Pak. J. Sci.* 64, 49–53.

Awah Ndukum, J., Kudi, A. C., Bradley, G., Ane-Anyangwe, I. N., Fon-Tebug, S., and Tchoumboue, J. (2010). Prevalence of bovine tuberculosis in abattoirs of the littoral and Western highland regions of cameroon: a cause for public health concern. *Vet. Med. Int.* 2010:495015. doi: 10.4061/2010/495015

Aziz, J. (2005). Management of source and drinking-water quality in Pakistan. *EMHJ-East. Mediterr. Health J.* 11, 1087–1098.

Azizullah, A., Khattak, M. N. K., Richter, P., and Häder, D.-P. (2011). Water pollution in Pakistan and its impact on public health—a review. *Environ. Int.* 37, 479–497. doi: 10.1016/j.envint.2010.10.007

Baig, S. A., Xu, X., and Khan, R. (2012). Microbial water quality risks to public health: potable water assessment for a flood-affected town in northern Pakistan. *Rural Remote Health* 12:2196.

Bartges, J., Kushner, R. F., Michel, K., Sallis, R., and Day, M. (2017). One health solutions to obesity in people and their pets. *J. Comp. Pathol.* 156, 326–333. doi: 10.1016/j.jcpa.2017.03.008

Barton, B. C. (2019). Introduction. One Health: over a decade of progress on the road to sustainability. *Rev. Sci. Tech.* 38, 21–50. doi: 10.20506/rst.38.1.2939

Baudouin, C., Charveron, M., Tarroux, R., and Gall, Y. (2002). Environmental pollutants and skin cancer. *Cell Biol. Toxicol.* 18, 341–348. doi: 10.1023/a:1019540316060

Bhowmik, A. K., Alamdar, A., Katsoyiannis, I., Shen, H., Ali, N., Ali, S. M., et al. (2015). Mapping human health risks from exposure to trace metal contamination of drinking water sources in Pakistan. *Sci. Total Environ.* 538, 306–316. doi: 10.1016/j.scitotenv.2015.08.069

Bilal, C., Khan, M., Avais, M., Ijaz, M., and Khan, J. (2009). Prevalence and chemotherapy of Balantidium coli in cattle in the River Ravi region, Lahore (Pakistan). *Vet. Parasitol.* 163, 15–17. doi: 10.1016/j.vetpar.2009.04.023

Bokhari, H., Shah, M. A., Asad, S., Akhtar, S., Akram, M., and Wren, B. W. (2013). *Escherichia coli* pathotypes in Pakistan from consecutive floods in 2010 and 2011. *Am. J. Trop. Med. Hyg.* 88, 519–525. doi: 10.4269/ajtmh.12-0365

Bosan, A., Qureshi, H., Bile, K. M., Ahmad, I., and Hafiz, R. (2010). A review of hepatitis viral infections in Pakistan. *J. Pak. Med. Assoc.* 60, 1045–1058.

Bostan, N., Javed, S., Nabgha, E. A., Eqani, S. A., Tahir, F., and Bokhari, H. (2017). Dengue fever virus in Pakistan: effects of seasonal pattern and temperature change on distribution of vector and virus. *Rev. Med. Virol.* 27:e1899. doi: 10.1002/rmv.1899

Braam, D. H., Jephcott, F. L., and Wood, J. L. N. (2021). Identifying the research gap of zoonotic disease in displacement: a systematic review. *Glob. Health Res. Policy* 6:25. doi: 10.1186/s41256-021-00205-3

Breslin, G., Shannon, S., Haughey, T., Donnelly, P., and Leavey, G. (2017). A systematic review of interventions to increase awareness of mental health and well-being in athletes, coaches and officials. *Syst. Rev.* 6:177. doi: 10.1186/s13643-017-0568-6

Brooker, S., Mohammed, N., Adil, K., Agha, S., Reithinger, R., Rowland, M., et al. (2004). Leishmaniasis in refugee and local Pakistani populations. *Emerg. Infect. Dis.* 10, 1681–1684. doi: 10.3201/eid1009.040179

Brown, H., and Nading, A. M. (2019). Introduction: human animal health in medical anthropology. *Med. Anthropol. Q.* 33, 5–23. doi: 10.1111/maq.12488

Butt, A. S., and Sharif, F. (2016). Viral Hepatitis in Pakistan: past, Present, and Future. *Euroasian J. Hepatogastroenterol.* 6, 70–81. doi: 10.5005/jp-journals-10018-1172

Castañeda, H., Holmes, S. M., Madrigal, D. S., Young, M. E., Beyeler, N., and Quesada, J. (2015). Immigration as a social determinant of health. *Annu. Rev. Public Health* 36, 375–392.

Central Intelligence Agency [CIA] (2016). *The World Factbook*. Langley, Virginia: Central Intelligence Agency

Chandio, T. A., Khan, M. N., Muhammad, M. T., Yalcinkaya, O., Wasim, A. A., and Kayis, A. F. (2020). Fluoride and arsenic contamination in drinking water due to mining activities and its impact on local area population. *Environ. Sci. Pollut. Res.* 28, 1–14. doi: 10.1007/s11356-020-10575-9

Chapman, B., and Gunter, C. (2018). "Local food systems food safety concerns," in *Preharvest Food Safety*, eds S. Thakur and K. E. Kniel (Hoboken: John Wiley & Sons, Inc), 249–260. doi: 10.1128/microbiolspec.PFS-0020-2017

Claeys, W. L., Cardoen, S., Daube, G., De Block, J., Dewettinck, K., Dierick, K., et al. (2013). Raw or heated cow milk consumption: review of risks and benefits. *Food Control* 31, 251–262.

Cunningham, A. A., Daszak, P., and Wood, J. L. (2017). One Health, emerging infectious diseases and wildlife: two decades of progress? *Philos. Trans. R. Soc. B Biol. Sci.* 372:20160167. doi: 10.1098/rstb.2016.0167

Dascalu, M. A., Wasniewski, M., Picard-Meyer, E., Servat, A., Bocaneti, F. D., Tanase, O. I., et al. (2019). Detection of rabies antibodies in wild boars in north-east Romania by a rabies ELISA test. *BMC Vet. Res.* 15:466. doi: 10.1186/s12917-019-2209-x

Daud, M., Nafees, M., Ali, S., Rizwan, M., Bajwa, R. A., Shakoor, M. B., et al. (2017). Drinking water quality status and contamination in Pakistan. *Biomed Res. Int.* 2017:7908183. doi: 10.1155/2017/7908183

Doganay, M., and Demiraslan, H. (2015). Human anthrax as a re-emerging disease. *Recent Pat. Anti-Infect. Drug Discov.* 10, 10–29. doi: 10.2174/1574891x10666150408162354

Du, R. Y., Stanaway, J. D., and Hotez, P. J. (2018). Could violent conflict derail the London Declaration on NTDs? *PLoS Negl. Trop. Dis.* 12:e0006136. doi: 10.1371/journal.pntd.0006136

Dubie, T., and Amare, T. (2020). Isolation, Serotyping, and Molecular Detection of Bovine FMD Virus from Outbreak Cases in Aba'ala District of Afar Region, Ethiopia. *Vet. Med. Int.* 2020:8847728. doi: 10.1155/2020/8847728

El-Sayed, A., and Kamel, M. (2020). Climatic changes and their role in emergence and re-emergence of diseases. *Environ. Sci. Pollut. Res.* 27, 22336–22352. doi: 10.1007/s11356-020-08896-w

Espinosa, R., Tago, D., and Treich, N. (2020). Infectious diseases and meat production. *Environ. Resour. Econ.* 76, 1019–1044. doi: 10.1007/s10640-020-00484-3

Fatima, M., Kumar, S., Hussain, M., Memon, N. M., Vighio, A., Syed, M. A., et al. (2021). Morbidity and Mortality Associated with Typhoid Fever Among Hospitalized Patients in Hyderabad District, Pakistan, 2017-2018: retrospective Record Review. *JMIR Public Health Surveill.* 7:e27268. doi: 10.2196/27268

Feng, Y., and Xiao, L. (2011). Zoonotic potential and molecular epidemiology of Giardia species and giardiasis. *Clin. Microbiol. Rev.* 24, 110–140. doi: 10.1128/CMR.00033-10

Fouque, F., and Reeder, J. C. (2019). Impact of past and on-going changes on climate and weather on vector-borne diseases transmission: a look at the evidence. *Infect. Dis. Poverty* 8, 1–9. doi: 10.1186/s40249-019-0565-1

Garshasbi, M., Ramazani, A., Sorouri, R., Javani, S., and Moradi, S. (2014). Molecular detection of Brucella species in patients suspicious of Brucellosis from Zanjan, Iran. *Braz. J. Microbiol.* 45, 533–538. doi: 10.1590/s1517-83822014005000048

Gayer, M., Legros, D., Formenty, P., and Connolly, M. A. (2007). Conflict and emerging infectious diseases. *Emerg. Infect. Dis.* 13, 1625–1631.

George, J., Häsler, B., Mremi, I., Sindato, C., Mboera, L., Rweyemamu, M., et al. (2020). A systematic review on integration mechanisms in human and animal health surveillance systems with a view to addressing global health security threats. *One Health Outlook* 2, 1–15. doi: 10.1186/s42522-020-00017-4

Gizaw, Z. (2019). Public health risks related to food safety issues in the food market: a systematic literature review. *Environ. Health Prev. Med.* 24:68. doi: 10.1186/s12199-019-0825-5

Hammer, C. C., Brainard, J., and Hunter, P. R. (2018). Risk factors and risk factor cascades for communicable disease outbreaks in complex humanitarian emergencies: a qualitative systematic review. *BMJ Glob. Health* 3:e000647. doi: 10.1136/bmjgh-2017-000647

Hatami, H., Qaderi, S., and Omid, A. M. (2019). Investigation of Crimean-Congo hemorrhagic fever in patients admitted in Antani Hospital, Kabul, Afghanistan, 2017–2018. *Int. J. Prev. Med.* 10:117. doi: 10.4103/ijpvm.IJPVM_391_18

He, H., Sun, D.-W., Pu, H., Chen, L., and Lin, L. (2019). Applications of Raman spectroscopic techniques for quality and safety evaluation of milk: a review of recent developments. *Crit. Rev. Food Sci. Nutr.* 59, 770–793. doi: 10.1080/10408398.2018.1528436

Huang, Y.-J. S., Higgs, S., and Vanlandingham, D. L. (2019). Emergence and re-emergence of mosquito-borne arboviruses. *Curr. Opin. Virol.* 34, 104–109. doi: 10.1016/j.coviro.2019.01.001

Hussain, M., Butt, A. R., Uzma, F., Ahmed, R., Irshad, S., Rehman, A., et al. (2020). A comprehensive review of climate change impacts, adaptation, and mitigation on environmental and natural calamities in Pakistan. *Environ. Monit. Assess.* 192:48. doi: 10.1007/s10661-019-7956-4

Ijaz, M., Abbas, S. N., Farooqi, S. H., Aqib, A. I., Anwar, G. A., Rehman, A., et al. (2018). Sero-epidemiology and hemato-biochemical study of bovine leptospirosis in flood affected zone of Pakistan. *Acta Trop.* 177, 51–57. doi: 10.1016/j.actatropica.2017.09.032

Ilyas, M., Ahmad, W., Khan, H., Yousaf, S., Yasir, M., and Khan, A. (2019). Environmental and health impacts of industrial wastewater effluents in Pakistan: a review. *Rev. Environ. Health* 34, 171–186. doi: 10.1515/reveh-2018-0078

Iqbal, M., Fatmi, Z., and Khan, M. A. (2020a). Brucellosis in Pakistan: a neglected zoonotic disease. *JPMA J. Pak. Med. Assoc.* 70, 1625–1626. doi: 10.5455/JPMA.24139

Iqbal, M., Saleem, M. S., Imran, M., Khan, W. A., Ashraf, K., Yasir Zahoor, M., et al. (2020b). Single tube multiplex PCR assay for the identification of banned meat species. *Food Addit. Contam. Part B Surveill.* 13, 284–291. doi: 10.1080/19393210.2020.1778098

Ishaq, A. R., Manzoor, M., Hussain, A., Altaf, J., Rehman, S. U., Javed, Z., et al. (2021). Prospect of microbial food borne diseases in Pakistan: a review. *Braz. J. Biol.* 81, 940–953. doi: 10.1590/1519-6984.232466

Jackson, A. (2018). Rabies: a medical perspective. *Rev. Sci. Tech.* 37, 569–580. doi: 10.20506/rst.37.2.2825

Jafar, K., Sultan, A., Abd El-Salam, N. M., Riaz, U., and Taif, S. (2014). Prevalence of tuberculosis in buffalo and cattle. *J. Pure Appl. Microbiol.* 8, 721–726.

Javed, A. (2016). Food Borne Health issues and their relevance to Pakistani society. *Am. Sci. Res. J. Eng. Technol. Sci.* 26, 235–251.

Junaidi, I. (2019). *Dengue outbreak sets new record in Pakistan*. Pakistan: Dawn.

Kämink, S., Abdi, A., Kamau, C., Ashraf, S., Ansari, M. A., Qureshi, N. A., et al. (2019). Failure of an innovative low-cost, noninvasive thermotherapy device for treating cutaneous leishmaniasis caused by leishmania tropica in Pakistan. *Am. J. Trop. Med. Hyg.* 101, 1373–1379. doi: 10.4269/ajtmh.19-0430

Kasi, K. K., von Arnim, F., Schulz, A., Rehman, A., Chudhary, A., Oneeb, M., et al. (2020). Crimean-Congo haemorrhagic fever virus in ticks collected from livestock in Balochistan, Pakistan. *Transbound. Emerg. Dis.* 67, 1543–1552. doi: 10.1111/tbed.13488

Khalid, S., Shahid, M., Bibi, I., Sarwar, T., Shah, A. H., and Niazi, N. K. (2018). A review of environmental contamination and health risk assessment of wastewater use for crop irrigation with a focus on low and high-income countries. *Int. J. Environ. Res. Public Health* 15:895. doi: 10.3390/ijerph15050895

Khaliq, A., Khan, I., Akhtar, M., and Chaudhry, M. (2015). Environmental risk factors and social determinants of pulmonary tuberculosis in Pakistan. *Epidemiology* 5:201.

Khan, J., and Khan, A. (2015). Incidence of dengue in 2013: dengue outbreak in District Swat, Khyber Pakhtunkhwa, Pakistan. *Int. J. Fauna Biol. Stud.* 2, 1–7.

Khan, K., Wahid, S., and Khan, N. H. (2019). Habitat characterization of sand fly vectors of leishmaniasis in Khyber Pakhtunkhwa, Pakistan. *Acta Trop.* 199:105147. doi: 10.1016/j.actatropica.2019.105147

Khan, N. H., Bari, A. U., Hashim, R., Khan, I., Muneer, A., Shah, A., et al. (2016). Cutaneous leishmaniasis in Khyber Pakhtunkhwa province of Pakistan: clinical diversity and species-level diagnosis. *Am. J. Trop. Med. Hyg.* 95, 1106–1114. doi: 10.4269/ajtmh.16-0343

Khan, S. U., and Hussain, I. (2020). Inequalities in health and health-related indicators: a spatial geographic analysis of Pakistan. *BMC Public Health* 20:1800. doi: 10.1186/s12889-020-09870-4

Kilpatrick, A. M., and Randolph, S. E. (2012). Drivers, dynamics, and control of emerging vector-borne zoonotic diseases. *Lancet* 380, 1946–1955. doi: 10.1016/S0140-6736(12)61151-9

Kim, J., Gedi, V., Lee, S.-C., Cho, J.-H., Moon, J.-Y., and Yoon, M.-Y. (2015). Advances in anthrax detection: overview of bioprobes and biosensors. *Appl. Biochem. Biotechnol.* 176, 957–977. doi: 10.1007/s12010-015-1625-z

Klumb, C., Scheftel, J., and Smith, K. (2020). Animal agriculture exposures among Minnesota residents with zoonotic enteric infections, 2012–2016. *Epidemiol. Infect.* 148:e55. doi: 10.1017/S0950268819002309

Kolton, C. B., Marston, C. K., Stoddard, R. A., Cossaboom, C., Salzer, J. S., Kozel, T. R., et al. (2019). Detection of Bacillus anthracis in animal tissues using InBios

active anthrax detect rapid test lateral flow immunoassay. *Lett. Appl. Microbiol.* 68, 480–484. doi: 10.1111/lam.13134

Lammie, S. L., and Hughes, J. M. (2016). Antimicrobial resistance, food safety, and one health: the need for convergence. *Annu. Rev. Food Sci. Technol.* 7, 287–312. doi: 10.1146/annurev-food-041715-033251

Lee, D., and Murphy, H. M. (2020). Private Wells and Rural Health: groundwater Contaminants of Emerging Concern. *Curr. Environ. Health Rep.* 7, 129–139. doi: 10.1007/s40572-020-00267-4

Lin, S., Fu, Y., Jia, X., Ding, S., Wu, Y., and Huang, Z. (2020). Discovering Correlations between the COVID-19 Epidemic Spread and Climate. *Int. J. Environ. Res. Public Health* 17:7958. doi: 10.3390/ijerph17217958

Ma, L., Chen, H., Yan, H., Wu, L., and Zhang, W. (2019). Food safety knowledge, attitudes, and behavior of street food vendors and consumers in Handan, a third tier city in China. *BMC Public Health* 19:1128. doi: 10.1186/s12889-019-7475-9

Majeed, M. M., and Munir, A. (2020). Pakistan: country report on children's environmental health. *Rev. Environ. Health* 35, 57–63. doi: 10.1515/reveh-2019-0087

Mangili, A., Vindenes, T., and Gendreau, M. (2016). "Infectious risks of air travel," in *Infections of Leisure*, ed. D Schlossberg (Washington, DC: ASM Press), 333–344. doi: 10.1128/microbiolspec.IOL5-0009-2015

McArthur, D. B. (2019). Emerging Infectious Diseases. *Nurs. Clin. North Am.* 54, 297–311.

McEwen, S. A., and Collignon, P. J. (2018). "Antimicrobial resistance: a one health perspective," in *Antimicrobial Resistance in Bacteria from Livestock and Companion Animals*, eds S. Schwarz, L. M. Cavaco and J. Shen (Washington, DC: American Society for Microbiology), 521–547.

McMichael, A. J., Patz, J., and Kovats, R. S. (1998). Impacts of global environmental change on future health and health care in tropical countries. *Br. Med. Bull.* 54, 475–488. doi: 10.1093/oxfordjournals.bmb.a011702

Moayeri, M., Leppla, S. H., Vrentas, C., Pomerantsev, A. P., and Liu, S. (2015). Anthrax pathogenesis. *Annu. Rev. Microbiol.* 69, 185–208.

Mohammadi, E., and Golchin, M. (2018). Detection of Brucella abortus by immunofluorescence assay using anti outer membrane protein of 19 kDa antibody. *Adv. Clin. Exp. Med.* 27, 643–648. doi: 10.17219/acem/85081

Nanan, D., White, F., Azam, I., Afsar, H., and Hozhabri, S. (2003). Evaluation of a water, sanitation, and hygiene education intervention on diarrhoea in northern Pakistan. *Bull. World Health Organ.* 81, 160–165.

Ngeleja, R. C., Luboobi, L. S., and Nkansah-Gyekye, Y. (2017). The effect of seasonal weather variation on the dynamics of the plague disease. *Int. J. Math. Math. Sci.* 2017, 1–25. doi: 10.1016/j.mbs.2018.05.013

Nieto, N. C., Khan, K., Uhllah, G., and Teglas, M. B. (2012). The emergence and maintenance of vector-borne diseases in the khyber pakhtunkhwa province, and the federally administered tribal areas of pakistan. *Front. Physiol.* 3:250. doi: 10.3389/fphys.2012.00250

Nisar, M., Mushtaq, M. H., Shehzad, W., Hussain, A., Nasar, M., Nagaraja, K. V., et al. (2018). Occurrence of Campylobacter in retail meat in Lahore, Pakistan. *Acta Trop.* 185, 42–45. doi: 10.1016/j.actatropica.2018.04.030

Noureen, R. (2018). Knowledge, attitude and practice regarding rabies in rural area of Lahore. *Int. J. Sci. Eng. Res.* 9.

Ochiai, R. L., Acosta, C. J., Danovaro-Holliday, M. C., Baiqing, D., Bhattacharya, S. K., Agtini, M. D., et al. (2008). A study of typhoid fever in five Asian countries: disease burden and implications for controls. *Bull. World Health Organ.* 86, 260–268. doi: 10.2471/blt.06.039818

Ondrejková, A., Suli, J., Ondrejka, R., Slepecká, E., Prokeš, M., Čechvala, P., et al. (2015). Detection of rabies antibodies in dog sera. *Pol. J. Vet. Sci.* 18, 47–51. doi: 10.1515/pjvs-2015-0006

Owczarczak-Garstecka, S. (2018). Understanding risk in human–animal interactions. *Forced Migr. Rev.* 58, 78–80.

Ozawa, Y. (2003). Risk management of transmissible spongiform encephalopathies in Asia. *Rev. Sci. Tech.* 22, 237–249. doi: 10.20506/rst.22.1.1397

Pakistan Bureau of Statistics [PBS] (2017). *Provisional Summary Results of 6th Population and Housing Census–2017*. Islamabad: Pakistan Bureau of Statistics.

Pandey, S. (2006). Water pollution and health. *Kathmandu Univ. Med. J.* 4, 128–134.

Paterson, D. L., Wright, H., and Harris, P. N. A. (2018). Health Risks of Flood Disasters. *Clin. Infect. Dis.* 67, 1450–1454. doi: 10.1093/cid/ciy227

Patz, J., Githeko, A., McCarty, J., Hussein, S., Confalonieri, U., and De Wet, N. (2003). Climate change and infectious diseases. *Clim. Chang. Hum. Health Risks Responses* 6, 103–137.

Petrin, C. E., Steele, R. W., Margolis, E. A., Rabon, J. M., Martin, H., and Wright, A. (2020). Drug-Resistant *Salmonella* typhi in Pakistan. *Clin. Pediatr.* 59, 31–33. doi: 10.1177/0009922819881203

Qasim, M., Anees, M. M., and Bashir, A. (2014). Unhygienic water is the cause of water borne disease among villagers: a case of Gujrat-Pakistan. *World Appl. Sci. J.* 29, 1484–1491.

Qin, L., Nan, W., Wang, Y., Zhang, Y., Tan, P., Chen, Y., et al. (2019). A novel approach for detection of brucella using a real-time recombinase polymerase amplification assay. *Mol. Cell. Probes* 48:101451. doi: 10.1016/j.mcp.2019.101451

Rab, M. A., Bile, M. K., Mubarik, M. M., Asghar, H., Sami, Z., Siddiqi, S., et al. (1997). Water-borne hepatitis E virus epidemic in Islamabad, Pakistan: a common source outbreak traced to the malfunction of a modern water treatment plant. *Am. J. Trop. Med. Hyg.* 57, 151–157. doi: 10.4269/ajtmh.1997.57.151

Rahman, M., Sobur, M., Islam, M., Ievy, S., Hossain, M., El Zowalaty, M. E., et al. (2020). Zoonotic Diseases: etiology, Impact, and Control. *Microorganisms* 8:1405. doi: 10.3390/microorganisms8091405

Rossati, A. (2017). Global warming and its health impact. *Int. J. Occup. Environ. Med.* 8, 7–20.

Rothenburger, J. L., Himsworth, C. G., Nemeth, N. M., Pearl, D. L., Treuting, P. M., and Jardine, C. M. (2019). The devil is in the details—Host disease and co-infections are associated with zoonotic pathogen carriage in Norway rats (*Rattus norvegicus*). *Zoonoses Public Health* 66, 622–635. doi: 10.1111/zph.12615

Saad-Roy, C., Van den Driessche, P., and Yakubu, A.-A. (2017). A mathematical model of anthrax transmission in animal populations. *Bull. Math. Biol.* 79, 303–324. doi: 10.1007/s11538-016-0238-1

Samad, A., Abbas, F., Ahmad, Z., Pokryrshko, O., and Asmat, T. M. (2018). Prevalence of foodborne pathogens in food items in Quetta, Pakistan. *Pak. J. Zool.* 50, 1–4.

Shabbir, M. Z., Jamil, T., Muhammad, K., Yaqub, T., Bano, A., MIrza, A. I., et al. (2015). Prevalence and distribution of soil-borne zoonotic pathogens in Lahore district of Pakistan. *Front. Microbiol.* 6:917. doi: 10.3389/fmicb.2015.00917

Shah, T., Hayat, A., Jadoon, A., Ahmad, S., and Bahadar Khan, S. (2017). Molecular detection of multi drug resistant tuberculosis (MDR-TB) in MDR-TB patients' attendant in North Western Pakistan. *PAFMJ* 67, 982–987.

Shahid, M., Khalid, S., Murtaza, B., Anwar, H., Shah, A. H., Sardar, A., et al. (2020). A critical analysis of wastewater use in agriculture and associated health risks in Pakistan. *Environ. Geochem. Health* 1–20. doi: 10.1007/s10653-020-00702-3

Shaikh, B. T., and Hatcher, J. (2005). Health seeking behaviour and health service utilization in Pakistan: challenging the policy makers. *J. Public Health* 27, 49–54. doi: 10.1093/pubmed/fdh207

Singh, C., and Ahmad, A. (2018). Molecular approach for ante-mortem diagnosis of rabies in dogs. *Indian J. Med. Res.* 147, 513–516. doi: 10.4103/ijmr.IJMR_1705_15

Sleeman, J., Richgels, K., White, C., and Stephen, C. (2019). Integration of wildlife and environmental health into a One Health approach. *Rev. Sci. Tech.* 38, 91–102. doi: 10.20506/rst.38.1.2944

Sohail, M. L., Khan, M. S., Ijaz, M., Naseer, O., Fatima, Z., Ahmad, A. S., et al. (2018). Seroprevalence and risk factor analysis of human leptospirosis in distinct climatic regions of Pakistan. *Acta Trop.* 181, 79–83. doi: 10.1016/j.actatropica.2018.01.021

Suk, J. E., Van Cangh, T., Beauté, J., Bartels, C., Tsolova, S., Pharris, A., et al. (2014). The interconnected and cross-border nature of risks posed by infectious diseases. *Glob. Health Action* 7:25287. doi: 10.3402/gha.v7.25287

Suk, W. A., Ruchirawat, K. M., Balakrishnan, K., Berger, M., Carpenter, D., Damstra, T., et al. (2003). Environmental threats to children's health in Southeast Asia and the Western Pacific. *Environ. Health Perspect.* 111, 1340–1347. doi: 10.1289/ehp.6059

Supramaniam, A., Lui, H., Bellette, B. M., Rudd, P. A., and Herrero, L. J. (2018). How myeloid cells contribute to the pathogenesis of prominent emerging zoonotic diseases. *J. Gen. Virol.* 99, 953–969. doi: 10.1099/jgv.0.001024

Tiwananthagorn, S., Bhutto, A. M., Baloch, J. H., Soomro, F. R., Kawamura, Y., Nakao, R., et al. (2012). Zoophilic feeding behaviour of phlebotomine sand flies in the endemic areas of cutaneous leishmaniasis of Sindh Province, Pakistan. *Parasitol. Res.* 111, 125–133. doi: 10.1007/s00436-011-2808-3

Torquato, R. B., Iamamoto, K., Fernandes, E. R., Achkar, S., Silva, S. R., Katz, I. S., et al. (2020). Detection of rabies virus antigen by the indirect rapid immunohistochemistry test in equines and comparisons with other diagnostic techniques. *Zoonoses Public Health* 67, 651–657. doi: 10.1111/zph.12745

Turnbull, P. C. B. (2008). *Anthrax In Humans And Animals*. Geneva: World Health Organization.

Ur-Rehman, S., Arshad, M., Hussain, I., and Iqbal, Z. (2014). Detection and seroprevalence of foot and mouth disease in sheep and goats in Punjab, Pakistan. *Transbound. Emerg. Dis.* 61, 25–30. doi: 10.1111/tbed.12194

Velraj, R., and Haghighat, F. (2020). The contribution of dry indoor built environment on the spread of Coronavirus: data from various Indian states. *Sustain. Cities Soc.* 62:102371. doi: 10.1016/j.scs.2020.102371

Vincent, A. T., Schiettekatte, O., Goarant, C., Neela, V. K., Bernet, E., Thibeaux, R., et al. (2019). Revisiting the taxonomy and evolution of pathogenicity of the genus Leptospira through the prism of genomics. *PLoS Negl. Trop. Dis.* 13:e0007270. doi: 10.1371/journal.pntd.0007270

Vincent, S. S. (2016). Socio-Economic Inequalities and their Impact on Health in Pakistan. *Int. J. Res. Nurs.* 7, 12–18.

Warraich, H., Zaidi, A. K., and Patel, K. (2011). Floods in Pakistan: a public health crisis. *Bull. World Health Organ.* 89, 236–237. doi: 10.2471/BLT.10.083386

World Health Organization [WHO] (2004). *Public health response to biological and chemical weapons: WHO guidance*. Geneva: World Health Organization.

World Health Organization [WHO] (2017). *News: Eap-pd: chikungunya reported in Pakistan*. Geneva: World Health Organization.

World Health Organization [WHO] (2018). *WHO expert consultation on rabies: third report*. Geneva: World Health Organization.

World Health Organization [WHO] (2019). *1 in 3 people globally do not have access to safe drinking water – UNICEF, WHO. News release New York*. Geneva: World Health Organization.

Yousaf, M. Z., Ashfaq, U. A., Anjum, K. M., and Fatima, S. (2018). Crimean-Congo Hemorrhagic Fever (CCHF) in Pakistan: the "Bell" is Ringing Silently. *Crit. Rev. Eukaryot. Gene Expr.* 28, 93–100. doi: 10.1615/CritRevEukaryotGeneExpr.2018020593

Zahid, J. (2018). *Impact Of Clean Drinking Water And Sanitation On Water Borne Diseases In Pakistan*. Islamabad: Sustainable Development Policy Institute.

Conflict of Interest: The authors declare that the research was conducted in the absence of any commercial or financial relationships that could be construed as a potential conflict of interest.

frontiers in Microbiology

ORIGINAL RESEARCH
published: 14 March 2022
doi: 10.3389/fmicb.2022.793348

In vitro Susceptibility of Human Cell Lines Infection by Bovine Leukemia Virus

Nury N. Olaya-Galán[1,2], Skyler Blume[3], Kan Tong[3], HuaMin Shen[3], Maria F. Gutierrez[2] and Gertrude C. Buehring[3]**

[1] Ph.D. Program in Biomedical and Biological Sciences, School of Medicine and Human Health, Universidad del Rosario, Bogotá, Colombia, [2] Grupo de Enfermedades Infecciosas, Laboratorio de Virología, Departamento de Microbiología, Pontificia Universidad Javeriana, Bogotá, Colombia, [3] School of Public Health, University of California, Berkeley, Berkeley, CA, United States

Evidence of the presence of bovine leukemia virus (BLV) in human beings and its association with breast cancer has been published in the literature, proposing it as a zoonotic infection. However, not enough evidence exists about transmission pathways nor biological mechanisms in human beings. This study was aimed at gathering experimental evidence about susceptibility of human cell lines to BLV infection. Malignant and non-malignant human cell lines were co-cultured with BLV-infected FLK cells using a cell-to-cell model of infection. Infected human cell lines were harvested and cultured for 3 to 6 months to determine stability of infection. BLV detection was performed through liquid-phase PCR and visualized through *in situ* PCR. Seven out of nine cell lines were susceptible to BLV infection as determined by at least one positive liquid-phase PCR result in the 3-month culture period. iSLK and MCF7 cell lines were able to produce a stable infection throughout the 3-month period, with both cytoplasmic and/or nuclear BLV-DNA visualized by IS-PCR. Our results support experimental evidence of BLV infection in humans by demonstrating the susceptibility of human cells to BLV infection, supporting the hypothesis of a natural transmission from cattle to humans.

Keywords: bovine leukemia virus, *in vitro* infection, human cell lines, zoonotic potential, cell-to-cell infection

OPEN ACCESS

Edited by:
Xiao-Nong Zhou, National Institute of Parasitic Diseases, China

Reviewed by:
Naoyoshi Maeda, Hokkaido University, Japan
Luiz Carlos Kreutz, The University of Passo Fundo, Brazil

****Correspondence:***
Nury N. Olaya-Galán
nury.olaya@urosario.edu.co
Gertrude C. Buehring
buehring@berkeley.edu

Specialty section:
This article was submitted to Infectious Agents and Disease, a section of the journal Frontiers in Microbiology

Received: *12 October 2021*
Accepted: *28 January 2022*
Published: *14 March 2022*

Citation:
Olaya-Galán NN, Blume S, Tong K, Shen H, Gutierrez MF and Buehring GC (2022) In vitro Susceptibility of Human Cell Lines Infection by Bovine Leukemia Virus. Front. Microbiol. 13:793348. doi: 10.3389/fmicb.2022.793348

INTRODUCTION

Viral agents have been linked to approximately 20% of human cancer types, and some causative relationships have been established (Morales-Sánchez and Fuentes-Pananá, 2014). The most common examples of those relationships include human papilloma virus (HPV) with cervical cancer, hepatitis B and C viruses (HBV, HCV) with liver cancer, Epstein–Barr virus (EBV) with Burkitt's lymphoma, and human herpes virus 8 (HHV8) with Kaposi's sarcoma. Breast cancer has long been studied as a possible candidate for a virus-caused human cancer due to the evidence of some viral markers present on breast cancer tissues (Lehrer and Rheinstein, 2019; Al Hamad et al., 2020; Lawson and Glenn, 2021). In the last decade, bovine leukemia virus (BLV) has been proposed as a possible risk factor for breast cancer development in different regions as a result of case–control studies in which statistically significant associations of the presence of the virus with breast cancer patients has been identified (Buehring et al., 2015; Lendez et al., 2018; Schwingel et al., 2019; Delarmelina et al., 2020; Olaya-Galán et al., 2021b).

Bovine leukemia virus is an exogenous retrovirus, grouped with human T-cell leukemia virus (HTLV) in the deltaretrovirus genus. These viruses cause leukemia/lymphoma both in cattle and humans, respectively (Lairmore, 2014). Cancer development could take more than 5–10 years post-infection to occur, although a low percentage (about 5–10%) of the infected population develops the last stages of the disease. BLV is distributed worldwide with prevalence rates between 10 and 90% in cattle, although North and South America have some of the highest prevalence rates (70–90%) (Polat et al., 2017). One of the biggest challenges of BLV infection is that most of the infected animals remain asymptomatic in the herds favoring the transmission and dissemination processes as no vaccine is available and diagnosis is not performed broadly (OIE, 2021).

Previous research has reported the presence of BLV biomarkers in humans, such as gene segments, viral proteins, and antibodies against BLV, which provides clear evidence of the presence of the virus in this host (Buehring et al., 2003, 2014, 2019; Ochoa Cruz et al., 2006; Mesa et al., 2013; Robinson et al., 2016; Khalilian et al., 2019). Studies of BLV in humans have been based on epidemiological analyses for the viral detection and association with breast cancer, but still there is a gap in the knowledge, viz. how does this virus (which naturally infects cattle) reach the human population and infect human beings. Therefore, concerns about the zoonotic potential of BLV have been present for some time in the BLV research, and for several years, researchers have tried to show the implications of BLV in human beings (Burridge, 1981; Burny et al., 1985; Buehring et al., 2003). In early BLV research, it was not possible to identify any relationship between humans and BLV (Burridge, 1981), but now there is increasing evidence about the presence of the virus in human beings, strengthening the hypothesis of BLV being a zoonotic agent (Cuesta et al., 2018; Buehring and Sans, 2020; Canova et al., 2021; Corredor-Figueroa et al., 2021).

Even if cattle is the natural host of the virus, evidence of the presence of BLV has also been reported in other species (Lee et al., 2012; Barez et al., 2015; Olaya-Galán et al., 2021a). Thus, BLV has been described as a versatile agent that could infect multiple hosts both naturally and under controlled conditions in the laboratory (Gillet et al., 2007). In cattle, the target cells of the virus are the B lymphocytes (Domenech et al., 2000), although in other studies *in vitro* infection has been evaluated in cell lines of different origins/sources including other bovine tissues, and some other animal species (Inabe et al., 1998; Domenech et al., 2000; Camargos et al., 2014; Iwan et al., 2014; Martinez Cuesta et al., 2018). However, few studies have been carried out regarding the infection of BLV in human cell lines and its implications of infection (Altaner et al., 1989; Tajima et al., 2003; Suzuki et al., 2018).

For BLV and its close relative HTLV, low amounts of free viral particles are released in the viral cycles compared with other retroviruses, and thus, a cell-to-cell transmission is needed to reach uninfected cells (Lairmore, 2014; Gross and Thoma-Kress, 2016). Although it is rare and less efficient, free viral particles could also be released from infected cells and perform a classic viral cycle of infection mediated by cellular receptors such as AP3D1 or CAT1/SLC7A1 proteins (Corredor et al., 2018; Bai et al., 2019). This research was focused on investigating if human cell lines from different tissues were susceptible of infection with the BLV under controlled conditions in the laboratory. Our results provide evidence supporting the hypothesis of the zoonotic potential of the virus and providing a model of human infection for further studies, as stable infection was reached in two different human cell lines.

MATERIALS AND METHODS

Cell Lines and Culture Conditions

Fetal Lamb Kidney (FLK) cells, constitutively infected with BLV, served as a repository of the virus. Minimal Essential Medium (MEM) was used for cell passage every 3–4 days after 80% confluency. Human cell lines used and growing conditions are described in **Table 1** (Pulvertaft, 1964; Soule et al., 1973, 1990; Pattillo et al., 1977; Peebles et al., 1978; Dexter et al., 1979; DuBridge et al., 1987; Roecklein and Torok-Storb, 1995; Stürzl et al., 2013). For each experiment, viability was verified by trypan blue stain and cells were counted through Neubauer's chamber technique.

TransWell Infections

To recreate a plausible scenario of infection of BLV, TransWells (Costar Corning Inc.) with 0.4-μm polyester pore membrane were inserted above a 12-well plate to co-culture BLV-infected cells with human cell lines. The TransWell pores do not allow whole cells to pass through the pores but do allow extensions of cells (e.g., nanotubes or cellular conduits) to make contact below the insert, allowing a cell-to-cell transmission of the virus. Before infections, cell lines were verified to be negative to BLV (**Supplementary Figure 1**).

Uninfected human cell lines were cultured in the lower compartments with an approximate concentration of 10^5 cells/ml until 70–80% confluency was reached in their respective media (**Table 1**). Thereafter, FLK cells were seeded in the TransWells (6,000 cells per well). For experimental infections, co-cultures were incubated for 48 h and then the human cell lines in the lower compartment were harvested. The BLV-infected human cell lines were scaled up into T25 cell culture flasks for follow-up of the infection, for up to 3–6 months to determine the stability of BLV infection.

As experimental controls, human cell lines with PBS 1X instead of FLK cells in the TransWell were also collected and maintained simultaneously with infected ones to compare morphology or any other visible change caused due to the viral infection. Infection experiments were repeated twice for the study, at two independent and different times. Manipulation of cell lines was carried out independently, reducing the risk of cross-contamination of cell cultures. Infections per cell line were performed on different days, and for the maintenance and follow-up, separate hoods for infected and non-infected cell lines were used as well. In addition, cell lines were initially validated to be negative to BLV prior infection with the PCRs used for viral detection (see next section).

TABLE 1 | Cell lines used in *in vitro* infection experiments and growth conditions.

Cell line	Cell/tissue type	Biological status	Medium + 10% FBS	Passage(days)
RaJi (ATCC CCL-86)	B cell—Lymphoblast	Burkitt's lymphoma + EBV	RPMI-1640	2–3
HS-27 (ATCC CRL-1634)	Fibroblast—skin	Non-malignant	DMEM	7–8
MCF 102A (ATCC CRL-10781)	Epithelial—mammary gland	Non-malignant	DMEM/F12, 1:1	3–4
MCF 7 (ATCC HTB-22)	Epithelial—mammary gland	Adenocarcinoma	DMEM	4–5
CaSki (ATCC CRL-1550)	Epithelial—cervix	Epidermoid carcinoma + HPV	RPMI-1640	3–4
G361 (ATCC CRL-1424)	Epithelial—skin	Malignant melanoma	MEM	3–4
293T (ATCC CRL-3216)	Epithelial—embryonic kidney	Non-malignant + adenovirus	DMEM	2–3
DLD-I (ATCC CCL-221)	Epithelial—colon	Colorectal carcinoma	RPMI-1640	4–5
iSLK (UC Berkeley donation)	Epithelial—kidney	Renal carcinoma + latent KSHV	DMEM	4–5

TABLE 2 | Evidence of BLV-GRE genomic region in human cell lines after infection through nPCR in a follow-up of 12 weeks post-infection.

Cell line	Replicate	Evidence of BLV post-infection				
		t0	Week 2	Week 4	Week 8	Week 12
RaJi (ATCC CCL-86)	1	Pos	Pos	Neg	Neg	Neg
	2	Pos	Pos	Neg	Neg	Neg
HS-27 (ATCC CRL-1634)	1	Pos	Pos	Pos	Pos	Neg
	2	Pos	Pos	Pos	Neg	Neg
MCF 102A (ATCC CRL-10781)	1	Pos	Pos	Pos	Neg	Neg
	2	Pos	Pos	Pos	Neg	Neg
MCF 7 (ATCC HTB-22)	1	Pos	Pos	Pos	Pos	Pos
	2	Pos	Pos	Pos	Neg	Neg
CaSki (ATCC CRL-1550)	1	Neg	–	–	–	–
	2	Neg	–	–	–	–
G361 (ATCC CRL-1424)	1	Neg	–	–	–	–
	2	Neg	–	–	–	–
293T (ATCC CRL-3216)	1	Pos	Neg	Neg	Neg	Neg
	2	Pos	Pos	Neg	Neg	Neg
DLD-I (ATCC CCL-221)	1	Pos	Pos	Pos	Neg	Neg
	2	Pos	Pos	Pos	Neg	Neg
iSLK	1	Pos	Pos	Pos	Pos	Pos
	2	Pos	Pos	Pos	Pos	Pos

Bovine Leukemia Virus Detection and Follow-up of Infection

After 48 h post-infection (hpi) with the TransWells, an aliquot of the cells in the bottom plate was recovered to perform DNA extraction with the DNeasy Kit from QIAgen following the manufacturer's instructions. Total DNA recovered was stored at −20°C until further use. Human GAPDH housekeeping gene was used as a validation control of the DNA extraction. Sheep *cytochrome C oxidase* housekeeping gene was used to verify that FLK cells did not trespass the membrane of the TransWells and human cell lines were not contaminated with FLK.

Viral genome was detected by PCR (see next section). Successful infected human cell lines were considered those in which BLV-DNA was detected in the initial DNA extraction post-infection and were maintained in cell culture with its respective conditions (**Table 1**). A follow up of the positive cell lines was performed every 2 weeks in which an aliquot of infected cells and controls without infection were taken for DNA extraction and PCR detection (**Table 2**).

Viral genes *LTR*, *gag*, *pol*, *env*, and *tax* were tested by liquid-phase nested PCR (nPCR) with GoTaq Promega to verify the presence of the complete genome of the virus at time 0 post-infection. Primers used for the viral detection and PCR conditions were used from previous studies (Buehring et al., 2014; Corredor et al., 2018). For the follow-up, detection of the GRE region of the LTR of the virus was used as a biomarker of viral infection, as it is one of the most conserved genes of the virus and belong to the 5′ limit of the viral genome. Results were visualized by electrophoresis in a 1.5% agarose gel, TBE1x, stained with ethidium bromide, and run conditions for 30 min—100 V in TBE1x. PCR conditions and primers are shown in the **Supplementary Table 1**.

For those cell lines that showed a stable infection of BLV during the total time of the follow-up, an *in situ* PCR (IS-PCR) was performed after 16 weeks of infection to confirm the presence of the virus inside the cells using methodology adapted from Nuovo (1995). Cell cultures were detached, rinsed, and smeared on enhanced adherence glass microscope slides (SuperFrost—Fisher). The slides were air dried and fixed for 18 h in 10% formalin neutral buffer. Digestion was performed with 2 mg/ml pepsin in 0.1 N HCl (20 min), followed by pepsin inactivation solution (100 mmol/L Tris–HCl, 100 mmol/L NaCl, pH 7.4) applied for 1 min, and were rinsed in DPBS and a final wash in absolute ethanol. Samples, run in duplicate, were surrounded with a 15 mm × 15 mm frame seal chamber (Bio-Rad, Hercules, CA, United States) for the PCR mix.

The PCR mixture was 4.0 mmol/L $MgCl_2$, 0.4 mmol/L dNTPs, 1 μmol/L primers (Operon Biotechnologies, Huntsville, AL, United States), 0.06% bovine serum albumin, 8 μmol/L digoxigenin-11-dUTP (dig) (Hoffman-La Roche, Basel, Switzerland), and 0.053 U/μl of HotStart Amplitaq Gold DNA Polymerase (Applied Biosystems, Foster City, CA, United States). IS-PCR was directed to a segment of the *tax* region of the BLV genome (nt 7197–7570, F: CTTCGGGATCCATTACCTGA and R: GCTCGAAGGGGGAAAGTGAA), with an expected product of 373 bp. PCR mix was placed into the chambers of the slides and was sealed with the plastic cover of BioRad. Slides were placed into an IS-PCR machine (Hybaid Thermo OmniSlide; Cambridge Biosystems, Cambridge, United Kingdom) for amplification. Thermal profile was used as previously described (Buehring et al., 2014). After amplification, endogenous peroxidase was quenched 30 min in 3% hydrogen-peroxide solution prepared in methanol. Dig-labeled nucleotides incorporated into PCR products were detected by anti-dig antibodies in an avidin–biotin-immunoperoxidase reaction (Hoffman-La Roche) and were revealed by diaminobenzidine (DAB) solution followed by the manufacturer's instruction (Vector, Burlingame, CA, United States). Smears of FLK cell line were used as a positive control. As a negative control of reaction, an adjacent smear for each cell line prepared without Taq polymerase and without primers was evaluated to verify that no cross-reaction or non-specific attachment occurred by the DIG-labeled uracil and/or by the anti-dig monoclonal antibody. Results were visualized in a Nikon Eclipse E200 optical microscope under × 40 magnification. Visualization of dark brown-red stain was considered a positive result. After verification of stable infection after 16 weeks, cells were stored in liquid nitrogen for further analyses.

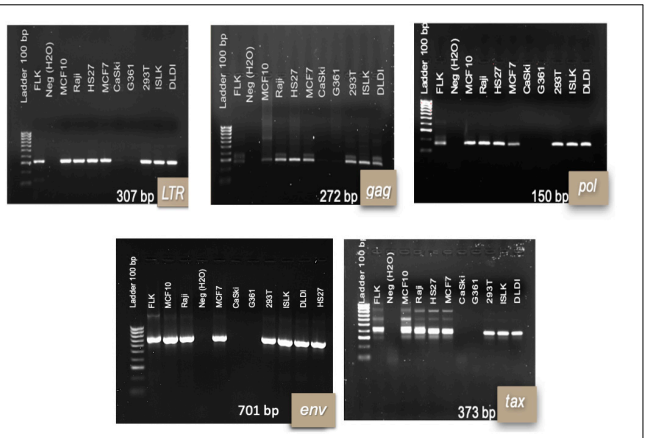

FIGURE 1 | Bovine leukemia virus genes' fragments for infected human cell lines at time 0 post-infection. 1.5% agarose electrophoresis gels with representative results per cell line. Results are shown at 48 hpi of the TransWell system. Each infection of the cell lines was repeated twice in two independent moments. DNA from FLK cell line was used as a positive control for PCR reactions.

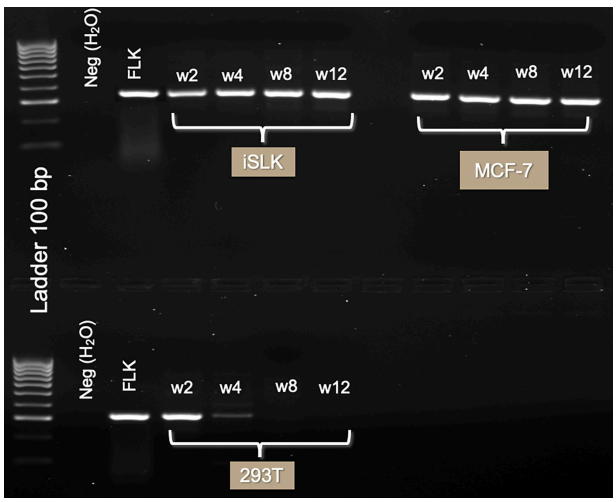

FIGURE 2 | Three-month follow-up of BLV infection in human cell lines with GRE region. Gel electrophoresis of PCR product (285 bp) run on 1.5% agarose TBE gel, stained with ethidium bromide. Lanes in order are of DNA extracted 2 weeks, 1 month, 2 months, and 3 months after TransWell infection. Notice the high intensity of the bands on iSLK and MCF-7 cell lines. In 293T cell line, viral infection was lost after week 4 post-infection.

RESULTS

All of the aliquots obtained from cell culture were validated for human GAPDH after 48 hpi and in each aliquot after DNA extraction for the follow-up. *Cytochrome C oxidase* of sheep was negative in all of them, confirming that it was not a cross-contamination from FLK (**Supplementary Figures 2, 3**).

Success of TransWell infection and stability of infection varied among different cell lines. CaSki and G361 cell lines were negative for most BLV genes following incubation in TransWells. DLDI, 293T, Raji, MCF-102A, HS-27, MCF-7, and iSLK cell lines were susceptible to BLV infection, as detected by nPCR amplification of viral genes. In time zero post-infection, all of the amplified regions for viral detection were present in 7 out of the 9 cell lines (**Figure 1**).

The DLDI, 293T, Raji, MCF-102A, and HS-27 cells were unable to sustain infection. In these cells, detection of BLV DNA decreased with time and became non-detectable over the follow-up period. The results of nested and *in situ* PCR are represented

on **Figures 2**, **3**, respectively, in which cell lines that reached a stable infection are described.

The presence of the GRE biomarker in the cell lines throughout the 3-month follow-up (**Figure 2**) is evidence of a stable infection. MCF-7 and iSLK were positive during the complete follow-up. No discernable changes in morphology of the cells infected with BLV were noted.

Figure 3 shows the results of *in situ* PCR as an end-point experiment performed on MCF-7 and iSLK after 16 weeks post-infection to visually validate the results of nPCR on cell lines with stable infection. Areas of the cells stained red/dark brown indicate regions containing BLV DNA. The cell lines iSLK and MCF7 showed BLV-*tax* gene segment inside the cells evenly distributed, with some darker spots visualized in the nucleus of iSLK (**Figure 3**—100 ×).

After 18 months of freezing in liquid nitrogen, cells were recovered again in cell culture to verify if they still were infected. An immunohistochemistry directed to p24 protein of the virus was carried out and detection was performed with DAB reagent in an immunoperoxidase system. Presence of the virus was confirmed in MCF-7 cells as visualized with dark coloring inside the cells. In addition, multinucleated cells were visualized suggesting the presence of syncytia formation (**Supplementary Figure 4**). iSLK cells were not possible to recover after thawing.

DISCUSSION

Understanding the impact that BLV infection could have in human beings is a topic of concern. Previous evidence of BLV in humans has reported its presence in blood, lung, and breast tissues from people with and without cancer (Mesa et al., 2013; Buehring et al., 2014; Robinson et al., 2016; Khalilian et al., 2019). This study shows that several human cell lines from different tissues were susceptible to BLV infection, and that a stable infection was obtained in two of the evaluated cell lines (MCF-7 and iSLK). Results showed the presence of viral DNA, which could be as a provirus, as total DNA was extracted for the follow-ups. Susceptibility of infection was shown in cells from different tissues such as kidney, colon, fibroblasts, and breast. These results open the possibility that BLV could be present in other organs in human beings, and considering its oncogenic potential, it will be interesting to evaluate if there is an association with other cancer etiologies in addition to breast (Buehring and Sans, 2020) and lung cancer (Kim et al., 2018).

Previous evidence of BLV *in vitro* infections has been focused on understanding specific pathways and molecular mechanisms of the virus (Inabe et al., 1998; Domenech et al., 2000; Takahashi et al., 2005; Camargos et al., 2014; Iwan et al., 2014; Murakami et al., 2017; Cuesta et al., 2019). However, few studies included human cell lines in the experimental designs (Altaner et al., 1989; Murakami et al., 2017; Suzuki et al., 2018). Results published by Altaner et al. (1989) were directed to evaluate the implications of BLV infection in humans' cells of neurotropic origin. Establishing an *in vitro* model that will allow the research community for further studies in the biological mechanisms of BLV infection in humans is still a priority in the research field. We propose that iSLK and MCF-7 cell lines could be used in the future for further analyses.

Previously, Suzuki et al. (2018) analyzed the early stages of the *in vitro* infection of the virus, in which it was determined that one of the crucial stages for viral producing cell lines and for stable infections was the retrotransciption. As a retrovirus, once BLV enters the host cell, its RNA genome is expected to be retrotranscribed to viral DNA and remains as extrachromosomal double-stranded DNA (E-DNA). Unlike retroviruses such as HIV, translocation of the viral genome into the nucleus is weak and mainly relies on cell division processes (MacLachlan and Dubovi, 2017). However, once into the nucleus, integration in the host genome occurs mediated by viral integrases in which a proviral state is acquired, generating stable and persistent infections in the host (Grandgenett et al., 2015; Martin et al., 2016). When E-DNA remains in the cytoplasm of the cell and does not manage to be translocated into the nucleus, viral DNA is more likely to degrade inside the cells and is not possible to obtain stable infections (Reyes and Cockerell, 1996).

Our results showed that seven out of the nine cell lines were able to overpass the initial steps of the viral cycle, such as attachment, entrance, and retrotranscription. Even if it was expected a cell-to-cell infection as few amounts of free viral particles are released, independently of which was the mechanism used by the virus for the entrance in human cell lines, evidence of DNA obtained from the extractions in the follow-up indicated that initial steps were successfully fulfilled. Viral receptors proposed for BLV (AP3D1 and CAT1/SLC7A1) (Corredor et al., 2018; Bai et al., 2019) are proteins that are widely distributed in most of the eukaryotic cells, as are proteins involved in intracellular transport processes. Those proteins could be favoring the interactions between the virus and different host cells due to the high identity and similarity percentages among species (Dell'Angelica and Angelica, 2009; Fotiadis et al., 2013), and their low specificity with tissues and specific cells. For the case of CaSki and G361 cell lines, which were the only two cell lines in which the infection was not successful, it might be due to lower amounts of expression of the receptor proteins compared with other cell types (Human Protein Atlas, 2021a,b) or to the lack of capacity of inducing nanotube formation for the viral entrance (Pique and Jones, 2012; Gross and Thoma-Kress, 2016).

The cell lines in which BLV genome was detected for a longer term support the hypothesis of a stable infection in MCF-7 (breast), iSLK (kidney), and DLD-I (colon) cell lines. Even if in our study we did not measure active viral production, nor functionality of the viral genes, the identification of these cell lines with the presence of viral DNA after a long-term infection suggests that a stable infection in the human body may occur as well. Although the present study does not suggest a mechanism as to why certain cell lines were unable to maintain a stable BLV infection, we hypothesize that it could be related with the process of integration in the host genome. Considering that BLV does not have a specific profile for integration within the host genome, and that it occurs randomly in different regions, with different patterns and in several chromosomes in cattle without a

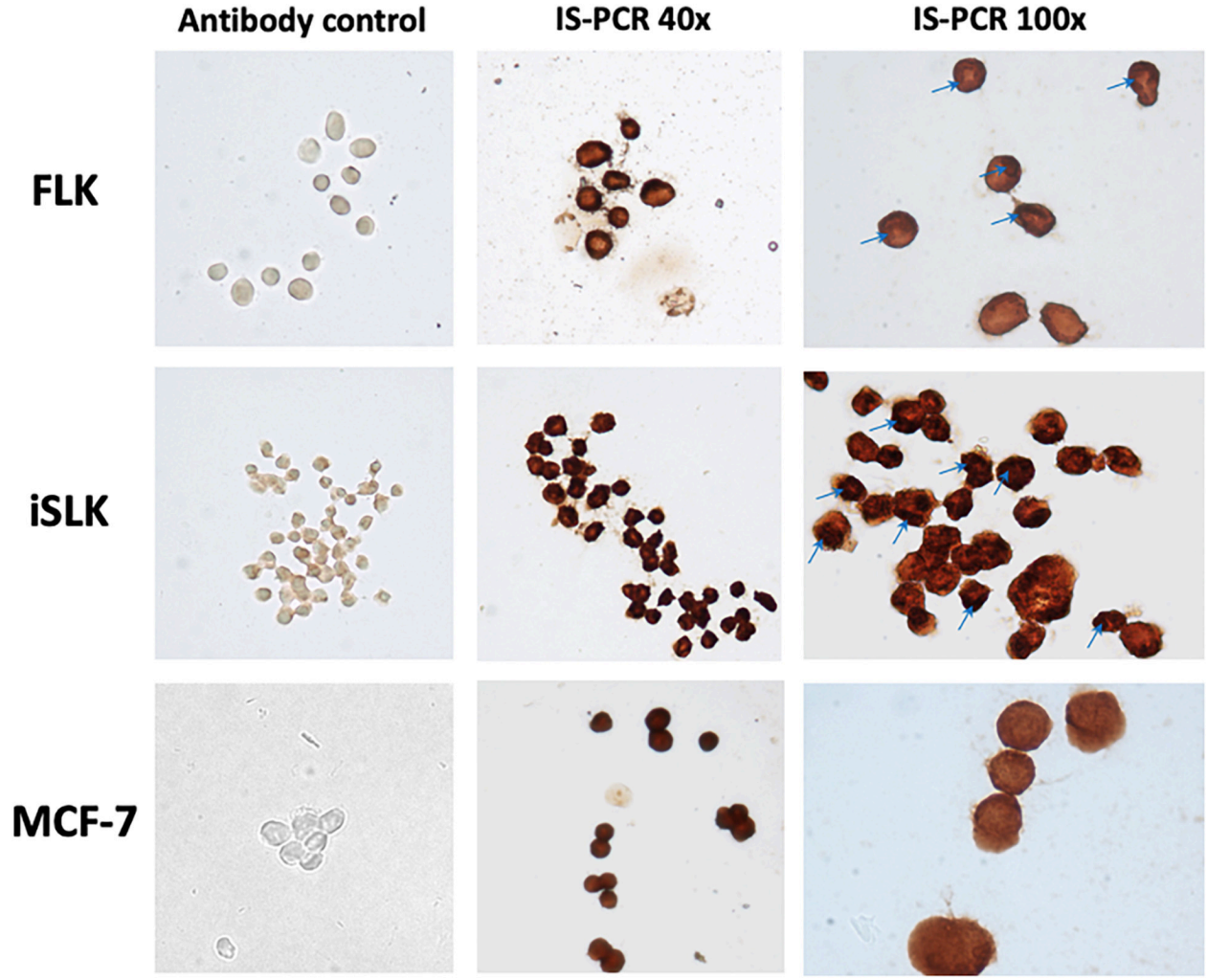

FIGURE 3 | Evidence of BLV inside the cells through *in situ* PCR (*tax* region). Smear of infected cell lines. FLK—positive control cell line. iSLK-BLV positive (kidney). MCF-7 BLV positive (breast). Antibody control—*in situ* PCR without primers and TaqPolymerase control, verification of no cross-reaction of anti-dig antibody. *In situ* PCR with complete reaction. Stain is visualized by DAB reaction against anti-dig system. Images visualized at 40 × and 100 × on a Nikon Eclipse E200 optical microscope. All images were treated with the same conditions of color and contrast.

specific association with disease progression (Onuma et al., 1982; Miyasaka et al., 2015), this also could be occurring in the human cells. In cattle, it is expected to integrate about 2 to 6 copies of BLV genome in the host cells, what favors to the increase of proviral load in the host due to the clonal expansion related to the disease (Gillet et al., 2007). As there is no correlation for the integration profiles in which different number of copies could be integrated, in our experiments, changes in the intensity of the bands present in the electrophoresis and darker colors in the *in situ* PCR could be associated with higher amounts of viral genome. The localization of BLV in the nucleus in iSLK *versus* the cytoplasm for MCF-7 based on the results from IS-PCR could be interpreted as differences in the integration profiles of the BLV in the form of provirus. It could be associated with more copies integrated in iSLK in contrast with MCF-7; however, in this study, we did not look for the integration sites of the virus, as it was not the main objective of the article. Finally, stable and persistent infections could also be related with the cell cycles of the different cell lines, in which initial cells that were infected with BLV could die before its mitotic cycle or could be displaced by uninfected cells replacing the cell populations.

One of the strengths of this study were the steps taken to ensure that the results obtained were free from cross-contamination. All DNA samples extracted from the human cell cultures were negative in PCR amplification of sheep cytochrome *C*, which makes it unlikely that positive nested PCR results were due to FLK cell-line contamination. Furthermore, FLK control DNA and cell line were handled in different areas, separate from the human cell culture samples to avoid cross-contamination while processing and to ensure the positive results obtained from DNA within the human cell culture samples. Two different detection techniques were used as well to ensure reliability of our

results. IS-PCR visualization showed presence of the viral genome inside the cells, which could be both in the cytoplasm of the cells or in the nucleus. Even if liquid-phase PCR is unable to provide any information as to the location of the source of the DNA, it showed the presence of viral genome after a total DNA extraction, indicating that early steps of the viral cycle were performed.

In addition, more than one BLV genome region was used for the follow-up of the experiments. The LTR (long terminal repeat) promoter region of BLV was used for liquid-phase PCR, and *tax* region, which codes an auxiliary protein with oncogenic potential, was used for IS-PCR. Those regions were chosen because they are the most highly conserved regions of BLV genome (Zhao et al., 2007; Barez et al., 2015). It is thought that in BLV and HTLV, the gag–pol (polymerase)–env segment of the BLV genome is often deleted during the progression of the disease to escape the host's immune response (Gillet et al., 2007; Zhao and Buehring, 2007). Detection of genomic biomarkers as evidence of the viral infection by PCR could result in false negatives if these regions were the primary or sole target for assays. Furthermore, it is important to highlight that both LTR region and Tax protein are crucial for active transcription of the virus within the host cells, as Tax protein acts as the main transactivator of the LTR promoter region, inducing active transcription of the virus (Fox et al., 2016; Pluta et al., 2020). In further studies, it will be interesting to determine levels of expression of both biomarkers and to identify if is there any correlation with the cell cycle, viral transcription, and cellular transformation patterns.

A limitation of our current study is that the positive results from the liquid-phase PCR do not provide information as to the integration status of BLV with respect to the host genome. While these results show that viral retro-transcription occurred (Inabe et al., 1998), we could not be sure if the virus was able to integrate its genome with that of the host cell, which is an essential step for its replication and persistent infection. This is an area of future research as inverse PCR techniques allow for determination of the integration status of the retrovirus, and can also provide information about where in the host's genome the virus integrates, which could give an insight of its localization in the host genome and of possible cellular genes' alteration (Murakami et al., 2011). However, inverse PCR assays are challenging as large amounts of PCR products are required for sequencing, which could be influenced by the proviral load in the host. Further studies are needed to understand the impact of the infection of BLV in these cell lines and in human beings.

Of special interest, the mammary epithelial cell line MCF-7 was both susceptible to BLV infection and able to maintain a stable infection over the 3-month culture period. Both conditions seem to be important in the progression of the disease in its host (Lairmore, 2014). This result is significant as it provides *in vitro* experimental evidence consistent with the hypothesis of BLV as an exogenous etiological agent of human breast cancer, obtained through a zoonotic infection (Corredor-Figueroa et al., 2021). Nevertheless, the varying susceptibility and capacity of maintaining a stable infection of BLV in human cell lines as well as from other mammal species opens new questions in BLV research in which further studies are needed toward the characterization of the mechanisms involved in BLV infection in other hosts than cattle. Our results provide evidence of BLV being capable of infecting human cell lines, what supports the hypothesis of natural infection of BLV in human beings, with huge possibilities of infecting different tissues among the human body.

CONCLUSION

Bovine leukemia virus was able to infect human cell lines through a cell-to-cell model. BLV biomarkers were identified in the cell lines as evidence of a stable infection. iSLK and MCF-7 cell lines were those that showed positive for a longer term, even after freezing and thawing. Our results support the hypothesis of BLV being a zoonotic infection and are the basis for further studies for a better understanding of BLV mechanisms in human beings. Stable infected cell lines will be useful for future studies to be performed under controlled conditions at the laboratory level.

DATA AVAILABILITY STATEMENT

The original contributions presented in the study are included in the article/**Supplementary Material**, further inquiries can be directed to the corresponding author/s.

AUTHOR CONTRIBUTIONS

NO-G and GB: conceptualization and visualization. NO-G, KT, SB, and HS: methodology. NO-G: software. GB: validation, resources, project administration, and funding acquisition. NO-G, SB, HS, and GB: formal analysis. NO-G, MG, and GB: investigation. NO-G and SB: writing—original draft preparation. NO-G, MG, and GB: writing—review and editing. MG and GB: supervision. All authors have read and agreed to the published version of the article.

FUNDING

This research did not receive any specific grant from funding agencies in the public, commercial, or not-for-profit sectors in the United States. This work was performed as part of the research areas of zoonotic infections supported by Ministerio de Ciencia, Tecnología e Innovación de Colombia (MinCiencias) through Fondo de Ciencia Tecnología e Innovación/Sistema General de Regalías, in the national call 009/2020 (BPIN project 2020000100127) granted to MG, which supported Publication Fees.

ACKNOWLEDGMENTS

Special thanks to Stephens at UC Berkeley for reagents and supplies. We would like to thank Gary Firestone and Fenyong Liu for cell lines' donation. Special thanks to Fundación Instituto de Inmunología de Colombia (FIDIC),

particularly to Manuel A. Patarroyo and Darwin Andres Moreno for supporting experimental design and shipping of cell lines. Gratitude to Fulbright Colombia, for grant awarded to NOG as a visiting student researcher (2017) supporting her fellowship at UC Berkeley in the United States.

SUPPLEMENTARY MATERIAL

The Supplementary Material for this article can be found online at: https://www.frontiersin.org/articles/10.3389/fmicb.2022.793348/full#supplementary-material

REFERENCES

Al Hamad, M., Matalka, I., Al Zoubi, M. S., Armogida, I., Khasawneh, R., Al-Husaini, M., et al. (2020). Human Mammary Tumor Virus, Human Papilloma Virus, and Epstein-Barr Virus Infection Are Associated With Sporadic Breast Cancer Metastasis. *Breast Cancer Basic Clin. Res.* 14:1178223420976388. doi: 10.1177/1178223420976388

Altaner, C., Altanerová, V., Bán, J., Niwa, O., and Yokoro, K. (1989). Human cells of neural origin are permissive for bovine leukemia virus. *Neoplasma* 36, 691–695. Available online at: http://www.ncbi.nlm.nih.gov/pubmed/2559338 [Accessed April 12, 2017]

Bai, L., Sato, H., Kubo, Y., Wada, S., and Aida, Y. (2019). CAT1/SLC7A1 acts as a cellular receptor for bovine leukemia virus infection. *FASEB J.*:fj201901528R. doi: 10.1096/fj.201901528R

Barez, P.-Y., de Brogniez, A., Carpentier, A., Gazon, H., Gillet, N., Gutiérrez, G., et al. (2015). Recent Advances in BLV Research. *Viruses* 7, 6080–6088. doi: 10.3390/v7112929

Buehring, G. C., DeLaney, A., Shen, H., Chu, D. L., Razavian, N., Schwartz, D. A., et al. (2019). Bovine leukemia virus discovered in human blood. *BMC Infect. Dis.* 19:297. doi: 10.1186/s12879-019-3891-9

Buehring, G. C., Philpott, S. M., and Choi, K. Y. (2003). Humans have antibodies reactive with Bovine leukemia virus. *AIDS Res. Hum. Retroviruses* 19, 1105–1113. doi: 10.1089/088922203771881202

Buehring, G. C., and Sans, H. M. (2020). Breast cancer gone viral? Review of possible role of bovine leukemia virus in breast cancer, and related opportunities for cancer prevention. *Int. J. Environ. Res. Public Health* 17:209. doi: 10.3390/ijerph17010209

Buehring, G. C., Shen, H. M., Jensen, H. M., Choi, K. Y., Sun, D., and Nuovo, G. (2014). Bovine Leukemia Virus DNA in Human Breast Tissue. *Emerg. Infect. Dis.* 20, 772–782. doi: 10.3201/eid2005.131298

Buehring, G. C., Shen, H. M., Jensen, H. M., Jin, D. L., Hudes, M., and Block, G. (2015). Exposure to Bovine Leukemia Virus Is Associated with Breast Cancer: A Case-Control Study. *PLoS One* 10:e0134304. doi: 10.1371/journal.pone.0134304

Burny, A., Bruck, C., Cleuter, Y., Mammerickx, M., Marbaix, G., Portetelle, D., et al. (1985). Bovine Leukemia Virus, a Versatile Agent with Various Pathogenic Effects in Various Animal Species. *Cancer Res.* 45, 4578–4583.

Burridge, M. J. (1981). The zoonotic potential of bovine leukemia virus. *Vet. Res. Commun.* 5, 117–126. doi: 10.1007/BF02214976

Camargos, M. F. F., Rajão, D. S., Leite, R. C. C., Stancek, D., Heinemann, M. B. B., Reis, J. K., et al. (2014). Genetic variation of bovine leukemia virus (BLV) after replication in cell culture and experimental animals. *Genet. Mol. Res.* 13, 1717–1723. doi: 10.4238/2014.January.22.11

Canova, R., Weber, M. N., Budaszewski, R. F., da Silva, M. S., Schwingel, D., Canal, C. W., et al. (2021). Bovine leukemia viral DNA found on human breast tissue is genetically related to the cattle virus. *One Heal* 13:100252. doi: 10.1016/j.onehlt.2021.100252

Corredor, A. P., Gonzales, J., Baquero, L. A., Curtidor, H., Olaya-Galán, N. N., Patarroyo, M. A., et al. (2018). In silico and in vitro analysis of boAP3d1 protein interaction with bovine leukaemia virus gp51. *PLoS One* 13:e0199397. doi: 10.1371/journal.pone.0199397

Corredor-Figueroa, A. P., Olaya-Galán, N. N., Velandia, S., Muñoz, M., Salas-Cárdenas, S. P., Ibáñez, M., et al. (2021). Co-Circulation of Bovine Leukemia Virus Haplotypes among Humans, Animals, and Food Products: New Insights of Its Zoonotic Potential. *Int. J. Environ. Res. Public Health* 18:4883doi: 10.3390/ijerph18094883

Cuesta, L. M., Lendez, P. A., Victoria, M., Farias, N., Guillermina, D. L., and Ceriani, M. C. (2018). Can Bovine Leukemia Virus Be Related to Human Breast Cancer? A Review of the Evidence. *J. Mammary Gland. Biol. Neoplasia.* doi: 10.1007/s10911-018-9397-z

Cuesta, L. M., Nieto Farias, M. V., Lendez, P. A., Rowland, R. R. R., Sheahan, M. A., Cheuquepán Valenzuela, F. A., et al. (2019). Effect of Bovine leukemia virus on bovine mammary epithelial cells. *Virus Res.* 271:197678. doi: 10.1016/j.virusres.2019.197678

Delarmelina, E., Buzelin, M. A., de Souza, B. S., Souto, F. M., Bicalho, J. M., Falcão Câmara, R. J., et al. (2020). High positivity values for bovine leukemia virus in human breast cancer cases from Minas Gerais. Brazil. *PLoS One* 15:e0239745. doi: 10.1371/journal.pone.0239745

Dell'Angelica, E. C., and Angelica, E. C. D. A. P. - (2009). 3-dependent trafficking and disease: the first decade. *Curr. Opin. Cell. Biol.* 21, 552–559. doi: 10.1016/j.ceb.2009.04.014

Dexter, D. L., Barbosa, J. A., and Calabresi, P. N. (1979). N–Dimethylformamide–induced alteration of cell culture characteristics and loss of tumorigenicity in cultured human colon carcinoma cells. *Cancer Res.* 39, 1020–1025.

Domenech, A., Goyache, J., Llames, L., Payá, J., Suarez, G., and Gomez-Lucía, E. (2000). In vitro infection of cells of the monocytic/macrophage lineage with bovine leukaemia virus. *J. Gen. Virol.* 81, 109–118. doi: 10.1099/0022-1317-81-1-109

DuBridge, R. B., Tang, P., Hsia, H. C., Leong, P. M., Miller, J. H., and Calos, M. P. (1987). Analysis of mutation in human cells by using an Epstein-Barr virus shuttle system. *Mol. Cell Biol.* 7, 379–387. doi: 10.1128/mcb.7.1.379

Fotiadis, D., Kanai, Y., and Palacín, M. (2013). The SLC3 and SLC7 families of amino acid transporters. *Mol. Aspects Med.* 34, 139–158. doi: 10.1016/j.mam.2012.10.007

Fox, J., Hilburn, S., Demontis, M.-A., Brighty, D., Rios Grassi, M., Galvão-Castro, B., et al. (2016). Long Terminal Repeat Circular DNA as Markers of Active Viral Replication of Human T Lymphotropic Virus-1 in Vivo. *Viruses* 8:80. doi: 10.3390/v8030080

Gillet, N., Florins, A., Boxus, M., Burteau, C., Nigro, A., Vandermeers, F., et al. (2007). Mechanisms of leukemogenesis induced by bovine leukemia virus: prospects for novel anti-retroviral therapies in human. *Retrovirology* 4:18. doi: 10.1186/1742-4690-4-18

Grandgenett, D. P., Pandey, K. K., Bera, S., and Aihara, H. (2015). Multifunctional facets of retrovirus integrase. *World J. Biol. Chem.* 6, 83–94. doi: 10.4331/wjbc.v6.i3.83

Gross, C., and Thoma-Kress, A. K. (2016). Molecular mechanisms of HTLV-1 cell-to-cell transmission. *Viruses* 8:74. doi: 10.3390/v8030074

Human Protein Atlas. (2021a). *AP3D1 protein expression summary | The Human Protein Atlas*. Available online at: https://www.proteinatlas.org/ENSG00000065000-AP3D1 (Accessed December 26, 2021)

Human Protein Atlas. (2021b). *Tissue expression of SLC7A1 | The Human Protein Atlas*. Available online at: https://www.proteinatlas.org/ENSG00000139514-SLC7A1/tissue (Accessed on December 26, 2021)

Inabe, K., Ikuta, K., and Aida, Y. (1998). Transmission and propagation in cell culture of virus produced by cells transfected with an infectious molecular clone of bovine leukemia virus. *Virology* 245, 53–64. doi: 10.1006/viro.1998.9140

Iwan, E., Szczotka, M., and Kuźmak, J. (2014). Application of in situ PCR for the detection of bovine leukaemia virus (BLV) infection in dendritic cell cultures. *Bull. Vet. Inst. Pulawy.* 58, 347–352. doi: 10.2478/bvip-2014-0054

Khalilian, M., Hosseini, S. M., and Madadgar, O. (2019). Bovine leukemia virus detected in the breast tissue and blood of Iranian women. *Microb. Pathog.* 135:103566. doi: 10.1016/j.micpath.2019.103566

Kim, Y., Pierce, C. M., and Robinson, L. A. (2018). Impact of viral presence in tumor on gene expression in non-small cell lung cancer. *BMC Cancer* 18:843. doi: 10.1186/s12885-018-4748-0

Lairmore, M. D. (2014). Animal models of bovine leukemia virus and human T-lymphotrophic virus type-1: insights in transmission and pathogenesis. *Annu. Rev. Anim. Biosci.* 2, 189–208. doi: 10.1146/annurev-animal-022513-114117

Lawson, J. S., and Glenn, W. K. (2021). Catching viral breast cancer. *Infect. Agent Cancer* 16:37. doi: 10.1186/s13027-021-00366-3

Lee, L. C., Scarratt, W. K., Buehring, G. C., and Saunders, G. K. (2012). Bovine leukemia virus infection in a juvenile alpaca with multicentric lymphoma. *Can Vet journal La Rev veìteìrinaire Can* 53, 283–286.

Lehrer, S., and Rheinstein, P. H. (2019). The virology of breast cancer: viruses as the potential causative agents of breast tumorigenesis. *Discov Med* 27, 163–166.

Lendez, P. A., Martinez-Cuesta, L., Nieto Farias, M. V., Shen, H., Dolcini, G. L., Buehring, G. C., et al. (2018). Bovine leukemia virus presence in breast tissue of Argentinian women. Its association with cell proliferation and prognosis markers. *Multi. Cancer Invest.* 2, 16–24. doi: 10.30699/acadpub.mci.4.16

MacLachlan, N. J., and Dubovi, E. J. (2017). "Retroviridae," in Fenner's Veterinary Virology N. J. MacLachlan and E. J. Dubovi (Cambridge: Academic Press) 269–297.

Martin, J. L., Maldonado, J. O., Mueller, J. D., Zhang, W., and Mansky, L. M. (2016). Molecular studies of HTLV-1 replication: An update. *Viruses* 8:31.

Martinez Cuesta, L., Nieto Farias, M. V., Lendez, P. A., Barone, L., Elizabeth Pérez, S., Dolcini, G. L., et al. (2018). Stable infection of a bovine mammary epithelial cell line (MAC-T) with bovine leukemia virus (BLV). *Virus Res.* 256, 11–16. doi: 10.1016/j.virusres.2018.07.013

Mesa, G., Ulloa, J. C., Uribe, A. M., Gutierrez, M. F., Giovanna, M., Carlos, U. J., et al. (2013). Bovine Leukemia Virus Gene Segment Detected in Human Breast Tissue. *Open J. Med. Microbiol.* 3, 84–90. doi: 10.4236/ojmm.2013.31013

Miyasaka, T., Oguma, K., and Sentsui, H. (2015). Distribution and characteristics of bovine leukemia virus integration sites in the host genome at three different clinical stages of infection. *Arch. Virol.* 160, 39–46. doi: 10.1007/s00705-014-2224-y

Morales-Sánchez, A., and Fuentes-Pananá, E. (2014). Human Viruses and Cancer. *Viruses* 6, 4047–4079. doi: 10.3390/v6104047

Murakami, H., Asano, S., Uchiyama, J., Sato, R., Sakaguchi, M., and Tsukamoto, K. (2017). Bovine leukemia virus G4 enhances virus production. *Virus Res.* 238, 213–217. doi: 10.1016/j.virusres.2017.07.005

Murakami, H., Yamada, T., Suzuki, M., Nakahara, Y., Suzuki, K., and Sentsui, H. (2011). Bovine leukemia virus integration site selection in cattle that develop leukemia. *Virus Res.* 156, 107–112. doi: 10.1016/j.virusres.2011.01.004

Nuovo, G. J. (1995). In situ PCR: protocols and applications. Genome Res. 4, S151–S167. Available online at: http://genome.cshlp.org/content/4/4/S151.abstract

Ochoa Cruz, A., Uribe, A., and Gutiérrez, M. (2006). Estudio del potencial zoonótico del Virus de la Leucosis Bovina y su presencia en casos de cáncer de seno. *Univ. Sci.* 11, 31–40. sci.v11i2.4968 doi: 10.11144/univ

OIE (2021). *Bovine Leukemia Virus (Chapter 11.6), Terrestrial Animal Health Code 2021 (29th Edition; Vol I–II)*. Paris, France: World Organization of Animal Health.

Olaya-Galán, N. N., Corredor-Figueroa, A. P., Velandia-Álvarez, S., Vargas-Bermudez, D. S., Fonseca-Ahumada, N., Nuñez, K., et al. (2021a). Evidence of bovine leukemia virus circulating in sheep and buffaloes in Colombia: insights into multispecies infection. *Arch Virol.* 11,1-11. doi: 10.1007/s00705-021-05285-7

Olaya-Galán, N. N., Salas-Cárdenas, S. P., Rodriguez-Sarmiento, J. L., Ibáñez-Pinilla, M., Monroy, R., Corredor-Figueroa, A. P., et al. (2021b). Risk factor for breast cancer development under exposure to bovine leukemia virus in Colombian women: A case-control study. *PLoS One* 16:e0257492. doi: 10.1371/journal.pone.0257492

Onuma, M., Sagata, N., Okada, K., Ogawa, Y., Ikawa, Y., and Oshima, K. (1982). Integration of Bovine Leukemia Virus DNA in the Genomes of Bovine Lymphosarcoma Cells. *Microbiol. Immunol.* 26, 813–820. doi: 10.1111/j.1348-0421.1982.tb00227.x

Pattillo, R., Hussa, R., Story, M., Ruckert, A., Shalaby, M., and Mattingly, R. (1977). Tumor antigen and human chorionic gonadotropin in CaSki cells: a new epidermoid cervical cancer cell line. *Science* 196, 1456–1458. doi: 10.1126/science.867042

Peebles, P. T., Trisch, T., and Papageorge, A. G. (1978). 727 - ISOLATION OF FOUR UNUSUAL PEDIATRIC SOLID TUMOR CELL LINES. *Pediatr. Res.* 12:485. doi: 10.1203/00006450-197804001-00732

Pique, C., and Jones, K. S. (2012). Pathways of cell-cell transmission of HTLV-1. *Front. Microbiol.* 3:378. doi: 10.3389/fmicb.2012.00378

Pluta, A., Willems, L., Douville, R. N., and Kuźmak, J. (2020). Effects of naturally occurring mutations in bovine leukemia virus 5′-ltr and tax gene on viral transcriptional activity. *Pathogens* 9, 1–28. doi: 10.3390/pathogens9100836

Polat, M., Takeshima, S., and Aida, Y. (2017). Epidemiology and genetic diversity of bovine leukemia virus. *Virol J.* 14:209. doi: 10.1186/s12985-017-0876-4

Pulvertaft, R. J. V. (1964). CYTOLOGY OF BURKITT'S TUMOUR (AFRICAN LYMPHOMA). *Lancet* 283, 238–240. doi: 10.1016/S0140-6736(64)92345-1

Reyes, R. A., and Cockerell, G. L. (1996). Unintegrated bovine leukemia virus DNA: association with viral expression and disease. *J. Virol.* 70, 4961–4965. doi: 10.1128/JVI.70.8.4961-4965.1996

Robinson, L. A., Jaing, C. J., Pierce Campbell, C., Magliocco, A., Xiong, Y., Magliocco, G., et al. (2016). Molecular evidence of viral DNA in non-small cell lung cancer and non-neoplastic lung. *Br. J. Cancer* 115, 497–504. doi: 10.1038/bjc.2016.213

Roecklein, B. A., and Torok-Storb, B. (1995). Functionally distinct human marrow stromal cell lines immortalized by transduction with the human papilloma virus E6/E7 genes. *Blood* 85, 997–1005. doi: 10.1182/blood.v85.4.997.bloodjournal854997

Schwingel, D., Andreolla, A. P., Erpen, L. M. S., Frandoloso, R., and Kreutz, L. C. (2019). Bovine leukemia virus DNA associated with breast cancer in women from South Brazil. *Sci. Rep.* 9:2949. doi: 10.1038/s41598-019-39834-7

Soule, H. D., Maloney, T. M., Wolman, S. R., Brenz, R., Russo, J., Pauley, R. J., et al. (1990). Isolation and Characterization of a Spontaneously Immortalized Human Breast Epithelial Cell Line. MCF-10. *Cancer Res.* 50, 6075–6086.

Soule, H. D., Vazquez, J., Long, A., Albert, S., and Brennan, M. A. (1973). human cell line from a pleural effusion derived from a breast carcinoma1,2. *J. Natl. Cancer Inst.* 51, 1409–1416. doi: 10.1093/jnci/51.5.1409

Stürzl, M., Gaus, D., Dirks, W. G., Ganem, D., and Jochmann, R. (2013). Kaposi's sarcoma-derived cell line SLK is not of endothelial origin, but is a contaminant from a known renal carcinoma cell line. *Int. J. Cancer* 132, 1954–1958. doi: 10.1002/ijc.27849

Suzuki, T., Ikeda, H., and Mase, M. (2018). Restricted viral cDNA synthesis in cell lines that fail to support productive infection by bovine leukemia virus. *Arch. Virol.* 163, 2415–2422. doi: 10.1007/s00705-018-3887-6

Tajima, S., Takahashi, M., Takeshima, S. N., Konnai, S., Yin, S. A., Watarai, S., et al. (2003). Mutant Form of the Tax Protein of Bovine Leukemia Virus (BLV), with Enhanced Transactivation Activity, Increases Expression and Propagation of BLV In Vitro but Not In Vivo. *J. Virol.* 77, 1894–1903. doi: 10.1128/JVI.77.3.1894-1903.2003

Takahashi, M., Tajima, S., Okada, K., Davis, W. C., and Aida, Y. (2005). Involvement of bovine leukemia virus in induction and inhibition of apoptosis. *Microbes. Infect.* 7, 19–28. doi: 10.1016/j.micinf.2004.09.014

Zhao, X., and Buehring, G. C. (2007). Natural genetic variations in bovine leukemia virus envelope gene: possible effects of selection and escape. *Virology* 366, 150–165. doi: 10.1016/j.virol.2007.03.058

Zhao, X., Jimenez, C., Sentsui, H., and Buehring, G. C. (2007). Sequence polymorphisms in the long terminal repeat of bovine leukemia virus: evidence for selection pressures in regulatory sequences. *Virus Res.* 124, 113–124. doi: 10.1016/j.virusres.2006.10.010

Conflict of Interest: The authors declare that the research was conducted in the absence of any commercial or financial relationships that could be construed as a potential conflict of interest.

Publisher's Note: All claims expressed in this article are solely those of the authors and do not necessarily represent those of their affiliated organizations, or those of the publisher, the editors and the reviewers. Any product that may be evaluated in this article, or claim that may be made by its manufacturer, is not guaranteed or endorsed by the publisher.

frontiers in Microbiology

ORIGINAL RESEARCH
published: 17 March 2022
doi: 10.3389/fmicb.2022.799942

Bacterium-Like Particles Displaying the Rift Valley Fever Virus Gn Head Protein Induces Efficacious Immune Responses in Immunized Mice

Shengnan Zhang[1†], Feihu Yan[1†], Dongping Liu[2], Entao Li[1], Na Feng[1], Shengnan Xu[1], Hualei Wang[3], Yuwei Gao[1], Songtao Yang[1], Yongkun Zhao[1*] and Xianzhu Xia[1*]*

[1] Changchun Veterinary Research Institute, Chinese Academy of Agricultural Sciences, Changchun, China, [2] The Nanjing Unicorn Academy of Innovation, Institute Pasteur of Shanghai, Chinese Academy of Sciences, Nanjing, China, [3] College of Veterinary Medicine, Jilin University, Changchun, China

Rift Valley fever virus (RVFV), a mosquito-borne zoonotic phlebovirus, causes serious disease in humans and ruminants. According to the World Health Organization, Rift Valley fever is classified as a priority disease, and as such, vaccine development is of high priority due to the lack of licensed vaccines. In this study, a bacterium-like particle vaccine (BLP), RVFV-BLPs, is constructed. A novel display system is described, which is based on non-living and non-genetically modified Gram-positive bacterial cells, designated as Gram-positive enhancer matrix (GEM). The RVFV Gn head protein was displayed on the surface of GEM by co-expression with the peptidoglycan-binding domain (protein anchor) at the C-terminus. We determined that the RVFV Gn head-PA fusion protein was successfully displayed on the GEM. Mice immunized with RVFV-BLPs produced humoral and cellular immunity. Interestingly, comparing the production of RVFV Gn head-specific IgG and its subtype by vaccinating with different antigen doses of the RVFV-BLPs determined that the RVFV-BLPs (50 μg) group showed a greater effect than the other two groups. More importantly, antibodies produced by mice immunized with RVFV-BLPs (50 μg) exhibited potent neutralizing activity against RVFV pseudovirus. RVFV-BLPs (50 μg) also could induce IFN-γ and IL-4 in immunized mice; these mice generated memory cells among the proliferating T cell population after immunization with RVFV-BLPs with effector memory T cells as the major population, which means that RVFV-BLPs is an effective vaccine to establish a long-lived population of memory T cells. The findings suggest that the novel RVFV-BLPs subunit vaccine has the potential to be considered a safe and effective candidate vaccine against RVFV infection.

Keywords: Rift Valley fever (RVF) virus, bacterial like-particles, fusion protein, neutralizing antibody, specific IgG antibodies, protein anchoring

OPEN ACCESS

Edited by:
Axel Cloeckaert, Institut National de Recherche pour L'Agriculture, L'Alimentation et L'Environnement (INRAE), France

Reviewed by:
Shawn Babiuk, National Centre for Foreign Animal Disease (NCFAD), Canada
James Tristan Gordy, Johns Hopkins University, United States

***Correspondence:**
Songtao Yang
yst62041@163.com
Yongkun Zhao
zhaoyongkun1976@126.com
Xianzhu Xia
xiaxzh@cae.cn

[†] These authors have contributed equally to this work

Specialty section:
This article was submitted to Infectious Agents and Disease, a section of the journal Frontiers in Microbiology

Received: *22 October 2021*
Accepted: *03 February 2022*
Published: *17 March 2022*

Citation:
Zhang S, Yan F, Liu D, Li E, Feng N, Xu S, Wang H, Gao Y, Yang S, Zhao Y and Xia X (2022) Bacterium-Like Particles Displaying the Rift Valley Fever Virus Gn Head Protein Induces Efficacious Immune Responses in Immunized Mice. Front. Microbiol. 13:799942. doi: 10.3389/fmicb.2022.799942

INTRODUCTION

First reported in 1931 in Kenya (Daubney et al., 1931), Rift Valley fever (RVF) is a zoonotic disease caused by the RVF virus (RVFV), which primarily affects ruminants but also has the capacity to infect and cause disease in humans. Since its emergence nearly 90 years ago, RVFV has been attributed to a number of recurrent epidemics and epizootics mostly across Africa (Clark et al., 2018). As a mosquito-borne virus, RVFV is most commonly transmitted among animals and humans *via* mosquito bites; however, humans can also become infected upon exposure to infectious blood, bodily fluids, and tissues (van Velden et al., 1977; McIntosh et al., 1980; Anyangu et al., 2010; LaBeaud et al., 2015). The severity of RVFV zoonosis as well as its ability to cause major epidemics in both ruminants and humans prompted authorities to list RVFV as a notifiable disease and a potential biological weapon (Borio et al., 2002). RVFV is one of the 10 priority pathogens on the 2018 WHO Blueprint List of Priority Diseases.

RVFV (genus *Phlebovirus*; family *Phenuiviridae*; order *Bunyavirales*) is a negative-sense, single-stranded RNA virus with a tripartite genome consisting of three segments, namely, large (L), medium (M), and small (S) (Elliott, 1997; Bouloy and Weber, 2010). The L segment encodes for the viral RNA polymerase (L), whereas the M segment encodes two glycoproteins, which are cleaved during translation by cellular proteases into glycoproteins Gn and Gc, respectively (Bouloy and Weber, 2010). Additionally, the M segment encodes two non-structural proteins, namely, NSm1 and NSm2, corresponding to 78 and 14 kDa non-structural proteins, respectively (Bouloy and Weber, 2010). The S segment encodes the nucleocapsid (N) protein as well as a third non-structural protein (NSs), which functions as a virulence factor (Struthers et al., 1984). Both the viral RNA polymerase and N proteins are necessary for viral RNA replication and transcription while the glycoproteins make up the viral envelope and are strong antigenic determinants, thus eliciting potent neutralizing antibodies (Allen et al., 2018).

Historically, vaccination is proven to be an effective strategy for the prevention of viral diseases. While three veterinary vaccines are commercially available for use in endemic countries (Barteling and Woortmeyer, 1984; Minke et al., 2004; Faburay et al., 2013; Chamchod et al., 2015), there currently remains no licensed human vaccines for preventing RVFV infection (Kortekaas, 2014). However, a number of RVF vaccine platforms are reported in recent years, including a DNA vaccine (Bhardwaj et al., 2010), equine herpesvirus type 1 (EHV-1) vector vaccine (Said et al., 2017), a DNA prime with modified vaccinia virus Ankara (MVA) boost (Lorenzo et al., 2018), Newcastle disease virus (NDV)-based vector vaccine (Kortekaas et al., 2010), Lumpy skin disease virus (LSDV) vector vaccine (Wallace et al., 2020), and virus-like particle (VLP) vaccines (Mandell et al., 2010; Li et al., 2016).

In recent years, a novel antigen delivery system consisting of non-living, non-genetically modified cell wall particles derived from the food-grade bacterium *Lactococcus lactis* MG1363 is described for a number of pathogens, including shigellosis (Heine et al., 2015), human papillomavirus (HPV) (Ribelles et al., 2013), influenza virus (H1N1) (Saluja et al., 2010), porcine circovirus type 2 (PCV2) (Qiao et al., 2019), hepatitis E virus (HEV) (Gao et al., 2015), foot-and-mouth disease virus (FMDV) (Cheng et al., 2019), severe acute respiratory syndrome coronavirus (SARS) (Lee et al., 2006), and porcine reproductive and respiratory syndrome virus (PRRSV) (Li et al., 2018). This novel antigen delivery system allows for the display of multiple antigens on the particle surface in the form of recombinant fusion proteins containing a heterogeneous antigen and a peptidoglycan protein anchor (PA). The PA is derived from the C-terminus of the lactococcal cell-wall hydrolase AcmA and comprises one or more lysine motifs (LysMs), which are recognized in more than 4,000 prokaryotic and eukaryotic proteins as carbohydrate-binding protein modules (Brinster et al., 2007; Buist et al., 2008) and can be bound to the peptidoglycan (PGN) surface of bacterium-like particles (BLPs) *via* high-affinity non-covalent binding.

Here, we describe RVFV-BLPs consisting of Gram-positive enhancer matrix (GEM) particles displaying the RVFV Gn head-PA fusion protein on their surface as a novel vaccine candidate for the prevention of RVF. The RVFV Gn head-PA fusion protein was produced using a baculovirus expression system and, through the addition of a honeybee melittin signal (HBM), was successfully secreted into the supernatant. Immunization of BALB/c mice with these RVFV-BLPs resulted in RVFV-specific humoral and cellular immune responses, supporting RVFV-BLPs as a novel vaccine candidate for RVFV.

MATERIALS AND METHODS

Ethics Statement

All BALB/c mice were purchased from Changchun Yisi Laboratory Animal Technology Co., Ltd. (Changchun, China) and kept under specific-pathogen-free (SPF) conditions, fed standard rodent chow, and provided water *ad libitum*. All BALB/c mice were handled in compliance with the guidelines for the Welfare and Ethics of Laboratory Animals of China (GB 14925-2001), and all protocols were approved by the Animal Welfare and Ethics Committee of the Veterinary Institute at the Changchun Veterinary Research Institute (Laboratory Animal Care and Use Committee Authorization, permit number JSY-DW-2018-02).

Bacteria and Cell Culture

Lactococcus lactis MG1363 was generously provided to us by Jianzhong Wang and cultured in M17 medium (Qingdao Hope Bio-Technology Co., Ltd., China) supplemented with 1% glucose (GM17) (Thermo Fisher Scientific, United States) at 30°C in standing cultures. Adherent *Spodoptera frugiperda* (Sf9) cells (Life Technologies, United States) were cultured at 27°C and maintained in SFM 900 II medium (Life Technologies, United States) supplemented with 10% heat-inactivated fetal bovine serum (FBS) and 1% penicillin-streptomycin. Huh7 cells (ATCC) were cultured at 37°C

with 5% CO_2 and maintained in Dulbecco's modified eagle medium (DMEM, Life Technologies, United States) supplemented with 10% FBS.

Construction of Recombinant Bacmid

The M sequence of the RVFV and the PA sequence were retrieved from the RVFV MP-12 strain (GenBank: DQ380208, 426–1,427 nt) and the *L. lactis* MG1363 strain (GenBank: U17696.1, from 820 to 1,488 nt) and were synthesized by Sangon Biotech (Shanghai, China). The Gn head domain was fused with PA and HBM (ATGAAATTCTTAGTCAACGTTGCCCT TGTTTTTATGGTCGTGTACATTTCTTACATCTATGCG) by overlap PCR using the specific primers (**Table 1**). The Gn head domain was designed from the fifth ATG of the M segment (426–1,427 nt), which includes a specific 54-nucleotide signal peptide (SP) sequence (Faburay et al., 2013) with an HBM signal sequence at the N-terminus and a PA sequence at C-terminus (**Figure 1**). The sequence was cloned into a pFast Bac 1 vector (Invitrogen-Life Technologies, United States) and confirmed by restriction enzyme digest and DNA sequencing, and then the plasmids were transformed into DH10 Bac-competent *E. coli* to generate the recombinant bacmid pFBac 1-HBM-Gn head-PA.

Rescue and Identification of Recombinant Baculovirus

Rescue of the recombinant baculovirus, rpFB1-Gn head-PA, was done by transfection of Sf9 cells with the recombinant bacmid, pFBac 1-HBM-Gn head-PA, using the Cellfectin II Reagent (Life Technologies, United States). Briefly, Sf9 cells were seeded 24 h prior to transfection in a six-well plate at a density of 8×10^5 cells/well to achieve a confluency of 80–90%. For transfection, 3 μg of recombinant bacmid was diluted in 100 μL Grace's Insect Medium (Thermo Fisher Scientific, United States) and combined with 8 μL Cellfectin II Reagent diluted in Grace's Insect Medium to a final volume of 210 μL. The resulting transfection mixture was vortexed briefly and incubated at room temperature for 15–30 min, after which the DNA–lipid mixture was added onto the Sf9 cells and incubated at 27°C. Supernatants containing first generation (P1) recombinant baculovirus were harvested 72 h post-transfection and passaged for three additional generations on Sf9 cells to yield fourth generation (P4) recombinant baculovirus. All passaging was done upon observation of cytopathic effects (CPE), typically within 24 h post-infection. Expression of the RVFV Gn head-PA fusion gene was confirmed by PCR (primers in **Table 1**) for both P3 and P4 recombinant baculovirus.

TABLE 1 | Sequences of the primers used in the present study.

Primer name	Sequence (5′–3′)
HBM-*EcoRI*-F1	CG**GAATTC**ATGAAATTCTTAGTCAACGTTGCCCT TGTTTTTATGGTCGTGTACATTTCTTACA
HBM-*XbaI*-His-Gn head-F2	GTGTACATTTCTTACATCTATGCGGCCGCT**TCTA** CATCACCATCACCATCACATGACTGTGCTCCC AGCCCTG
Gn head-PA-F3	GAAGCGTGAACTGAGCGGTGCTTCTTCAGCTG
Gn head-PA-R1	CAGCTGAAGAAGCACCGCTCAGTTCACGCTTC
PA-*KpnI*-R2	GG**GGTACC**TAACTTGATACGCAGGTATTGAC CGATCAGG

[a]*Restriction enzyme sites EcoR I, Xba I, and Kpn I; are shown in bold. The HBM sequence is underlined.*

Identification of Rift Valley Fever Virus Gn Head-Protein Anchor Fusion Protein Expressed by Recombinant Baculovirus

Expression of RVFV Gn head-PA fusion protein by the rescued recombinant baculovirus was confirmed by indirect immunofluorescence analysis (IFA). Briefly, Sf9 cells were seeded in a 96-well plate to a density of 4×10^4 cells/well and infected with recombinant baculovirus at a multiplicity of infection (MOI) of 0.5 and cultured at 27°C for 48 h. Mock infected cells were included as a negative control. Following infection, the cells were fixed in 80% ice-cold acetone for 2 h at -20°C, washed with phosphate buffered saline (PBS) and incubated for 1 h at 37°C with a 1:1,000 dilution of rabbit anti-RVFV eGn serum produced in-house. Next, the cells were washed three times with PBST (0.5% Tween-20) and incubated for 1 h at 37°C with a 1:10,000 dilution of goat antirabbit IgG/FITC antibody (Bioss Antibodies, China) containing 1% Evans blue (Sigma-Aldrich, United States). The cells were then washed three times with PBST (0.5% Tween-20) and imaged using a ZEISS fluorescence microscope (Zeiss, Germany).

Both cell lysate and supernatant from recombinant baculovirus-infected Sf9 cells were subjected to Western blot analysis to confirm the expression of the RVFV Gn head-PA fusion protein. Briefly, Sf9 cells were seeded in a six-well plate at a density of 4×10^5 cells/well and subsequently infected with recombinant baculovirus at an MOI of 0.5. Cell lysate and supernatants were harvested 4 days post-infection and subjected to Western blot analysis. Proteins within the cell lysate and supernatant were denatured at 95°C for 10 min and resolved on a 12% SDS-polyacrylamide gel followed by transfer onto a 0.45 μm nitrocellulose membrane (GE Healthcare Life Science, Germany) using the wet transfer method. The nitrocellulose membrane was then blocked for 2 h at room temperature with the QuickBlock Blocking Buffer (Beyotime Biotechnology, China). After blocking, the membrane was washed three times with PBST (0.5% Tween-20) and subsequently incubated overnight at 4°C with rabbit anti-RVFV eGn protein serum diluted 1:200 in QuickBlock Primary Antibody Dilution buffer (Beyotime Biotechnology, China). The following day, the membrane was washed five times (6 min/wash) with PBST (0.5% Tween-20) and then incubated for 1 h at room temperature with goat antirabbit IgG/HRP secondary antibody (Bioss Antibodies, China) diluted 1:10,000 in QuickBlock Secondary Antibody Dilution buffer (Beyotime Biotechnology, China). The nitrocellulose membrane was then washed five times (6 min/wash) in PBST (0.5% Tween-20) and Western blots imaged using the Gel Image System analysis software, version 4.2 (Tanon, China).

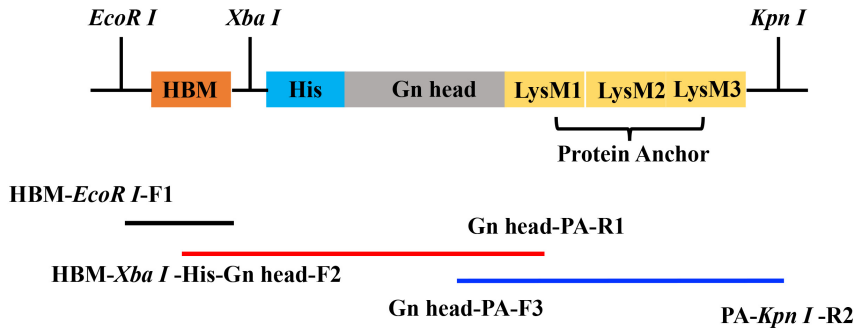

FIGURE 1 | Schematic representation of the plasmid. The primers in **Table 1** were used to amplify the HBM-Gn head-PA fragment according to the illustration.

Gram-Positive Enhancer Matrix Preparation

GEM particles were prepared as previously described (van Roosmalen et al., 2006). Briefly, *L. lactis* MG1363 cells were cultured in GM17, on a temperate orbital shaker at 30°C and 175 rpm for 15 h. The *L. lactis* MG1363 cells were harvested by centrifugation at 8,000 rpm for 15 min once the culture reached an OD_{600} value of 2 and the resulting cell pellet washed three times with PBS. Upon washing, the bacterial pellet was resuspended in 10% trichloroacetic acid (Sigma-Aldrich, United States) and boiled at 99°C for 30 min, effectively lysing the bacteria, degrading released proteins and DNA. The resulting lysate was washed three times with PBS and then resuspended in PBS. One unit (1U) of GEM particles was defined as approximately 2.5×10^9 particles (Bosma et al., 2006). Prepared GEM particles were stored at -20°C.

Binding and Dissociating of the Rift Valley Fever Virus Gn Head-Protein Anchor Fusion Protein to Gram-Positive Enhancer Matrix Particles

1U of GEM particles were added to the supernatant containing RVFV Gn head-PA fusion protein and slowly mixed at 37°C for 30 min. After binding, the GEM particles bound to the RVFV Gn head-PA fusion protein were collected by centrifugation at 5,000 rpm for 10 min and subsequently washed with and resuspended in PBS. RVFV Gn head-PA fusion proteins were dissociated from the GEM particles using 2% Mercaptoethanol. The mixture was then centrifuged at 10,000 rpm for 5 min and supernatants containing RVFV Gn head-PA protein collected. Samples were then analyzed by SDS-PAGE and Western blot.

Identification of Gram-Positive Enhancer Matrix Particles Loaded With Rift Valley Fever Virus Gn Head-Protein Anchor Fusion Protein

The surface localization of RVFV Gn head-PA on GEM particles was confirmed by immunofluorescence microscopy, flow cytometry, transmission electron microscopy (TEM), and immune-electron microscopy.

For TEM, the GEM particles loaded with RVFV Gn head-PA fusion protein were prefixed with 2.5% glutaraldehyde in 0.1 M PBS (pH 7.4) for 24 h at 4°C. The GEM particles were post-fixed with 1% osmium tetroxide for 1 h at 4°C. After dehydration through a series of ethanol gradients followed by acetone solutions, the samples were embedded in Epon 812 resin mixture. Ultrathin sections (70 nm) were stained with 2% uranyl acetate in 70% ethanol and Reynold's lead solution and examined with a JEM 1200EXII electron microscope (JEOL, Japan).

For immunofluorescence microscopy and flow cytometry, the GEM particles loaded with RVFV Gn head-PA fusion protein were fixed with 4% paraformaldehyde for 30 min at room temperature and then IFA performed as described in section "Rescue and Identification of Recombinant Baculovirus." The GEM particles loaded with RVFV Gn head-PA fusion protein were resuspended in sterile water, GEM particles used as a negative control were treated in parallel. The samples were separated into two batches. In batch I, samples were spread on a glass slide and observed with a fluorescence microscope. In batch II, samples were analyzed by flow cytometry using a FACSAria Cell Sorter (BD Biosciences, United States).

For immune-electron microscopy, the GEM particles loaded with RVFV Gn head-PA fusion protein were absorbed on copper grids for 30 min at room temperature followed by three washes with PBS. The grids were incubated for 2 h at room temperature with rabbit anti-RVFV eGn protein serum diluted 1:200 in PBS supplemented with 2% BSA. Following incubation, the grids were washed five times with PBS and incubated for 1 h at 37°C with donkey antirabbit IgG H&L (10 nm Gold) (Abcam, United States) diluted 1:100 in 30 μL PBS. Last, grids were washed three times with PBS and examined with a JEM 1200EXII electron microscope.

Maximum Binding Capacity of Rift Valley Fever Virus Gn Head-Protein Anchor Fusion Protein on Gram-Positive Enhancer Matrix Particles

The maximum amount of RVFV Gn head-PA fusion protein bound to 1U GEM particles was determined by SDS-PAGE. Briefly, 1U of GEM particles was combined with a range of supernatant volumes (1, 2, 3, 4, 6, 8, and 10 mL) containing

the RVFV Gn head-PA fusion protein. After binding for 1 h, the complexes were washed three times with PBS. At the same time, a BSA standard was twofold serially diluted. Samples were denatured with 5 × protein loading buffer at 95°C for 10 min. Equal volumes of samples were loaded on the gel, and the samples were separated by 12% SDS-polyacrylamide gel. After Coomassie blue (Beyotime Biotechnology, China) staining for 20 min followed by 10 washes, the maximum amount of RVFV Gn head-PA fusion protein that bound to 1U GEM particles was determined based on the BSA standard using the Quantity One image analysis software.

Vaccine Preparation and Immunization of Mice

GEM particles loaded with RVFV Gn head-PA fusion protein were defined as RVFV-bacteria like particles (RVFV-BLPs). Upon verifying that the GEM particles could bind the RVFV Gn head-PA fusion protein, we further evaluated the immunogenicity of RVFV-BLPs *in vivo* using BALB/c mice.

Six-week-old female BALB/c mice were randomly divided into four groups of 10 and each group vaccinated intramuscularly in the quadriceps with three different doses, namely, 20, 50, and 100 μg of RVFV-BLPs diluted in PBS. Mice in the control group were vaccinated with PBS. Animals in each group received a prime immunization, followed by two repeated immunizations at 2 and 4 weeks post primary immunization. Sera was harvested weekly until 4 weeks after the second repeated (third immunization).

ELISA Measurement of Rift Valley Fever Virus Gn Head-Specific IgG Antibodies

Sera from vaccinated animals were tested for the presence of RVFV Gn head-specific IgG, IgG1, IgG2a, and IgG3 antibodies by indirect ELISA. Briefly, 96-well microtiter plates were coated overnight at 4°C with 10 μg/mL purified RVFV Gn head protein (100 μL/well) prepared in 0.05 M carbonate-bicarbonate buffer. Purified RVFV Gn head protein was produced in-house by expression in 293F cells. After coating, the plates were washed three times with PBST (0.5% Tween-20) followed by blocking for 2 h at 37°C with 5% skim milk (Solarbio, China). The plates were then incubated for 1 h at 37°C with twofold serially diluted sera prepared in 5% skim milk. Following incubation, the plates were washed three times with PBST (0.5% Tween-20) and subsequently incubated for 1 h at 37°C with 1:10,000 dilutions (100 μL/well) of either goat antimouse IgG (H&L)-HRP (Bioworld, United States), goat antimouse IgG1-HRP (Southern Biotechnology, United States), goat antimouse IgG2a-HRP (Southern Biotechnology, United States), or goat antimouse IgG3-HRP (Southern Biotechnology, United States) diluted in 5% skim milk. After washing, tetramethylbenzidine (TMB) substrate (Sigma-Aldrich, United States) was added and incubated at room temperature for 10 min in a dark room. The reaction was stopped with 50 μL/well H_2SO_4 (0.5 M), and the absorbance was measured at 450 nm using an automated ELISA plate reader (Thermo Fisher Scientific, United States).

Pseudotyped Virus Neutralization Assay

An RVFV pseudotyped virus neutralization assay (PsVNA) was performed as described previously (Ma et al., 2019). Briefly, 200 pfu RVFV-pseudovirus was incubated with an equal volume of threefold serially diluted serum samples from immunized mice at 2 weeks after the third immunization in 96-well plates for 1 h at 37°C. Huh7 cells were then added to each well at a density of 3×10^4 cells/well and incubated at 37°C with 5% CO_2 for 24 h. The relative light unit (RLU) values were then measured (Nie et al., 2017), and the reduction in values was compared with those in the control wells, which were then used to determine the 50% inhibitory dilution (ID_{50}) values of the sera using the Reed–Muench method.

Lymphocyte Proliferation Assay

In vitro lymphocyte proliferation studies were performed with splenocytes from immunized mice. Two weeks after the third immunization, three mice from each group were randomly selected and euthanized. Harvested spleens were transferred to a tissue culture dish and mechanically minced followed by treatment in red blood cell lysing agent. The resulting splenocytes were washed with RPMI 1640 medium (Gibco, United States) containing 10% FBS. Next, the splenocytes were seeded in 96-well plates to a density of 2×10^3 cells/well (100 μL/well) and stimulated for 24 h with 10 μg/mL purified RVFV Gn head protein at 37°C and 5% CO_2. Lymphocyte proliferation was monitored according to the technical manual of the TransDetect Cell Counting kit (CCK) (TransGen Biotech, China).

Detection of IFN-γ and IL-4 Cytokine by ELISpot Assay

ELISpot IFN-γ and IL-4 cytokine assays were performed as described previously (Zhang et al., 2019). Splenocytes were cultured in RPMI 1640 medium containing 10% FBS and stimulated with or without purified RVFV Gn head protein (10 μg/mL) for 36 h at 37°C and 5% CO_2. Following incubation, splenocytes producing IFN-γ and IL-4 were measured using mouse enzyme-linked immunospot (ELISpot) kits (Mabtech AB, Sweden) according to the manufacturer's instructions. Spot-forming cells (SFCs) were enumerated using an automated ELISpot reader (AID ELISPOT reader-iSpot, Germany).

Analysis of Splenic T Lymphocyte Subtypes

T cell subset populations and memory T lymphocytes in splenocytes were analyzed by flow cytometry. Splenocytes were seeded into six-well plates at a density of 5×10^6 cells/mL and stimulated with or without purified RVFV Gn head protein (10 μg/mL) for 36 h at 37°C and 5% CO_2. Cells were then labeled with equal volumes of 1:250 dilutions of anti-CD3-PE-Cy5, anti-CD4-FITC, anti-CD8-PE, anti-CD44-APC, and anti-CD62-PerCP-Cy5 (BD Biosciences, United States) for 30 min at 4°C. After washing, labeled cells were analyzed in a FACSAria™ Cell Sorter (BD Biosciences, United States).

RESULTS

Expression of the Rift Valley Fever Virus Gn Head-Protein Anchor Fusion Protein

The recombinant baculovirus, rpFB1-Gn head-PA, was successfully rescued by transfection of Sf9 cells with the recombinant bacmid pFBac 1-HBM-Gn head-PA. Sf9 cells infected with the recombinant baculovirus showed CPE at 24 hpi, whereas mock-infected cells exhibited no CPE as expected (**Figures 2A,B**). Furthermore, IFA analysis revealed a pronounced green fluorescence signal for infected Sf9 cells, whereas mock-infected cells showed no signal (**Figures 2C,D**). The RVFV Gn head-PA gene (1776bp) was detected in the P3 and P4 recombinant baculovirus by PCR and sequenced (**Figure 2E**). Last, Western blot analysis of both the supernatant and cell lysate from Sf9 cells infected with recombinant baculovirus revealed a 70 kDa band corresponding to the RVFV Gn head-PA fusion protein confirming its expression and secretion into the supernatant (**Figure 2F**).

Analysis of Gram-Positive Enhancer Matrix Particles Loaded With Rift Valley Fever Virus Gn Head-Protein Anchor Fusion Protein

RVFV-BLPs were subjected to both SDS-PAGE (**Figure 3A**) and Western blot (**Figure 3B**) analysis to confirm whether the RVFV Gn head-PA fusion protein was capable of binding to the GEM particles *via* PA. From the SDS-PAGE it can be observed that *L. lactis* MG1363 showed itself proteins (**Figure 3A**, lane 2) and GEM particles contained no proteins, confirming that treatment of *L. lactis* MG1363 with 10% TCA resulted in complete protein degradation (**Figure 3A**, lane 3). The RVFV-BLPs (**Figure 3A**, lane 6) contained fewer protein impurities by comparison with supernatant alone containing RVFV Gn head-PA fusion protein (**Figure 3A**, lane 7). In addition, Western blot analysis confirmed that the GEM particles alone contained no detectable RVFV Gn head-PA fusion protein as expected; the RVFV-BLPs confirmed the presence of the RVFV Gn head-PA fusion protein and were present in higher amounts when compared with supernatant alone containing RVFV Gn head-PA fusion protein (**Figure 3B**). Last, Western blot analysis of RVFV-BLPs treated with 2-mercaptoethanol revealed that the RVFV Gn head-PA fusion protein could be dissociated from the GEM particles following treatment with a reducing agent (**Figure 3B**). Together these data demonstrate that GEM particles can be used to enrich and purify the RVFV Gn head-PA fusion protein, and the non-covalent bond is very stable.

Next, fluorescence microscopy, flow cytometry, TEM, and immuno-electron microscopy were performed to verify that the RVFV Gn head-PA fusion protein was displayed on the surface of the GEM particles. Immunofluorescence microscopy revealed that only the RVFV-BLPs showed fluorescence (**Figure 4A**), whereas the GEM particles alone did not (**Figure 4B**). Flow cytometry results showed that fluorescence was significantly increased in RVFV-BLPs compared with GEM particles (**Figure 4C**). Together, these results confirm that the RVFV Gn head-PA fusion protein was properly and efficiently displayed on the GEM particles. TEM was used to further evaluate differences in the morphology among untreated *L. lactis* MG1363 and GEM particles. Untreated *L. lactis* MG1363 had a uniform internal texture, and the bacterial cell wall was clearly visible (**Figure 4D**). In contrast, the GEM particles (*L. lactis* MG1363 treated with TCA) had structurally intact peptidoglycan with a morphology resembling a smooth outer sphere with a hollow interior (**Figure 4E**). Furthermore, the intracellular protein and DNA contents of the GEM particles appeared to be partially released or degraded as expected (Bosma et al., 2006). TEM analysis of the RVFV-BLPs revealed the RVFV Gn head-PA fusion protein adhered to the surface of the GEM particles like cotton wool (**Figure 4F**, red arrow). Last, immuno-electron microscopy revealed that the surface-exposed RVFV Gn head-PA fusion protein was evenly distributed on the GEM particles (**Figure 4G**).

Maximum Binding Capacity of Rift Valley Fever Virus Gn Head-Protein Anchor Fusion Protein on Gram-Positive Enhancer Matrix Particles

The maximum binding capacity of the RVFV Gn head-PA fusion protein displayed on the GEM particles was evaluated by resuspending 1U of GEM particles in either 1, 2, 3, 4, 6, 8, or 10 mL of supernatant containing RVFV Gn head-PA fusion protein and subsequently subjected to SDS-PAGE. The result demonstrates that with the increase of supernatant volume binding with 1U GEM particles, the relative quality of binding increased (**Figure 4H**). Due to the similarity of the combination with 6, 8, and 10 mL, it was already saturated (**Figure 4I**, lane 7–9). Furthermore, we estimated that 1U GEM particles could bind 100 μg RVFV Gn head-PA fusion protein by Quantity One image analysis software.

Detection and Measurement of Serum Antibody Response in Mice

BALB/c mice were immunized intramuscularly in groups of 10 with three different doses of RVFV-BLPs, namely, 20, 50, and 100 μg with control animals receiving PBS alone. Animals in each group received a prime immunization, followed by two repeated immunizations at 2 and 4 weeks post prime immunization and sera subsequently collected every week until 4 weeks after the second repeated immunization (**Figure 5**). For all groups, no RVFV Gn head specific IgG nor any of the IgG subtypes (IgG1, IgG2a, or IgG3) were detectable before 3 weeks post-primary immunization (**Figure 6**).

RVFV Gn head-specific IgG antibody titers were detectable for all groups starting at 3 weeks post-primary vaccination and peaked at 5 weeks post-primary vaccination, after which titers began to decrease with this decrease being most pronounced among the RVFV-BLPs (20 μg) group (**Figure 6A**). Interestingly, the comparison in IgG responses among the three different vaccine dose groups, revealed no positive correlation between antigen dose and the immunogenicity

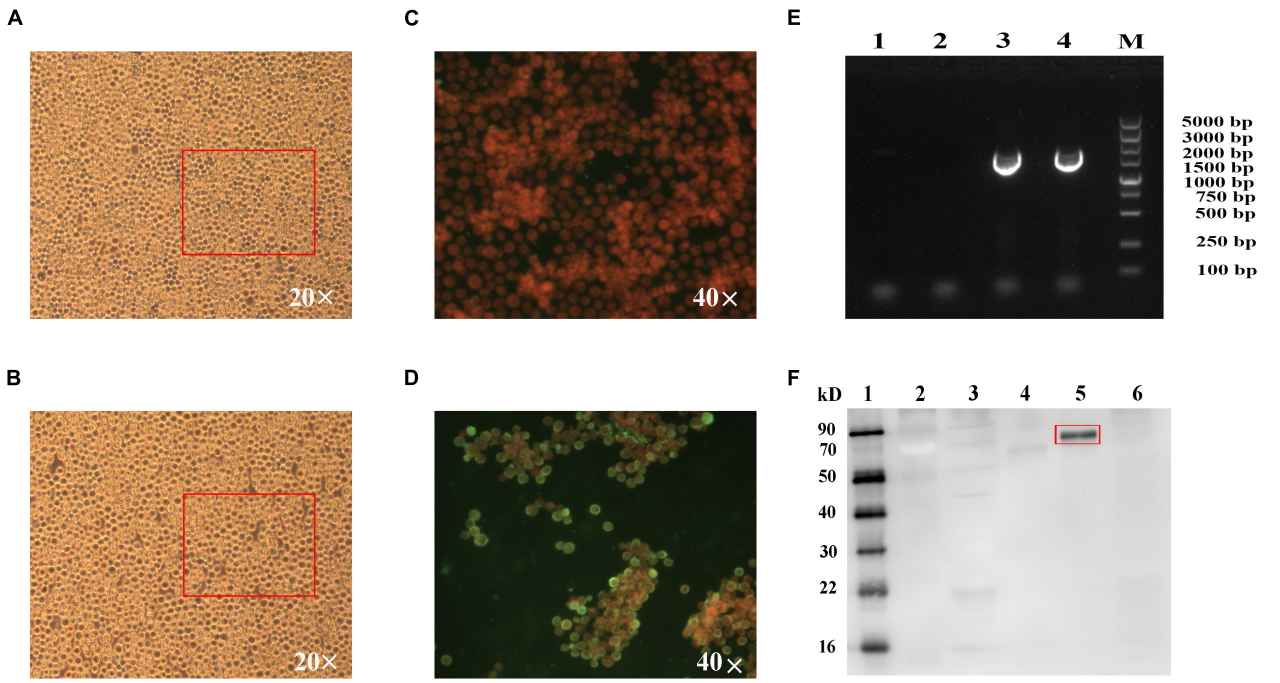

FIGURE 2 | Identification of the fusion protein. Normal Sf9 cells **(A,C)**, Sf9 cells infected with 3% recombinant baculovirus for 24 h, cells showed CPE of big and round **(B)** and were fixed, permeabilized, and stained with rabbit anti-RVFV eGn serum produced in-house and fusion protein is labeled by goat antirabbit IgG/FITC **(D)**. Identification of the stability of recombinant baculovirus by PCR **(E)**, lane 1 is Sf9 cells, lane 2 is control baculovirus, and lanes 3 and 4 are the third- and fourth-generation recombinant baculovirus, RVFV Gnhead-PA is 1776 bp. The fusion proteins secreted into the cell supernatant detected by WB **(F)**, lanes 1 and 2 are a protein marker, lane 3 is Sf9 cells, lane 4 is a mixture of Sf9 cells infected with control baculovirus, the supernatant (lane 5) and cell lysis fragment (lane 6) of the Sf9 cells infected with the recombinant baculovirus. RVFV Gn head-PA is 70 kD.

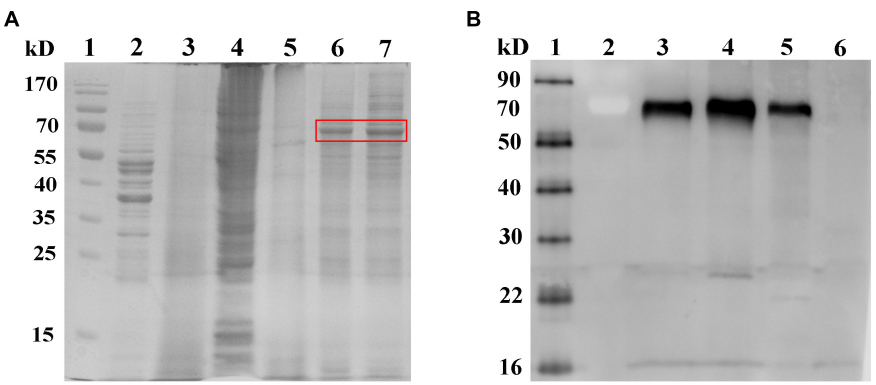

FIGURE 3 | Identification of binding and dissociating of the RVFV Gn head-PA fusion protein to GEM particles. SDS-PAGE analyses of binding between RVFV Gn head-PA fusion protein and GEM particles **(A)**, lane 1 is protein marker, lane 2 is *L. lactis* MG1363, lane 3 is GEM particles, lane 4 is Sf9 cells, lane 5 is control baculovirus, lane 6 is RVFV-BLPs, and lane 7 is the supernatant containing RVFV Gn head-PA fusion protein. Western blot analyses of binding and dissociating between RVFV Gn head-PA fusion protein and GEM particles **(B)**, lanes 1 and 2 are protein marker, lane 3 is the supernatant after dissociated by using 2% Mercaptoethanol, lane 4 is RVFV-BLPs, lane 5 is the supernatant containing RVFV Gn head-PA fusion protein, and lane 6 is GEM particles.

of the RVFV-BLPs, where the 50 μg dosage demonstrated the greatest immunogenicity, yielding the highest RVFV Gn head-specific IgG titers when compared with the 20 and 100 μg RVFV-BLP groups (**Figure 6A**). While the RVFV-BLPs (100 μg) group received the greatest amount of antigen, the appearance of RVFV Gn head-specific IgG antibodies was delayed compared with the 20- and 50 μg groups, only reaching comparable titers 4 weeks post-primary vaccination (**Figure 6A**).

To better characterize the antibody responses mounted against the RVFV Gn head protein, the levels of RVFV Gn head-specific IgG subtypes (IgG1, IgG2a, and IgG3) elicited following

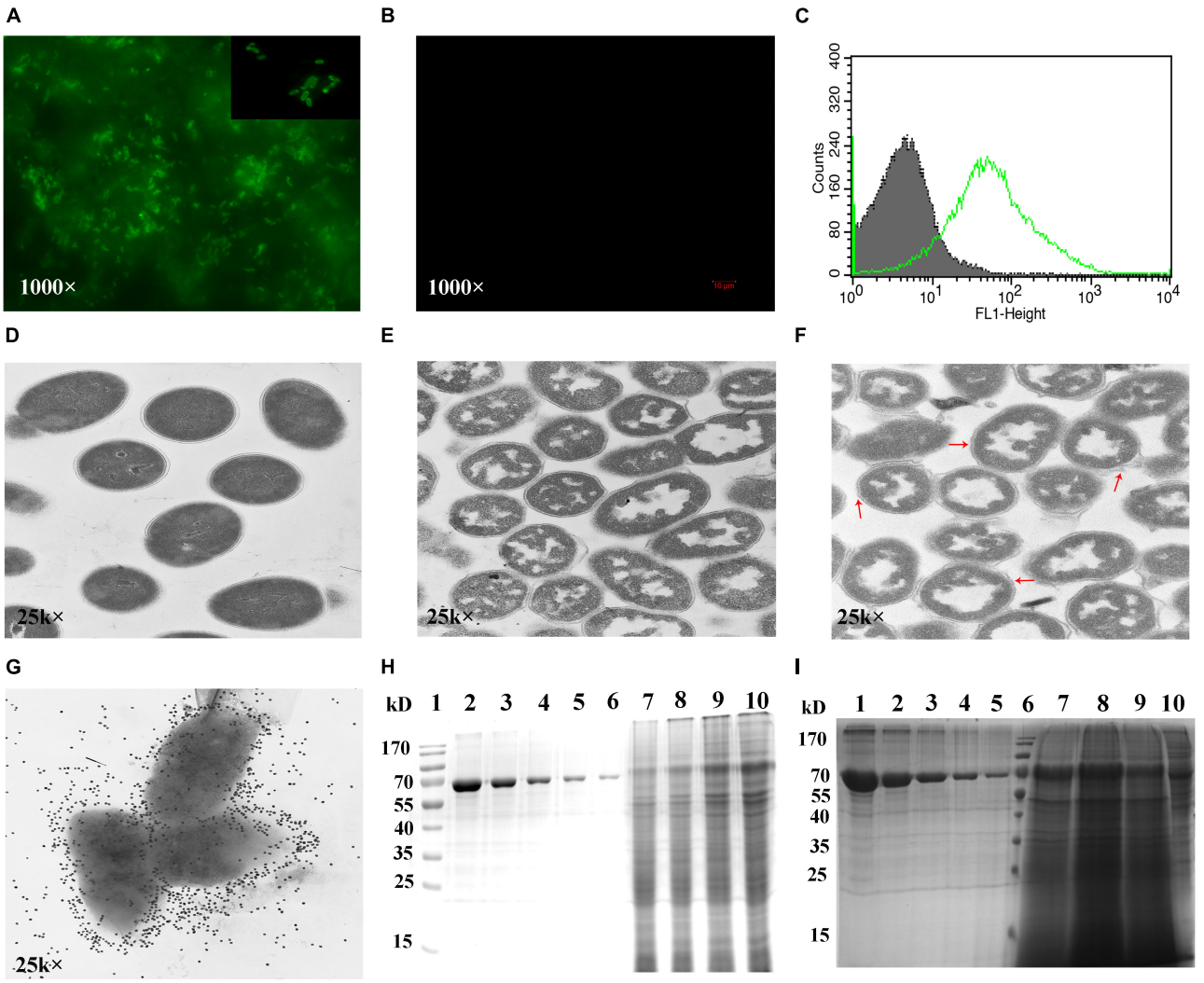

FIGURE 4 | Detection of fusion protein displayed on the surface of GEM particles. IFA experiment detection of RVFV-BLPs labeled by goat antimouse FITC **(A)** and no fluorescence found in GEM particles **(B)**. FACS histograms of RVFV-BLPs (green) and GEM particles (gray) **(C)**. TEM and immunogold labeling images of RVFV-BLPs, *L. lactis* MG1363 **(D)**, GEM particles **(E)** and RVFV-BLPs **(F)**. Fusion protein on the surface of GEM particles detected by immunogold labeling **(G)**. The maximum binding capacity of the fusion protein displayed on GEM particles was determined by SDS-PAGE **(H,I)**. In **(H)**, lane 1 is protein marker, lanes 2–6 are BSA, 0.5–0.03125 mg/ml. 1U GEM particles mixed with 1 (lane 7), 2 (lane 8), 3 (lane 9), and 4 mL (lane 10). In **(I)**, lanes 1–5 are BSA, 0.5–0.03125 mg/ml. Lane 6 is protein marker, 1U GEM particles mixed with 6 (lane 7), 8 (lane 8), 10 (lane 9), and lane 10 is the supernatant containing RVFV Gn head-PA fusion protein.

immunization with three different doses of RVFV-BLP were assessed by ELISA. The ratio of IgG2a/IgG1 is an indicator of Th1/Th2 deviation markers (type 1 cellular immune response or type 2 humoral immune response) with ratios > 1 being indicative of a Th1 response and ratios < 1 being indicative of a Th2 response. For all vaccine groups the IgG2a/IgG1 ratio was less than 1, suggesting that the RVFV-BLPs elicited a predominantly Th2 humoral immune response in BALB/c mice.

In all groups, RVFV Gn head-specific IgG1 subtype antibodies were detectable across all groups starting at 3 weeks post-primary vaccination (**Figures 6B–D**). In contrast, subtype IgG2a was only detectable in the 50 and 100 μg groups starting at 6 and 5 weeks post-primary immunization, respectively (**Figures 6C,D**) with no IgG2a being detected in the 20 μg group at any time point (**Figure 6B**). Surprisingly, RVFV Gn head-specific subtype IgG3 was only present in animals vaccinated with 50 μg RVFV-BLPs and was detectable starting at 5 weeks post-primary vaccination (**Figure 6C**). For all vaccinated animals, IgG1 was the dominant subtype induced by the RVFV-BLPs regardless of dosage.

Rift Valley Fever Virus Neutralizing Activity

Sera collected 6 weeks post-primary immunization from the RVFV-BLPs (50 μg) group was further analyzed to determine whether the anti-RVFV Gn head protein antibodies induced following vaccination exhibited neutralizing activity. The results demonstrate that immunized mice serum collected from

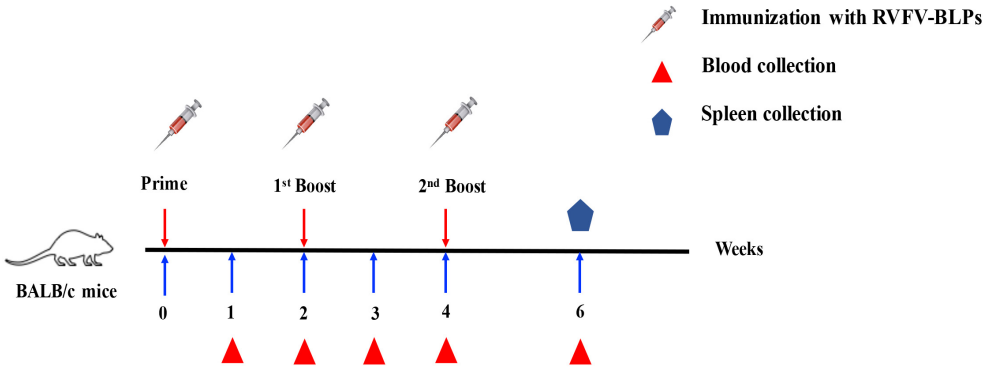

FIGURE 5 | Immunization schedule. BALB/c mice were immunized intramuscularly with different doses of RVFV-BLPs and boosted two times with the same amount on days 14 and 28.

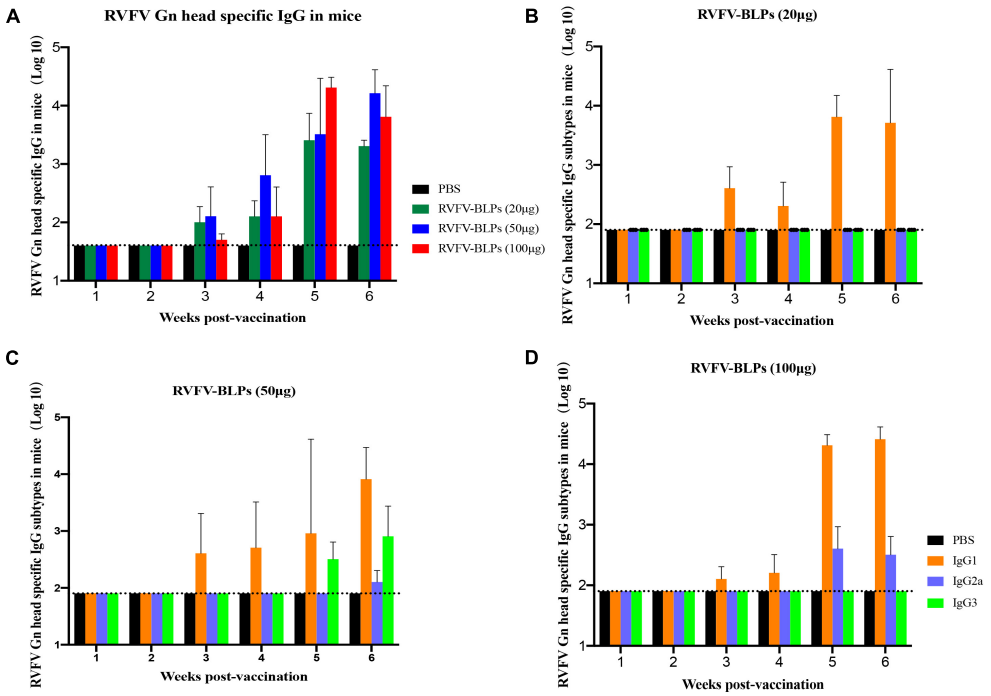

FIGURE 6 | Detection of antibody levels in immunized mice sera. Sera collection from mice immunized with different amounts of RVFV-BLPs. RVFV Gn head-specific IgG ($p > 0.05$), IgG1, IgG2a, and IgG3 levels in the serum were assessed by indirect ELISA; data are shown as the means ± SD. RVFV Gn head-specific IgG levels in mice immunized with different amounts of RVFV-BLPs **(A)**, and the levels of IgG subtypes in RVFV-BLPs (20 μg) **(B)**, RVFV-BLPs (50 μg) **(C)** and RVFV-BLPs (100 μg) **(D)**. Dotted line is cutoff values, calculated as OD450 of control × 2.1. Data are shown as the mean ± SEM and were analyzed by an unpaired *t*-test.

2 weeks after the third immunization could inhibit 50% RVFV pseudovirus infection (**Figure 7A**).

Rift Valley Fever Virus-Bacterium-Like Particle Vaccines Induced T Cell Proliferative Responses

Splenocytes from mice immunized with RVFV-BLPs (50 μg) were harvested 6 weeks post-primary vaccination to evaluate whether immunization with RVFV-BLPs could induce antigen-specific T cell proliferation in the spleen. Splenocytes harvested from immunized mice were found to proliferate more efficiently than those from the PBS group ($^*p < 0.05$) following stimulation with purified RVFV Gn head protein *in vitro* (**Figure 7B**).

Rift Valley Fever Virus-Bacterium-Like Particle Vaccines Induced Antigen-Specific IFN-γ and IL-4 Secretion

The results demonstrate that RVFV-BLPs are capable of inducing the production of RVFV Gn head-specific antibodies

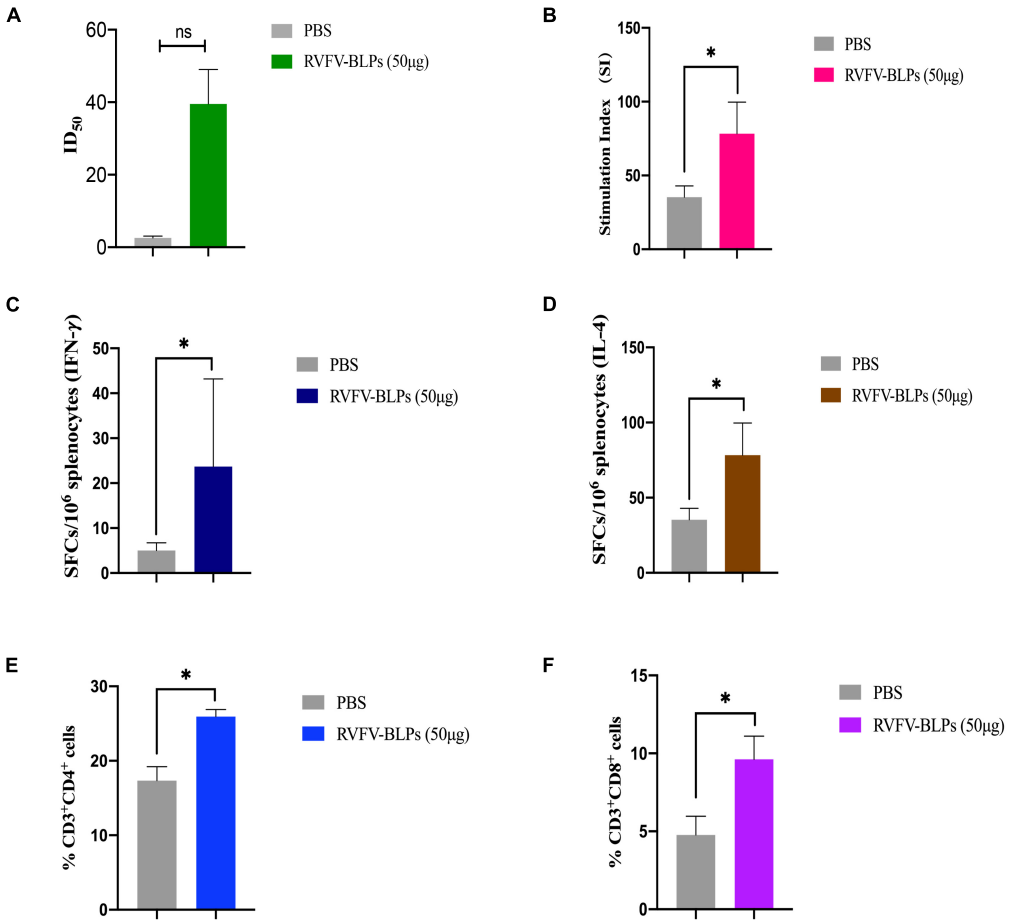

FIGURE 7 | Humoral and cellular responses detection of mice immunized with RVFV-BLPs (50 μg). The neutralizing RVFV-pseudovirus activity of mice immunized with RVFV-BLPs (50 μg) of 2 weeks after the third immunization were represented by 50% inhibition dilution (ID_{50}) **(A)**. Antigen-specific T cell proliferation, the stimulation index of the splenocytes was detected using a CCK assay by stimulating the cells with purified RVFV Gn head protein **(B)**. The RVFV Gn head-specific IFN-γ and IL-4 activity of splenocytes were evaluated using commercial ELISpot kits. SFC secreting IFN-γ **(C)** and IL-4 **(D)** were enumerated in an automated ELISpot reader. T cell proliferation was analyzed by using the following gating strategy: live→single cells→$CD3^+ \rightarrow CD4^+/CD8^+$ **(E,F)**. Data are shown as the mean ± SEM and were analyzed by an unpaired *t*-test (*$p < 0.05$).

and effectively stimulate splenocyte proliferative responses in immunized mice. As such, we set out to investigate whether RVFV-BLPs could promote cytokine secretion by evaluating through ELISpot assays IFN-γ and IL-4 responses in proliferating splenic T cells from immunized mice. From the results, it can be observed that the levels of IFN-γ and IL-4 in splenocytes harvested from the RVFV-BLPs (50 μg) group were significantly higher than those in the PBS control group (*$p < 0.05$) (**Figures 7C,D**), indicating that RVFV-BLPs could promote cytokine secretion.

Rift Valley Fever Virus-Bacterium-Like Particle Vaccines Induced Antigen-Specific Cellular Immune Response

To evaluate the cellular immune response induced by RVFV-BLPs, splenocytes from the RVFV-BLPs (50 μg) group were harvested 6 weeks post-primary vaccination and subjected to flow cytometry to characterize T cell subset populations in splenocytes (**Figures 7E,F**). Analysis by flow cytometry revealed that the number of $CD3^+CD4^+$ (**Figure 7E**) and $CD3^+CD8^+$ (**Figure 7F**) T cells in splenocytes harvested from mice immunized with 50 μg RVFV-BLPs were significantly elevated (*$p < 0.05$) when compared with the PBS control group.

DISCUSSION

While several types of RVFV vaccines (Barteling and Woortmeyer, 1984; Minke et al., 2004; Bhardwaj et al., 2010; Kortekaas, 2014; Chamchod et al., 2015; Said et al., 2017) have been reported in recent years, there still remains no fully licensed vaccines for use in non-endemic countries for either humans or veterinary animals. In contrast, a limited number of vaccines are available for veterinary use in endemic countries; however, there

is no clear policy or practice of routine livestock vaccinations as a preventive strategy against potential RVF disease outbreaks. In this study, we describe a novel RVFV-BLPs vaccine platform, consisting of *L. lactis* MG1363–derived GEM particles displaying on their surface the RVFV Gn head-PA fusion protein *via* a transmembrane protein anchor. The display of large antigens on bacterial surfaces can at times be problematic as they perturb the membrane topology (Lee et al., 2006), and as such, to overcome this, we used the head domain of RVFV Gn starting with the fifth ATG (426–1,427 nt), which is an ideal region recognized by neutralizing antibodies (Wu et al., 2017). Secretory expression is a major criterion for large-scale production of vaccines, and as such, an HBM signal was added upstream of the RVFV Gn head domain (**Figure 1**) to allow for secretion of the RVFV Gn head-PA fusion protein into the supernatant following infection of Sf9 cells with the constructed recombinant baculovirus. Sf9 cells infected with the constructed recombinant baculovirus displayed CPE within 24 h post infection (**Figures 2A,B**), and not only was the fusion protein expressed (**Figure 2D**), but it was also secreted into the supernatant (**Figure 2F**).

The GEM particles used to display the RVFV Gn head-PA fusion protein were prepared through treatment of *L. lactis* MG1363 with 10% TCA. Following treatment, the GEM particles appeared as peptidoglycan spheres with all proteins and intracellular DNA degraded as observed by TEM (**Figure 4E**). In contrast, TEM of untreated *L. lactis* MG1363 revealed an intact bacterial cell wall (**Figure 4D**). Both SDS-PAGE and Western blot analysis of the RVFV-BLPs confirmed that the RVFV Gn head-PA fusion protein was bound to the GEM particles (**Figures 3**, **4**) and displayed on the surface of the GEM particles *via* PA with an appearance similar to cotton filaments as observed by TEM (**Figures 4A,F,G**). Last, the maximum amount of RVFV Gn head-PA fusion protein capable of binding to 1 U (2.5×10^9 particles) of GEM particles was empirically determined to be 100 μg (**Figures 4H,I**).

To evaluate the immunogenicity of the RVFV-BLPs, BALB/c mice were immunized intramuscularly with three different doses, namely, 20, 50, and 100 μg of RVFV-BLPs. Mice were given a prime immunization followed by two repeated immunizations at 2 and 4 weeks post prime immunization and sera harvested weekly until 4 weeks after the second repeated (third immunization) (**Figure 5**). For all groups, RVFV Gn head-specific IgG antibodies were detectable 1 week after the second immunization; however, the 50 μg group had the highest titers compared with the 20 and 100 μg groups (**Figure 6A**). The specific IgG in the 50 μg group showed higher than the 100 μg group in early immunization and faded slowly. Further evaluation of the IgG subtypes (IgG1, IgG2a, and IgG3) among the three vaccine doses revealed that the level of the IgG subtypes had no linear relationship with the level of IgG, and the RVFV-BLPs elicited a predominantly Th2 humoral immune response in BALB/c mice.

The comprehensive analysis of the RVFV Gn head-specific IgG suggests that the RVFV-BLPs were capable of inducing a humoral immune response. With these findings, we selected the RVFV-BLPs (50 μg) group for further investigation to test for the presence of neutralizing antibodies as well as characterize the cellular immune response induced by the RVFV-BLPs. The immunized mice serum harvested 2 weeks after the second repeated immunization was evaluated for neutralizing activity by using a RVFV pseudovirus and revealed that mice immunized with RVFV-BLPs could produce a neutralizing RVFV pseudovirus antibody (**Figure 7A**). Together, these data reveal that BALB/c mice immunized with RVFV-BLPs mount a productive humoral immune response. For cellular immune response, the results show that RVFV-BLPs (50 μg) can induce antigen-specific T cell proliferation in the spleen (**Figure 7B**) and also effectively stimulate splenocytes to secrete IFN-γ (**Figure 7C**) and IL-4 (**Figure 7D**). IFN-γ is a Th1-type cytokine involved in the cellular immune response, and IL-4 is a Th2-type cytokine associated with humoral immune responses, which indicates that RVFV-BLPs (50 μg) could effectively stimulate the production of both Th1 and Th2 cytokines in mice, thereby enhancing cellular and humoral immune responses.

Last, we further characterize the cellular immune response mounted following immunization with 50 μg RVFV-BLPs and find that vaccination with RVFV-BLPs significantly increased numbers of $CD4^+$ (**Figure 7E**) and $CD8^+$ (**Figure 7F**) T cells compared with the PBS control group.

In short, the described RVFV-BLPs were found to induce both humoral and cellular immune responses in immunized BALB/c mice and, thus, represent a novel and promising vaccine candidate for the prevention of RVF infection in both humans and veterinary animals. Furthermore, the low cost and scalable production of the RFVF BLPs make them appealing for immunization on a large scale. Last, an additional benefit of RVFV-BLPs is that they could enable differentiation between infected and non-infected vaccinated animals (DIVA). While these RVFV-BLPs represent a novel vaccine candidate, further investigation is required to determine whether they can confer protection *in vivo* following challenge with RVFV.

DATA AVAILABILITY STATEMENT

The original contributions presented in the study are included in the article/supplementary material, further inquiries can be directed to the corresponding author/s.

ETHICS STATEMENT

The animal study was reviewed and approved by the Welfare and Ethics of Laboratory Animals of China (GB 14925-2001).

AUTHOR CONTRIBUTIONS

SZ and FY conceived and designed the experiments. SZ, FY, and EL performed the experiments. DL, HW, and YG analyzed the data. SZ wrote the manuscript. XX, YZ, and SY reviewed the manuscript. All authors read and approved the final manuscript.

FUNDING

This research was funded by the Jiangsu Science and Technology Plan Project (SBE2019740307) and the National Project for Prevention and Control of Transboundary Animal Diseases (Grant No. 2017YFD0501804).

ACKNOWLEDGMENTS

We thank Youchun Wang (Division of HIV/AIDS and Sex-transmitted Virus Vaccines, National Institutes for Food and Drug Control) for help with the antibody neutralization experiments using the VSV pseudovirus.

REFERENCES

Allen, E. R., Krumm, S. A., Raghwani, J., Halldorsson, S., Elliott, A., Graham, V. A., et al. (2018). A protective monoclonal antibody targets a site of vulnerability on the surface of rift valley Fever Virus. *Cell Rep.* 25, 3750–3758.e4. doi: 10.1016/j.celrep.2018.12.001

Anyangu, A. S., Gould, L. H., Sharif, S. K., Nguku, P. M., Omolo, J. O., Mutonga, D., et al. (2010). Risk factors for severe Rift Valley fever infection in Kenya, 2007. *Am. J. Trop. Med. Hyg.* 83, 14–21. doi: 10.4269/ajtmh.2010.09-0293

Barteling, S. J., and Woortmeyer, R. (1984). Formaldehyde inactivation of foot-and-mouth disease virus. Conditions for the preparation of safe vaccine. *Arch. Virol.* 80, 103–117. doi: 10.1007/BF01310652

Bhardwaj, N., Heise, M. T., and Ross, T. M. (2010). Vaccination with DNA plasmids expressing Gn coupled to C3d or alphavirus replicons expressing gn protects mice against Rift Valley fever virus. *PLoS Negl. Trop. Dis.* 4:e725. doi: 10.1371/journal.pntd.0000725

Borio, L., Inglesby, T., Peters, C. J., Schmaljohn, A. L., Hughes, J. M., Jahrling, P. B., et al. (2002). Hemorrhagic fever viruses as biological weapons - Medical and public health management. *JAMA* 287, 2391–2405. doi: 10.1001/jama.287.18.2391

Bosma, T., Kanninga, R., Neef, J., Audouy, S. A., van Roosmalen, M. L., Steen, A., et al. (2006). Novel surface display system for proteins on non-genetically modified gram-positive bacteria. *Appl. Environ. Microbiol.* 72, 880–889. doi: 10.1128/AEM.72.1.880-889.2006

Bouloy, M., and Weber, F. (2010). Molecular biology of rift valley Fever virus. *Open Virol. J.* 4, 8–14. doi: 10.2174/1874357901004010008

Brinster, S., Furlan, S., and Serror, P. (2007). C-terminal WxL domain mediates cell wall binding in *Enterococcus faecalis* and other gram-positive bacteria. *J. Bacteriol.* 189, 1244–1253. doi: 10.1128/JB.00773-06

Buist, G., Steen, A., Kok, J., and Kuipers, O. P. (2008). LysM, a widely distributed protein motif for binding to (peptido)glycans. *Mol. Microbiol.* 68, 838–847. doi: 10.1111/j.1365-2958.2008.06211.x

Chamchod, F., Cosner, C., Cantrell, R. S., Beier, J. C., and Ruan, S. (2015). Transmission dynamics of rift valley fever virus: effects of live and killed vaccines on epizootic outbreaks and enzootic maintenance. *Front. Microbiol.* 6:1568. doi: 10.3389/fmicb.2015.01568

Cheng, H., Chen, J., Cai, Z., Du, L., Hou, J., Qiao, X., et al. (2019). Development of GEM-PA-nanotrap for purification of foot-and-mouth disease virus. *Vaccine* 37, 3205–3213. doi: 10.1016/j.vaccine.2019.04.078

Clark, M. H. A., Warimwe, G. M., Di Nardo, A., Lyons, N. A., and Gubbins, S. (2018). Systematic literature review of Rift Valley fever virus seroprevalence in livestock, wildlife and humans in Africa from 1968 to 2016. *PLoS Negl. Trop. Dis.* 12:e0006627. doi: 10.1371/journal.pntd.0006627

Daubney, R., Hudson, J. R., and Gamham, P. C. (1931). Enzootic hepatitis of Rift Valley fever: an undescribed virus disease of sheep, cattle and man from East Africa. *J. Pathol. Bacteriol.* 34, 545–549. doi: 10.1002/path.1700340418

Elliott, R. M. (1997). Emerging viruses: the Bunyaviridae. *Mol. Med.* 3, 572–577. doi: 10.1007/bf03401814

Faburay, B., Wilson, W., McVey, D. S., Drolet, B. S., Weingartl, H., Madden, D., et al. (2013). Rift Valley fever virus structural and nonstructural proteins: recombinant protein expression and immunoreactivity against antisera from sheep. *Vector Borne Zoonotic Dis.* 13, 619–629. doi: 10.1089/vbz.2012.1285

Gao, S., Li, D., Liu, Y., Zha, E., Zhou, T., and Yue, X. (2015). Oral immunization with recombinant hepatitis E virus antigen displayed on the *Lactococcus lactis* surface enhances ORF2-specific mucosal and systemic immune responses in mice. *Int. Immunopharmacol.* 24, 140–145. doi: 10.1016/j.intimp.2014.10.032

Heine, S. J., Franco-Mahecha, O. L., Chen, X., Choudhari, S., Blackwelder, W. C., van Roosmalen, M. L., et al. (2015). *Shigella* IpaB and IpaD displayed on *L. lactis* bacterium-like particles induce protective immunity in adult and infant mice. *Immunol. Cell Biol.* 93, 641–652. doi: 10.1038/icb.2015.24

Kortekaas, J. (2014). One Health approach to Rift Valley fever vaccine development. *Antiviral Res.* 106, 24–32. doi: 10.1016/j.antiviral.2014.03.008

Kortekaas, J., Dekker, A., de Boer, S. M., Weerdmeester, K., Vloet, R. P., de Wit, A. A., et al. (2010). Intramuscular inoculation of calves with an experimental Newcastle disease virus-based vector vaccine elicits neutralizing antibodies against Rift Valley fever virus. *Vaccine* 28, 2271–2276. doi: 10.1016/j.vaccine.2010.01.001

LaBeaud, A. D., Pfeil, S., Muiruri, S., Sutherland, L. J., Traylor, Z., Gildengorin, G., et al. (2015). Factors associated with severe human Rift Valley fever in Sangailu, Garissa County, Kenya. *PLoS Negl. Trop. Dis.* 9:e0003548. doi: 10.1371/journal.pntd.0003548

Lee, J. S., Poo, H., Han, D. P., Hong, S. P., Kim, K., Cho, M. W., et al. (2006). Mucosal immunization with surface-displayed severe acute respiratory syndrome coronavirus spike protein on Lactobacillus casei induces neutralizing antibodies in mice. *J. Virol.* 80, 4079–4087. doi: 10.1128/JVI.80.8.4079-4087.2006

Li, L., Qiao, X., Chen, J., Zhang, Y., Zheng, Q., and Hou, J. (2018). Surface-displayed porcine reproductive and respiratory syndrome virus from cell culture onto gram-positive enhancer matrix particles. *J. Ind. Microbiol. Biotechnol.* 45, 889–898. doi: 10.1007/s10295-018-2061-1

Li, Y. T., Wang, C. L., Zheng, X. X., Wang, H. L., Zhao, Y. K., Gai, W. W., et al. (2016). Development and characterization of Rift Valley fever virus-like particles. *Genet. Mol. Res.* 15:gmr7772. doi: 10.4238/gmr.15017772

Lorenzo, G., Lopez-Gil, E., Ortego, J., and Brun, A. (2018). Efficacy of different DNA and MVA prime-boost vaccination regimens against a Rift Valley fever virus (RVFV) challenge in sheep 12 weeks following vaccination. *Vet. Res.* 49:21. doi: 10.1186/s13567-018-0516-z

Ma, J., Chen, R., Huang, W., Nie, J., Liu, Q., Wang, Y., et al. (2019). *In vitro* and *in vivo* efficacy of a Rift Valley fever virus vaccine based on pseudovirus. *Hum. Vaccin Immunother.* 15, 2286–2294.

Mandell, R. B., Koukuntla, R., Mogler, J. L., Carzoli, A. K., Freiberg, A. N., Holbrook, M. R., et al. (2010). A replication-incompetent Rift Valley fever vaccine: chimeric virus-like particles protect mice and rats against lethal challenge. *Virology* 397, 187–198. doi: 10.1016/j.virol.2009.11.001

McIntosh, B. M., Russell, D., dos Santos, I., and Gear, J. H. (1980). Rift Valley fever in humans in South Africa. *S. Afr. Med. J.* 58, 803–806.

Minke, J. M., Audonnet, J. C., and Fischer, L. (2004). Equine viral vaccines: the past, present and future. *Vet. Res.* 35, 425–443. doi: 10.1051/vetres:2004019

Nie, J., Wu, X., Ma, J., Cao, S., Huang, W., Liu, Q., et al. (2017). Development of in vitro and in vivo rabies virus neutralization assays based on a high-titer pseudovirus system. *Sci. Rep.* 7:42769. doi: 10.1038/srep42769

Qiao, X. W., Yu, X. M., Li, P. C., Yu, S. S., Chen, J., Zhang, Y. P., et al. (2019). Immune efficacy of a porcine circovirus type 2 vaccine purified using Gram-positive enhancer matrix surface display technology. *J. Appl. Microbiol.* 127, 658–669. doi: 10.1111/jam.14346

Ribelles, P., Benbouziane, B., Langella, P., Suárez, J. E., and Bermúdez-Humarán, L. G. (2013). Protection against human papillomavirus type 16-induced tumors in mice using non-genetically modified lactic acid bacteria displaying E7 antigen at its surface. *Appl. Microbiol. Biotechnol.* 97, 1231–1239. doi: 10.1007/s00253-012-4575-1

Said, A., Elmanzalawy, M., Ma, G., Damiani, A. M., and Osterrieder, N. (2017). An equine herpesvirus type 1 (EHV-1) vector expressing Rift Valley fever virus (RVFV) Gn and Gc induces neutralizing antibodies in sheep. *Virol. J.* 14:154. doi: 10.1186/s12985-017-0811-8

Saluja, V., Visser, M. R., van Roosmalen, M. L., Leenhouts, K., Huckriede, A., Hinrichs, W. L., et al. (2010). Gastro-intestinal delivery of influenza subunit

vaccine formulation adjuvanted with Gram-positive enhancer matrix (GEM) particles. *Eur. J. Pharm. Biopharm.* 76, 470–474. doi: 10.1016/j.ejpb.2010.08.003

Struthers, J. K., Swanepoel, R., and Shepherd, S. P. (1984). Protein synthesis in Rift Valley fever virus-infected cells. *Virology* 134, 118–124. doi: 10.1016/0042-6822(84)90277-0

van Roosmalen, M. L., Kanninga, R., El Khattabi, M., Neef, J., Audouy, S., Bosma, T., et al. (2006). Mucosal vaccine delivery of antigens tightly bound to an adjuvant particle made from food-grade bacteria. *Methods* 38, 144–149.

van Velden, D. J., Meyer, J. D., Olivier, J., Gear, J. H., and McIntosh, B. (1977). Rift Valley fever affecting humans in South Africa: a clinicopathological study. *S. Afr. Med. J.* 51, 867–871.

Wallace, D. B., Mather, A., Kara, P. D., Naicker, L., Mokoena, N. B., Pretorius, A., et al. (2020). Protection of cattle elicited using a bivalent lumpy skin disease virus-vectored recombinant rift valley fever vaccine. *Front. Vet. Sci.* 7:256. doi: 10.3389/fvets.2020.00256

Wu, Y., Zhu, Y., Gao, F., Jiao, Y. M., Oladejo, B. O., Chai, Y., et al. (2017). Structures of phlebovirus glycoprotein Gn and identification of a neutralizing antibody epitope. *Proc. Natl. Acad. Sci. U.S.A.* 114, E7564–E7573. doi: 10.1073/pnas.1705176114

Zhang, S., Hao, M., Feng, N., Jin, H., Yan, F., Chi, H., et al. (2019). Genetically modified rabies virus vector-based rift valley fever virus vaccine is safe and induces efficacious immune responses in mice. *Viruses* 11:919.

Conflict of Interest: The authors declare that the research was conducted in the absence of any commercial or financial relationships that could be construed as a potential conflict of interest.

Publisher's Note: All claims expressed in this article are solely those of the authors and do not necessarily represent those of their affiliated organizations, or those of the publisher, the editors and the reviewers. Any product that may be evaluated in this article, or claim that may be made by its manufacturer, is not guaranteed or endorsed by the publisher.

frontiers | Frontiers in Microbiology

REVIEW
published: 04 April 2022
doi: 10.3389/fmicb.2022.825828

Bacteriophage-Mediated Control of Biofilm: A Promising New Dawn for the Future

Cheng Chang[1†], Xinbo Yu[1,2†], Wennan Guo[1†], Chaoyi Guo[1], Xiaokui Guo[1], Qingtian Li[3*] and Yongzhang Zhu[1*]*

[1] School of Global Health, Chinese Center for Tropical Diseases Research, Shanghai Jiao Tong University School of Medicine, One Health Center, Shanghai Jiao Tong University-The University of Edinburgh, Shanghai, China, [2] College of Stomatology, Shanghai Jiao Tong University School of Medicine, Shanghai, China, [3] Department of Laboratory Medicine, Ruijin Hospital, Shanghai Jiao Tong University School of Medicine, Shanghai, China

OPEN ACCESS

Edited by:
Pilar García, Spanish National Research Council (CSIC), Spain

Reviewed by:
Gina Ann Suh, Mayo Clinic, United States
Hao Chen, University of Texas Southwestern Medical Center, United States

***Correspondence:**
Xiaokui Guo
microbiology@sjtu.edu.cn
Qingtian Li
qingtianli@sjtu.edu.cn
Yongzhang Zhu
yzhzhu@sjtu.edu.cn;
yzhzhu@hotmail.com

[†] These authors have contributed equally to this work

Specialty section:
This article was submitted to Antimicrobials, Resistance and Chemotherapy, a section of the journal Frontiers in Microbiology

Received: *30 November 2021*
Accepted: *11 February 2022*
Published: *04 April 2022*

Citation:
Chang C, Yu X, Guo W, Guo C, Guo X, Li Q and Zhu Y (2022) Bacteriophage-Mediated Control of Biofilm: A Promising New Dawn for the Future. Front. Microbiol. 13:825828. doi: 10.3389/fmicb.2022.825828

Biofilms are complex microbial microcolonies consisting of planktonic and dormant bacteria bound to a surface. The bacterial cells within the biofilm are embedded within the extracellular polymeric substance (EPS) consisting mainly of exopolysaccharides, secreted proteins, lipids, and extracellular DNA. This structural matrix poses a major challenge against common treatment options due to its extensive antibiotic-resistant properties. Because biofilms are so recalcitrant to antibiotics, they pose a unique challenge to patients in a nosocomial setting, mainly linked to lower respiratory, urinary tract, and surgical wound infections as well as the medical devices used during treatment. Another unique property of biofilm is its ability to adhere to both biological and man-made surfaces, allowing growth on human tissues and organs, hospital tools, and medical devices, etc. Based on prior understanding of bacteriophage structure, mechanisms, and its effects on bacteria eradication, leading research has been conducted on the effects of phages and its individual proteins on biofilm and its role in overall biofilm removal while also revealing the obstacles this form of treatment currently have. The expansion in the phage host-species range is one that urges for improvement and is the focus for future studies. This review aims to demonstrate the advantages and challenges of bacteriophage and its components on biofilm removal, as well as potential usage of phage cocktail, combination therapy, and genetically modified phages in a clinical setting.

Keywords: bacteriophages, phage therapy, biofilms, depolymerase, endolysin

INTRODUCTION

Ancient Chinese warfare often had soldiers, in an arranged formation, form a fortress-like circle to shield themselves from and strike their opponents, as depicted in **Figure 1**. Similarly, bacteria benefit from working in a group by building a protective system that individual bacteria find difficult to achieve. Working together also allows bacteria to effectively conduct a collective assault on the host's defense or immune system. Having a medium to host a community of bacteria, therefore, is vital, and is achieved by the formation of biofilm. Biofilm is a microbial aggregate composed of an extracellular polymeric substance matrix secreted by the microbes themselves.

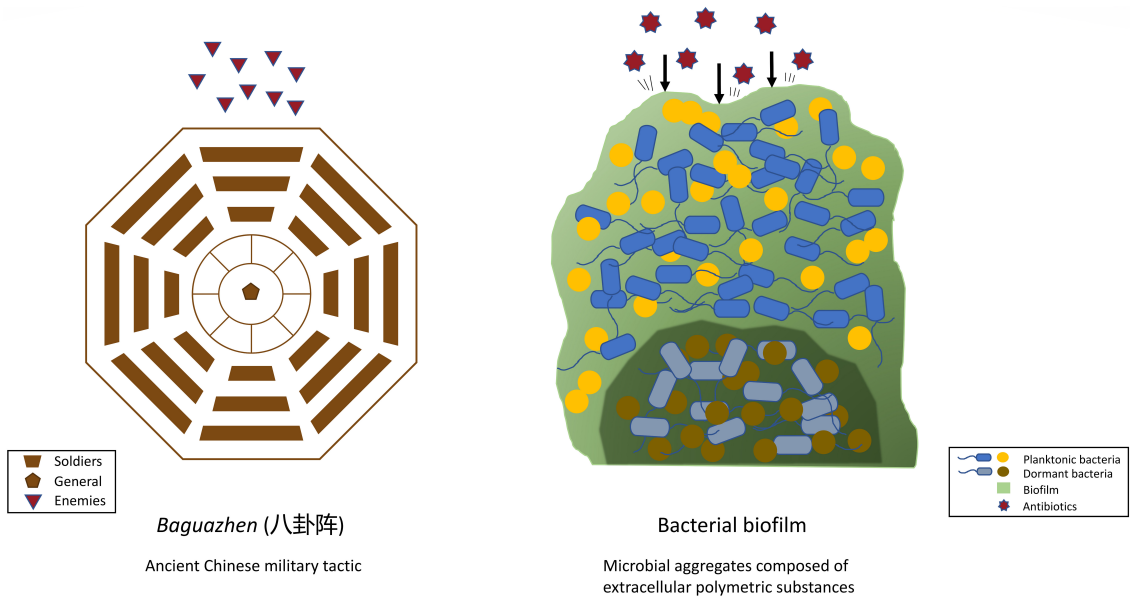

FIGURE 1 | Comparing the structural mechanism of ancient Chinese military tactics and bacterial biofilm.

The topic of biofilm raises global health concerns as the presence of biofilm is responsible for the majority of bacterial infections due to its ability to promote microbial survival against external stimuli, including antibiotics (Harrison et al., 2007; Høiby et al., 2011; Lebeaux et al., 2013; Wu et al., 2019; Yin et al., 2019). In addition, the presence of biofilm formation on medical devices presents a major challenge for modern medicine, especially on artificial joint restorations and catheters (Morris et al., 2019; Cano et al., 2021).

Hence, new strategies to eliminate biofilm function are in demand and bacteriophage therapy is an option regaining attention in recent decades. Bacteriophages—commonly simplified as phages—are the most abundant micoorganisms on the planet. Phages are viruses that selectively target and specifically kill bacteria through a replication cycle that involves attachment, injection of genetic information, replication within the cell, viral assembly, and—in lytic phages—kill the host bacteria cell by lysing the cell wall. Phages provide researchers and clinicians alike with a new dimension in antibacterial combat.

WHAT IS BIOFILM?

The extracellular polymeric substance (EPS) matrix composed in biofilm consists of exopolysaccharides, secreted proteins, lipids, extracellular DNA, and other minor components (Whitchurch et al., 2002; Rabin et al., 2015). The characteristics of the matrix components as well as the interactions of molecules provide mechanisms to biofilm's adherence to varieties of surfaces, preservation of nutrient reservoirs, and protection from outer environment (Yan and Bassler, 2019). Biofilm is commonly formed on surfaces such as dental deposits and medical implants, while it is also capable of forming without said surfaces (O'Toole et al., 2000; Alhede et al., 2011). The formation of biofilm is a complex yet well-regulated process that can be categorized into five main steps, as demonstrated in **Figure 2**: (i) surface sensing operated by the planktonic bacteria's flagella that facilitates such signaling through surface swarming (Armbruster and Parsek, 2018). (ii) attachment stage that involves the initial reversible attachment, responsible for loosely adhering the surface and detaching, and the subsequent irreversible attachment, responsible for more specific and stable adherence that is carried out by the bacterial adhesions (Rabin et al., 2015; Armbruster and Parsek, 2018). (iii) excretion of EPS matrix produced by the recently attached bacteria that signifies the creation of biofilm (Rabin et al., 2015). (iv) maturation of biofilm that involves interactions between bacteria cells that leads to the formation of microcolonies (Muhammad et al., 2020). (v) dispersal of biofilm structure following the release of planktonic bacteria and initiate the formation of biofilm at other sites (Rabin et al., 2015).

The adaptation and survival of biofilm are further accomplished via quorum sensing (QS), a communication system between resident bacteria cells that lead to a collective behavioral adjustment to change in cell density or other surrounding conditions (Remy et al., 2018). QS also plays an important role in regulating virulence factors in biofilm and contributing additional defensive mechanisms against foreign stress (Høyland-Kroghsbo et al., 2013).

Biofilm-resident bacteria can be categorized based on its Gram stain (Gram-positive or Gram-negative) or its growth site. The most encountered Gram-positive bacterial species include *Staphylococcus aureus (S. aureus), Listeria monocytogenes (L. monocytogenes), Bacillus subtilis (B. subtilis)*, and *Enterococcus faecalis (E. faecalis)* (Abee et al., 2011; Cruz et al., 2018). Gram-negative bacteria, on the other hand, are more prevalent

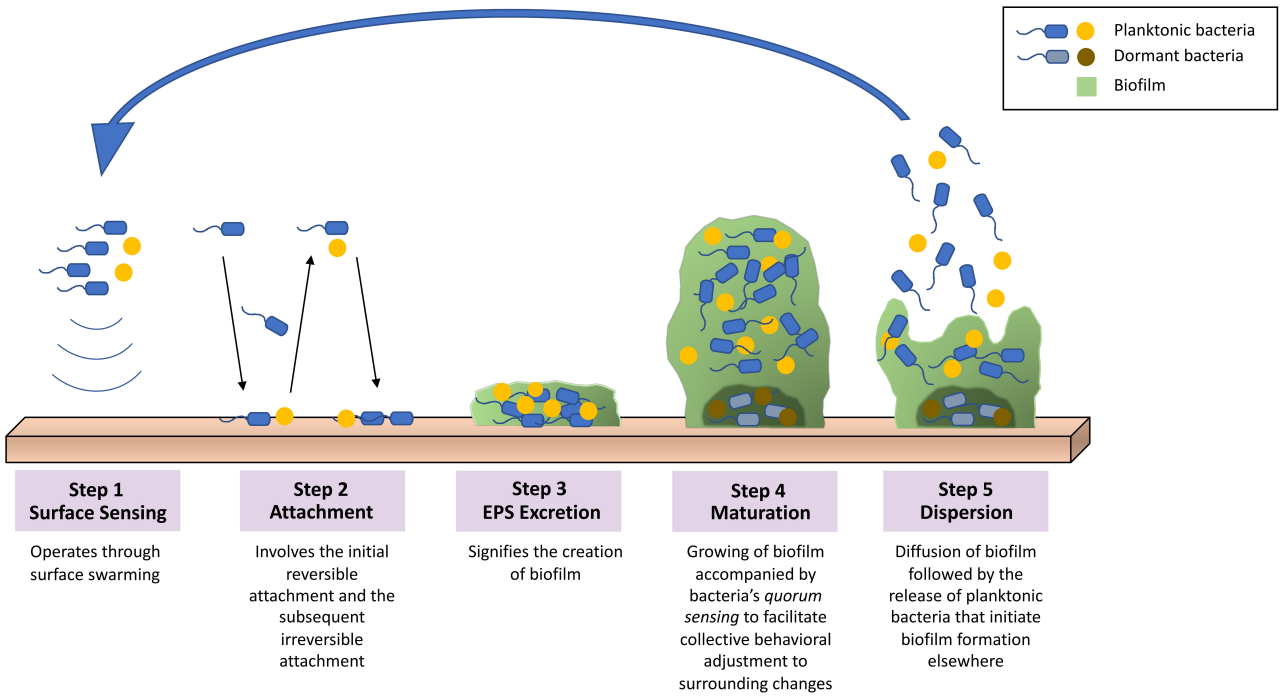

FIGURE 2 | Overview of the biofilm formation process. (1) Surface sensing operated by surface swarming. (2) Attachment stage involving the initial reversible attachment and the subsequent irreversible attachment. (3) Excretion of EPS that signifies the creation of biofilm. (4) Maturation of biofilm that involves quorum sensing to facilitate collective behavioral adjustments to surrounding changes. (5) Dispersal of biofilm structure following the release of planktonic bacteria initiating biofilm formation elsewhere.

and clinically significant specifically in the nosocomial setting due to its higher multidrug resistance rate (Spellberg et al., 2013). Frequently isolated Gram-negative bacteria include *Pseudomonas aeruginosa (P. aeruginosa)* (Bisht et al., 2021), *Klebsiella pneumoniae (K. pneumoniae)* (Tabassum et al., 2018), *Acinetobacter baumannii (A. baumannii)* (Shahed-Al-Mahmud et al., 2021), *Escherichia coli (E. coli)* (Sharma et al., 2016), *Proteus mirabilis (P. mirabilis)* (Wasfi et al., 2020), and *Streptococcus pneumoniae (S. pneumoniae)* (van der Kamp et al., 2020). In addition, bacteria and its biofilm could also be classified depending on whether a foreign body is involved or not. Common bacteria that cause infection through the formation of biofilm on medical devices include *P. mirabilis* (Wasfi et al., 2020), *S. aureus* (Lister and Horswill, 2014), *Staphylococcus epidermidis (S. epidermidis)* (Walker et al., 2020), *P. aeruginosa* (Walker et al., 2020), and *Streptococcus viridans (S. viridans)* (Veerachamy et al., 2014). Moreover, due to the complex, yet exceptionally humid and nutritional environment, the dental cavity is highly susceptible to biofilm formation (Dewhirst et al., 2010). Bacteria that are responsible for such activity include *Corynebacterium*, *Streptococcus*, *Porphyromonas*, *Haemophilus/Aggregatibacter*, *Neisseriaceae*, *Fusobacterium*, *Leptotrichia*, *Capnocytophaga*, and *Actinomyces* (Mark Welch et al., 2016).

Biofilm, acting as 'protective clothing', allows the bacteria to thrive well in inhospitable environments such as extreme temperatures and poor nutrient conditions (Harrison et al., 2007; Yin et al., 2019). Due to biofilm's strong resistance to external stimuli, it is estimated that 65% to 80% of the bacterial infections in the human body are correlated with biofilm (Lebeaux et al., 2013). There are two ways of biofilm infections: through direct infection of body tissue such as via lung infections in cystic fibrosis patients (Lebeaux et al., 2013), and contaminated medical devices or prostheses such as urinary catheters and dentures in patients with urinary tract infections and periodontal infections, respectively (Donlan, 2001; Murakami et al., 2015). Hence, since a broad spectrum of diseases is associated with the presence of biofilm, the ability of bacteria to form biofilms determines its pathogenicity and is of great significance in the course of infection.

ANTIMICROBIAL COMPOUNDS ON BIOFILM TREATMENT

Among biofilm's resistance to external pressures, one that presents immense clinical threat is its opposition against antimicrobial activities, chiefly during its mature stage (Wolcott et al., 2010; Wu et al., 2015). Bacteria clustered in biofilm could become up to a thousand times more resistant to antibiotics than the planktonic bacteria cells (Høiby et al., 2011; Wu et al., 2015). Several mechanisms could account for such resistance, as shown in **Table 1**: (1) Limitation of antibiotic diffusion through EPS matrix. (2) Limitation of antibiotic

TABLE 1 | Biofilm's antibiotic-resistant approaches and their mechanisms.

Antibiotic-resistant approach	Mechanisms
Limitation of antibiotic diffusion via EPS matrix	The structure of the EPS matrix, notably the exopolysaccharides, provides physical layers of protection against antimicrobial agents by creating permeability barriers that limit its diffusion (Yasuda et al., 1999). Moreover, biofilm EPS contains anionic and cationic molecules that can bind charged antimicrobial agents and accumulate antibacterial molecules up to 25% of its weight (Nadell et al., 2015; Sugano et al., 2016). Hence, the thick layers of EPS matrix may not be responsible for complete antibiotic resistance but provide the time necessary for biofilm to form adaptive phenotypic response to reduce susceptibility (Tseng et al., 2013).
Limitation of antibiotic diffusion via extracellular DNA (eDNA)	The inhibition of bacterial mobility due to the increase of cell density in the biofilm environment creates ideal conditions for direct interaction between conjugative plasmids (eDNA) as well as eDNA and exopolysaccharides (Hu et al., 2012; Rabin et al., 2015). Both interactions lead to the construction of more defined biofilm structures due to the increase in adhesion factors, hence further limiting the diffusion of antimicrobial compounds.
Antibiotic-degrading enzymes in the matrix	Biofilm possesses the ability to collect large amounts of β-lactamase, an antibiotic-degrading enzyme, in the matrix, creating a defensive mechanism that leads to hydrolysis of antibiotics when struck (Schmelcher et al., 2012).
Horizontal gene transfer	The accumulation of bacterial cells within the biofilm facilitates the horizontal gene transfer of the genes responsible for resistance (Bowler et al., 2020).
Multispecies interactions	Interactions between microorganisms that are different species in a biofilm can change the general antimicrobial resistance of the population (Bowler et al., 2020).

diffusion via extracellular DNA. (3) Activation of antibiotic-degrading enzymes in the matrix. (4) Horizontal gene transfer. (5) Multispecies interactions.

Furthermore, the biofilm matrix also protects bacteria from host immune responses. When activating the immune system, biofilm prevents bacteria from neutrophilic phagocytosis by containing the bacteria cells within a thick layer of coating (Yan and Bassler, 2019). Because neutrophils are only capable of engulfing pathogens that are smaller than 10 μm, they would find it impossible to ingest biofilm that could range up to 500 μm in horizontal dimension (Ferkinghoff-Borg and Sams, 2014; Yan and Bassler, 2019).

Despite difficulties combating biofilm, there are potential antimicrobial strategies that have shown to be partly effective. Wolcott et al. have demonstrated the use of sharp debridement techniques to remove the entire biofilm structure at its early stage of formation (Wolcott et al., 2010). While this method of physical scraping led to a decrease in the resistance to gentamicin in biofilm formed on fresh wounds, the regaining of antibiotic resistance after the 24-h therapeutic window as well as the limitation to function only on exposed infected regions have shown that this method is impractical in most cases (Wolcott et al., 2010; Yan and Bassler, 2019). In addition, bacterial enzyme-mediated biofilm dispersal has also gained clinical relevance especially in the eradication of biofilms in the oral cavity, where bacteria may secrete enzymes that downgrade biofilm matrix polymers produced by other pathogens (Kaplan, 2010). Nevertheless, due to the continuous upsurge in the number of multi-drug resistant bacterial strains, clinical and scientific research are in demand for finding alternative strategies to cope with biofilm development (Morris and Cerceo, 2020). Phages, the natural predator of bacteria, could be a solution worth exploring.

HOW PHAGES COMBAT BIOFILM

Phage-based treatment is capable of combating biofilm via several mechanisms using various phage components. Phages are strictly host-specific viruses that infect bacteria and are host-dependent during self-replication. In recent years, with the reduction in new antibiotic discoveries and the increase of antimicrobial resistance (AMR), phage and phage therapy research have gradually made a comeback since the discovery of antibiotics. Thousands of phages have been discovered (Ackermann and Prangishvili, 2012), but its basic structural forms can be categorized into four types: tailed phages, polyhedral phages, filamentous phages, and pleomorphic phages (Ackermann, 2009). The highly specific interaction with the host cell relies upon the receptor-binding protein positioned on the tail fiber of phages (Dams et al., 2019). The antibacterial activity of phage is carried out by two main enzymes—depolymerase and lysins—which are responsible for degrading capsular polysaccharides and peptidoglycan in bacterial cells, respectively (Schmelcher et al., 2012; Yan et al., 2014). The domain of a depolymerase is often displayed at the tip of the phage as tail fibers. On the other hand, lysins are encoded either inside or on the tail of the virion, which cleave the peptidoglycan cell wall from the inside and outside respectively (Sharma et al., 2018).

Phages are capable of destroying the bacterial hosts and therefore preventing the formation of biofilm (Domingo-Calap and Delgado-Martinez, 2018). Phages could also penetrate existing biofilm and eliminate the biofilm structure with or without killing the resident bacteria (Domingo-Calap and Delgado-Martinez, 2018). In nature, biofilm removal using phages could be categorized into three ways: (i) intra- to extracellular degradation of the bacterial structure. (ii) extra- to intracellular degradation of the bacterial structure. (iii) chemical dispersion of biofilm matrix, notably the EPS structure (Chan and Abedon, 2015). The corresponding modes by which phage-based treatment works are through basic phage therapy, phage-derived lysins, and phage-derived depolymerases (Young, 1992; Schmelcher et al., 2012; Yan et al., 2014). In addition, phages could be structurally engineered or bind with other antimicrobial compounds to produce genetically modified or combination therapies that could enhance the efficacy of eliminating microbial activity. The five ways of biofilm removal mentioned above are

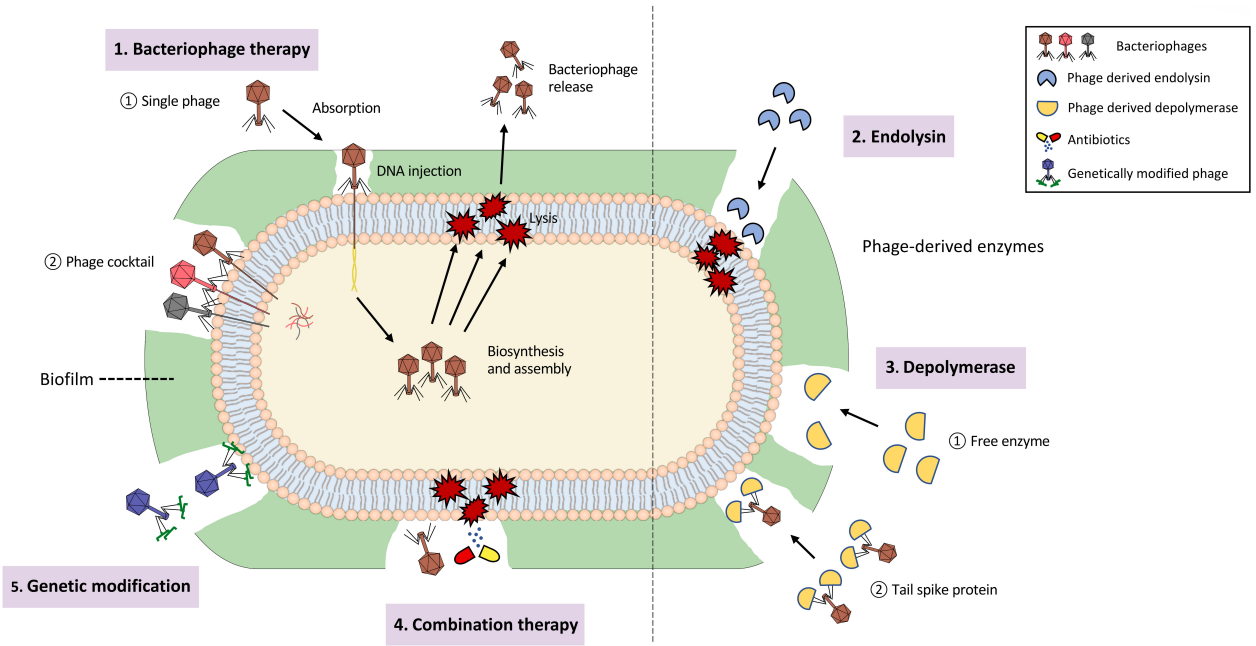

FIGURE 3 | Depiction of biofilm removal using phages and its derived enzymes. (1). Bacteriophage therapy, consisting of single phage therapy and cocktail therapy, that is used for intra- to extracellular degradation of the bacterial structure. (2). Phage-derived endolysin used for extra- to intracellular degradation of the bacterial structure. (3). Phage-derived depolymerase, presented as free enzyme or tail spike protein, that is used for chemical dispersion of the biofilm matrix. (4). Combination therapy using both phages and other antimicrobial compounds, such as antibiotics. (5). Genetically-modified phages that enlarge the host-species interaction range.

depicted in **Figure 3**. Biofilm is like a "baguazhen," a fortress-like circle previously mentioned, that is almost insurmountable to common antibiotics. Hence, this paper provides each potential phage-based approach toward this 'insurmountable fortress' that will be further discussed in the following sections.

Phage Therapy

Exploiting phage against bacterial activity can be identified as a form of microorganism-mediated biocontrol, which includes the adoption of the whole organism or solely the organism-derived products as the bacterial antagonist (Chan and Abedon, 2015). On that account, the treatment mediated by the entire phage structure is defined as phage therapy and has shown to be effective in eradicating bacterial biofilm through killing bacteria hosts from "within" (Parasion et al., 2014; Chan and Abedon, 2015; Domingo-Calap and Delgado-Martinez, 2018).

Prior to attaching to the host cell, phages infiltrate biofilm using depolymerases, encoded at the tail structure of the virion, to aid its affinity toward target bacteria (Parasion et al., 2014). Subsequently, the initial interaction between phages and bacteria hosts that leads to viral infection is activated by the receptor-binding protein on the long tail fiber that specifically attaches to the receptors on the surface of the host cell (Islam et al., 2019). Following the irreversible attachment phase are the tail sheesh contraction, tail tube penetration, genome injection, and finally cell lysis (Islam et al., 2019). The intra- to extracellular degradation of the host cell is unique to virulent phages which induce the release of progeny phages from the infected cells at the final stage of the lytic cycle (Cisek et al., 2017). Additionally, this discharge of lytic progeny virions is accompanied by the activation of holins and endolysins, two phage proteins that trigger cell lysis (Cisek et al., 2017). Holins are responsible for piercing the cytoplasmic membrane of the host, while also enabling endolysin to give access to and degrade bacterial peptidoglycan, a major component of the bacterial cell wall (Cisek et al., 2017).

Many studies have been carried out using phage therapy to combat biofilm formation, as shown in **Supplementary Table 1**. The first case study was conducted by Doolittle et al. in 1995, where Escherichia virus T4, or commonly known as phage T4, was used to eliminate the existing biofilm secreted by *E. coli* (Doolittle et al., 1995). Phage therapy has since then proven to be effective in eradicating biofilm secreted by various bacterial strains, while its studies in clinical settings are also extensive. Amongst them is the eradication of biofilms on the surfaces of medical devices, such as prostheses and catheters (Morris et al., 2019; Cano et al., 2021; Manoharadas et al., 2021). For instance, Morris et al. assessed the anti-biofilm activity of phage toward prosthesis-related infections caused by *S. aureus*. The study mimicked clinical settings by applying a phage cocktail on biofilm-coated three-dimensional-printed titanium that is frequently used in orthopedic implants. The result demonstrated a 3.3-fold reduction in biofilm biomass, as well as a decrease in the thickness and area of the biofilm after 48 h of cocktail exposure (Morris et al., 2019). On the other hand, catheter-associated biofilm clearance may involve with an alternative approach where phage is used as a gel-like coating on the catheter to reduce the bacterial adhesion to the surfaces (Curtin and

Donlan, 2006; Maszewska et al., 2018). Furthermore, since the excessive misuse of traditional antibiotics has led to a striking rise in cases related to drug-resistant bacterial infections (World Health Organization [WHO], 2020), phage therapy has recently shifted the focus on eradicating biofilms produced by multi-drug resistant (MDR) bacteria such as MDR *Enterobacter cloacae* (*E. cloacae)* (Jamal et al., 2019), MDR *S. aureus* (Cha et al., 2019), MDR *P. aeruginosa* (Yuan et al., 2019; Adnan et al., 2020), and MDR *Salmonella gallinarum* (*S. gallinarum)*, (Rizzo et al., 2020) to name a few. The diagnostic assays for measuring anti-biofilm activity of phages include fluorescence microscopy (Shahed-Al-Mahmud et al., 2021), LIVE/DEAD BacLight Bacterial Viability Kit (Latka and Drulis-Kawa, 2020), etc. Additionally, biofilm clearance in the oral cavity using phage therapy is also observed in recent years.

Dental Biofilm and Related Health Concerns

The oral cavity provides an ideal inhabiting environment for biofilm formation. These biofilms can form on natural dentition and tissues, alongside abiotic surfaces including dental prostheses and implants. Dental biofilms form in a similar process as biofilms in other parts of the body, with planktonic, biofilm, and dispersal phases. Heller et al. detailed a biofilm formation process whereupon immersion in oral cavity fluid, a thin pellicle composed of saliva and glycoproteins is adsorbed onto the tooth surface (Heller et al., 2016). Bacteria aggregate toward this pellicle in a variety of ways, including but not limited to pellicle-bacteria surface molecule interactions and charge-related attachment. As stated above, the main species of bacteria inhabiting oral biofilms can be categorized into nine taxa: *Corynebacterium*, *Streptococcus*, *Porphyromonas*, *Haemophilus*/*Aggregatibacter*, *Neisseriaceae*, *Fusobacterium*, *Leptotrichia*, *Capnocytophaga*, and *Actinomyces*. Mark Welch et al. observed complex microbial coagulation, with *Corynebacterium* acting as a bridge microbe within the biofilm structure. It is known that dental biofilm and related plaque are a direct causes of periodontal diseases such as gingivitis and periodontitis, as well as dental caries (Mark Welch et al., 2016). Certain bacteria within the biofilm, for instance, *Porphyromonas gingivalis (P. gingivalis)*, have shown interactions with stem cells and are linked to several immune diseases including Alzheimer's disease and rheumatoid arthritis (Kriebel et al., 2018; Olsen and Singhrao, 2020). Many phages have been derived and isolated as of date from several oral pathogenic bacteria including *Fusobacterium*, *Aggregatibacter*, etc. Kabwe et al. (2019) discovered a novel phage FNU1 capable of significantly reducing *Fusobacterium nucleatum* (*F. nucleatum*) biofilm mass by 70%. The study determined that the FNU1 phage was capable of breaking down the biofilm of *F. nucleatum* and lysing the bacteria cells within, thus presenting another viable option in periodontitis treatment.

Phage Cocktails Addressing the Limitations of Single Phage Therapy

As seen in **Supplementary Table 1**, phage therapy entails the preparation of a single phage or a mix of various phages, also known as phage cocktails (Lusiak-Szelachowska et al., 2020). Despite the success of a single type of phage against bacteria activity, the demand for phage cocktails emerged because high specificity in a single phage strain often leads to limitations in identifying the fitting strain. The search for a corresponding strain of phage before treatment can often be problematic especially for emergency cases (Domingo-Calap and Delgado-Martinez, 2018). As a result, the implemented strategy is the preparation of a phage cocktail, which increases the efficiency of such pairing by increasing the range of action (Kifelew et al., 2020). Phage cocktails could also delay the emergence of phage-resistant bacteria by including multiple phages for bacteria to interact with (Domingo-Calap and Delgado-Martinez, 2018). Moreover, different strains of phages could also complement one another by providing the necessary antimicrobial elements that one may be short of. An example of this is demonstrated by Chhibber et al. (2015) who applied phage cocktail therapy against mixed-species biofilm of *K. pneumoniae* and *P. aeruginosa*. The phage cocktail consists of *K. pneumoniae*-specific depolymerase-producing phage KP01K2 and *P. aeruginosa*-specific non-depolymerase-producing phage Pa29. The former phage with degrading enzyme hydrolyzed the outer structure of *K. pneumoniae* to enable the access of Pa29 to *P. aeruginosa* located underneath, hence resulting in a significant reduction of biofilm biomass for both bacteria that may not be possible to eradicate without cocktail approach (Chhibber et al., 2015). All in all, since biofilms are multi-bacterial communities, cocktail therapy is more in demand (O'Toole et al., 2000).

Apart from the limitations in the narrow range of action, growing resistance, and other constraints that could be solved by the use of phage cocktail, phage therapy also presents fundamental concerns (Chan and Abedon, 2015) in its relative usage safety in treating biofilm and other microbial activities. The issue lies in the phage release of inflammatory bacterial proteins, notably endotoxins, due to impure phage preparations (Steele et al., 2020). Poor phage purification may result in having high concentrations of lysed bacteria with inflammatory proteins that instigate the immune system and trigger the inflammatory response (Steele et al., 2020). Nevertheless, researchers such as Luong et al. (2020) have demonstrated the combinational use of centrifugation, microfiltration, and cross-flow ultrafiltration that could remove up to 10^6 fold of endotoxins in phage preparations, while other researchers have also displayed different effective strategies (Szermer-Olearnik and Boratynski, 2015; Van Belleghem et al., 2017). In order to introduce phage therapy to the masses, the ethical acceptance and social compliance of injecting viruses into the body and potentially treating diseases must also be addressed (Domingo-Calap and Delgado-Martinez, 2018).

Phage-Derived Enzymes

Phage therapy combats microbial activities largely through two substances: lysin and depolymerase. As these phage-encoded enzymes have also shown effectiveness against biofilm formation, the purification and recombining of the derived enzymes enable alternative choices to withstand challenges related to host specificity and resistance.

Lysin

Phage lysins are hydrolytic enzymes and depending on its target bacteria can be labeled as either Gram-positive or Gram-negative lysins. Lysins are generally considered as enzymes produced at the end of the phage lytic replication cycle to cleave the bacterial cell wall from within the cell for release, but can also work externally by assisting bacterial cell penetration of the parental phage. In addition to its phage-related abilities, lysins can degrade the biofilm extracellular polymeric matrix and target the associated bacteria within the matrices.

It is known that lysins generally have the best effect on Gram-positive bacteria, since Gram-negative bacteria have an outer membrane (OM) that restricts lysins from reaching their peptidoglycan cell walls. Despite the challenges faced when combating Gram-negative bacteria, studies have shown promising results, for instance Vasina et al. (2021) found that the four Gram-negative bacteria-targeting endolysins LysAm24, LysAp22, LysECD7, and LysSi3, have high antibacterial activity both *in vitro* and *in vivo*.

In Gram-positive lysins, the C-terminal (cell-binding domain, CBD) is responsible for binding to the cell wall, whereas the N-terminal (enzymatically active domain, EAD) is responsible for catalyzing peptidoglycan hydrolysis. Gram-negative lysins have no use for a CBD and generally utilize a globular configuration with a single EAD to interfere with the bacterial cell wall (Becker et al., 2008). Some Gram-negative lysins have been found to have a modular configuration that consist of an N-terminal peptidoglycan binding domain (PBD) that recognizes the peptidoglycan in Gram-negative bacteria and also the C-terminal EAD similar to Gram-positive lysins (Briers et al., 2009; Walmagh et al., 2012). In addition, some Gram-negative lysins have been found to have a domain, CHAP (cysteine, histidine-dependent amidohydrolase/peptidase), which has the ability to facilitate hydrolysis of the peptidoglycan layer (Sanz-Gaitero et al., 2013; Becker et al., 2015). This ability allows enhancement of its catalytic capabilities, allowing a lysin to be enzymatically active on the peptidoglycan of multiple Gram-negative strains (Walmagh et al., 2013).

Due to the ability of bacteria to form antibiotic-resistant and multidrug-resistant biofilms, lysins used as free enzymes (independently without the parental phage) have shown to be a potential alternative to antibacterial drugs in treating bacterial biofilms. **Table 2** demonstrates the antibiofilm lysins trials conducted on a variety of growth sites. As mentioned earlier, biofilm can be a serious threat clinically due to the tendency of it forming in human infections and certain medical devices. As seen in **Table 2**, *S. aureus*, especially multi-drug resistant *S. aureus* (MRSA) is one of the major target bacteria when it comes to research on lysins, as they are common in clinical settings. In studies from both 2014 and 2017, ClyH and ClyF (both chimeric lysins) have been found to have effect against MRSA (Yang et al., 2014, 2017). Both studies showed a large percentage of biofilm mass reduction when treated with chimeric lysin ClyH or ClyF. In this review, we focus on endolysin (as a free enzyme) activity on combating biofilm and biofilm formation in clinical use.

While the mechanism for antibiofilm disruption by lysins is not fully understood, lysins possess the ability to degrade a substantial amount of the extracellular polymeric matrix of the biofilm. Optimally, lysins or antibiofilm agents in general should have the ability to penetrate biofilm, disrupt its matrix and then combat the bacteria (Rabin et al., 2015). This can be made possible through inhibiting bacterial surface attachment and disruption or destabilization of matured biofilms (Miquel et al., 2016).

The promising future of lysins has a lot to do with its advantages over other antibacterial agents, such as antibiotics or its parental phage. One of the major advantages lysins have over broad-spectrum antibiotics is higher specificity against its target bacteria, which also prevents it from targeting the normal flora (Landlinger et al., 2021). Some other advantages include fast lysis of host cell, synergism when combined with other antibacterials, ability to combat biofilms and lower chance of developing resistance (Schuch et al., 2014; Oliveira et al., 2018). Although lysins are antibacterials with great potential, there are some disadvantages worth mentioning. These include factors like the challenge of finding a suitable drug delivery method, its exceptionally high of a specificity and regulatory body approval, as Murray et al., 2021 has summarized in her review relating to the challenges of lysins used in a clinical setting (Murray et al., 2021).

Depolymerase

Depolymerases are a type of enzyme that possesses the ability to degrade the capsular polysaccharides on Gram-negative bacteria, thus providing an entry point for other forms of attack, such as the use of antibacterial drugs. Depolymerases are typically encoded as part of phage structure and several known depolymerases able to function against a range of bacteria species have been identified. Based on the different mechanisms of phage depolymerases, they can be further categorized into two groups: hydrolases and lyases (Knecht et al., 2019). Hydrolases, in contrast to lyases, cleave substrates by hydrolysis—a process that involves the use of a water molecule (Ozaki et al., 2017).

As mentioned above, the main component of biofilm is EPS, which can make up 50 to 90 percent of the total biofilm organic components (Flemming and Wingender, 2010). Hence, these enzymes also hold the ability to inhibit biofilm formation. Phage-derived depolymerases may present two facets of approach toward anti-biofilm treatment, (i) as tail spike protein (TSP), or (ii) as free enzymes. The former approach pertains to purifying the protein present in biofilm-degrading phages and heterologously expressing it as recombinant protein on virion structures. Free depolymerase, on the other hand, presents a certain set of advantages not present when part of a virion (TSP), these include but are not limited to greater molecular stability, reduced chances for resistance formation, and more efficient delivery via diffusion (Chan and Abedon, 2015).

Guo et al. (2017) conducted a trial that analyzed the ORF42 of the vB_EcoM_ECOO78 *E. coli* phage and extracted the depolymerase Dpo42. The enzyme, after further purification, was expressed as a free protein via *E. coli* BL21. The team

TABLE 2 | Anti-biofilm lysin studies.

Author, year	Biofilm-forming bacteria	Phage strain(s)/lysin	Growth site	Results
Landlinger et al., 2021	*Gardnerella*	PM-477 (engineered lysin)	vaginal swabs from BV (bacterial vaginosis) patients	For the majority of the samples, PM-477 demonstrated disruption of biofilm without affecting the remaining vaginal microbiome
Sosa et al., 2020	*S. aureus*	PlySs2	Murine tibial implant	PlySs2 and vancomycin used together *in vivo* reduced the number of CFUs on the surface of implants by 92%
Fursov et al., 2020	*K. pneumoniae*	Prophage/LysECD7	diffusion chambers implanted in outbred rats	Substantial number of viable bacteria in the formed biofilms was disrupted by 50 μg of LysECD7 injected intraperitoneally
Idelevich et al., 2020	*S. aureus*	HY-133 (chimeric lysin)	Vascular graft surface	HY-133 on graft surface-adherent cells was moderate
Schuch et al., 2017	*S. aureus*	Bacterial specific phage/CF-301	Surgical mesh, catheters	In catheters, CF-301 removed all biofilm within 1 h
				Antibiofilm activity of CF-301 was improved in combinations with lysostaphin
				Highly effective for destroying biofilms and biofilm bacteria
Yang et al., 2017	*S. aureus*	187, bacterial specific phage/ ClyF (chimeric lysin)	Mouse model of burn wound	ClyF treated burn wounds showed clear degradation of biofilm compared with control group
Yang et al., 2016	*Streptococcus mutans (S. mutans)*	Prophage/ClyR (chimeric lysin)	hydroxyapatite disks	Biofilms formed on hydroxyapatite disks (representing the tooth enamel) reduced by ∼1 log at 50 μg/ml, ∼2 logs at 100 μg/ml, and ∼3 logs at 200 μg/ml
Thandar et al., 2016	*A. baumannii*	P307 and P307SQ-8C (engineered lysins)	polyvinyl chloride (PVC) catheter tubing	After 2 h, approximately 3- and 4-log decreases in CFU/ml were observed with P307 and P307SQ-8C
				After 24 h, an additional ∼1.3-log decrease was observed with P307
Lood et al., 2015	*A. baumannii*	Prophage/PlyF307	Catheters, mouse model	Catheters treated with PlyF307 displayed an approximately 1.6-log-unit decrease in the number of *A. baumannii*
				Mouse models treated with PlyF307 displayed an approximately 2-log-unit decrease in bacterial viability
Yang et al., 2014	*S. aureus*	ClyH (chimeric lysin)	96-well plates	ClyH treated clinical S. aureus isolates showed a > 60% biofilm mass reduction

tested the protein's ability on *E. coli* and determined that Dpo42 effectively degraded the capsular polysaccharides (CPS) surrounding the *E. coli* as well as prevention of *E. coli* biofilm formation. An advantage of depolymerases may be its ability to degrade the glycocalyx, the main component of both biofilm matrices as well as bacterial capsules (Chan and Abedon, 2015). Moreover, as part of the phage composition, depolymerase also shares advantages including a high specificity toward a specific bacteria species without harming the normal flora, usage in tackling multidrug-resistant (MDR) bacteria, etc. (Lin et al., 2017; Al-Wrafy et al., 2019).

Further research conducted using TSP depolymerase has opened the field to medical device applications. Shahed-Al-Mahmud et al. (2021) utilized tail spike proteins to treat *A. baumannii*-adhered catheters and observed significantly fewer bacteria cells after 4 h of treatment. The study was designed by immersing the catheters into *A. baumannii* culture, thus allowing the formation and growth of biofilm, for seven days and treating with either TSP or PBS control. Zebrafish tested using Ab-54149 with and without the depolymerase demonstrated that after 4 days, TSP-treated zebrafish presented significantly higher survival rates compared to those without TSP treatment. Shahed-Al-Mahmud et al. (2021) proposed that φAB6 TSP would provide potential treatment against MDR *A. baumannii* infections in the near future. Additional anti-biofilm depolymerase trials are demonstrated in **Table 3**.

The inclusion of bacterial capsules as a target may lead to a decrease in bacterial virulence and open a pathway for not only phages but also antibiotics as a potential treatment option. It should also be mentioned that depolymerase also presents the ability to be extensively genetically engineered to increase its effectiveness (Topka-Bielecka et al., 2021).

Combination of Phage and Antimicrobials

The application of phage therapy and virion proteins has displayed immense progress in eradicating biofilm. Yet, some studies have suggested a combinational therapy of phage and other antimicrobial activity, as using phages alone may not be sufficient to eradicate biofilm effectively or permanently. For instance, when Nzakizwanayo et al. (2015) applied phage therapy to eradicate crystalline biofilm formed by *P. mirabili*s on urinary catheters after 10 h of infections, the levels of biofilm formation were significantly reduced but not the number of resident planktonic cells that are available to repeatedly secrete biofilm. While a revised approach was not investigated further by Nzakizwanayo et al. (2015) an

TABLE 3 | Anti-biofilm depolymerase studies.

Author, year	Biofilm-forming bacteria	Phage(s)	Growth site	Results
Shahed-Al-Mahmud et al., 2021	*A. baumannii*	φAB6	96-well microtiter plate	Showed a therapeutic effect in the treatment of *A. baumannii*-induced infections
Chen et al., 2021	*A. baumannii*	vB_AbaM-IME-AB2	96-well plate	Total eradication of human serum bacteria at 50% volume ratio when combination of phage and colistin was applied.
Ku et al., 2021	*P. mirabilis*	KMI8	96 well polystyrene plates	Capable of degrading mono-biofilms of a strain of *Klebsiella michiganensis (K. michiganensis)* that carried the polysaccharide capsule KL70 locus
Rice et al., 2021	*K. michiganensis*	vB_PmiS_PM-CJR	LB agar plates	Characterized a biofilm depolymerase from a *Proteus* phage
Wu et al., 2019	*K. pneumoniae*	SH-KP152226	96-well plate	Specific enzymatic activities in the depolymerization of the K47 capsule Enhance polymyxin activity against *K. pneumoniae* biofilms
Guo et al., 2017	*E. coli*	vB_EcoM_ECOO78	96-well microtiter plate	New potential strategy for preventing *E. coli* biofilm formation

advanced elimination of biofilm could be achieved by the combination of phage with other antimicrobial approaches. Doub et al. (2021) presented a successful clinical case where a patient with intractable *S. epidermidis* prosthetic knee infection is recovering without clinical recurrence after being treated with phage therapy and debridement, antibiotics, irrigation, and retention of the prosthesis (DAIR) surgery. This combinational approach by DAIR benefits phage therapy by manually removing the overlying planktonic bacteria as well as parts of the chronic biofilm structure to allow for direct exposure of phage to deep-seated bacteria, thus resulting in complete eradication of biofilm biomass and improvement in clinical therapeutic effect (Doub et al., 2021).

The combination of phages and antibiotics could also address the challenges in the emergence of increasing tolerant bacterial populations against phages. Antibiotics have shown immense success in combating bacterial activity in the last few decades but have gradually unveiled its flaws. As mentioned earlier, the increase in antibiotic-resistant bacteria strains and the inhibition of antibiotic diffusion inside thick EPS matrix led to new opportunities for phage applications. While phages can penetrate the biofilm matrix and the communities within, treatment of biofilms with solely phages could also lead to the emergence of phage-resistant strains and thus, the inability for phages to eradicate biofilm. For instance, Henriksen et al. (2019) examined the effect of repeated phage treatments on *P. aeruginosa* biofilms over time and showed growth of biovolume from 22.24 to 31.07 $\mu m^3/\mu m^2$ when treated with phages twice and thrice, respectively. Nonetheless, the biovolume of phage-treated biofilm decreased up to 0.14 $\mu m^3/\mu m^2$ after ciprofloxacin was added in Henriksen et al. (2019). Hence, as an increase of phage resistance from bacteria enables its higher sensitivity to antibiotics (Kortright et al., 2019), instead of replacing antibiotics, phages could combine with antibiotics to provide two divergent pressures for resistance prevention (Tagliaferri et al., 2019). This has also been demonstrated in the *K. pneumoniae* biofilm treated with the combinational use of lytic phage KP34 and ciprofloxacin, which led to a significant reduction in the number of resistant variants (Latka and Drulis-Kawa, 2020), as well as in other numerous biofilms (Coulter et al., 2014; Wang et al., 2020).

Recent studies have shed light on the potential of combining depolymerases with other compounds. Chen et al. (2021) identified during a trial, a depolymerase Dpo71 from an *A. baumannii* phage in the heterologous host *E. coli* to combat multidrug-resistant *A. baumannii*. The team concluded after further research that Dpo71 presented the ability to enhance antibiotic activity, specifically colistin, and demonstrated that at 10 μg/ml, Dpo71 enabled a total eradication of human serum bacteria at 50% volume ratio. Dpo71 was also able to inhibit both existing as well as new biofilm formation. Chen et al. further proposed that the potential combination therapy of Dpo71 with colistin could enhance antibiofilm capabilities, therefore, increasing the survival rate of infected patients (Chen et al., 2021). A further list of recent combination therapy is demonstrated in **Table 4**.

Genetically Engineered Phages

The final strategy this paper wishes to present comes via genetic engineering, a recombination process pioneered in 1973 by American biochemists Stanley N. Cohen and Herbert W. Boyer. (Britannica, 2021). The concept presented a multitude of opportunities for scientists to recombine DNA strands to create a phage phenotype suitable for a specific host. In the past 30 years, phages have seen a period of rapid growth, thus leading to different categories and types of recombined, genetically modified phages and phage proteins being developed. Phages can be engineered using several different protocols including but not limited to homologous recombination, phage recombineeringm of electroporation DNA, CRISPR-Cas-based phage engineering, *in vivo* recombineering, etc. (Pires et al., 2016; Chen et al., 2019).

Current research regarding genetically engineered phages can be broadly split into two categories, phage therapy and phage proteins. Lu et al. conducted a trial involving the use of a lysogenic phage M13mp18 with overexpressed lexA3 to increase the antibiotic-induced killing ability toward *E. coli* (Lu and Collins, 2009). The team demonstrated that the lexA3-producing phage together with ofloxacin, an antibiotic, significantly increased the antibacterial effect against wild-type *E. coli* EMG2. Edgar et al. conducted a trial by means of gene delivery via homologous recombination (Edgar et al., 2012).

TABLE 4 | Anti-biofilm combination therapy studies.

Author, year	Biofilm-forming bacteria	Phage strain	Growth site	Results
Chen et al., 2021	*A. baumannii*	vB_AbaM-IME-AB2	96-well plate	Total eradication of human serum bacteria at 50% volume ratio when combination of phage and colistin was applied.
Doub et al., 2021	*S. epidermidis*	PM448	Bacterial site in the intraarticular space of the patient's prosthetic knee	Combination therapy of phage and debridement, antibiotics, irrigation, and retention of the prosthesis surgery led the patient to recover from recalcitrant prosthetic joint infection by having thorough eradication of biofilm biomass.
Latka and Drulis-Kawa, 2020	*K. pneumoniae*	KP34	96 well plates	Best antibiofilm results where lytic phage KP34 was applied in combination with ciprofloxacin
Kifelew et al., 2020	*S. aureus*	AB-SA01	96-well polystyrene tissue culture plate	Application of phage cocktails led to a significant reduction in bacterial host population within mixed-species biofilm, while combination with tetracycline led to more bacterial population reduction.
Henriksen et al., 2019	*P. aeruginosa*	ATCC 12175-B1, ATCC 14203-B1, ATCC 14205-B1	Flow cells	Single phage treatment led to an 85% to 95% reduction in biofilm's biovolume. Repeated phage treatment enhanced the biovolume of the biofilm after the second and third treatments. The combination of phages and ciprofloxacin led to biomass reduction of 6 log units. Demonstrated the possibility of bacterial resistance to phages and the effectiveness of combination therapy of phages and antibiotics.
Papadopoulou et al., 2019	*Flavobacterium psychrophilum (F. psychrophilum)*	Fpv-9, Fpv-10	96-well polystyrene microtitre plates	Phage cocktail led to a significant reduction in biofilm biomass after 24-hour exposure Anti-biofilm compounds (2-aminoimidazole, emodin, parthenolide, and D-leucine) inhibited biofilm formation for up to 80%. Suggesting the higher efficacy of combinational therapy of phage and inhibiting compounds against biofilm.
Chhibber et al., 2015	*K. pneumoniae, P. aeruginosa*	KP01K2, Pa29	Black polycarbonate membrane, 96-well microtiter plates with TSB medium	Led to log-CFU/cm2 biofilm reduction of 3.9 when using KP01K2 for *Klebsiella*, while no significant reduction was observed when using Pa29 for *Pseudomonas*. Led to log-CFU/cm2 biofilm reduction of 2.8 when both phages were used. Led to complete eradication or log-CFU/cm2 biofilm reduction of 4 when combinational use of KP01K2 and xylitol was used for *Klebsiella* or *Pseudomonas*, respectively. Led to log-CFU/cm2 biofilm reduction of 6 when combinational use of KP01K2, Pa29. and xylitol was used for *Pseudomonas*. Suggesting the higher efficacy of combinational therapy of phage and xylitol against biofilm
Seth et al., 2013	*S. aureus*	Bacteria-specific phages	Six-millimeter dermal punch wounds in New Zealand rabbit ears	The combination of phage therapy and sharp debridement decreased bacterial biofilm cell counts by a 2-log fold (99% removal). Illustrated the effective approach of combining phage therapy and sharp debridement technique.

Phages carrying the homologously recombinant genes rpsL (sensitive to streptomycin) and gyrA (sensitive to nalidixic acid) were administered to induced antibiotic-resistant E. coli and a significant MIC decrease was later observed. Lu et al. also engineered a T7 phage expressing an *Aggregatibacter actinomycetemcomitans (A. actinomycetemcomitans)* biofilm-degrading enzyme dispersion B (Lu and Collins, 2007). The team discovered that the T7 phage was effective against *E. coli* TG1 biofilms by a log4.5 reduction.

Phage proteins, especially lysins previously discussed, also present the potential to be genetically engineered to maximize and broaden their effectiveness. There has been growing interest in modified lysins with novel characteristics, especially engineered lysins and chimeric lysins when combating biofilm. Engineered lysins are novel lysins with customized features created by swapping its modular domains, for instance, artificial lysins (artilysins) that are created by combining a natural lysin fragment with peptides or other proteins

(Rodriguez-Rubio et al., 2016; Schirmeier et al., 2018). Chimeric lysins (also known as chimeolysins) are formed by switching the domains of the natural lysin, such as the cell wall binding domains (CBDs) and the catalytic domains (CDs) (Huang et al., 2020; Li et al., 2021). Engineered lysins used in countering biofilm are well represented in anti-biofilm lysin trials as shown in **Table 2**. Landlinger et al., 2021 conducted a study that found an engineered lysin, PM-477 to be active against *Gardnerella* biofilms (Landlinger et al., 2021). Lysin PM-477 was created by recombining EADs and CBDs, testing various combinations on bacterial strains to find a final combination that is the most efficient.

CONCLUDING REMARKS

There are five main approaches to countering the biofilm matrix. (1) Phage therapy that entails the use of the whole organism, which eradicates bacterial biofilm through killing bacteria hosts from "within" via the initial penetration of the matrix by depolymerase followed by the lytic cycle. (2) Phage-derived depolymerase which could be used as a TSP or free enzyme and works by degrading the EPS, CPS, and glycocalyx. (3) Phage-derived endolysins that infiltrate the EPS structure and combat the local bacteria externally. (4) Combination therapy that is associated with the application of phage and other antimicrobial compounds for more complete eradication of both the matrix and the dormant bacteria, as well as decrease in resistance toward phages. (5) Genetically engineered phages enlarge the host-species interaction range by modifying the proteins involved in the phage attachment and/or insertion. The future of phage therapy focuses on expanding the scope of phage and its derived enzymes which could be achieved by further exploration of: (i) combinational therapy with phage and antibiotics; (ii) genetically engineered phages; (iii) genetically engineered proteins such as artilysins, chimeolysins that overcome the limitations allowing endolysins to target gram-negative bacteria.

AUTHOR CONTRIBUTIONS

CC, XY, and WG wrote this article. CG provided some comments. XG, QL, and YZ conducted the research and revised the manuscript. All authors contributed to the article and approved the submitted version.

SUPPLEMENTARY MATERIAL

The Supplementary Material for this article can be found online at: https://www.frontiersin.org/articles/10.3389/fmicb.2022.825828/full#supplementary-material

REFERENCES

Abee, T., Kovács, A. T., Kuipers, O. P., and van der Veen, S. (2011). Biofilm formation and dispersal in Gram-positive bacteria. *Curr. Opin. Biotechnol.* 22, 172–179. doi: 10.1016/j.copbio.2010.10.016

Ackermann, H. W. (2009). Phage classification and characterization. *Methods Mol. Biol.* 501, 127–140. doi: 10.1007/978-1-60327-164-6_13

Ackermann, H. W., and Prangishvili, D. (2012). Prokaryote viruses studied by electron microscopy. *Arch. Virol.* 157, 1843–1849. doi: 10.1007/s00705-012-1383-y

Adnan, M., Ali Shah, M. R., Jamal, M., Jalil, F., Andleeb, S., Nawaz, M. A., et al. (2020). Isolation and characterization of bacteriophage to control multidrug-resistant *Pseudomonas aeruginosa* planktonic cells and biofilm. *Biologicals* 63, 89–96. doi: 10.1016/j.biologicals.2019.10.003

Alhede, M., Kragh, K. N., Qvortrup, K., Allesen-Holm, M., van Gennip, M., Christensen, L. D., et al. (2011). Phenotypes of non-attached *Pseudomonas aeruginosa* aggregates resemble surface attached biofilm. *PLoS One* 6:e27943. doi: 10.1371/journal.pone.0027943

Al-Wrafy, F., Brzozowska, E., Gorska, S., Drab, M., Strus, M., and Gamian, A. (2019). Identification and characterization of phage protein and its activity against two strains of multidrug-resistant *Pseudomonas aeruginosa*. *Sci. Rep.* 9:13487. doi: 10.1038/s41598-019-50030-5

Armbruster, C. R., and Parsek, M. R. (2018). New insight into the early stages of biofilm formation. *Proc. Natl. Acad. Sci. U. S. A.* 115, 4317–4319. doi: 10.1073/pnas.1804084115

Becker, S. C., Foster-Frey, J., and Donovan, D. M. (2008). The phage K lytic enzyme LysK and lysostaphin act synergistically to kill MRSA. *FEMS Microbiol. Lett.* 287, 185–191. doi: 10.1111/j.1574-6968.2008.01308.x

Becker, S. C., Swift, S., Korobova, O., Schischkova, N., Kopylov, P., Donovan, D. M., et al. (2015). Lytic activity of the staphylolytic Twort phage endolysin CHAP domain is enhanced by the SH3b cell wall binding domain. *FEMS Microbiol. Lett.* 362, 1–8. doi: 10.1093/femsle/fnu019

Bisht, K., Moore, J. L., Caprioli, R. M., Skaar, E. P., and Wakeman, C. A. (2021). Impact of temperature-dependent phage expression on *Pseudomonas aeruginosa* biofilm formation. *NPJ Biofilms Microbiomes* 7:22. doi: 10.1038/s41522-021-00194-8

Bowler, P., Murphy, C., and Wolcott, R. (2020). Biofilm exacerbates antibiotic resistance: is this a current oversight in antimicrobial stewardship? *Antimicrob. Resist. Infect. Control* 9:162. doi: 10.1186/s13756-020-00830-6

Briers, Y., Schmelcher, M., Loessner, M. J., Hendrix, J., Engelborghs, Y., Volckaert, G., et al. (2009). The high-affinity peptidoglycan binding domain of *Pseudomonas* phage endolysin KZ144. *Biochem. Biophys. Res. Commun.* 383, 187–191. doi: 10.1016/j.bbrc.2009.03.161

Britannica, T. (2021). *Genetic Engineering [Online]*. Available online at: https://www.britannica.com/science/genetic-engineering (accessed August 2021).

Cano, E. J., Caflisch, K. M., Bollyky, P. L., Van Belleghem, J. D., Patel, R., Fackler, J., et al. (2021). Phage Therapy for Limb-threatening Prosthetic Knee *Klebsiella pneumoniae* Infection: case Report and In Vitro Characterization of Anti-biofilm Activity. *Clin. Infect. Dis.* 73, e144–e151. doi: 10.1093/cid/ciaa705

Cha, Y., Chun, J., Son, B., and Ryu, S. (2019). Characterization and Genome Analysis of Staphylococcus aureus Podovirus CSA13 and Its Anti-Biofilm Capacity. *Viruses* 11:54. doi: 10.3390/v11010054

Chan, B. K., and Abedon, S. T. (2015). Bacteriophages and their enzymes in biofilm control. *Curr. Pharm. Des.* 21, 85–99. doi: 10.2174/1381612820666140905112311

Chen, X., Liu, M., Zhang, P., Xu, M., Yuan, W., Bian, L., et al. (2021). Phage-Derived Depolymerase as an Antibiotic Adjuvant Against Multidrug-Resistant *Acinetobacter Baumannii*. *bioRxiv* [Preprint]. doi: 10.1101/2021.05.26.445908

Chen, Y., Batra, H., Dong, J., Chen, C., Rao, V. B., and Tao, P. (2019). Genetic Engineering of Bacteriophages Against Infectious Diseases. *Front. Microbiol.* 10:954. doi: 10.3389/fmicb.2019.00954

Chhibber, S., Bansal, S., and Kaur, S. (2015). Disrupting the mixed-species biofilm of *Klebsiella pneumoniae* B5055 and *Pseudomonas aeruginosa* PAO using bacteriophages alone or in combination with xylitol. *Microbiology* 161, 1369–1377. doi: 10.1099/mic.0.000104

Cisek, A. A., Dabrowska, I., Gregorczyk, K. P., and Wyzewski, Z. (2017). Phage Therapy in Bacterial Infections Treatment: one Hundred Years After the

Discovery of Bacteriophages. *Curr. Microbiol.* 74, 277–283. doi: 10.1007/s00284-016-1166-x

Coulter, L. B., McLean, R. J., Rohde, R. E., and Aron, G. M. (2014). Effect of bacteriophage infection in combination with tobramycin on the emergence of resistance in *Escherichia coli* and *Pseudomonas aeruginosa* biofilms. *Viruses* 6, 3778–3786. doi: 10.3390/v6103778

Cruz, C. D., Shah, S., and Tammela, P. (2018). Defining conditions for biofilm inhibition and eradication assays for Gram-positive clinical reference strains. *BMC Microbiol.* 18:173. doi: 10.1186/s12866-018-1321-6

Curtin, J. J., and Donlan, R. M. (2006). Using bacteriophages to reduce formation of catheter-associated biofilms by Staphylococcus epidermidis. *Antimicrob. Agents Chemother.* 50, 1268–1275. doi: 10.1128/AAC.50.4.1268-1275.2006

Dams, D., Brondsted, L., Drulis-Kawa, Z., and Briers, Y. (2019). Engineering of receptor-binding proteins in bacteriophages and phage tail-like bacteriocins. *Biochem. Soc. Trans.* 47, 449–460. doi: 10.1042/BST20180172

Dewhirst, F. E., Chen, T., Izard, J., Paster, B. J., Tanner, A. C., Yu, W. H., et al. (2010). The human oral microbiome. *J. Bacteriol.* 192, 5002–5017. doi: 10.1128/JB.00542-10

Domingo-Calap, P., and Delgado-Martinez, J. (2018). Bacteriophages: protagonists of a Post-Antibiotic Era. *Antibiotics* 7:66. doi: 10.3390/antibiotics7030066

Donlan, R. M. (2001). Biofilms and device-associated infections. *Emerg. Infect. Dis.* 7, 277–281. doi: 10.3201/eid0702.010226

Doolittle, M. M., Cooney, J. J., and Caldwell, D. E. (1995). Lytic infection of *Escherichia coli* biofilms by bacteriophage T4. *Can. J. Microbiol.* 41, 12–18. doi: 10.1139/m95-002

Doub, J. B., Ng, V. Y., Wilson, E., Corsini, L., and Chan, B. K. (2021). Successful Treatment of a Recalcitrant Staphylococcus epidermidis Prosthetic Knee Infection with Intraoperative Bacteriophage Therapy. *Pharmaceuticals* 14:231. doi: 10.3390/ph14030231

Edgar, R., Friedman, N., Molshanski-Mor, S., and Qimron, U. (2012). Reversing bacterial resistance to antibiotics by phage-mediated delivery of dominant sensitive genes. *Appl. Environ. Microbiol.* 78, 744–751. doi: 10.1128/AEM.05741-11

Ferkinghoff-Borg, J., and Sams, T. (2014). Size of quorum sensing communities. *Mol. Biosyst.* 10, 103–109. doi: 10.1039/c3mb70230h

Flemming, H. C., and Wingender, J. (2010). The biofilm matrix. *Nat. Rev. Microbiol.* 8, 623–633. doi: 10.1038/nrmicro2415

Fursov, M. V., Abdrakhmanova, R. O., Antonova, N. P., Vasina, D. V., Kolchanova, A. D., Bashkina, O. A., et al. (2020). Antibiofilm activity of a broad-range recombinant endolysin LysECD7: in vitro and in vivo study. *Viruses* 12:545. doi: 10.3390/v12050545

Guo, Z., Huang, J., Yan, G., Lei, L., Wang, S., Yu, L., et al. (2017). Identification and Characterization of Dpo42, a Novel Depolymerase Derived from the *Escherichia coli* Phage vB_EcoM_ECOO78. *Front. Microbiol.* 8:1460. doi: 10.3389/fmicb.2017.01460

Harrison, J. J., Ceri, H., and Turner, R. J. (2007). Multimetal resistance and tolerance in microbial biofilms. *Nat. Rev. Microbiol.* 5, 928–938. doi: 10.1038/nrmicro1774

Heller, D., Helmerhorst, E. J., Gower, A. C., Siqueira, W. L., Paster, B. J., and Oppenheim, F. G. (2016). Microbial Diversity in the Early In Vivo-Formed Dental Biofilm. *Appl. Environ. Microbiol.* 82, 1881–1888. doi: 10.1128/AEM.03984-15

Henriksen, K., Rorbo, N., Rybtke, M. L., Martinet, M. G., Tolker-Nielsen, T., Hoiby, N., et al. (2019). P. aeruginosa flow-cell biofilms are enhanced by repeated phage treatments but can be eradicated by phage-ciprofloxacin combination. *Pathog. Dis.* 77:ftz011. doi: 10.1093/femspd/ftz011

Høiby, N., Ciofu, O., Johansen, H. K., Song, Z. J., Moser, C., Jensen, P., et al. (2011). The clinical impact of bacterial biofilms. *Int. J. Oral Sci.* 3, 55–65. doi: 10.4248/ijos11026

Høyland-Kroghsbo, N. M., Maerkedahl, R. B., and Svenningsen, S. L. (2013). A quorum-sensing-induced bacteriophage defense mechanism. *mBio* 4, e00362–12. doi: 10.1128/mBio.00362-12

Hu, W., Li, L., Sharma, S., Wang, J., McHardy, I., Lux, R., et al. (2012). DNA builds and strengthens the extracellular matrix in Myxococcus xanthus biofilms by interacting with exopolysaccharides. *PLoS One* 7:e51905. doi: 10.1371/journal.pone.0051905

Huang, L., Luo, D., Gondil, V. S., Gong, Y., Jia, M., Yan, D., et al. (2020). Construction and characterization of a chimeric lysin ClyV with improved bactericidal activity against Streptococcus agalactiae in vitro and in vivo. *Appl. Microbiol. Biotechnol.* 104, 1609–1619. doi: 10.1007/s00253-019-10325-z

Idelevich, E. A., Knaack, D., Nugroho, N. T., Peters, G., Bisdas, T., Molinaro, S., et al. (2020). Comparative in vitro activity of bacteriophage endolysin HY-133 against *Staphylococcus aureus* attached to vascular graft surface. *Med. Microbiol. Immunol.* 209, 51–57. doi: 10.1007/s00430-019-00638-1

Islam, M. Z., Fokine, A., Mahalingam, M., Zhang, Z., Garcia-Doval, C., van Raaij, M. J., et al. (2019). Molecular anatomy of the receptor binding module of a bacteriophage long tail fiber. *PLoS Pathog.* 15:e1008193. doi: 10.1371/journal.ppat.1008193

Jamal, M., Andleeb, S., Jalil, F., Imran, M., Nawaz, M. A., Hussain, T., et al. (2019). Isolation, characterization and efficacy of phage MJ2 against biofilm forming multi-drug resistant *Enterobacter cloacae*. *Folia Microbiol.* 64, 101–111. doi: 10.1007/s12223-018-0636-x

Kabwe, M., Brown, T. L., Dashper, S., Speirs, L., Ku, H., Petrovski, S., et al. (2019). Genomic, morphological and functional characterisation of novel bacteriophage FNU1 capable of disrupting *Fusobacterium nucleatum* biofilms. *Sci. Rep.* 9:9107. doi: 10.1038/s41598-019-45549-6

Kaplan, J. B. (2010). Biofilm dispersal: mechanisms, clinical implications, and potential therapeutic uses. *J. Dent. Res.* 89, 205–218. doi: 10.1177/0022034509359403

Kifelew, L. G., Warner, M. S., Morales, S., Thomas, N., Gordon, D. L., Mitchell, J. G., et al. (2020). Efficacy of Lytic Phage Cocktails on Staphylococcus aureus and *Pseudomonas aeruginosa* in Mixed-Species Planktonic Cultures and Biofilms. *Viruses* 12:559. doi: 10.3390/v12050559

Knecht, L. E., Veljkovic, M., and Fieseler, L. (2019). Diversity and Function of Phage Encoded Depolymerases. *Front. Microbiol.* 10:2949. doi: 10.3389/fmicb.2019.02949

Kortright, K. E., Chan, B. K., Koff, J. L., and Turner, P. E. (2019). Phage Therapy: a Renewed Approach to Combat Antibiotic-Resistant Bacteria. *Cell Host Microbe* 25, 219–232. doi: 10.1016/j.chom.2019.01.014

Kriebel, K., Hieke, C., Engelmann, R., Potempa, J., Muller-Hilke, B., Lang, H., et al. (2018). Porphyromonas gingivalis Peptidyl Arginine Deiminase Can Modulate Neutrophil Activity via Infection of Human Dental Stem Cells. *J. Innate Immun.* 10, 264–278. doi: 10.1159/000489020

Ku, H., Kabwe, M., Chan, H. T., Stanton, C., Petrovski, S., Batinovic, S., et al. (2021). Novel *Drexlerviridae* bacteriophage KMI8 with specific lytic activity against *Klebsiella michiganensis* and its biofilms. *PLoS One*. 16:e0257102. doi: 10.1371/journal.pone.0257102

Landlinger, C., Tisakova, L., Oberbauer, V., Schwebs, T., Muhammad, A., Latka, A., et al. (2021). Engineered Phage Endolysin Eliminates Gardnerella Biofilm without Damaging Beneficial Bacteria in Bacterial Vaginosis Ex Vivo. *Pathogens* 10:54. doi: 10.3390/pathogens10010054

Latka, A., and Drulis-Kawa, Z. (2020). Advantages and limitations of microtiter biofilm assays in the model of antibiofilm activity of Klebsiella phage KP34 and its depolymerase. *Sci. Rep.* 10:20338. doi: 10.1038/s41598-020-77198-5

Lebeaux, D., Chauhan, A., Rendueles, O., and Beloin, C. (2013). From in vitro to in vivo Models of Bacterial Biofilm-Related Infections. *Pathogens* 2, 288–356. doi: 10.3390/pathogens2020288

Li, X., Wang, S., Nyaruaba, R., Liu, H., Yang, H., and Wei, H. (2021). A Highly Active Chimeric Lysin with a Calcium-Enhanced Bactericidal Activity against Staphylococcus aureus In Vitro and In Vivo. *Antibiotics* 10:461. doi: 10.3390/antibiotics10040461

Lin, D. M., Koskella, B., and Lin, H. C. (2017). Phage therapy: an alternative to antibiotics in the age of multi-drug resistance. *World J. Gastrointest. Pharmacol. Ther.* 8, 162–173. doi: 10.4292/wjgpt.v8.i3.162

Lister, J. L., and Horswill, A. R. (2014). Staphylococcus aureus biofilms: recent developments in biofilm dispersal. *Front. Cell. Infect. Microbiol.* 4:178. doi: 10.3389/fcimb.2014.00178

Lood, R., Winer, B. Y., Pelzek, A. J., Diez-Martinez, R., Thandar, M., Euler, C.W., et al. (2015). Novel phage lysin capable of killing the multidrug-resistant Gram-negative bacterium *Acinetobacter baumannii* in a mouse bacteremia model. *Antimicrob. Agents Chemother.* 59, 1983–1991. doi: 10.1128/AAC.04641-14

Lu, T. K., and Collins, J. J. (2007). Dispersing biofilms with engineered enzymatic bacteriophage. *Proc. Natl. Acad. Sci. U. S. A.* 104, 11197–11202. doi: 10.1073/pnas.0704624104

Lu, T. K., and Collins, J. J. (2009). Engineered bacteriophage targeting gene networks as adjuvants for antibiotic therapy. *Proc. Natl. Acad. Sci. U. S. A.* 106, 4629–4634. doi: 10.1073/pnas.0800442106

Luong, T., Salabarria, A. C., Edwards, R. A., and Roach, D. R. (2020). Standardized bacteriophage purification for personalized phage therapy. *Nat. Protoc.* 15, 2867–2890. doi: 10.1038/s41596-020-0346-0

Lusiak-Szelachowska, M., Weber-Dabrowska, B., and Gorski, A. (2020). Bacteriophages and Lysins in Biofilm Control. *Virol. Sin.* 35, 125–133. doi: 10.1007/s12250-019-00192-3

Manoharadas, S., Altaf, M., Alrefaei, A. F., Hussain, S. A., Devasia, R. M., Badjah Hadj, A. Y. M., et al. (2021). Microscopic analysis of the inhibition of staphylococcal biofilm formation by *Escherichia coli* and the disruption of preformed staphylococcal biofilm by bacteriophage. *Microsc. Res. Tech.* 84, 1513–1521. doi: 10.1002/jemt.23707

Mark Welch, J. L., Rossetti, B. J., Rieken, C. W., Dewhirst, F. E., and Borisy, G. G. (2016). Biogeography of a human oral microbiome at the micron scale. *Proc. Natl. Acad. Sci. U. S. A.* 113, E791–E800. doi: 10.1073/pnas.1522149113

Maszewska, A., Zygmunt, M., Grzejdziak, I., and Rozalski, A. (2018). Use of polyvalent bacteriophages to combat biofilm of *Proteus mirabilis* causing catheter-associated urinary tract infections. *J. Appl. Microbiol.* 125, 1253–1265. doi: 10.1111/jam.14026

Miquel, S., Lagrafeuille, R., Souweine, B., and Forestier, C. (2016). Anti-biofilm Activity as a Health Issue. *Front. Microbiol.* 7:592. doi: 10.3389/fmicb.2016.00592

Morris, J., Kelly, N., Elliott, L., Grant, A., Wilkinson, M., Hazratwala, K., et al. (2019). Evaluation of Bacteriophage Anti-Biofilm Activity for Potential Control of Orthopedic Implant-Related Infections Caused by Staphylococcus aureus. *Surg. Infect.* 20, 16–24. doi: 10.1089/sur.2018.135

Morris, S., and Cerceo, E. (2020). Trends, Epidemiology, and Management of Multi-Drug Resistant Gram-Negative Bacterial Infections in the Hospitalized Setting. *Antibiotics* 9:196. doi: 10.3390/antibiotics9040196

Muhammad, M. H., Idris, A. L., Fan, X., Guo, Y., Yu, Y., Jin, X., et al. (2020). Beyond Risk: bacterial Biofilms and Their Regulating Approaches. *Front. Microbiol.* 11:928. doi: 10.3389/fmicb.2020.00928

Murakami, M., Nishi, Y., Seto, K., Kamashita, Y., and Nagaoka, E. (2015). Dry mouth and denture plaque microflora in complete denture and palatal obturator prosthesis wearers. *Gerodontology* 32, 188–194. doi: 10.1111/ger.12073

Murray, E., Draper, L. A., Ross, R. P., and Hill, C. (2021). The Advantages and Challenges of Using Endolysins in a Clinical Setting. *Viruses* 13:680. doi: 10.3390/v13040680

Nadell, C. D., Drescher, K., Wingreen, N. S., and Bassler, B. L. (2015). Extracellular matrix structure governs invasion resistance in bacterial biofilms. *ISME J.* 9, 1700–1709. doi: 10.1038/ismej.2014.246

Nzakizwanayo, J., Hanin, A., Alves, D. R., McCutcheon, B., Dedi, C., Salvage, J., et al. (2015). Bacteriophage Can Prevent Encrustation and Blockage of Urinary Catheters by *Proteus mirabilis*. *Antimicrob. Agents Chemother.* 60, 1530–1536. doi: 10.1128/aac.02685-15

Oliveira, H., Sao-Jose, C., and Azeredo, J. (2018). Phage-Derived Peptidoglycan Degrading Enzymes: challenges and Future Prospects for In Vivo Therapy. *Viruses* 10:292. doi: 10.3390/v10060292

Olsen, I., and Singhrao, S. K. (2020). Porphyromonas gingivalis infection may contribute to systemic and intracerebral amyloid-beta: implications for Alzheimer's disease onset. *Expert Rev. Anti Infect. Ther.* 18, 1063–1066. doi: 10.1080/14787210.2020.1792292

O'Toole, G., Kaplan, H. B., and Kolter, R. (2000). Biofilm formation as microbial development. *Annu. Rev. Microbiol.* 54, 49–79. doi: 10.1146/annurev.micro.54.1.49

Ozaki, T., Abe, N., Kimura, K., Suzuki, A., and Kaneko, J. (2017). Genomic analysis of Bacillus subtilis lytic bacteriophage varphiNIT1 capable of obstructing natto fermentation carrying genes for the capsule-lytic soluble enzymes poly-gamma-glutamate hydrolase and levanase. *Biosci. Biotechnol. Biochem.* 81, 135–146. doi: 10.1080/09168451.2016.1232153

Papadopoulou, A., Dalsgaard, I., and Wiklund, T. (2019). Inhibition Activity of Compounds and Bacteriophages against Flavobacterium psychrophilum Biofilms In Vitro. *J. Aquat. Anim. Health* 31, 225–238. doi: 10.1002/aah.10069

Parasion, S., Kwiatek, M., Gryko, R., Mizak, L., and Malm, A. (2014). Bacteriophages as an alternative strategy for fighting biofilm development. *Pol. J. Microbiol.* 63, 137–145. doi: 10.33073/pjm-2014-019

Pires, D. P., Cleto, S., Sillankorva, S., Azeredo, J., and Lu, T. K. (2016). Genetically Engineered Phages: a Review of Advances over the Last Decade. *Microbiol. Mol. Biol. Rev.* 80, 523–543. doi: 10.1128/MMBR.00069-15

Rabin, N., Zheng, Y., Opoku-Temeng, C., Du, Y., Bonsu, E., and Sintim, H. O. (2015). Biofilm formation mechanisms and targets for developing antibiofilm agents. *Future Med. Chem.* 7, 493–512. doi: 10.4155/fmc.15.6

Remy, B., Mion, S., Plener, L., Elias, M., Chabriere, E., and Daude, D. (2018). Interference in Bacterial Quorum Sensing: a Biopharmaceutical Perspective. *Front. Pharmacol.* 9:203. doi: 10.3389/fphar.2018.00203

Rice, C. J., Kelly, S. A., O'Brien, S. C., Melaugh, E. M., Ganacias, J. C. B., Chai, Z. H., et al. (2021). Novel phage-derived depolymerase with activity against *Proteus mirabilis* biofilms. *Microorganisms* 9:2172. doi: 10.3390/microorganisms9102172

Rizzo, N. N., Pottker, E. S., Webber, B., Borges, K. A., Duarte, S. C., Levandowski, R., et al. (2020). Effect of two lytic bacteriophages against multidrug-resistant and biofilm-forming *Salmonella* Gallinarum from poultry. *Br. Poult. Sci.* 61, 640–645. doi: 10.1080/00071668.2020.1805724

Rodriguez-Rubio, L., Chang, W. L., Gutierrez, D., Lavigne, R., Martinez, B., Rodriguez, A., et al. (2016). 'Artilysation' of endolysin lambdaSa2lys strongly improves its enzymatic and antibacterial activity against streptococci. *Sci. Rep.* 6:35382. doi: 10.1038/srep35382

Sanz-Gaitero, M., Keary, R., Garcia-Doval, C., Coffey, A., and van Raaij, M. J. (2013). Crystallization of the CHAP domain of the endolysin from Staphylococcus aureus bacteriophage K. *Acta Crystallogr. Sect. F Struct. Biol. Cryst. Commun.* 69, 1393–1396. doi: 10.1107/S1744309113030133

Schirmeier, E., Zimmermann, P., Hofmann, V., Biebl, M., Gerstmans, H., Maervoet, V. E. T., et al. (2018). Inhibitory and bactericidal effect of Artilysin((R)) Art-175 against colistin-resistant mcr-1-positive *Escherichia coli* isolates. *Int. J. Antimicrob. Agents* 51, 528–529. doi: 10.1016/j.ijantimicag.2017.08.027

Schmelcher, M., Donovan, D. M., and Loessner, M. J. (2012). Bacteriophage endolysins as novel antimicrobials. *Future Microbiol.* 7, 1147–1171. doi: 10.2217/fmb.12.97

Schuch, R., Khan, B. K., Raz, A., Rotolo, J. A., and Wittekind, M. (2017). Bacteriophage lysin CF-301, a potent antistaphylococcal biofilm agent. *Antimicrob. Agents Chemother.* 61:e02666-16. doi: 10.1128/AAC.02666-16

Schuch, R., Lee, H. M., Schneider, B. C., Sauve, K. L., Law, C., Khan, B. K., et al. (2014). Combination therapy with lysin CF-301 and antibiotic is superior to antibiotic alone for treating methicillin-resistant Staphylococcus aureus-induced murine bacteremia. *J. Infect. Dis.* 209, 1469–1478. doi: 10.1093/infdis/jit637

Seth, A. K., Geringer, M. R., Nguyen, K. T., Agnew, S. P., Dumanian, Z., Galiano, R. D., et al. (2013). Bacteriophage therapy for Staphylococcus aureus biofilm-infected wounds: a new approach to chronic wound care. *Plast. Reconstr. Surg.* 131, 225–234. doi: 10.1097/PRS.0b013e31827e47cd

Shahed-Al-Mahmud, M., Roy, R., Sugiokto, F. G., Islam, M. N., Lin, M. D., Lin, L. C., et al. (2021). Phage phiAB6-Borne Depolymerase Combats *Acinetobacter baumannii* Biofilm Formation and Infection. *Antibiotics* 10:279. doi: 10.3390/antibiotics10030279

Sharma, G., Sharma, S., Sharma, P., Chandola, D., Dang, S., Gupta, S., et al. (2016). *Escherichia coli* biofilm: development and therapeutic strategies. *J. Appl. Microbiol.* 121, 309–319. doi: 10.1111/jam.13078

Sharma, U., Vipra, A., and Channabasappa, S. (2018). Phage-derived lysins as potential agents for eradicating biofilms and persisters. *Drug Discov. Today* 23, 848–856. doi: 10.1016/j.drudis.2018.01.026

Sosa, B. R., Niu, Y., Turajane, K., Staats, K., Suhardi, V., Carli, A., et al. (2020). 2020 John Charnley Award: the antimicrobial potential of bacteriophage-derived lysin in a murine debridement, antibiotics, and implant retention model of prosthetic joint infection. *Bone Joint* J 102-B(7_Supple_B), 3–10. doi: 10.1302/0301-620X.102B7.BJJ-2019-1590.R1

Spellberg, B., Bartlett, J. G., and Gilbert, D. N. (2013). The future of antibiotics and resistance. *N. Engl. J. Med.* 368, 299–302. doi: 10.1056/NEJMp1215093

Steele, A., Stacey, H. J., de Soir, S., and Jones, J. D. (2020). The Safety and Efficacy of Phage Therapy for Superficial Bacterial Infections: a Systematic Review. *Antibiotics* 9:754. doi: 10.3390/antibiotics9110754

Sugano, M., Morisaki, H., Negishi, Y., Endo-Takahashi, Y., Kuwata, H., Miyazaki, T., et al. (2016). Potential effect of cationic liposomes on interactions with oral bacterial cells and biofilms. *J. Liposome Res.* 26, 156–162. doi: 10.3109/08982104.2015.1063648

Szermer-Olearnik, B., and Boratynski, J. (2015). Removal of endotoxins from bacteriophage preparations by extraction with organic solvents. *PLoS One* 10:e0122672. doi: 10.1371/journal.pone.0122672

Tabassum, R., Shafique, M., Khawaja, K. A., Alvi, I. A., Rehman, Y., Sheik, C. S., et al. (2018). Complete genome analysis of a Siphoviridae phage TSK1 showing biofilm removal potential against *Klebsiella pneumoniae*. *Sci. Rep.* 8:17904. doi: 10.1038/s41598-018-36229-y

Tagliaferri, T. L., Jansen, M., and Horz, H. P. (2019). Fighting Pathogenic Bacteria on Two Fronts: phages and Antibiotics as Combined Strategy. *Front. Cell. Infect. Microbiol.* 9:22. doi: 10.3389/fcimb.2019.00022

Thandar, M., Lood, R., Winer, B. Y., Deutsch, D. R., Euler, C. W., and Fischetti, V. A. (2016). Novel engineered peptides of a phage lysin as effective antimicrobials against multidrug-resistant *Acinetobacter baumannii*. *Antimicrob. Agents Chemother.* 60, 2671–2679. doi: 10.1128/AAC.02972-15

Topka-Bielecka, G., Dydecka, A., Necel, A., Bloch, S., Nejman-Falenczyk, B., Wegrzyn, G., et al. (2021). Bacteriophage-Derived Depolymerases against Bacterial Biofilm. *Antibiotics* 10:175. doi: 10.3390/antibiotics10020175

Tseng, B. S., Zhang, W., Harrison, J. J., Quach, T. P., Song, J. L., Penterman, J., et al. (2013). The extracellular matrix protects *Pseudomonas aeruginosa* biofilms by limiting the penetration of tobramycin. *Environ. Microbiol.* 15, 2865–2878. doi: 10.1111/1462-2920.12155

Van Belleghem, J. D., Merabishvili, M., Vergauwen, B., Lavigne, R., and Vaneechoutte, M. (2017). A comparative study of different strategies for removal of endotoxins from bacteriophage preparations. *J. Microbiol. Methods* 132, 153–159. doi: 10.1016/j.mimet.2016.11.020

van der Kamp, I., Draper, L. A., Smith, M. K., Buttimer, C., Ross, R. P., and Hill, C. (2020). A New Phage Lysin Isolated from the Oral Microbiome Targeting Streptococcus pneumoniae. *Pharmaceuticals* 13:478. doi: 10.3390/ph13120478

Vasina, D. V., Antonova, N. P., Grigoriev, I. V., Yakimakha, V. S., Lendel, A. M., Nikiforova, M. A., et al. (2021). Discovering the Potentials of Four Phage Endolysins to Combat Gram-Negative Infections. *Front. Microbiol.* 12:748718. doi: 10.3389/fmicb.2021.748718

Veerachamy, S., Yarlagadda, T., Manivasagam, G., and Yarlagadda, P. K. (2014). Bacterial adherence and biofilm formation on medical implants: a review. *Proc. Inst. Mech. Eng. H* 228, 1083–1099. doi: 10.1177/0954411914556137

Walker, J. N., Poppler, L. H., Pinkner, C. L., Hultgren, S. J., and Myckatyn, T. M. (2020). Establishment and Characterization of Bacterial Infection of Breast Implants in a Murine Model. *Aesthet. Surg. J.* 40, 516–528. doi: 10.1093/asj/sjz190

Walmagh, M., Boczkowska, B., Grymonprez, B., Briers, Y., Drulis-Kawa, Z., and Lavigne, R. (2013). Characterization of five novel endolysins from Gram-negative infecting bacteriophages. *Appl. Microbiol. Biotechnol.* 97, 4369–4375. doi: 10.1007/s00253-012-4294-7

Walmagh, M., Briers, Y., dos Santos, S. B., Azeredo, J., and Lavigne, R. (2012). Characterization of modular bacteriophage endolysins from Myoviridae phages OBP, 201phi2-1 and PVP-SE1. *PLoS One* 7:e36991. doi: 10.1371/journal.pone.0036991

Wang, L., Tkhilaishvili, T., Trampuz, A., and Gonzalez Moreno, M. (2020). Evaluation of Staphylococcal Bacteriophage Sb-1 as an Adjunctive Agent to Antibiotics Against Rifampin-Resistant Staphylococcus aureus Biofilms. *Front. Microbiol.* 11:602057. doi: 10.3389/fmicb.2020.602057

Wasfi, R., Hamed, S. M., Amer, M. A., and Fahmy, L. I. (2020). *Proteus mirabilis* Biofilm: development and Therapeutic Strategies. *Front. Cell. Infect. Microbiol.* 10:414. doi: 10.3389/fcimb.2020.00414

Whitchurch, C. B., Tolker-Nielsen, T., Ragas, P. C., and Mattick, J. S. (2002). Extracellular DNA required for bacterial biofilm formation. *Science* 295:1487. doi: 10.1126/science.295.5559.1487

Wolcott, R. D., Rumbaugh, K. P., James, G., Schultz, G., Phillips, P., Yang, Q., et al. (2010). Biofilm maturity studies indicate sharp debridement opens a time-dependent therapeutic window. *J. Wound Care* 19, 320–328. doi: 10.12968/jowc.2010.19.8.77709

World Health Organization [WHO]. (2020). *Antibiotic Resistance [Online]*. Available online at: https://www.who.int/news-room/fact-sheets/detail/antibiotic-resistance (accessed August 2021).

Wu, H., Moser, C., Wang, H. Z., Hoiby, N., and Song, Z. J. (2015). Strategies for combating bacterial biofilm infections. *Int. J. Oral Sci.* 7, 1–7. doi: 10.1038/ijos.2014.65

Wu, Y., Wang, R., Xu, M., Liu, Y., Zhu, X., Qiu, J., et al. (2019). A Novel Polysaccharide Depolymerase Encoded by the Phage SH-KP152226 Confers Specific Activity Against Multidrug-Resistant *Klebsiella pneumoniae* via Biofilm Degradation. *Front. Microbiol.* 10:2768. doi: 10.3389/fmicb.2019.02768

Yan, J., and Bassler, B. L. (2019). Surviving as a Community: antibiotic Tolerance and Persistence in Bacterial Biofilms. *Cell Host Microbe* 26, 15–21. doi: 10.1016/j.chom.2019.06.002

Yan, J., Mao, J., and Xie, J. (2014). Bacteriophage polysaccharide depolymerases and biomedical applications. *BioDrugs* 28, 265–274. doi: 10.1007/s40259-013-0081-y

Yang, H., Bi, Y., Shang, X., Wang, M., Linden, S. B., Li, Y., et al. (2016). Antibiofilm activities of a novel chimeolysin against streptococcus mutans under physiological and cariogenic conditions. *Antimicrob. Agents Chemother.* 60, 7436–7443. doi: 10.1128/AAC.01872-16

Yang, H., Zhang, H., Wang, J., Yu, J., and Wei, H. (2017). A novel chimeric lysin with robust antibacterial activity against planktonic and biofilm methicillin-resistant Staphylococcus aureus. *Sci. Rep.* 7:40182. doi: 10.1038/srep40182

Yang, H., Zhang, Y., Huang, Y., Yu, J., and Wei, H. (2014). Degradation of methicillin-resistant Staphylococcus aureus biofilms using a chimeric lysin. *Biofouling* 30, 667–674. doi: 10.1080/08927014.2014.905927

Yasuda, H., Koga, T., and Fukuoka, T. (1999). In vitro and in vivo models of bacterial biofilms. *Methods Enzymol.* 310, 577–595. doi: 10.1016/s0076-6879(99)10045-4

Yin, W., Wang, Y., Liu, L., and He, J. (2019). Biofilms: the Microbial "Protective Clothing" in Extreme Environments. *Int. J. Mol. Sci.* 20:3423. doi: 10.3390/ijms20143423

Young, R. (1992). Bacteriophage lysis: mechanism and regulation. *Microbiol. Rev.* 56, 430–481. doi: 10.1128/mr.56.3.430-481.1992

Yuan, Y., Qu, K., Tan, D., Li, X., Wang, L., Cong, C., et al. (2019). Isolation and characterization of a bacteriophage and its potential to disrupt multi-drug resistant *Pseudomonas aeruginosa* biofilms. *Microb. Pathog.* 128, 329–336. doi: 10.1016/j.micpath.2019.01.032

Conflict of Interest: The authors declare that the research was conducted in the absence of any commercial or financial relationships that could be construed as a potential conflict of interest.

Publisher's Note: All claims expressed in this article are solely those of the authors and do not necessarily represent those of their affiliated organizations, or those of the publisher, the editors and the reviewers. Any product that may be evaluated in this article, or claim that may be made by its manufacturer, is not guaranteed or endorsed by the publisher.

frontiers | Frontiers in Veterinary Science

ORIGINAL RESEARCH
published: 18 July 2022
doi: 10.3389/fvets.2022.799710

Microbiological Quality and Presence of Foodborne Pathogens in Raw and Extruded Canine Diets and Canine Fecal Samples

*Doina Solís[1], Magaly Toro[1], Paola Navarrete[1], Patricio Faúndez[2] and Angélica Reyes-Jara[1]**

[1] Laboratorio de Microbiología y Probióticos, Instituto de Nutrición y Tecnología de los Alimentos (INTA), Universidad de Chile, Santiago, Chile, [2] Red de Atención Veterinaria, Hospital de Alta Complejidad Bilbao, Universidad de Chile, Santiago, Chile

Pet food can be a source of microbiological hazards that might affect companion animals and owners. Even though owners usually rely on conventional pet diets, such as extruded diets, new feeding practices, such as raw meat-based diets (RMBDs), have grown. RMBDs' benefits are still scientifically uncertain, while its risks have been documented. The use of canine RMBDs might increase the exposure to zoonotic pathogens, such as *Salmonella* spp., *Listeria monocytogenes*, *Campylobacter* spp., among others. Identifying pathogen prevalence in canine food and pets is required to contribute to public health measures. The aims of this study were: (1) to compare the microbiological quality of RMBDs and extruded diets (2) to identify and compare the prevalence of *Salmonella spp., Campylobacter jejuni,* and *L. monocytogenes* from raw and extruded canine diets and canine fecal samples, and (3) to characterize pet owners according to the diet chosen to be used on their pets, their motivations for using RMBDs, and their knowledge about benefits and risks related to this feeding practice. Conventional and molecular microbiological methods were used to identify pathogen presence from food and fecal samples, while pulsed-field gel electrophoresis (PFGE) was performed to evaluate the clonal relationship between isolates. Aerobic plate counts for RMBDs were higher than those detected for extruded diets. *Salmonella* spp. and *L. monocytogenes* were isolated from 35.7% (15/42) RMBDs, while *Salmonella* spp., *C. jejuni,* and *L. monocytogenes* from 33.3% (11/33) fecal samples from RMBD-fed dogs. From the RMBD samples positive to *Salmonella* spp., chicken was the main meat ingredient composing the diets. PFGE analysis confirmed a genetic association between *Salmonella* spp. isolates from fecal and raw food samples from the same household. We did not detect pathogens from extruded food samples or feces from extruded-fed dogs. Using a survey, we identified dog owners' unawareness and/or underestimation of risks related to RMBDs. We demonstrated that canine raw pet food might be a source of zoonotic foodborne pathogens that represent a health risk for both humans and pets. While clinical findings caused by the mentioned pathogens vary among pets, the zoonotic potential implies a significant concern.

Keywords: raw meat-based diets, foodborne pathogens, pet food, pet food safety, *Listeria monocytogenes*, *Salmonella* spp., *Campylobacter* spp.

OPEN ACCESS

Edited by:
Sibao Wang,
Shanghai Institutes for Biological Sciences (CAS), China

Reviewed by:
Marie-Lou Gaucher,
Université de Montréal, Canada
Sampathkumar Balamurugan,
Agriculture and Agri-Food Canada (AAFC), Canada
Devon Radford,
Agriculture and Agri-Food Canada (AAFC), Canada

***Correspondence:**
Angélica Reyes-Jara
areyes@inta.uchile.cl

Specialty section:
This article was submitted to Veterinary Infectious Diseases, a section of the journal Frontiers in Veterinary Science

Received: *04 November 2021*
Accepted: *23 June 2022*
Published: *18 July 2022*

Citation:
Solís D, Toro M, Navarrete P, Faúndez P and Reyes-Jara A (2022) Microbiological Quality and Presence of Foodborne Pathogens in Raw and Extruded Canine Diets and Canine Fecal Samples.
Front. Vet. Sci. 9:799710.
doi: 10.3389/fvets.2022.799710

INTRODUCTION

It is estimated that around 470 million dogs and 370 million cats are owned and kept as pets globally (1). The constant growth of the pet population and the close bond between humans and pets influence a high demand for high-quality pet products. In pet foods, safety is one of the most critical characteristics that must be assured along the production chain (2).

Since the mid-1,800 s, when the first commercial pet foods appeared, the pet food industry has continuously grown. By 2005 and subsequent years, dog's and cat's nutrition mainly consisted of conventional commercial diets, such as dry, moist, and semi-moist food (3). These diets are produced mostly through extrusion processes and have been historically considered safe to feed pets (4, 5).

Food safety threats that might be present through the pet food manufacturing process include physical, chemical, and biological hazards that are also present in the food industry intended for human consumption (6). Leading causes of pet food recall include mycotoxins, *Salmonella* spp., contamination with veterinary drugs, ingredient adulteration, and errors in the nutritional formulation (5, 6). The most significant sources of contamination are raw materials (6). Although extrusion is considered an effective critical control point (CCP) to eliminate microbiological hazards–such as *Salmonella* spp.—throughout the conventional production process, post-extrusion contamination and pet illnesses are still possible (5–7).

The close interaction between humans and pets has promoted companion animal lifestyle changes, including different dietary choices related to the owner's interests and beliefs (8). Although conventional commercial diets are still the preferred type of pet food chosen among pet owners, the interest in new feeding practices, such as the use of raw meat-based diets (RMBDs), has grown (4). Proponents believe this type of food is more natural and healthier for pets (9).

RMBDs consist of uncooked ingredients, including meats, organs, meaty bones, vegetables, and fruits (7, 10). Some of these ingredients, especially those of animal origin, are frequently contaminated with foodborne pathogens such as *Salmonella* spp. *L. monocytogenes*, *Campylobacter* spp., Shiga-toxigenic *Escherichia coli,* among others (9–11). Pathogen detection in RMBDs has been studied in countries where this feeding practice has been established for at least 30 years (11). The prevalence of these pathogens in RMBDs varies among countries, ranging between 7.1 and 80% for *Salmonella* spp. (11, 12), 16–54% for *L. monocytogenes* (10, 13), and 0–22% for *C. jejuni* (11).

Pets might also get ill due to pathogen infection, and raw diets have been recognized as a risk factor for fecal pathogen shedding in pets (9, 11). Moreover, contact with ingredients contaminated with antimicrobial-resistant bacteria might also be a public health concern for both the owner and the pet (4, 9). To date, most microbiological hazards present in the pet food industry still need effective control measures (2).

The present study sought to determine pet food safety based on the presence of zoonotic pathogens in extruded and RMBDs and to determine the prevalence of *Salmonella* spp., *C. jejuni*, and *L. monocytogenes* in canine fecal samples. Moreover, the genetic relationship between bacteria isolated from pet food and fecal bacterial isolates was studied. Additionally, to understand the factors that determined the adoption of the raw diets feeding practice, we examined the owners' motivations for feeding their dogs these diets. Finally, we characterized some in-home hygiene practices adopted by owners while manipulating RMBDs.

MATERIALS AND METHODS

Pet Food Samples

A total of 66 dog food samples (RMBDs = 42; extruded diets = 24) were analyzed. RMBDs were divided into raw commercial (n = 31) and home-prepared raw diets (n = 11). Canine raw commercial diets were obtained from every participant or purchased by the investigators. All homemade RMBDs analyzed were obtained from owners. Commercial RMBDs came from the six most representative RMBD producers in the market, and selected companies were legally registered by the country's veterinary and health authorities (14). The numbers of samples from each manufacturer were: A = 5, B = 4, C = 5, D = 5, E = 6, F = 6. RMBDs were transported in coolers containing ice packs to the laboratory as previously described (9). Extruded diets (n = 24) were received from participants in sterile containers and transported at room temperature for further analysis.

Fecal Samples

Pet owners were recruited through a public announcement emphasizing on RMBD-fed dogs. Upon the owner's acceptance of the terms of the study, a physical examination was performed by veterinarians. Dogs enrolled in the study were healthy, did not have any gastrointestinal symptoms, and did not use antibiotics for at least 6 weeks before the sample collection. The demographics of dogs enrolled in the study are shown in **Supplementary Table 1**. Rectal swabs (Copan® Transystem™ 132C) were obtained from 33 RMBD-fed dogs and 22 extruded-fed dogs; every dog was sampled once, except one dog (T20–40), which was sampled on two different occasions. Samples were transported in coolers containing ice packs to the laboratory and processed within the same day. The study was approved by the Institutional Committee for the Care and Use of Animals (CICUA) from the University of Chile under the CICUA code 20411-VET-UCH.

Microbiological Analysis of Pet Food Samples

All dog food samples (RMBDs = 42; extruded = 24; total = 66) were analyzed following methodologies described in the Bacteriological Analytical Manual (BAM) with minor modifications for aerobic plate counts (APC), *Salmonella* spp, *L. monocytogenes,* and *C. jejuni* isolation and identification (15–18).

For the APC analysis, 25 g from each sample were homogenized in 225 ml buffered peptone water (Bacto™,

212367, Australia), and decimal dilutions were prepared. Afterward, 1 ml of each dilution was transferred into separate Petri dishes, and 15 ml of warm plate count agar was poured over the sample (Oxoid^{TM}, CM0463, USA). Petri dishes were incubated at 37°C for 48 ± 2 h (18). An acceptable APC level ($<1 \times 10^6$ UFC/g) was defined according to the maximum level suggested by Kukier et al. (19).

Salmonella spp. isolation was conducted through a two-step enrichment procedure. Briefly, 25 g of each food sample were homogenized in 225 ml lactose broth (Difco^{TM}, 241,000) and incubated at 37°C for 24 h. Then, 0.1 ml of the homogenate was inoculated onto Rappaport-Vassiliadis broth (Oxoid^{TM}, CM0669, USA) and 1 ml onto tetrathionate broth (Oxoid^{TM}, CM0671, USA). Both enrichments were incubated at 42°C for 24 h and then plated into Hektoen agar (BD Difco^{TM}, 11703543, USA) and XLD agar (BD Difco^{TM}, 11783503, USA) and incubated at 37°C for 24 h (15). Typical colonies were characterized by biochemical tests (15) and confirmed as *Salmonella* spp. through a polymerase chain reaction (PCR) for the *invA* gene with the primers *invA*F (5′-GAATCCTCAGTTTTTCAACGTTTC-3′) and *invAR* (5′-TAGCCGTAACAACCAATACAAATG-3′) (20).

For *L. monocytogenes* isolation, 25 g of sample were homogenized in 225 ml *Listeria* enrichment broth (BD Difco^{TM}, 11718333, USA) and incubated at 30°C for 48 h. The enrichment was plated onto Palcam agar (Oxoid^{TM}, CM0877, USA) and Chromogenic *Listeria* agar (Oxoid^{TM}, CM1084, USA) and incubated at 37°C for 48 h (16). Presumptive *L. monocytogenes* colonies from each plate were confirmed by Gram stain observation and a PCR with the primers lmo3F (5′-GTCTTGCGCGTTAATCATTT-3′) and lmo4R (5′-ATTTGCTAAAGCGGGAATCT-3′) (21).

For *C. jejuni* isolation, food samples (25 g) were homogenized in 225 ml Bolton broth (Oxoid^{TM}, CM0983, USA) with supplement SR0183 (Oxoid^{TM}, USA) and 5% horse blood. Homogenates were incubated at 37°C for 24 h in microaerophilic conditions, followed by plating onto Skirrow agar (Oxoid^{TM}, CM0331, USA) with supplement SR0069 (Oxoid^{TM}, USA) and 5% horse blood and onto CCDA agar (Oxoid^{TM}, CM0739, USA) with supplement SR0155 (Oxoid^{TM}, USA). Plates were incubated at 42°C for 24−48 h in a microaerophilic atmosphere (17). Presumptive *C. jejuni* colonies were confirmed by microscopic observation (wet mount slides and Gram staining) and biochemical tests, including catalase and hippurate tests (17).

Microbiological Analysis of Pet Fecal Samples

Canine fecal samples (RMBD-fed dog samples = 33; extruded-fed dog sample s = 22; total = 55) were also analyzed for the presence of the *Salmonella* spp., *L. monocytogenes,* and *C. jejuni.*

For *Salmonella* spp isolation, stool samples were inoculated into 10 ml buffered peptone water and incubated at 37°C for 24 h. Then, 0.1 ml were transferred to Rappaport-Vassiliadis and 1 ml to tetrathionate broth and incubated at 42°C for 24 h. Enrichments were plated onto Hektoen and XLD agar and incubated at 37°C for 24 h (15). Presumptive colonies were characterized by biochemical tests and confirmed as *Salmonella* spp. through a PCR for the *invA* gene as described in the previous section.

For *L. monocytogenes* isolation, stool samples were inoculated into 10 ml *Listeria* enrichment broth and incubated at 30°C for 48 h. Enrichment cultures were plated onto Palcam and Chromogenic *Listeria* agar and incubated at 37°C for 48 h (16, 22). Presumptive colonies were confirmed by PCR with primers lmo3F and lmo4R as described in the previous section.

For *C. jejuni* detection, fecal samples were inoculated into 10 ml Bolton broth with antibiotics and 5% horse blood and incubated at 37°C for 24 h in microaerophilic conditions. Enrichment cultures were plated onto Skirrow agar with supplement SR0069 and 5% horse blood and onto CCDA agar with supplement SR0155. Plates were incubated at 42°C for 24–48 h in a microaerophilic atmosphere and *C. jejuni* was identified as described in the previous section.

All bacterial isolates were stored at −20°C for further analysis.

Pulse-Field Gel Electrophoresis

Salmonella spp. isolates ($n = 10$) obtained simultaneously from pet food and fecal samples from the same households were genetically characterized to assess their clonal relationship. Every isolate analyzed was obtained from a different dog, except two *Salmonella* spp. isolates (T20–40 A and B), obtained from fecal samples taken 1 month apart from the same dog. Pulsenet PFGE protocols were used (23). Briefly, isolated colonies were plated onto Trypticase Soy Agar (TSA) (BD Difco^{TM}, 236950, USA) and incubated at 37°C for 14–18 h. Cell suspension plugs were prepared the next day in 1% Pulsed Field Certified Agarose (Bio-Rad, 1620137, USA) and transferred to lysis buffer (50 mM Tris:50 mM EDTA, pH 8.0 + 1% Sarcosyl) and Proteinase K (20 mg/ml). After washing the agarose plugs, digestion was performed with the *Xba*I enzyme (Promega, Wisconsin, USA) at room temperature for 15 min. The electrophoresis was performed on the CHEF DR III unit (Bio-Rad Laboratories Canada, Ltd., Mississauga, Ontario, Canada) using the conditions described in the *Salmonella* spp. protocol (initial switch time: 2.2 s, final switch time: 63.8 s, voltage:6 V, included angle:120°, run time: 17–20 h). BioNumerics version 7.1 (Applied Maths, Sint-Martens-Latem, Belgium) was used to interpret PFGE patterns and build a neighbor-joining (NJ) tree. Similarities of PFGE patterns were calculated using the Dice coefficient with a 1% tolerance.

Owner's Motivations and Habits

A questionnaire to understand the owner's motivations and habits was developed by veterinarians and filled out by every owner. Surveys consisted of close-ended questions including three categories: (i) animal and diet-specific factors, (ii) owners' motivations for feeding the type of diet they had selected for their pets, and (iii) food hygiene practices. Open-ended questions were used to describe the owner's knowledge about risks and benefits related to raw feeding. The questionnaire for RMBD-fed dog owners ($n = 22$) included 22 questions, while only 14 questions were included for the extruded-fed group ($n = 14$). Extra questions answered by RMBD-fed dog owners consisted

of the main raw ingredients used to feed their pets. Some participants had more than one dog, but those owners filled a single questionnaire.

Statistical Analysis

Aerobic plate count data for RMBDs and extruded diets were tested for normality (Shapiro-Wilk test) (24) and homoscedasticity (Fligner-Killeen test) (25). Welch's two-sample *t*-test was used to contrast raw and extruded diets APC levels (26), while ANOVA was used for the multiple comparison analysis among RMBDs producers (27). Fischer's exact test was used to evaluate the association between pathogen prevalence and type of diet (RMBDs or extruded) (28). The Kruskal Wallis test was applied to analyze associations between a) pathogen presence and APC levels and b) pathogen presence and type of meat used in raw diets (29). A p-value of $\leq$0.05 was considered significant. Analyses were performed with the statistical software STATA (STATA® MP 16.0, StataCorp, USA). Descriptive statistics were employed for the questionnaire's categorical variables, such as participants' gender/sex, age, and type of food used/consumed (30).

RESULTS

Pet Food Microbiological Analysis

RMBDs ($n = 42$) and extruded ($n = 24$) pet food samples were analyzed using conventional and molecular microbiological methods to compare APC levels and pathogen presence. APC levels for the RMBDs, including commercially and homemade diets, were significantly higher than those detected for extruded diets (p-value $< 2.2 \times 10^{-16}$) (**Figure 1**). For the RMBDs, APCs ranged from 1.4×10^5 to 4.3×10^8 CFU/g (Median $= 3.0 \times 10^6$), while for extruded diets it fluctuated from <10 to 1.8×10^3 CFU/g (Median $= 9.1 \times 10^1$) (**Figure 1**). No statistical difference was detected between commercial and homemade RMBD APCs (p-value $= 0.17$) (**Supplementary Figure 1**). Furthermore, from the six commercial RMBD manufacturers (A–F) analyzed, B and D showed the highest APCs (p-value < 0.05) (**Figure 2**). Statistical analysis showed that APCs were independent of the type of meat used to manufacture the RMBDs (p-value $= 0.063$, Kruskal Wallis).

None of the pathogens were isolated from the extruded diets, whereas 15/42 (35.7%) RMBD samples—commercial and homemade— carried bacterial pathogens. *Salmonella* spp. was isolated from 26.2% ($n = 11$) RMBD samples and *L. monocytogenes* from 19% ($n = 8$). *C. jejuni* was not isolated from any food sample. Chicken meat was the main ingredient in most of the food samples contaminated with *Salmonella* spp. (6/11; 54.5%) (**Supplementary Table 2**). *L. monocytogenes* was isolated from samples made with chicken ($n = 2$), beef ($n = 2$), salmon ($n = 1$), and guanaco (*Lama guanicoe*; $n = 1$) (**Supplementary Table 2**).

Pet Fecal Samples Microbiological Analysis

A total of 55 fecal samples (RMBD-fed dog samples = 33; extruded-fed dog samples = 22) were analyzed for the presence of selected pathogens. We detected a higher prevalence of pathogen shedding from RMBD-fed dogs (33.3%; 11/33) than from extruded-fed dogs, in which samples did not carry any of the tested pathogens (0%; 0/22) (p-value $= 0.002$) (**Table 1**). Among the RMBD-fed dogs, *Salmonella* spp. was the pathogen most frequently isolated (24.2%, 8/33), while *L. monocytogenes* was isolated from 3% (1/33) and *C. jejuni* from 6% (2/33) fecal samples (**Table 1**).

Association Between Bacterial Pathogen Shedding and Pet Food Contamination

An additional analysis was performed to evaluate the pathogen co-occurrence between isolates from fecal and food samples. Only bacterial contaminated pet food consumed by dog participants ($n = 11$) and canine pathogen carriers ($n = 11$) were considered for this analysis (**Table 2**).

Fecal samples from five dogs tested positive for pathogens, but their food tested negative (**Table 2**). Similarly, pathogens were detected in five RMBD samples obtained from households where dogs' fecal results did not evidence pathogen presence. However, in five cases, *Salmonella spp.* was obtained simultaneously from the pet fecal sampling and the dog's food. A dog fecal sample carried *C. jejuni,* but the pet consumed a RMBD contaminated with *Salmonella* spp. and *L. monocytogenes* (**Table 2**).

Salmonella isolates ($n = 10$) obtained simultaneously from a dog's fecal sample and the RMBD the dog was fed with were analyzed by PFGE to assess their clonal relationship. The Neighbor-Joining tree, built with the restriction patterns resulting from the PFGE analysis, grouped isolates in two clusters with $\geq$90% similarity among isolates (**Figure 3**). Cluster 1 included five highly related *Salmonella* spp. isolates: food isolate A20–32 and fecal isolates T20–45 and T20–46 were obtained from "household l," and food isolate A20–24 and fecal isolate T20–34 were associated with "household j." Cluster 2 was formed by three *Salmonella* spp. from "household k:" A20–28 from pet food and two isolates (T20–40 A and B) from dog 40's fecal samples obtained 1 month apart (**Figure 3**). Interestingly, all these isolates came from households that used diets made with chicken as a primary meat ingredient.

Characterization of Pet Owners

A total of 36 dog owners from 55 healthy dogs (RMBD-fed dogs = 33; extruded-fed dogs = 22) agreed to participate in the study and responded to the questionnaire. In some cases, participants owned more than one dog, which were fed the same type of diet. Since recruitment emphasized RMBD-fed dog owners, 61.1% ($n = 22$) of participants reported using RMBDs for their dogs, while 38.9% ($n = 14$) preferred conventional extruded diets. A summary of the most relevant demographic data from the respondents is shown in **Supplementary Table 3**.

The questions, mainly focusing on RMBD-fed dog owners, were intended to describe the owner's reasons and habits for using unconventional diets. Regarding the preferred ingredients for feeding their pets, the most common meat sources were beef and chicken, while liver was the main organ used. Apple and carrots were the most common fruit and vegetable used (**Supplementary Figure 2**).

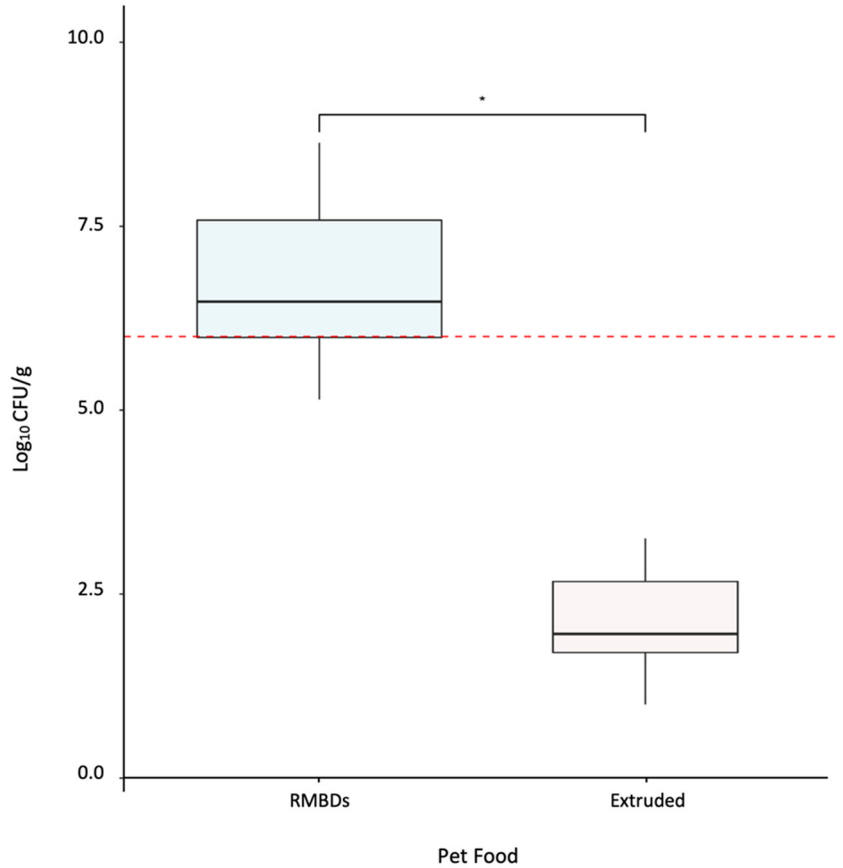

FIGURE 1 | Aerobic bacterial counts (APC) for RMBDs ($n = 42$) and extruded ($n = 24$). The Fligner-Killeen test was used to determine the homogeneity of variances (homoscedasticity) and Shapiro-Wilk test for normality. The level of APC between both diets was compared using *Welch's Two-Sample T-test* *p-value $< 2.20 \times 10^{-16}$. The red line shows the suggested APC upper limit for animal compound feed according to Kukier et al. (19). RMBD's APC $>1 \times 10^6$ CFU/g = 31.

The owners' perception of the risks and benefits of RMBDs was analyzed. All RMBD-fed dogs owners ($n = 22$) considered this feeding practice to provide numerous health benefits to their pets, mainly related to improved cutaneous and gastrointestinal health and better feces quality (**Table 3**; **Supplementary Table 4**). Nevertheless, only 12/22 (54.5%) declared knowing about the risks related to raw feeding. Moreover, 50% of extruded-fed dog owners knew about the risks and/or benefits of raw feeding (**Table 3**). Microbiological contamination of food and foreign bodies, such as bones, were the main risks perceived by the owners (**Supplementary Table 4**).

RMBD-fed dog owners' habits showed that 68.2% (15/22) stored raw ingredients and prepared raw food in the same space/fridge used for human food storage. Also, 81.8% (18/22) of owners manipulated raw pet diets in the same space they prepared food for human consumption (**Supplementary Table 5**).

DISCUSSION

Pet ownership has grown throughout the years, and the human-animal bond has strengthened. Studies have shown that companion animals play an essential role in human health and wellbeing. Dog's role has diversified from simple companionship to new applications such as assistance and working and supporting humans in several therapeutic ways (31). Increasing pet ownership has also played an essential role in dogs' lifestyles, behaviors, and habits. Owners have changed their pet's feeding habits, including providing unconventional pet food like RMBDs (8). Raw diets might represent a source of microbiological hazards for pets, and these risks could even affect owners through contact with their pets or manipulation of contaminated pet food (8).

In this study, 31/42 raw diets analyzed showed an elevated APC level (**Figure 1**). Since Chilean regulation does not establish microbiological criteria exclusively for raw pet food (32), we defined an APC level of 10^6 CFU/g as the maximum accepted level of microbial contamination as previously suggested by Kukier et al. (19). Since APC is a hygienic indicator used to estimate the bacterial population in a food sample (18), our results reveal the importance of strengthening good manufacturing practices in the RMBD industry. Overall, the microbiological quality for the extruded food in this study was adequate. Even though the microbiological quality of pet foods

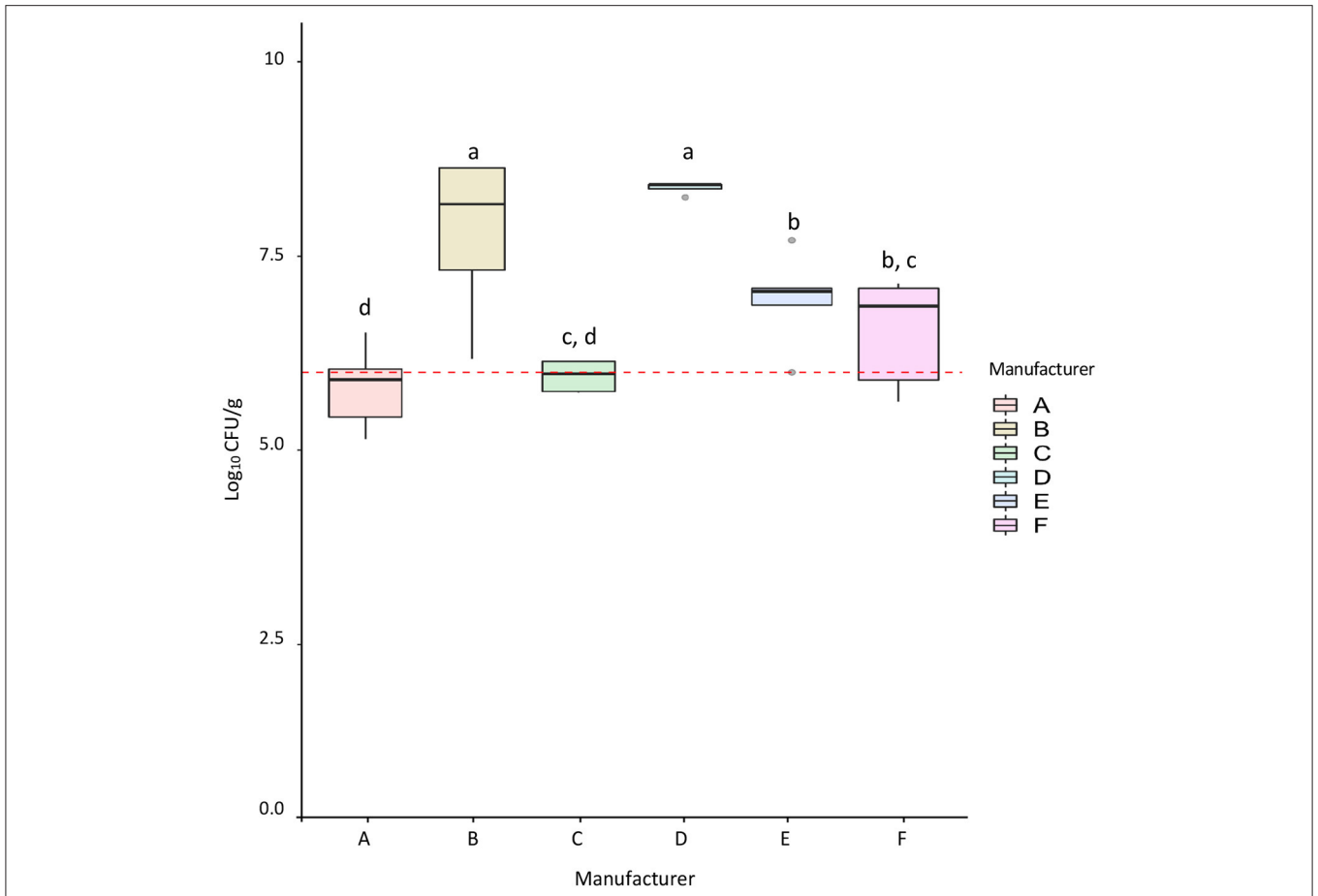

FIGURE 2 | Aerobic bacterial counts (APC) for commercial RMBDs from different manufacturers. The number of samples from each manufacturer was: A = 5, B = 4, C = 5, D = 5, E = 6, F = 6. The Fligner-Killeen test was used to determine the homogeneity of variances and the Shapiro-Wilk test for normality. Multiple comparison analysis of ANOVA for the APC was performed between manufacturers. Different letters marked for bars represent significant differences (p-value < 0.05). The red line shows the suggested APC upper limit for animal compound feed according to Kukier et al. (19).

TABLE 1 | Total fecal samples analyzed (n = 55) and number of positive samples for *Salmonella* spp., *L. monocytogenes, and C. jejuni* according to the type of pet food.

Type of pet food	Fecal samples n	Fecal samples with pathogens *n* (%)	*Salmonella* spp. *n* (%)	*L. monocytogenes* *n* (%)	*C. jejuni n* (%)
RMBDs	33	11 (33.3%)*	8 (24.2%)	1 (3%)	2 (6%)
Extruded	22	0 (0%)*	0 (0%)	0 (0%)	0 (0%)

**Fisher's Exact Test (p-value = 0.002).*

has been previously reported, only a few studies have compared the microbial load between raw and extruded diets (19), as shown in the present work.

Commercial RMBDs should be produced following strict safety measures (HACCP systems, handling of raw materials, hygienic and sanitary practices) and kept frozen; therefore, a lower microbiological load would be expected (33, 34). However, in the present study, we did not find significant differences in the APCs between homemade and commercial RMBDs (**Supplementary Figure 1**).

Pet diets are not exempt from microbiological hazards (5, 7). Even conventional diets that undergo an extrusion process might exhibit post extrusion contamination (5). From March 2020 to August 2021, the FDA started 28 recalls due to possible or confirmed microbiological contamination of pet food; 18 recalls for raw pet food, seven for extruded food, and three for pet treats. *Salmonella* spp., *L. monocytogenes*, Shiga toxin-producing *Escherichia coli* O128, and *Clostridium botulinum* were the cause of these recalls (35). Raw pet diets have shown to be a significant source of pathogenic bacteria (7, 9, 10). Our results support these findings since bacterial pathogens were

TABLE 2 | Analysis of the co-occurrence between isolates from pet food consumed by dog participants ($n = 11$) and the pathogen dog carriers ($n = 11$).

		Fecal samples			RMBD samples		
Dog no.	**Household**	***Salmonella* spp.**	***C. jejuni***	***L. monocytogenes***	***Salmonella* spp.**	***C. jejuni***	***L. monocytogenes***
5	a		x				
8	b						x
9	b						
11	c	x					
13	c	x					
14	d				x		
15	e				x		x
17	f				x		x
25	g	x			x		
28	h	x					
32	i		x		x		x
34	j	x			x		
40	k	x*			x		
45	l	x			x		
46	l	x			x		
52	m			x			

**Dog no. 40 was sampled twice. Both analyzes were positive for Salmonella spp. Pathogen co-occurrence (fecal and RMBD samples) is shown in gray.*

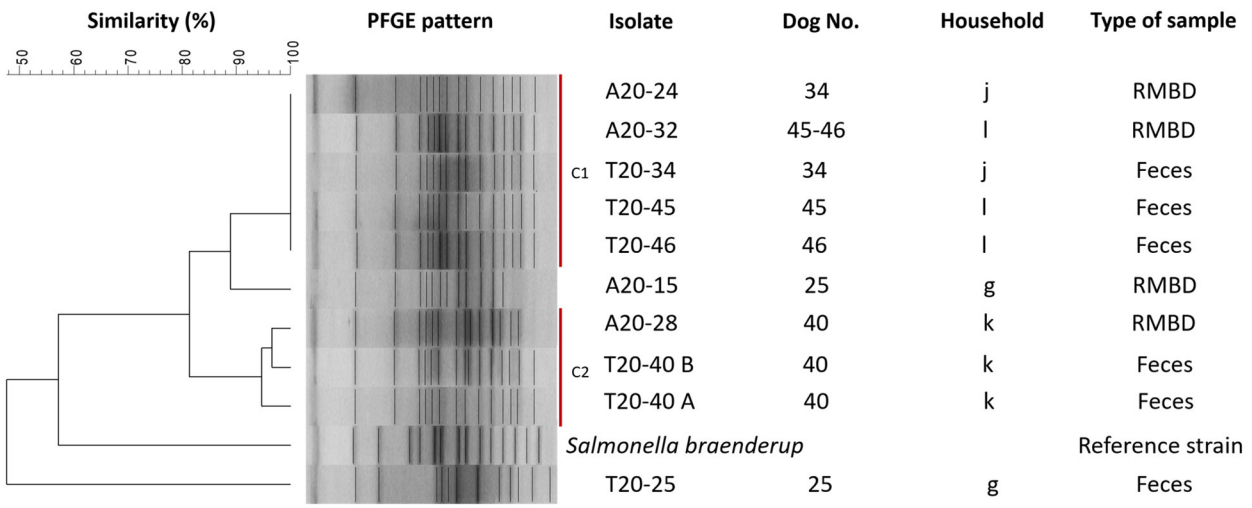

FIGURE 3 | Dendrogram of pulsed-field gel electrophoresis (PFGE) cluster analysis of ten *Salmonella spp.* isolates from RMBD and fecal samples from RMBD-fed dogs. PFGE was performed for *Salmonella* spp. with the restriction enzyme *Xba*I. Sample T20–40 represents two different samples from the same patient taken 1 month apart. C1, cluster 1; C2, cluster 2.

isolated from 35.7% of the RMBD samples. We identified a similar detection rate for *Salmonella* spp. than other studies (10, 36, 37), and a lower detection rate for *L. monocytogenes* than previously reported (10).

In the present study, chicken was the primary source of animal protein in RMBDs contaminated with *Salmonella* spp, while diets contaminated with *L. monocytogenes* were made of diverse meat types (**Supplementary Table 2**). Chicken is a food matrix frequently linked to *Salmonella* spp. contamination (38, 39), while *L. monocytogenes* contamination has been linked to various food matrices, such as raw meat, fruits, and vegetables (40).

Worldwide, official microbial quality standards regulating raw pet foods are still limited (11), especially in regions where raw feeding is relatively new, such as Latin America. Even though regions such as the UK regulate the pet food industry, microbiological analysis for pet foods only consider *Enterobacteriaceae* counts and *Salmonella* spp. detection. Nevertheless, studying other possible microbial pathogens is supported by guidelines and recommendations that promote

TABLE 3 | Answers to questions to evaluate owners' knowledge about benefits (QA) and risks (QB) related to RMBDs.

Variable	RMBD-fed dog owners ($n = 22$), n (%)	Extruded-fed dog owners ($n = 12$*), n (%)
QA: Knowledge about health benefits related to RMBDs		
Yes	22 (100)	6 (50)
No	0 (0)	6 (50)
QB: Knowledge about risks related to RMBDs		
Yes	12 (54.5)	6 (50)
No	10 (45.5)	6 (50)

*Two owners refused to answer QA and QB.

best practices throughout the pet food industry (41–43). For instance, the Pet Food Manufacturers Association (PFMA) guidelines for manufacturing raw pet food in the UK mention *L. monocytogenes*, *C. jejuni*, and *E. coli* as part of the microbiological hazards that should be considered in a risk assessment for raw pet foods. These pathogens are not yet legally regulated within the pet food industry but are closely related to human foodborne diseases (13, 40, 42, 44, 45). Including these foodborne pathogens in the regulation could reinforce the existing regulatory measures to safeguard pet and human health since these pathogens might cause severe human illness through direct contact with RMBDs or cross-contaminated surfaces while manipulating raw ingredients and products.

It should be considered that indicator microorganisms are not suitable as a direct assessment of safety, since the analyses does not differentiate between bacterial species. In the present study, we analyzed APCs instead of counting *Enterobacteriaceae*. APC is a quality indicator that estimates the number of total aerobic microorganisms that grow at mesophilic temperatures. It is used to evaluate the quality of raw materials, cross-contamination, and appropriate hygiene measures, among others (46). In the food industry, *Enterobacteriaceae* counts are used as an indicator of hygiene and post-processing contamination. This latter analysis is usually applied to heat-treated products, such as extruded pet diets, to assess the adequacy of processing and hygiene practices (46, 47). Although *Enterobacteriaceae* counts were not performed in this study, the resulting information could have been helpful as an indirect estimation of enteropathogen loads.

The information generated in this study supports the importance of implementing more robust measures, such as requiring HACCP implementation along the production chain and validating such systems. Moreover, sampling guidelines and microbiological criteria explicitly developed for RMBDs should be a requirement, and further studies will be necessary to identify other possible microbiological hazards in this type of product (9, 11).

The risk of pathogen shedding in pets has been previously studied. Authors have reported *Salmonella* fecal excretion in 3–50% of RMBD-fed dogs, and other pathogens have also been detected (7). For instance (48), in a recent study comparing fecal pathogen excretion between dry and raw-fed dogs, concluded that RMBD-fed dogs were 30 times more likely to excrete *Salmonella* than dogs fed with extruded diets (48). Nevertheless, a comparison of *L. monocytogenes* and *C. jejuni* shedding between raw and extruded-fed dogs has not been reported to date.

Reports indicate that *Salmonella* spp. is shed by 0–44% of dogs, and percentages vary among countries, feeding behaviors, and health status (48, 49). In our study, *Salmonella* spp. fecal excretion in RMBD-fed dogs (24.2%) was higher than in other existing reports (48) but inferior to data reported in Canada and other locations by Finley et al. (34, 50). Although *L. monocytogenes* was isolated in one fecal sample (3%), our study is one of the few available to report the canine fecal shedding of this pathogen. Moreover, our study is the first in comparing the fecal excretion of *L. monocytogenes* between raw and extruded-fed healthy dogs. Kocabiyik et al. (22) reported an *L. monocytogenes* fecal carriage of 1.22% in stray dogs; however, the study did not inform the type of food consumed by the dogs or whether a medical examination was performed on the dogs enrolled in the study before sampling.

The link between canine fecal pathogen shedding and consumption of contaminated RMBDs has been studied for *Salmonella* spp. (11, 48). Evidence for this link is limited for *C. jejuni* (11) and is not available for *L. monocytogenes*. In the present study, fecal isolation of *C. jejuni* and *L. monocytogenes* was independent of the detection of these pathogens in pet food samples.

Even though infections caused by *Salmonella*, *L. monocytogenes,* and *C. jejuni* are usually uncommon in dogs, cases have been strongly associated with ingesting contaminated meat or meat by-products (51). More importantly, the zoonotic potential, implicit public health risks (10), and severity of diseases caused by these pathogens represent the main risk of these types of pet food (52).

In this study, *C. jejuni* was detected only in 6% of stool samples, which is lower than previous findings (53). However, the pathogen was not detected in any of the food samples. Studies have shown an isolation rate of *C. jejuni* ranging from 0 to 50% in dogs with and without gastrointestinal disease (51). While the *Campylobacter* infection can be attributed to meat products, pathogen isolation from feces might not be simultaneous since the fecal shedding can last for prolonged periods after infection recovery (51). Moreover, viable non-culturable *Campylobacter* forms might also interfere with the isolation of the pathogen, even though bacteria in this form might still cause infection (54).

It has been described that RMBD-fed dogs can shed *Salmonella* shortly after the ingestion of contaminated pet food, and shedding might last up to 3–6 weeks in most cases. Usually, pathogen shedding is continual for the first week, but afterward, it becomes intermittent (34, 51). Dogs whose fecal sample tested positive for *Salmonella* spp., but the pathogen was not detected from their food were possibly sampled several days after ingesting contaminated raw food. Other factors might affect the bacterial detection from food samples, including the microbial distribution and the sample's heterogeneous structure,

which might affect the sample representativeness and cause false-negative results (55, 56). Also, animal carriers might shed *Salmonella* due to an unrelated event, such as contact with contaminated fomites (food bowls, hospital cages), consumption of animals that act as reservoir hosts, coprophagy, among others (51). For dogs who showed a positive RMBD sample with a negative fecal result, the intermittency of the fecal shedding should also be considered, as well as the amount of ingested bacteria to produce gastrointestinal colonization and the pet's immune status, among other factors, since bacterial shedding and further bacterial isolation depends on the amount of bacteria that previously survived the passage through the stomach (51).

The genetic similarity among strains simultaneously isolated from dog fecal samples and RMBDs suggests the survival and spread of *Salmonella* spp. from the ingredients commonly used to prepare RMBDs (57). More dogs and a higher sampling frequency are required to perform a conclusive evaluation regarding clonal spread. In contrast, the possible clonal strains' spread among pets and owners might be assessed by studying both human and pet samples.

Evidence shows a high association between RMBDs and health hazards for both humans and animals (7, 9, 10); however, in this study, pet owners demonstrated a strong belief that RMBDs provide numerous benefits at minimal or no risks. These results are also in concordance with previously published data where authors reported owners' tendency to underestimate the risks related to raw feeding or their unawareness (30, 48). The questionnaire also revealed that owners' attitudes, practices, and motivations for using an unconventional raw diet were similar to those reported in other countries such as Brazil and Italy (30, 48).

Owners might be exposed to pathogens through contact with pet food, direct contact with the pet excretions, and the dog's environment. For example, cross-contamination while manipulating pet RMBDs is another critical factor that might cause human illness (9). It is crucial to promote the interdisciplinary work between health professionals and national and international agencies to provide guidance and work in safety strategies for minimizing the risks that might be present in pet products, especially in pet food. The One Health approach is mandatory to guarantee the optimum and healthy interconnection between humans and pets and the health of their shared environment (58).

CONCLUSION

We concluded that RMBDs are more likely to be contaminated by pathogenic bacteria than extruded pet diets. Along the raw pet food manufacturing process, safety measures should be strengthened to control possible microbiological hazards that might affect dogs and owners, and implemented in countries where regulation is absent. Novel microbial inactivation technologies and strategies, or the improvement of already known technologies, such as high-pressure processing, should be studied to control contaminating pathogens. Enteropathogen excretion was higher in RMBD-fed dogs than in extruded-fed dogs. At the same time, the eventual spread of bacterial clones such as *Salmonella* spp. from RMBD to dogs or owners might represent a significant public health concern. Furthermore, owners who preferred raw diets for their pets underestimated the risks related to this feeding practice or knew the risks but still chose to use these diets. Education, guidance, and proper communication between health professionals and pet owners are required, especially for the owners who prefer raw diets for their pets, since the correct use of RMBDs might minimize the risk of food-borne contamination to both owners and pets. Since this is the first Chilean study addressing this topic, further research in this area, the analysis of different zoonotic pathogens, and a larger sample size will be a useful complement to the reported data.

DATA AVAILABILITY STATEMENT

The original contributions presented in the study are included in the article/**Supplementary Material**, further inquiries can be directed to the corresponding author/s.

ETHICS STATEMENT

The animal study was reviewed and approved by Institutional Committee for the Care and Use of Animals (CICUA) from the University of Chile under the CICUA code 20411-VET-UCH. Written informed consent was obtained from the owners for the participation of their animals in this study.

AUTHOR CONTRIBUTIONS

DS and AR-J: conceptualization of the study and conceived the original idea. DS and PF: sample collection. DS: carried out the experiments. DS, MT, and AR-J: microbiological data analysis, application of statistical analysis, and contributed to the interpretation of the results. DS, MT, PN, PF, and AR-J: writing–reviewing and editing. All authors read and approved the final manuscript.

FUNDING

The ENL12/20, a grant from University of Chile support the pay of supplies to perform the research.

ACKNOWLEDGMENTS

We would like to thank all the owners and dogs who participated and made this study possible. Ángel Parra and Bárbara Leyton for contributing to the statistical data analysis. The authors appreciate the assistance given by all the staff from the Microbiology and Probiotics Laboratory from the Institute of Nutrition and Food Technology (INTA), University of Chile.

SUPPLEMENTARY MATERIAL

The Supplementary Material for this article can be found online at: https://www.frontiersin.org/articles/10.3389/fvets.2022.799710/full#supplementary-material

Supplementary Figure 1 | Aerobic bacterial counts (APC) for commercial (n = 31) and homemade (n = 11) RMBDs. The Fligner-Killeen test was used to determine the homogeneity of variances and the Shapiro-Wilk test for normality. The level of APC between both diets was compared using *Welch's Two-Sample T-test*, p-value = 0.17. The red line shows the suggested APC upper limit for animal compound feed according to Kukier et al. (19).

Supplementary Figure 2 | Most common raw ingredients preferred by pet owners for commercial and/or homemade RBMDs (n = 42). **(A)** Meat, **(B)** Organ meats, **(C)** Fruits, **(D)** Vegetables.

Supplementary Table 1 | Demographics of dogs enrolled in the study (n = 55).

Supplementary Table 2 | Characterization of the RMBDs analyzed (n = 42).

Supplementary Table 3 | Demographics of dog owners (n = 36).

Supplementary Table 4 | RMBD-fed dog owners' perceptions about risks and benefits related to RMBDs.

Supplementary Table 5 | RMBD-fed dog owners' main characteristics and habits.

REFERENCES

1. Jalongo MR. The effects of COVID-19 on early childhood education and care: research and resources for children, families, teachers, teacher educators. *Early Child Educ J.* (2021) 49:763–74. doi: 10.1007/s10643-021-01208-y
2. Kepinska-Pacelik J, Biel W. Microbiological hazards in dry dog chews and feeds. *Animals.* (2021) 11:631. doi: 10.3390/ani11030631
3. Crane SW, Cowell CS, Stout NP, Moser EA, Millican J, Romano P, et al. Commercial pet foods. In: Hand MS, Thatcher CD, Remillard RL, Roudebush P, Novotny J, editorss. *Small animal clinical Nutrition.* Topeka, KS: Elsevier Health Sciences. (2010). p. 157–90
4. Dodd S, Cave N, Abood S, Shoveller AK, Adolphe J, Verbrugghe A. An observational study of pet feeding practices and how these have changed between 2008 and 2018. *Vet Rec.* (2020) 186:643. doi: 10.1136/vr.105828
5. Dzanis DA. Anatomy of a recall. *Top Companion Anim Med.* (2008) 23:133–6. doi: 10.1053/j.tcam.2008.04.005
6. Carrión PA, Thompson LJ. Pet food. In: Motarjemi Y, Lelieveld H, editors. *Food Safety Management: A Practical Guide for the Food Industry.* San Diego, CA: Academic Press (2014). p. 379–96. doi: 10.1016/B978-0-12-381504-0.00015-9
7. Freeman LM, Chandler ML, Hamper BA, Weeth LP. Current knowledge about the risks and benefits of raw meat–based diets for dogs and cats. *J Am Vet Med Assoc.* (2013) 243:1549–58. doi: 10.2460/javma.243.11.1549
8. Overgaauw PAM, Vinke CM, Hagen M, Lipman LJA. A one health perspective on the human-companion animal relationship with emphasis on zoonotic aspects. *Int J Environ Res Public Health.* (2020) 17:3789. doi: 10.3390/ijerph17113789
9. Nuesch-Inderbinen M, Treier A, Zurfluh K, Stephan R. Raw meat-based diets for companion animals: a potential source of transmission of pathogenic and antimicrobial-resistant enterobacteriaceae. *R Soc Open Sci.* (2019) 6:191170. doi: 10.1098/rsos.191170
10. van Bree FPJ, Bokken G, Mineur R, Franssen F, Opsteegh M, van der Giessen JWB, et al. Zoonotic bacteria and parasites found in raw meat-based diets for cats and dogs. *Vet Rec.* (2018) 182:50. doi: 10.1136/vr.104535
11. Davies RH, Lawes JR, Wales AD. Raw diets for dogs and cats: a review, with particular reference to microbiological hazards. *J Small Anim Pract.* (2019) 60:329–39. doi: 10.1111/jsap.13000
12. Joffe DJ, Schlesinger DP. Preliminary assessment of the risk of salmonella infection in dogs fed raw chicken diets. *Can Vet J.* (2002) 43:441.
13. Nemser SM, Doran T, Grabenstein M, McConnell T, McGrath T, Pamboukian R, et al. Investigation of liste-ria, Salmonella, and toxigenic Escherichia coli in various pet foods. *Foodborne Pathog Dis.* (2014) 11:706–9. doi: 10.1089/fpd.2014.1748
14. Servicio Agrícolay Ganadero. *Reglamento de Alimentos para Animales. Departamento de Comunicaciones y Participación Ciudadana.* (2018). Available online at: https://www.sag.gob.cl/sites/default/files/d_4-2017_regl_alimentos_pdf-difusion_tapa.pdf (accessed March 3, 2022).
15. Andrews WH, Hua W, Jacobson A, Beilei G, Guodong Z, Hammack T. *Bacteriological Analytical Manual (BAM) Chapter 5: Salmonella.* (2021). Available online at: https://www.fda.gov/food/laboratory-methods-food/bam-chapter-5-salmonella (accessed October 1, 2021).
16. Hitchins AD, Jinneman K, Chen Y. *Bacteriological Analytical Manual (BAM) Chapter 10: Detection of Listeria Monocytogenes in Foods and Environmental Samples, and Enumeration of Listeria Monocytogenes in Foods.* (2017). Available online at: https://www.fda.gov/food/laboratory-methods-food/bam-chapter-10-detection-listeria-monocytogenes-foods-and-environmental-samples-and-enumeration (accessed October 1, 2021).
17. Hunt JM, Abeyta C, Tran T. *Bacteriological Analytical Manual (BAM) Chapter 7: Campylobacter.* (2021). Available online at: https://www.fda.gov/food/laboratory-methods-food/bam-chapter-7-campylobacter(accessed October 1, 2021).
18. Maturin L, Peeler JT. *Bacteriological Analytical Manual (BAM): Aerobic Plate Count.* (2001). Available online at: https://www.fda.gov/food/laboratory-methods-food/bam-chapter-3-aerobic-plate-count (accessed October 1, 2021).
19. Kukier E, Goldsztejn M, Grenda T, Kwiatek K, Wasy D, Hoszowski A. Microbiological quality of compound feed used in Poland. *Bull Vet Inst Pulawy.* (2012) 56:349–54. doi: 10.2478/v10213-012-0061-x
20. Kim JS, Lee GG, Park JS, Jung YH, Kwak HS, Kim SB, et al. A novel multiplex PCR assay for rapid and simultaneous detection of five pathogenic bacteria: Escherichia coli O157:H7, Salmonella, staphylococcus aureus, listeria monocytogenes, vibrio parahaemolyticus. *J Food Prot.* (2007) 70:1656–62. doi: 10.4315/0362-028X-70.7.1656
21. Parra A, Toro M, Jacob R, Navarrete P, Troncoso M, Figueroa G, et al. Antimicrobial effect of copper surfaces on bacteria isolated from poultry meat. *Braz J Microbiol.* (2018) 49:113–8. doi: 10.1016/j.bjm.2018.06.008
22. Kocabiyik AL, Çetin C, Özakin C. Faecal carriage of listeria monocytogenes in stray dogs in Bursa Province, Turkey. *Turkish J Vet Anim Sci.* (2006) 29:1357–9.
23. Centers for Disease Control and Prevention. *Standard Operating Procedure for PulseNet PFGE of Escherichia coli O157: H7, Escherichia coli non-O157 (STEC), Salmonella Serotypes, Shigella Sonnei and Shigella Flexneri.* (2013). Available online at: https://www.cdc.gov/pulsenet/pdf/ecoli-shigella-salmonella-pfge-protocol-508c.pdf (accessed December 2, 2021).
24. Ghasemi A, Zahediasl S. Normality tests for statistical analysis: a guide for non-statisticians. *Int J Endocrinol Metab.* (2012) 10:486–9. doi: 10.5812/ijem.3505
25. Beyene K, Bekele SA. Assessing univariate and multivariate homogeneity of variance: a guide for practitioners. *J Mathematical Theory Model.* (2016) 6:13–7.
26. Kim HY. Statistical notes for clinical researchers: the independent samples. *Restor Dent Endod.* (2019) 44:e26. doi: 10.5395/rde.2019.44.e26
27. McHugh ML. Multiple comparison analysis testing in ANOVA. *Biochem Med.* (2011) 21:203–9. doi: 10.11613/BM.2011.029
28. Kim HY. Statistical notes for clinical researchers: Chi-squared test and Fisher's exact test. *Restor Dent Endod.* (2017) 42:152–5. doi: 10.5395/rde.2017.42.2.152
29. Sheskin DJ. The kruskal-wallis one-way analysis of variance by ranks. In: Sheskin DJ, editor. *Handbook of Parametric and Nonparametric Statistical Procedures.* Boca Raton: Chapman and Hall/CRC (2011). p. 1001–21.

30. Morelli G, Bastianello S, Catellani P, Ricci R. Raw meat-based diets for dogs: survey of owners' motivations, attitudes and practices. *BMC Vet Res.* (2019) 15:74. doi: 10.1186/s12917-019-1824-x
31. Gee NR, Rodriguez KE, Fine AH, Trammell JP. Dogs supporting human health and well-being: a biopsychosocial approach. *Front Vet Sci.* (2021) 8:630465. doi: 10.3389/fvets.2021.630465
32. Servicio Agrícolay Ganadero. *Resolución 7885 exenta. Departamento de Comunicaciones y Participación Ciudadana.* (2018). Available online at: https://www.bcn.cl/leychile/navegar?idNorma=1114058 (accessed March 3, 2022).
33. European Comission. *Commission Regulation (EU) No 142/2011.* (2011). Available at: https://eur-lex.europa.eu/legal-content/EN/TXT/PDF/?uri=CELEX:32011R0142&from=EN (accessed April 6, 2022).
34. Finley R, Ribble C, Aramini J, Vandermeer M, Popa M, Litman M, et al. The risk of salmonellae shedding by dogs fed Salmonella-contaminated commercial raw food diets. *Can Vet J.* (2007) 48:69–75.
35. Food and Drug Administration (FDA). *Recalls, market withdrawals, and safety alerts.* (2021). Available online at: https://www.fda.gov/safety/recalls-market-withdrawals-safety-alerts (accessed October 1, 2021).
36. Finley R, Reid-Smith R, Ribble C, Popa M, Vandermeer M, Aramini J. The occurrence and antimicrobial susceptibility of salmonellae isolated from commercially available canine raw food diets in three Canadian cities. *Zoonoses Public Health.* (2008) 55:455–61. doi: 10.1111/j.1863-2378.2008.01147.x
37. Strohmeyer RA, Morley PS, Hyatt DR, Dargatz DA, Scorza V, Lappin MR. Evaluation of bacterial and protozoal contamination of commercially available raw meat diets for dogs. *J Am Vet Med Assoc.* (2006) 228:537–42. doi: 10.2460/javma.228.4.537
38. Centers for Disease Control and Prevention. *Chicken and Food Poisoning.* (2021). Available online at: https://www.cdc.gov/foodsafety/chicken.html#:~:text=In%20fact%2C%20about%201%20in,eat%20raw%2C%20such%20as%20salad (accessed March 10, 2022).
39. Tack DM, Ray L, Griffin PM, Cieslak PR, Dunn J, Rissman T, et al. Preliminary incidence and trends of infections with pathogens transmitted commonly through food-Foodborne diseases active surveillance Network, 10 US Sites, 2016–2019. *Morbidity Mortality Weekly Rep.* (2020) 69:509. doi: 10.15585/mmwr.mm6917a1
40. Food and Drug Administration. *Listeria (Listeriosis).* (2019). Available online at: https://www.fda.gov/food/foodborne-pathogens/listeria-listeriosis (accessed March 10, 2022).
41. Food and Drug Administration. *Guidance for Industry: Manufacture and Labeling of Raw Meat Foods for Companion and Captive Non Companion Carnivores and Omnivores.* (2004). Available online at: https://www.regulations.gov/document/FDA-2002-D-0148-0007 (accessed March 4, 2022).
42. Pet Food Manufacturer's Association. *Guidelines for the Manufacture of Raw Pet Food in the UK.* (2017). Available online at: https://www.pfma.org.uk/news/guidelines-for-producers-of-raw-pet-food-launched-by-pfma (accessed March 4, 2022).
43. Food and Drug Administration. *Current Good Manufacturing Practice and Hazard Analysis and Risk-Based Preventive Controls for Food for Animals.* (2014). Available online at: https://www.regulations.gov/document/FDA-2011-N-0922-0269 (accessed April 6, 2022).
44. World Health Organization. *Campylobacter.* (2020). Available online at: https://www.who.int/news-room/fact-sheets/detail/campylobacter (accessed April 06, 2022).
45. Mughini-Gras LM, Smid JH, Wagenaar JA, Koene MG, Havelaar AH, Friesema IH, et al. Increased risk for Campylobacter jejuni and C. coli infection of pet origin in dog owners and evidence for genetic association between strains causing infection in humans and their pets. *Epidemiol Infect.* (2013) 141:2526–35. doi: 10.1017/S0950268813000356
46. Food Standards Australia New Zealand. *Compendium of Microbiological Criteria for Food.* (2018). Available online at: https://www.foodstandards.gov.au/publications/Documents/Compedium%20of%20Microbiological%20Criteria/Compendium_revised-jan-2018.pdf (accessed April 30, 2022).
47. Halkman HBD, Halkman AK. Indicator organisms. In: Batt CA, Tortorello ML, editors. *Encyclopedia of Food Microbiology*. London: Academic Press (2014) p. 358–63.
48. Viegas FM, Ramos CP, Xavier RGC, Lopes EO, Junior CAO, Bagno RM, et al. Fecal shedding of *Salmonella* spp., *Clostridium perfringens, and clostridioides difficile* in dogs fed raw meat-based diets in Brazil and their owners' motivation. *PLoS ONE.* (2020) 15:e0231275. doi: 10.1371/journal.pone.0231275
49. Lowden P, Wallis C, Gee N, Hilton A. Investigating the prevalence of Salmonella in dogs within the midlands region of the United Kingdom. *BMC Vet Res.* (2015) 11:1–6. doi: 10.1186/s12917-015-0553-z
50. Morley PS, Strohmeyer RA, Tankson JD, Hyatt DR, Dargatz DA, Fedorka-Cray PJ. Evaluation of the association between feeding raw meat and Salmonella enterica infections at a greyhound breeding facility. *J Am Vet Med Assoc.* (2006) 228:1524–32. doi: 10.2460/javma.228.10.1524
51. Greene CE. Salmonellosis. In: Greene CE, editor. *Infectious Diseases of the Dog and Cat*. St. Louis, MO: Elsevier-Saunders (2012). p. 383–8.
52. Schlech WF. Epidemiology and clinical manifestations of *Listeria monocytogenes* infection. *Microbiol Spectr.* (2019) 7:GPP3-0014-2018. doi: 10.1128/microbiolspec.GPP3-0014-2018
53. Rodrigues CG, Melo RT, Fonseca BB, Martins PA, Ferreira FA, Araújo MB, et al. Occurrence and characterization of Campylobacter spp. isolates in dogs, cats and children. *Pesqui Vet Bras.* (2015) 35:365–70. doi: 10.1590/S0100-736X2015000400009
54. Ruiling LV, Wang K, Feng J, Heeney DD, Liu D, Lu X. Detection and quantification of viable but non-culturable *Campylobacter jejuni. Front Microbiol.* (2020) 10:2920. doi: 10.3389/fmicb.2019.02920
55. Food and Drug Administration. *Guidance for Industry Testing for Salmonella Species in Human Foods and Direct-Human-Contact Animal Foods.* (2012). Available online at: https://www.fda.gov/regulatory-information/search-fda-guidance-documents/guidance-industry-testing-salmonella-species-human-foods-and-direct-human-contact-animal-foods (accessed December 2, 2021).
56. Zadernowska A, Chajecka W. Detection of Salmonella spp. presence in food. In: Barakat SM, editor. *Salmonella-A Dangerous Foodborne Pathogen*. Rijeka: InTech. (2012). p. 393–412.
57. Valdezate S, Vidal A, Herrera-León S, Pozo J, Rubio P, Usera MA, et al. Salmonella derby clonal spread from pork. *Emerg Infect Dis.* (2005) 11:694. doi: 10.3201/eid1105.041042
58. Mackenzie JS, Jeggo M. The one health approach-why is it so important? *Trop Med Infect Dis.* (2019) 4:88. doi: 10.3390/tropicalmed4020088

Conflict of Interest: The authors declare that the research was conducted in the absence of any commercial or financial relationships that could be construed as a potential conflict of interest.

frontiers | Frontiers in Veterinary Science

TYPE Original Research
PUBLISHED 30 September 2022
DOI 10.3389/fvets.2022.913622

OPEN ACCESS

EDITED BY
Lester J. Perez,
Abbott, United States

REVIEWED BY
Maria Irene Pacini,
University of Pisa, Italy
Francisco Rivera-Benítez,
Instituto Nacional de Investigaciones Forestales, Agrícolas y Pecuarias (INIFAP), Mexico

*CORRESPONDENCE
Changsun Choi
cchoi@cau.ac.kr

SPECIALTY SECTION
This article was submitted to Veterinary Infectious Diseases, a section of the journal Frontiers in Veterinary Science

RECEIVED 05 April 2022
ACCEPTED 06 September 2022
PUBLISHED 30 September 2022

CITATION
Yeo D, Hossain MI, Jung S, Wang Z, Seo Y, Woo S, Park S, Seo DJ, Rhee MS and Choi C (2022) Prevalence and phylogenetic analysis of human enteric emerging viruses in porcine stool samples in the Republic of Korea. *Front. Vet. Sci.* 9:913622. doi: 10.3389/fvets.2022.913622

Prevalence and phylogenetic analysis of human enteric emerging viruses in porcine stool samples in the Republic of Korea

Daseul Yeo[1], Md. Iqbal Hossain[1], Soontag Jung[1], Zhaoqi Wang[1], Yeeun Seo[1], Seoyoung Woo[1], Sunho Park[1], Dong Joo Seo[2], Min Suk Rhee[3] and Changsun Choi[1,4]*

[1]Department of Food and Nutrition, Chung-Ang University, Anseong-si, South Korea, [2]Department of Food and Nutrition, Gwangju University, Gwangju, South Korea, [3]Division of Food Bioscience and Technology, College of Life Sciences and Biotechnology, Korea University, Seoul, South Korea, [4]Bio and Environmental Technology Research Institute, Chung-Ang University, Seoul, South Korea

Emerging infectious diseases (EID) in humans and animals are proving to be a serious health concern. This study investigated the prevalence of emerging or re-emerging human enteric viruses in porcine stools and swabs. Eleven enteric EID viruses were selected as target viruses for the current study and ranked based on their impact on public health and food safety: enterovirus (EV), hepatitis E virus, norovirus GI and GII, sapovirus (SaV), adenovirus (AdV), astrovirus, rotavirus, hepatitis A virus, aichivirus, and bocavirus. Using real-time RT-PCR or real-time PCR, EID viruses were detected in 129 (86.0%) of 150 samples. The most prevalent virus was EV, which was detected in 68.0% of samples, followed by AdV with a detection rate of 38.0%. In following sequencing and phylogenetic analyses, 33.0% (58/176) of the detected viruses were associated with human enteric EID viruses, including AdV-41, coxsackievirus-A2, echovirus-24, and SaV. Our results show that porcine stools frequently contain human enteric viruses, and that few porcine enteric viruses are genetically related to human enteric viruses. These findings suggest that enteric re-emerging or EID viruses could be zoonoses, and that continuous monitoring and further studies are needed to ensure an integrated "One Health" approach that aims to balance and optimize the health of humans, animals, and ecosystems.

KEYWORDS

enteric virus, emerging virus, phylogenetic analysis, enterovirus, adenovirus, foodborne virus, pig

Introduction

Emerging infectious diseases (EID) are defined as newly recognized infectious diseases in a community or existing diseases that rapidly increase in incidence or expand in geographic range. Many emerging diseases are zoonotic—the disease-causing organism first incubates in an animal host and then spreads to humans at random (1).

Zoonotic diseases spread from animals to humans *via* direct contact, contaminated food and/or water, or the environment, and account for about 61% of the infectious organisms affecting humans (2). Viral pathogens transmitted *via* the fecal-oral route are often reported as EID infectious agents. EID viruses can spread between humans and have pandemic potential, which has recently led to the COVID-19 pandemic (3).

Worldwide, 3,618 cases of EID have been reported from 2016 to 2018 (4), with 331 cases of infectious diseases recorded in the United States during the first 6 months of 2019 (4). The Republic of Korea has noted an increase in EID virus-related deaths between 1996 and 2015, with the rate increasing from 16.5 per 100,000 to 44.6 per 100,000 (5). Recently, EID viruses were identified as the main pathogenic agents in cases of intestinal infections, viral hepatitis, respiratory tract infections, and sepsis (5), and enteric EID viruses were the main cause of disease in such cases. The hepatis A virus (HAV) and the hepatitis E virus (HEV), for example, are representative EID viruses that cause viral hepatitis and intestinal infections, and the HEV and the enterovirus (EV) have become the leading causes of infections in humans overall. As a zoonotic viral disease, numbers of HEV infections escalated from 514 in 2005 to 5,617 in 2015 across Europe (6). Similarly, different serotypes of EV are prevalent at different frequencies in different parts of the world. For example, since the 1980s, seasonal endemic EV-A71 has been prevalent in the U.S., causing small sporadic outbreaks (7). Similarly, EV-A71 continues to cause large epidemics of hand foot and mouth disease (HFMD) and neurological diseases every 1–3 years in the Asian region since the 1990s (7).

There are various causes underlying the emergence of EID viruses, including increasing human and livestock densities, altering patterns of wild-to-domestic animal contact, direct human-to-wild animal contact, and changes in host species diversity (8). As a reservoir of viral EID, pigs represent the major livestock with the most human contact. Various viruses (e.g., picornaviruses, arboviruses, circoviruses, flaviviruses, and herpesviruses) can infect both pigs and humans (9). Because various viruses use pigs as their host, the investigation of the role of pigs as a potential EID virus reservoir is essential to understand the circumstances under which these pathogens emerge and evolve, especially in light of the "One Health" approach that is needed to control zoonoses. However, although research on human enteric viruses has extensively covered waterborne transmission, little information is so far available on enteric EID virus transmission in animals (10). Therefore, we focused on the role of pigs as a potential EID virus reservoir in this study.

The aim of this study was to identify potential enteric EID viruses by examining detection rates and analyzing the genetic relationships between the detected viruses in the Republic of Korea. We selected enteric viruses that are being monitored in eight countries around the world and identified their prevalence in pigs, the livestock closest to humans.

Materials and methods

Ethical approval

The study design, animal handling, and experimental protocols were reviewed and approved by the Institutional Animal Care and Use Committee (IACUC) of Chung-Ang University, Republic of Korea (IACUC approval number: CAU2018-00112). All experiments were conducted in accordance with the IACUC guidelines and regulations.

Selection of enteric EID viruses

The potential enteric EID viruses were identified from pathogen lists regulated by the relevant organizations or institutions of each country and from previous publications. A total of 20 human and animal health agencies and food safety administrations were included in our selection process (Supplementary Table 1). Enteric EID viruses were ranked based on their priority for and impact on public health and food safety (Figure 1). The selection of target viruses is depicted in Supplementary Table 2. Following the decision process illustrated in Figure 1, eleven target viruses were selected: norovirus (NoV)-GI, NoV-GII, sapovirus (SaV), HEV, adenovirus (AdV), aichivirus (AiV), astrovirus (AstV), HAV, and rotavirus (RotaV) in rank 1; human bocavirus (BoV) and EV including coxsackievirus (CV), echovirus (EchoV), and poliovirus in rank 3. No enteric EID was classified as rank 2.

Sample preparation and nucleic acid extraction

One hundred nineteen porcine stool samples and 31 porcine rectal swabs were collected from 14 pig farms located in Gyeonggi-do, Gyeongsang-do, Jeolla-do, and Chungcheong-do provinces in the Republic of Korea. A total of 87 piglets and 63 sows were tested for enteric EID virus prevalence (Table 1). All samples were collected from healthy pigs and transferred to a laboratory for analysis. To minimize sampling stress, veterinarians collected pig stools and rectal swabs from several different pens at each farm, following the IACUC protocol guidelinesWe used the BD CultureSwab MaxV collection and transport systems (Becton, Dickinson and Company, NJ, USA) for rectal swabs and Norgen Biotek's Stool Nucleic Acid Collection and Preservation system (Lubio Science, Zurich, Switzerland) to collect porcine stools. Each sample was composed of 10% (v/v) stool suspension in phosphate-buffered saline (PBS; 0.1 M, pH 7.4). The suspension was prepared as previously described (11). Viral RNA and DNA were extracted using

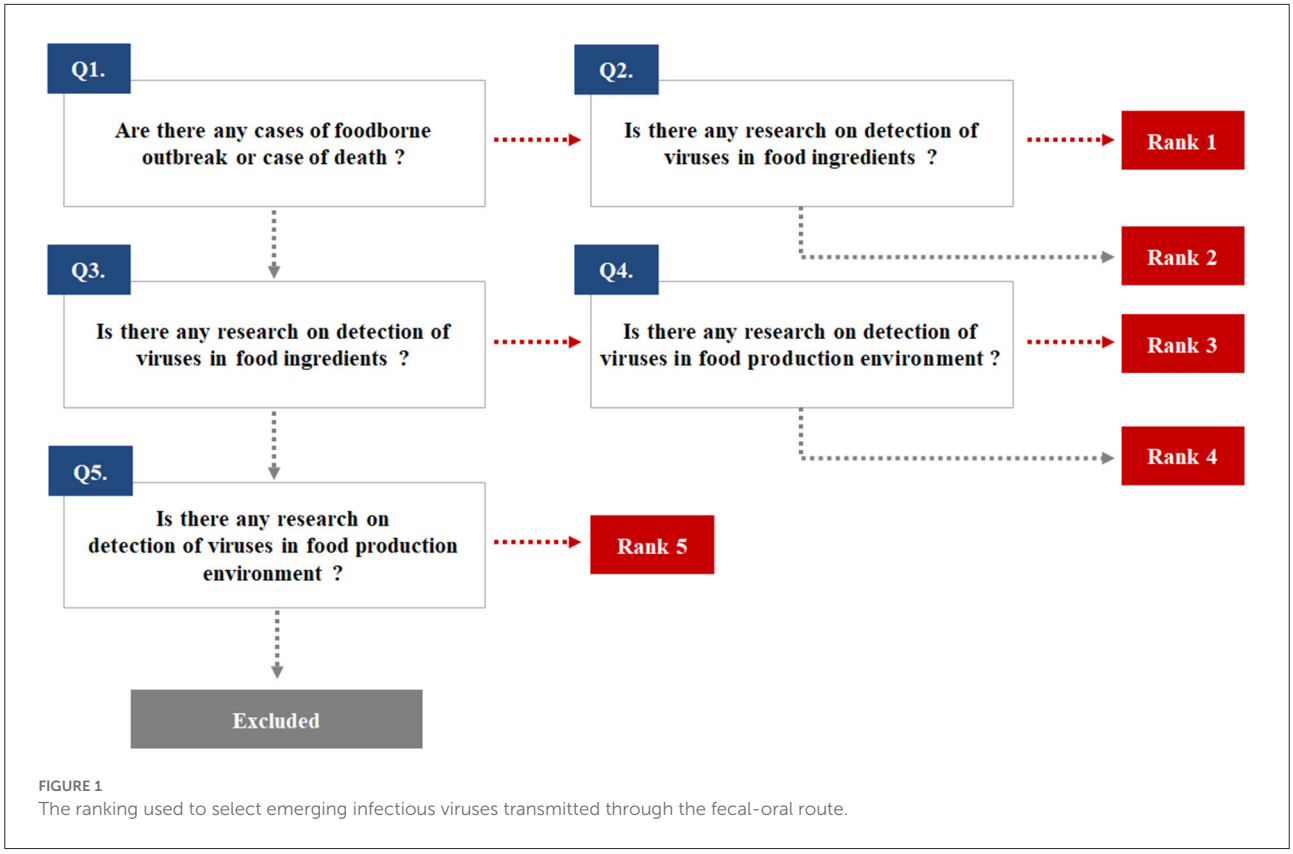

FIGURE 1
The ranking used to select emerging infectious viruses transmitted through the fecal-oral route.

TABLE 1 Stages and sample types of 150 pigs at a pig farm in the Republic of Korea.

Region	Stage		Total
Sample type	Sows	Piglets	
Gyeonggi-do	9	11	20
Stools	9	11	20
Gyeongsang-do	47	47	94
Stools	46	19	65
Swabs	1	28	29
Jeolla-do	2	8	10
Stools	2	8	10
Chungcheong-do	5	21	26
Stools	3	21	24
Swabs	2	0	2
Total	**63**	**87**	**150**

the RNeasy Mini kit (Qiagen, Hilden, Germany) according to the manufacturer's instructions. The extracted RNA and DNA samples were stored at −80°C until real-time reverse transcription PCR (RT-qPCR) or real-time PCR (qPCR) was performed.

RT-qPCR or qPCR for the detection and titration of enteric EID viruses

The primers and probes used for one-step RT-qPCR and qPCR are presented in Supplementary Table 3. One-step RT-qPCR for detecting each RNA virus was performed with the one-step RT-PCR kit (Qiagen, Hilden, Germany), while qPCR was performed using the Premix Ex Taq (2X)™ kit (Takara, Shiga, Japan) to identify the DNA viruses. RT-qPCR and qPCR were performed on the CFX96™ Real-Time PCR system (Bio-Rad, CA, USA); the titration of each virus sample was determined using either RT-qPCR or qPCR. Synthetic RNA and DNA sequences were used in the assay as standard templates for titration. Synthetic templates, including quantitative synthetic DNA of human AdV-41 (ATCC® VR-930DQ, Virginia, US) and quantitative synthetic RNA of NoV-GII (ATCC® VR-3235SD, Virginia, US), were used as standard templates for AdV and NoV, respectively, and IDT-synthetic RNA oligo (IDT, IA, USA) was used as the standard template for EV, HEV, and RotaV.

For RT-qPCR- or qPCR-positive samples, nested (RT)-PCR was performed to obtain amplicons for sequence analysis. The primers used for nested (RT)-PCR are presented in Supplementary Table 4. Nested (RT)-PCR was performed using a one-step RT-PCR kit (Bioneer, Daejeon, Republic of

Korea). Amplicon size was confirmed on 1.0% agarose gel electrophoresis and then used for the sequencing analysis.

Sequence analysis and phylogenetic tree

Purification of PCR product was performed using a nucleospin gel and a PCR Clean-up Mini Kit (Macherey-Nagel, Düren, Germany). The sequence analysis was performed with capillary electrophoresis on a SeqStudio Genetic Analyzer (Thermo Fisher Scientific, MA, USA). Sequence data were edited using the SeqMan programme (DNASTAR, WI, USA). The sequences were analyzed by comparison with different viral genotype sequences using BLAST and the Norovirus Typing Tool version 2 (https://www.rivm.nl/mpf/typingtool/norovirus/) (12).

To establish the genetic relationships between the detected viruses, phylogenetic analyses were carried out using the nucleotide sequences. During the phylogenetic analysis of the detected EID viruses, with the MEGA X software (http://www.megasoftware.net), the RNA-dependent RNA polymerase (RdRp) gene was targeted for EV, the hexon and fiber genes for AdV, ORF2 and VP1 overlapping regions for HEV, the VP1 region for SaV, and the ORF1-ORF2 junction region for NoV-GII. For the sequencing analysis, a bootstrap consensus tree inferred from 1,000 replicates was taken to represent the evolutionary history of the analyzed taxa. Branches corresponding to partitions reproduced in <50% of the bootstrap replicates were collapsed (13).

Results

Prevalence of EID viruses detected in porcine stools and swabs

One hundred twenty-nine (86.0%) of the 150 samples tested were positive for the presence of at least one EID virus (Table 2). A total of 85 (56.6%) and 44 (29.3%) of the 129 positive samples were identified as containing single and multiple viruses, respectively. In the single virus-containing samples, EV (including EV-G, CV-A2, and EchoV) and AdV were most commonly detected, in 61 and 22 of the 85 samples, respectively. In contrast, 31 of the 44 samples containing multiple viruses tested positive for both EV-G and AdV.

Table 2 shows that overall, EV was detected in 102 (68.0%) of the 150 samples, while EV-G was the most prevalent genotype, detected in 95 (93.1%) of the 102 EV-positive samples. AdV, HEV, SaV, and NoV-GII were found in 57 (38.0%), eight (5.3%), five (3.3%), and four (2.7%) out of 150 samples, respectively. Further, HEV was not identified as a single virus in any sample but only detected alongside EV-G, CV-A2, AdV, NoV-GII, and SaV. Moreover, depending on the host tropism characteristics, 33.0% (58/176) of the viruses were determined to be human enteric viruses, including CV-A2, EchoV, AdV, and SaV-GI; in contrast, 59.1% (104/176) and 8.0% (14/176) of the viruses detected in this study were porcine enteric viruses (including EV-G, porcine AdV-5, and porcine AdV-3) and zoonotic enteric viruses (including NoV-GII.11, NoV-GII.18, HEV-GIII, and SaV-GV).

Additionally, the viral loads of EV-G, CV-A2, and EchoV-24 ranged between 1.3 and 6.8, 2.3 and 5.9, and 3.7 log10 genome copies/mL, respectively. The viral loads of AdV, HEV, and NoV-GII ranged between 0.1 and 5.1, 0.5 and 3.5, and 0.6 and 3.0 log10 genome copies/mL (average values, 2.4, 1.9, and 1.3 log10 genome copies/mL). In addition, the viral load of SaV was not determined in this study. Although 82.6% (124/150) porcine samples tested positive for RotaV on RT-qPCR, nested RT-PCR failed to obtain amplicons for sequence analysis. NoV-GI, AstV, HAV, BoV, and AiV were not detected in any of the porcine samples (data not shown).

Genotype and phylogenetic analysis of enteric EID viruses detected in porcine samples

Enterovirus

Amplicons derived from positive samples were further characterized by sequencing. The phylogenetic analysis of RdRp region fragments for EV is shown in Figure 2. Six EV sequences belonged to the EV-A genogroup and clustered with a reference sequence of NC038306 (CV-A2). The nucleotide sequence identity is shown in Supplementary Table 5, exhibiting a nucleotide sequence identity of 98.8–100.0%. On the other hand, only one EchoV-E24 (MK415773) was identified as belonging to genogroup EV-B, and it clustered with the AY302548 reference sequence, demonstrating 100.0% nucleotide sequence identity. The EV-G genogroup was identified in five genotypes: EV-G1, EV-G2, EV-G6, EV-G9, and EV-G10. Moreover, 53 sequences belonged to a large cluster of EV-G9, which contained reference sequences of LC316821, LC316825, and LC316824, demonstrating a high percentage of nucleotide sequence identity, around 84.1–95.1%, with porcine strain LC316825. Thirteen EV-G2 sequences clustered with porcine reference sequences (LC316792 and AF363455), while their nucleotide sequence identity with LC316792 and AF363455 was 86.6–95.1% and 86.6–91.5%, respectively. Twelve EV sequences clustered with EV-G1 and exhibited 52.4–58.5% nucleotide sequence identity with the KF985175 reference sequence. The ten EV-G6 sequences showed 75.6–89.0% nucleotide sequence identity with the JQ818253 reference sequence, which was not reported on before the Republic of Korea. The seven sequences of EV-G matched with EV-G10. The nucleotide identity of

TABLE 2 Profiles of enteric EID viruses detected in porcine stools and swabs.

		Number of positive samples (%)		
		Stools ($n = 119$)	Rectal swabs ($n = 31$)	Total ($n = 150$)
Detected virus type				
None		17 (14.3)	4 (12.9)	21 (14.0)
Single				
	EV-G	50 (42.0)	5 (16.1)	55 (36.6)
	CV-A2	0 (0.0)	5 (16.1)	5 (3.3)
	EchoV	1 (0.8)	0 (0.0)	1 (0.7)
	AdV	17 (14.3)	5 (16.1)	22 (14.6)
	NoV-GII	1 (0.8)	0 (0.0)	1 (0.7)
	SaV	1 (0.8)	0 (0.0)	1 (0.7)
	Total	**70 (58.8)**	**15 (48.3)**	**85 (56.6)**
Multiple				
	EV-G + AdV	21 (17.6)	10 (32.3)	31 (20.6)
	EV-G + HEV	4 (3.4)	0 (0.0)	4 (2.6)
	EV-G + SaV	3 (2.5)	0 (0.0)	3 (2.0)
	EV-G + NoV-GII	0 (0.0)	1 (3.2)	1 (0.7)
	CV-A2 + HEV	0 (0.0)	1 (3.2)	1 (0.7)
	EV-G + NoV-GII + AdV	1 (0.8)	0 (0.0)	1 (0.7)
	HEV + AdV	1 (0.8)	0 (0.0)	1 (0.7)
	HEV + AdV + NoV-GII	1 (0.8)	0 (0.0)	1 (0.7)
	HEV + AdV + SaV	1 (0.8)	0 (0.0)	1 (0.7)
	Total	**32 (26.9)**	**12 (38.7)**	**44 (29.3)**
Susceptible host type				
	Human	39 (22.2)	19 (10.8)	58 (33.0)
	Porcine	86 (48.7)	18 (10.2)	104 (59.1)
	Zoonotic	12 (6.8)	2 (1.1)	14 (8.0)
	Total[¶]	**137 (77.9)**	**39 (22.2)**	**176**

[¶]Susceptible host classification was based on the total number of detected virus (176) including multiple detection.

the clusters of EV-G10 with the KP982873 reference sequence was 78.0–82.9%.

Adenovirus

The sequences of AdV positive samples were analyzed for the hexon and fiber genes using a phylogenetic tree as depicted in Figure 3; the nucleotide sequence identities are listed in Supplementary Tables 6, 7. For the hexon gene, our analysis shows that 48, seven, and two AdV sequences clustered with the human AdV-41, porcine AdV-5, and porcine AdV-3 genogroups, respectively (Figure 3A). However, the sequence identity range of the human AdV-41 genogroup with the AB330122 (human AdV-41 Tak strain) reference sequence was 97.3–99.1%; likewise, the porcine AdV-5 genogroup clustered with the AC000009 (porcine AdV C strain) reference sequence and showed 93.8–95.9% nucleotide sequence identity, while the porcine AdV-3 genogroup showed 81.4–83.2% nucleotide sequence identity with the KU761583 (porcine AdV-3 strain) reference sequence. Four sequences of AdV were also analyzed for fiber genes using a phylogenetic tree (Figure 3B), and we found that the resulting sequences clustered with human AdV-41 and exhibited 99.1–99.3% nucleotide sequence identity with the reference sequence DQ315364 (human AdV-41 Tak strain). A comparison of the AdV sequences with those obtained for the hexon gene also confirmed the presence of human AdV-41 strains but not porcine AdV strains.

Hepatitis E virus

Phylogenetic analysis of HEV was based on ORF2 and VP1 overlapping regions (Figure 4). All investigated HEV

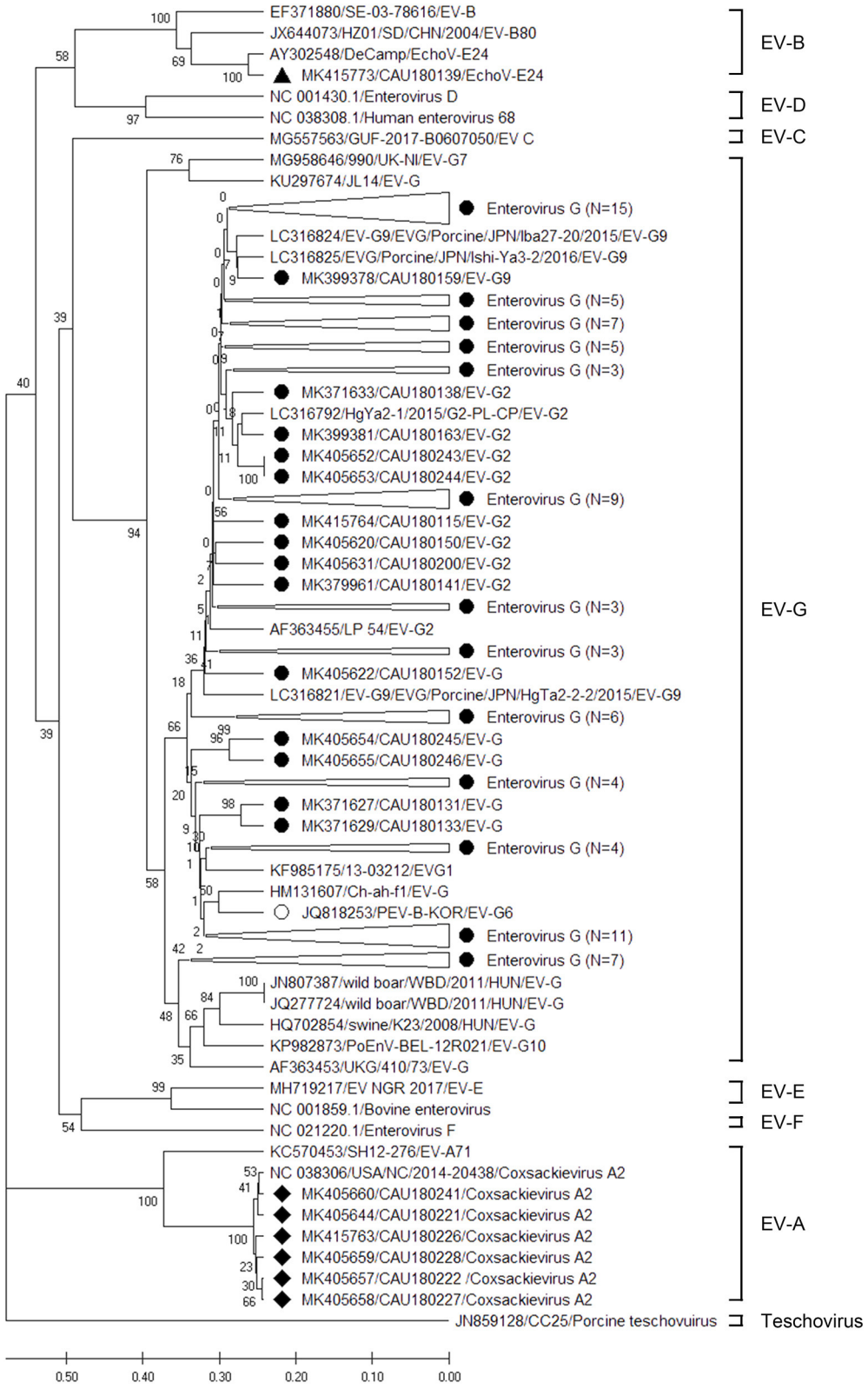

FIGURE 2
Phylogenetic analysis of the EVs detected in porcine stools and swabs. The EV phylogenetic tree was constructed using the Unweighted Pair Group Method with Arithmetic Mean (UPGMA) and based on the 191-bp sequence of the RdRp region. The black circles (•), black squares (■),
(Continued)

FIGURE 2 (Continued)
and black triangle (▲) indicate the EV-G, CV- A2, and EchoV-E24 sequences detected in this study, respectively. The white circle (○) represents an EV-G (JQ818253/PEV-B-KOR/EV-G6) reference sequence that was reported in the Republic of Korea. The phylogenetic analysis included the EV genotype: EV-A (two strains), EV-B (three strains), EV-C (one strain), EV- D (two strains), EV-G (16 strains), EV-E (two strains), EV-F (one strain), and teschovirus (one strain) as reference sequences. Large triangles (△) on the phylogenetic tree represent the compression of a subtree with a genetic relationship, with the numbers of compressed sequences shown in parentheses. The numbers at the nodes of the tree indicate bootstrap values and the scale bar indicates nucleotide substitutions per site.

sequences in this study were confirmed to belong to the GIII genogroup. During the phylogenetic analysis, eight HEV sequences (MK341089, MK341088, MK341086, MK341081, MK341087, MK341082, MK341080, and MK341083) clustered with the porcine HEV reference sequences (FJ426403 and KR027506). Particularly, the MK341082 sequence showed a high nucleotide sequence identity of 93.9% with the FJ426403 reference sequence (Supplementary Table 8).

Sapovirus

The phylogenetic analysis of SaV was based on the VP1 region, as depicted in Figure 5, and the nucleotide sequence identities are listed in Supplementary Table 9. According to our analysis, three (MK450329, MK450330, and MK450331) and two (MK361037 and MK36103) sequences of SaV belonged to the GI and GV genogroups, respectively. Moreover, the SaV-GI cluster showed 94.1–94.6% nucleotide sequence identity with the human SaV reference sequences (AY694184 and KP298674), while the SaV-GV cluster exhibited 77.2–77.5% nucleotide sequence identity with the porcine SaV reference sequence (AB521772).

Norovirus GII

Three NoV-GII.11 and one NoV-GII.18 sequence were confirmed by phylogenetic analysis of the RdRp region, as shown in Figure 6. According to analysis, the three sequences (MK355709, MK355707, and MK355706) belonging to the NoV-GII.11 genotype clustered with a porcine NoV reference sequence (HQ392821). Their nucleotide sequence identity with the HQ392821 reference sequence was 88.2–88.6%, and that with the human NoV reference sequence (KC662537) 72.0–73.3% (Supplementary Table 10).

Discussion

In this study, eleven enteric EID viruses were chosen based on their priority for and impact on public health and food safety. We observed a high prevalence of enteric EID viruses in porcine samples collected from domestic pig farms in the Republic of Korea. A total of 176 viruses were detected, including several viruses that were detected in multiple cases per same porcine stools and rectal swabs. The positivity rate for EID viruses in individual porcine stools and rectal swabs was 86.0%. As for single viruses, EV and AdV were the most commonly detected viruses in the 150 samples tested. As for multiple detection, 31 of the 44 positive samples were positive for both EV and AdV. We detected human enteric viruses, CV-A2, EchoV, AdV, and SaV-GI, and porcine enteric viruses, EV-G, porcine AdV-5, and porcine AdV-3. Moreover, the zoonotic viruses NoV-GII.11, NoV-GII.18, HEV-GIII, and SaV-GV were detected (representing 9.3% of all detected viruses). The porcine enteric virus detection rate was 69.3% (104/150), with most being EV-G, while human enteric viruses were detected in 38.7% (58/150) of samples. To our knowledge, there is no prior report on the detection of CV-A2, EchoV, AdV-41, and SaV-GI in pigs in the Republic of Korea.

Detection was often prolonged, due to the ability of the viruses to survive on environmental surfaces, in foods, and in water (14). Viruses detected in stools have three possible sources: direct shedding from infected pigs, contaminated pig farm environments, and contaminated workers (15). Regarding the prevalence of enteric EID viruses, porcine stools and rectal swabs showed detection rates of 85.7% (102/119) and 87.0% (27/31), possibly indicating direct virus infection of the animals, although most of the detected viruses were EV and AdV in both sample types. However, among the detected viruses (EV and AdV), AdV-41 and CV-A2 are known to infect only humans. Moreover, enteric viruses were extremely stable on pork chops when stored at low temperatures (16, 17). The infectivity of the viruses was not confirmed since they were only detected *via* PCR, but the presence of human enteric viruses in porcine samples indicates the possibility of the virus spreading to animals, thereby providing a possible cause of zoonotic infection. In addition, a virus can be transmitted from an infected pig to humans through direct contact with the environment or contaminated instruments as well as through the consumption of contaminated undercooked meat (18).

Our study based on phylogenetic analyses evaluated the genotypes and sub-genotypes of enteric EID viruses in porcine stools and swabs. The RdRp genomic region that was analyzed for EV is a highly conserved genomic region, according to previous reports (19). During our phylogenetic analysis of the detected EV, three EV genogroups were identified, which belonged to EV-A, EV-B, and EV-G. Within these genogroups, EV-A included six sequences of CV-A2 detected on porcine

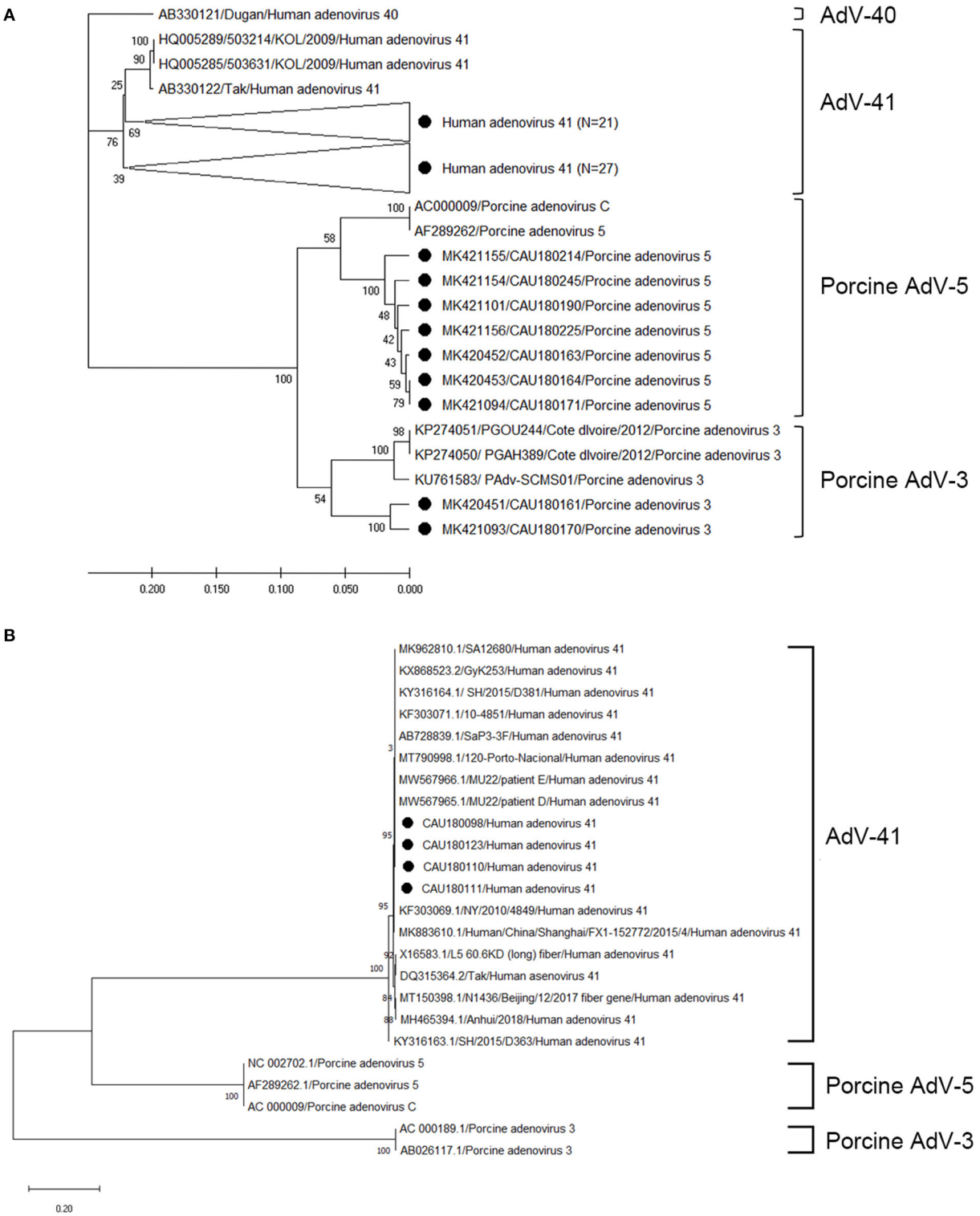

FIGURE 3
Phylogenetic tree of AdV detected in porcine stools and swabs. Sequences detected in this study are represented as black circles (•). **(A)** Phylogenetic tree analysis for the AdV hexon gene using the UPGMA method and based on the 171-bp sequence. Here, AdV-41 (three strains), AdV-40 (one strain), porcine AdV-5 (two strains), and porcine AdV-3 (three strains) were used as reference sequences. Large triangles (◁) on the phylogenetic tree represent the compression of a subtree with a genetic relationship, with the numbers of compressed sequences shown in parentheses. **(B)** Phylogenetic tree analysis for AdV (662-bp of the fiber gene) using the maximum likelihood method. Here, AdV-41 (15 strains), porcine AdV-5 (three strains), and porcine AdV-3 (two strains) were used as reference sequences. The numbers at the nodes of the tree indicate bootstrap values and the scale bar indicates nucleotide substitutions per site.

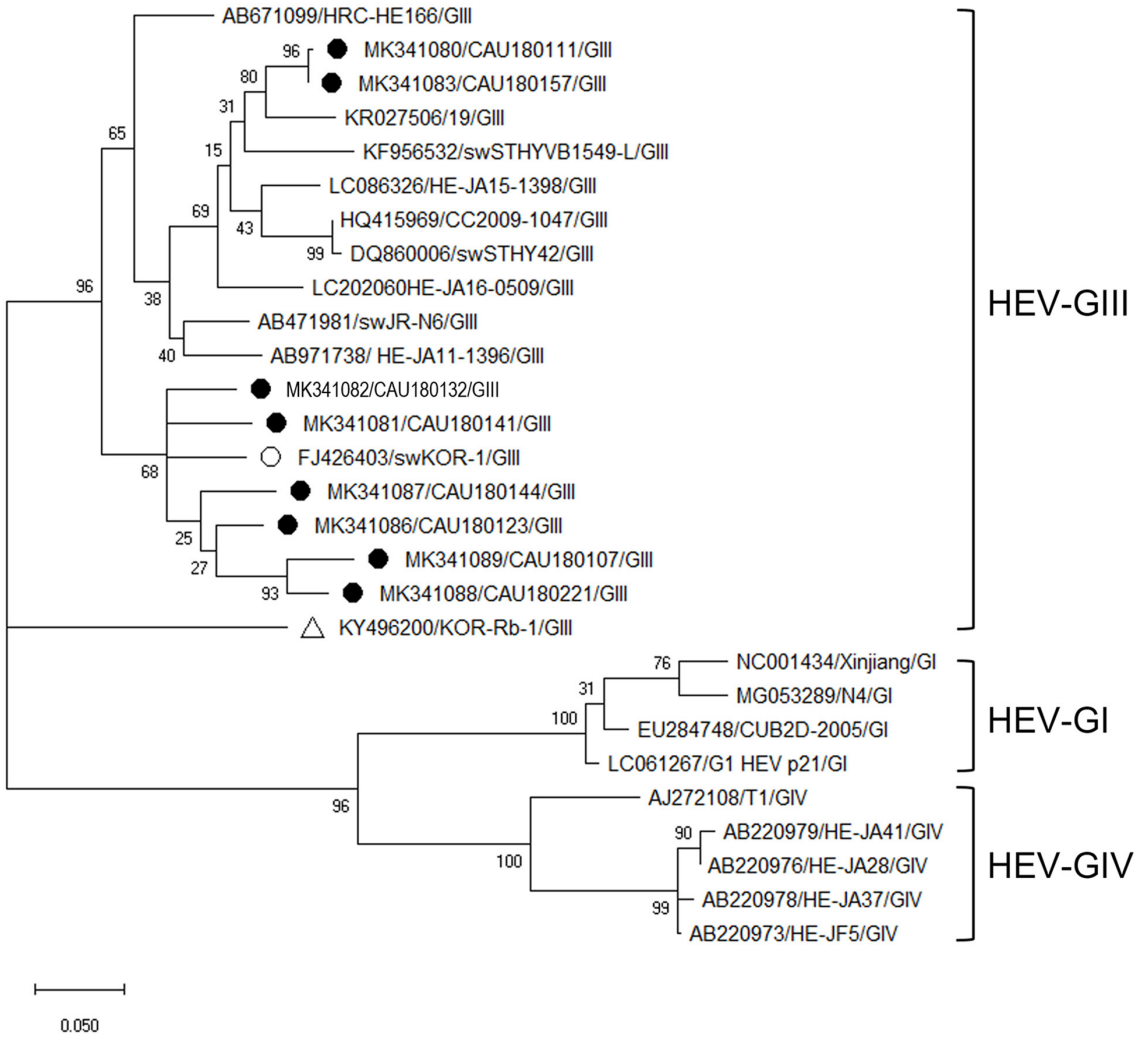

FIGURE 4
Phylogenetic analysis of HEV detected in porcine stools and swabs. The HEV phylogenetic tree was constructed following the UPGMA method and based on 348-bp sequences of ORF2 and VP1 overlapping region. Sequences detected in this study are represented as black circles (•). The reference sequences of porcine HEV (FJ426403/swKOR-1) and rabbit HEV (KY496200/KOR-Rb-1) strains detected in the Republic of Korea are labeled with white circle (○) and triangle (Δ), respectively. The phylogenetic analysis included HEV-GI (four strains), HEV-GIII (11 strains), and HEV-GIV (five strains) as reference sequences. The numbers at the nodes of the tree indicate bootstrap values and the scale bar indicates nucleotide substitutions per site.

rectal swabs only, with a high nucleotide sequence identity (98.8–100.0%) with the NC038306 (CV-A2) reference sequence discovered in the US (20). CV is one of the major public health problems among children in the Republic of Korea, with ∼214,642 (0.53%) of 40,461,309 outpatients surveilled in a study from 2010 to 2013 diagnosed with CV-induced HFMD (21). In addition, the EV-B genogroups show frequent recombination within species (22), and one sequence of EchoV-E24 (MK415773) that was detected in porcine stool clustered with the AY302548 (EchoV-E24) reference sequence isolated from humans in the US in 2004 (22). This indicates that the capsid region of the corresponding EchoV-E24 (MK415773) sequence also needs to be analyzed for more accurate genotyping. In the Republic of Korea, no cases of infection or hospitalization due to EchoV-E24 have been reported, but one out of 579 HFMD pediatric patients is diagnosed with an EchoV-E24 infection in China in 2010 (23). Moreover, the EV-G genogroup consists of three large clusters. Among them, the largest clade contains 89 sequence groups with EV-G1, EV-G2, EV-G6, and EV-G9, while the EV-G10 group includes seven sequence groups. Reports from Japan and Germany have stated that 51 sequences belong to a large cluster of EV-G9 (24, 25). To date, the EV-G genogroup consists of 17 types of genotypes from EV-G1 to EV-G17 (25), of which EV-G1, EV-G2,

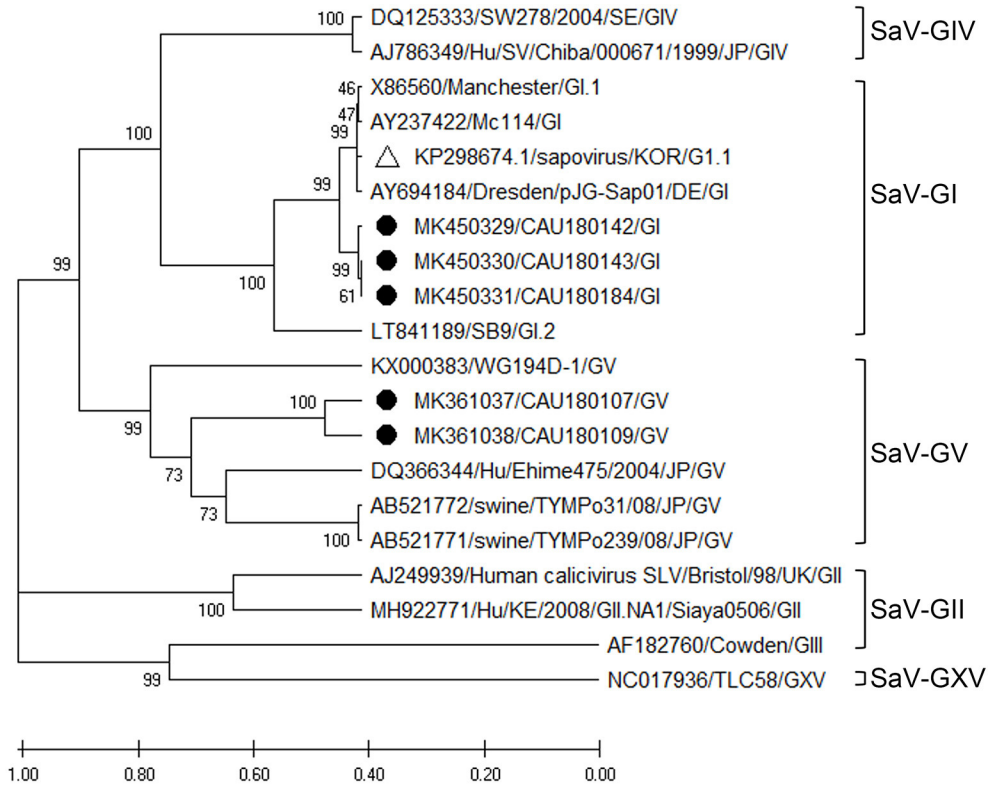

FIGURE 5
Phylogenetic analysis of SaV detected in porcine stools and swabs. The SaV phylogenetic tree was constructed following the UPGMA method and based on 416-bp sequences of the VP1 region. Sequences detected in this study are represented as black circles (•). The white triangle (Δ) represents the human SaV strain (KP298674/KOR/G1.1) that was confirmed in the Republic of Korea. The phylogenetic analysis included SaV-GI (four strains), SaV-GII (two strains), SaV-GIII (one strain), SaV-GIV (two strains), SaV-GV (four strains), and SaV-GXV (one strain) as reference sequences. The numbers at the nodes of the tree indicate bootstrap values and the scale bar indicates nucleotide substitutions per site.

EV-G6, EV-G9, and EV-G10 were identified in this study. In the Republic of Korea, EV-G6 (JQ818253) was first reported in 2009, also isolated from porcine stool (26). According to our findings, 11 sequences of EV-G6 clustered with the JQ818253 strain, exhibiting a 75.6–89.0% nucleotide sequence identity. The other 84 sequences' average nucleotide sequence identity with the JQ818253 strain was 80.9%. This is presumed to be from a similar era than the ancient JQ818253 strain. For a higher phylogenetic resolution, the capsid region of VP1 also needs to be analyzed in future studies.

The sequences positive for AdV were analyzed for hexon and fiber genes. The hexon gene is highly conserved (27), making it the best single region of the AdV genome for genus-specific detection; other major capsid protein regions were identified to target the fiber gene that was used for the subgroup determinant validation. Our phylogenetic analysis of the detected AdV revealed that the sequences belonged to the human AdV-41, porcine AdV-5, and porcine AdV-3 genogroups. An additional analysis of some fiber genes confirmed a higher sequence identity with the AdV reference sequences, of 99.1–99.3%, as that reported in Asian countries (28). Porcine AdV infections were usually asymptomatic, but some cases of mild diarrhea or mild respiratory signs in porcine have been reported (29); however, no signs of pig infections were recorded in this study. In particular, in view of the potential application of porcine AdV as virus vectors for vaccines and the use of animal AdV as vectors for gene therapy, the results of this study indicate that attention should be paid to health and infectious disease management and vaccine development.

The HEV prevalence rate varies by country, region, and even farms within a country (30). Our phylogenetic analysis of all detected HEV sequences belonging to the same genotype, HEV-GIII, showed a high nucleotide identity (93.9%) with FJ426403 (swine HEV isolate swKOR-1). Meanwhile, the six HEV-positive sequences found in this study clustered with sub-genotype GIIIa containing reference strain FJ426403 (31), while two other positive sequences (MK341080, MK341083) were grouped with KR027506, which has been found to infect humans in France, belonging to the sub-genotype GIIIc (32). However, HEV-positive sequences belonging to sub-genotype GIIIa were detected at higher rates than GIIIc, in line with reports that the HEV-GIIIa sub-genotype is predominantly prevalent in the

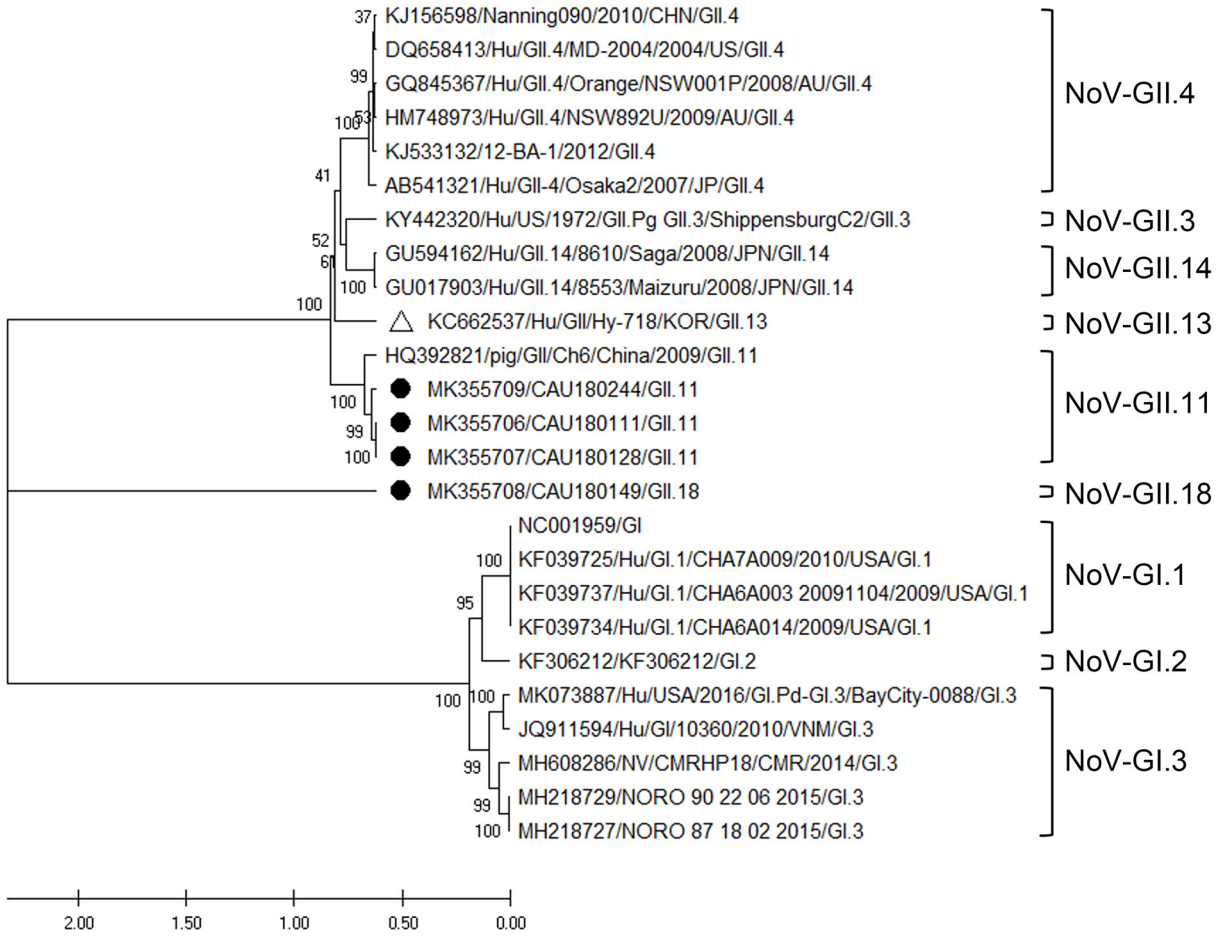

FIGURE 6
Phylogenetic analysis of NoV detected in porcine stools and swabs. The NoV phylogenetic tree was constructed following the UPGMA method and based on 310-bp sequences of the RdRp region. Sequences detected in this study are labeled with black circles (•). The white triangle (Δ) represents the human NoV strain (KC662537/Hu/GII/Hy-718) that was confirmed in the Republic of Korea. As reference sequences, NoV-GII.4 (six strains), GII.3 (one strain), GII.14 (two strains), GII.13 (one strain), GII.11 (one strain), and GI (10 strains) were used. The numbers at the nodes of the tree indicate bootstrap values and the scale bar indicates nucleotide substitutions per site.

Republic of Korea and Japan while the GIIIc sub-genotype is predominantly prevalent in Europe (32). Likewise, our study also confirmed the genetic association of the detected HEV to infect both humans and porcine HEV. In the Republic of Korea, the sub-genotype GIIIa detected in cats and oysters was found to be genetically close to porcine and human HEV (31). According to Wilhelm et al. (33), HEV sequences identified in Canadian retail pork livers closely match human strains. It is widely known that HEV is an emerging zoonotic agent and that pigs represent an important reservoir (31). Moreover, ingestion of HEV-contaminated raw or undercooked pig products is the main source of HEV transmission through food (34). Therefore, to prevent indigenous human HEV infections in the Republic of Korea, one should be careful about coming in contact with infected animals and consuming contaminated meat.

SaV has been detected in humans, pigs, mink, dogs, sea lions, bats, chimpanzees, and rats (25, 35). The SaV genome contains two overlapping open reading frames (ORFs): ORF1 and ORF2. ORF1 encodes the non-structural proteins and the capsid protein, VP1, while ORF2 encodes the minor structural protein, VP2. Furthermore, SaV is genetically highly diverse and classified into nineteen genogroups based on the VP1 sequences (35, 36). Among the nineteen SaV genogroups, four genogroups (GI, GII, GIV, and GV) and eight genogroups (GIII, GV, GVI, GVII, GVIII, GIX, GX, and GXI) have been found to be linked to human and pig infections, respectively (36). However, as far as we are aware, this is the first time that the SaV-GV genogroup (in two detected sequences, MK361037 and MK36103) has been detected in porcine stools in the Republic of Korea. In addition, based on our phylogenetic analysis, the SaV-GV genogroup was more closely related to porcine SaV than human SaV. Accordingly, the SaV-GI genogroup clusters with the KP298674 reference strain isolated from human stools (37). Overall, detected isolates and reference strains differ between

porcine and human stool, and it is presumed that there may be genetic differences, even within the same GI genogroup.

The NoV genus covers viruses that infect a variety of hosts such as humans, pigs, cattle, and mice, and this broad range of hosts provides the opportunity for its zoonotic spread (38). Among the various hosts, asymptomatic infected pigs are known as natural reservoirs of NoV. Moreover, porcine NoV is genetically most similar to human NoV. In addition, NoV-GII.11 and GII.18 genotypes have been reported as sources of infections in pigs (39). Accordingly, porcine NoV has been mainly detected in pigs (40). Among the diverse range of human NoV genotypes in GII, NoV-GII.18 shares the highest amino acid identity with the human GII.3 (39). Our study results also show the genetic similarity of NoV-GII.18 (MK355708) to human NoV-GII.4. Furthermore, in the Republic of Korea, the NoV-GII.11 was detected in fecal samples from asymptomatic food handlers (41). According to a phylogenetic analysis, the MK355709, MK355707, and MK355706 sequences cluster with the HQ392821 reference sequence isolated from pigs with diarrhea symptoms in China (40). These results indicate that porcine NoV has a high potential for zoonotic transmission of enteric EID.

Several enteric viruses are very similar to human viruses found in pigs, and some are thought to have zoonotic potential. In this study, all of the target viruses were detected, which shows how common they are in Korean pig populations (42–44). Sequence analyses were conducted to determine how likely these viruses are to spread to humans. However, only few positive RT-qPCR samples could be used for conventional RT-PCR and sequencing, potentially due to the fact that the assays have different sensitivities and we could therefore not successfully amplify the samples using conventional RT-PCR. However, it cannot be ruled out that the primer systems we used were not able to detect certain viruses. Therefore, RT-PCR systems that can reliably identify different porcine viruses should be designed in the future. Our sequence analysis shows that the few viruses that are typical to pigs are only weakly related to human strains. Another result of our phylogenetic analysis is that pig and human strains were grouped together on different branches of the phylogenetic trees.

The emergence of enteric EID viruses exemplifies the complex interaction of humans, animals, and the environment (45). Many viruses have been shown to survive for a long period in their natural reservoirs (46), and viruses are constantly spreading from natural hosts to humans and other animals (47), due to human activities such as modern agriculture and urbanization (48). Keeping in mind the "One Health" philosophy, the best strategy to prevent viral zoonosis is to maintain the natural viral reservoirs separate from human society. Zoonotic agents have been responsible for the majority of current human health threats (49). One of the most important facets of public health is veterinary public health (VPH), where veterinarians are responsible for safeguarding animal and human health and wellbeing. Viral pathogenesis studies for domestic and wild animals, as well as for human diseases, are coordinated by veterinary virologists working in VPH. This coordination is essential to our understanding of how viruses spread and affect individual health and populations over time; it is also important for preparing for the emergence of new human diseases. However, veterinarians must be aware of the disease's prevalence, risk factors, control strategies, and associated costs and benefits in order to adequately advise producers on disease management. Good hygienic practices during slaughtering are required to reduce the danger of these viruses being introduced into the food chain. Furthermore, highly exposed individuals, such as slaughterers and veterinarians, should be made more aware of the need to prevent direct transmissions.

In further studies, the prevalence and zoonotic potential of all pig viruses suspected to infect humans should be assessed using larger samples and including more geographical regions to precisely evaluate the risk of zoonotic virus transmission. Furthermore, whole-genome sequence analyses are needed for a more comprehensive approach, rather than genotyping of specific genes.

Conclusion

This study documents the molecular detection and diversity of human enteric EID viruses in porcine stools and swabs collected from pig farms in the Republic of Korea. Our results indicate that human enteric viruses detected in pigs and some porcine enteric viruses are genetically related to human enteric viruses. In addition, the previously known zoonotic viruses, such as HEV-GII, NoV-GII, SaV, EV, and AdV, were detected in porcine samples, indicating the zoonotic potential of porcine enteric viruses as potential EIDs.

Data availability statement

The datasets presented in this study can be found in online repositories. The names of the repository/repositories and accession number(s) can be found in the article/Supplementary material.

Ethics statement

The study design, animal handling, and experimental protocols were reviewed and approved by the Institutional Animal Care and Use Committee (IACUC) of Chung-Ang University, Republic of Korea (IACUC approval number: CAU2018-00112). All experiments were conducted in accordance with the IACUC guidelines and regulations. Written informed consent was obtained from the owners for the participation of their animals in this study.

Author contributions

DS, MR, and CC: conceptualization and supervision. DY, MH, SJ, and ZW: validation. DY and SJ: formal analysis and software. DY, SJ, ZW, YS, SW, and SP: investigation and methodology. DY, MH, and SJ: visualization. DY, DS, MR, and CC: project administration. DY, SJ, and SP: data curation. CC: resources. DY: writing—original draft preparation. DY, MH, SJ, and CC: writing—review and editing. MR and CC: funding acquisition. All authors have read and agreed to the published version of the manuscript.

Funding

This research was supported by a grant (17162MFDS034) from the Ministry of Food and Drug Safety in 2017-2019. YS was supported by the Chung-Ang University Graduate Research Scholarship in 2021.

Conflict of interest

The authors declare that the research was conducted in the absence of any commercial or financial relationships that could be construed as a potential conflict of interest.

Publisher's note

Supplementary material

The Supplementary Material for this article can be found online at: https://www.frontiersin.org/articles/10.3389/fvets.2022.913622/full#supplementary-material

SUPPLEMENTARY TABLE 1
List of institutions reviewed for selection of enteric EID.

SUPPLEMENTARY TABLE 2
Rank of emerging infectious viruses.

SUPPLEMENTARY TABLE 3
Primers used for the screening of target viruses.

SUPPLEMENTARY TABLE 4
Primers used for the sequencing analysis.

SUPPLEMENTARY TABLE 5
Comparison of nucleotide sequence identity of EV.

SUPPLEMENTARY TABLE 6
Comparison of nucleotide sequence identity of the AdV hexon gene region.

SUPPLEMENTARY TABLE 7
Comparison of nucleotide sequence identity of the AdV fiber gene region.

SUPPLEMENTARY TABLE 8
Comparison of nucleotide sequence identity of HEV.

SUPPLEMENTARY TABLE 9
Comparison of nucleotide sequence identity of SapoV.

SUPPLEMENTARY TABLE 10
Comparison of nucleotide sequence identity of NoV.

SUPPLEMENTARY TABLE 11
GenBank accession numbers for all viral sequences confirmed in this study.

References

1. McArthur DB. Emerging infectious diseases. *Nurs Clin.* (2019) 54:297–311. doi: 10.1016/j.cnur.2019.02.006

2. Rahman M, Sobur M, Islam M, Ievy S, Hossain M, El Zowalaty ME, et al. Zoonotic diseases: etiology, impact, and control. *Microorganisms.* (2020) 8:1405. doi: 10.3390/microorganisms8091405

3. Singh S, McNab C, Olson RM, Bristol N, Nolan C, Bergstrøm E, et al. How an outbreak became a pandemic: a chronological analysis of crucial junctures and international obligations in the early months of the Covid-19 pandemic. *Lancet.* (2021) 398:2109–24. doi: 10.1016/S0140-6736(21)01897-3

4. Choi SY, Kim JH, Kim J, Hwang ES. World outbreak trend of infectious diseases with surveillance. *J Bacteriol Virol.* (2019) 49:141–51. doi: 10.4167/jbv.2019.49.3.141

5. Choe YJ, Choe SA, Cho SI. Trends in infectious disease mortality, South Korea, 1983–2015. *Emerg Infect Dis.* (2018) 24:320. doi: 10.3201/eid2402.170862

6. Aspinall EJ, Couturier E, Faber M, Said B, Ijaz S, Tavoschi L, et al. Hepatitis E virus infection in Europe: surveillance and descriptive epidemiology of confirmed cases, 2005 to 2015. *Eurosurveillance.* (2017) 22:30561. doi: 10.2807/1560-7917.ES.2017.22.26.30561

7. Fischer TK, Simmonds P, Harvala H. The importance of enterovirus surveillance in a post-polio world. *Lancet Infect Dis.* (2021) 23:352–354. doi: 10.1016/S1473-3099(20)30852-5

8. Chiesa F, Tomassone L, Savic S, Bellato A, Mihalca AD, Modry D, et al. A survey on one health perception and experiences in europe and neighboring areas. *Front Public Health.* (2021) 9:92. doi: 10.3389/fpubh.2021.609949

9. Firth C, Charleston MA, Duffy S, Shapiro B, Holmes EC. Insights into the evolutionary history of an emerging livestock pathogen: porcine circovirus 2. *J Virol.* (2009) 83:12813–21. doi: 10.1128/JVI.01719-09

10. Nieuwenhuijse DF, Koopmans MP. Metagenomic sequencing for surveillance of food-and waterborne viral diseases. *Front Microbiol.* (2017) 8:230. doi: 10.3389/fmicb.2017.00230

11. Seo DJ, Jung D, Jung S, Ha SK, Ha SD, Choi IS, et al. Experimental miniature piglet model for the infection of human norovirus GII. *J Med Virol.* (2018) 90:655–62. doi: 10.1002/jmv.24991

12. Kroneman A, Vennema H, Deforche K, Avoort H, Peñaranda S, Oberste M, et al. An automated genotyping tool for enteroviruses and noroviruses. *J Clin Virol.* (2011) 51:121–5. doi: 10.1016/j.jcv.2011.03.006

13. Kumar S, Stecher G, Li M, Knyaz C, Tamura K. Mega X: molecular evolutionary genetics analysis across computing platforms. *Mol Bio Evol.* (2018) 35:1547. doi: 10.1093/molbev/msy096

14. Kotwal G, Cannon JL. Environmental persistence and transfer of enteric viruses. *Curr Opin Virol.* (2014) 4:37–43. doi: 10.1016/j.coviro.2013.12.003

15. Salines M, Andraud M, Rose N. From the epidemiology of hepatitis E virus (Hev) within the swine reservoir to public health risk mitigation strategies: a comprehensive review. *Vet Res.* (2017) 48:1–15. doi: 10.1186/s13567-017-0436-3

16. Brandsma S, Muehlhauser V, Jones T. Survival of murine norovirus and F-RNA coliphage Ms2 on pork during storage and retail display. *Int J Food Microbiol.* (2012) 159:193–7. doi: 10.1016/j.ijfoodmicro.2012.09.015

17. Jones T, Muehlhauser V. Survival of porcine teschovirus as a surrogate virus on pork chops during storage at 2° C. *Int J Food Microbiol.* (2015) 194:21–4. doi: 10.1016/j.ijfoodmicro.2014.11.003

18. Monini M, Di Bartolo I, Ianiro G, Angeloni G, Magistrali CF, Ostanello F, et al. Detection and molecular characterization of zoonotic viruses in swine fecal samples in italian pig herds. *Arch Virol.* (2015) 160:2547–56. doi: 10.1007/s00705-015-2538-4

19. Bo S, Peng G. Structural basis of viral RNA-dependent RNA polymerase catalysis and translocation. *PNAS.* (2016) 113:E4005–14. doi: 10.1073/pnas.1602591113

20. Oberste MS, Penaranda S, Maher K, Pallansch MA. Complete genome sequences of all members of the species human enterovirus A. *J Gen Virol.* (2004) 85:1597–607. doi: 10.1099/vir.0.79789-0

21. Joshi YP, Kim JH, Kim H, Cheong HK. Impact of drinking water quality on the development of enteroviral diseases in Korea. *Int J Environ Res Public Health.* (2018) 15:2551. doi: 10.3390/ijerph15112551

22. Oberste MS, Maher K, Pallansch MA. Evidence for frequent recombination within species human enterovirus B based on complete genomic sequences of all thirty-seven serotypes. *J Virol.* (2004) 78:855–67. doi: 10.1128/JVI.78.2.855-867.2004

23. Zhang X, Wang H, Ding S, Wang X, Chen X, Wo Y, et al. Prevalence of enteroviruses in children with and without hand, foot, and mouth disease in China. *BMC Infect Dis.* (2013) 13:1–8. doi: 10.1186/1471-2334-13-606

24. Bunke J, Receveur K, Oeser AC, Fickenscher H, Zell R, Krumbholz A. High genetic diversity of porcine enterovirus G in Schleswig-Holstein, Germany. *Arch Virol.* (2018) 163:489–93. doi: 10.1007/s00705-017-3612-x

25. Nagata A, Sekiguchi Y, Oi T, Sunaga F, Madarame H, Imai R, et al. Genetic diversity of enterovirus G detected in faecal samples of wild boars in Japan: identification of novel genotypes carrying a papain-like cysteine protease sequence. *J Gen Virol.* (2020) 101:840–52. doi: 10.1099/jgv.0.001446

26. Moon HJ, Song D, Seon BH, Kim HK, Park SJ, An DJ, et al. Complete genome analysis of porcine enterovirus B isolated in Korea. *J Virol.* (2012) 86:10250. doi: 10.1128/JVI.01548-12

27. José G, Marta PI, Natalia MG, Carmen M. Adenovirus structure: what is new? *Int J Mol Sci.* (2021) 22:5240. doi: 10.3390/ijms22105240

28. Ishiko H, Shimada Y, Konno T, Hayashi A, Ohguchi T, Tagawa Y, et al. Novel human adenovirus causing nosocomial epidemic keratoconjunctivitis. *J Clin Microbiol.* (2008) 46:2002–8. doi: 10.1128/JCM.01835-07

29. Fong TT, Lipp EK. Enteric viruses of humans and animals in aquatic environments: health risks, detection, and potential water quality assessment tools. *Microbiol Mol Biol Rev.* (2005) 69:357–71. doi: 10.1128/MMBR.69.2.357-371.2005

30. Primadharsini PP, Nagashima S, Okamoto H. Genetic variability and evolution of hepatitis E Virus. *Viruses.* (2019) 11:456. doi: 10.3390/v11050456

31. Song YJ, Jeong HJ, Kim YJ, Lee SW, Lee JB, Park SY, et al. Analysis of complete genome sequences of swine hepatitis E virus and possible risk factors for transmission of HEV to humans in Korea. *J Med Virol.* (2010) 82:583–91. doi: 10.1002/jmv.21730

32. Lhomme S, Abravanel F, Dubois M, Chapuy-Regaud S, Sandres-Saune K, Mansuy JM, et al. Temporal evolution of the distribution of hepatitis E virus genotypes in southwestern France. *Infect Genet Evol.* (2015) 35:50–5. doi: 10.1016/j.meegid.2015.07.028

33. Wilhelm B, Muellner P, Pearl DL, Rajić A, Houde A, McEwen SA. Preliminary molecular epidemiological investigation of hepatitis E virus sequences from Quebec, Canada. *Prev Vet Med.* (2015) 118:359–69. doi: 10.1016/j.prevetmed.2014.12.011

34. Meng XJ. Zoonotic and foodborne transmission of hepatitis E virus. *Semin Liver Dis.* (2013) 33:041–9. doi: 10.1055/s-0033-1338113

35. Oka T, Lu Z, Phan T, Delwart EL, Saif LJ, Wang Q. Genetic characterization and classification of human and animal sapoviruses. *PLoS ONE.* (2016) 11:e0156373. doi: 10.1371/journal.pone.0156373

36. Yinda CK, Conceição-Neto N, Zeller M, Heylen E, Maes P, Ghogomu SM, et al. Novel highly divergent sapoviruses detected by metagenomics analysis in straw-colored fruit bats in cameroon: divergent bat sapoviruses. *Emerg Microbes infect.* (2017) 6:1–7. doi: 10.1038/emi.2017.20

37. Choi HL, Suh CI, Park SW, Jin JY, Cho HG, Paik SY. Whole-genome sequencing analysis of sapovirus detected in South Korea. *PLoS ONE.* (2015) 10:e0132328. doi: 10.1371/journal.pone.0132328

38. Verma AK, Bhat S, Sircar S, Dhama K, Malik YS. Enteric viral zoonoses: counteracting through one health approach. *J Exp Biol Agric Sci.* (2018) 6:42–52. doi: 10.18006/2018.6(1).42.52

39. Wang QH, Costantini V, Saif LJ. Porcine enteric caliciviruses: genetic and antigenic relatedness to human caliciviruses, diagnosis and epidemiology. *Vaccine.* (2007) 25:5453–66. doi: 10.1016/j.vaccine.2006.12.032

40. Shen Q, Zhang W, Yang S, Cui L, Hua X. Complete genome sequence of a new-genotype porcine norovirus isolated from piglets with diarrhea. *J Vriol.* (2012) 86:7015–6. doi: 10.1128/JVI.00757-12

41. Jeong AY, Jeong HS, Lee JS, Park YC, Lee SH, Hwang IG, et al. Occurrence of norovirus infections in asymptomatic food handlers in South Korea. *J Clin Microbiol.* (2013) 51:598–600. doi: 10.1128/JCM.01856-12

42. Choi IS, Kwon HJ, Shin NR, Yoo HS. Identification of swine hepatitis E virus (HEV) and prevalence of anti-hev antibodies in swine and human populations in Korea. *J Clin Microbiol.* (2003) 41:3602–8. doi: 10.1128/JCM.41.8.3602-3608.2003

43. Jung K, Saif LJ. Porcine epidemic diarrhea virus infection: etiology, epidemiology, pathogenesis and immunoprophylaxis. *Vet J Vet.* (2015) 204:134–43. doi: 10.1016/j.tvjl.2015.02.017

44. Lee C. Porcine epidemic diarrhea virus: an emerging and re-emerging epizootic swine virus. *Virol J.* (2015) 12:1–16. doi: 10.1186/s12985-015-0421-2

45. Dixon MA, Dar OA, Heymann DL. Emerging infectious diseases: opportunities at the human-animal-environment interface. *Vet Rec.* (2014) 174:546–51. doi: 10.1136/vr.g3263

46. Han HJ, Wen Hl, Zhou CM, Chen FF, Luo LM, Liu Jw, et al. Bats as reservoirs of severe emerging infectious diseases. *Virus Res.* (2015) 205:1–6. doi: 10.1016/j.virusres.2015.05.006

47. Parrish CR, Holmes EC, Morens DM, Park EC, Burke DS, Calisher CH, et al. Cross-species virus transmission and the emergence of new epidemic diseases. *MMBR.* (2008) 72:457–70. doi: 10.1128/MMBR.00004-08

48. Howard CR, Fletcher NF. Emerging virus diseases: can we ever expect the unexpected? *Emerg Microbes infect.* (2012) 1:1–9. doi: 10.1038/emi.2012.47

49. Meslin F. Global aspects of emerging and potential zoonoses: a who perspective. *Emerg Infec Dis.* (1997) 3:223. doi: 10.3201/eid0302.970220

Frontiers in Microbiology

Explores the habitable world and the potential of microbial life

The largest and most cited microbiology journal which advances our understanding of the role microbes play in addressing global challenges such as healthcare, food security, and climate change.

Discover the latest Research Topics

See more →

Frontiers

Avenue du Tribunal-Fédéral 34
1005 Lausanne, Switzerland
frontiersin.org

Contact us

+41 (0)21 510 17 00
frontiersin.org/about/contact